Title
PROCEEDINGS OF THE WORKSHOP ON PARTICLE PHYSICS AT INTERMEDIATE ENERGIES

Author
Field, R.D.

Publication Date
1971-06-01

WEN2E1

UCRL-20655
UC-34 Physics
TID-4500 (57th Ed)

Proceedings of the Workshop on Particle Physics at Intermediate Energies

Held on March 29-30, 1971, at
The California Institute of Technology
Pasadena, California

June 1971

Edited by R.D. Field Jr.
Lawrence Radiation Laboratory
University of California
Berkeley, California
94720

Printed in the United States of America
Available from
National Technical Information Service
U.S. Department of Commerce
5285 Port Royal Road
Springfield, Virginia 22151
Price: Printed Copy $6.00; Microfiche $0.95

DISCLAIMER

PROCEEDINGS OF THE WORKSHOP ON

PARTICLE PHYSICS AT INTERMEDIATE ENERGIES*

Held on March 29-30, 1971, at the
California Institute of Technology,
Pasadena, California.

Edited by: R. D. Field, Jr.
Lawrence Radiation Laboratory
University of California
Berkeley, California 94720

Organized by: G. C. Fox, J. D. Jackson, H. M. Steiner,
and G. Zweig

Sponsored by: California Institute of Technology
Pasadena, California 91109 and
Lawrence Radiation Laboratory
University of California
Berkeley, California 94720

* This work was supported in part by the U.S. Atomic Energy Commission.

Papers in this Proceedings are
reproduced directly from contributor's copy

Discussion Leaders

C. Lovelace
A. Yokosawa
A. H. Rosenfeld
G. Zweig
J. Ballam
B. Cork
G. Manning
W. A. Wenzel

Speakers

G. Manning
B. Cork
D. Jovanovic
E. J. Lofgren
D. Berley
F. Muller
J. Ballam
H. K. Ticho
G. Shapiro
J. L. Rosner
R. G. Moorhouse
M. J. Moravcsik
R. D. Tripp
L. Wolfenstein
R. J. Cashmore
G. Goldhaber
C. Quigg
R. E. Diebold
C. B. Chiu

Other Contributors

G. C. Fox
H. M. Steiner
C. Schmid
G. A. Ringland
E. L. Berger
J. Weyers
W. R. Holley
R. L. Kelly
L. Galtieri
G. Gidal
G. Conforto
J. Mandula
F. Halzen
R. C. Sah

Foreword

Does the intermediate energy machine have a role to play in the coming era of the giant 300-GeV-and-up accelerators? Is there any interesting physics left to be done on the intermediate energy machines? If so, what? The answers to these questions can only come from many discussions between both theoretical and experimental physicists. The workshop was intended to "bridge the gap" between theory and experiment and to begin to answer the above questions.

The workshop was held on Monday and Tuesday, March 29-30, 1971, at the California Institute of Technology in Pasadena, California. It was organized as follows:

Program

Session I, Monday Morning

Chairman, C. Lovelace (Introductory Remarks)

9:00-10:45 Accelerator Programs and Improvements
(<20 min. formal presentation by each speaker, plus discussion)

Nimrod (RHEL): G. Manning
ZGS (Argonne): B. Cork
Bevatron (LRL): E. J. Lofgren

Coffee

11:00-12:15 Intermediate Energy Programs at Higher Energy Laboratories
(10-15 min. presentation by each speaker, plus discussion)

BNL: D. Berley
CERN: F. Muller
SLAC: J. Ballam

Session II, Monday Afternoon

Chairman, A. Yokosawa

1:30-2:30 Techniques
(20 min. presentation by each speaker, plus discussion)

Streamer Chambers: H. K. Ticho
Polarized Targets: G. Shapiro

Resonances and Phase Shift Analysis

2:30 Spectroscopy: J. L. Rosner (30 min. + 10 min. discussion)
3:10 πN Scattering: R. G. Moorhouse (20 min. + 10 min. discussion)

Coffee

3:50 KN and NN Scattering: M. J. Moravcsik (10 min. + 10 min. discussion)
4:10 Multichannel Analysis: R. D. Tripp (20 min. + 10 min. discussion)
4:40 General Discussion

Session III, Tuesday Morning

Chairman, A. H. Rosenfeld

9:00 Weak Interactions: L. Wolfenstein (40 min. + 20 min. discussion)

Coffee

Multiparticle Final States

10:15 Phase Shift Analysis of Multiparticle Final States:
R. J. Cashmore (25 min. + 10 min. discussion)
10:50 Resonances Observed in Production Experiments (mainly bosons):
G. Goldhaber (25 min. + 10 min. discussion)
11:25 Multiparticle Processes at Intermediate Energies:
C. Quigg (25 min. + 10 min. discussion)
12:00 Discussion

Session IV, Tuesday Afternoon

Chairman, G. Zweig

Quasi-Two Body Processes

1:30 Experiments: R. E. Diebold (20 min. + 10 min. discussion)
2:00 Line-reversal Comparisons and Other Tests of the Regge Phase:
C. B. Chiu (25 min. + 10 min. discussion)
The Importance of Being an Amplitude (if time permits):
G. C. Fox

Coffee

3:15 Summary and Open Discussion

Discussion Leaders: J. Ballam
B. Cork
G. Manning
W. A. Wenzel

These Proceedings contain texts from all of the invited speakers on the program, except for J. Ballam and H. K. Ticho. However, as can be seen from the above program, the emphasis was on discussion. There were indeed many interesting and worthwhile discussions, most of which are included in the Proceedings. But because of the difficulty in transcribing discussions from the tape recorder, I have only reproduced those discussions that I felt would be of benefit to the reader. I apologize to any participant who feels slighted by the choice of discussions included.

I would like to thank those at Cal Tech and especially Geoffrey Fox for their excellent job as host of the workshop. I also wish to thank all those who contributed to the Proceedings. The following graduate students helped me to varying degrees with the Proceedings: P. Robrish, D. Lissauer, T. Mast, and A. Skudja. Finally, I would like to thank Genece Hoskin and Chris Graham, without whose help in typing there would be no Proceedings.

R. D. Field, Jr.

May 20, 1971
Lawrence Radiation Laboratory
University of California
Berkeley, California 94720

CONTENTS

SESSION I

Introductory Remarks: C. Lovelace 1

NIMROD Experimental Programme
G. Manning 2

ZGS Program
D. Jovanovic and B. Cork 38a

The Bevatron Program
E. J. Lofgren, W. R. Holley, R. C. Sah 59

Intermediate Energy Program at the AGS
D. Berley 72a

CERN Programme
F. Muller 91

SESSION II

Polarized Target Techniques
G. Shapiro 117

The Spectrum of Low-Lying Hadron States
J. L. Rosner 129

Partial Wave Analysis and Experiment in πN Reactions
R. G. Moorhouse 169

Remarks on K-N and N-N Partial Wave Analysis
M. J. Moravcsik 176a

Low and Intermediate Energy $\bar{K}N$ Experiments
R. D. Tripp 190a

SESSION III

Workshop Talk on Weak Interactions
L. Wolfenstein 203

Partial Wave Analyses in Multiparticle Final States
R. J. Cashmore 220a

Interfering Boson Resonances as a Tool in Strong Interactions and Search for C Violation in the Electromagnetic or Semi-Strong Interactions
G. Goldhaber 250a

Multiparticle Reactions at Intermediate Energies
C. Quigg 277

SESSION IV

Intermediate Energy Experiments on Quasi-Two-Body Production
R. Diebold 341

Tests of an Empirical Rule for Cuts and Discussion of Line Reversal Relations
C. B. Chiu 396

ADDITIONAL CONTRIBUTIONS

Some Useful Hadronic Experiments at Intermediate Energies
E. L. Berger, G. C. Fox, C. Quigg, and G. A. Ringland 453b

Quantum Numbers of Cross-Channel Exchanges
J. Mandula, J. Weyers, G. Zweig, and F. Halzen 457

Introductory Remarks

by C. Lovelace

This meeting is to find out what physics can be done with old accelerators. First let me describe the situation I would like to improve on: Some pen club sticks a pin into a list of beams, orders a few 100 K bubble chamber photos, runs them through automatic measuring devices and reconstruction programs, and publishes half a dozen papers untouched by human brain. This is politely known as a "survey experiment." Given an accelerator big enough to make quarks, any idiot can find quarks. To discover something new at the energies of existing machines requires a certain degree of intelligence. This explains why so many experimentalists are anxious to work at NAL.

What could be more suitable to high energy machines than Regge phenomenology? The biggest advance in Regge theory in the last decade was certainly the discovery of duality. Almost all Regge fits done without FESR turned out to have wrong amplitudes. Duality could never have been discovered without the πN phase shifts. The πN phase shift analyses were made possible by the polarized target experiments from Rutherford Laboratory and Berkeley. If all accelerators except Brookhaven and CERN had been closed down in 1961, duality would never have been discovered, and Regge theorists would still be groping in the dark. This is just one historical example of the importance of low energy measurements.

NIMROD EXPERIMENTAL PROGRAMME

G. Manning
Department of Physics

Rutherford High Energy Laboratory
Chilton, Didcot
Berkshire, England

1. INTRODUCTION

There are about nine groups using Nimrod for counter work in High Energy Physics and one for Nuclear Structure work. All of the groups are also making growing use of the CERN accelerators.

During the last year the British Bubble Chamber Groups have received two thirds of their film from the CERN bubble chambers thus enabling the 150 cm hydrogen chamber to be devoted predominantly to development of the track sensitive target technique. This work is being done in collaboration with CERN.

This growing utilization of the CERN accelerators by the counter and bubble chamber physicists who have previously based the major part of their programme on Nimrod is an intentional policy aimed at supporting about two thirds of the British High Energy Physics groups on the CERN accelerators during the period after the start-up of the 300 GeV accelerator in 1975-6. If this aim is realized then either Nimrod or Nina (the 5 GeV electron accelerator) will be able to support the remaining demand and one or other of the National accelerators could be phased out. No decision has yet been made that this should happen or which of the two would be stopped should the decision ultimately be made.

Meanwhile it is clear that the experimental programme on Nimrod and Nina will be reduced during the coming years as funds and effort are

diverted to the fuller utilization of the CERN PS, CERN SC and ISR and eventually the 300 GeV accelerator. This reduction is not due to a declining interest in the Physics but to a deliberate policy to concentrate on the international accelerators and to a shortage in overall funds.

2. BEAMS AVAILABLE

Figures 1 and 2 show the present layout of beams in the three experimental halls of Nimrod. There are a total of four counter beams derived from internal targets and six from two extracted beams. One of these extracted beams (X2) has a single target feeding two beams and the second (X3) has two sequential targets each feeding two counter beams. A low energy pion irradiation beam (π11) is also derived from one of these targets. A third extracted proton beam (x1) feeds a separated beam for the bubble chamber.

The three extracted proton beams all use the Piccioni system and have extraction efficiencies of 30-40%, see table 1. A short spill in X1 for the bubble chamber followed by a long spill for the counters, in either X2 or X3, can be given on the same flat top. Similarly a short spill for parasitic setting-up can be given during current rise, in X2 prior to a long spill in X3 (or vice versa). All internal beams can be fed in parallel with the extracted proton beams. This very flexible arrangement, coupled with the adequate intensity of Nimrod 2.5 - 3.0 x 10^{12} ppp, means that many users can be satisfied at once and the average utilization could be well above 6 users if the demand existed. Table 2 summarizes the operation of Nimrod since its start-up. The higher average number of users since 1968 has resulted from the greater use of external beams.

Table 3 gives brief details of the properties of the current beams. In general, there is adequate pion flux for normal demands up to about 5 GeV/c. The kaon yields are adequate for physics up to about 3 GeV/c, and beyond that it is normal to use the CERN PS. There is currently no neutral beam although it is easy to provide if required and an obvious addition would be an optimised stopped kaon beam - this may be added from a target in X2 in the future.

3. COUNTER PHYSICS PROGRAMME

Tables 4 - 6 list experiments carried out on Nimrod and still under analysis, those currently being run and those planned for the immediate future.

3.1 πN Elastic Scattering

In the past a considerable effort has been placed upon the study of πp elastic scattering including the use of polarized targets. Figure 3 shows a downwards pointing arrows measurements made at Nimrod and upwards pointing arrows measurements made elsewhere. It can be seen that greater than 50% of the world's data on πp elastic scattering has been taken at Nimrod. This programme is now practically completed although one proposal, No. 83 by the Bristol/Soton/RHEL group, is for further measurements on πp scattering where phase shift analysis show they are necessary. A larger body of data on $\pi^+ \vec{p}$ scattering at 68 momentum between 0.6 and 2.7 GeV/c has just been taken (Proposal 55 by the RHEL Group C) and Fig. 4 shows typical result at two momenta. The new data considerably enhances the information available on the πN system and a new phase shift analysis is under way.

3.2 KN Elastic Scattering

A considerable effort is also being made on KN elastic scattering. Four experiments have been completed on $K^{\pm}p$ elastic scattering and are currently being analyzed. Proposals 30 and 74 by UCL, studies $K^{-}p$ at 32 momenta between 1 and 2.4 GeV/c and $K^{+}p$ at 28 momenta between 1.4 and 2.3 GeV/c. Analysis is well under way and should be fully published in the near future. A phase shift analysis has been made of the $K^{+}p$ data and there is no requirement to invoke resonances in the $K^{+}p$ system, see figure 5. Proposals 40 and 63 by Birmingham/RHEL, studied $K^{\pm}p$ scattering at 14 momenta between 0.43 and 0.93 GeV/c. A preliminary analysis of the K^{+} has been made and a phase shift analysis is in progress. The first indications are that the elastic cross section is isotropic at low momenta (see figure 6) and that the total elastic cross section shows no structure, see figure 7. Total cross section measurements had indicated structure in this region. Analysis is continuing and should be able to determine the real part of the amplitude from Coulomb interference at least at the lowest momenta.

This same group are currently studying $K^{\pm}n$ scattering (Proposal 73) over the same momentum region 0.43 - 0.93 GeV/c.

The Bristol/Soton/RHEL group are currently studying $K^{+}p$ elastic scattering in the momentum region 0.9 - 1.6 GeV/c (Proposal 43). They have started data taking and figure 8 shows a preliminary result at 1.45 GeV/c with limited data over part of their angular range. Their angular coverage should be very good ($\cos\theta^{*}$ - 1.0 - 0.97) and they are aiming at greater than 2×10^{4} events per angular distribution.

3.3 Inelastic Channels in the πN System

The considerable study of N^* states made using elastic scattering is now being extended by study of inelastic scattering. This programme should provide independent confirmation of resonant states found and will provide branching ratios to test SU3 predictions. One experiment (Proposal 87 by Cambridge/RHEL) plans to study $\pi^- p \rightarrow \Lambda^o K^o$ from threshold to 1.5 GeV/c and will provide both angular distributions and polarization information. The aim is to obtain $\sim 10^4$ events per momentum at 17 separate momenta. A possible extension for the future would be to use a polarized target to measure A and R.

A second experiment (Proposal 81 by Glasgow/RHEL) plans to study $\pi^- \vec{p} \rightarrow \pi^o n$ and $\eta^o n$ from 0.6 - 3.5 GeV/c. It is due to start in June 1971 and will use a new type of polarized target called a "frozen target" that polarizes in an accurate superconducting solenoid and then transfers the target to a holding field of poor uniformity but with good access.

One further experiment, proposal 50 by IC/Soton/RHEL, was a search for new narrow bosons using $\pi^- p \rightarrow n X^o$ and $p X^-$, using time-of-flight on the n and p. It will yield information on the splitting of the A_2^- and A_2^o over a region of t from 0.1 - 0.7. Analysis is under way.

3.4 Inelastic Channels in the K-p System

One experiment, Proposal 33 by the Oxford group, studied $K^- p \rightarrow$ neutral final states, over the momentum region 0.68 - 0.99 GeV/c. These are states not easily studied in a bubble chamber, particularly the $\Sigma^o \pi^o$ final state. Preliminary analysis has been made and a phase shift analysis is being made. Further data will be taken by the same group with

an improved set-up over the momentum region 0.9 - 1.05 GeV/c, Proposal 92. The experiment should yield 1500 events in the $\pi^{o}\Sigma^{o}$ channel/momentum at 7 different momenta and about a factor of 2 more in the $\Lambda^{o}\pi^{o}$ channel.

3.5 Weak Interactions

Three experiments on the weak interaction have been completed and analysis is almost complete. One, Proposal 31 by the Westfield/RHEL, studied the decay parameters of the Σ^{+} and should provide a test of the $\Delta I = 1/2$ rule in nonleptonic decays. The expected accuracy is about 5% in amplitude.

A second, Proposal 45 by Cambridge/RHEL, studied the $\Delta S = \Delta Q$ rule in K^{o} decay. The production reaction was $\pi^{-}p \rightarrow \Lambda^{o}K^{o}$. A sample of ~4000 Ke3 decay from an initially pure K^{o} state were obtained and an accuracy of ~ 4% is expected on the $\Delta S = -\Delta Q/\Delta S = \Delta Q$ amplitude.

The third experiment, Proposal 26 by the QMC/AERE/RHEL group studied Σ β decay using Σ's produced by $\pi^{-}p \rightarrow K^{+}\Sigma^{-}$. Analysis is practically complete but only a small sample of events (~ 49) have been obtained.

3.6 E-M Interactions

An experiment, Proposal 70 by the Westfield/RHEL group, is studying the charge asymmetry in $\eta^{o} \rightarrow \pi^{+}\pi^{-}\pi^{o}$ and $\eta^{o} \rightarrow \pi^{+}\pi^{-}\gamma$. A powerful detector using 60 neutron counters in time-of-flight to select η from the reaction $\pi^{-}p \rightarrow \eta^{o}n$ has been set up in which the η decay particles are detected in optimum spark chambers situated in a large magnet viewed by a videcon system. An effective mass resolution for the η of $\pm$ 4.5 MeV has been achieved. About 100,000 $\eta \rightarrow \pi^{+}\pi^{-}\pi^{o}$ decays have already been recorded and the ultimate target is 400,000 which should yield an accuracy on the

asymmetry of $\sim \pm 0.2\%$. A second proposal, number 76 by the same group, will be carried out by the addition of electron Cerenkov counters to the same equipment. This will search for the C violating decay $\eta^{o} \rightarrow \pi^{o} e^{+} e^{-}$ and should be able to improve the present limit on the branching ratio of 2×10^{-4} by about a factor of 10. The experiment should also be able to study the C allowed decay $\eta \rightarrow \gamma e^{+} e^{-}$ and could yield information on the form factor of the η. About 100-200 events should be collected.

A second experiment, Proposal 78 by the Cambridge/RHEL group, search for new particles of mass between that of the electron and muon and for anomalies in the Bremsstrahlung of particles of mass close to that of the electron. This work was a follow-up of reported anomalies observed in a bubble chamber experiment. No supporting evidence was found. No new particles were discovered at a level of 1/1000 of the electron intensity.

4. BUBBLE CHAMBER PROGRAMME

Table 7 lists bubble chamber exposures taken at Nimrod that are still under analysis.

The only proposals remaining are in the 150 cm hydrogen chamber with a track sensitive hydrogen or deuterium target and a neon-hydrogen filling for the chamber. The development of this technique is being made in collaboration with CERN. One target worked during 1970 and made 40,000 expansions before breaking. Fig. 9 is a typical picture. The targets have now been modified to provide a cooling loop in the hydrogen to maintain a temperature difference between the target and the chamber. This gives an extra degree of freedom and it is hoped that when running commences in April the system

will be easier to operate.

Four proposals have been made for experiments using the target facility, see table 8, and if the system is successful, it will provide a valuable complement to the CERN chambers. Proposals will be accepted from both British and other European groups.

5. PROPOSED AND POSSIBLE IMPROVEMENTS IN NIMROD AND ITS FACILITIES

5.1 Machine Developments

Only one improvement is currently approved for Nimrod. That is the construction of an additional R-F cavity working at the second harmonic of the main frequency. This should improve the circulating intensity by a factor of about 1.4 and should give an intensity, limited by space charge effects, $\sim 4 \times 10^{12}$ ppp. Any further improvement in the circulating beam will require an increase in injection energy. A design study has been made of a 400 MeV booster, which would also be suitable to feed into a super conducting 22 GeV replacement of Nimrod. This injector would cost $\sim$ £0.75M.

A complete design study has been made of a super conducting replacement of Nimrod fitting in the existing experimental hall. Assuming a maximum field of 60.7 Kg a momentum of 22 GeV/c could be obtained. Fig. 10 shows a diagram of the layout and table 9 gives some of the relevant parameters. It is very difficult to make an accurate costing of the conversion as the technical feasibility depends upon the success of the current R and D programme on superconducting magnets. Nevertheless, an approximate and conservative cost estimate is given in table 10. The progress on superconducting magnets is satisfactory and a realistic

prototype pulsed magnet with a suitable field accuracy and configuration should be produced in the next 18 months.

Whether a proposal is made to make the conversion is clearly dependent upon the success of the magnet programme and also upon whether it is decided that Nimrod should continue to operate in the long term.

5.2 Beam Improvements

A design has been made for a stopped kaon beam and the relevant parameters are given in table 11. The yield for K^+ in flight is in the region $4 - 7 \times 10^4$ depending upon settings of the mass and momentum slits. The yield for K^- is down by a factor of ~ 4. Separation could be improved at the cost of a reduced yield. Several groups have expressed interest in physics requiring this beam and it could be installed during the winter shut-down of 1971/72.

A further growing requirement is for higher momentum pion beams and hence some of the beams will be redesigned to go to higher momentum including one capable of reaching 7 GeV/c.

A third interest is in improved K beams, particularly with some separation to improve the K/π rates. A development programme is under way on superconducting R-F separators using lead cavities. This work shows considerable promise and a full-size structure has produced fields of 225 gauss which are as good as those obtained on full size niobium cavities. R and D work is continuing.

All of the above beam developments would greatly benefit from an improved beam intensity and if a new injector could be built a factor of 5 could be gained. Further factors of 1.4 could be gained from the second harmonic cavity and improvements in extraction efficiency. If all

could be achieved the overall gain in extracted beam could be a factor of 10 resulting in 10^{13} ppp extracted.

6. SUMMARY OF FUTURE NIMROD PROGRAMME

In the past a large fraction of the RHEL programme has been concentrated on a study of pion nucleon elastic scattering and more than half of the world's data has been collected at Nimrod. In general, the region up to 3 GeV/c is now well covered in fine momentum steps (~ 30 MeV/c) and with a precision approaching the level where E-M corrections are relevant. Data is available on polarization as well as total and differential cross sections.

During the last year or so effort has shifted to the KN system and Nimrod has contributed strongly to the data on differential cross sections over the region 0.4 - 2.5 GeV/c. Much remains to be done in this field especially in K^-N where copious resonances are found. The K^+p system has so far shown no evidence of resonant structure but continued work is required.

Emphasis is now turning to inelastic channels in both πN and KN channels. Many higher mass baryon resonances are known to be highly inelastic and hence inelastic scattering to an accuracy comparable with the elastic studies should be a productive line of research. The work will provide a completely independent analysis of the resonances and should states of the same mass, width and quantum numbers be found as those found from elastic reactions, it will give added confidence in the significance and uniqueness of the interpretation of phase shift analyses. The additional information on branching ratios will give further crucial tests on theories such as quark models, SU3 models and Regge models.

In final states involving hyperons, a single experiment gives information on differential cross-sections and polarization and an obvious development for the future is to use polarized targets to yield A and R parameters.

In weak interaction physics a study of the validity of selection rules and conservation laws will continue to dominate the field accessible to Nimrod. The many decay modes of the kaon constitute one of the best fields of investigations for the study of the weak interaction and particularly of the CP violating process which is still not understood. An intense low energy caon beam is planned to be in operation on Nimrod in about a year. There are many uses for such a beam; for example, the study of kaon-nucleon interactions at very low energies; the study of the decay of stopped kaons; to form sources of polarized hyperons and to study their decays; to form excited atoms involving capture of kaons or Σ hyperons into "electron like" orbits, etc. This beam could be of great interest for both elementary particle physics and nuclear structure physics.

The track-sensitive target facility mentioned earlier will be used in the 150 cm liquid hydrogen bubble chamber. It enables the characteristics of hydrogen and heavy liquid chamber to be combined in one instrument (in particular having a high sensitivity to neutral particles) and will be the only European bubble chamber operating in this mode for several years.

This physics programme will provide a viable and front line research programme for many years to come. It is not second rate physics and is essential for a full understanding of the subject - the resonance region may prove to be the crucial key to High Energy Physics.

Nimrod is capable of considerable improvement; it is the second highest energy proton accelerator in Western Europe and is a facility we cannot afford to lose.

TABLE 1

EXTRACTED PROTON BEAMS					
Beam Number	Max $\Delta p/p$	$\Delta\Omega$ (msterads)	Particle	Momentum (GeV/c)	Yield/pulse quoted for 5×10^{11} on internal tgt
X1	0.2%	~ 0.2	p	up to 7.8	1.4×10^{11}
X2	0.2%	~ 0.2	p	up to 7.8	1.8×10^{11}
X3	0.2%	~ 0.2	p	up to 7.8	2.0×10^{11}

BRIEF OPERATIONAL SUMMARY FOR NIMROD

TABLE 2

Period	Hrs at 7GeV for high energy physics		Efficiency	Total of hrs at 7GeV used by experimental teams	Average no of experiments running simultaneously	Total no of accelerated protons	Notes
	Scheduled	Achieved					
1.10.64 to 31.12.65	1770	1330	75%	2811	2.1	1.67×10^{18}	7GeV operation for $\sim 4\frac{1}{2}$ months of period only
11.1.66 to 31.12.66	5840	4850	83%	18906	3.9	7.63×10^{18}	
1.1.67 to 31.12.67	4758	3723	78%	10705	2.9	5.88×10^{18}	7GeV operation for ~ 9 months of period only
1.1.68 to 31.12.68	6152	5170	84%	24907	4.8	7.19×10^{18}	~ 7 months of period at half normal repetition rate
1.1.69 to 31.12.69	5145	4521	88%	26044	5.8	1.04×10^{19}	
1.1.70 to 31.12.70	5297	4708	89%	21429	4.6	1.29×10^{19}	Totals include time at 5 & 6 GeV, at the experimental teams' request

TABLE 3

NIMROD BEAMS - PRESENT AND PROPOSED

Beam Number	Max $\Delta p/p$	$\Delta\Omega$ (msterads)	Particle	Momentum (GeV/c)	Yield/pulse quoted for 5.10^{11} on internal tgt or 10^{11} on external tgt with $\Delta p/p$ = 1% FWHH
π7	2%	0.93	π^-	1.0 - 4.0	1 - 2.5 x 10^5
π8	2%	1.0	$\pi^{\pm}$	0.5 - 1.7	10^5 - 1 GeV/c
π9	12%	1.4	π^-	0.4 - 4.1	estimated as $\sim 2 \times 10^4$ at central momentum
π10	4%	0.7 - 1.0	$\pi^{\pm}K^{\pm}p$	0.7 - 2.0	π^+ 2 x 10^4 π^- 5 x 10^4 K^- 1.5 x 10^2 at 1.2 GeV/c
π11	10%	10	$\pi^{\pm}$	0-0.200	$\sim 10^5$ (2 rads/hour)
K9 for Bubble Chamber	3%	0.185	$\pi^{\pm}K^{\pm}p$	$K^{\pm}$ 2-3 $\pi^{\pm}$ 0.8-6 p 0.8-7.5	2 GeV/c ~ $3K^-$, $20K^+$
K10S	3%	1.3	K^-	0.65 - 1.2	1 GeV/c - 200
K12A	6%	5.1	$K^{\pm}$	0.4 - 1.0	0.8 GeV/c - 500
K13C	2%	1.3	$\pi^{\pm}$	0.5 - 2.0	2 x 10^5
K15	2%	~ 3	$\pi^{\pm}K^{\pm}$	1.0 - 2.0	K^+ 300 K^- 50
P71	1.5%	0.81	p	1.5 - 3.7	5 x 10^4 at 2 GeV/c

TABLE 4

Nimrod Experiments Elastic Scattering

	Group	Proposal No.	Experiment	State	Measurements
πN	UCL	74	$\pi^+ p$ $\frac{d\sigma}{d\Omega}$	Analysis	14 momenta; 1.0 - 1.4 GeV/c and 1.715 GeV/c
	RHEL (C)	55	$\pi^+ p$ polarised target	Analysis	68 momenta; 0.6 - 2.70 GeV/c
	Bristol/Soton/ RHEL	83	$\pi^+ p$ $\frac{d\sigma}{d\Omega}$	Running	30 momenta; 0.6 - 2.0 GeV/c
KN	B'ham/RHEL	40	$K^- p$ $\frac{d\sigma}{d\Omega}$	Analysis	14 momenta; 0.60 - 0.93 GeV/c
	"	63	$K^+ p$ $\frac{d\sigma}{d\Omega}$	Analysis	13 momenta; 0.43 - 0.93 GeV/c
	"	73	$K^+ n$ $\frac{d\sigma}{d\Omega}$	Running	To match Props. 40, 63 above
	UCL/RHEL	30	$K^- p$ $\frac{d\sigma}{d\Omega}$	Analysis	13 momenta; 1.0 - 1.4 GeV/c 19 momenta; 1.7 - 2.4 GeV/c
	"	74	$K^+ p$ $\frac{d\sigma}{d\Omega}$	Analysis	28 momenta; 1.4 - 2.3 GeV/c
	Bristol/Soton/ RHEL	43	$K^+ p$ $\frac{d\sigma}{d\Omega}$	Running	24 momenta; 0.9 - 1.6 GeV/c
pp	QMC/Bergen/RHEL	61	pp $\frac{d\sigma}{d\Omega}$	Analysis	14 momenta; 1.3 - 3.6 GeV/c

Nimrod Experiments on Inelastic Reactions

TABLE 5

	Group	Proposal No.	Experiment	State	Measurements
πN	IC/Soton/RHEL	50	$\pi^- p \to p X^-$ resonance $n X^0$ search	Analysis	$p\pi^-$ 0.7 - 4 GeV/c $M(X^0)$ covered 500 - 2000 MeV/c^2
	Camb/RHEL(B)	87	$\pi^- p \to \Lambda^0 K^0$ $\frac{d\sigma}{d\Omega}$ P	Setting-up	17 momenta 10^4 events/momentum
	Glasgow/RHEL(C)	81	$\pi^- \vec{p} \to \pi^0 n$ P $\to \eta^0 n$	Setting-up	0.6 - 3.5 GeV/c
KN	Oxford	33	$K^- p \to$ neutral	Analysis	16 momenta 0.685 - 0.990 MeV/c $\sim$ 3,500 $\Lambda\pi^0$; $\sim$ 1,600 $\Sigma^0\pi^0$
	Oxford	92	$K^- p \to$ neutral	Setting-up	7 momenta 0.9 - 1.05 GeV/c Expected yield $\sim$ 20,000 $\Lambda\pi^0$; $\sim$ 10,000 $\Sigma^0\pi^0$
	B'ham/RHEL	73	$K^+ n \to K^0 p$ $\frac{d\sigma}{d\Omega}$	Running	13 momenta 0.45 - 0.95 GeV/c

TABLE 6

Nimrod Experiments on WEAK and Electro-Magnetic Interaction

	Group	Proposal No.	Experiment	State	Measurements
Weak Interaction	Westfield/RHEL	31	$\Sigma^+ \rightarrow p\pi^o$	Analysis	Measurement of non-leptonic decay parameters
	Camb/RHEL	45	Test of $\Delta S = \Delta Q$ rule	Analysis	Test of $\Delta S = \Delta Q$ rule using $K \rightarrow \pi e \nu$ produced by $\pi^- p \rightarrow \Lambda^o K^o$
	QMC/AERE/RHEL	26	Σ^- beta decay	Analysis	Measurement of electron asymmetry, 43 events
E-M Interaction	Westfield/RHEL	70	$\eta^o \rightarrow \pi^+\pi^-\pi^o$ $\rightarrow \pi^+\pi^-\gamma$	Running	Aim at 400,000 $\pi^+\pi^-\pi^o$ decays Measure of charge asymmetry
	Westfield/RHEL	76	$\eta^o \rightarrow e^+e^-\pi^o$	Setting-up	Search for C violating decay
	Camb/RHEL	78	Search for anomalies in Bremsstrahlung	Analysis	Search for new particles and for anomalies in Bremsstrahlung

TABLE 7

Bubble Chamber Experiments at Nimrod, being analysed

Group	Proposal No.	Experiment	Measurements
CEN (Saclay)/College de France/Strasbourg/ RHEL	18	K^-p interactions; 1.25 - 1.85 GeV/c	1.65 x 10^6 pictures; 13 momenta. Formation of S = -1 baryon resonances
B'ham/Edinburgh/ Glasgow/Imp. Coll.	18	K^-d interactions; 1.45 and 1.65 GeV/c	0.72 x 10^6 pictures. Study of $K^-d \rightarrow \Lambda\pi^-p$ to select $K^-n \rightarrow \Lambda\pi^-$
Univ.Coll/Tufts Univ./ Brussels/CERN	38	2.2 GeV/c K^- exposure in the 1.4m Heavy Liquid Bubble Chamber	0.68 x 10^6 pictures. Lifetime of Ξ^o. Study of Λ-Λ interaction and Ξ^-, Ξ^* resonances. Search for X^o, ϕ^o neutral decays and radiative Y^* decays
Imp.Coll./Westfield	39, 57, 86	π^+p interactions 0.8 - 1.7 GeV/c	0.62 x 10^6 pictures; 11 momenta. Formation of baryon resonances with S = 0, I = 3/2
Cambridge	Addendum to 49	n-p interactions; 1 - 7.5 GeV/c	1.12 x 10^5 pictures. Single and multiple pion production. Strange particle production
CEN (Saclay)/Imp. College/Westfield	56	K^+n interactions in the 2 to 3 GeV/c region	0.2 x 10^6 pictures K^+p 0.8 x 10^6 pictures k^+d Search for exotic baryon states, e.g. Z^*
Cambridge	77	1 GeV/c electrons into hydrogen bubble chamber	0.31 x 10^6 pictures. Anomalies in electromagnetic processes
Cambridge	85	n-p interactions from 1 - 3.5 GeV/c	0.9 x 10^5 pictures; improved n beam. High statistics study of $np \rightarrow pp\pi^-$ $\rightarrow pp\pi^+\pi^-\pi^o$ $pn\pi^+\pi^-$

TABLE 8

Bubble Chamber Proposals to use Target Facility

Group	Proposal No.	Target Filling	Chamber Filling Neon/H_2	Exposure	Aims of Experiment
RHEL/Durham/CERN/ UCL	91	H_2	50/50	250,000 pictures 4 GeV/c π^+	Investigate A_2^+ splitting and H Meson
Oxford	68	D_2	95/5	500,000 pictures 2 GeV/c π^+	$\pi^+ d \rightarrow pp\pi^o\pi^o$ investigate $\pi^o\pi^o$ interaction
UCL	84	H_2	90/10 if possible	500,000 pictures p_K 0.4 - 0.8 GeV/c	$K^- p \rightarrow \Sigma^o\pi^o$ and other final states involving γ's
RHEL	L of I 44	H_2	50/50	1,000,000 pictures stopping K^-	Hyperon β decay

Table 9

Maximum Momentum	25.38 GeV/c
Maximum Bending Field	7 T
Protons per Pulse	1.5×10^{13}
Cycle Time	6.75 sec
Ejection Efficiency	> 95 %
Injection Energy (Kinetic)	400 MeV
Field at Injection	0.267 T
Transition Energy	3.82 GeV
Aperture Diameter	0.12 m
Stored Energy	51 MJ
Circumference	175 m
Circumference Ratio	2.3
Mean Radius	27.85 m
Bending Radius	12.09 m
Maximum Quadrupole Gradient	63.2 T/m
Number of Focusing Periods	20
Number of Superperiods	4
Number of Betatron Oscillations per Revolution: Q_H, Q_V	4.8, 4.85
Resonant Q Value	4.66
Phase Advance per Period	86.4°
Maximum β Value	13.7 m
Effective Length of Bending Magnets	0.95 m
Effective Length of Quadrupoles	0.5 m
Length of one Period	8.75 m
Length of Long Straights	6.05 m
RF Frequency: Injection	7.32 MHz
: Ejection	10.26 MHz
RF Harmonic Number	6
Number of Pulses Injected	12
Injection Platform	0.75 sec
Peak RF Volts	54 kV
Average Power in Beam	30.5 kW
Length of RF Cavity	2 x 2.0 m

SCS MAIN RING PARAMETERS

TABLE 10

PRELIMINARY SCS COSTING

SUPERCONDUCTING ASPECTS	ITEMS, (£k)	SUB-TOTALS (£M)
SUPERCONDUCTOR	1,000	
MAGNET CONSTRUCTION & IRON SHIELDING	650	
CRYOSTATS & SUPPORTS	600	
REFRIGERATION	900	
		3.15
NON-SUPERCONDUCTING ASPECTS		
LINAC IMPROVEMENTS, 15 MeV TRANSFER	170	
400 MeV BOOSTER	550	
400 MeV TRANSFER & INJECTION, INC. CONTROL	215	
RF SYSTEM	200	
MODS. TO POWER SUPPLY	200	
CONTROL, CORRECTION, STEERING, DIAGNOSTICS	425	
CONTROL COMPUTER	100	
EJECTION (2 EPB's)	350	
NEW BEAM TRANSPORT EQUIPMENT	1,020	
ENGINEERING WORK	500	
CONTINGENCIES & INFLATIONS	750	
		4.48
TOTAL	£k 7,630	£M 7.63

TABLE 11

STOPPING K^+ BEAM - ESTIMATED PROPERTIES AT FINAL FOCUS

Production Angle = 5°

Target = 4mm x 4mm x 100mm copper

	Momentum Slit (Half-Width) mm	Mass Slit (Half-Width) mm	Integrated acceptance for K^+ (m st.%Δp/p)	K^+ flux at final focus (600 MeV/c 10^{12} protons)	% Momentum bite (FWHH)	π^+/K^+ at focus
BBB/22	50	10	28.4	3.2×10^4	2.5	20:1
	75	15	37.3	4.0×10^4	3.4	30:1
	100	20	40.4	4.4×10^4	3.5	50:1
BBB/BB	50	10	40.9	4.4×10^4	3.1	25:1
	75	15	57.4	6.4×10^4	4.0	35:1
	100	20	64.2	7.2×10^4	4.2	60:1

BBB/22 ≡ 3 Berkeley Type Quadrupoles + 2 RHEL Type 2 Quadrupoles

BBB/BB ≡ 5 Berkeley Type Quadrupoles

FIGURE CAPTIONS

Fig. 1 Beam layout in Halls 1 and 2.

Fig. 2 Beam layout in Halls 2 and 3.

Fig. 3 Data taken in πp elastic scattering experiments. Downward pointing arrows indicate data taken at Nimrod and upward arrows data taken elsewhere.

Fig. 4 Typical polarization data taken at two momenta for $\pi^+ p$ by RHEL (Group C). A total of 68 momenta were taken in the experiment between 0.6 and 2.7 GeV/c

Fig. 5 Phase shift analysis of $K^+ p$ including preliminary data taken at 28 momenta between 1.4 and 2.3 GeV by the UCL/RHEL Group. Four solutions are shown. None require a resonance in the $K^+ p$ system.

Fig. 6 Angular distributions for $K^+ p$ scattering in the momentum range 0.43 - 0.93 GeV/c from the Birmingham/RHEL group. This preliminary data does not cover the full angular range that will finally be available.

Fig. 7 $K^+ p$ total elastic cross sections. The new data from the Birmingham/RHEL group is determined by integrating the differential cross sections shown in figure 6. It disagrees with the values of Bowen et al. determined by attenuation of a K beam. The previous indication of a shoulder at 0.6 GeV/c is not confirmed.

Fig. 8 A preliminary angular distribution for $K^+ p$ scattering at 1.45 GeV/c from the experiment of the Bristol/Soton/RHEL group. Only a limited amount of data is shown for the forward and backward angular region.

Fig. 9 A typical picture of the track sensitive target in the 150 cm chamber. The target filling was hydrogen and the chamber filling was 50/50 Mol. neon/hydrogen.

Fig. 10 A layout of a super conducting replacement for Nimrod in the existing machine hall. Assuming a peak field of 60.7 Kg a momentum of 22 GeV/c can be obtained.

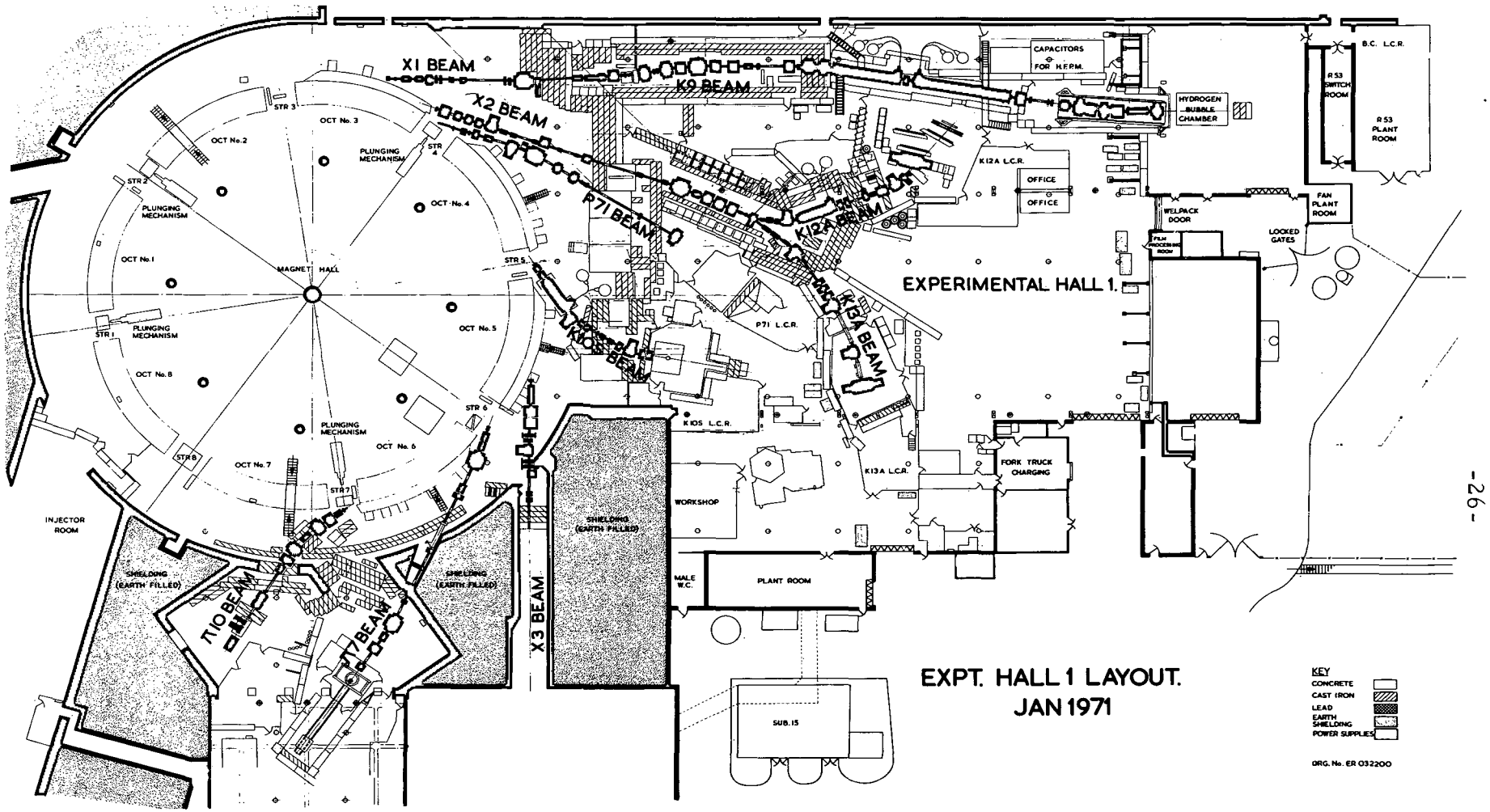
X1 BEAM
X2 BEAM
K9 BEAM
P71 BEAM
K12A BEAM
K13A BEAM
K10S BEAM
X3 BEAM
T10 BEAM
T17 BEAM
CAPACITORS FOR H.F.P.M.
HYDROGEN BUBBLE CHAMBER
B.C. L.C.R.
R53 SWITCH ROOM
R53 PLANT ROOM
K12A L.C.R.
OFFICE
OFFICE
FAN PLANT ROOM
WELPACK DOOR
LOCKED GATES
FILM PACKING ROOM
EXPERIMENTAL HALL 1.
P71 L.C.R.
K10S L.C.R.
K13A L.C.R.
FORK TRUCK CHARGING
WORKSHOP
MALE W.C.
PLANT ROOM
SUB.15
INJECTOR ROOM
SHIELDING (EARTH FILLED)
SHIELDING (EARTH FILLED)
SHIELDING (EARTH FILLED)
MAGNET HALL
OCT No.1
OCT No.2
OCT No.3
OCT No.4
OCT No.5
OCT No.6
OCT No.7
OCT No.8
PLUNGING MECHANISM
PLUNGING MECHANISM
PLUNGING MECHANISM
STR 1
STR 2
STR 3
STR 4
STR 5
STR 6
STR 7
STR 8
EXPT. HALL 1 LAYOUT.
JAN 1971
KEY
CONCRETE
CAST IRON
LEAD
EARTH SHIELDING
POWER SUPPLIES
DRG. No. ER 032200

Fig. 1.

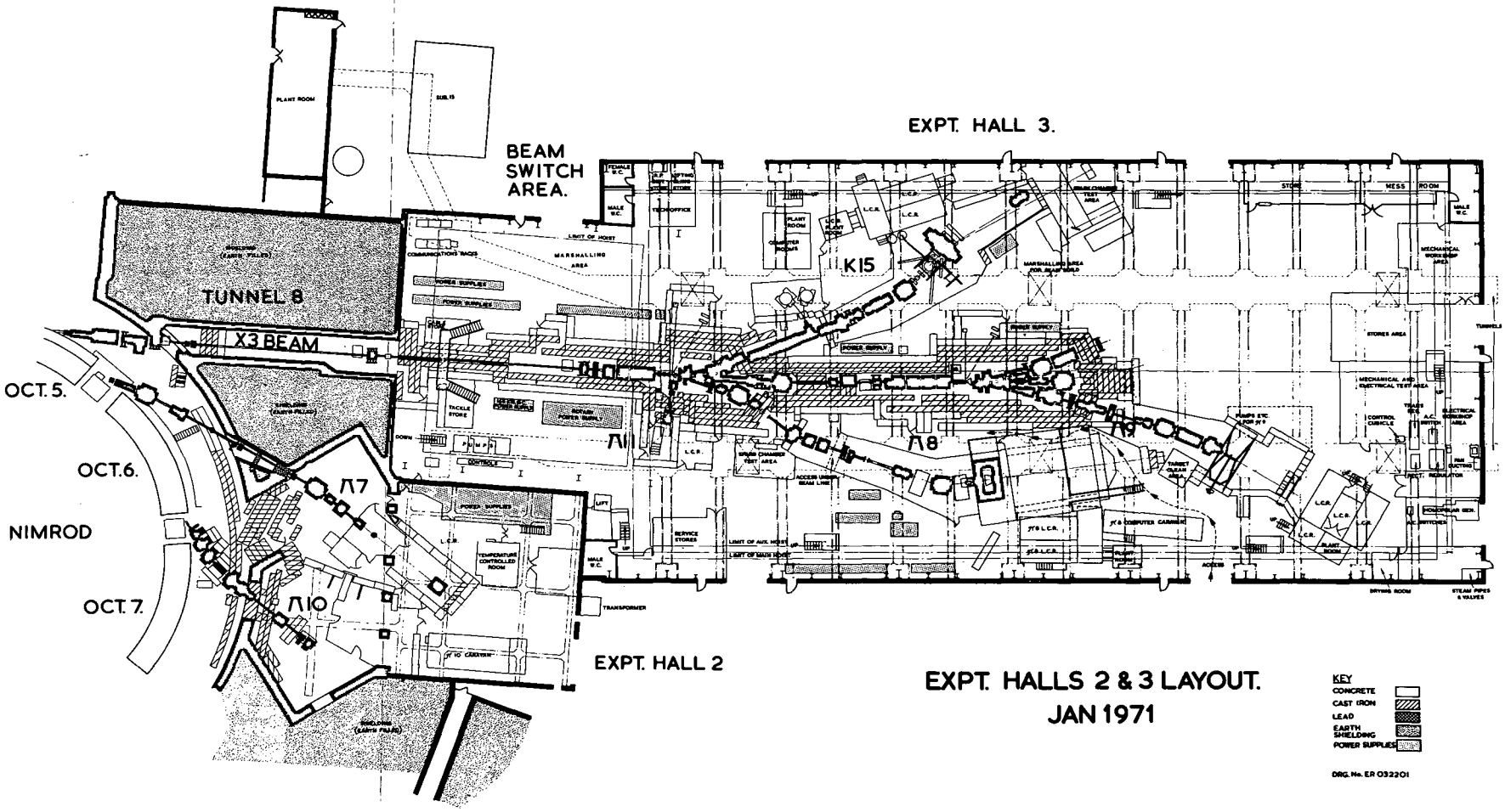
EXPT. HALL 3.
BEAM SWITCH AREA.
TUNNEL 8
X3 BEAM
OCT. 5.
OCT. 6.
NIMROD
OCT. 7.
Λ7
Λ10
Λ11
Λ8
K15
EXPT. HALL 2
EXPT. HALLS 2 & 3 LAYOUT.
JAN 1971
KEY
CONCRETE
CAST IRON
LEAD
EARTH SHIELDING
POWER SUPPLIES
DRG. No. ER 032201

Fig. 2.

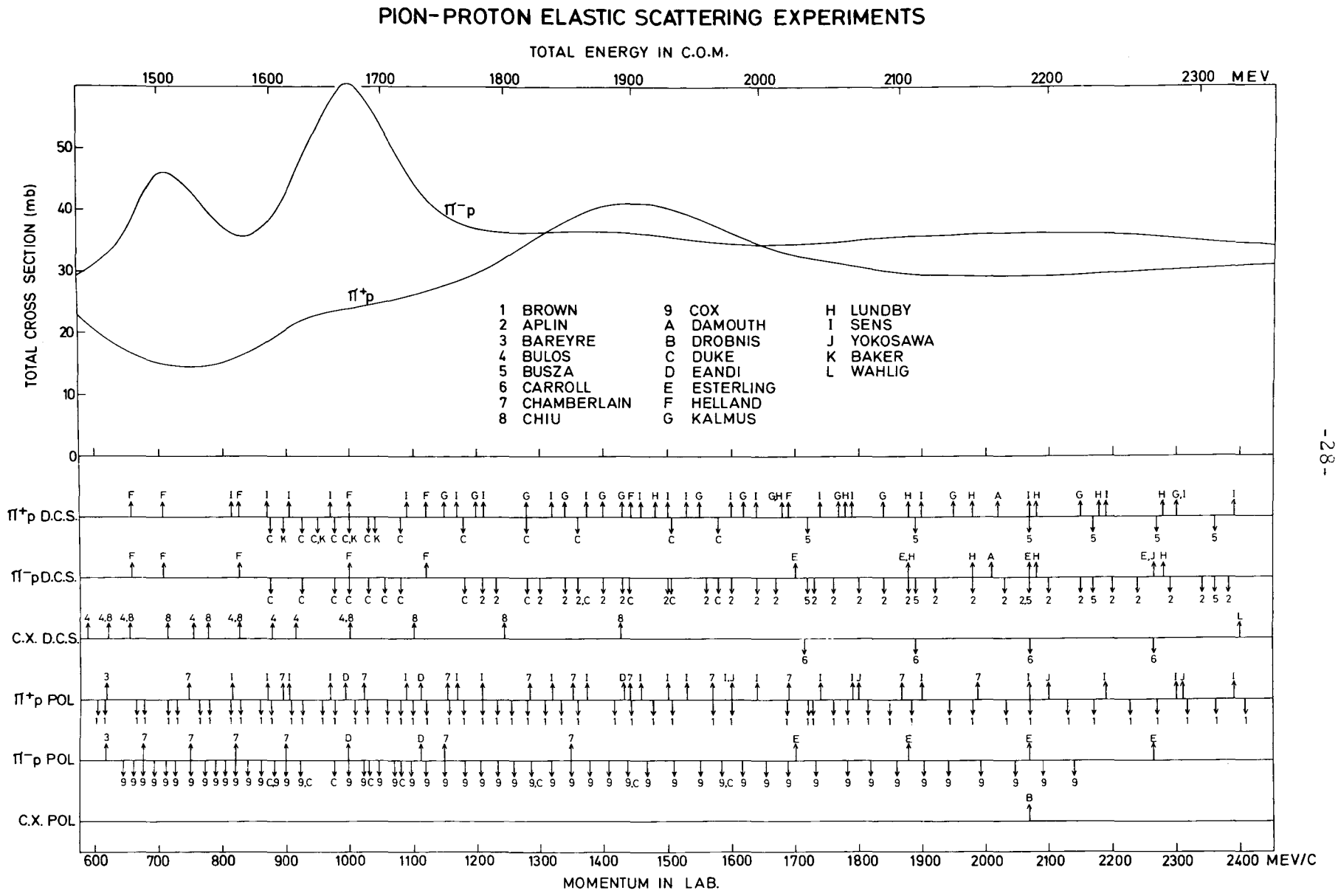
PION-PROTON ELASTIC SCATTERING EXPERIMENTS
TOTAL ENERGY IN C.O.M.
1500 1600 1700 1800 1900 2000 2100 2200 2300 MEV
TOTAL CROSS SECTION (mb)
50
40
30
20
10
0
π⁻p
π⁺p
1 BROWN
2 APLIN
3 BAREYRE
4 BULOS
5 BUSZA
6 CARROLL
7 CHAMBERLAIN
8 CHIU
9 COX
A DAMOUTH
B DROBNIS
C DUKE
D EANDI
E ESTERLING
F HELLAND
G KALMUS
H LUNDBY
I SENS
J YOKOSAWA
K BAKER
L WAHLIG
π⁺p D.C.S.
π⁻p D.C.S.
C.X. D.C.S.
π⁺p POL
π⁻p POL
C.X. POL
600 700 800 900 1000 1100 1200 1300 1400 1500 1600 1700 1800 1900 2000 2100 2200 2300 2400 MEV/C
MOMENTUM IN LAB.

Fig. 3.

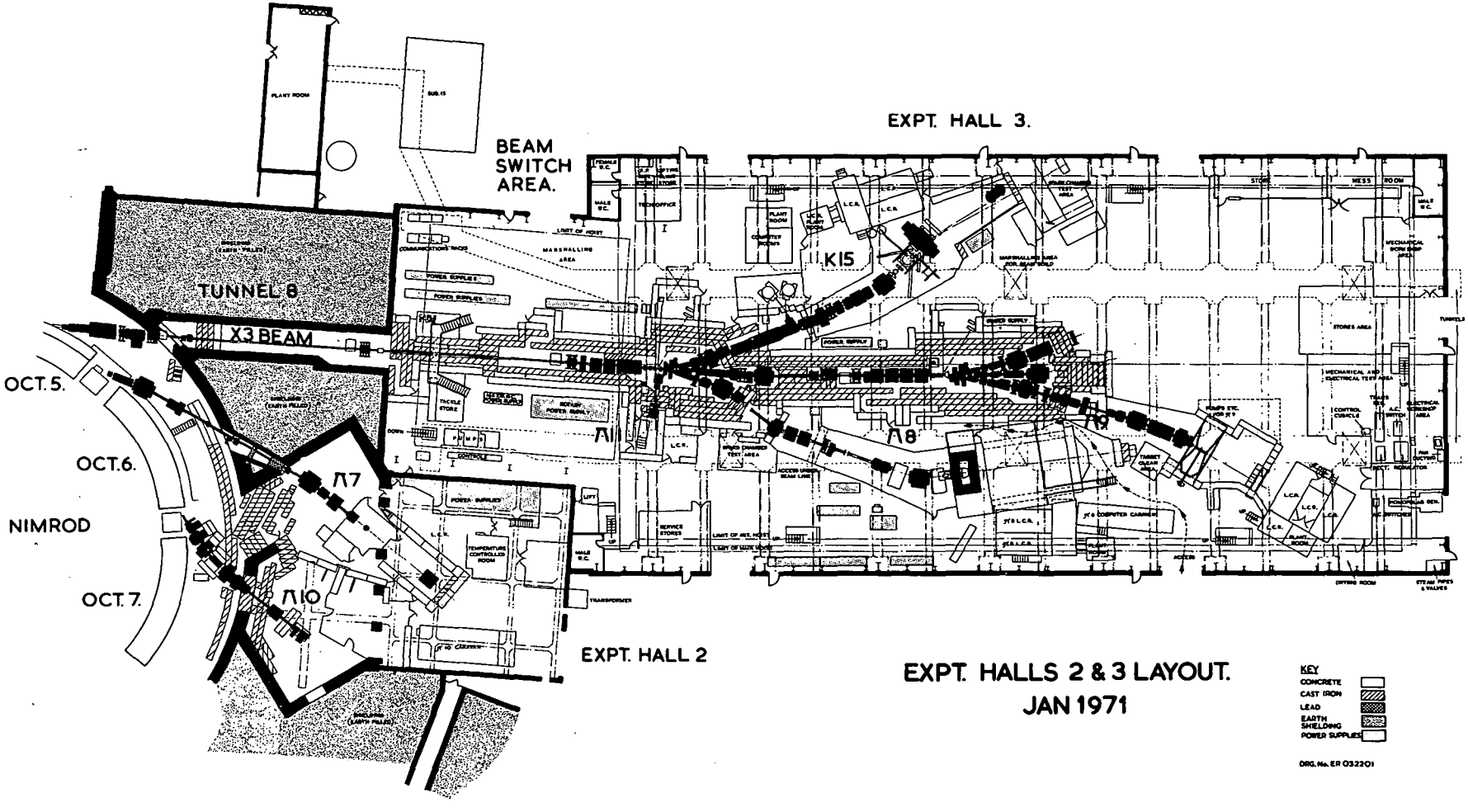
EXPT. HALL 3.
BEAM SWITCH AREA.
TUNNEL 8
X3 BEAM
OCT. 5.
OCT. 6.
NIMROD
OCT. 7.
K15
Λ1
Λ7
Λ8
Λ9
Λ10
EXPT. HALL 2
EXPT. HALLS 2 & 3 LAYOUT.
JAN 1971
KEY
CONCRETE
CAST IRON
LEAD
EARTH SHIELDING
POWER SUPPLIES
DRG. No. ER 032201

Fig. 2.

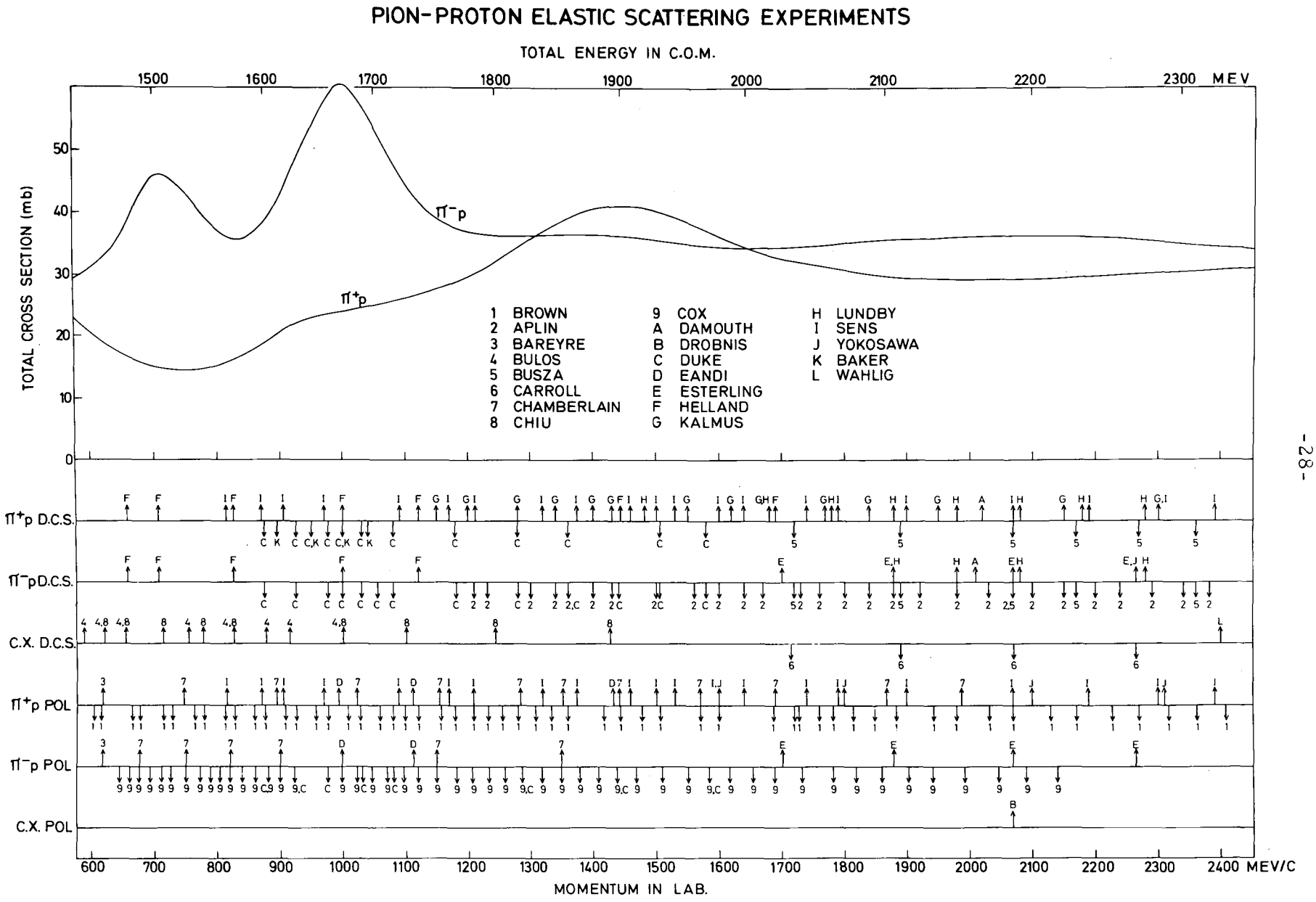
PION-PROTON ELASTIC SCATTERING EXPERIMENTS
TOTAL ENERGY IN C.O.M.
1500 1600 1700 1800 1900 2000 2100 2200 2300 MEV
TOTAL CROSS SECTION (mb)
50
40
30
20
10
0
π⁻p
π⁺p
1 BROWN
2 APLIN
3 BAREYRE
4 BULOS
5 BUSZA
6 CARROLL
7 CHAMBERLAIN
8 CHIU
9 COX
A DAMOUTH
B DROBNIS
C DUKE
D EANDI
E ESTERLING
F HELLAND
G KALMUS
H LUNDBY
I SENS
J YOKOSAWA
K BAKER
L WAHLIG
π⁺p D.C.S.
π⁻p D.C.S.
C.X. D.C.S.
π⁺p POL
π⁻p POL
C.X. POL
600 700 800 900 1000 1100 1200 1300 1400 1500 1600 1700 1800 1900 2000 2100 2200 2300 2400 MEV/C
MOMENTUM IN LAB.

Fig. 3.

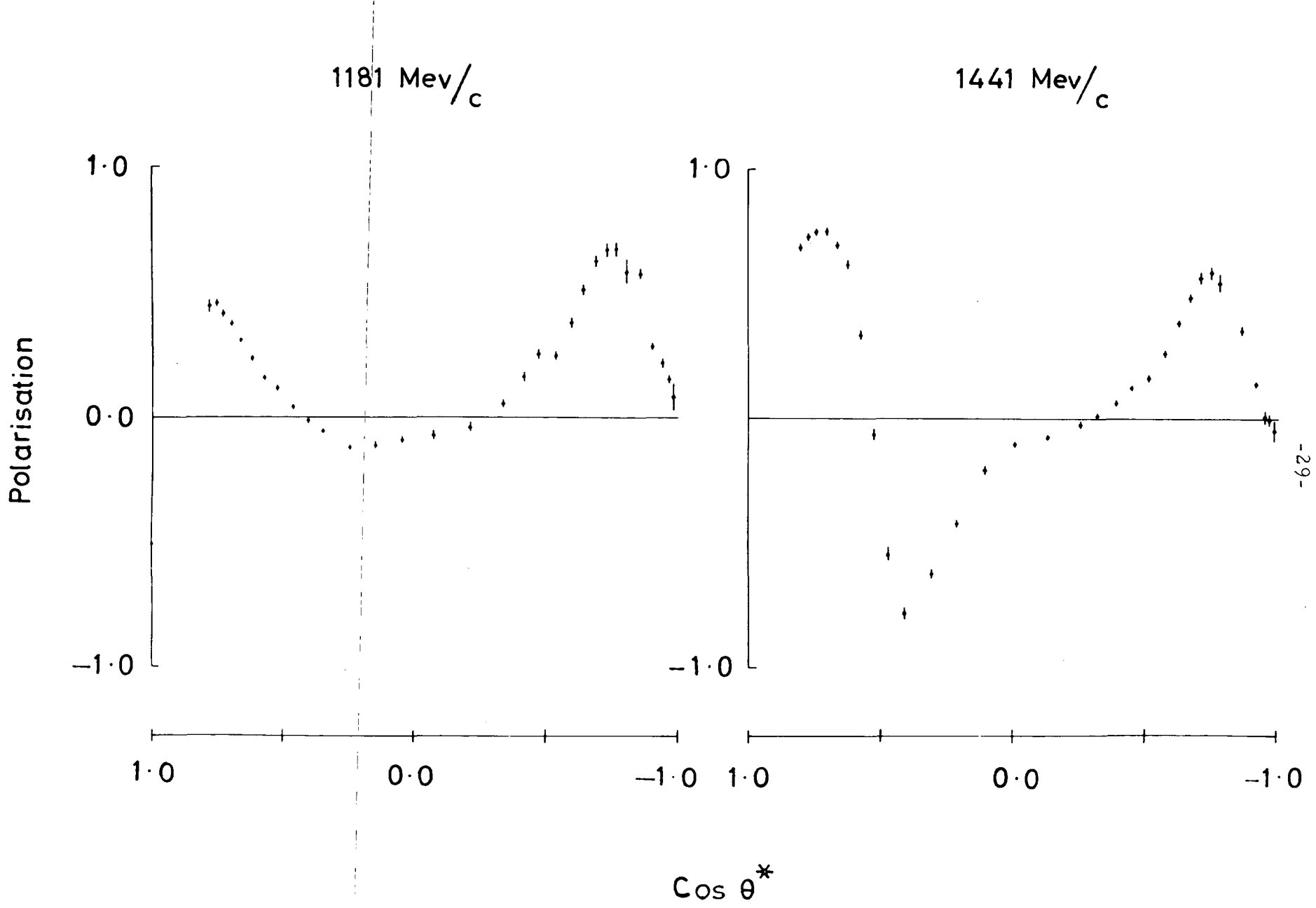

Fig. 4.

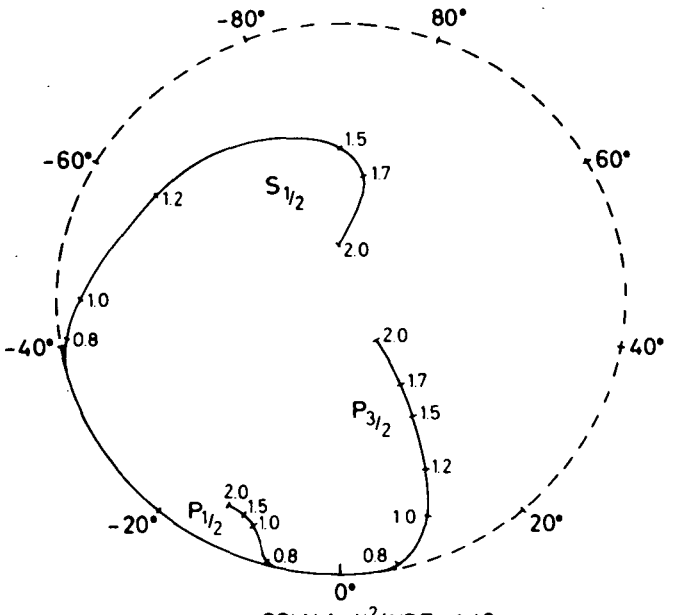

SOLN.A, X^2/NDF =1.43

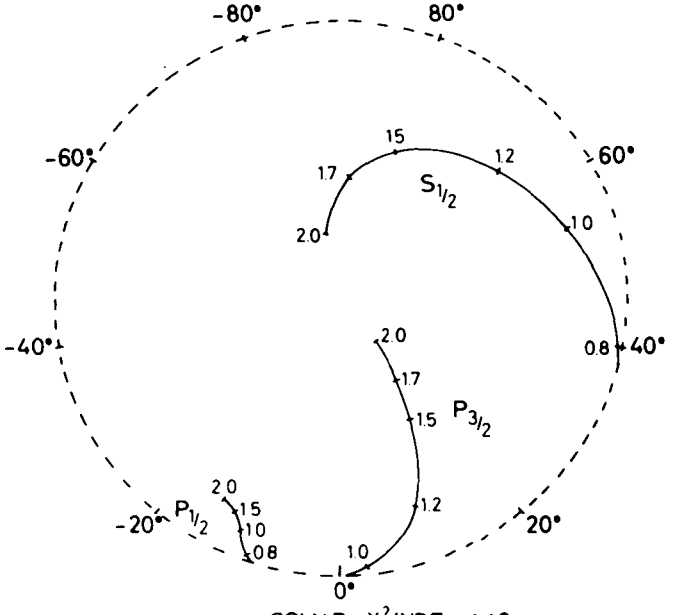

SOLN.B, X^2/NDF = 1.42

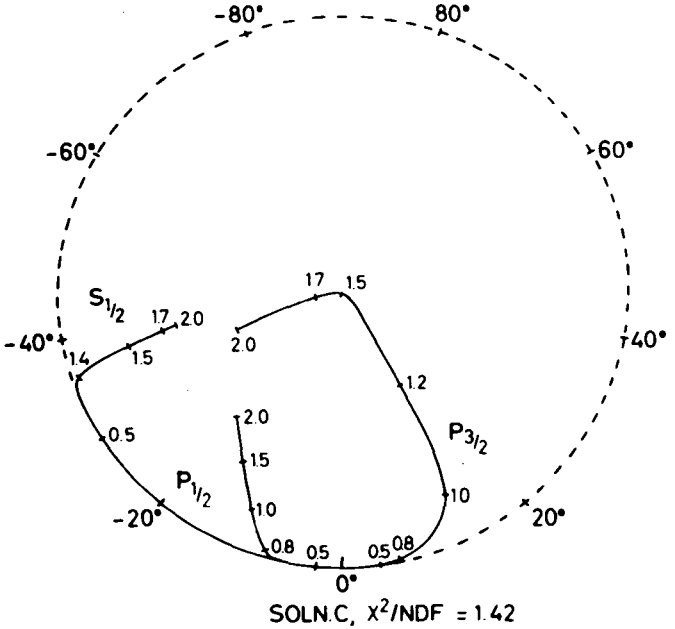

SOLN.C, X^2/NDF = 1.42

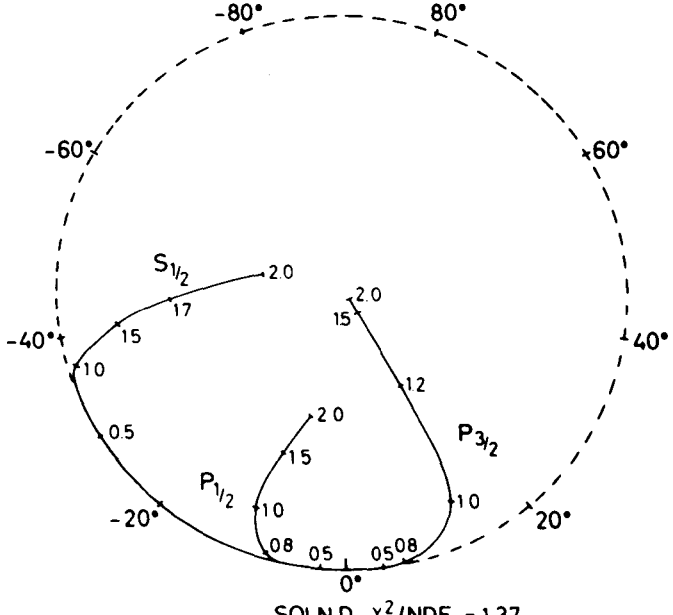

SOLN.D, X^2/NDF = 1.37

Fig. 5.

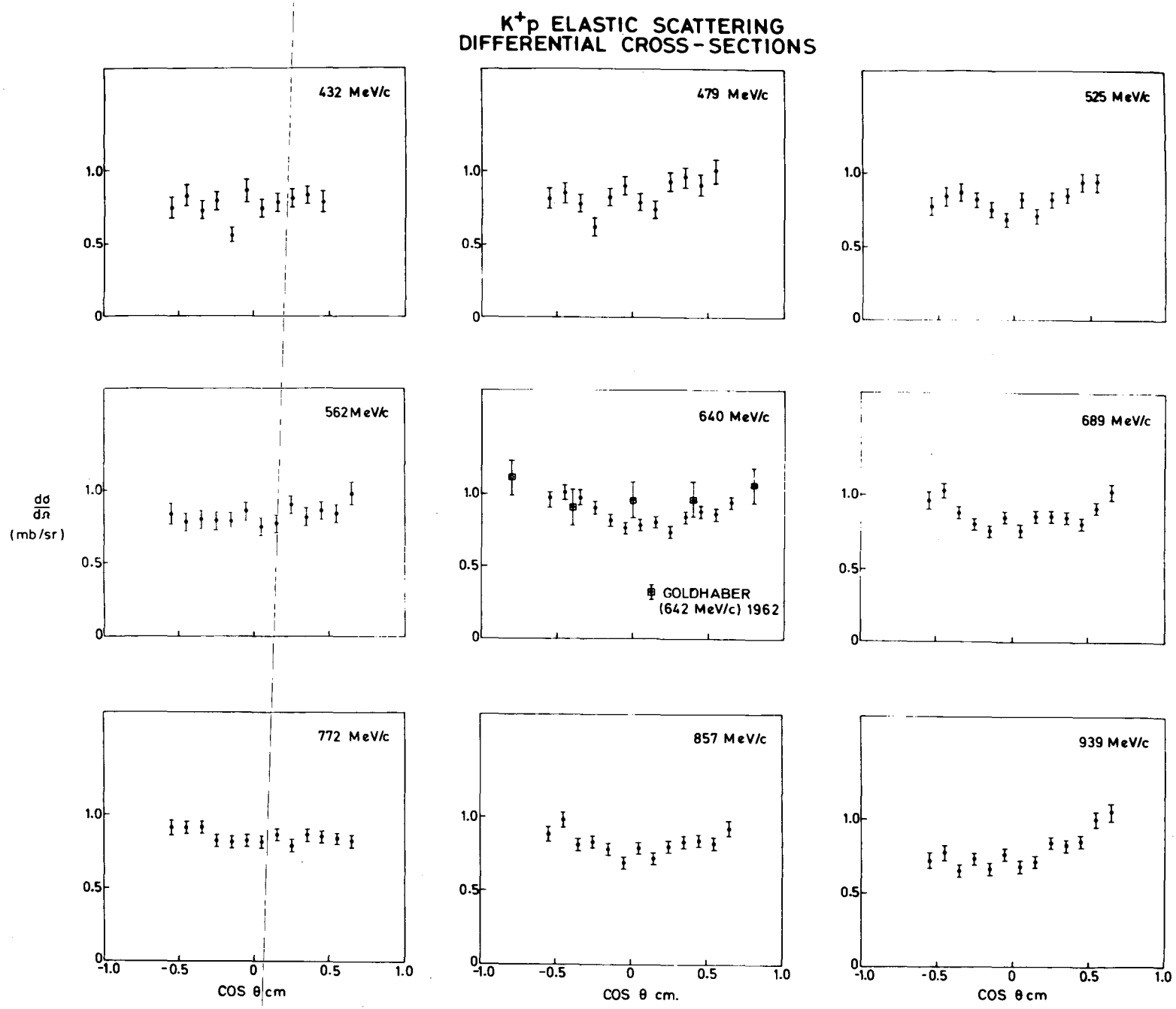
K+p ELASTIC SCATTERING
DIFFERENTIAL CROSS-SECTIONS
432 MeV/c
479 MeV/c
525 MeV/c
562 MeV/c
640 MeV/c
689 MeV/c
772 MeV/c
857 MeV/c
939 MeV/c
GOLDHABER
(642 MeV/c) 1962
dσ/dΩ
(mb/sr)
COS θ cm
COS θ cm.
COS θ cm

Fig. 6.

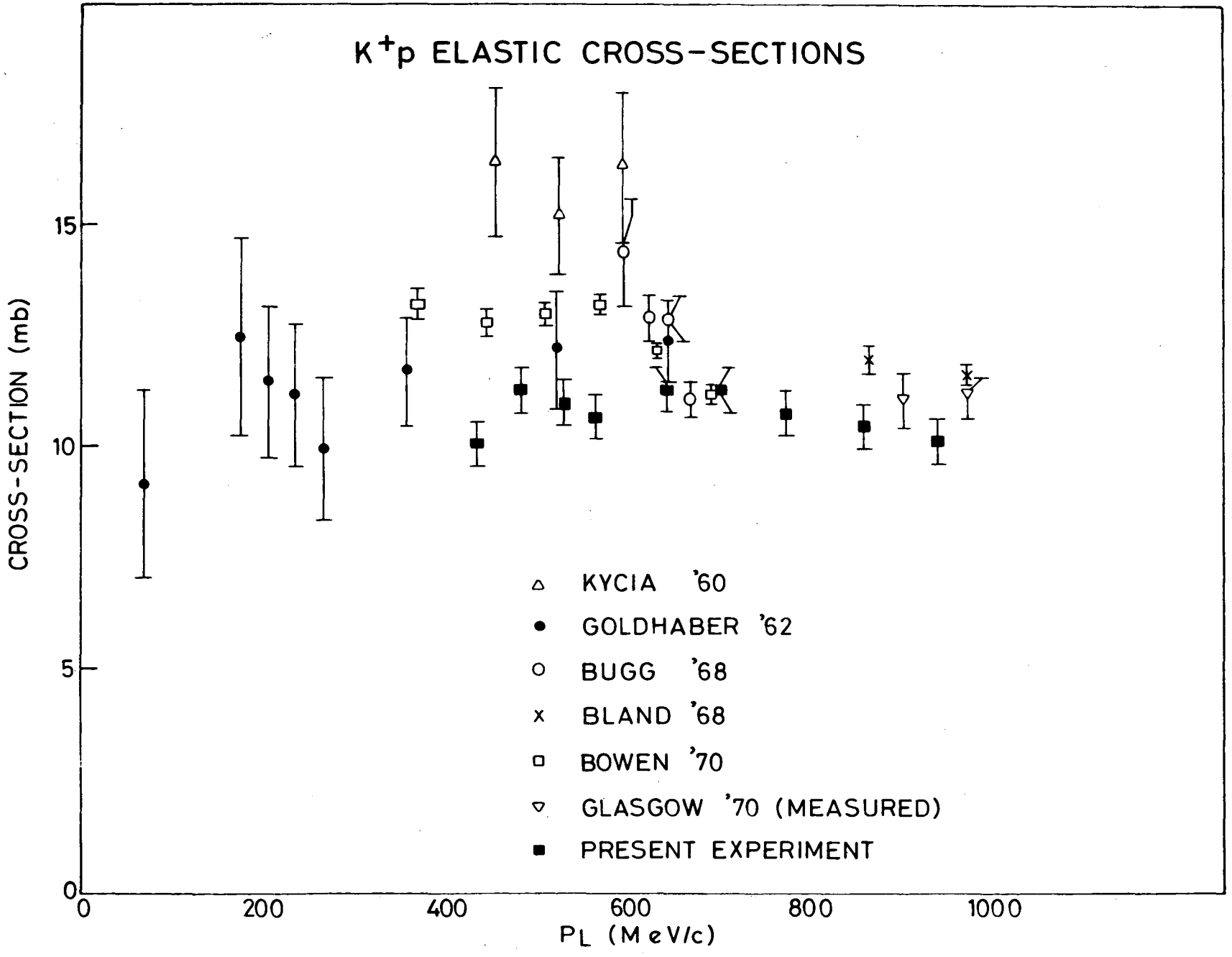
K+p ELASTIC CROSS-SECTIONS
CROSS-SECTION (mb)
0
5
10
15
0
200
400
600
800
1000
PL (MeV/c)
KYCIA '60
GOLDHABER '62
BUGG '68
BLAND '68
BOWEN '70
GLASGOW '70 (MEASURED)
PRESENT EXPERIMENT

Fig. 7.

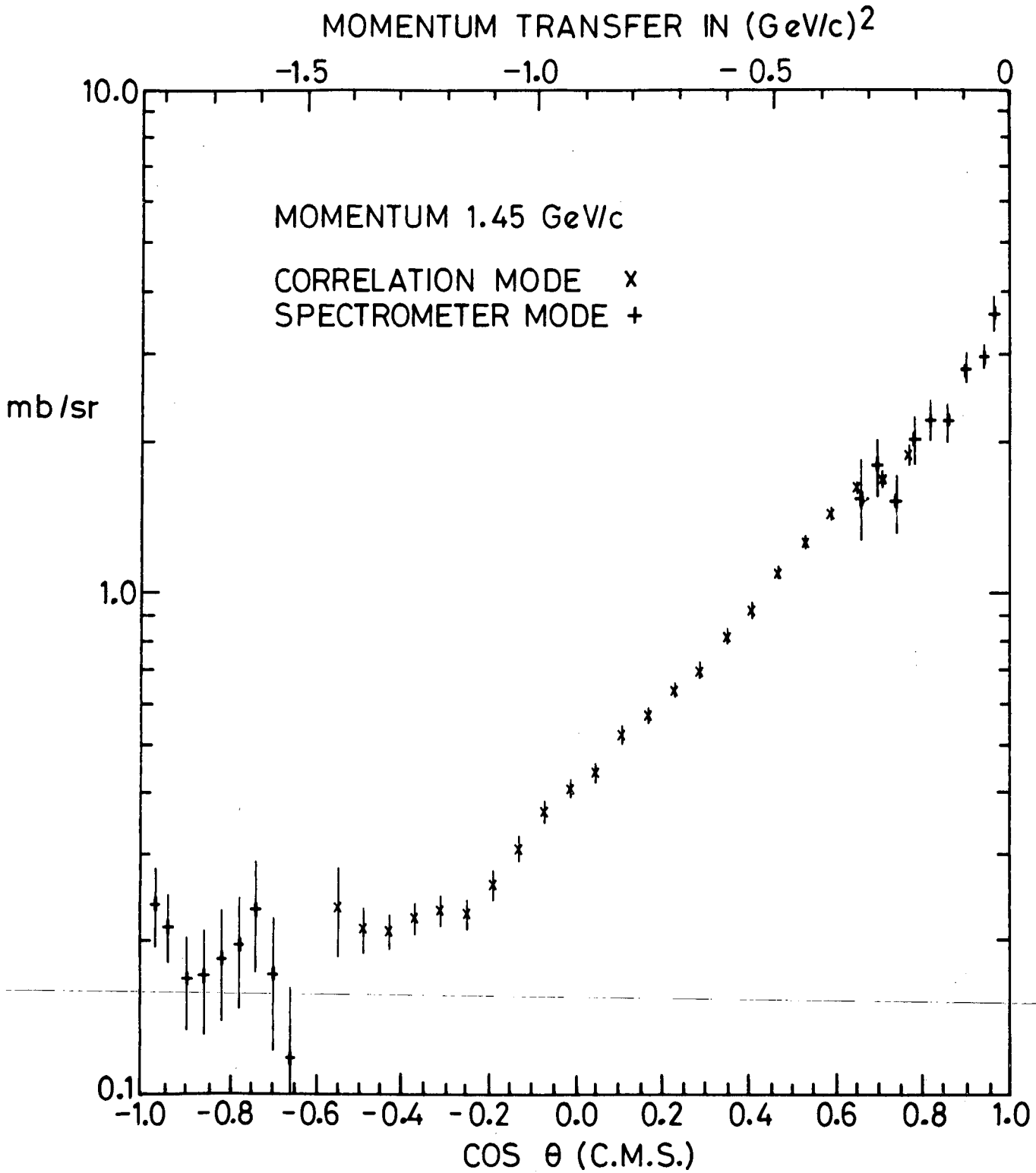
MOMENTUM TRANSFER IN (GeV/c)2
-1.5
-1.0
- 0.5
0
10.0
MOMENTUM 1.45 GeV/c
CORRELATION MODE x
SPECTROMETER MODE +
mb/sr
1.0
0.1
-1.0
-0.8
-0.6
-0.4
-0.2
0.0
0.2
0.4
0.6
0.8
1.0
COS θ (C.M.S.)

Fig. 8.

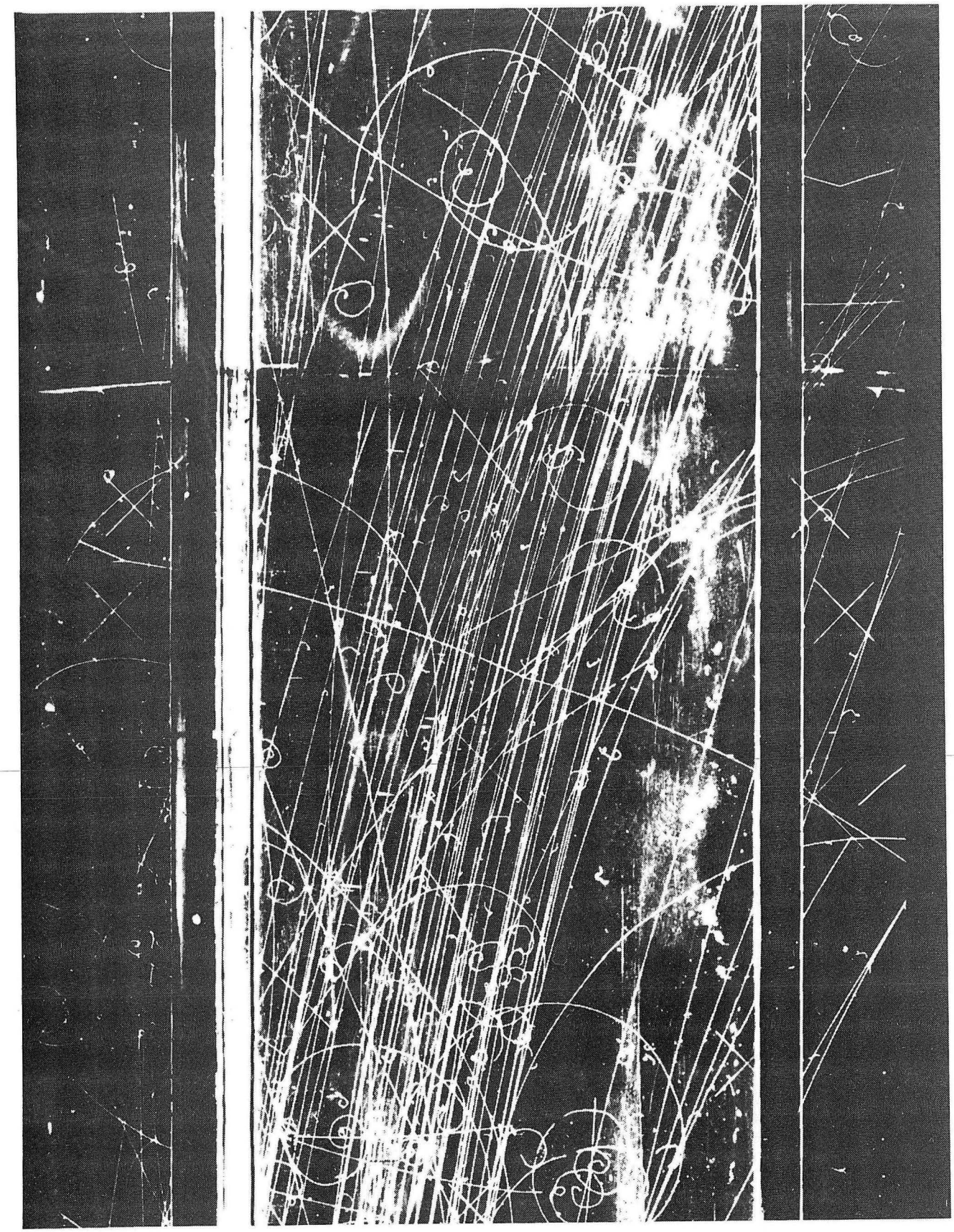

Fig. 9

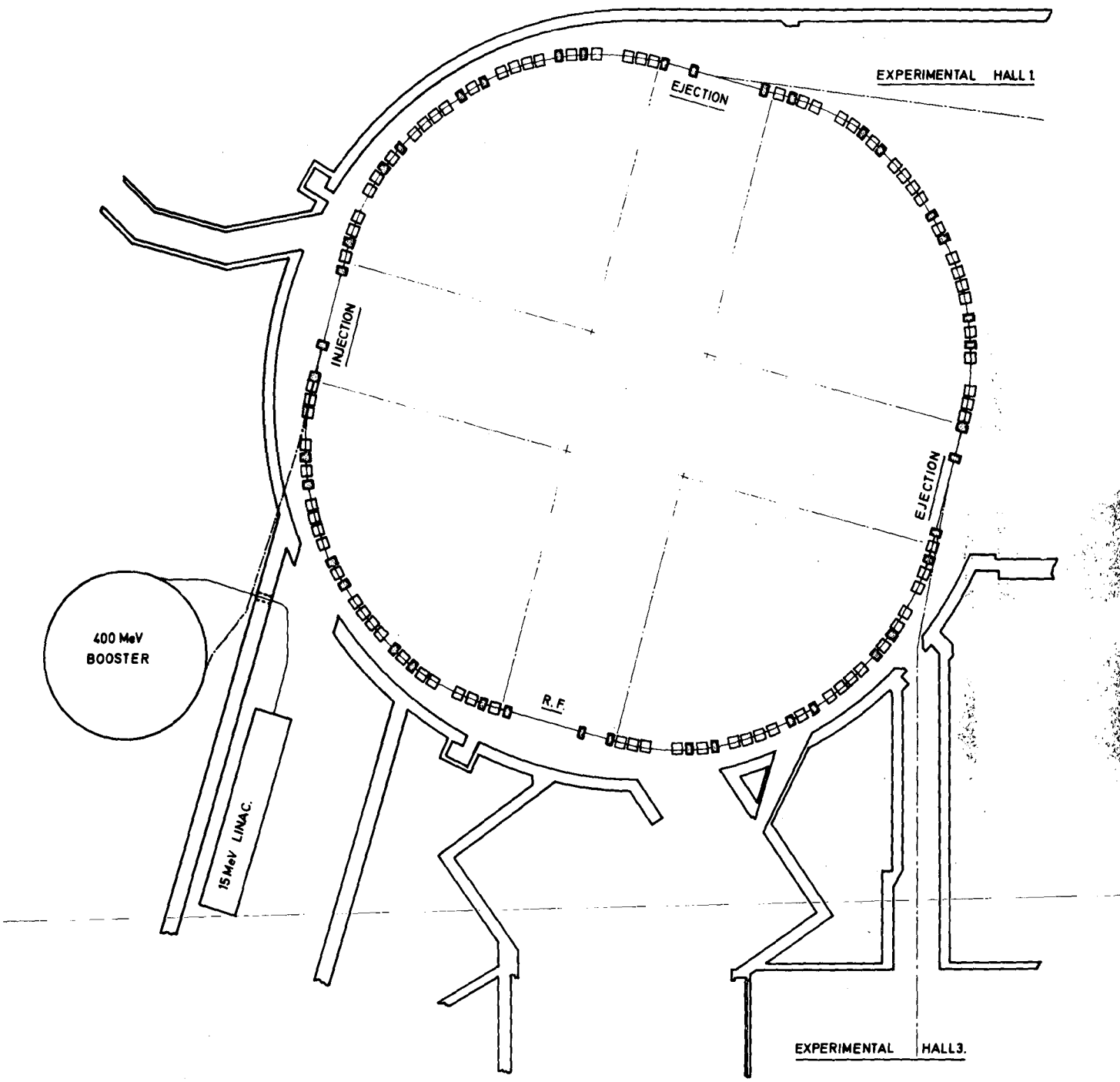
EXPERIMENTAL HALL 1
EJECTION
INJECTION
EJECTION
400 MeV
BOOSTER
R.F.
15 MeV LINAC.
EXPERIMENTAL HALL 3.

Fig. 10.

Discussion

Lovelace (Rutgers):

1. The K^+p data from the UCL Collaboration was not very adequate for phase shift analysis. The limitations on finding K^+p resonances come mainly from the inaccuracy of the differential cross section and its large normalization errors, rather than from energy gaps. I think it would be better to cut down the number of energies and increase the accuracy and improve the normalization.
2. When doing πN charge exchange polarization you ought to measure the differential cross section as well. It is by no means covered, in fact present experiments disagree with each other.
3. The $K\Lambda$ experiment should be extended up from 1.5 GeV/c to higher energies. This is a process in which we can easily get the full amplitudes, and it will be interesting to use FESR and investigate the status of EXD for the K^* and K^{**} exchanges.

Yokosawa (Argonne): Why are you interested in cutting down the number of energies in K^+p scattering?

Lovelace (Rutgers): There is no evidence of fine structure in K^+p scattering. The K^+p DCS and polarization change very slowly with energy. In πp and K^-p, one would like data at many energies. However, in K^+p it is more important to measure DCS accurately at a few energies. Even if there were fine structure, you would have to measure accurately, as well as closely, to see it.

Goldhaber (LRL): At RHEL are you doing anything on Kd total cross sections.

Manning (RHEL): There are no total cross sections measurements as such. There are measurements of $K^+n \rightarrow K^+n$; $K^+n \rightarrow K^0p$ and $K^-n \rightarrow K^-n$ over the momentum region 0.45 - 0.95 GeV/c.

Goldhaber (LRL): I am very interested in the discrepancy between the new Rutherford Laboratory K^+p σ_{TOTAL} data and the Arizona University data which agreed with the old Rutherford Laboratory data of Bugg et al. As you know the previous dip in $\sigma_{TOT}(K^+p)$ contributes importantly to the $I = 0$ peak or shoulder at 1760 MeV. If the dip in $\sigma_{TOT}(K^+p)$ goes away the $I = 0$ effect at 1760 would be considerably reduced.

ZGS PROGRAM

ARGONNE NATIONAL LABORATORY

Drasko Jovanovic and Bruce Cork

April 5, 1971

A. DRASKO JOVANOVIC

This brief description of the ZGS program will consist of two parts:

1) A discussion of the experimental area beam configuration, and

2) A list of experiments that either were completed in the last year or are presently set up in the experimental area.

1) The central feature of the beam configuration at the ZGS is the presence of the two full energy external proton beams. The positioning of these beams is such that the circulating beam in the ZGS can be extracted into both of them simultaneously. Extraction is accomplished using energy loss targets (Piccioni - targets); extraction efficiencies of approximately 30% are obtained in this manner. The secondary beams are derived from Be targets, 2 - 4 in. in length, positioned in the external proton beams. Generally, the transmitted portion of the primary proton beam is refocused on other targets further downstream. Thus, the External Proton Beam-I (EPB-I) is used on three secondary beam targets, the last one a heavy target. In this furthest downstream area, it is planned to have four beams originating at the heavy target. Currently, only one of these is operational.

The 12-ft bubble chamber is located at the end of the External Proton Beam-II (EPB-II) area and will have an rf separated beam operating up to 9 GeV/c serving it. Currently, only a neutrino beam is in operation. All secondary beams at the ZGS can be in operation simultaneously; the distribution

of intensity is adjusted by varying the amount of the circulating beam extracted into each of the primary proton beams and the secondary beam target thicknesses. This allows a given experiment to carry on tuning with a small amount of beam without interfering with other experiments that are taking data.

The ZGS circulating intensity is nominally 2.5×10^{12} ppp with a repetition rate of 3.5 - 4 sec and a flat top of 1 sec. A typical beam division would be $3 - 4 \times 10^{11}$ protons extracted into EPB-I and $2 - 3 \times 10^{11}$ into EPB-II.

In addition to the EPB experimental areas, there is an internal target area where operations center around two beams derived from the EPB-I extraction target. The 17° beam is a π^- beam operating up to 5.5 GeV/c. The other beam is a neutral 0° beam. The 7° separated beam was used in conjunction with the 30-in. bubble chamber, now planned to be moved to NAL in the early fall (1971).

The two enriched secondary beams (Beam 6 and Beam 42) are K meson beams, 1 - 2.3 GeV/c and stopping, respectively. The pion contamination in these beams can be as low as 4:1 π/K at low momenta, and 20:1 at the highest momenta. Beams 1, 8, and 21 are all secondary pion beams operating up to 8 GeV/c with nominal intensities of a few hundred thousand $\pi^{\pm}$/pulse.

2) List of experiments. Three groups of experiments either recently finished or currently in progress are given in the three attached tables.

These experiments represent a rather diverse range of experimental program activities. Note that most of the experiments are university collaborations with Argonne internal groups.

WEAK INTERACTIONS

University of Chicago Ohio St. ANL	$\Lambda^o \rightarrow pe\nu$.	Optical Chambers and Magnet	Completed 1000 events Analysis in Progress
Yale	$K_L^o \rightarrow \pi\mu\nu$ Polarization	Counters Sigma 2	10^6 events Analysis in Progress
University of Chicago	Precision measurement of the $K_L^o - K_S^o$ mass difference Phase of η_{+-}		Completed Published
University of Illinois	$\frac{K^o \rightarrow 2\pi}{\bar{K}^o \rightarrow 2\pi} = R(t/\varepsilon)$ for $4 < t/\tau < 16$	Wire Spark Chamber No Magnet	In Progress
University of Chicago	$\frac{K_L^o \rightarrow \ell\pi^{+-}\nu}{K_L^o \rightarrow \ell^-\pi^+\nu} = R(t/\tau)$	Wire Spark Chamber and Magnet	Setting Up
University of Chicago	$\Lambda^o \rightarrow P\mu\nu$	Optical Chambers	Planning

INELASTIC CHANNELS

ANL University of Michigan	$\pi^+ P \rightarrow K^+ \Sigma^+$	Wire Spark Chamber Magnet	Completed Published
University of Illinois	$\pi^- P \rightarrow \omega/\eta\, N$		Completed Analyses in Progress
University of Michigan	$\pi^- P \rightarrow K^+ \Sigma^-$ etc.	Wire Spark Chamber Magnet	Completed Analyses in Progress
Notre Dame	$\pi^+ P \rightarrow \pi^+ \pi^+ N$	Wire Spark Chamber Magnet	Completed Analyses in Progress
University of Chicago University of Wisconsin	$\pi^- P \rightarrow P\, A_2^-$ $\hookrightarrow \pi^- \gamma\gamma$	Optical Chamber	In Progress
Iowa State	$\pi^- P \rightarrow X^o N$	Counter	In Progress
ANL (1, 2)	$\pi^- P \rightarrow K^o\, \Lambda^o/\Sigma$	Wire Spark Chamber Magnet	Setting Up
Indiana	$\pi^- P \rightarrow A_2 P$	Wire Spark Chamber 6050	Setting Up

ELASTIC CHANNELS

Experimental Group	Description		Status
University of Indiana	$\pi^{\pm}P$, 2 -5 GeV/c	Wire Spark Chamber	Completed Published
University of Michigan, ANL	$\pi^{+}P$ 3, 4, 5 GeV/c		Completed Published
ANL, NAL Northwestern	Polarized $\pi^{\pm}P$ backward	Counter Polarized Target	Completed Analyses in Progress
Ohio State Michigan State	NP el. 6- 12 GeV/c	Wire Spark Chamber N-Counters	Completed Published
University of Minnesota	$\pi^{-}P \rightarrow \pi^{o}N$	Optical Chamber Counter	Completed Published
University of Michigan ANL	$\pi^{+}P$ el. at t = 3	Wire Spark Chamber Magnet	Completed Analyses in Progress
ANL, NAL Northwestern	$K^{+}P$ Polarized 1.5 - 2.1 GeV/c	Polarized Target Counter	Completed Published
Ohio State Michigan State	NP - Polarized Backward	Polarized Target Wire Spark Chamber	Setting Up
University of Maryland, ANL	$K^{+}P$ Elastic 1.5-2.3 GeV/c	Wire Spark Chamber Entr.	Setting Up

B. BRUCE CORK

The characteristics of the primary and secondary beams at the ZGS have been discussed by Drasko Jovanovic. I would like to add a few supplementary remarks.

During 1970 the ZGS logged 4500 hours of operation for high energy physics research purposes. Frequently, as many as seven experiments were in operation simultaneously. Twenty experiments, including eight bubble chamber experiments, were completed during the year. Most of the experiments were collaborations between university groups and Argonne internal groups, as Drasko has mentioned.

The relatively new external proton beam experimental area (EPB-II) was used extensively during the year for counter experiments. The beam was also transported to the 12-ft hydrogen bubble chamber; an exposure of 10,000 photographs of 12 GeV/c protons in hydrogen was made, as well as an exposure of 75,000 photographs of neutrinos in hydrogen. Eleven neutrino interactions have been observed to date in the analysis of this film. Some of these aspects are summarized in the table which follows.

It is our plan at present, that the 30-in. hydrogen bubble chamber will be moved to NAL this summer. The 40-in. heavy liquid chamber has been given an inactive status and will continue as such for the foreseeable future. We feel that these bubble chambers will be advantageously replaced

by a 1.2 m streamer chamber which will be located in an unseparated beam (8 GeV/c, or less). The streamer chamber is, at present, undergoing development in a test beam. Excellent cosmic ray traces have been observed. After initial testing the chamber will be installed in the 500-liter bubble chamber magnet which will be operated at a magnetic field of 18 kG. Experiments with this chamber will supplement many of the experiments to be carried out in the 12-ft bubble chamber.

The number of secondary beams in use at the ZGS has reached the point that increased intensity is required to satisfy the needs of the numerous experiments. Fast spill resonant extraction of the circulating proton beam for the neutrino experiment in the 12-ft bubble chamber has been achieved with 70% extraction efficiency. To achieve increased circulating beam intensity, development work is well under way on a 200-MeV booster injector that will double charge exchange 50-MeV negative hydrogen ions and accelerate these to 200 MeV. The goal of this project is to obtain a factor of four increase in the ZGS circulating intensity. To test the ideas involved, the 2.2 GeV Cornell electron synchrotron has been modified to accelerate protons. The degree to which this project is ultimately successful may be somewhat limited by the very small aperture of the machine.

Another project that should be mentioned involves the acceleration of polarized protons. The ZGS has properties that appear to be favorable for this purpose; further work is being done to determine if the plan is truely

feasible.

It seems very apparent to us that the energy range accessible with the ZGS still represents a very fertile source for new information. All of the known resonances can be produced with 12-GeV protons; detailed understanding of their properties is far from complete. There are still large gaps in the differential cross section data in this range, as well as in the polarization data. This region has been an excellent one for investigating CP violation effects; we believe it will continue to be so. The neutrino spectrum peaks at 1 GeV, ideal for the study of two and three body neutrino interactions in the 12-ft bubble chamber.

The number of approved experiments has reached the point that the ZGS is now scheduled for more than a year in advance. This is already such a long lead time that it is necessary to periodically review the status of the approved experiments during the intervening time period. We see in all of this many challenges and many opportunities for the years ahead.

FIGURE CAPTIONS

Fig. 1: ZGS beams.

Fig. 2: External proton beam I area and meson area.

Fig. 3: External proton beam II area.

Fig. 4: Expected π^+ yields from ZGS counter beams.

Fig. 5: Expected π^- yields from ZGS counter beams.

Fig. 6: Expected K^+ and K^- yields from ZGS counter beams.

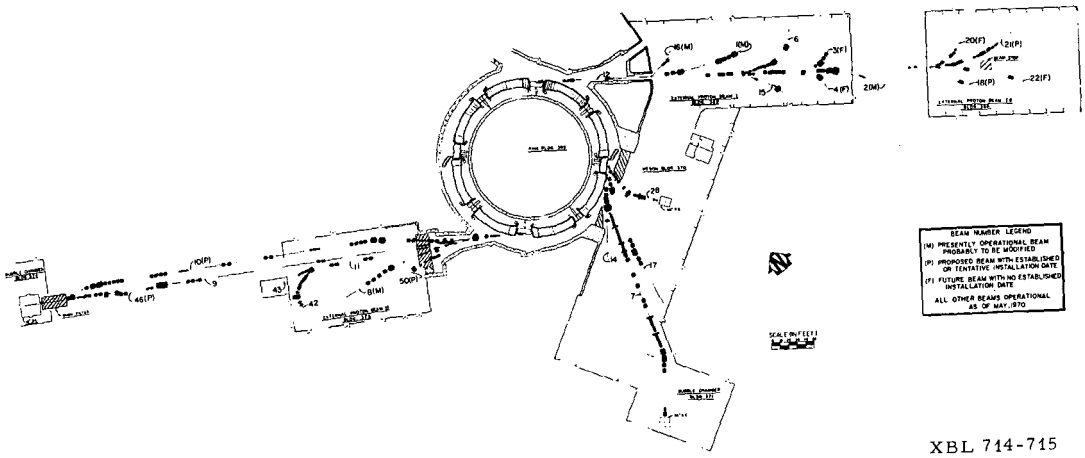
BEAM NUMBER LEGEND
(M) PRESENTLY OPERATIONAL BEAM PROBABLY TO BE MODIFIED
(P) PROPOSED BEAM WITH ESTABLISHED OR TENTATIVE INSTALLATION DATE
(F) FUTURE BEAM WITH NO ESTABLISHED INSTALLATION DATE
ALL OTHER BEAMS OPERATIONAL AS OF MAY, 1970
SCALE IN FEET
XBL 714-715

Fig. 1.

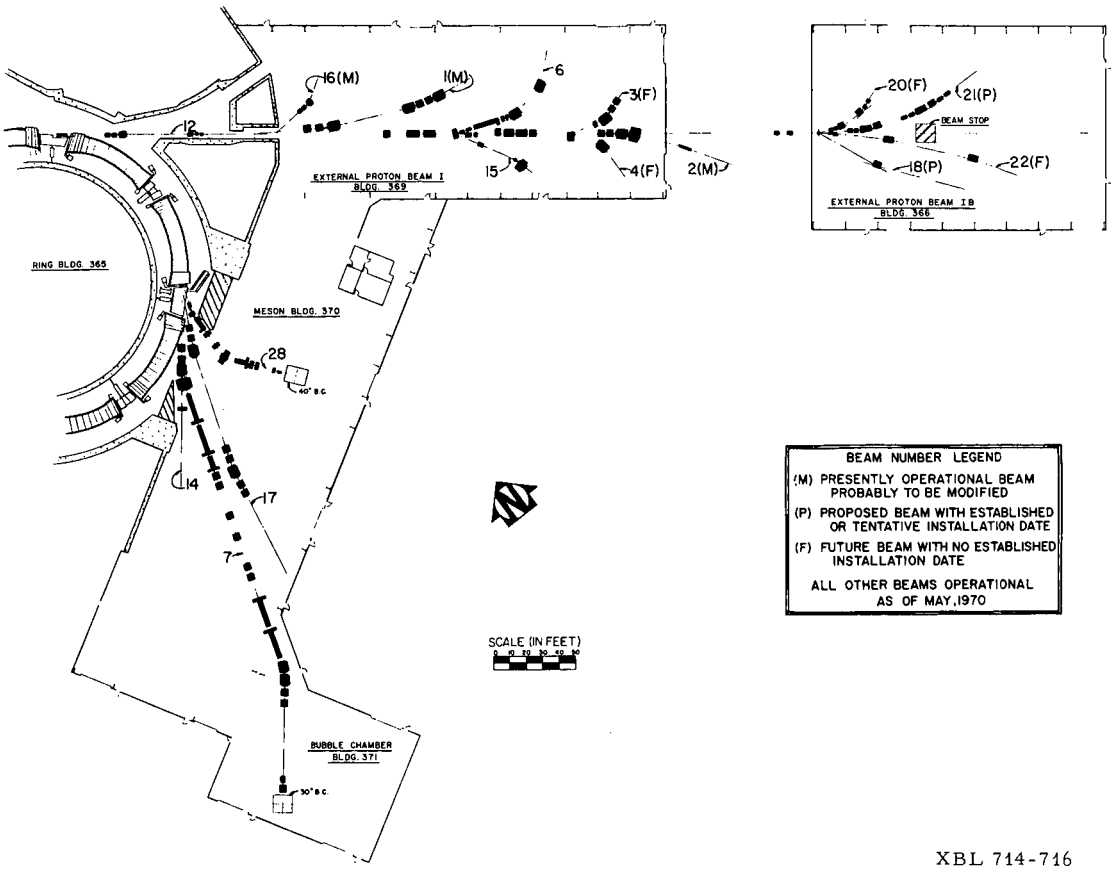
16(M)
1(M)
6
3(F)
12
15
4(F)
2(M)
EXTERNAL PROTON BEAM I
BLDG. 369
20(F)
21(P)
BEAM STOP
18(P)
22(F)
EXTERNAL PROTON BEAM IB
BLDG. 366
RING BLDG. 365
MESON BLDG. 370
28
40° B.C.
14
17
7
BEAM NUMBER LEGEND
(M) PRESENTLY OPERATIONAL BEAM PROBABLY TO BE MODIFIED
(P) PROPOSED BEAM WITH ESTABLISHED OR TENTATIVE INSTALLATION DATE
(F) FUTURE BEAM WITH NO ESTABLISHED INSTALLATION DATE
ALL OTHER BEAMS OPERATIONAL AS OF MAY, 1970
SCALE (IN FEET)
0 10 20 30 40 50
BUBBLE CHAMBER
BLDG. 371
30° B.C.
XBL 714-716

Fig. 2.

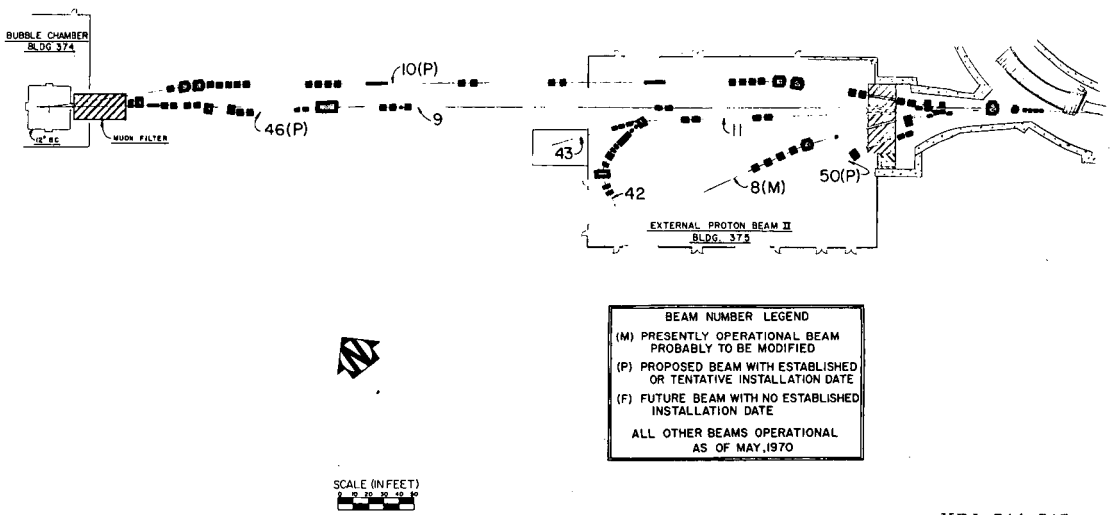

XBL 714-717

Fig. 3.

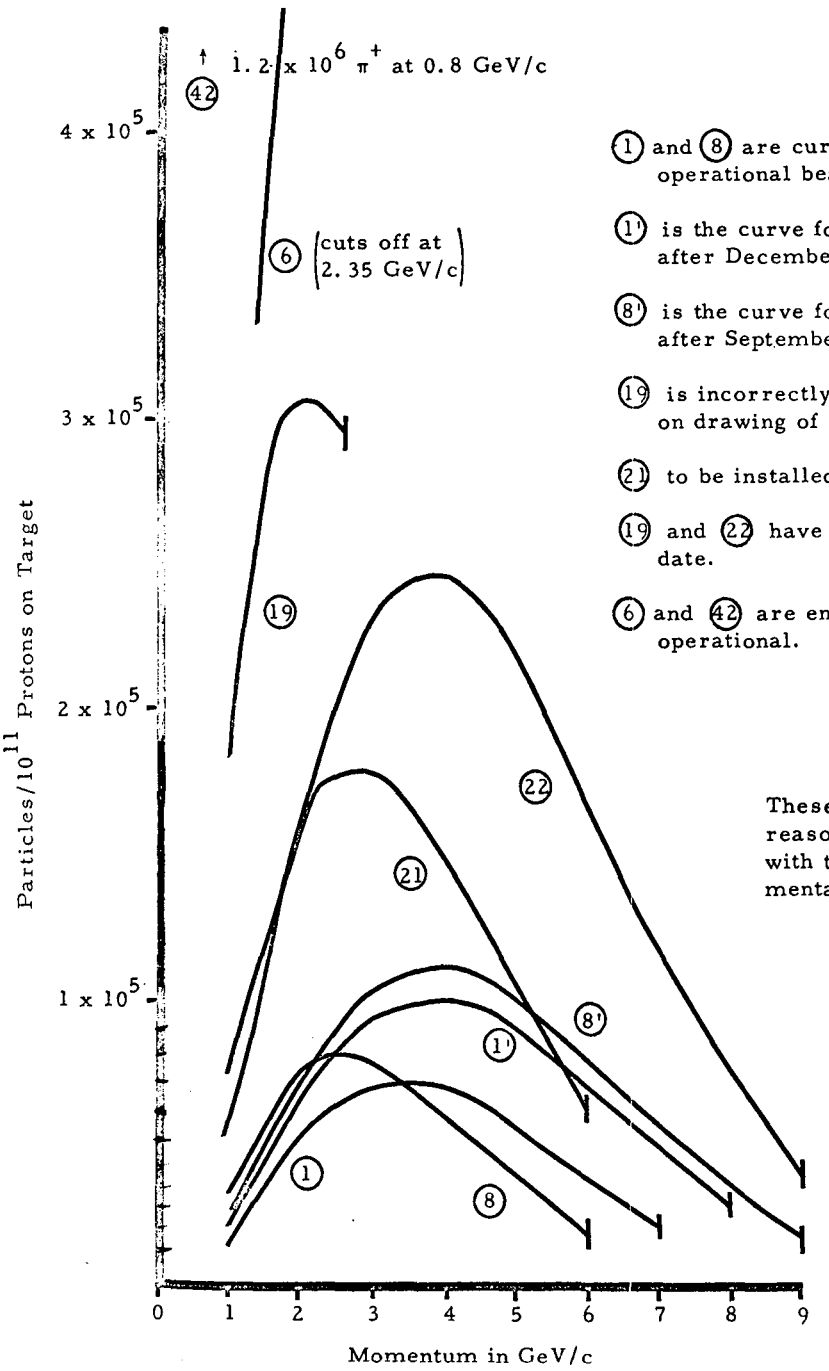
† 1.2 x 10^6 π+ at 0.8 GeV/c
42
4 x 10^5
6 (cuts off at 2.35 GeV/c)
3 x 10^5
19
2 x 10^5
22
21
1 x 10^5
8'
1'
1
8
Particles/10^11 Protons on Target
0 1 2 3 4 5 6 7 8 9
Momentum in GeV/c
1 and 8 are curves for currently operational beams.
1' is the curve for modification after December 1970.
8' is the curve for modification after September 1970.
19 is incorrectly labeled Beam 3 on drawing of experimental areas.
21 to be installed November 1970.
19 and 22 have no definite installation date.
6 and 42 are enriched beams presently operational.
These curves are in reasonable agreement with the limited experimental data available.
XBL 714-718

Fig. 4.

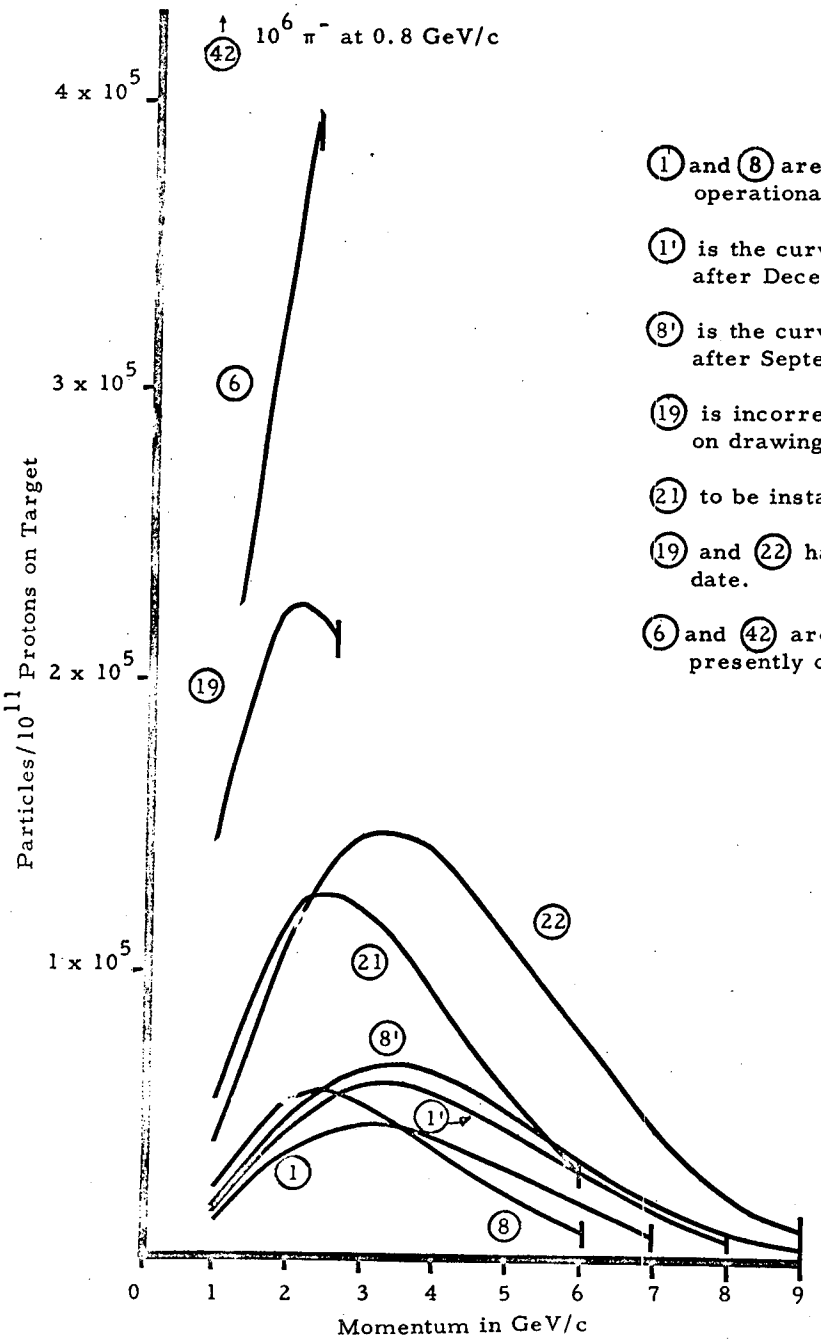

(1) and (8) are curves for currently operational beams.

(1') is the curve for modification after December 1970.

(8') is the curve for modification after September 1970.

(19) is incorrectly labeled Beam 3 on drawing of experimental areas.

(21) to be installed November 1970.

(19) and (22) have no definite installation date.

(6) and (42) are enriched beams presently operational.

These curves are in reasonable agreement with the limited experimental data available.

XBL 714-719

Fig. 5.

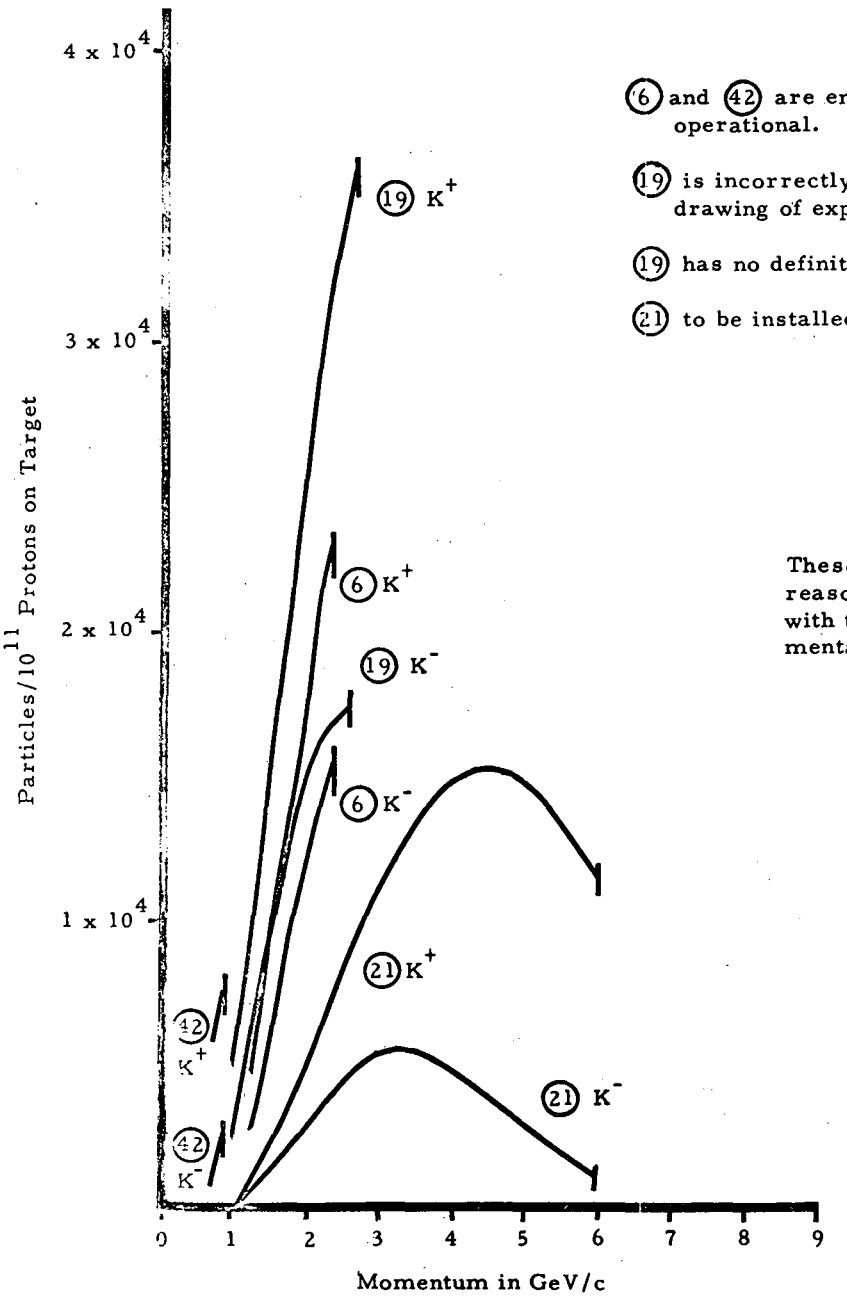

(6) and (42) are enriched beams currently operational.

(19) is incorrectly labeled Beam 3 on drawing of experimental areas.

(19) has no definite installation date.

(21) to be installed November 1970.

These curves are in reasonable agreement with the limited experimental data available.

XBL 714-720

Fig. 6.

Discussion

Yokosawa (Argonne): I would like to have someone comment on what physics you can learn by using polarized beams. Is it worthwhile? Will it contribute to very crucial physics.

Fox (CIT): I think it will!

Lovelace (Rutgers): What can you do with polarized beams except pp phase shift analysis?

Fox (CIT):

A. Uses of Polarized Beam

There are several extremely interesting experiments that can be performed with a polarized proton beam.

(i) Polarized p beam on polarized (p,d) target. This is presumably a counter experiment. Uses have been mentioned by Lovelace and Steiner: (a) low energy phase shift analysis, (b) test of models for high energy inelastic and elastic exchange processes. Such experiments measure the pp analogues of R and A in meson-baryon scattering. E. L. Berger and G. C. Fox [Phys. Rev. Letters 25, 1783 (1970)] have shown the latter are decisive signatures of the various models. The same will be true in pp scattering. Moreover, the technical difficulties in measuring final baryon polarizations limits meson-baryon scattering studies to $\pi N \leftarrow K(\Sigma,\Lambda)$, $\bar{K}N \rightarrow \pi(\Sigma,\Lambda)$ and elastic scattering. This is a very limited subset of reactions--in particular it includes none of the dominant π, ρ, A_2 exchange processes. The p(p,d) experiment will allow study of these exchanges, e.g., $pn \rightarrow np$ and $pp \rightarrow n\Delta^{++}$

(π, ρ, A_2), backward $pp \to \pi d$ (N_α, N_γ exchange) as well as the elastic case mentioned by Steiner.

(ii) Polarized p beam on unpolarized target (p,d) at low energy. The unambiguous identification of an exotic resonance in KN or NN scattering would be of major importance. Both KN phase shift analysis and theoretical work [R. Aaron, R. D. Amado, R. R. Silbar, Phys. Rev. Letters 26, 407 (1971)--hereafter AAS] suggest such resonances will be very inelastic. Unfortunately simple $d\sigma/dt$ measurements of $KN \to K\Delta$ are insufficient to distinguish a cross section rising from threshold and falling at high energy, i.e., 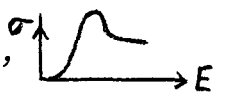

from background $\oplus$ a Z^* resonance, i.e.,

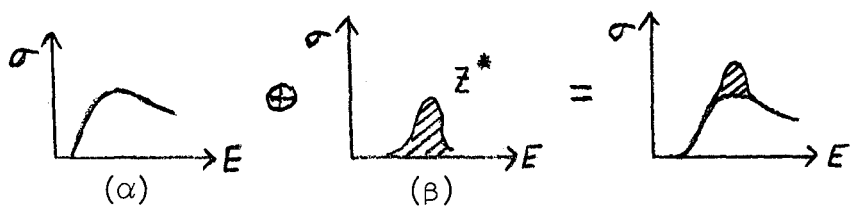

Polarization measurements will pick out the distinctive Breit-Wigner form of (β) by interference with the dominant and purely real (from duality) diagram (α). [In $d\sigma/dt$ (α) and (β) were incoherent.] So measurements of $KN \to KN\pi$ and $NN \to NN\pi$ off a polarized target should provide decisive tests for an exotic resonance. The model of AAS predicted a resonance in $KN \to K^*N$: the same mechanism will apply in p(p,d) scattering and lead to an exotic B = 2 resonance in $NN \to N\Delta$. The KN experiment requires new techniques (cf. my

reply on page 126)--the NN experiment with polarized beam around the $N\Delta^{++}$ threshold requires only a bubble chamber.

(iii) Bubble Chamber (Yes, they are alive and well) experiment: polarized p beam on unpolarized (p,d) target at, say, $p_{lab} \gtrsim 3$ GeV/c. According to duality, all non-Pomeron pp scatterings are purely real and hence should have no polarization. This is contradicted by polarization in np CEX. There is no understanding of this data because no one knows how duality is broken. The early bubble chamber experiments established the usual peripheral peaks and so stimulated the current theoretical models--Regge exchange, quark model quantum numbers, etc. This experiment will establish the systematics of the "forbidden" polarization over a wide range of final states. Unlike results on single reaction (np CEX), such data should allow an understanding of the mechanism of duality breaking and the energy dependence thereof--hence one can build a new theory. Further, one will be able to study the systematics of diffractive polarizations $pp \to pp$, $pp \to pN^*_{1400}$ and so learn all about the Pomeron.

There are probably other exciting experiments. It is clear that a polarized beam allows study of important and otherwise inaccessible physics. It should be a major priority if a good quality beam is technically possible.

Steiner (LRL): I think the kind of physics to be done with high energy polarized proton beams is rather limited. There are however a number of potentially interesting experiments. For example one could test factorization by measuring various polarization correlation and polarization transfer parameters in high energy proton-nucleon scattering. In the polarization correlation experiments one would scatter a polarized beam from a polarized target, whereas in the polarization transfer processes one analyzes the polarization of the low energy recoiling particle produced by the interaction of a high energy polarized proton with an unpolarized target. If factorization is a good approximation then these correlation and transfer effects are expected to be very small.

April 9, 1971

THE BEVATRON PROGRAM

Edward J. Lofgren, William R. Holley, Richard C. Sah

Lawrence Radiation Laboratory
University of California
Berkeley, California

The first section of this note will give the present operating capabilities of the Bevatron. The second section will outline the planned improvement program and the final section will give a brief account of the experimental program.

1. Capability of the Bevatron

The Bevatron operates at a maximum energy of 6.2 GeV and the usual maximum intensity is about $5 \cdot 10^{12}$ protons per pulse at 10 to 12 pulses per minute or about 10^{12} protons per second. The record maxima are about 20% higher. About 80% of the beam can be extracted with a newly installed resonant extraction system. The extracted beam can be divided and directed down three proton channels which are shown in Figure 1. Each channel is shielded to take up to $3 \cdot 10^{12}$ protons per pulse. A more usual value of beam in a channel is, however 10^{12} protons per pulse. That suffices for most experiments and it permits a greater degree of multiple running. The bending and focusing elements in these channels are controlled by a computer system which gives great flexibility in the control of the beams in the three channels. The amount of beam in each channel, the energy and the pulse length may be varied from pulse to pulse or during a pulse. The beam pulse may be as long as two seconds depending on the pulse mode and the energy of the extracted beam. Recent improvements in the suppression of magnet ripple will make it possible to limit beam variation in the frequency

range of several kilo Hertz to less than 50%. The duty cycle resulting from the r.f. structure is greater than 70%.

Three secondary beam lines can be set up at each channel giving a capacity of 9 simultaneous beams from the external proton beam system. (Seven are set up at the present time.) Two internal target stations may also be used for secondary π^- beams or for neutral particle beams.

A summary of the characteristics of the secondary beams presently in use is given in Figure 2. The beams are identified on Figure 1 by the beam numbers. More detailed information on these beams is given in the Bevatron Experimenters' Handbook.[1]

The Bevatron is scheduled to run about two thirds of the time, and the actual running time is about 90% of the scheduled time. Of the one-third of the time not scheduled to run, one-third is the minimum required for maintenance, improvements and holidays. The remaining two-thirds is ascribable to curtailed budgets. Some of the operating statistics are given in graphical form in Figure 3.

2. Improvement Program

A modest continuing program of improvements is being carried out on the Bevatron. Recently completed improvements have centered on improved control of the external beam of the Bevatron and on an increase of the extraction efficiency. The efficiency of the old energy loss extraction system was 40%, while the new resonant extraction system is 80% efficient. The planned use of thinner septa for the first extraction magnets will increase further the efficiency to more than 90%. The importance of these

---

[1] UCRL-17333, Bevatron Experimenters' Handbook. A copy may be obtained by writing to: Mrs. A. M. Morrish, Building 50, Room 149, Lawrence Radiation Laboratory, Berkeley, California 94720.

developments is even greater than the direct saving of beam, because radiation damage to the vacuum tank is one of the beam limits and a lower loss will permit higher circulating beam and more beam in the external channels.

The improvements now underway center on increased intensity, both of the circulating beam and of the secondary beams. The most important change is the replacement of the present 20 MeV injection system with the 50 MeV system of the Brookhaven AGS. A new 200 MeV injection system is now being installed on the latter accelerator. The installation of the 50 MeV system on the Bevatron should be completed by Spring 1972. The expected increase in beam is about a factor of 2-1/2 to 3 and comes from a reduction of losses due to space charge effects and to gas scattering. An additional planned change is the introduction of auxiliary cryogenic pumping to improve the vacuum from the present value of $2 \cdot 10^{-6}$ torr to $5 \cdot 10^{-7}$ torr.

Together these changes should increase the circulating beam to $2 \cdot 10^{13}$ ppp and with the expected improvement in extraction the external beam should be $1.8 \cdot 10^{13}$ ppp.

High intensity K beams are being designed for low momentum ($\lesssim 1.5$ GeV/c) and stopping K experiments. One goal is a separated beam which will yield 10^5 stopped K^+ per pulse, with a background of 10^6 pions. This is 40 to 50 times greater than the present beam, although the incident proton requirements will increase only modestly, perhaps to $2 \cdot 10^{12}$ ppp. The design is based on very short specially designed separators and magnets. Two stages of mass separation will be used. The solid angle of acceptance will be about 30 msr. Sextupole magnets and sextupole components in bending magnets will be used to correct partially the large second order aberrations resulting from the large acceptance of the system.

3. Experimental Program

The experimental program at the Bevatron is summarized in Figure 4 and the experiments are briefly described in this section.

In a continuation of a previous experiment on backward $\pi^- p$ elastic scattering between 600 and 1280 MeV/c, a group from Iowa State University, McGill University and St. Louis University is extending their measurements to higher energies. The new experiment, which uses a magnet and scintillation counters, is now being set up and will measure the differential cross section for $\pi^- p$ elastic scattering over an angular range of $\sim 160^\circ$ to 177° in the center of mass. Measurements will be taken at 31 incident pion momenta in the range 1300 to 2500 MeV/c. The data will be used to search for new resonances and to provide tests of the various phase shift analyses at these energies.

In another potentially useful experiment from the point of view of phase shift analyses a collaboration between members of several LRL groups is currently setting up to measure the polarization asymmetry in the reactions $\pi^- p \to \pi^0 n$ and $\pi^- p \to \eta n$ at four momenta between 800 and 2000 MeV/c. The experiment will use optical spark chambers to detect events originating from a polarized ethelene glycol target. The momenta have been carefully chosen so that the new data will be most useful in resolving present ambiguities in pion–nucleon phase shift solutions. Future plans of the group include measurements of R and A parameters in πN scattering and also the investigation of associated production reactions such as $\pi N \to K\Lambda$ using a polarized target.

In an experiment which will be setting up at the Bevatron shortly a group from the University of Arizona and the University of Michigan propose

to measure the K^+p and K^+d total cross sections with an accuracy of ± 0.25 mb in the momentum range 0.60 to 1.4 GeV/c. The purpose is to resolve the question of whether the I=0 structure in K^+–n total cross section is double peaked at .8 GeV/c and 1.2 GeV/c. A Z^{o*} resonance has been claimed for the lower peak, and the key question is whether or not the peak exists experimentally. The proposed experiment should settle this point.

A collaborative effort involving the University of Chicago, Carleton University and the National Research Council, Canada is setting up an experiment to study in detail the reaction $pp \to d\pi^+$ at 10 momenta between 3.0 and 7.0 GeV/c. Multi–wire proportional chambers, Cherenkov counters and a large magnet will be used to analyze both final state particles. The aim of the experiment is to obtain the accurate data (5%) needed to disentangle the contributions of various mechanisms possibly involved in the reaction. The reaction $pp \to dM^+$ for arbitrary missing mass will also be studied, especially where M^+ is the ρ^+.

In the field of meson resonances, an experiment by a UCLA and UC Riverside group has been approved to study with high statistics and good mass resolution the production t–dependence and properties of the A_2^o in the reactions

$$\pi^- p \to A_2^o\, n$$
$$\hookrightarrow \pi^+\pi^-\pi^o,\ K^+K^-,\ K_1^o K_1^o\ .$$

These reactions will be studied in the streamer chamber developed by UCLA. In addition other mesons such as the $f^o(1260)$, $D^o(1285)$ and $\pi_N(1016)$ will be investigated. The experiment has been approved for running in the Fall of 1971.

In addition to the above strong interaction experiments there is an extensive list of experiments investigating weak interactions, electromagnetic interactions and nuclear chemistry.

A group from UCSD is currently running an experiment measuring hyperon leptonic decays. A 1.2 GeV/c pion beam is used to produce Λ and Σ hyperons in a CH_2 target by associated production. Detection apparatus utilizing scintillation counters, Cherenkov counters, wire spark chambers, Charpak chambers, optical chambers and a large analyzing magnet is used to measure the branching ratio of the decays $\Sigma^{\pm} \rightarrow e^{\pm}\nu n$ and the values of G_A/G_V for the decays $\Sigma^{\pm} \rightarrow ne^{\pm}\nu$, $\Sigma^{\pm} \rightarrow \Lambda^{o}e^{\pm}\nu$, and $\Lambda^{o} \rightarrow ne^{-}\nu$.

An LRL group is currently modifying apparatus recently used to obtain stringent limits on the decays $K_L^o \rightarrow \mu\mu$, ee, μe in order to measure the muon polarization in $K_L^o \rightarrow \pi^- \mu^+ \nu$. The double spectrometer containing wire spark chambers which was used for the previous experiment will be modified by addition of a polarimeter. The polarimeter can have its magnetic field along either of two mutually perpendicular directions. The two orientations of magnetic field will allow the determination of both the real and imaginary parts of the $K_{\ell 3}^o$ form factor $\xi(q^2)$.

The initial experiment (being set up now) using the UCLA streamer chamber is an investigation of possible C-violating effects in the $\pi\pi\gamma$ decay mode of the X^o meson produced in the reaction

$$\pi^- p \rightarrow X^o n$$

$$\hookrightarrow \pi^+ \pi^- \gamma.$$

Scintillation counters, photon counters and neutron counters will be used to trigger the streamer chamber.

In the late Spring of 1971 an LRL group will set up an experiment in the stopping K^+ beam at the Bevatron to search for the reaction $K^+ \rightarrow \mu^+ \nu \bar{\nu} \nu$ and simultaneously for the reaction $K^+ \rightarrow \pi^+ \nu \bar{\nu}$. These reactions may reveal an interaction between neutrinos which could be quite strong in comparison with the weak interaction. Second order weak interaction effects will also be explored in the experiment.

An extensive experiment at the Bevatron studying kaonic atoms by means of K^- mesic X-rays is now drawing to a close. High resolution solid state detectors have been used to measure the detailed X-ray spectra emitted from kaonic atoms formed in targets of various elements placed in a 500 MeV/c K^- beam. Nuclear sizes and information on the structure of the nuclear surface may be obtained from these measurements. In addition Σ^- hyperonic atoms, Coulomb excitation coupling between nuclear energy levels and energy levels of kaonic orbits, and hypernuclei will be studied.

To round out the present Bevatron program mention should be made of two experiments by a collaboration between an LRL-Chemistry group and Simon Fraser University. In one of the experiments thin foils of metals are placed in the Bevatron external proton beam and the properties of collision fragments, especially new isotopes, are studied. This experiment is a continuation of a project of over five years duration during which a number of new isotopes have been discovered, including ^{11}Li, ^{14}B, ^{15}B, and ^{17}C. The other experiment also uses thin metal foils placed in the Bevatron EPB and studies α-emitting products in order to search for very short lived isotopes (half-lives of milliseconds to minutes). The apparatus has just been installed and data taking will begin soon.

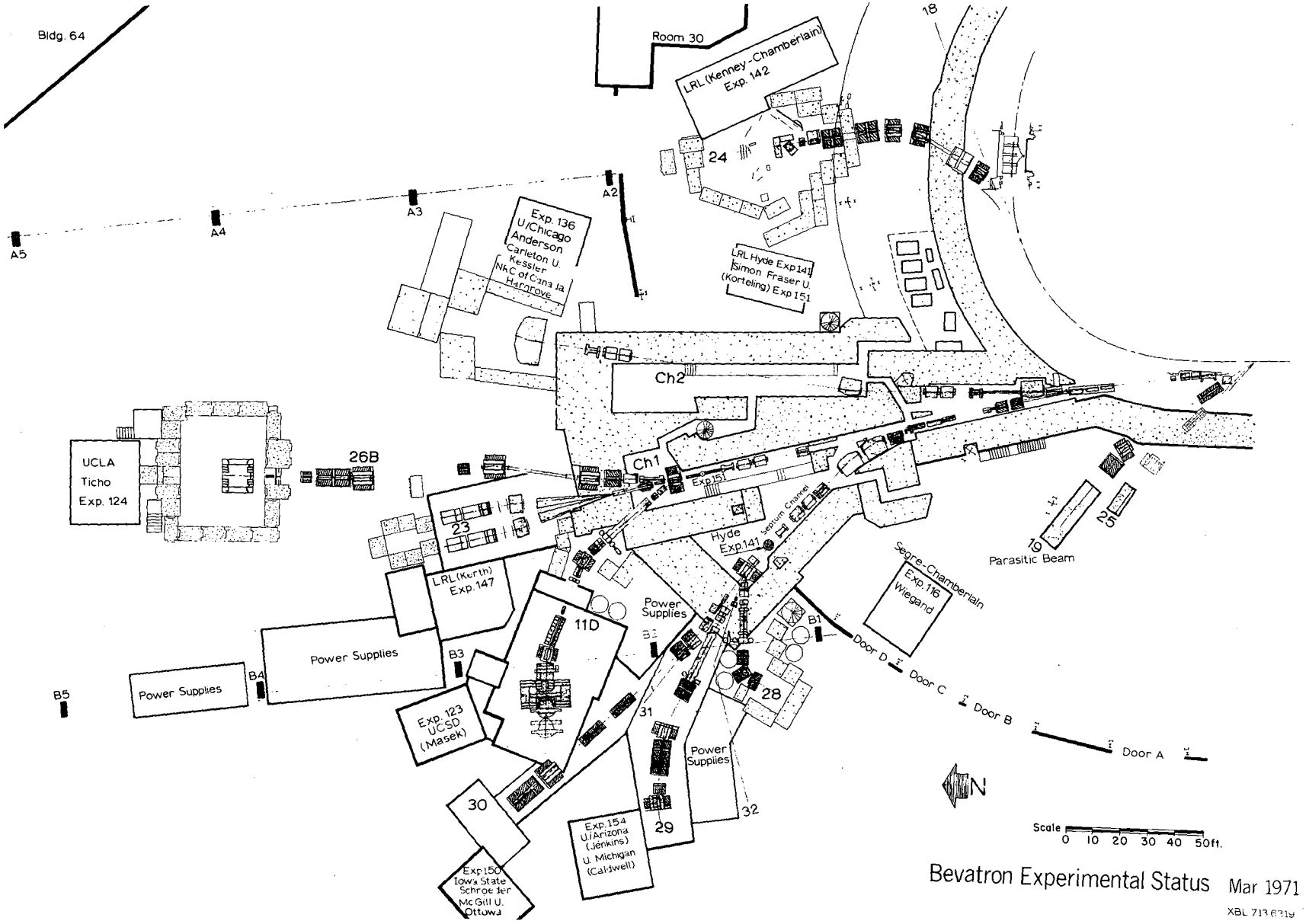
Bldg. 64
Room 30
LRL (Kenney-Chamberlain) Exp. 142
18
24
A2
A3
A4
A5
Exp. 136 U/Chicago Anderson Carleton U. Kessler NRC of Canada Harrower
LRL Hyde Exp 141 Simon Fraser U. (Korteling) Exp 151
Ch2
Ch1
Exp 151
UCLA Ticho Exp. 124
26B
23
Hyde Exp141
Septum Channel
Parasitic Beam
Segre-Chamberlain Exp. 116 Wiegand
LRL (Kerth) Exp. 147
Power Supplies
11D
B1
B2
B3
B4
B5
Door D
Door C
Door B
Door A
28
31
30
29
32
Exp. 123 UCSD (Masek)
Exp. 154 U/Arizona (Jenkins) U. Michigan (Caldwell)
Exp 150 Iowa State Schroeder McGill U. Ottowa
N
Scale 0 10 20 30 40 50ft.
Bevatron Experimental Status Mar 1971
XBL 713 6319

Fig. 1.

SUMMARY OF BEVATRON BEAMS

	Beam No.	Separated Beam	Momentum Range (GeV/c)	Type of Particles +	Type of Particles −	Type of Particles 0	**Flux @ 10^{12} protons	(%) $\Delta p/p$	(msr) $\Delta\Omega$	Prod. Angle
External Proton Beam		No	3–7	p	– –	– –	10^{12}	.05	< .1	– –
	11D	Yes	0–1.5	p K π	K π	– –	8×10^6 $\pi^{\pm}$ 5×10^4 K^+ @ 1.2 GeV/c 5×10^3 K^- @ 1.2 GeV/c	± 2	2.2	5°
	23	– –		– – –	– –	n K	1.2×10^6 K_L^o @ 50 feet from target		.9	4°
	26B	No	0–4	p K π	K π	– –	6×10^6 $\pi^{\pm}$ @ 2 GeV/c	± 3	1.0	2°
	28	Yes	0–.5	p K π	K π	– –	2200 K^+ stopped 200 K^- stopped	± 2	5.0	0°
	29	Yes	0–2	p K π	K π	– –	7×10^4 K^+ @ 1.5 GeV/c 7×10^3 K^- @ 1.5 GeV/c	± 3	1.3	0°
	30	No	0–5	p K π	K π	– –	8×10^6 $\pi^{\pm}$ @ 1–2 GeV/c 8×10^5 $\pi^{\pm}$ @ 4 GeV/c	± 4	1.0	2°
Internal Proton Beam										
	18	– –		– – –	– –	n K			0.5	0°
	19*	No	2–3	– – –	π	– –		± 4	~.5	0°
	24	No	1.5–2.5	– – –	K π	– –	3.3×10^6 π^- @ 2 GeV/c			

*Beam 19 is a TEST beam.

Fig. 2

** Some fluxes can be improved by increasing acceptance; however, the optical properties of the beams would then deteriorate.

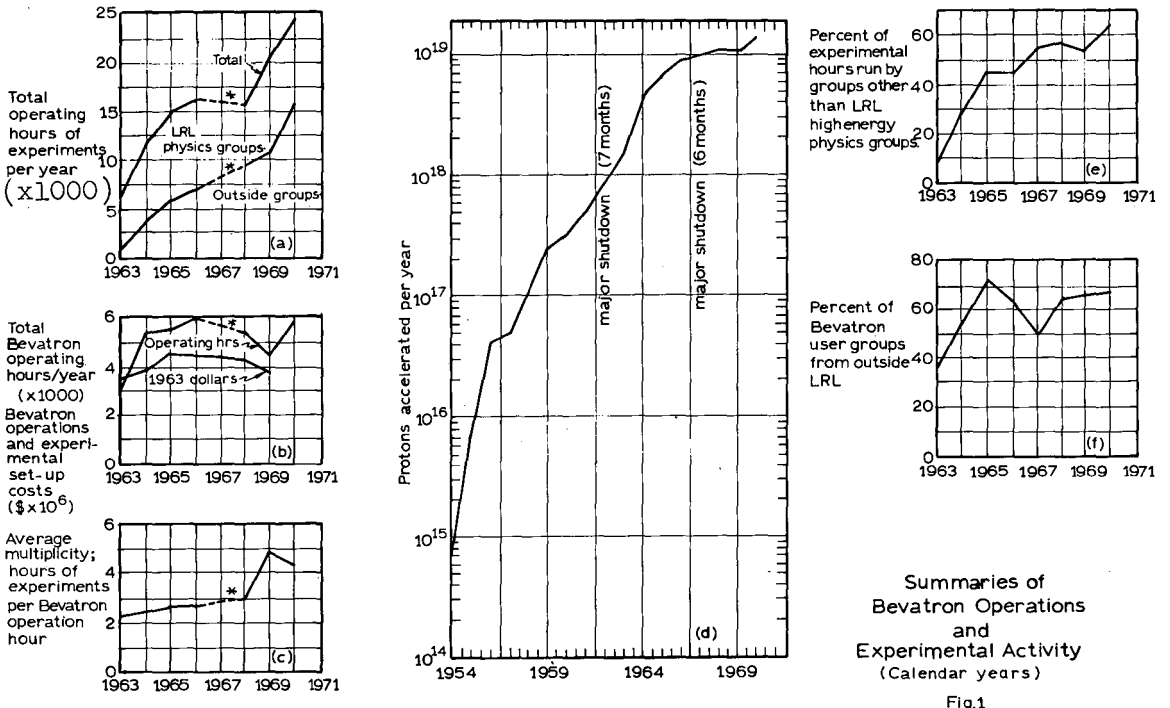

* Major Bevatron shutdown in 1967

Summaries of Bevatron Operations and Experimental Activity
(Calendar years)

Fig.1
B-05-15

XBL 711 6221

Fig. 3

CURRENTLY SCHEDULED BEVATRON EXPERIMENTS

EXP. NO.	GROUP (IN CHARGE)	SECONDARY BEAM CHARACTERISTICS	BEAM NO.	TITLE OF EXPERIMENTS	4/1/71 STATUS
		STRONG INTERACTION EXPERIMENTS			
150	Iowa State (Schroeder) St. Louis U. (Crabb) McGill U. (Ott)	1.3–2.5 GeV/c π^-	30	Backward $\pi^- p$ Elastic Scattering (31 momenta)	Setting-up
142	LRL (Chamberlain) LRL (Kenney)	.8–2 GeV/c π^-	24	Polarization $\pi^- p \rightarrow \pi^o n$ (3–4 momenta)	Setting-up
154	U. Arizona (Jenkins) U. Michigan (Caldwell)	0.6–1.4 GeV/c	29	K^+–Nucleon Total Cross-Sections (about 25–30 momenta)	Setting-up
136	U. Chicago (Anderson) Carleton U. (Kessler) NRC of Canada (Hargrove)	EPB 3–7 GeV/c Protons	CH–II	$pp \rightarrow d\pi$ (9 momenta)	Setting-up
152	UCR (Shen) UCLA (Ticho)	3.0 GeV/c π^-	26B	A_2^o Decay in Streamer Chamber	Accepted
		WEAK AND ELECTROMAGNETIC INTERACTIONS			
123	UCSD (Masek)	1.3 GeV/c π^+ and π^-	11D	Σ and Λ Leptonic Decays	Running
147	LRL (Kerth)	Neutral Beam	23	Muon Polarization in K_L^o ($\mu 3$)	Setting-up
124	UCLA (Ticho)	2.3 GeV/c π^-	26B	$X^o \rightarrow \pi^+ \pi^- \gamma$ in Streamer Chamber	Setting-up
145	LRL (Stiening)	0.5 GeV/c K^+	28	Search for $K^+ \rightarrow \mu^+ \nu \bar{\nu} \bar{\nu}$	Accepted
		OTHER EXPERIMENTS			
116	LRL (Wiegand)	0.5 GeV/c K^-	28	K^-–Mesic X-rays	Running
141	LRL–Chemistry (Hyde) Simon Fraser U. (Korteling)	EPB – CH I	F3A	Light Fragments Ejected from Complex Nuclei	Running
151	LRL–Chemistry (Hyde) Simon Fraser U. (Korteling)	EPB	F3D	Spallation, Fission and Fragmentation from Heavy Nuclei	Running

Fig. 4

Discussion

Ringland (RHEL): You talked about a K^+ beam, however, some weak interaction physicists feel that perhaps a K^0 beam would be more interesting. What are the possibilities of doing weak interaction K^0 experiments on the Bevatron.

Wenzel (LRL): A large part of the Bevatron program is weak interaction physics, at least one-half. Although much has been done on K decay, one limitation on doing K^0 experiments is the lack of suitable RF structure. We plan to improve this situation in the future. We have not discussed this research here because we feel that this conference should emphasize strong interactions.

Quigg (Stony Brook): Are you going to fill in any of the gaps left in Manning's slide. (See page 28)

Steiner (LRL): We plan to do πN charge exchange polarization at 1080, 1280, and 1580 MeV/c.

Lovelace (Rutgers): Are these the energies at which accurate $\pi^+ p$ elastic polarization has already been measured?

Steiner (LRL): These are energies where excellent data exist in all other channels.

Wenzel (LRL): The external beam at the Bevatron is very flexible because the magnets are designed to track the accelerator. That is, the beam can be put out at any energy from two up to six GeV. You don't have to turn off the rest of the program. This is obviously valuable for the systematic study of reactions with s-channel dependence. If it turns out that protons can't be

accelerated and maintain their polarization, there is the possibility of using deuterons which would depolarize less because of the small anomalous moment. Then you can strip the deuteron and get a reasonably good polarized proton beam.

INTERMEDIATE ENERGY PROGRAM AT THE AGS
(Less than 8 GeV)

David Berley

BROOKHAVEN NATIONAL LABORATORY

INTERMEDIATE ENERGY PROGRAM AT THE AGS*
(Less than 8 GeV)

David Berley
Brookhaven National Laboratory
Upton, L.I., N.Y.

The AGS is a 33 GeV proton synchrotron which is presently undergoing an improvement program. At the end of the improvement program about a year or a year and a half from now the accelerator should produce a proton intensity of 10^{13} protons per pulse. The maximum duty cycle of the beam will be about 50%, the repetition period between one and two seconds depending upon the duty cycle.

The AGS complex is shown schematically in the first slide. The experimental program centers around a number of target stations. There are three target stations available for the bubble chamber program, two of them external and one of them internal.

The counter spark chamber program centers around one internal target station and two external target stations. Either of the external stations can be operated simultaneously with the internal target. We are in the process of building up a third target station shown at B. There are on the AGS floor about ten operating electronic experiments from seven charged particle beams coming from the sources shown in the slide.

The experimental facilities available for counter spark chamber experiments are summarized in Table I. There is one purified beam now in operation and the second one under construction. Together

*Work performed under the auspices of the U.S. Atomic Energy Commission

they provide fluxes of particles from rest up to 2.5 GeV/c. Typical intensities at 1 GeV/c are 3×10^5 particles per AGS cycle and at 2 GeV/c 30,000 K^+ particles per AGS cycle. The intensities of kaons and antiprotons are summarized in Figs. 2 and 3.

There are two neutral beams, one of which has a momentum spectrum which extends from 1 to 4 GeV/c, the other from 3 to 10 GeV/c.

In addition to the separated and neutral beams there are also some high precision unseparated beams at the AGS which may be of interest at this conference. There is a small angle charged beam which produces between 10^6 and 10^7 pions per sec., and the second of these is soon to be constructed.

There are other beams which utilize the high energy aspects of the AGS. There is a hyperon beam, a muon beam and a diffracted proton beam.

The particles available to bubble chambers are summarized in Table II. During the next running period we shall have two chambers available for physics experiments. One is in a slow K beam that has a maximum momentum of 1 GeV/c and can be used for stopping particle experiments in the BNL 30-in. bubble chamber. The 80-in. bubble chamber will be able to do experiments with pions, kaons, protons and antiprotons from 3 GeV up to the maxima shown in the table.

The additions to the AGS program which are contemplated now are separated beams for counter/spark chamber experiments which will

cover the entire range available at the AGS from stopping particles to 20 GeV/c kaons and π^+. Table I summarizes what is foreseen in the way of separated beams at the AGS in the future. In Fig. 2 the kaon fluxes are indicated (the solid lines are for K^+; the dashed lines are for K^-) and in Fig. 3 the antiproton fluxes are indicated. The idea is to have separated beams which cover the complete spectrum available at the AGS, the lower energy ones now in operation.

A summary of the AGS experimental program in the intermediate energy region will now be summarized. This accounts for about half of the entire program. Some of the experiments are listed in Table III and a brief description of them is given below.

1. A very precise set of total cross section measurements have already been done in an existing separated beam. These will be continued and extended down to lower energy.

2. There have been a series of experiments with antiproton annihilations. One of these is an experiment designed to study antiproton charge exchange, both forward and backward to uncover new resonances and try to understand the exchange processes responsible for the backward charge exchange. Now being set up is an experiment to study the annihilation of antiprotons in hydrogen into neutral bosons $\pi^o\pi^o$, $\pi^o\eta^o$, $\pi^o\rho^o$, etc. It turns out that the neutral boson decay modes are useful for determining quantum numbers of resonant states. There is a third antiproton annihilation experiment in which two or more

charged particles at large angle will be detected in order to measure the cross section for processes involving large momentum transfer.

3. Considerable work has already been done by a Yale group to do a phase shift analysis on Kp Scattering. They are continuing their measurements at lower energy on the scattering of K^+, K^- and $\bar{p}$'s, on polarized protons.

4. A number of experiments are in the process of being done or recently been completed to study quasi two-body reactions. Examples of these are π^- or K^- on protons to yield negative bosons and protons. The B minus could be an A meson, R, S etc. A second experiment on two body reactions is a double-V spectrometer. Here pions on protons can give two V's which are an $N^*\rho$ or a K^oA^o. These are in the process of being analyzed.

5. A three-arm spectrometer from the BNL Collins group is now being set up looking at multiparticle processes. These processes correspond to a diagram in which two fast protons emerge and from a pionization bubble come a splash of pions all of which are detected and kinematically reconstructed. Soon the spectrometer will be in a pion beam and reactions like $\pi^+p \rightarrow \pi^+p +$ many π^- pions will be possible to study.

6. There is a large program at the AGS to study the weak decays of kaons and hyperons. In the neutral kaon beams we have had a series of three experiments in quick succession to measure the leptonic charge asymmetry in Ke_3 decay.

Other experiments with neutral kaons measure the decay parameters η_{+-}, η_{oo}. There are others to study the regeneration of K_L into K_S by electrons, K_L to lepton pairs and K_L to K_S regeneration amplitudes in hydrogen and deuterium. The latter experiment uses the weak interactions to learn something about the strong interactions.

K decays in flight have produced a number of AGS experiments. Most recent ones ar the K^{+-} decay into $\pi\pi\gamma$. A comparison of the Dalitz plots for the two kaon charges will yield information about CP conservation in this decay mode. Another charged kaon decay experiment is the K_{e4} experiment. Here several thousand K^+ and K^- decays into these two modes will yield some information about the $\pi\pi$ phase shifts. A comparison of the K^+ and the K^- decay also yields information on the CP violation in these decays.

There are two experiments to study the decay of hyperons. In one the hyperon source is from stopped K^- in hydrogen and in the second the source of negative hyperons is a target bombarded with a high proton intensity. A beam of hyperons is extracted and 6 meters from the production target is a decay region which is viewed by a pair of spectrometers. The purpose of both of these experiments is to measure the Gv/Ga ratio in Σ^- decay. The hyperon beam is also capable of studying other hyperons like Ξ^- and Ω^-.

It is planned to have a large aperture spectrometer which will be set up in the two higher energy separated beams. In this facility physics with kaons and antiprotons as well as pions and protons will be done from 3 GeV/c to the maximum available at the accelerator.

Table Captions

Table I Summary of AGS beams used for counter spark chamber experiments.

Table II Summary of AGS beams used for bubble chamber experiments.

Table III Overview of AGS experimental program at intermediate energies.

TABLE I

Separated Beams K^+ K^- $\bar{p}$		
$1.3 < p < 2.6$	Operating	dc separators
$0 < p < 1.2$	1971	dc separators
$1.5 < p < (5 - 8)$	1973	dc or rf
$5 < p < 20$	$\geq$ 1974	rf superconducting
Neutral Beams K_L^o		
$1 < p < 4$	Operating	1.6×10^5 K_L/GeV/c/pulse
$3 < p < 10$	"	5×10^5
Unseparated Beams		
$5 < p < 28$	Operating	
$5 < p < 28$	1972	
diffracted proton beam	Operating	
$2 < p < 17.5$	Test	
Special Beams		
$p < 9$	Operating	$\sim 10^7$ μ^+/pulse
$p \cong 25$	"	$\sim$ 300 Σ^-/pulse

TABLE II

	Pmin Pmax (GeV/c)			
	30-in. Bubble Chamber	31-in. Bubble Chamber	80-in. Bubble Chamber	7-ft Bubble Chamber
π	0.4 - 1.1	0.5 - 4.0	3 - 25	- 11
K	0 - 0.9	1.7 - 3.0	3.5- 15	
p	0 - 1.1	0.5 - 4.0	3 - 29	
$\bar{p}$	0 - 1.1	1.0 - 4.0	3 - 18	
D			20 - 29	
		O F F in April 71		1972 ν- beam

TABLE III

OVERVIEW OF THE EXPERIMENTAL PROGRAM AT INTERMEDIATE ENERGIES

1. Total cross section			
$K^{\pm}\begin{pmatrix} p \\ N \end{pmatrix}$	$1 < p < 2.5$	complete	BNL
$\bar{p}\begin{pmatrix} p \\ N \end{pmatrix}$	$.5 < p < 1.1$	planned	BNL
2. Antiproton annihilations			
$\bar{p}p \rightarrow \bar{N}N$, $N\bar{N}$	$.6 < p < 2.5$		Stony Brook/Wisconsin
$\bar{p}p \rightarrow$ neutral bosons			
$\pi^o\pi^o$, $\pi^o\eta^o$, $\pi^o\rho^o$, $\pi^o f^o$ etc.	$.4 < p < 2$		MIT/Brown/Bari
$\bar{p}p \rightarrow$ more than two charged particles, large momentum transfer	$.6 < p < 2.5$		Rutgers
Bubble Chamber Experiments			
3. Phase Shift Analysis			
$K^+p_{\phi} \rightarrow K^+p$	$1.2 < p < 2.3$	complete	Yale
$K^-p_{\phi} \rightarrow K^-p$	$0.7 < p < 1.2$	planned	Yale
$\bar{p}p_{\phi} \rightarrow \bar{p}p\pi^+\pi^-$			
4. Quasi two body reactions			
$\pi^{\pm}, K^{\pm}\ p \rightarrow p\ B^{\pm}$	$5 < p < 20$		NE/Stony Brook
$\pi^{\pm}, K^{\pm}\ p \rightarrow p\ A_2^-$, $N^*\rho$, $K^o\Lambda^o$, V V	$p = 20$ 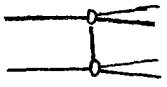		BNL
5. Multiparticle processes			
$pp \rightarrow pp +$ up to 6 charged pions	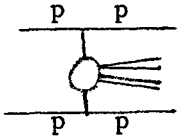		BNL
$\pi p \rightarrow \pi p +$ many pions			

TABLE III (Cont'd)

6. Weak decays of kaons and hyperons

$K_L^o \to 2\pi$ $\eta_{\pm}$ η_{oo}		Princeton(Cronin) Princeton(Fitch) Columbia(Steinberger)
$K_L \to \ell\ \nu\ \pi^{\mp}$		Columbia
$K_L \to \mu^+ \mu^-,\ e^+e^-$	Proposed	Columbia
$K^{\pm} \to e^{\pm} \nu\ \pi^+\pi^-$		Pennsylvania
$K^{\pm} \to \pi^{\pm}\pi^o\gamma$		BNL
$K_L^o\ p \to K^+\ \Xi^o$, $\Xi^o \to \Lambda^o\ \pi^o$	Proposed	Carnegie Mellon
$\Sigma^- \to e^-\ \nu\ N$ Ξ^- Ω^-		Princeton Yale

7. K^-, $\bar{p}$ atomic x rays — VARC; Yale/Columbia

Figure Captions

Figure 1. Layout of AGS Complex

Figure 2. Kaon fluxes at existing and proposed separated beams. The beam labeled 5 is in operation, Z is under construction and the others are in the planning stage. The top abscissa is the Kp invariant mass and the right ordinate scale is the number of events per microbarn foot produced in liquid hydrogen per second.

Figure 3. Antiproton fluxes at existing and proposed separated beams. Beam 5 exists and Z is under construction. The upper abscissa scale is the $\bar{p}$ p invariant mass and the right ordinate scale is the number of events per microbarn foot per second.

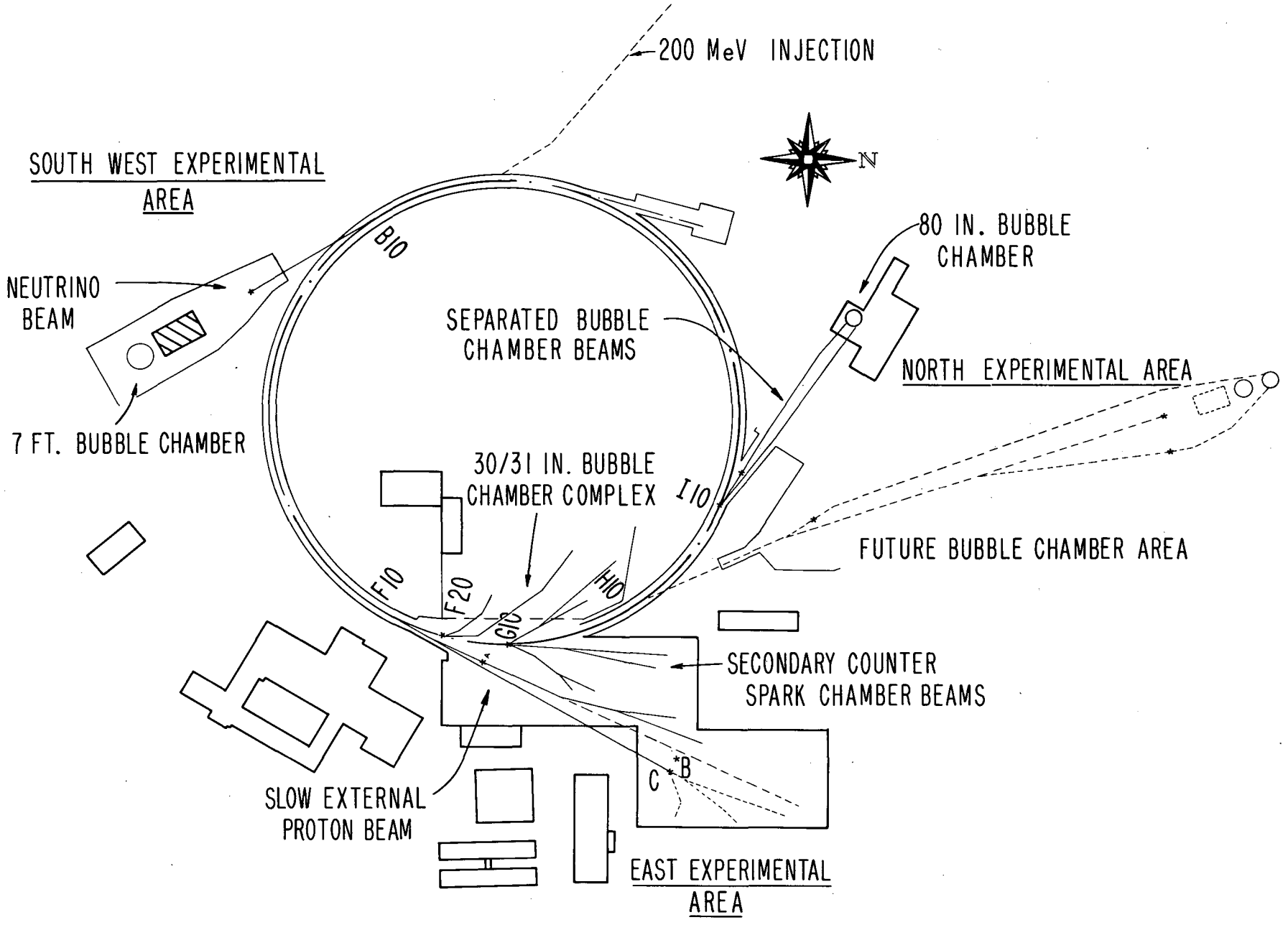
200 MeV INJECTION
N
SOUTH WEST EXPERIMENTAL AREA
B10
80 IN. BUBBLE CHAMBER
NEUTRINO BEAM
SEPARATED BUBBLE CHAMBER BEAMS
NORTH EXPERIMENTAL AREA
7 FT. BUBBLE CHAMBER
30/31 IN. BUBBLE CHAMBER COMPLEX
I10
FUTURE BUBBLE CHAMBER AREA
F10
F20
H10
G10
SECONDARY COUNTER SPARK CHAMBER BEAMS
B
C
SLOW EXTERNAL PROTON BEAM
EAST EXPERIMENTAL AREA

Fig. 1.

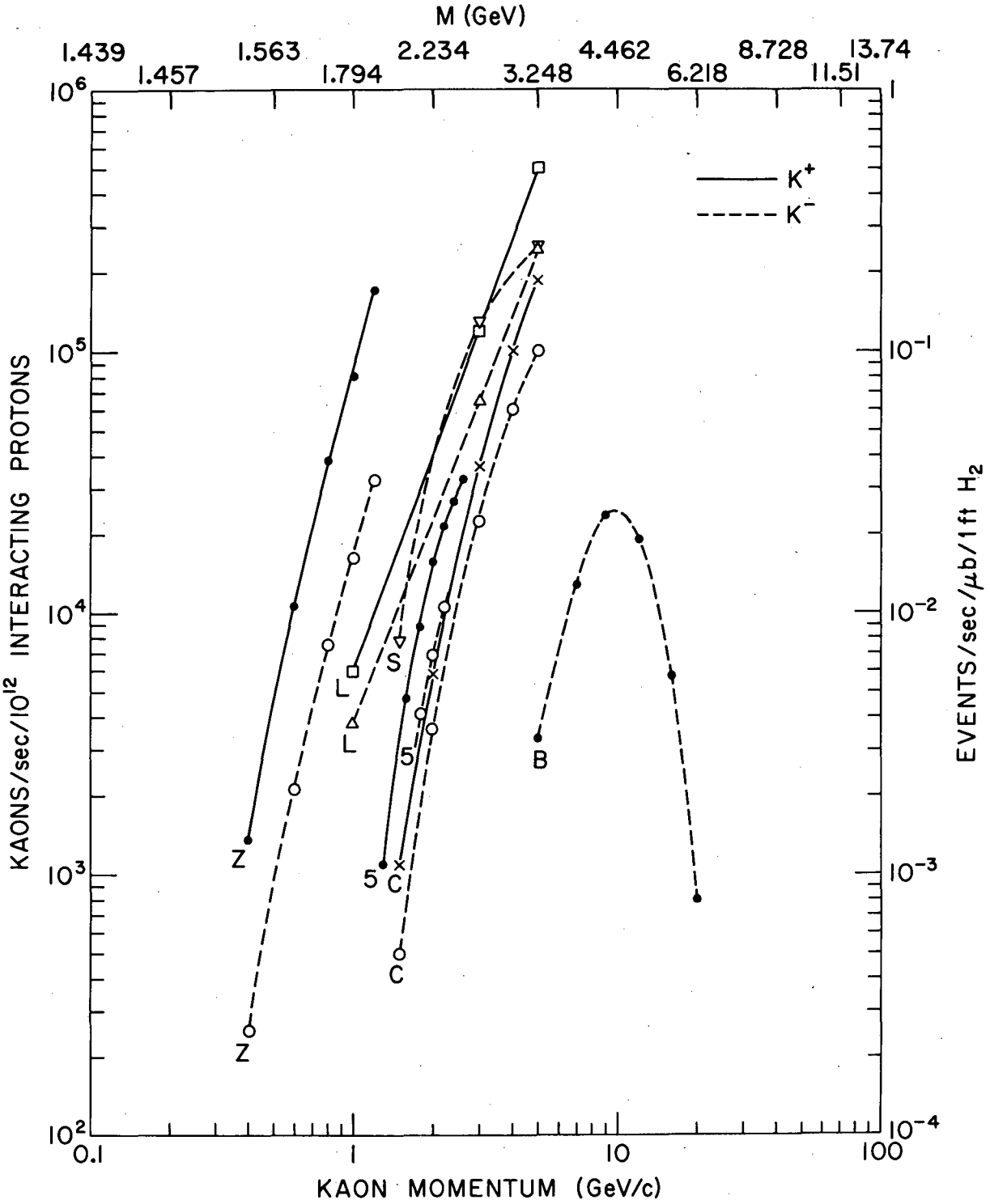
M (GeV)
1.439
1.457
1.563
1.794
2.234
3.248
4.462
6.218
8.728
11.51
13.74
10^6
10^5
10^4
10^3
10^2
1
10^{-1}
10^{-2}
10^{-3}
10^{-4}
0.1
1
10
100
K^+
K^-
KAONS/sec/10^{12} INTERACTING PROTONS
EVENTS/sec/μb/1 ft H_2
KAON MOMENTUM (GeV/c)
Z
Z
L
L
S
5
5
C
C
B

Fig. 2.

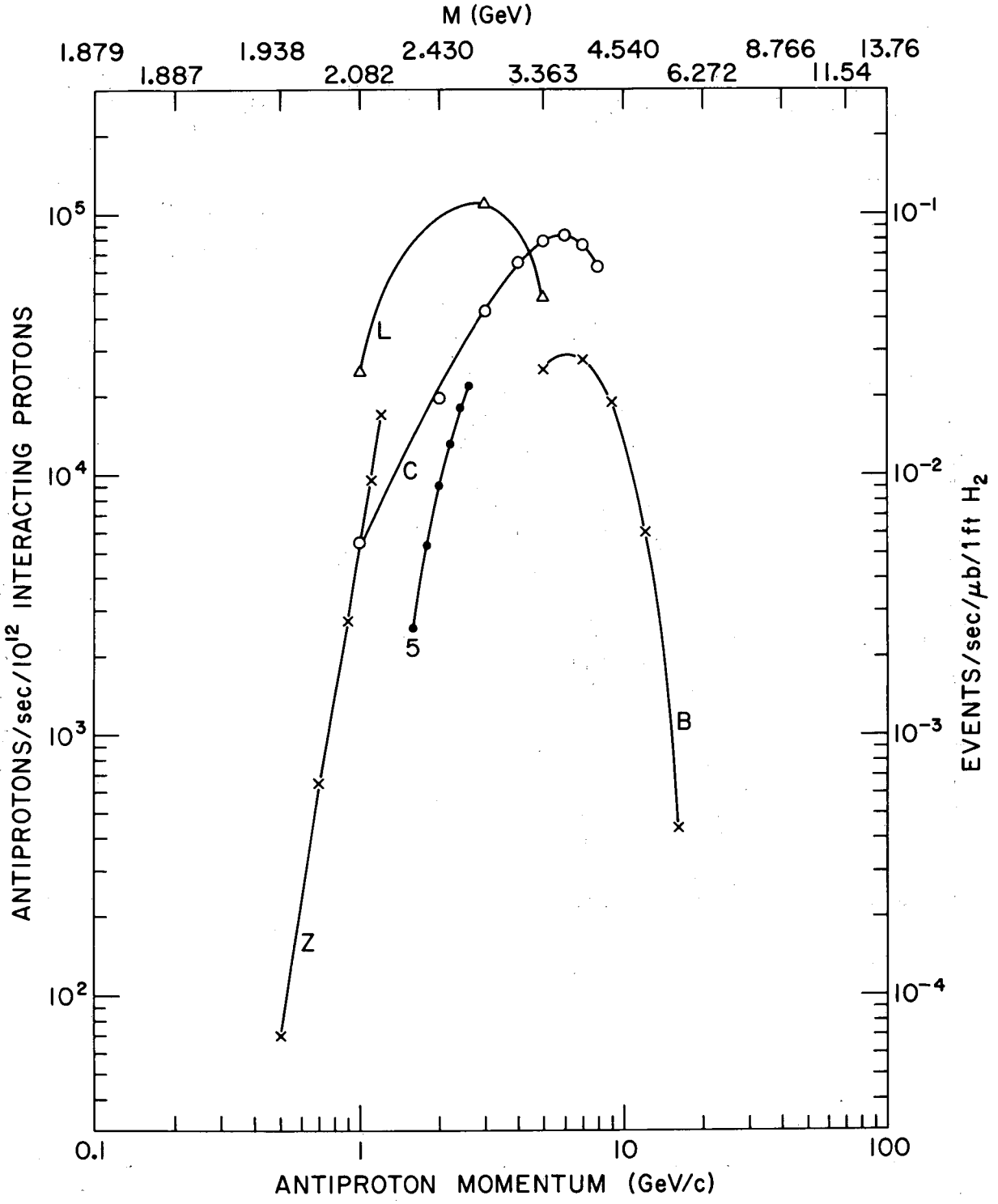
M (GeV)
1.879
1.887
1.938
2.082
2.430
3.363
4.540
6.272
8.766
11.54
13.76
ANTIPROTONS/sec/10^12 INTERACTING PROTONS
EVENTS/sec/μb/1ft H2
ANTIPROTON MOMENTUM (GeV/c)
L
C
5
Z
B
0.1
1
10
100

Fig. 3.

Discussion

Berger (Argonne): What is the liquid in the 30 in. chamber?

Berley (BNL): Hydrogen-deuterium or hydrogen-neon mixtures.

Lovelace (Rutgers): I have a comment on the low energy K^-p polarization. As far as I can find, the lowest K^-p elastic polarization experiment with decent statistics is the CERN-Holland measurement at 980 MeV/c and this is just below an F5 resonance. So you are already in a region where F waves are important. The reason why πp and K^+p phase shift analyses were successful was that you could start from the lowest energy, where there is essentially only one partial wave contributing, and work up continuously. In K^-p this is not possible, because there are no polarizations measured at energies where one partial wave dominates (nor even 2 or 3). Polarizations in the inelastic channels $\pi\Lambda$ and $\pi\Sigma$ help a little bit, but are really no substitute for elastic polarization. This is because in $K^-p \to \pi\Lambda$ or $\pi\Sigma$ you have an overall phase ambiguity which you can never resolve. In elastic channels you can resolve it by the optical theorem. It seems to me that one is never really going to put the Y^*'s on the same footing as the N^*'s until the K^-p elastic polarizations are taken down to at most 500 MeV/c. The experimental difficulty is that the beam intensities die as you go down in energy, and so there is not enough flux to get reasonable running time. I think it is very important for anyone who has high intensity low-energy K^- beams to do these polarized target experiments.

This applies also to $\bar{p}p \rightarrow \bar{p}p$, etc. At rest it is pure S wave, but by the time you see it in flight at several hundred MeV/c it is already diffractive. The high partial waves come in very rapidly in $\bar{P}P$. Obviously for looking at high mass mesons, it would be interesting to do a phase shift analysis on $\bar{p}p$ some day. It would be necessary, however, to bring the annihilations in flight much closer to the annihilations at rest, if one is ever to do this.

Lovelace (Rutgers): Who is going to have the best low energy K^- beam?

Berley (BNL): I think we are.

Lovelace (Rutgers): Then you certainly should emphasize K^-p polarized target experiments.

Berley (BNL): This experiment is coming up.

Moravcsik (Oregon) I have a general question. The usual argument against intermediate energy machines is that high energy machines can do anything an intermediate energy machine can do. What can we say in defense of intermediate energy machines?

Lovelace (Rutgers): Look at it historically. How many experiments used in phase shift analysis came from high energy machines?

Moravcsik (Oregon): True. High energy machines are geneally used at high energy and not much time is allotted to intermediate energy work. But is it true as far as technology is concerned that anything that can be done at intermediate energy machines can also be done on the AGS?

Berley (BNL): Yes.

Manning (RHEL): One point that is relevant is that if you are going to do a systematic survey you have to sit on the floor for several thousand hours. In practice it is not possible to get on at the PS or AGS for this length of time.

Wenzel (LRL): I think it is a question of economics. The higher energy machines cost more to build, improve, and operate, and you expect them to concentrate on the higher energies. The study of the intermediate energy region can be done more cheaply at an intermediate energy machine. Proton induced interactions cannot be studied systematically near transition energy and shielding is more expensive for the higher energy machines.

Galtieri (LRL): There seems to be duplication at the various labs in the various experiments they are doing. Can I learn about what experiments are running or going to be running by asking for the proposals that have been approved? Better communication between the laboratories at this level would certainly reduce duplication of effort.

Berley (BNL): The proposals at Brookhaven are open for inspection.

Lovelace (Rutgers): The theorists say to the experimenters "do this experiment." Nothing happens. The next year they shout "do this experiment." The next year they scream "do this experiment." Then suddenly five people do it simultaneously!

Manning (RHEL): At Nimrod the proposals are certainly available.

Rosenfeld (LRL): I want to ask everyone a question. Would it be useful to produce a compilation of the experiments going on at the various laboratories as well as the proposals for the following year?

Audience: Yes!!!

[Editors Note: As a result of this response, a meeting was held to discuss the scope of such a compilation, and the Particle Data Group agreed to undertake it. Work is underway.]

CERN Programme

F. Muller, LRL and CERN

This review is intended to give a general idea of the experimental facilities and of the evolution of the physics programme. It does not pretend to completeness nor to accuracy of detail and should not be quoted as a source of information.

1. General Description

The existing and future main features of CERN are displayed on fig. 1. This figure does not show the recently decided upon European 300 GeV, which would lie at the top of this drawing, i. e. in the North of the present site. The dotted line across the site is the French-Swiss boundary.

a. PS operation

Peak energy	28 GeV
Intensity	2×10^{12} protons/pulse in 20 bunches
Working schedule	2 weeks out of 3, 1 month or longer shutdown each year.
Typical cycles	2 sec at 19.2 GeV, 600 m sec flat top 2 sec at 24 GeV, 440 m sec flat top (above 24 GeV, the cycle time increases more rapidly, due to necessity of supplementary cooling time between pulses)

b. Hall, targets and external beams

They are schematized on figure 2.

The North and South Hall existed at the beginning of PS operation. Their beams come from 3 internal targets, two (1 and 8) for counter experiments in the South Hall, one (6) used up to now in the RBE (rapid beam extraction)

mode to feed the 81 cm Saclay HBC.

The East Hall, built later, is equipped with two ejected beams, a fast extracted one (FE58) for the 2 m CERN-HBC, and a slow extracted one (SE62) for counter experiments.

The Last Hall to have come in use is the South-East Hall for the 1.2 m CERN-HLBC, now replaced by Gargamelle, and fed by a fast extracted beam (FE74).

Recently a new extracted beam (FE16) has come into use for feeding the Intersecting Storage Rings (ISR).

Beam-sharing is the normal operating mode. Typically, 10% of the beam can be taken on the rise of the PS pulse for the 81 cm HBC, then a few bunches are extracted for each expansion of Gargamelle (one per pulse) and the 2 m HBC (usually 2 per pulse, at the beginning of the flat-top, using a total time of 150 msec) and then either the slow extraction (East Hall) or the internal targets (South Hall) can operate for the rest of the flat-top. Sharing is not possible between these two last operations (when East Hall operates, 1% of the beam can be used, on the rise of the PS pulse, to test equipment in South Hall).

Fig. 2 (not on scale) illustrates these possibilities.

c. Beams

The beams (and experiments) presently installed in the South, North and East Halls are shown in Figs. 3 and 4. The beams used for experiments in the South Hall are:

(1) Three medium energy unseparated beams (m_{11}, q_{10}, m_g). Typical intensities are about 10^6 π^+ in q_{10} at 2.5 GeV/c and 8×10^5 π^+

in m_{11} at 5 GeV. In both cases with 10^{12} incident protons at 24 GeV, and ± 2% momentum bite.

(2) A medium energy beam, partially separated by an electrostatic cavity, m_7, giving for instance 10^5 K^+ (1 K^+ for $6\pi^+$) at 2.2 GeV/c ± 2%, with 10^{12} protons at 19 GeV.

(3) A high energy beam, d_{29}, giving 2×10^6 π^- at 16 GeV ± 0.75%, with 10^{12} protons at 24 GeV.

In the East Hall, the slow extracted beam is subdivided in three by two septums and several secondary beams are taken from the three targets:

(1) Two neutral beams, b_{17} and b_{19}.

(2) Two high energy beams, P_4 and P_5, giving $2\text{-}3 \times 10^6$ π^- between 6 and 10 GeV/c, for a momentum bite of ± 1%, on about 2×2 cm^2 targets, all that with 10^{12} protons at 24 GeV. At maximum energy (16-18 GeV), there are still about $.5 \times 10^6 \pi^-$.

(3) Two special purpose beams: a short slow $K^\pm$ beam k_{12} providing stopped kaons, and a short beam, with supraconducting quadrupoles, S103, in which it is hoped to obtain 1000 Σ^- hyperons for 10^{12} incident protons.

The bubble chamber beams are:

(1) For the 81 cm HBC, a low-energy separated beam, k_{13} (.6-.8 GeV/c for $K^\pm$)

(2) For the 2 m HBC, a low energy beam k_8 (1-2 GeV/c), a medium energy beam m_6 (from 2 to 4.6 GeV/c $K^\pm$) an R. F. separated high energy beam U_6 (5.5, 8.25, 10, 14.3 and 16 GeV/c $K^\pm$, up to 16 GeV π^+ and 24 GeV protons).

(3) For Gargamelle, a neutrino beam. Proton and pion beams are foreseen.

d. Future improvements

The extracted beam from FE 16 which feeds the ISR can also go into a new

Hall on the western end of the site (West Hall). This Hall will contain the 3.70 m HBC and the Omega set-up (to be described later), to be operative respectively beginning and middle of 1972, as well as a new g-2 experiment, scheduled for 1973. Later (76?) an extracted beam from the recently decided "300 GeV" European accelerator will go into this West Hall.

Also in construction is a Booster, which will inject protons into the PS at 800 MeV, instead of the 50 MeV of the present linac, allowing to raise the circulating beam intensity to 10^{13} protons. This booster was originally scheduled for 1973.

2. Bubble Chambers

Bubble chamber operations in the past three years are summarized in table 1:

a. Hydrogen Chambers

Rather than giving a complete list of various exposures, these have been grouped in domains of energy, corresponding for the 2 m chamber to its three beams (the 81 cm was, for all that time, low energy < 1.3 GeV/c). Incident particles are listed in order of frequency of use. The period of three years was chosen so as to average out the fluctuations due to scheduling practice of the 2 m chamber, which runs usually for a period of about 6 months in a given beam (also, deuterium operation is blocked in rather long, hence infrequent, periods).

(i) The 81 cm chamber will be definitely stopped this spring. Since 1966, it has been devoted to low energy experiments of which the numerically most important have been:

(1) $\bar{p}p$ at 0, .7 and 1.2 GeV/c (10^6 pictures, CERN College de France): boson resonances

(2) $\bar{p}d$ at 0 and .7 GeV. (Padua-Roma-College de France)

(3) K^-p (some D^2) from .4 to 1.3 GeV/c (1.4×10^6 pictures, CERN-Heidelberg - Saclay): strange baryon resonances by phase-shift analysis.

(4) K^-p stopped (Heidelberg, 1.5×10^6 pictures): hyperon decays.

It now finishes to take two series, each of 1.5×10^6 pictures: $\bar{p}$ at .7 GeV/c and K^- in H^2 and D^2 between .6 and .8 GeV/c.

(ii) The 2m chambers program has had a heavy emphasis on high energy (i. e., $p > 8$ GeV/c). From the proposals, there is no great marked change, except possibly a greater interest in medium energies and deuterium, and a definite decrease of interest for low energy. The total lack of proton experiments, except a few at high energies, should be noted, as well as the lack, up to now, of low-energy π experiments and the low present interest in antiprotons.

Recent experiments, with at least $.3 \times 10^6$ pictures (an asterisk denotes more than $.6 \times 10^6$ pictures) are:

	p GeV/c	Hydrogen	
K^-	.8 - 1.4		Rutherford
K^-	1.4 - 1.8		CERN-Heidelberg
K^+	1.2 - 1.7*		CERN-Saclay ($\Delta S/\Delta Q$)
$\bar{p}$	1.5 - 2		Glasgow-IPN Paris-Lausanne-Liverpool-Neuchatel
K^-	2. 2. 8		Saclay-College de France
K^-	3. 3, 3. 6; 3. 9; 4. 2		Oxford; Amsterdam-Nijmegen Ecole Polytechnique-Saclay
π^-	3.9		CERN-Saclay
K^-	10*		ABCHLV
K^-	14.3*		Ecole Polytechnique-Rutherford-Saclay
K^+	16*		Birmingham-Bruxelles-CERN IPN Paris-Saclay
π^+	16		ABBCHKW
p	12-24		Bonn-Hamburg-Munich
p	19		Copenhagen-Helsinki-Oslo Stockholm
		Deuterium	
K^-	1.2 - 1.8		Birmingham
π^+	4		Birmingham-Durham-Rutherford
K^+	5.45		Oxford
K^+	8.25		Brussels, IPN Paris, Saclay
π^-	9		Bari, Bologna, Florence, IPN Paris

Proposals include, besides continuation of some of above experiments:

H_2		p(GeV/c)		
Low	$\pi^{\pm}$	1-1.8	(Saclay)	1.2×10^6 pictures
Medium	K^-	4.6	(Pisa)	1.0×10^6
High	K^-	16	(ABCHLV)	$.3\times10^6$
	π^+	9-11	Bologna, Florence Genoa, Milan	$.5\times10^6$
	π^+	16	Aachen, Bonn, CERN Warsaw	$.4\times10^6$
D_2				
Low	K^-	.94	Munich	$.35\times10^6$
Medium	$\bar{p}$	3	Padua, Rome, Scandinavian Collaboration	$.6\times10^6$
High	K^-	8.25	Bologna, Messina	$.3\times10^6$
	π^-	9-11	Bologna, Florence Genoa, Milan	$.5\times10^6$

(iii) Hydorgen (and deuterium) physics

Few of the experiments listed above have yet given results; this is due to the inherent time delay for measurements, etc., still much longer in Europe than in the U. S., and also to the widespread collaborations, which are like Esope's tongue.

Glamorous results, obtained quite a while ago in low energy $\bar{p}$ and K^- have been quoted. The high energy domain is very promising but still mostly in the exploratory stage. Quid of the medium energies, which have been slightly in the dark in the recent years? Actually one should not forget that, as early as 1963, they have provided the first quantitative

checks of peripheral production (K^* production in $K^\pm$ at 3 GeV/c; ρ production in $\pi^\pm$ at 4 GeV/c, pole extrapolation in π^- at 2.7 GeV/c.)

As of today, it seems that medium energy reactions are analyzed more easily in terms of t-channel than s-channel, and they have, over higher energies, the advantage of much bigger cross-sections for quasi-two body processes, not to speak of better resolution, less ambiguities, etc., which might more than compensate for higher background.

An interesting recent development is the investigation of very small angle scattering at the beginning of the region of Coulomb interference (in K^- at 4.2 GeV/c and K^+ at 5 GeV/c by Amsterdam, Nijmegen, and now in 10 GeV/c K^- at CERN through the FSD). More generally a few experiments (10 GeV/c K^-, 3-3.5-5 GeV/c K^+, 2.7 GeV/c π^-) have shown that elastic angular distributions of high quality, in the low t-region (and even in the intermediate region), can be obtained from bubble chambers.

(iv) Heavy liquid chambers

The CERN 1.2 meter Heavy Liquid Chamber has finished its career in 1970 by taking mainly pictures for strong interaction physics (~ 1 GeV/c K^- for investigation of baryon resonances, and 3.5 GeV π^+ for detection of the $\pi^0\pi^0$ system). It is now replaced by Gargamella, a chamber built at Saclay. This has 4.8 m length, 1.9 m diameter, 20 Kgauss field and is seen by 2 longitudinal rows of 4 cameras. With a mixture of 90% propane, 10% CF_3Br, the radiation length is 60 cm, 25% of the events are on free hydrogen, and the average measuring accuracy is ±3% for charged particles, ±10% for photons.

The chamber has been tested recently and should start soon on a programme of 10^6 neutrino pictures, 25 GeV protons, and 2 GeV π^+ (for investigation of the $\gamma\gamma$ and $\pi\pi\gamma$ decay modes of the η' meson).

v) Chambers to come

BEBC (Big European Bubble Chamber) is being installed in the West Hall. Its main characteristics are given in Table I, its programme is not yet fixed. Besides physics experiments, there will be trials of various means for detecting the photons: plates or neon-hydrogen mixture around a hydrogen target. The prospect of using BEBC with the future European accelerator should certainly influence this programme.

Finally, a special purpose chamber, HYBUC (Hyperon Bubble Chamber) built at Munich, is being tested now at CERN. It has a field of 10 Kgauss parallel to the axis of the chamber, which is 32 cm long and 13 cm in diameter. It purposes to measure the magnetic moment of hyperons.

3. Counter Physics

a) Experimental programme

Statistics on that subject are harder to establish than in bubble chamber physics, where the number of pictures (or of events per microbarn) provides a unit of about the same quality as the r. e. m for the effect of radiation. Here the unit could be the number of weeks on the floor,* but there is a well known time factor (dilating for an outside observer, contracting for an observer

*Typically an experiment will be given about 8 weeks running time but may occupy the floor for a year (technically, it can run only half the time, add to those 16 weeks the setup time and compare with the 30 weeks per year the PS works). This checks with the about 20 experiments completed in 2 years, using 10 beams.

tied to the experiment). So Table II gives a list of experiments finished in the two last years, and a list of experiments approved for 1971, including limited continuation of some of the previous ones. Experiments are grouped according to broad subjects, in order to detect eventual shifts in physicists' interests.

With due respect for the small numbers involved, it would seem that interest is somewhat shifting from weak interactions and search of resonances to study of reaction mechanisms, with or without polarized targets (this conclusion is confirmed by the experimental proposals for the Omega project, see below). Inside that last category (20 experiments in the 3 years), 4 are in the low energy region, and 4 in the medium energy region, roughly the same proportion as in bubble chambers, reflecting here the popularity of Regge models and duality. A well-known difference with bubble chamber physics is that the study of reactions is up to now limited to two-body final states. Exceptions are the CERN-Munich experiment, a possible study of N^* production in the $K^0 p\pi^+$ final state used for the $\Delta S/\Delta Q$ experiment, the production of N^*N final states in the $pp \rightarrow$ 2 body experiment, the experiment on π^- diffraction on helium (and other older experiments in the CERN-ETH magnet). With the Ω project (see below) and other techniques, the field of 3 or more body should be investigated better.

A vast variety of techniques is used:

(1) optical chambers for instance for γ detection in the Pisa-Karlsruhe experiment on neutral resonances and the first η_∞ experiment (the new η_∞ experiment uses big scintillators) and in the "little omega", inside the CERN-ETH magnet.

(2) scintillator arrays, for instance in $\pi^{\pm}p$ scattering on polarized targets (CERN-Orsay)

(3) wire chambers, for instance in the $K^{\pm}p$ backward scattering experiments (CERN-Ecole Polytechnique-Orsay-Stockholm) and the $n\pi^{+}\pi^{-}$ experiment (CERN-Munich).

(4) proportional (Charpak) wire chambers in the CERN-Heidelberg ϕ_{+-} experiment and the $K^{-}n$ elastic scattering experiment.

Bigger intensity, better and longer flat-top, use of larger magnets, technical increase in data-taking capacity have led to higher statistics experiments (example: 300000 $\pi^{+}\pi^{-}n$ events recorded in two weeks in the CERN-Munich experiment) or to investigation of small-cross section reactions (example: study of $\pi^{\pm}$, $K^{\omega}p$ backward scattering near 10 GeV/c, with or without polarized target).

b) The Omega Project

i) Description

The Omega (Ω) is essentially a large magnet filled with spark-chambers. This kind of device has been used since 1964 in the ω apparatus, (optical spark-chambers in the CERN-ETH magnet).

The following table shows the main characteristics of the two systems:

	ω	Ω
Field	10.5 Kgauss	18 Kgauss
Distance between pole pieces	.9 m	1.5 m
Transverse dimensions	$1.7 \times .9$ m^2	3 m diameter
Useful volume	1.4 m^3	13.4 m^3

The magnet coils are made of superconducting Nb-Ti wires cooled by the helium flowing in an inside copper tube. The magnet has movable poles and yoke to adjust to the needs of particular experiments. (See Figure 5)

The Omega will be first equipped with optical spark-chambers, 1.4×2 m^2, with 1 cm gap, made of 10μ Al foil. This should give a momentum error of about 1% for 5-10 GeV/c particles. It has been recently decided not to take photographs, but to scan the chambers with a Plumbicon, a system analogous to the Vidicon, but faster (less than 10 μ sec between two operations). Fig. 6 shows a possible spark chamber arrangement.

The Omega will be installed in the West Hall and start operating middle 72. Two sets of beams are planned: 15 GeV/c unseparated, medium (3-4 GeV) energy ES separated, neutral beam, from a target at about 50 m; high resolution, high energy beam (and later on RF separated beam) from a target at about 110 m.

In the future, the optical chambers may be replaced by digitized chambers, and the use of polarized targets inside the Omega is also planned (butanol target will be operated this summer for the $K^- p \rightarrow K^0 n$ experiment, using the ω-magnet, properly shimmed to create a local uniform 25 Kgauss field). The target for the Ω may be of the frozen type.

ii) Experimental programme

Broadly speaking, the proposals fall in two categories: those which trigger on a slow recoil particle (proton, neutron or lambda) and look for the decay products of the associated missing mass, and those which trigger on a fast forward particle to study low cross-section reactions such as baryon exchange, forbidden exchanges.

For the first year of operation, 6 proposals have been approved:

(1) study of charged non-strange bosons (in the mass-region 1.5-2 GeV), using a proton time-of-flight trigger (Bari-Bonn-CERN-Milano).

(2) study of neutral non-strange bosons, using a neutron trigger (Birmingham-Rutherford-Westfield College).

(3) study of non-diffractively produced $K\pi\pi$ systems in the reaction $K^- p \rightarrow \overline{K}^0 \pi^+ \pi^- n$ (forward trigger) (CERN-ETH).

(4) baryon exchange, triggering on a forward lambda (CERN-ETH. Karlsruhe-Saclay).

(5) baryon-antibaryon production using a forward antiproton trigger (Glasgow-Saclay).

(6) baryonic exchanges, triggering on a forward proton (CERN-College de France-Ecole Polytechnique-Orsay).

All these experiments are with incident beam around 8-10 GeV/c. Fig. 7 and 8 demonstrate the two main triggering modes, as planned for experiments 1 and 2, on the one hand, and 4, on the other hand.

Table I. Bubble Chambers

	68-69-70 (operating chambers)		Proposals and plans (≥ 71)	
	(10^6 pictures)		(10^6 pictures)	
K_8 - Low	2.9	K^-, K^+, $\bar{p}$	1.6	$\pi^\pm$, K^-
m_L - Med	2.1	$K^-, \pi, \bar{p}, K^+$	2.1	$K^-, \pi, K^+, \bar{p}$
U_5 - High	4.3	$K^\pm, \pi, p, \bar{p}$	3.3	$K^\pm, \pi, p, \bar{p}$
Total (2 m)	9.3	(2.1 in D_2)	7.0	(≈ 2 in D_2)
81 cm	5.3	$K^-, \bar{p}, K^+$	Finishes this spring to stock 1.5 K^-, 1.5 $\bar{p}$ of ≈ .7 GeV/c	
1.2 m HLBC	1.6 in 70 (π^+ 3.5, slow K^- stop K^+)		Replaced by Gargamelle	
Gargamelle	Installed 70		1.0 neutrinos, 25 GeV p, 2 GeV $\pi^+(\eta')$	
B. E. B. C ϕ = 3.7 m h = 2 m B = 3.5 T 4 cameras, (105° Fish Eye) 70 mm film	Construction		Cool-down End 71 Technical runs 72 Physics not fixed - neutrinos (D_2 ?) - R. F. beam	
HyBUC	Test in 71		Hyperon magnetic moment	

Table II. PS Counter Experiments

69 - 70	71 (Approved)
Weak Interactions and Symmetries	
η_{oo}, ϕ_{oo} (CERN-Rutherford)	ϕ_{+-} (CERN-Heidelberg)
η_{+-}, $K^0 \to \ell\bar{\ell}$, Δm (CERN-Aachen-Torino)	K_{e_2}/K_{μ_2} (CERN-Heidelberg)
K_{e_4} (Geneva-Saclay)	
$\Lambda\beta$ (CERN-Heidelberg)	
$\Delta S/\Delta Q$ (CERN-Orsay-Vienna)	
η_{oo} (CERN-Aachen-Torino)	
$K^{\pm} \to \pi^{\pm}\pi^0\gamma$, $\pi^{\pm}\pi^0\pi^0$ (Glasgow - Liverpool-Oxford-Rutherford)	
Search for quarks (CERN)	Hyperon beam (CERN, Ecole, Polytechnique, Orsay)
Nuclear Physics	
On line mass spectrometer (Orsay)	
K-mesonic atoms (CERN-Karlsruhe-Heidelberg)	
Hypernuc. γ-rays (CERN-Heidelberg-Warsaw)	
Resonances (beam momentum in GeV/c)	
$\geq$ 2.6 charged bosons (CERN-Geneva-Munich)	$\pi^- p \to \Lambda_0 X_0$ (Roma)
2.13 neutral m. m. (CERN-Bologna)	
6 $\pi^- p \to n + \gamma$'s (Pisa-Karlsruhe)	
17 $\pi^- p \to n\pi\pi$ (CERN-Munich) $\to$ pK^-K^0 etc.	9 GeV (CERN-Munich)

Table II. Continued. PS Counter Experiments

69 - 70		71 (Approved)
Reaction Mechanisms		
1-3 GeV/c $\sigma(K^- p \to K^0 n)$ (CERN-Caen-Saclay)		1-2 GeV/c $K^- n \to K^- n$ (CERN-Caen-Brussels)
8-26 GeV/c $pp \to$ 2 body (CERN)		
8-24 GeV/c $np \to pn$ (Karlsruhe-CERN)	→	Serpukhov
4-8 GeV/c $\bar{p}p \to \bar{n}n$ (CERN-ETH-Imperial College)		
9-16 GeV/c π^- He diffraction (CERN-ETH-Uppsala)		
4 GeV/c $pp \to \pi^+\pi^-$ (Padua-College de France)		6-2 GeV/c $\bar{p}p \to \bar{p}p$, $\pi\pi$, ·· (Rutherford-Queen Mary-Liverpool-DNPL)
$\leq$ 5 GeV/c $\pi^\pm$, $K^\pm p$ backward (CERN-Ecole Polytechnique-Orsay-Stockholm)	→	10 GeV/c $K^\pm p$; $\bar{p}p \to \pi^+\pi^-$
9-13-15 GeV/c πd (CERN-Trieste)		5 GeV/c $\pi^- p \to K^+\Sigma^-, d\bar{p}$ (CERN-Orsay)
9.7-12.8-15.8 GeV/c pd (CERN-Trieste)		
Polarized Targets (proton)		
6-16 A&R parameters (Saclay)		4 GeV/c $\pi^+ p \to p\pi^+, \Sigma^+ K^+$ (CERN-Trieste)
0.8 - 3 GeV/c $K^\pm, \pi$ el. (CERN-Holland)		8 GeV/c $K^- p \to \bar{K}^0 n$ (CERN-ETH-Imperial College-Saclay)
6 GeV/c $\pi^- p \to \pi^0 n$ (CERN-Desy)		
6-18 GeV/c π, K el. (CERN-Orsay-Pisa)		
6-8 GeV/c π, K backward (CERN-Orsay-Oxford)	→	Continuation

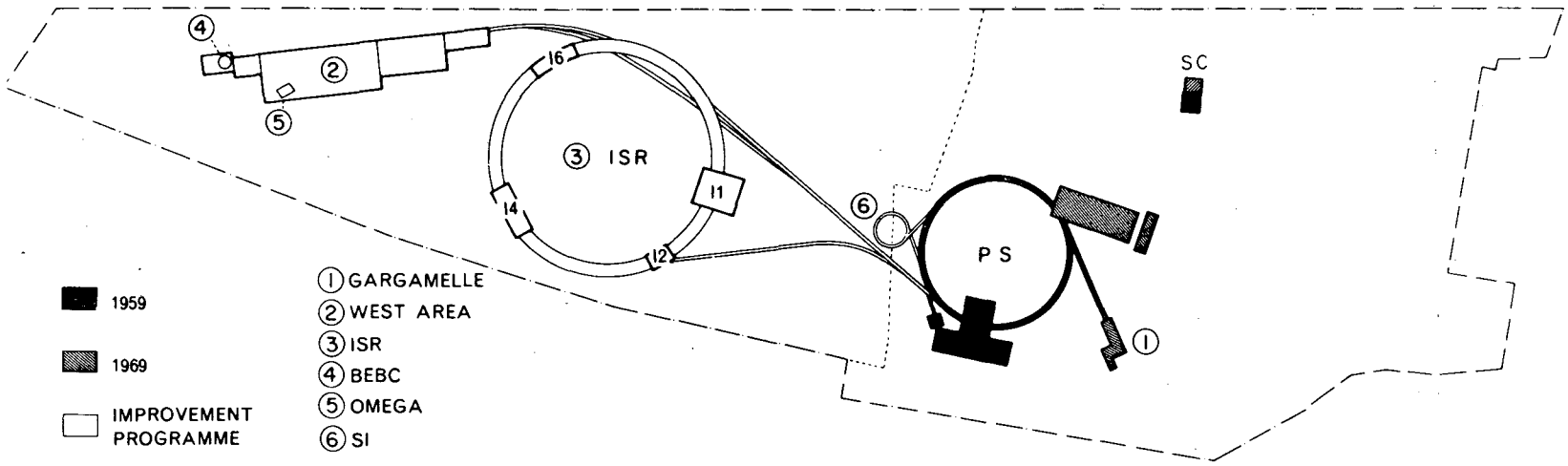

XBL 715-976

Fig. 1.

CERN - General lay-out

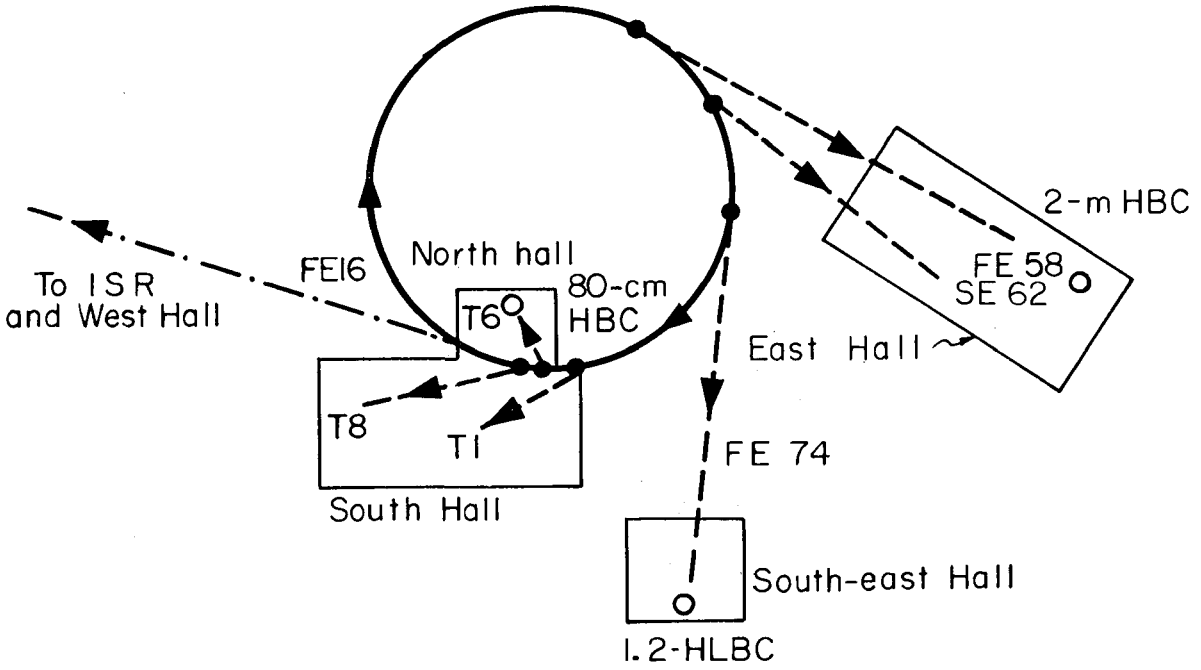
To ISR
and West Hall
FE16
North hall
T6
80-cm
HBC
2-m HBC
FE 58
SE 62
East Hall
T8
T1
South Hall
FE 74
South-east Hall
1.2-HLBC

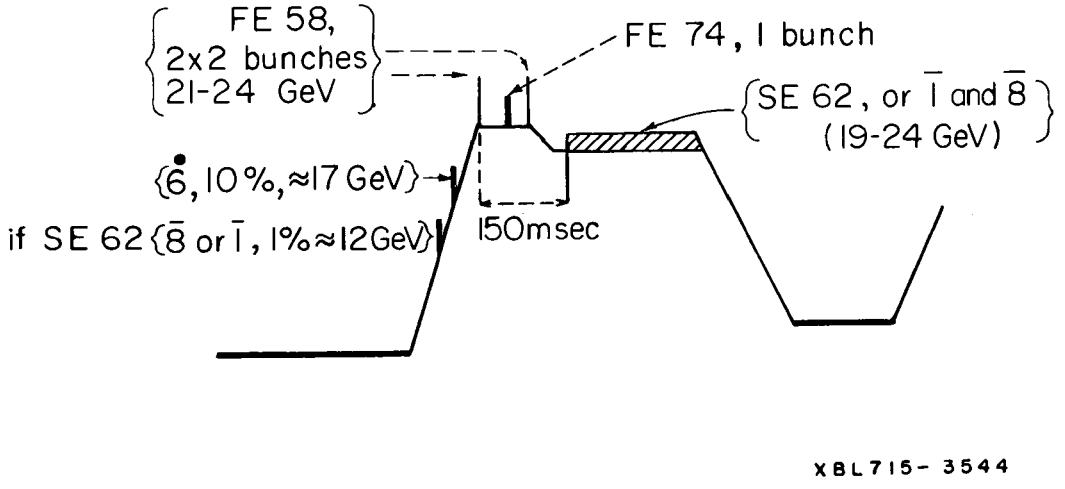
FE 58,
2x2 bunches
21-24 GeV
FE 74, 1 bunch
SE 62, or $\bar{1}$ and $\bar{8}$
(19-24 GeV)
{6, 10%, ≈17 GeV}
if SE 62 {$\bar{8}$ or $\bar{1}$, 1% ≈ 12GeV}
150msec
XBL715-3544

Fig. 2.

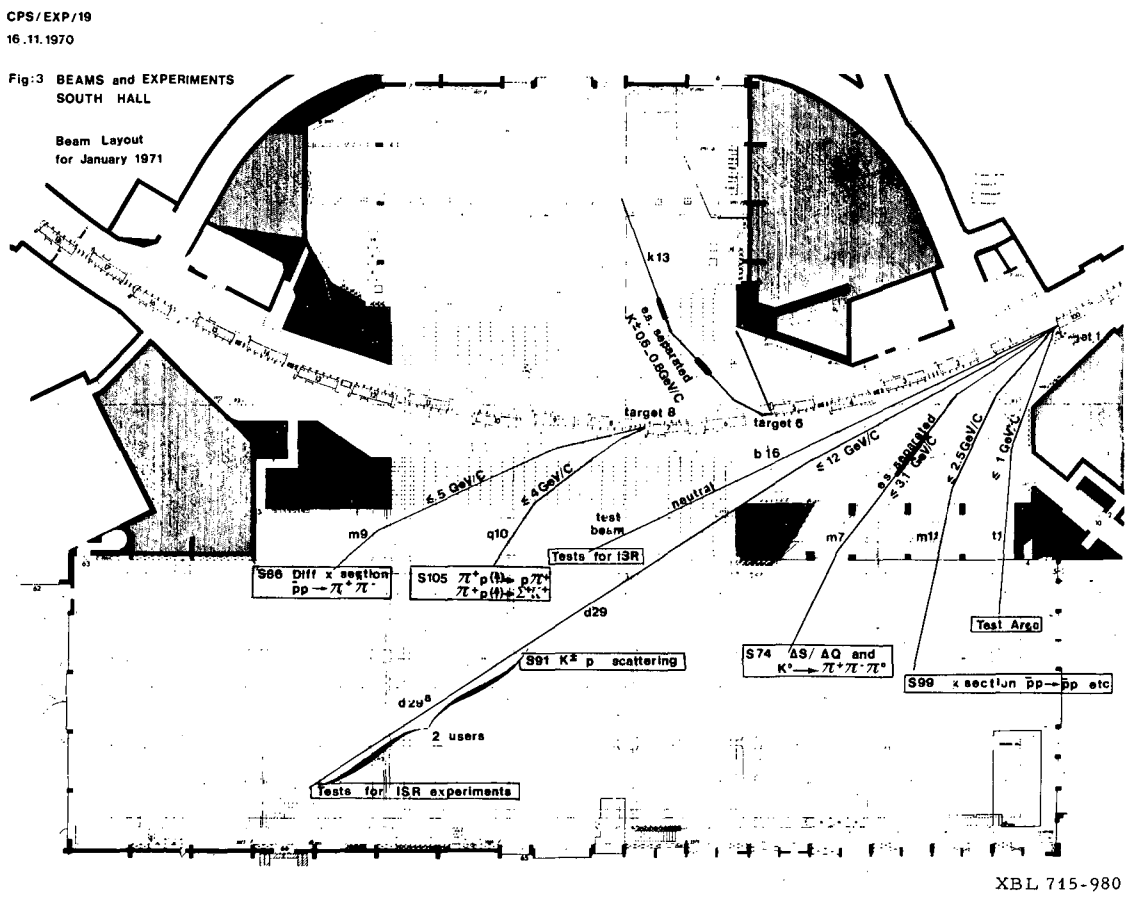

Fig. 3.

South Hall

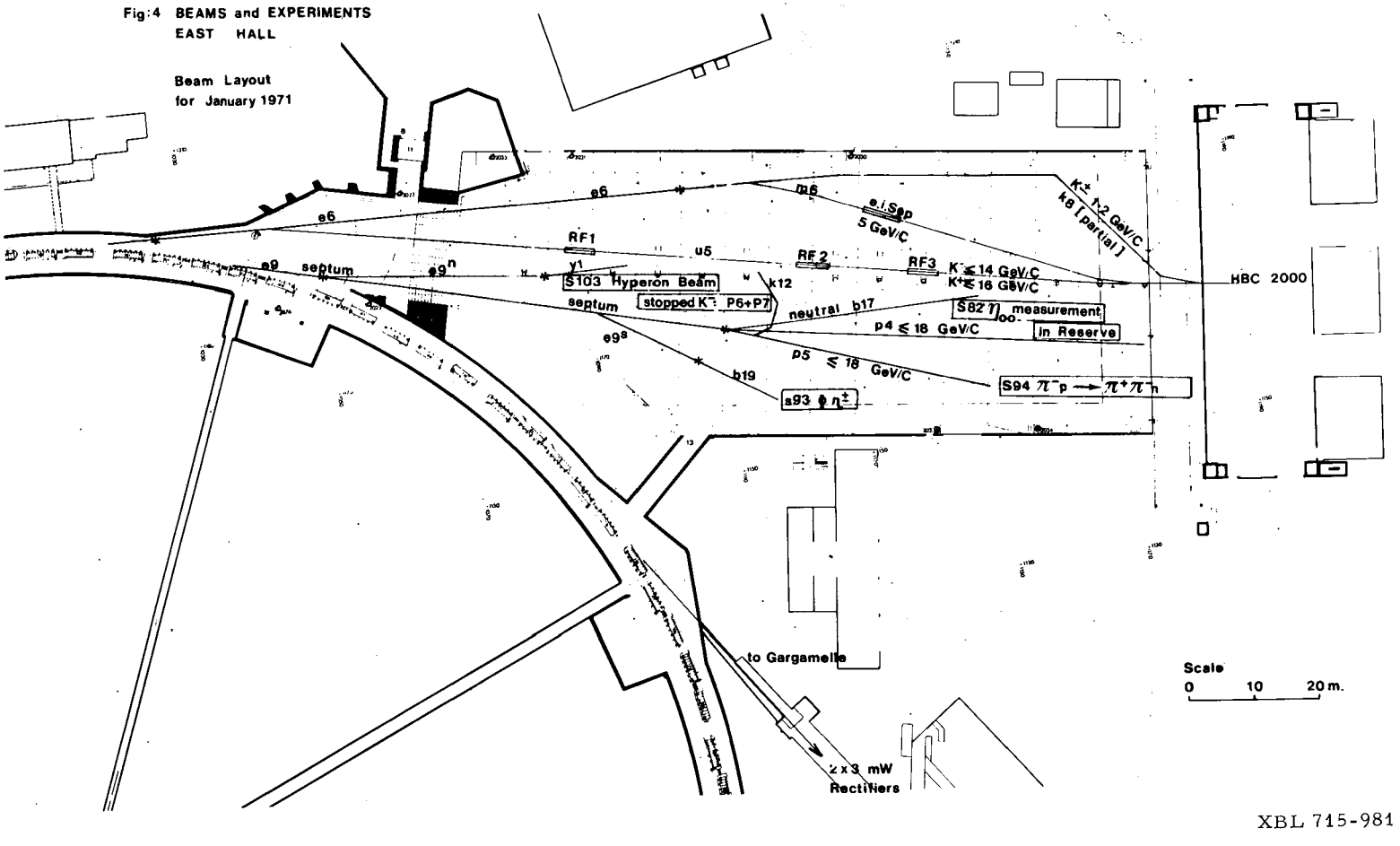

Fig.4.

East Hall

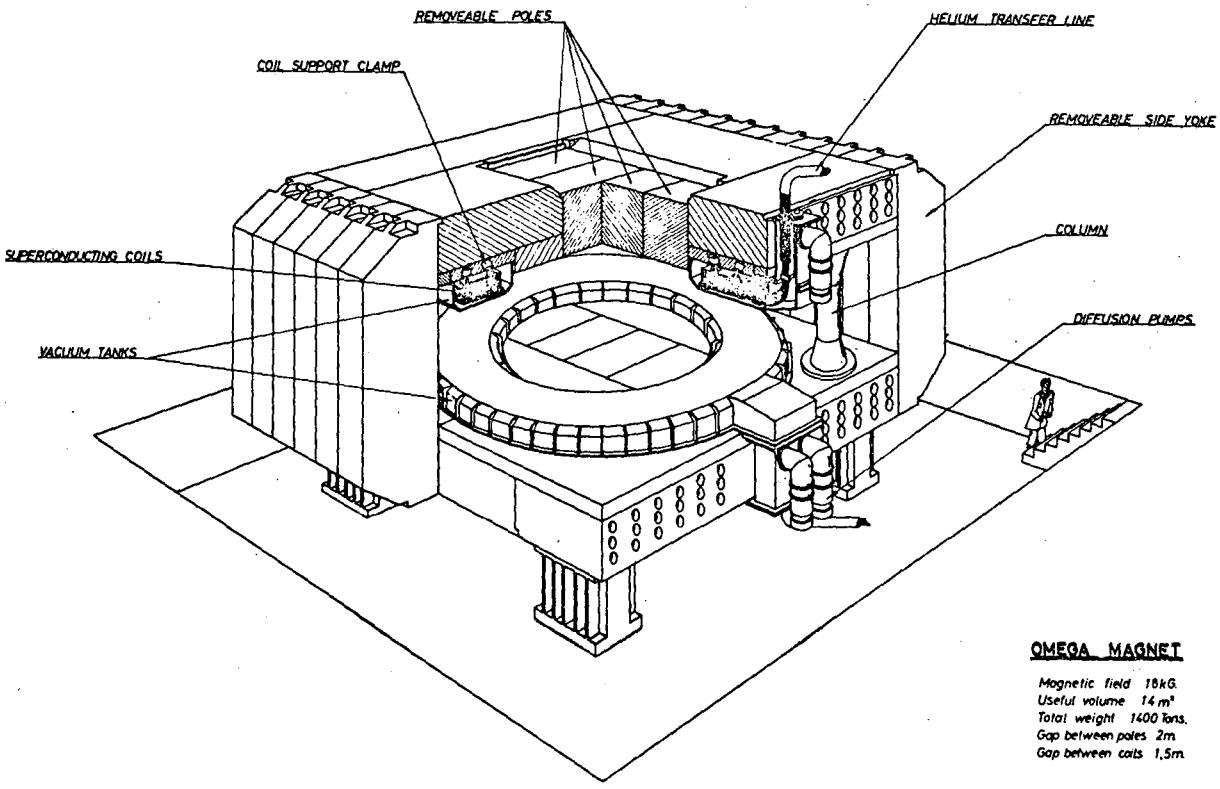

Fig. 5.

Sketch of the Omega Project

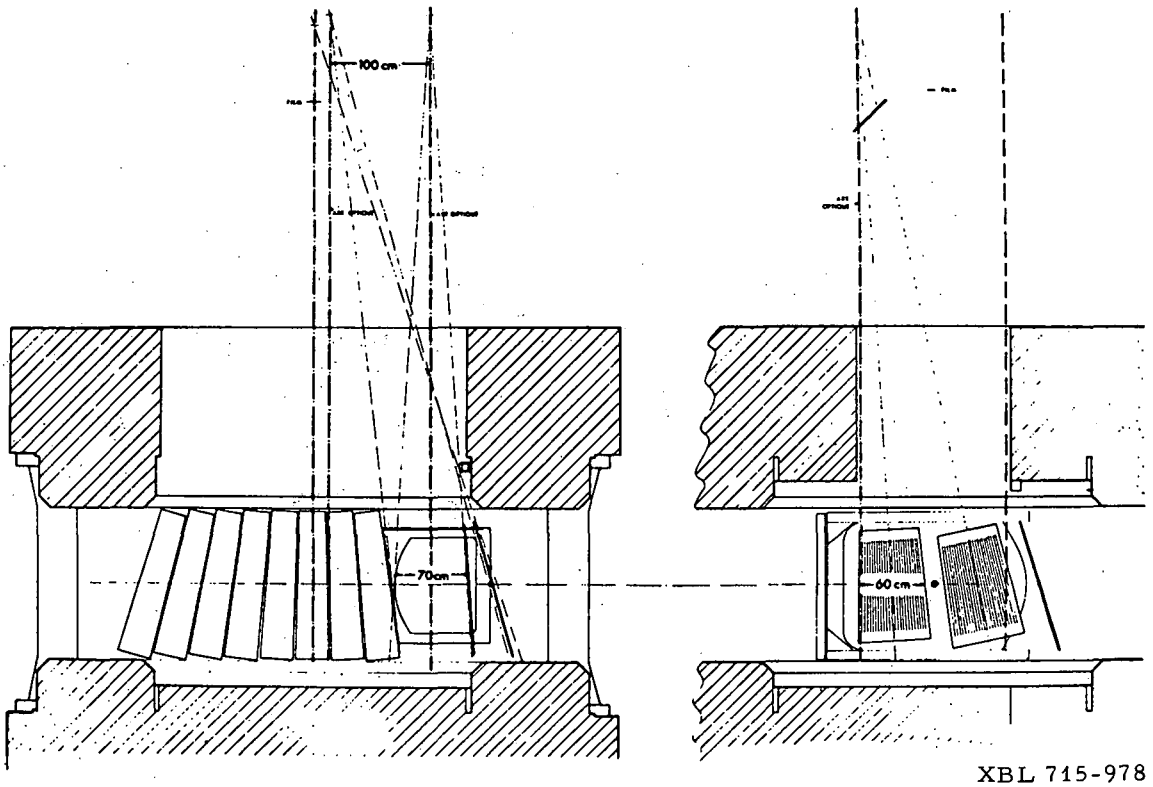

Fig. 6.

One Possible Spark Chamber Set-up

for the Omega

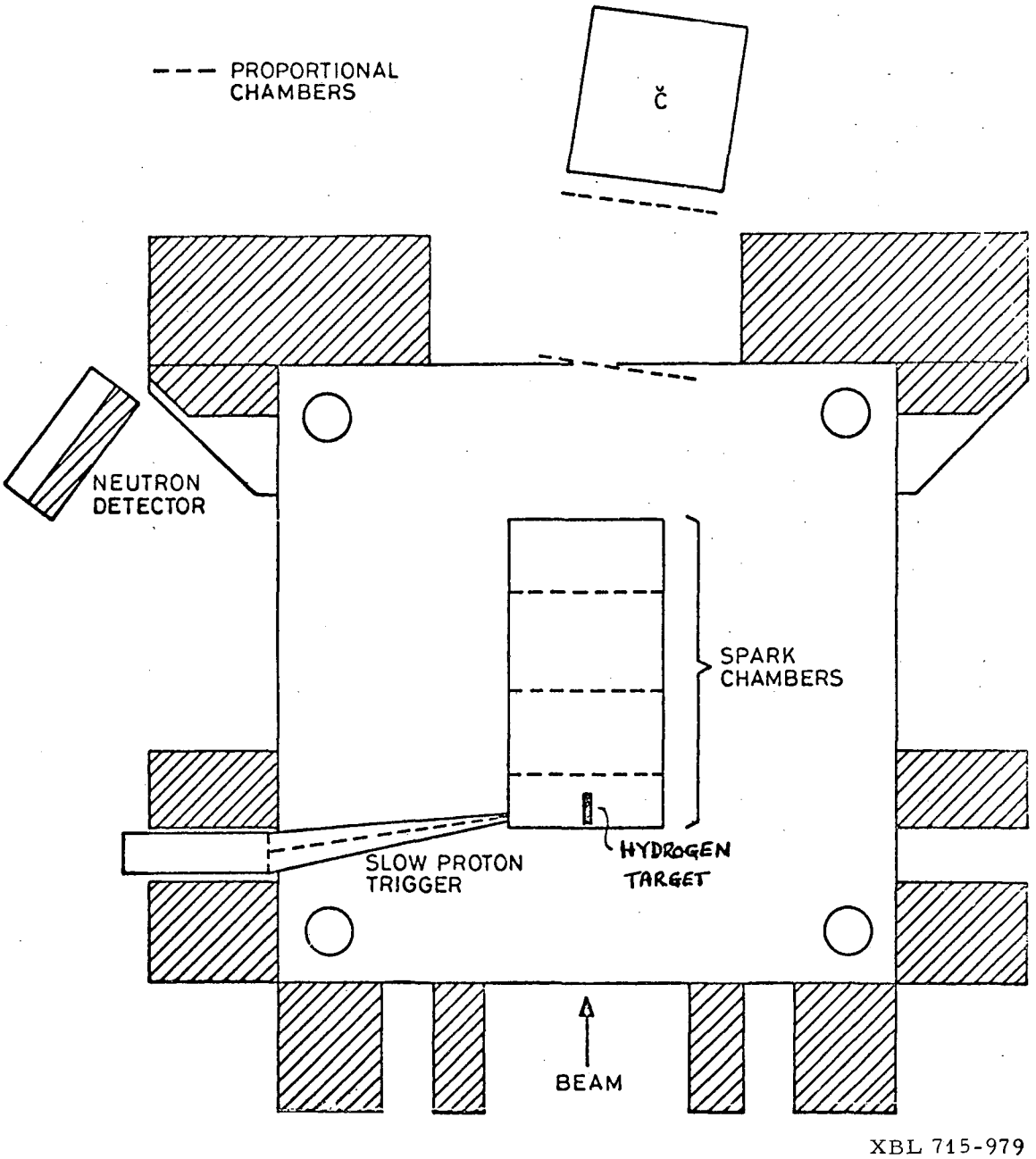

Fig. 7.

Search for Boson Resonances in the Omega

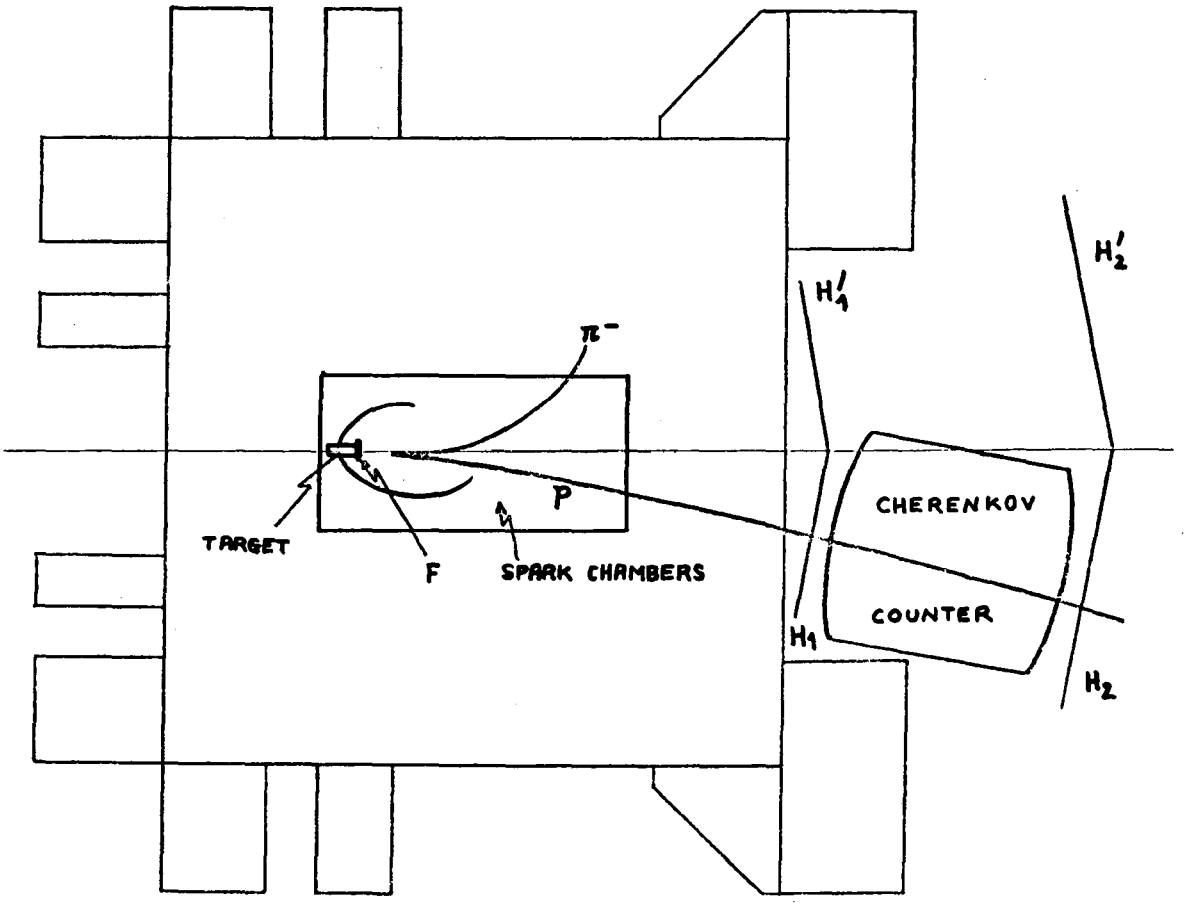

XBL 715-982

Fig. 8.

Study of Baryon Exchange in the Omega

Discussion

Goldhaber (LRL): One experiment of interest that has not been mentioned as yet is K^+ scattering off polarized deuterons. What you want to get is K^+n charge exchange polarization around 0.5-1.0 GeV. This is where people are claiming several Z_0^*'s. To study this one needs to do a phase-shift analysis which requires some knowledge on K^+n charge exchange polarization.

Yokosawa (Argonne): The polarized deuteron target is indeed working. All that remains is to do the experiment.

Steiner (LRL): I have a question for the theorists. What role might the strong interaction machines play in studying radiative provesses?

Lovelace (Rutgers): I think $\pi^-p \to \gamma n$ is interesting at low energies, where the dueterium corrections for the inverse process are uncertain.

Steiner (LRL): At the LRL 184" synchrocyclotron a group from UCLA is going to try to measure the magnetic moment of the $\Delta(1236)$ by studying $\pi^+p \to \pi^+p\gamma$. From the experimental point of view it is probably feasible to study reactions of this general type at other energies and in other processes. It might well be possible to study the radiative decay modes of say one N^* into another. There are quark model and other predictions for many of these processes. Of the existing accelerators the Bevatron, the ZGS, and NIMROD are especially well suited for experiments of this type. I think it would be worthwhile to look in more detail into the theoretical and experimental aspects of this type of physics.

Moorhouse (LRL): There are other interesting reactions such as the electromagnetic decays of the $\Sigma(1385)$. This could be used to check U-spin conservation which allows $\Sigma^-(1385) \rightarrow \Sigma^- + \gamma$ but forbids $\Sigma^+(1385) \rightarrow \Sigma^+ + \gamma$. Both in the case of the $\Sigma(1385)$ and the $Y_0^*(1520)$ (on which some electromagnetic decay measurements already exist) a rather clean separation of resonance and background is possible, whereas for the electromagnetic decays of the N^* resonances, which are broader, the extraction of partial widths is more critically dependent on a complete phase-shift analysis.

SESSION II

POLARIZED TARGET TECHNIQUES

Gilbert Shapiro

POLARIZED TARGET TECHNIQUES

Gilbert Shapiro
University of California
Berkeley, CA. 94720

The experiments which have been performed using polarized targets can be grouped into three categories:

(1) measurement of the normal polarization parameter in elastic scattering;

(2) tests of discrete symmetries and measurement of intrinsic parity in hadron interactions;

(3) analysis of the polarization of the recoil particle after elastic scattering in a plane containing the target polarization vector--the so-called R and A measurements.

In category (1) rather extensive measurements have been carried out in elastic $\pi^{\pm}p$, pp and $K^{\pm}$ scattering. The range of beam momenta studied has extended from 0.25 up to 25 Gev/c. The range of momentum transfers covered has been typically from 0.1 $(\text{Gev/c})^2$ to as much as 3 $(\text{Gev/c})^2$. The results of these measurements have generally been used as inputs to phase-shift analyses at the lower energies. At these and higher energies polarization measurements are sensitive to the presence of the smaller amplitudes which interfere with the dominant amplitude in the process under study.

In many cases polarization measurements have been made at closely spaced energy intervals. The accuracy is as good as ± .05 to ± .10 in most cases. While the range of experiments has been quite extensive, it appears profitable to repeat some of the experiments with accuracy in the ±.01 to ±.03 range. Such accuracy would help to pin down the phase shifts with sufficient precision to (1) remove ambiguities remaining in the phase shift solutions, and (2) to pin down the scattering amplitudes so they can be more useful in, say, finite-energy-sum-rule calculations.

More recently polarization measurements have been made in charge-exchange experiments, such as $\pi^- p \rightarrow \pi^o n$, $\pi^- p \rightarrow \eta^o n$, $np \rightarrow pn$. Other possibilities suggest themselves, such as $K^- p \rightarrow \bar{K}^o n$. This type of measurement can be important as input to phase shift analyses, since it represents a different kind of measurement, and can be as effective as getting better accuracy in repetitions of the older polarization measurements. Charge exchange reactions are also interesting because they can be mediated only by the exchange of an object with $I \geqslant 1$. By measuring the polarization, which arises from the interference of two such amplitudes, of opposite parity, we have the opportunity to observe the effect of low-lying trajectories.

Polarization effects of the type I have so far discussed can be, and have been, measured by classical double scattering experiments not using polarized targets. Naturally the use of polarized targets can reduce systematic errors, and extend the range of angles of useful measurements. Experiments of the second and third category cannot be done at all without polarized targets.

Polarized targets have been used to test time reversal invariance in inelastic electron-proton scattering. One of the important conclusions we reached in this experiment was that, in measuring a null effect, it was possible to keep systematic errors down to a level of $\pm.0005$ in the raw asymmetry. That is, over a period of several weeks, with the target polarization being reversed every two or three minutes, it was possible to accumulate 4 million counts in each channel without apparently incurring systematic errors as great as the statistical errors. This demonstrates that in measurements with polarized targets, given sufficient counting rate and running time, it is possible to attain at least this level of precision.

In another experiment of this type, it was possible to confirm that the KΣN parity is negative. In a related measurement one could determine the polarization in the reaction $\pi^- p \rightarrow K^+ \Sigma^-$. This particular polarization would not be measurable without a polarized target, since the Σ^- decays isotropically.

The R and A type measurements involve, as I have mentioned before, an elastic scattering from a polarized target, in a plane containing the polarization vector, followed by a second scattering of the recoil proton to analyze its polarization state. These parameters (R and A, or linear combinations thereof) are sensitive to the real part of the product of the spin-flip and the non-spin-flip amplitudes. The standard polarization measurement is proportional to the imaginary part of this product. Thus we can distinguish between the case where polarization vanishes because the spin-flip amplitude vanishes, and the case where it vanishes because the two amplitudes have the same phase.

So far only the Saclay Group has perfromed R and A measurements with polarized targets, but other groups are now building apparatus suitable for this type of experiment. A different design of the polarized target magnet is required. Particles must be able to approach the target, and to emerge from it, in a direction parallel to the magnetic field. Thus we cannot have solid iron pole-faces. Nevertheless field uniformity of ±10 gauss out of 25 kilogauss is required over the target volume, in order to polarize the target.

The performance of recently tested targets is illustrated in figure 1. Certain materials have advantages when it is necessary to reverse polarization direction at frequent intervals, or when radiation damage effects are important. If these considerations do not apply, we can apply a figure of merit as follows.

We assume that the target volume is determined by the magnetic field uniformity, and the total running time is fixed. Let H. F. (hydrogen fraction) be the ratio of hydrogen to total counts in the kinematic channel of interest. H.F. can be close to unity when we have a two-constraint fit or better, and when the cross-section is not falling too rapidly with angle. In situations where the background due to non-hydrogen events cannot be discriminated against kinematically, H.F. may be proportional to the fraction by weight of free hydrogen in the target material. Let ρ^H be the density of free protons in the target and P_T the target polarization available. The figure of merit for a target material is inversely proportional to the statistical error in the measured polarization parameter for a given length of running and is given by:

$$\text{figure of merit} \sim (\text{H.F.}) \times P_T \times \sqrt{\frac{\rho H}{\text{H.F.}}} = P_T \times \sqrt{\text{H.F.} \times \rho H}$$

There are other sources of error than statistical of course. One of these is the measurement of the target polarization. This can be tricky if, as often can happen, the polarization is not uniform throughout the target volume. For a near-null experiment this effect is not important. For experiments in which the measured parameter is large (i.e., of the order of unity) we are hopeful of reducing this source of error to not more than 3% of the measured result.

It has recently been pointed out that measurements of the R and A parameters in associated-production experiments can make a decisive test between competing absorptive cut models. These experiments appear to be soon within the range of feasability.

Another type of measurement which may be possible with polarized targets are those involving broad resonances as final states. One such example is $\pi^- p \rightarrow \rho^o n$ which can be compared to photoproduction polarization measurements in accordance with various rector dominance models.

In short, while I expect that I have not mentioned all possible experiments that will be done with polarized targets in the future, it appears that there remain a great many interesting and important ones to be done particularly in the energy range below 10 Gev.

Table I

Material	Paramagnetic Doping	ρH (g/cm^3)	Percent Hydrogen (by wt.)	Polarization Measured at T(°K)	H(Koe)	Polarization Achieved Maximum	Working	Polarization Build-Up Time(sec)	Radiation Damage Dose ($particles/cm^2$)
"LMN"-$La_2Mg_3(NO_3)_{12}.24H_2O$ (universally used until 1967)	1% $^{142}Nd^{+++}$	.06	3.2%	1.0	25	75%	55-65%	300-600	2×10^{12}
Ethanol C_2H_5OH	Porphyrexide	.10	13.0%	1.0	25	35%	15-25%	25 sec	4×10^{14}
Butanol C_4H_9OH	Porphyréxide	.11	13.5%	1.0 0.5 1.0	25 25 47	45% 67% 67%	35%	15	4×10^{14} (can be annealed)
Ethylene Glycol $C_2H_4(OH)_2$	Cr^Vcomplex	.14	9.7%	1.0 0.5 1.1	25 25 47.5	48% 80% 80%	40-45%	15 500 90(with 100 mw power)	4×10^{14} (cannot be annealed)
Propanediol $C_3H_6(OH)_2$	Cr^Vcomplex	.11	10.5%	1.0	25	50%	45-50%	150	
Ammonia NH_3	Cr^Vcomplex	.14	17.7%	1.0	25	45%	40%	1400	
Deuterated butanol C_4D_9OD	Porphyrexide	.13 (Deuterons)	23.8% (Deuterons)	.5	25	22%	20%	250	

Table II. He^3 Polarized Targets

Method	Temperature	Pressure	H (gauss)	Density (g/cm^3)	Polarization
Optical Pumping	Room	$\lesssim$ 10 mm	~100	10^{-6}	40%
Optical Pumping	Room	1 atm.	~100	10^{-4}	20%
Pomeranchuk Cooling	$< 0.01^{\circ}K$	34 atm.	> 40,000	0.1	Not yet tested

Discussion

Yokosawa (Argonne): The latest information from Borghini at CERN about the NH_3 target is that at 25 Kg and 0.05° K they obtained 60% polarization with a target of usable size. [Private communication, Borghini to Shapiro, April 22, 1971, 70%.]

Shapiro (LRL): How many hours does it take to build up the polarization?

Yokosawa (Argonne): The so-called build up time is a few hours.

Lately there have been many exciting papers about the importance of measurements of the R and A parameters. It would be helpful if a convention, similar to the Basel convention for the polarization parameter, could be adopted by theorists and experimentalists for R and A.

Shapiro (LRL): Anyone who writes a paper should be careful to show explicitly how they define A and R.

Romanouski: Has there been any success in polarizing HD?

Yokosawa (Argonne): Abragam and his colleagues have been trying to polarize it, but without success.

Shapiro (LRL): At one time Honig had a plan to make a Frozen HD target. One of my objections to such a frozen target is that its long relaxation time means that it is very difficult to reverse the target's polarization.

Manning (RHEL): You can, of course, take the time to reverse the polarization, though it might take several hours.

Shapiro (LRL): Yes, but systematic effects which can be minimized by frequent polarization reversals cannot be handled with such a target.

Manning (RHEL): There is a suggestion that one might use two targets, polarized in opposite directions.

Shapiro (LRL): There will still be some systematic effect because the two targets won't be identical.

Manning (RHEL): You would have to run each of the targets with both signs of polarization to minimize that systematic effect.

Fox (CIT):

On the Importance of Being a Multiparticle Final State Produced from a Polarized Target

In the following I would like to indicate the great interest in measuring, e.g., $\pi N \to \pi\pi N$ off a polarized target. This will require some technical advances, e.g., placing polarized target in a streamer chamber; it would be nice if some thought could be given to the necessary hardware developments. And so to physics.

(i) I have already mentioned (see page 56) the interest in measuring $KN(\uparrow) \to KN\pi$ [$N(\uparrow)$ = polarized N hereafter] at low energy. It will discover a Z^*. More generally, low energy phase shift analysis of multiparticle final states have been unsuccessful so far. Potentially they are rich in resonances [there is plenty of cross section and less angular momentum barrier, for, e.g., N^{**}(high spin) $\to \pi\Delta$ than $N^{**} \to \pi N$]. Good polarization data stimulated elastic scattering phase shifts: so it will in multiparticle reactions. Particularly so, as the latter have large real background (π exchange in $\pi N \to \rho N$, whole reaction $KN \to KN\pi$). This is disaster in

$d\sigma/dt$ where you measure $|\text{BACK}|^2 + |\text{RES}|^2$ (= large, = small) --polarization will pick up the interference $\text{Im(RES)} \times \text{Re(BACK)}$. Good reactions are $\pi N(\uparrow) \to \pi\pi N$ (plenty of events), $KN(\uparrow) \to K\pi N(Z^*)$, $\bar{K}N(\uparrow) \to \pi\pi\Lambda$ (R and A from final Λ polarization).

(ii) To find all the observables in $MB \to MB$ you must measure final baryon polarizations off a polarized target. This is only possible [cf. A(i) (see page 55)] for a <u>few</u> exchange processes $\pi N \to K(\Sigma,\Lambda)$, $\bar{K}N \to \pi(\Sigma,\Lambda)$. <u>But</u>, in, say, $\pi N \to \pi\Delta$, you have eight unknown quantities (real and Im of four amplitudes), four observables off unpolarized target ($d\sigma/dt$, ρ_{33}, ρ_{31}, ρ_{3-1}) plus six <u>extra</u> observables with a polarized target. Thus, in this reaction, a single experiment off a polarized target will (over) determine all amplitudes (up to overall phase). You do <u>not</u> need to measure final baryon polarization. Other examples: $\pi N \to \omega\Delta$, 24 unknown quantities, 20 observables off unpolarized target, 36 (!) extra observables off polarized target; $\pi N \to \rho N$, 12 unknown quantities, four unpolarized observables, six polarized observables. In latter case only, one does not have a complete set--one more observable is needed. (It could be, for instance, final baryon polarization observed by rescattering of p in Argonne giant 12-foot chamber.) These reactions test ρ, A_2, π and B exchange--segments <u>not</u> tested in $\pi N \to K\Sigma$ type experiments. Together with the polarized p experiment A(i) (see page 55) they represent a goldmine waiting to be observed.

Lovelace (Rutgers): If you are going to do three-particle states with a polarized target, an obvious place to start is the reaction $K^+p \to K\Delta$. One would expect that, if the Z_1^* exists, then that would be its main decay channel.

THE SPECTRUM OF LOW-LYING HADRON STATES*

Jonathan L. Rosner

School of Physics and Astronomy
University of Minnesota
Minneapolis, Minnesota 55455

(Invited talk at Workshop on Particle Physics at Intermediate Energies, California Institute of Technology, March 29-30, 1971.)

Abstract

The low-lying meson and baryon states are reviewed from various theoretical standpoints, with particular emphasis on the quark model scheme of classification. Experiments to fill in gaps are suggested where possible.

Contents

1. Mesons as $q\bar{q}$;L
2. Baryons as qqq;L
3. Higher spin resonances
4. Quark model "dynamics"
5. Exotic baryons
6. Exotic mesons
7. Predictions of duality
8. Scale invariance and 0^+ states
9. Uses of high statistics and resolution
10. Conclusions

*Work supported in part by the U. S. Atomic Energy Commission through Contract No. AT-(11-1)-1764.

The hadron spectrum is probably going to provide us with the key to hadron structure. It has regularities understood from many points of view, including SU(3), the quark model, superconvergence, and duality.

The most recent investigations of hadron structure are based on "direct" probes via deep inelastic lepton scattering. These are essential to any realistic "composite" model of hadrons, as they are uniquely sensitive to the properties of the "component parts". On the other hand, such experiments must be complemented by purely spectroscopic ones: elucidation of energy levels and decay schemes. Bohr was told about the Balmer formula only one month before his first paper on the hydrogen atom was written.[1] Until then he had been concerned only with more general properties of atomic structure. His calculations would not have been taken as seriously had they proved only the possibility of an atom stable against collapse.

I would like to suggest places where the gaps in our knowledge about low-lying hadron states need to be filled in. This pattern has not changed appreciably in the past couple of years, but is far from complete. An overall view of the hadron spectrum and its regularities may be had from several reviews,[2-5] prepared with more advance notice than I have had.[6]

Our guide to the regularities of the strongly interacting particles, especially in light of the uncertain status of the A_2 splitting,[7] continues to be the naive quark model,[8-12] whereby mesons all appear to behave as

$$M_2 = q\bar{q} \quad (\in \underset{\sim}{1}, \underset{\sim}{8} \text{ of SU(3)}) \tag{1}$$

and baryons as

$$B_3 = qqq \quad (\in \underset{\sim}{1}, \underset{\sim}{8}, \underset{\sim}{10} \text{ of SU(3)}) \ . \tag{2}$$

The quarks q are members of an SU(3) triplet $\underset{\sim}{3}$: an isospin doublet u, d and a singlet s:[8]

	I	I_3	Y	Q
u	1/2	1/2	1/3	2/3
d	1/2	-1/2	1/3	-1/3
s	0	0	-2/3	-1/3

(3)

These assignments are motivated by simplicity. Other schemes include ones without fractional charges, and involve more quarks.[13] Most are equivalent to eq. (3) for the purpose of low-lying hadron classification.[14] The distinction among various such schemes seems hard to press experimentally at the moment, though Z^*'s (K^+p and K^+n resonances, if they exist) may have some bearing on them.[15] We shall therefore stick with the usual assignment (3) in what follows.

The naiveté of the quark model lies in the assumption that particles lie on linear Regge trajectories with a more or less universal slope $\alpha' \simeq 1$ GeV^{-2}. This phenomenon is confirmed in the case of the baryons[4,5] and is supported by experience with dual models.[16,17] It would correspond to roughly harmonic forces in an oscillator model.[9,10] Serious distortions of such forces would then be needed to obtain a second 2^+ state at the mass of the A_2.[12] The existence of some such distortion is suggested by the low mass of "radial" excitation states[2] such as the N(1470) $1/2^+$ and E(1420) 0^-, but by and large the harmonic-oscillator nature of the spectrum is mysteriously well-obeyed (especially if the A_2 is unsplit.[7])

The quark model also allows one to state the apparent absence of "exotic" states such as:

$$M_4 = qq\bar{q}\bar{q} \quad (\in \underset{\sim}{1}, \underset{\sim}{8}, \underset{\sim}{10}, \underset{\sim}{\overline{10}}, \underset{\sim}{27} \text{ of SU(3)})^{18} \tag{4}$$

or

$$B_5 = qqqq\bar{q} \quad (\in \underset{\sim}{1}, \underset{\sim}{8}, \underset{\sim}{10}, \underset{\sim}{\overline{10}}, \underset{\sim}{27}, \underset{\sim}{35} \text{ of SU(3)})^{5,19} \tag{5}$$

in dynamical rather than algebraic terms:

Algebra: no $\left\{\begin{matrix} \underset{\sim}{10},\ \underset{\sim}{\bar{10}},\ \underset{\sim}{27} \text{ mesons} \\ \underset{\sim}{\bar{10}},\ \underset{\sim}{27},\ \underset{\sim}{35} \text{ baryons} \end{matrix}\right\}$ exist

Dynamics: forces between quarks are such that

no $\left\{\begin{matrix} \underset{\sim}{10},\ \underset{\sim}{\bar{10}},\ \underset{\sim}{27} \text{ mesons} \\ \underset{\sim}{\bar{10}},\ \underset{\sim}{27},\ \underset{\sim}{35} \text{ baryons} \end{matrix}\right\}$ exist

This sounds like an unsympathetic view! Actually I believe it is in the right direction. Rudimentary dynamics often allows one to rule out certain representations, as in the case of half-odd-integer values of ℓ when we make the dynamical identification $\vec{L} = \vec{r} \times \vec{p}$.[20]

1. Mesons as $q\bar{q}$; L.

We shall concentrate here on L = 0 and L = 1 states, where one has some hope of sorting out the experimental situation. The identification of a complete multiplet of $q\bar{q}$; L = 2 resonances seems prohibitively difficult at present, though some encouraging starts have been made which will be discussed in Section 3.

L = 0:

0^- states: π, K, η, $\eta'(\,^1S_0)$

This multiplet appears to act predominantly as an octet plus a weakly mixed singlet (η'), as predicted by SU(6)[11] or duality.[21] The presence of some mixing between octet and singlet[2,13] is suggested by the large value[13,22] of

$$\Gamma(\eta \to \gamma\gamma) / \Gamma(\pi^0 \to \gamma\gamma) \simeq 10^2 .$$

This mixing is almost certainly such that the η gains in nonstrange quarks relative to its content as a pure octet member.[13] A suggestion to the contrary,[2] namely that η be mostly $s\bar{s}$, was motivated by the apparent narrowness of $\delta(962)$ ($\Gamma \lesssim 5$ MeV), an effect which has since been called into question,[22] (see below in this section: "0^+ states")

and by superconvergence criteria which are very easily relaxed.[23]

Further evidence that the η' couples as we would expect it to in the quark model[2,13] comes from combining the recent branching ratio determination[24]

$$\Gamma(\eta' \to \gamma\gamma) / \Gamma(\eta' \to \text{all}) = 1.8 \pm 0.5\% \tag{6}$$

with the upper bound[22]

$$\Gamma(\eta' \to \text{all}) < 4 \text{ MeV} \tag{7}$$

This allows one to exclude the non-quark-model type coupling ($\eta \sim s\bar{s}$) for a mixing angle $|\theta_o| = 10^o$, the value preferred by a quadratic mass formula.[2] A further improvement in the combined bounds (6) and (7) by a factor of 2 is necessary to exclude a similar pathology for $|\theta_o| = 24^o$, the value preferred by a linear mass formula. Present theoretical estimates of $\Gamma(\eta' \to \gamma\gamma)$ [13,25] lie below 30 KeV, so that such improvements may be worthwhile. They could be made, for example, by a high-resolution study of the η', to improve the bound (7).

An anomaly in the $\pi\pi\gamma$ mode of the η' has recently been reported in the reaction[26]

$$K^- p \to K^- p \text{ "M(953)"}$$
$$\hookrightarrow \pi^+\pi^-\gamma \tag{8a}$$
$$\hookrightarrow \eta\pi\pi \ . \tag{8b}$$

In all previous reactions, including one which can be studied simultaneously with (8), i.e.

$$K^- p \to \eta' \Lambda \quad , \tag{9}$$

the $\pi\pi\gamma$ mode of the η' has been consistent with 100% $\rho\gamma$. Reaction (8a) shows no ρ signal. One suggestion[23] is that the "M(953)" has $J^{PC} = 1^{++}$, I = 0, and is indeed decaying into $\rho\gamma$ but with a highly distorted matrix element. That this is likely turns out to follow

from vector dominance. Another possibility is that C(M(953)) = -1, which would forbid its $\rho\gamma$ decay. In this case, since the decay (8b) implies G = +, one has I(M(953)) = 1, implying the existence of a charged mode. It is possible that $\delta(962)$ could be this effect, with a (much broader) $\eta\pi$ resonance,[22] seen by several groups, also lying nearby. However, the apparent absence of an $\omega\pi^{\pm}$ resonance at 953 MeV would then be surprising.

A third possibility, of course, is that of a "severe statistical fluctuation,"[26] and therefore it is of utmost importance to confirm the effect by re-opening the η' question in all ways possible.

The existence of <u>at least</u> a 0^- (or 2^-!) state around 960 MeV is confirmed by the observed decay[24] $\eta' \to \gamma\gamma$. (A J = 1 particle cannot decay to $\gamma\gamma$[27]). The 2^- hypothesis persists,[28] but one may be able to rule out such a low-mass, high-J state by certain very powerful inequalities based on duality.[29]

1^- states: ρ, K*, ω, ϕ ($^3S_1$)

The most remarkable effect associated with this nonet has been the observation of spectacular ρ-ω interference effects: destructive in

$$\pi^+ p \to \pi^+ \pi^- \Delta^{++} \qquad (10)^{30}$$

and constructive in

$$\pi^- p \to \pi^+ \pi^- n \qquad (11)^{31,32}$$

The stability of the result (11) between 2.3[31] and 15[32] GeV/c is particularly interesting. A theoretical explanation of these effects on the basis of degenerate π-B trajectory exchange[33] predicts a vast number of other cases which may be tested. We refer the interested reader to Refs. 30 and 33 for a complete treatment of the subject.

Quark model predictions have continued to fall into line with the observation[3] of

$$\phi \to \eta\gamma \qquad (12)$$

and the small rate for[3]

$$\phi \to \pi^o \gamma \tag{13}$$

(These decays are just SU(3) analogies of the familiar M1 transition $\omega \to \pi^o\gamma$ which accounts for roughly 10% of all ω decays.[22]) The decay

$$\rho^o \to \pi^o\gamma \tag{14}$$

still has not been observed; SU(3) and vector dominance would predict

$$\Gamma(\rho^o \to \pi^o\gamma)/\ \Gamma(\omega \to \pi^o\gamma) \simeq 1/9 \tag{15}$$

or a partial width $\Gamma(\rho^o \to \pi^o\gamma) \simeq 130$ KeV. Knowledge of this partial width turns out to be useful in estimating[34] the rate of the decay mode

$$\omega \to \pi\pi\gamma \tag{16}$$

This estimate is made by setting the strength of a dual amplitude through knowledge of the couplings in the two-step process

$$\begin{array}{l} \omega \to \rho\pi \\ \qquad \hookrightarrow \pi\gamma \end{array} \tag{17}$$

It is probably more reliable than a simple pole model, which must add contributions from $\omega \to \left\{\begin{matrix} f_o \\ \sigma \end{matrix}\right\}\gamma \to \pi\pi\gamma$ to Eq. (17). The amplitude of Ref. 34 implies such contributions to begin with. It leads to the bounds[34]

$$50 \text{ KeV} \leq \Gamma(\omega \to \pi\pi\gamma) \leq 400 \text{ KeV}. \tag{18}$$

The ability to distinguish $\pi^+\pi^-\gamma$ from $\pi^+\pi^-\pi^o$ final states[26] should be applied to the process (16). At the moment one has only neutral decays of ω which do not fit $\omega \to \pi^o\gamma$ [35] as candidates for reaction (16).

Process (16) is of special interest to theorists since it represents an E1 transition, of which there is not a single present example in the mesons except for the possible $D' \to \pi\pi\gamma$ decay.[23]

L = 1:

2^+ states: A_2, K^{**}, f, f' ($^3P_2$)

New branching ratios have become available on the A_2 [36] and the K^{**}. [37] These have been analyzed with respect to SU(3) (with attention to mixing and barrier effects) by K. W. Lai; no difficulty with SU(3) exists.[38] Using essentially the same data (see Table I), ignoring mixing, and taking a simple (barrier) x (phase space) factor (without an interaction radius) of the form $p(p/p_o)^4/M^2$, I prepared Fig. 1 to show the present situation. This figure is normalized so that the entries of the two boxes should lie on two independent vertical lines if SU(3) is good[39] and on a single vertical line if $SU(6)_W$ is good.[40,41] As one sees, no mixing or interaction radius is needed to make SU(3) work. (Neither correction affects the slight discrepancy between $A_2 \to \rho\pi$ and $K^{**} \to K^*\pi$. This discrepancy used to be worse[40] before the data of Ref. 37.)

It is amusing to note that the deviation suggested by Fig. 1, namely

$$\frac{\Gamma(2^+ \to 1^-0^-)}{\Gamma(2^+ \to 0^-0^-)} \gtrsim SU(6)_W \text{ value} \qquad (19)$$

is in the same direction as that suggested on the basis of super-convergence by Gilman and Harari[42] for the 1^- couplings, namely

$$\frac{g^2(1^- \to 1^-0^-)}{g^2(1^- \to 0^-0^-)} > SU(6)_W \text{ value} \qquad (20)$$

The rate $\Gamma(f' \to KK)$ is poorly known.[22] Furthermore, there is a claim for $f' \to \eta\pi\pi$,[43] a decay violating one's theoretical expectations,[44] which is responsible for the asymmetry in the last line of Fig. 1. (The central point ignores this claim, as does K. W. Lai in his analysis.[38]) This claim deserves further study in view of the possibility of another resonance near the mass of f', the F_1.[45]

I will refer you to the CalTech phenomenology conference proceedings[7] for a discussion of the A_2 splitting. Recent high-statistics

Table I. Experimental Partial Wdiths for decays of 2^+ mesons to 1^-0^- and 0^-0^- .

1^-0^-	Exptl. partial width, MeV
$A_2 \rightarrow \rho\pi$	67 ± 4
$K^{**} \rightarrow K^*\pi$	27 ± 5
$\rightarrow \rho K$	9 ± 4
$\rightarrow \omega K$	3 ± 2.5
$f' \rightarrow (K^*\bar{K}+\bar{K}^*K)$	≤ 21
0^-0^-	
$A_2 \rightarrow \eta\pi$	16 ± 2
$\rightarrow K\bar{K}$	6.5 ± 1.1
$K^{**} \rightarrow K\pi$	62 ± 7
$\rightarrow K\eta$	≤ 2.5
$f \rightarrow \pi\pi$	151^{+15}_{-29}
$\rightarrow K\bar{K}$	4.7 ± 2.0
$f' \rightarrow K\bar{K}$	73^{+23}_{-43}

(Based on Refs. 22, 36, and 37.)

experiments have shed light on the production mechanism of the A_2 (dominantly f_o exchange).[7] However, we seem to have lost the splitting in the process![46] At this point one could probably learn a great deal about 2^+ production mechanisms in general by looking at density matrix elements for $K^{**}(1420)$ and f_o for various incident beams.

1^{++} states: A_1, Q_A, D, (D'?) ($^3P_1$)

The case for the A_1 would be strengthened considerably by conclusive evidence for its non-diffractive production.[47] At present the best such evidence comes from the reaction[48]

$$\pi^- p \to p \text{ (forward) } X^-, \tag{21}$$

in which the "A_1" is identified only as a bump and not as a 3π, $\rho\pi$, or $\sigma\pi$ state.

One question regarding the A_1 is that of a visible D-wave component in $\rho\pi$ decay (seen only in one experiment[49] and nearly absent in others[50,51]). Both $SU(6)_W$[40] and superconvergence schemes[42] predict this D-wave component to be appreciable, but with opposite effects: in $SU(6)_W$ it suppresses $J_z = 0$ decay, while in the model of Ref. 42 it suppresses $J_z = \pm 1$ decay. The results of Ref. 50 and 51 show that neither is the case. The approach of Ref. 42 does not stand or fall on this one result, of course. The fact that appreciable transverse coupling of A_1 to $\rho\pi$ is seen only requires another low-lying resonance to saturate the appropriate superconvergence relation (SCR). The $h(J^{PC} = 1^{+-}, I = 0$; see below[3]) would do quite nicely if it were confirmed. The more transverse coupling of A_1 to $\rho\pi$, the more would be needed for $h \to \rho\pi$ to compensate in the SCR. High statistics on the h would be useful for this reason, to facilitate a careful Dalitz plot analysis of $h \to 3\pi$.

The $Q_A(^3P_1)$ and $Q_B(^1P_1)$ kaonic resonances can mix with one another, and the mixing goes away when SU(3) becomes exact. This was pointed out long ago.[52] The way exact SU(3) implies no mixing can be visualized

by assuming the two "bare" states Q_A and Q_B mix via the real transitions[53]

$$Q_A \rightarrow \pi K^* \rightarrow Q_B \qquad (22a)$$

and

$$Q_A \rightarrow K\rho \rightarrow Q_B \qquad (22b)$$

In the exact SU(3) limit the contributions of (22a) and (22b) cancel one another because of the (f-type, d-type) coupling to (Q_A, Q_B). An estimate of the mixing potential induced by SU(3) breaking in the phase space factors alone then can be made, but its effect will depend on the spacing of the "bare" levels. More studies of the Q region, especially with regard to separation of diffractive "background" (if any) are needed, but the problems are at least as great as those of the A_1.

The D meson[22] is one's best argument in favor of non-diffractively-produced $J^{PC} = 1^{++}$ states at the moment. Its continued good health is essential to that of the quark model. Recently its $\rho\pi\pi$ mode has been reported.[3]

The study of the D is crucial to that of its nonet partner, the as yet unconfirmed D'.[23,26] Both duality schemes[21,54] and the Gell-Mann-Okubo mass formula suggest the D is predominantly an I = Y = 0 octet member. The D' is then an SU(3) singlet, may lie low,[23] and may couple even more strongly than the D to nonstrange systems. The possibility has been raised[23] that it overlaps the η', at least given current experimental resolution, and has similar decay modes (except $\gamma\gamma$), thereby explaining the "M(953)" effect of Ref. 26 (see section on 0^- states). If this guess is correct, one should look for a D' in reactions where a D is produced.

The relaxation[23] of superconvergence schemes[42] necessary to accommodate $D \epsilon \underset{\sim}{8}$, $D' \epsilon \underset{\sim\sim}{1}$ is relatively minor, but it has the following beneficial effects:

(a) D(1285) $\rightarrow \delta\pi$ is no longer forbidden, but a width of some 35-40 MeV is predicted instead.

(b) $\delta \rightarrow \eta\pi$ is no longer forbidden.

(c) One is no longer tied to the prediction of an unseen D(1070)

degenerate with the $A_1(1070)$.

The exact mass of the D' predicted in Ref. 23 depends on whether $\Gamma(A_1^{\text{transverse}} \to \rho\pi)$ is small as predicted in Ref. 42, and comes out around 950 MeV only when the minimal extension of this model is made, namely:

Gilman-Harari:		Rosner-Colglazier:
$X^o(960)$	$\nearrow$	$\eta'(960) \in \underset{\sim}{1}$
	$\searrow$	$\eta\ (550) \in \underset{\sim}{8}$
$D(1070)$	$\nearrow$	$D(1285) \in \underset{\sim}{8}$
	$\searrow$	$D'(950) \in \underset{\sim}{1}$

The arrows indicate that the weight of the state on the left in the SCR is divided according to quark model couplings among the pair of states on the right. If $\Gamma(A_1^{\text{Tr}} \to \rho\pi) \neq 0$, the D' mass comes out smaller. On the other hand, the contributions of states such as B and f_o should then be taken into account as well; they involve a considerable extension of the algebraic structure of the model. Such extensions are probably desirable. First, however, comes the experimental confirmation of the missing D'!

The unlikely possibility[22] that E(1420) has $J^P = 1^+$ should also receive further study, although such a high-mass state does not "repair" the SCR properly.

1^{+-} states: B , Q_B, (h?), (h'??) ($^1P_1$)

The B meson has some D wave in its $\omega\pi$ decay, leading to a predominance of the transverse coupling.[2,40] Again, this is in contrast to the $SU(6)_W$ prediction,[40] and again (as in A_1 decay) one expects[40] $SU(6)_W$ to be broken in this manner. The reason is that (transverse/longitudinal) coupling ratios depend on the ratio of S wave to D wave amplitudes. This ratio is predicted by $SU(6)_W$ without due respect

for barrier factors,[55] but it is also predicted with the wrong sign. A simple model of meson decays as proceeding via creation of a $q\bar{q}$ pair with quantum numbers of the vacuum[56,40] leads to one degree of freedom more than $SU(6)_W$. This extra parameter is precisely the S/D ratio.

The D wave piece of $B \to \omega\pi$ is noticeable in contrast to that for $A_1 \to \rho\pi$ both because of the Clebsch-Gordan coefficients of the model and because $m_B > m_A$ so that centrifugal barrier suppression is less extreme.

Further experiments on the D wave component of $B \to \omega\pi$ are needed at different energies in view of differing conditions of background. (At present the cleanest data are in $\pi^- p \to \pi^-\pi^-\pi^o\pi^+ p$ and 5 and 7.5 GeV/c.[57])

The Q_B has already been mentioned as mixing with the Q_A. By analogy with the B, one might expect it to be produced non-diffractively. The h (as distinct from the non-existent[2,58] H) has recently appeared around 1010 MeV in 3π spectra,[3] and deserves further study (as mentioned above). However, there is no sign of a corresponding partner of higher mass (h'). If such a state were made predominantly of $s\bar{s}$ it could not decay to $\rho\pi$, and its most likely mode would be $K^*\bar{K}+\bar{K}^*K$. It could be the state seen in Ref. 45, for example, for which $J^{PC} = 1^{+-}$ is a possibility.[59] Alternatively, it could be degenerate with the E(1420), leading to confusion in claims for the J^P of this state. (The favored J^P of E(1420) is 0^-, and at least one $C = +$ state is present at this mass since the decay $K_1^oK_1^o\pi^o$ is seen.[60])

0^+ states: δ, $K_N(?)$, $\sigma(700)$, S^* (^3P_o)

Repeated attempts to confirm the narrow $\delta(962)$[61] have failed, the most recent being the observation of a broader such state[62] in an experiment where the narrow state was claimed:[63] $pp \to d(MM)^+$. That there seems to be a broader state, decaying to $\eta\pi$, at or slightly above this mass, seems quite likely however.[64] We shall denote this particle by δ; a synonym is "$\pi_N(980)$". (The narrow δ may exist as well, of course.)

The possibility of a $K\pi$ S-wave resonance (K_N) somewhere between

900 and 1200 MeV still remains in question[3]. One might expect such a state to be separated in (mass)^2 from the δ by the universal such separation: $M_K^2 - M_\pi^2 \simeq M_{K^*}^2 - M_\rho^2 \simeq M_{K^{**}}^2 - M_{A_2}^2 \simeq 0.2$ to 0.3 GeV^2. Arguments for such a separation follow from pictures of symmetry breaking in the quark model.[9-11] However, the data do not seem to have converged much since our optimism of 1968![2] The status of the σ is only marginally better experimentally. It is probably better to rely on various theoretical pictures[17,42,65,66] which predict that there should be an I = Y = 0 object with $J^{PC} = 0^{++}$ around $m_\sigma \simeq m_\rho$.

The $S^*(1060)$, an S-wave $K\bar{K}$ effect with I = Y = 0, also has not been pinned down conclusively, with vast differences in its quoted width.[22,67]

Schemes of broken $SU(6)_W$ which decouple the relative D wave and S wave decays of the $q\bar{q}$; L = 1 mesons to 1^-0^- or 0^-0^- pairs nonetheless relate the S wave decays to one another. In particular a narrow $\pi_N(980)$ ($\Gamma \lesssim 20$ MeV) and broad A_1 ($\Gamma > 200$ MeV) would be incompatible with such a picture.[40]

"Superfluous" states

As all of the I = 1, Y = 0 states of $q\bar{q}$; L = 1 have been associated with claimed effects, the possibility of additional such states in the 1 to 1.5 GeV region[22] should be viewed with particular interest. Not one such claim seems to have survived at present.[68] The existence of such states (possibly considerably narrower than those just described) is one possible solution[69] to the problem of duality in baryon-antibaryon scattering,[70] but such "exotics" may lie above $B\bar{B}$ threshold or may be absent altogether. This latter possibility would say duality is badly broken in $B\bar{B}$ scattering, as it seems to be in other reactions with high thresholds which are likely to be very inelastic.[21]

Similar remarks hold for the $K_N(1260)$ resonance reported at Kiev,[3] if both it and a $K_N(1080)$[2] were found to exist. High-statistics $K\pi$ spectra may be quite rich in effects, or they may wash out fluctuations! The question is by no means settled at present.

The $F_1(1540)$[3,22] seems to lie on the borderline between the $q\bar{q}$;

L = 1 and $q\bar{q}$; L = 2 mesons. Its J^P is probably 1^+ or 2^-; if the former, it is "superfluous". If the latter, one also has a puzzle. The claim that its neutral mode has been identified in $p\bar{p}$ annihilations suggests that if $J^P = 2^-$, $C = +$.[45] This would mean $G(F_1(1540)) = -$. Is this the same as the "$\pi_A(1640)$"[22]? Partical-wave $\rho\pi$ analyses suggest that this may indeed be the case, with the $J^P = 2^-$ $\rho\pi$ spectrum peaking below 1600 MeV.[51] However, (a) the $f\pi$ spectrum peaks above 1600 MeV,[51] and (b) the $F_1(1540)$ is supposed to be narrower than the $\pi_A(1640)$. There is no room for two I = 1, Y = 0, $J^{PC} = 2^{-+}$ mesons in the conventional quark model.

The alternative suggestion $G(F_1) = +$ would lead us to look for a $\pi\omega$ mode, as yet unobserved.

The only candidate for a "radial excitation" state is the E(1420) with probable $J^{PC} = 0^-$.[60] Its pion-like companion might lie lower and could decay to $\rho\pi$ and $\sigma\pi$. It is interesting that 3π partial-wave analyses[51,71] in $\pi^- p \to (3\pi)^- p$ show a large 0^- component around 1300 MeV which cuts off sharply somewhere above 1400 MeV. This effect bears watching, though it is not clear how one would ever identify it as a resonance.

2. Baryons as qqq;L

Here the statistics problem of quarks enters: as fermions, they would have to lie in a totally antisymmetric ground state, whereas the harmonic oscillator classification scheme prefers a symmetric state. We shall assume the latter to be the case; an important point of principle is thus glossed over, but we have nothing new to add on this score.[72]

L = 0

$\underset{\sim}{8}$ $1/2^+$ states: N, Λ, Σ, Ξ ($^{1/2}S_{1/2}$)

A cautionary note about taking quark model dynamics too seriously comes from its prediction $|G_A/G_V| = 5/3$, which is modified substantially as soon as configuration mixing[73] is introduced. This mixing affects

the quark model (or $SU(6)_W$) prediction[74]

$$(f/d)_{1/2+ \to 0^- 1/2+} \simeq 2/3 \qquad (25)$$

very little, which is fortunate since such values inferred from the axial vector currents of $1/2^+$ baryons agree very well with this prediction at present.[22]

$\underset{\sim}{10}$ $3/2^+$ states: Δ, Y_1^*, Ξ^*, Ω^- ($^{3/2}S_{3/2}$)

New things include a larger width for $\Xi^* \to \Xi\pi$ agreeing better with SU(3),[5] and the observation of the $\overline{\Omega}^+$.[75]

L = 1

$\underset{\sim}{8}$ $5/2^-$ states: N(1680), Λ(1830), Σ(1765), Ξ(1930) ($^{3/2}P_{5/2}$)

This multiplet requires more work on its S = -2 member, whose J^P is by no means certain.[76] The multiplet has $f \simeq -0.2$,[5,22,74] whereas $SU(6)_W$ would predict f = -1/2, but no gross violations of SU(3) have been demonstrated.[5]

$\underset{\sim}{8} + \underset{\sim}{1}$ $3/2^-$ states: N(1520), $\Lambda\begin{Bmatrix}1520\\1690\end{Bmatrix}$, Σ(1660), Ξ(1820) ($^{1/2}P_{3/2}$)

The Λ states of this multiplet mix strongly with one another.[5] The multiplet would have f = 5/8 in $SU(6)_W$,[77] and present fits[5,22] are not far from this. Unfortunately there are (i) another $3/2^-$ $\underset{\sim}{8}$ and (ii) a $3/2^-$ $\underset{\sim}{10}$ predicted in the qqq; L = 1 picture, whose states may be admixed into those just quoted, and the precise identification of $3/2^-$ resonances corresponding to all these slots, i.e.

$3/2^-$ states:		
$(\underset{\sim}{1}, \underset{\sim}{8}, \underset{\sim}{8}, \underset{\sim}{10})$	Δ	one
	N	one
	Λ	three
	Σ	three
	Ξ	three ,

(26)

will be needed before the mixing problem can be sorted out in a satisfactory manner. It is the likelihood of complications such as these that make the baryon resonances much harder to study than the mesons, even though for baryons one can make better use of the enormously powerful techniques of phase shift analysis.

$\underset{\sim}{8}$ $3/2^-$ N(claims), $\Lambda(?)$, $\Sigma'(1660)?\Xi?(^{3/2}P_{3/2})$

It does not seem we have made much progress in the study of these states since 1968.[2] A possible exception is the claim for a second $\Sigma(1660)$.[5] The Σ member of the present multiplet should have very different $f(f \simeq -1/2)$ by $SU(6)_W$ considerations than that of the previous multiplet, and in particular should have a large $\bar{K}N$ coupling. (The Λ member should almost decouple from $\bar{K}N$.) This difference and others point out the importance of studying all inelastic channels (including three-body ones[5,78]) when sorting out hyperon resonances.

$\underset{\sim}{8} + \underset{\sim}{1}$ $1/2^-$ $N(1530); \Lambda\begin{Bmatrix}1405\\1670\end{Bmatrix}$, $\Sigma(1730)$, Ξ ? $(^{1/2}P_{1/2})$

The rate for $N(1530) \to N\eta$ has recently come down, reducing a previous discrepancy with SU(3).[5]

$\underset{\sim}{10}$'s $3/2^-$, $1/2^-$ (Δ's available) $(^{1/2}P_{3/2}, {}^{1/2}P_{1/2})$

The $\underset{\sim}{10}$, $3/2^-$ multiplet is of interest since its coupling to $0^-1/2^+$ is very weak, both experimentally and in duality schemes.[21,79] It is therefore a prime object for study in inelastic phase shift analyses.[78] At the same time, its weak coupling to the elastic channel will mitigate the complexity of the situation depicted in Eq. (26) somewhat.

3. Quark model and higher spins.

Mesons

Some evidence for rising meson Regge trajectories has been accumulating slowly. The only firm example is the g meson[22], $J^P = 3^-$, a candidate for the recurrence of the $\rho(J^P = 1^-)$. The 2^- recurrence of the pion also may have been identified,[51] though there is not universal agreement on its properties at present. (See the discussion in Sec. 1 on the F_1, for example). A neutral three-pion state around 1680 MeV is consistent with being the 3^- recurrence of the ω.[80] Finally, in S = 0 systems one has the L,[51] a 2^- candidate for the recurrence of the kaon. The sequence of bumps in missing mass spectra[81] linear in $(\text{mass})^2$ requires observation of decay products and J^P analyses before it can be taken as evidence that meson trajectories rise any higher, though studies via $p\bar{p} \to \pi^+\pi^-$ and $p\bar{p} \to p\bar{p}$ have suggested that high meson spins are indeed present above $p\bar{p}$ threshold.[64]

I am surprised by the number of reviews which have claimed to understand the "R" region (the I = 1, Y = 0 mesons that would be formed of $q\bar{q}$; L = 2 : $J^{PC} = 3^{--}$, 2^{-+}, 2^{--}, 1^{--}). They differ from one another quite often! (Where does one put the F_1, for instance? Is it one of these?)

The discovery of a ρ-like state above 1500 MeV would have little to do with proving details of the dual $\pi\pi$ scattering model[17,82] correct (this model predicts a "ρ'" degenerate with f_o.) The point at issue is whether there are states which are "superfluous" from the standpoint of the quark model, and a ρ' below 1300 MeV would certainly be one of them. Any 1^{--} state above 1500 MeV fits most naturally into a $q\bar{q}$; $^3D_1$ classification (unless one can show there are two of them!)

The identification of the narrow bumps in the R region in missing mass spectra[81] with states of known decay properties[3,22,64] continues to be problematic.

Baryons

Recent phase shift analyses have suggested that linear Regge

trajectories may indeed exist for the baryons,[4,5] as shown by the sequences

$$N(\tfrac{1}{2}^+, \tfrac{5}{2}^+, \underline{\tfrac{9}{2}^+}) \tag{27}$$

$$\Delta(\tfrac{3}{2}^+, \tfrac{7}{2}^+, \underline{\tfrac{11}{2}^+}) \tag{28}$$

$$\Lambda(\tfrac{1}{2}^+, \tfrac{5}{2}^+, \underline{\tfrac{9}{2}^+}) \tag{29}$$

where the last (underlined) entry has been known as a bump for some time but claims for its J^P value have recently been registered.[4,5] The linearity of these trajectories in $(\text{mass})^2$ suggests a spectrum roughly like that of the three-particle harmonic oscillator, which was of course, the motivation for the discussion of the L = 0 and L = 1 qqq states of the previous section. If this is the case, it is of interest to confirm the additional degeneracy of the "n = 2" harmonic oscillator spectrum for baryons.[83] The low states are:

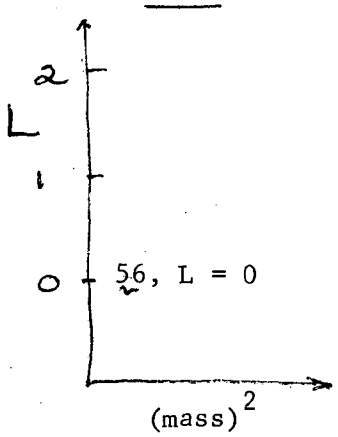

(30)

Certain duality schemes[21] seem not to require the states with question marks, so their confirmation is of particular interest in testing the quark model.

The 20 does not couple to 35 (0^- or 1^- mesons) x 56 ($1/2^+$ or $3/2^+$ baryons) and thus is not accessible in formation experiments. In this respect it is at least as hard to study as a boson multiplet. Both 70, L = 2 and 70, L = 0, however, should definitely be visible. The states they contain are:

70, L = 2:

$$\underset{\sim}{10}\text{'s: } 5/2^+,\ 3/2^+ \tag{31}$$

$$\underset{\sim}{8}\text{'s; } f \simeq -1/2\text{: } 7/2^+,\ 5/2^+,\ 3/2^+,\ 1/2^+ \tag{32}$$

$$g(N\bar{K}\Lambda) \simeq 0$$

$$\underset{\sim}{8}\text{'s; } f \simeq +1/2 : 5/2^+ ,\ 3/2^+ \tag{33}$$

$$g(N\bar{K}\Sigma) \simeq 0$$

$$\underset{\sim}{1}\text{'s} : 5/2^+ ,\ 3/2^+ \tag{34}$$

70, L = 0:

$$\underset{\sim}{10} : 1/2^+ \tag{35}$$

$$\underset{\sim}{8} ; f \simeq 1/2 : 3/2^+ \tag{36}$$

$$\underset{\sim}{8} , f \simeq -1/2 : 1/2^+ \tag{37}$$

$$\underset{\sim}{1} : 1/2^+ \tag{38}$$

The states associated with the $\underset{\sim}{56}$, L = 2 and $\underset{\sim}{56}$, L = 0 multiplets (already partially filled[2]) are

56, L = 2

$$\underset{\sim}{10}\text{'s} : 7/2^+,\ 5/2^+ ,\ 3/2^+ ,\ 1/2^+ \tag{39}$$

$$\underset{\sim}{8}\text{'s} : 5/2^+ ,\ 3/2^+ \ (f \simeq 1/2) \tag{40}$$

56, L = 0

$$\underset{\sim}{10} : 3/2^+ \tag{41}$$

$$\underset{\sim}{8} : 1/2^+ \ (f \simeq 1/2) \tag{42}$$

There are several characteristic positive-parity states which must belong to the group (31)-(38) and not to (39)-(42):

(1) An $I = 1/2$, $J^P = 7/2^+$ πN resonance (F_{17} in phase shift terminology). A claim for this state exists.[22] It should couple very weakly to $\bar{K}\Lambda$; much more strongly to $\bar{K}\Sigma'$.

(2) Any $J^P = 7/2^+$ Λ state. It should couple only weakly to $\bar{K}N$.

(3) Any Λ state coupling weakly to $\bar{K}N$ but strongly to other $0^-1/2^+$ channels. This would indicate $f \simeq -1/2$, a distinctive property of some $\underset{\sim}{70}$ octet members.

(4) Highly inelastic decimets (cf. $\underset{\sim}{70}$, $L = 1$ case).

(5) Any $I = 1/2$ N^* states coupling more to $\bar{K}\Sigma$ than to $\bar{K}\Lambda$ ($\Longrightarrow$ $f \underset{\sim}{\simeq} -1/2$).

These are only examples; others depend on sorting out <u>definite signs</u> of inelastic amplitudes by means of interference techniques[84] in phase shift analyses. One notices that several of the above predictions depend on one's observing a given resonance to <u>decouple</u> from the elastic channel. It is a pecularity of the SU(6) f-values[74] that they tend to make certain states decouple from $\bar{K}N$, but <u>not</u> characteristically from $\pi\Sigma$ or $\pi\Lambda$ (Σ states with $f \simeq -1/2$ have a larger $\Lambda\pi/\Sigma\pi$ branching ratio than do Σ' states with $f = 1/2$, however). <u>What we learn from formation experiments may not be the whole story with respect to the existence of $\underset{\sim}{70}$, $L = 2$ or 0 multiplets</u>, therefore. This can be redressed in part by emphasis on inelastic channels with high statistics experiments,[85] as the decoupling just mentioned is usually not exact.

4. <u>Quark Model "dynamics"</u>

We have already discussed this subject to some extent with respect to the mesons.[40] The question is to what extent clear-cut violations of $SU(6)_W$ can be demonstrated in those decays where two partial waves can and do contribute. Some of these are listed below.

DECAY	$SU(6)_W$ PRED.	P.W.RATIO SPECIFIED	EXPT.
$A_1 \to \rho\pi$	$J_z = \pm 1$	D/S	Mostly S wave; SLAC: D/S opp. sgn. to $SU(6)_W$
$B \to \omega\pi$	$J_z = 0$	D/S	D/S opp. sgn. to $SU(6)_W$
$D_{13}(1520) \to \Delta\pi$	$J_z = \pm 1/2$	D/S	?
$F_{15}(1688) \to \Delta\pi$	$J_z = \pm 1/2$	G/D	?
$\Delta(1950) \to \Delta\pi$	$\frac{\Gamma(J_z=\pm 3/2)}{\Gamma(J_z=\pm 1/2)} = 9$	H/F	?

(43)

The most reasonable result to expect is that the lower of the two partial waves will dominate in each of the last three processess in Eq. (43). However, it would be amusing if a small admixture of the higher partial wave were found to enter with relative sign opposite to the prediction of $SU(6)_W$, as seems to be indicated for the two meson decays listed. Again precise inelastic partial wave analyses are needed for the answer.

5. Exotic Baryons

The symmetric quark model is in some trouble if the lowest $qqqq\bar{q}$ objects do not have negative parity, as one might expect from a relative S-wave wavefunction. Most indications for Z*'s favor positive-parity effects if any.[5,19] One should recall the prediction of the strong-coupling theory[86] that P-wave $0^- - 1/2^+$ resonances lie in the ascending order:

$$(\underset{\sim}{8},1/2^+),\ (\underset{\sim\sim}{10},3/2^+),\ (\underset{\sim}{\bar{10}},1/2^+),\ (\underset{\sim\sim}{27},3/2^+),\ldots. \tag{44}$$

with average $\underset{\sim}{\bar{10}}$ and $\underset{\sim\sim}{27}$ masses probably below 2 GeV. Other predictions of positive-parity Z*'s exist.[15] Predictions of negative-parity

Z_o*'s include those based on consideration of the double pion-exchange Born term for

$$K^+n \to K^*N \to K^+n \tag{45}$$

The opening of the K*N inelastic channel is claimed to "drive" the $D_{3/2}$ and $S_{1/2}$ waves through resonance.[87] A similar mechanism for generation of $\Xi^*_{3/2}$ resonances would have to rely heavily on kaon exchange (short-range) so that it is not clear such resonances would be predicted at all by the model. One thus has the possibility of incomplete SU(3) multiplets for exotics.

The parity of the lowest Z*'s (if any exist) is thus of central theoretical importance.

Certain quark model selection rules[88] (based on duality) predict that if Z*'s exist, they are highly inelastic. A decisive test of this should be possible in the I = 0 channel, where one hint of a Z* is claimed to involve a bump in σ_{el}. The selection rules[88] fail to predict that n and p form a deuteron (they forbid high-rising elastically coupled trajectories of np resonances), so a similar isolated failure for the I = 0 K^+n system might be excusable (to be understood on the grounds of corrections to the selection rules via loop diagrams.[88])

For reference, the rules forbid all trilinear couplings of hadrons in which (a) each pair of hadrons is not connected by at least one quark line, or (b) a quark line begins and ends in the same hadron. I do not understand the dynamical basis of these rules in a satisfactory way at present, but they are tremendously compelling empirically.

6. Exotic Mesons

Mesons made of $qq\bar{q}\bar{q}$ ("M_4") are needed to "build" t-channel $q\bar{q}$ exchanges in baryon-antibaryon scattering if exact duality between poles in s and poles in t holds.[70] This question is independent of whether such objects may appear at low masses, as was speculated to hold purely on the basis of the A_2 splitting.[69] If the A_2 is not split,[46] there is no compelling reason for such mesons to lie so low

in mass. They should not lie much above baryon-antibaryon threshold, however, in any case.[69,70] One thus has to search only the region below about 3 GeV for such mesons, preferably via their couplings to baryons in annihilation processes[70,88,89] or backward scattering[88-90]. Another possibility, of course, is that M_4 mesons of ordinary I, Y could be produced diffractively: we do not understand the quark structure of the Pomeranchukon, so no objections to this occur in principle. The processes

$$M_4 \to M_4' M_2 \tag{46}$$

could then lead to states of unusual I, Y.

The complete absence of M_4 states would indicate that duality is badly broken for high-threshold processes, a possibility which has been suggested.[21]

Low-lying mesons of exotic I, Y (below $\simeq$ 1500 MeV) are almost certainly not present.[3,18] Rapid fall-offs of cross sections with increasing energy for such reactions as $\pi^- p \to K^+ \Sigma^-$ place bounds on the existence of some higher-mass states, depending on their couplings to the particles involved, by the lack of their exchange.

The selection rules of Ref. 88, however, predict <u>weak</u> couplings of exotics to the meson-meson system, so that more meaningful bounds follow from the process

$$\bar{p}p \to \bar{\Sigma}^+ \Sigma^- \tag{47}$$

The experimental fall-off as $s^{-6.5\pm2}$, compared with that of

$$\bar{p}p \to \begin{cases} \bar{\Lambda}\Lambda \\ \bar{\Lambda}\Sigma^\circ + \bar{\Sigma}^\circ\Lambda \\ \bar{\Sigma}^- \Sigma^+ \end{cases} \tag{48}$$

as $s^{-1.5}$, indicates that $\alpha(0)$ for any exotic trajectory contributing appreciably to process (47) lies at least 1.5 units below the corresponding non-exotic value in (48). In view of the entirely

reasonable likelihood that Regge cuts may contribute in process (47), one must view this as only an upper bound on $\alpha_{exotic}(0):\alpha(0) \lesssim -1.3$.

It is quite likely that the leading exotic trajectories would correspond to $qq\bar{q}\bar{q}$; $S_q = 2$, $L = 0$, $J = 2$ in the same manner as for the leading non-exotic ones $q\bar{q}$; $S_q = 1$, $L = 0$, $J = 1$. The bound just quoted then indicates that it is probably not worthwhile looking for any $I = 3/2$, $|Y| = 1$ meson below 1800 MeV.

A recent study of inclusive reactions[92] in the processes

$$A + B \rightarrow C + (\text{anything}) \tag{49}$$

predicts s dependence in the approach to a universal sealing law when $AB\bar{C}$ is non-exotic but no such dependence when $AB\bar{C}$ is exotic. This allows one to extend one's repertoire of total cross section measurements to targets composed of $B\bar{C}$ and to check Lipkin's rule for the energy dependence of such total cross sections. The rule[93] states that $\sigma_T(XY)$ falls whenever a quark in Y can be "eaten" by the corresponding antiquark in X. It was the original motivation for duality graphs,[94] and predicts correctly the cases listed below.

σ_T falling as $s \rightarrow \infty$	σ_T flat as $s \rightarrow \infty$
π^+p, K^-p, K^-n,	pp, pn, K^+p, K^+n,
$\bar{p}p$, $\bar{p}n$, ρp, ωp, γp	ϕp

(50)

The identification of such energy dependence with direct channel resonance effects[95] would lead one to expect[70] exotic resonances in (e.g.) the $\bar{\Sigma}^+p$ channel, where Lipkin's rule predicts energy dependence in σ_T. (To confirm the rule in further cases it would be interesting to check the energy dependence of $\sigma_T(\Lambda p)$, predicted to be flat. A measurement of this quantity to 5% or 10% would probably be able to give us further information about SU(3) breaking in the Pomeranchukon, available at present only from meson-nucleon total cross sections.)

Total cross sections such as $\sigma_T(\bar{\Sigma}^+p)$ are clearly unmeasurable, but

processes (49) allow one to check a host of exotic channels where Lipkin's rule and therefore duality graphs would predict energy dependence. Some of these channels are listed in Eq. (51). The entries denote particles C in reaction (49):

A / B	π^+	π^-	K^+	K^-	p
p	$n, \Lambda, \Sigma^0, \Xi^0$	Ξ^0, Ξ^-	Λ, Σ^+, Ξ^0	—	—
n	Ξ^0, Ξ^-	$p, \Lambda, \Sigma^0, \Xi^-$	Λ, Σ^+, Ξ^0	p, Σ^+	$\pi^+, K^+, \bar{K}^0$

(51)

with additional possibilities suggested by isospin rotations. If the distribution function[92] for (say) $\pi^- n \to p +$ (anything) were to show the s dependence characteristic of non-exotic channels, this would confirm Lipkin's rule in a much wider context than its present domain of validity (Eq. (50)). Assuming exact duality,[70] such behavior would also be indirect evidence for exotic mesons.

7. Predictions of duality

Here we make only a few brief remarks, as the field has been well-reviewed.[54]

(a) π-B exchange degeneracy. This follows from applying duality to the process $0^-1/2^+ \to 1^-1/2^+$. The t-channel trajectories are assumed to have cancelling imaginary parts for exotic s-channels. One can separate out various types of exchange, among them the π-B type. This particular degeneracy relates the production phases of ρ and ω (for $J_z = 0$ in the t channel) in such a way that the spectacular interference effects mentioned in Sec. 1 are correctly predicted.[33] Similar considerations apply to $\rho_\infty \frac{d\sigma}{dt}$ in

$$\pi^- p \to \left\{ \begin{matrix} A_2^0 \\ f_0 \end{matrix} \right\} n \tag{52}$$

$$\pi^+ p \to \left\{ \begin{matrix} A_2^0 \\ f_0 \end{matrix} \right\} \Delta^{++} \tag{53}$$

where the interference can be studied in great detail via the K^+K^- and $K_1^oK_1^o$ decay modes of the bracketed resonances.[7]

(b) Baryons. The f/d ratios mentioned earlier follow to some extent from duality in backward meson-baryon scattering[21,77] (further sources in Refs. 54 and 89). The pattern for the leading baryon trajectories is such that octets with $J^P = 5/2^-, 9/2^-, \ldots$ have $f \simeq -1/2$ while those with $J^P = 3/2^-, 5/2^+, 7/2^-, \ldots$ have $f \simeq 1/2$. The consequences of these values have been mentioned in Sec. 2 : $f \simeq -1/2$ makes $g(NK\bar{\Lambda}) \simeq 0$, while $f \simeq 1/2$ makes $g(NK\bar{\Sigma}) \simeq 0$.

(c) Mesons. A picture of "broken duality"[21] allows one to discard high-threshold constraints, such as those derived from VV → VV that would make the π and the η' degenerate. One is left with

$$\text{Nonets: } J^{PC} = 1^{--},\ 2^{++},\ 1^{+-},\ 2^{--}$$

$$\text{Octets: } J^{PC} = 0^{-+},\ 1^{++} \qquad (54)$$

in accord with experiment. The possibility[23] that the 1^{++} SU(3) singlet, unconstrained by duality, may have $M \simeq 950$ MeV and decay modes $\pi\pi\gamma$, $\pi\pi\eta$ has already been discussed in Sec. 1. The predicted nonet structure of the $J^{PC} = 1^{+-}$ multiplet does not seem to hold if the h (1010) (see Sec. 1) is the partner of the B(1235). However, if one breaks SU(3) from the start in processes

$$\begin{array}{ccc} 0^- & & 1^- \\ & \rightarrow & \\ 1^- & & 0^- \end{array} \qquad (55)$$

and considers the $P = -(-)^J$ exchanges in $\pi^+ f^+ \rightarrow \rho^+ \pi^+$, one finds that the π and the h ($J^{PC} = 1^{+-}$, I = 0) must be exchange degenerate,[96] which is not a bad prediction in light of the claim for h(1010) mentioned in Sec. 1.

8. Scale invariance and 0^+ states.

The suggestion has been made that a useful symmetry limit is that

in which, in addition to chiral SU(3) x SU(3), one has dilatation invariance by virtue of the existence of an SU(3) singlet, $J^{PC} = 0^{++}$ (Goldstone) boson of zero mass.[97] As symmetry breaking is turned on, the dilatation invariance and SU(3) x SU(3) are broken simultaneously. What this means is that one need not have an "ideal" 0^+ nonet with one I = Y = 0 member (σ?) degenerate with the I = 1, Y = 0 member (δ?). The "bare" SU(3) singlet starts out (before breaking) at zero mass, far from the mass of the "bare" ^3P_o octet. What is remarkable is that the singlet shift is so large compared to octet shifts; the mass of the σ is probably not very far below that of the δ. Apparently this effect is predicted satisfactorily.[98]

The claims for an $S^*(1060)$ and a $K_N(1080)$ cannot be associated with two members of the same "nonet" no matter what the mixing between octet and singlet, as long as the "bare" singlet has mass less than the "bare" octet as just mentioned. It is popular[98] to believe in the quoted mass of the $S^*(1060)$ and discard the claims[22] for an S-wave $K\pi$ resonance above this mass. We only note that the proximity of the S*(1060) to $K\bar{K}$ threshold could be responsible for misinterpretation of its parameters (for example, the possibility of a large scattering length is apparently not ruled out.[22])

It is therefore of <u>prime importance</u> to determine the mass of any S-wave $K\pi$ resonance in some model-independent way, and to cast further light on the exact nature of the S* effect. (See Sec. 1 regarding the expected magnitude of SU(3) breaking for 0^+ mesons).

The possibility of an S-wave I = 0 $\pi\pi$ resonance <u>appearing</u> to be much lower in mass than 700 MeV in inelastic reactions[99] (i.e. those other than off-mass-shell $\pi\pi$ scattering) has recently been suggested.[100] The motivation comes from writing the partial-wave amplitude as

$$t_{\pi\pi}^{I=J=0} = t_{\pi\pi}^{C.A.} / D_{\pi\pi}^{I=J=0} \qquad (56)$$

to unitarize[66,101] the current-algebra[102] $\pi\pi$ result $t_{\pi\pi}^{C.A.}$. Since $t_{\pi\pi}^{C.A.}$ has a zero very near threshold, and therefore an appreciable slope in s, $D_{\pi\pi}^{I=J=0}$ acquires a similar energy dependence. For inelastic processes such as $\gamma\gamma \to \pi\pi$[100] in which the numerator function has <u>no</u> current-

algebra zero near threshold the net result of the skewing in D is to weight the mass spectrum strongly toward low $m_{\pi\pi}$. This may be responsible for effects such as those reported in Ref. 99. Certainly the fundamental nature of the breaking of dilatation invariance[97,98] demands that the whole 0^+ "nonet" receive much further study.

9. Uses of high statistics and resolution

Production mechanisms require the measurement of $\rho_{ij} \frac{d\sigma}{dt}$, and to learn about possible distortions of Breit-Wigner shapes (e.g. ρ-ω or f_o-A_2 interference, see above) one must measure

$$\rho_{ij} \frac{d^2\sigma}{dm\, dt} \tag{57}$$

where m is the effective mass. As an example, to study f_o-A_2 interference in (say)

$$\pi^- p \rightarrow K^+K^- n \tag{58}$$

one probably needs 5000 events:

$$\begin{array}{lll} 20 & 20\ \text{MeV} \quad \text{bins} & 1100\text{-}1500 \text{ in m} \\ 5 & 0.1\ \text{GeV}^2 \text{ bins} & 0\text{-}0.5 \text{ in } |t'| \\ 50 & \text{Events / [20 MeV} \times \text{0.1 GeV}^2\text{] for } \rho_{ij} & \end{array} \tag{59}$$

The payoff is in learning branching ratios very precisely and in testing whether the apparent stability of interference between ρ and ω carries over to their 2^+ partners. This is only an example of the type of experiment one could perform with such statistics, of course.

Phase shift analyses in mesonic channels[51] would also benefit greatly from such improvements. An important question is whether there are really two 1^+ states in the "Q" bump, possibly with small amounts of D wave decay for $K^*\pi$.[40] The whole A_1 question, it seems, will only be settled in the backward direction[47,48] where partial-wave analyses will again be necessary.[103] A "Deck-type" background is

claimed to be expected, but it apparently will not have $J^P = 1^+$.[103] The A_1 may have substructure,[104] to add to our troubles. Again, high resolution and overwhelming statistics (to allow for t cuts) will be of great help in resolving such questions.

10. Conclusions

The quark model states are represented by several solid resonances which suggest a definite overall pattern more extensive than that of SU(3). Much of this pattern remains to be filled out, however, if we are to place any faith in even the taxonomic aspects of the quark model (the symmetry SU(6) x O(3)).

Many theories predict mesonic states in addition to those of the $q\bar{q}$; L picture[2,70,105]. These theories should be tested regardless of whether the A_2 is split, as they do not require this feature. Indeed, they are powerless to predict a degeneracy of the type "A_2-A_2'" without additional assumptions. (The degeneracy would seem to be a more essential feature of some other approaches.[106]) The additional states could easily be manifested as narrow resonances (produced with small cross sections). To distinguish present claims for these[22] from statistical fluctuations one needs considerably better data than available at present. This is not an unreasonable request: compare the primitive state of elementary particle spectroscopy to that of molecules, atoms, and nuclei!

We are probably some distance from a "Bohr Theory" of the hadrons: by comparison, optical spectra were painstakingly studied for a hundred years before Bohr. The real satisfaction in such work must have come from such breakthroughs as that of Michelson, who first saw the hydrogen fine structure using interferometric techniques.[107] (Fine structure in the sodium D lines dates back to Fraunhofer,[108] the father of optical spectroscopy).

I hope we are in for similar satisfaction as we continue to fill in the developing pattern of the strongly interacting particles.

References

1. See, e.g. Martin J. Klein, Paul Ehrenfest, Amsterdam and New York, North-Holland Publishing Co., 1970.
2. H. Harari, in Proceedings of the XIV International Conference on High Energy Physics, Vienna, 1968, eds. J. Prentki and J. Steinberger, Geneva, CERN, 1968, p. 195.
3. A. Astier, in Proceedings of the XV International Conference on High Energy Physics, Kiev, 1970, Moscow, Atomizdat, to be published. (Mesons).
4. R. Plano, Kiev, Conf. op. cit. (S = 0 baryons).
5. N. P. Samios, Kiev Conf. op. cit. (S $\neq$ 0 baryons).
6. In the three weeks since I was asked to prepare the present review I have also had to cope with considerable new data on the A_2 in preparing a review of that subject.
7. J. Rosner, "Theoretical Remarks on the A_2 Meson," CalTech Phenomenology Conference, 25-26 March, 1971 (to be published).
8. M. Gell-Mann, Phys. Lett. 8, 214 (1964).
9. G. Zweig, CERN preprints TH-401 and TH-412 (unpublished).
10. G. Zweig, in Meson Spectroscopy (1968 Phila. Meson Conf.), eds. C. Baltay and A. Rosenfeld, New York, Benjamin, 1968, p. 485.
11. R. H. Dalitz, in Meson Spectroscopy, op. cit., p. 497.
12. R. H. Dalitz, in Symmetries and Quark Models, ed. Ramesh Chand, New York, Gordon and Breach, 1970, p. 355.
13. See, e.g., S. Okubo, in Symmetries and Quark Models, op. cit., p. 59. We regard the question of whether decays such as $\pi^0 \to \gamma\gamma$ tell us about "bare charges" of quarks as essentially unsettled. All of our considerations will be insensitive to these "bare charges".
14. See, e.g., M. Y. Han and Y. Nambu, Phys. Rev. 139, B 1006 (1965).
15. O. W. Greenberg and C. A. Nelson, Phys. Rev. 179, 1354 (1969) (See esp. Table I.)
16. G. Veneziano, Nuovo Cimento 57A, 190 (1968).
17. C. Lovelace, Phys. Lett. 28B, 264 (1968).

18. J. Rosner, in Experimental Meson Spectroscopy (1970 Phila. Meson Conf.), eds. C. Baltay and A. Rosenfeld, New York, Columbia University Press, 1970, p. 499.
19. G. Goldhaber, in Hyperon Resonances-70, ed. Earle C. Fowler, Durham (N.C.), Moore Publ. Co., 1970, p. 407.
20. The author thanks P. Freund for this example.
21. J. Mandula, J. Weyers, and G. Zweig, Phys. Rev. Lett. 23, 266 (1969).
22. Particle Data Group, Rev. Mod. Phys., to be published.
23. J. Rosner and E. W. Colglazier, Phys. Rev. Lett. 26, 933 (1971).
24. D. Bollini, et al., Nuovo Cimento 58A, 289 (1968) and data presented at Bologna Meson Conference, April, 1971; E. Harvey, et. al., in Proc. of the Kiev Conference (1970), op. cit. and Bull. Am. Phys. Soc. 16, 111 (1971).
25. L. H. Chan, L. Clavelli, and R. Torgerson, Phys. Rev. 185, 1754 (1969).
26. M. Aguilar-Benitez, et.al., Phys. Rev. Lett. 25, 1635 (1970).
27. C. N. Yang, Phys. Rev. 77, 242 (1950).
28. A. N. Zaslavskii, V. I. Ogievetskii, and V. Tybor, Yad. Fiz. 9, 852 (1969) (Sov. J. Nucl. Phys. 9, 498 (1969)).
29. D. D. Coon and D. Geffen, to be published; D. D. Coon, private communication.
30. G. Goldhaber, in Experimental Meson Spectroscopy, op. cit., p. 59.
31. S. Hagopian, et. al., Phys. Rev. Lett. 25, 1050 (1970); S. Hagopian, et.al., Bull. Am. Phys. Soc. 16, 112 (1971).
32. D. W. G. S. Leith, CalTech Phenomenology Conference, op. cit.
33. A. Goldhaber, G. Fox, and C. Quigg, Phys. Lett. 30B, 249 (1969).
34. R. Aviv and S. Nussinov, Phys. Rev. D2, 209 (1970).
35. See, e.g., J. T. Dakin, et.al., Bull. Am. Phys. Soc. 16, 112 (1971).
36. M. Alston-Garnjost, et.al., Phys. Lett. 34B, 156 (1971).
37. M. Aguilar-Benitez, et.al., Phys. Rev. Lett. 25, 1362 (1970).
38. K. W. Lai, CalTech Phenomenology Conference, op. cit.
39. We make the familiar nonet ansatz for couplings whereby disconnected quark diagrams do not occur.
40. E. W. Colglazier and J. L. Rosner, Nucl. Phys. B27, 349 (1971).

41. The relations of Fig. 1 continue to be predicted in the model of broken $SU(6)_W$ adopted in this work, as they all involve D-wave decays. The breaking comes only in the comparison of D-wave and S-wave amplitudes, whose ratio is badly predicted by $SU(6)_W$.

42. F. Gilman and H. Harari, Phys. Rev. 165, 1803 (1968).

43. V. Barnes, et.al., Phys. Rev. Letters 19, 964 (1967).

44. The $\pi\pi$ system must have internal $\ell \geq 2$ and L with respect to the η of at least 1. The decay is strictly forbidden by quark model selection rules.

45. J. Duboc, et. al., Phys. Lett. 34B, 343 (1971).

46. M. Gettner, CalTech Phenomenology Conference, op. cit.; D. Bowen et.al., Phys. Rev. Lett., to be published. This is the only experiment which conclusively contradicts the splitting results (see Refs. 7 and 22), as variations with respect to charge state, s, and t would in principle be possible.

47. D. Garelick, in Experimental Meson Spectroscopy, op. cit., p. 205.

48. E. W. Anderson, et.al., Phys. Rev. Lett. 22, 1456 (1969).

49. J. Ballam, et.al., Phys. Rev. D1, 94 (1970).

50. D. J. Crennell, et.al., Phys. Rev. Letters 24, 781 (1970).

51. U. E. Kruse, in Experimental Meson Spectroscopy, op. cit., p. 359, and CalTech Phenomenology Conference, op. cit.

52. For a complete set of references, see Ref. 40.

53. One could also include the pair of intermediate states ($K\sigma$, $K_N\pi$), where K_N is an S-wave $K\pi$ resonance of unspecified properties (see section on 0^+ states.)

54. J. Mandula, J. Weyers, and G. Zweig, Ann. Rev. Nucl. Sci. 20, 289 (1970).

55. S. Meshkov, in Experimental Meson Spectroscopy, op. cit., p. 535.

56. L. Micu, Nucl. Phys. B10, 521 (1969).

57. D. Brockway, et.al., in Kiev Conf., op. cit; M. Ioffredo, private communication.

58. B. Chaudhary and E. Marquit, Phys. Rev. D2, 2110 (1970).

59. Then, the $\eta\pi\pi$ effect of Ref. 43 would have to come from something else, e.g. the $F_1(1540)$. (See Ref. 22).

60. P. Baillon, et.al., Nuovo Cimento 50A, 393 (1967).

61. W. Kienzle, et.al., Phys. Lett. 19, 438 (1965).
62. M. Abolins, in Experimental Meson Spectroscopy, op. cit., p. 171.
63. J. Oostens, et.al., Phys. Lett. 22, 708 (1966).
64. See the review by M. Derrick, in Proceedings of the Boulder Conference on High Energy Physics, 1969, eds. K. T. Mahanthappa, W. D. Walker, and W. E. Brittin, Boulder, Colo. Assoc. Univs. Press, 1969, p. 290.
65. S. L. Adler, Phys. Rev. 140, B736 (1965).
66. L. Brown and R. Goble, Phys. Rev. Lett. to be published.
67. W. Beusch, in Experimental Meson Spectroscopy, op. cit., p. 185.
68. See Ref. 18 for a brief list of these.
69. J. Rosner, Phys. Lett. 33B, 493 (1970).
70. J. Rosner, Phys. Rev. Lett. 21, 950, 1422(E) (1968).
71. D. Brockway, thesis, U. of Illinois, 1970 (unpublished).
72. For one review, see O. W. Greenberg, in Proceedings of the Lund International Conference on Elementary Particles, ed. G. von Dardel, Lund (Sweden), Berlingska Boktrykeriet, 1969.
73. See. e.g., H. Harari, Phys. Rev. Lett. 16, 964 (1966); Ibid., 17, 56 (1966), D. Horn, Ibid., 17, 778 (1966).
74. We take f+d = 1 in much of the subsequent discussion. In this notation $g(N\bar{K}\Lambda) = 0$ when $f = -\frac{1}{2}$ while $g(N\bar{K}\Sigma) = 0$ when $f = \frac{1}{2}$.
75. A. Firestone, et.al., Phys. Rev. Lett. 26, 410 (1971).
76. See the review by G. Yodh, in Symmetries and Quark Models, op. cit., for the general status of $\frac{1}{2}^-$ states. These are of tremendous interest, but difficult to study since they cannot be formed in the direct channel.
77. See, e.g., R. Capps, Phys. Rev. Lett. 22, 215 (1969).
78. R. Cashmore, this conference.
79. J. Rosner, Phys. Rev. Lett. 24, 173 (1970); J. Rosner, Phys. Rev. D1, 2701 (1970).
80. J. A J. Matthews, et.al., Bull. Am. Phys. Soc. 16, 112 (1971).
81. M. N. Focacci, et.al., Phys. Rev. Lett. 17, 890 (1966).
82. J. Shapiro, Phys. Rev. 179, 1345 (1969).
83. For a discussion of the harmonic oscillator spectrum of three particles, see R. L. Walker, in Proceedings of the International

Symposium on Electron and Photon Interactions at High Energy, Daresbury, 1969, eds. D. W. Braben and R. E Rand, Liverpool, Daresbury Nucl. Phys. Lab., 1969, p. 23; and G. Karl and E. Obryk, Nucl. Phys. B8, 609 (1968).

84. W. M. Smart, et.al., Phys. Rev. Lett. 17, 556 (1966); M. Ferro-Luzzi, et.al., in Proc. of Kiev Conference (1970), op. cit.

85. Photoexcitation amplitudes can also lead to information on this question. See, C. A. Heusch and F. Ravndal, Phys. Rev. Lett. 25, 253 (1970).

86. C. Goebel, Phys. Rev. Lett. 16, 1130; 17, 66(E) (1966).

87. R. Aaron, R. Amado, and R. Silbar, Phys. Rev. Lett. 26, 407 (1971).

88. P. Freund, R. Waltz, and J. Rosner, Nucl. Phys. B13, 237 (1969).

89. J. Rosner, in Proceedings of the Eastern Theoretical Physics Conference, October, 1969, Syracuse University.

90. M. Jacob and J. Weyers, Nuovo Cimento 70A,1970.

91. H. W. Atherton, et.al., Phys. Lett. 30B, 494 (1969).

92. Chan Hong-Mo, et.al., Phys. Rev. Lett. 26, 672 (1971).

93. H. Lipkin, Phys. Rev. Lett. 16, 1015 (1966).

94. H. Harari, Phys. Rev. Lett. 22, 562 (1969); J. Rosner, Ibid., 689 (1969).

95. P. G. O. Freund, Phys. Rev. Lett. 20, 235 (1968); H. Harari, Ibid., 1395 (1968).

96. J. Mandula, J. Weyers, and G. Zweig, unpublished.

97. M. Gell-Mann, Proceedings of the 3rd Hawaii Topical Conference in Particle Physics (1969), Los Angeles, Western Periodicals Co.

98. P. Carruthers, Phys. Rev. D3, 959 (1971); R. Crewther, Phys. Rev., to be published.

99. See, for example, H. Brody, et.al., Phys. Rev. Lett. 24, 948 (1970).

100. R. Goble and J. Rosner, to be published.

101. L. Brown and R. Goble, Phys. Rev. Lett. 20, 346 (1968).

102. S. Weinberg, Phys. Rev. Lett. 17, 616 (1966).

103. E. Berger, this conference.

104. C. Nef, Thesis, Univ. of Geneva, 1970 (unpublished); see also Ref. 3.

105. A partial list: D. Horn, J. Coyne, S. Meshkov, and J. Carter, Phys. Rev. 147, 980 (1966); D. Horn, Nuovo Cimento 62A, 581 (1969); R. Arnold and J. Uretsky, Phys. Rev. Lett. 23, 444 (1969).

106. See e.g., L. H. Chan, et.al., Phys. Rev. Lett. 25, 482 (1970); F. Gürsey and M. Koca, Nuovo Cimento 1A, 429 (1971).

107. A. A. Michelson, Phil. Mag. 34, 280 (1892).

108. J. v. Fraunhofer, "Prismatic and Diffraction Spectra," ed. and trans. J. S. Ames, New York, Harper and Bros. 1898.

Figure Caption

Figure 1: 2^+ partial widths into 1^-0^- and 0^-0^- pairs. Normalization is that of Ref. 40. The entries of the two boxes should lie on two independent vertical lines if SU(3) is good, and on a single vertical line if SU(6) is good.

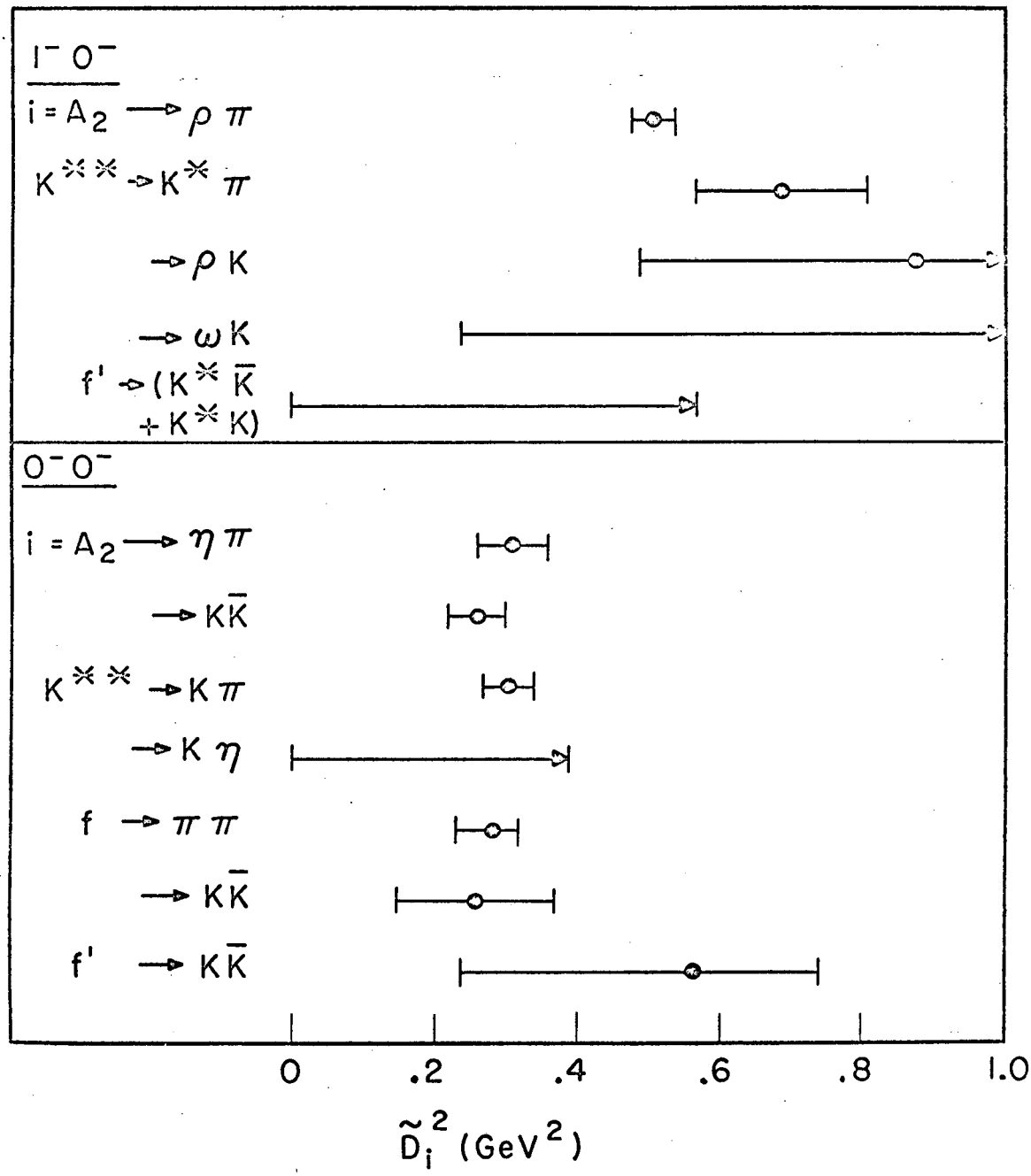
1⁻ 0⁻
i = A2 → ρ π
K** → K* π
→ ρ K
→ ω K
f' → (K* K̄ + K* K)
0⁻ 0⁻
i = A2 → η π
→ K K̄
K** → K π
→ K η
f → π π
→ K K̄
f' → K K̄
0
.2
.4
.6
.8
1.0
D̃i² (GeV²)
XBL 715-983

Fig. 1.

Discussion after Rosner's Talk:

BERGER: In order to determine whether the bump observed in backward A_1 production is really the A_1 "resonance," a phase shift analysis must be performed. The point is that this bump might be due to a mechanism similar to the Deck Effect. Such a kinematic enhancement may be distinguished from production of a 1^+ meson by a partial wave analysis.

ROSNER: Could such a Deck type effect produce an enhancement as narrow as that seen by the Collins group?

BERGER: Yes, although I haven't done a detailed calculation. You must recall that the Deck mechanism applies to the whole bump, not just to some small two-bin wide "signal" you think you observe on top of a broad bump.

BERGER: Let me add a few brief comments about backward A_1 production. First, one should look for backward A_1 production in $\pi^+ p$ scattering rather than in $\pi^- p$ scattering. The cross-section should be much larger in $\pi^+ p$ than in $\pi^- p$. This is true, whether you think A_1 is a resonance or a Deck (kinematic) effect, and follows as a simple deduction from the relative sizes of $\pi^\pm p$ backward elastic scattering cross-sections. If you insist on a model, recall that $\pi^- p$ backward elastic and backward A_1 production are mediated by Δ_δ exchange, which has notoriously small coupling in both $\pi^- p \to p\pi^-$

and $\gamma p \to N\pi^-$.

Second, even if you find an A_1-like bump in $\pi^- p \to A_1^- p$ (backward), which is not a diffractive channel, it doesn't necessarily imply that A_1 is a resonance. A simple reflection diagram (drawn below) will give you a kinematic bump.

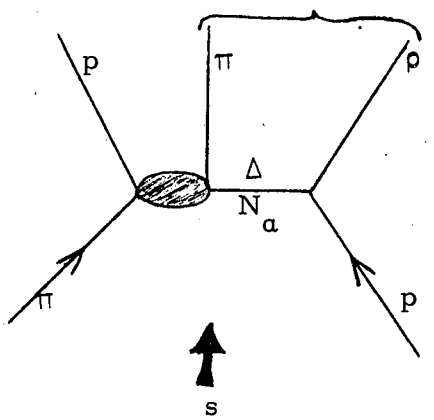

The shaded oval represents the complete πN backward scattering amplitude. In a practical calculation, measured πN backward data could be employed in the theoretical amplitude to provide absolute normalization. Symbols N_a and Δ denote exchanges, of which we have some knowledge (Berger and Fox, Nucl. Phys. B26, 1 (1971)). The reflection diagram will produce an enhancement just above $\pi\rho$ threshold, but it is (off hand) unlikely that this kinematic bump will have $J^P = 1^+$. In forward diffractive production of A_1, the kinematic Deck diagram does give a $J^P = 1^+$ bump; this arises because $\cos\theta$ dependence remarkably cancels out of the ratio $s_1/(t - m_\pi^2)$. Here, s_1 is a factor in the overall production amplitude which comes from Pomeron exchange and $(t - m_\pi^2)$ is just the pion propagator. This argument may be

found in my Irvine review talk (December, 1969). In the backward kinematic diagram, a similar cancellation does not occur; therefore, I do not expect the kinematic bump to be a pure J^P state, as it is in forward production. This would be a good problem for an industrious graduate student to work out carefully. Experimenters should get enough backward A_1 data so they can perform a spin-parity analysis similar to that done by Kruse, Ascoli, and collaborators at Illinois. If they see primarily $J^P = 1^+$ in backward production, then the resonance supporters will get a big boost.

My third remark concerns the momentum-transfer dependence of backward A_1 production. Collins, Turkot et al. observe a much sharper t distribution than for, say, backward $\pi p \to p\pi$ or $\pi p \to \rho p$. However, a very sharp t distribution is decidedly a characteristic signature of kinematic threshold enhancements. Again, the argument is given in my Irvine review talk.

PARTIAL WAVE ANALYSIS AND EXPERIMENT IN πN REACTIONS*

R. G. Moorhouse

Department of Physics and Lawrence Radiation Laboratory
University of California, Berkeley, California 94720

In this talk I will first discuss the probable structure of scattering amplitudes and how to make the best use of this structure in partial wave analysis. Afterwards I will briefly discuss the reactions $\pi^- p \to \pi^o n$, $\pi^- p \to K^o \Lambda^o$, $\pi^+ p \to K^+ \Sigma^+$ which are likely to be useful, and perhaps essential, in finding the higher energy low angular momentum N^* resonances.

I. HARARI-FREUND DUALITY AND PARTIAL WAVE ANALYSIS

If we write

$$\text{Im(Amplitude)} = \text{Im(Background)} + \text{Im(s-channel resonances)} \tag{1}$$

then the Harari-Freund[1] duality hypothesis is that Im(Background) is dual to the Pomeron (and Im(s-channel resonances) to ordinary Regge poles). Consequently we may express (1) as

$$\text{Im(Amplitude)} = \text{Im(Pomeron)} + \text{Im(s-channel resonances)}. \tag{2}$$

The Pomeron has t-channel isospin zero, $I_t = 0$. The most direct confirmation of the hypothesis (2) comes from the πN partial wave analysis. By making the t-channel isospin projections of the partial waves Harari and Zarmi[2] showed that there is considerable imaginary background in the $I_t = 0$ partial waves while only resonances were apparent in the $I_t = 1$ partial waves. Figure 1 shows the Harari-Zarmi diagrams.

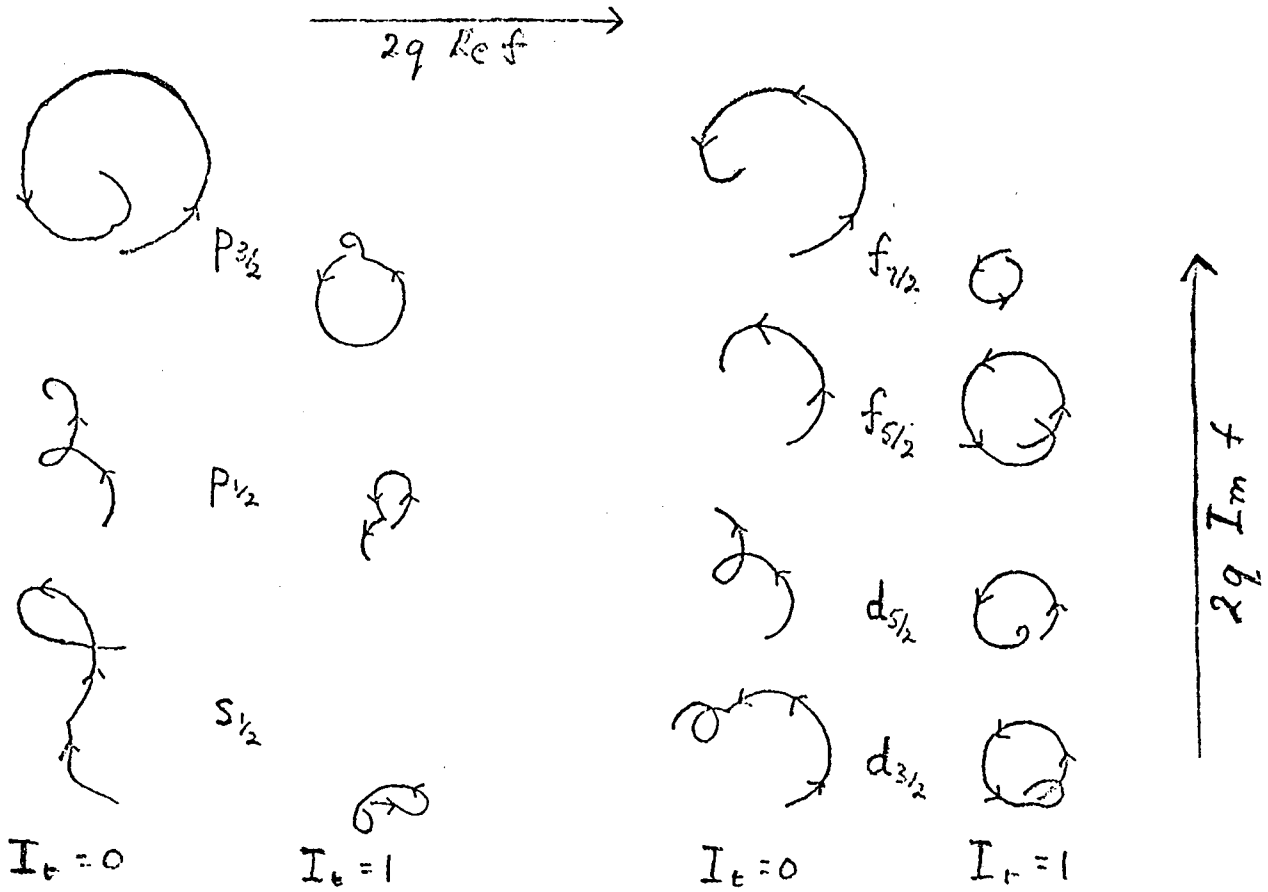

Fig. 1. The Harari-Zarmi[2] $I_t = 0$ and 1 projections of the πN partial waves showing nonresonant imaginary part in $I_t = 0$, but not in $I_t = 1$. The arrows show the direction of increasing energy.

Since πN partial wave analysis provides good evidence for the correctness of Harari-Freund duality (at any rate in the limited form (2)) it seems to me reasonable to use Harari-Freund duality to help πN partial wave analysis out of some of its difficulties. These difficulties arise in some or all of the energy regions T_π (pion kinetic energy) = 1.0 GeV $\leftrightarrow$ 2.5 Gev $\leftrightarrow$ 3.0 GeV corresponding to E(center of mass energy) = 1.7 GeV $\leftrightarrow$ 1.9 GeV $\leftrightarrow$ 2.4 GeV $\leftrightarrow$ 2.6 GeV and we may summarize the relevant points as follows:

(i) In partial wave analysis it is difficult to get accurate information on low angular momentum waves; at the same time it is important to get information on resonances in these states, which may be

radial excitations in the quark model and daughters in Regge theory.

(ii) The higher the energy, the greater the difficulty.

(iii) The Harari-Zarmi figures show bigger Pomeron content in the lower partial waves.

Points (i), (ii), and (iii) suggest that we should use the Harari-Freund hypothesis through the ansatz:

Amplitude = Pomeron + s-channel resonances + real background. (3)

The latest results in K^+p scattering suggest that the Pomeron may be parametrized in the form

$$\text{Pomeron} = a(s)e^{b(s)t} \tag{4}$$

in the range $0 > -t > 2.0$ $(\text{GeV}/c)^2$, where $a(s)$, $b(s)$ are smooth monotonic functions of energy. The operational meaning of the word Pomeron in using (3) and (4) in phase shift analysis, is that $I_t = 0$. Such a parametrization of the imaginary part of the background will certainly reduce the total number of parameters, and should improve the accuracy with which the resonance contributions to the lower angular momentum partial waves can be found.

There are of course some uncertainties about the nature of the Pomeron, so formulae such as (3) and (4) should be used tentatively and heuristically, and partly in the hope of illuminating the nature of the Pomeron. Such questions are whether the Pomeron has a considerable real part at, say, $t \sim -1.0$ $(\text{GeV}/c)^2$, and whether the Pomeron is helicity nonflip or spin nonflip or neither. Harari and Zarmi[3] present evidence for the helicity nonflip nature of the Pomeron in πN scattering but the situation may not be completely resolved.[4]

Wrighton, Ross, and Leith[5] have used a simplified form of (3) (pure imaginary Pomeron and no real background) in fitting $\pi^- p$ scattering. The results are encouraging, and some of us are working along the lines of (3) and (4).

II. THE IMPORTANCE OF EXPERIMENTS ON $\pi^- p \to \pi^o n$, $\pi^- p \to K^o \Lambda$ AND $\pi^+ p \to K^+ \Sigma^+$ IN THE 1-3 GeV/c REGION

Since for these reactions there can be no Pomeron exchange in the t-channel the Harari-Freund hypothesis implies that all the imaginary parts of the amplitudes are due to s-channel resonances. Consequently accurate experiments in these channels are an important test of the Harari-Freund hypothesis and, if that be valid, are good for resonance discovery. The importance of improving the data on $\pi^- p \to \pi^o n$ has been repeatedly emphasized by phase shift analysts so here I would like to comment particularly on $\underline{\pi^- p \to K^o \Lambda}$; $\underline{\pi^+ p \to K^+ \Sigma^+}$:

(a) These channels select respectively pure $T = 1/2$ and pure $T = 3/2$ in the s-channel, <u>without Pomeron exchange</u>.

(b) Λ and Σ^+ analyze their own polarization.

(c) Because of their higher threshold these reactions will tend to emphasize lower partial waves in the 1.0 - ~2.0 GeV/c region, and thus to provide independent evidence on just those interesting lower angular momentum resonances on which information may possibly also be obtained by use of the Harari-Freund hypothesis, as outlined in I above.

(d) In general partial wave analysis of these channels should have a valuable symbiotic interaction with $\pi^+ N \to \pi^+ N$ partial wave analysis (as the $\bar{K}N \to \pi\Sigma$, Λ interactions do in the less well measured $\bar{K}N \to \bar{K}N$ case).

(e) There should be interesting SU3 comparisons in a case where two $S \neq 0$ particles are created (strange quark pair production in the s-channel).

It will probably be necessary to measure the cross-section data over a full angular range and with say $\pm 3\%$ errors in differential cross section in > 20 angular bins per energy, and at energy intervals < 50 Mev/c apart. (The integrated $\pi^- p \to K^o \Lambda$ cross section over much of the energy range is ~ 20 μb.)

It is encouraging that a little has already been achieved using much worse data than this. For example in partial wave analysis of $\pi^- p \to K^o \Lambda$ Wagner and Lovelace[6] have recently obtained interesting results in the third resonance region, E ~ 1700 MeV. And in analysis of their own experiments on $\pi^+ p \to K^+ \Sigma^+$, Kalmus, Borreani, and Louie[7] have established the branching ratio of the f_{37} $\Delta^{++}(1920) \to K^+ \Sigma^+$ as $2.0 \pm 0.4\%$, against (their estimate of) the SU3 expected result of 13%. They also find an f_{35} at a mass of ~2050 MeV/c^2 (from πN elastic scattering, an f_{35} is found at ~1860 Mev/c^2).

One should remark finally that besides low angular momentum resonances (radial excitations or daughters) there are many resonances that one expects to occur at ~2.2 GeV/c^2-2.4 GeV/c^2, but whose confirmation is desirable, and whose absence would be revolutionary. The negative parity resonances in the 2nd and 3rd resonance regions are classified in the quark model as an SU6{70}, $L = 1^-$, and we may make the following table, also exhibiting the expected 'Regge recurrence' multiplet {70}, $L = 3^-$.

	$[70, 1^-]$	$[70, 3^-]$
$\{8,2\}$	$s_{11}(1530)$	d_{15}
	$d_{13}(1520)$	$g_{17}(2200)$?
$\{8,4\}$	$s_{11}(1700)$	d_{13}
	$d_{13}(1730)$?	d_{15}
	$d_{15}(1670)$	g_{17}
		d_{15}
$\{10,2\}$	$s_{31}(1640)$	d_{35}
	$d_{33}(1690)$	g_{37}

The particles listed under $[70, 3^-]$ are, except for the interesting case of the d_{13}, Regge recurrences of particles in the $[70, 1^-]$.

FOOTNOTES AND REFERENCES

* This work was supported in part by the U. S. Atomic Energy Commission.

1. H. Harari, Phys. Rev. Letters 20, 1395 (1968); P. G. O. Freund, Phys. Rev. Letters 20, 235 (1968).

2. H. Harari and Y. Zarmi, Phys. Rev. 187, 2230 (1969).

3. H. Harari and Y. Zarmi, Phys. Letters 32B, 291 (1970).

4. C. Meyers and P. Salin, Pomeron Structure from Low Energy K^+p Scattering, Bordeaux preprint.

5. G. C. Wrighton, W. A. Ross, and D. W. G. S. Leith, SLAC preprint.

6. F. Wagner and C. Lovelace, Nucl. Phys. B25, 411 (1971).

7. G. E. Kalmus, G. Borreani, and J. Louie, Phys. Rev. D2, 1824 (1970).

REMARKS ON K-N AND N-N PARTIAL WAVE ANALYSIS

Michael J. Moravcsik

Department of Physics and
Institute of Theoretical Science
University of Oregon
Eugene, Oregon 97403

REMARKS ON K-N AND N-N PARTIAL WAVE ANALYSIS

Michael J. Moravcsik

Department of Physics and
Institute of Theoretical Science

University of Oregon
Eugene, Oregon 97403

(Prepared for the meeting on Hadron Physics at Intermediate Energies, held at Cal. Tech. on March 29 and 30, 1971.)

The task given to me is to say something pertinent about K-N and N-N interactions from a partial wave point of view in 18 minutes including discussion. My remarks therefore will be, by necessity, telegraphic in style, with some references for further study.

The first remark pertains to whether partial wave decompositions can be expected to remain of interest when we push up the energy into the 3-10 GeV range. The answer appears to be affirmative, mainly because the concept of a resonance continues to dominate our thinking in particle physics. Although the question of what a resonance is has undergone various convulsions lately, resulting in a certain fuzzification of the old and simple concepts, one of the few trade marks of a resonance that has survived is its being connected to a definite state of the usual quantum members, and, in particular, of angular momentum. Thus, in looking for, and identifying the quantum members of resonances, the partial wave decomposition remains of considerable importance.

Against this, one must add that on the other hand, whatever dynamical "theories" we have of strong interactions, they do not lend themselves very naturally to an angular momentum representation. Specifically, the various

particle exchange mechanisms, Reggeized or not, absorption corrected or not, always appear inclosed forms which contain significant contributions to a very large number of angular momentum states. Comparison of experiments with those theories, therefore, might very well be done more effectively by measuring enough experimental observables at a given energy and angle so that the invariant amplitudes can be experimentally determined and then checked against theoretical predictions for these amplitudes.

Returning, however, to the partial wave representations, we might wonder about the feasibility of doing such an analysis at energies at which a large number of partial waves must be taken into account. In this connection, two recent phenomenological developments should be mentioned which indicate that partial wave decompositions might be feasible at all energies.

The first of these developments has the name of optimalized expansion[1], and has been championed by Cutkosky and Deo, together with some collaborators, and, independently, by Ciulli. The mathematical idea here is to perform a conformal mapping from the cos θ plane into a different variable so as to push the location of the singularities as far from the physical regions as possible. Consequently, an expansion in the new variable is likely to converge faster, and hence a given set of data could be described in terms of a fewer number of parameters. Physically, the method could be thought of as a spectral analysis of angular distributions in terms of a series other than the usual Legendre functions. In effect, the new expansion represents a different weighting of experimental data in the various angular ranges. I have not seen enough of this work in published form so as to be able to make useful statements about specific experimental implications of this different weighting, but it is, in any case, likely that in view of the new expansion, a different set of angles will merit special experimental attention than in the conventional Legendre expansion.

It should be remarked that the new parameters, obtained in the optimalized expansion, have no intuitive physical meaning, similar to the meaning of partial wave amplitudes or phase shifts. Since, however, they are just linear combinations of the conventional partial wave amplitudes, the latter can be determined from the former.

A similar method of optimalized transformations is also possible from a complex energy plane into an appropriately chosen other variable. This then permits an economical parametrization of the energy dependence of scattering amplitudes.

This method of optimalized expansion has been applied already to both reactions under discussions here, namely to K-N and N-N scatterings. The results, which we do not have time to review here, are promising enough so that further experiments should definitely count on utilizing it.

The second of the phenomenological developments which should aid in the partial wave description of experiments at intermediate energies is the so-called phase band method[2], developed by myself, and applied to pion-nucleon scattering in collaboration with Bridges and Yokosawa. This method is based on the following observation: Consider first the admittedly very idealized situation of a scattering involving spinless particles, with errorless measurements of the differential cross section at a continuous set of angles in the complete angular range, and let us describe these experiments in terms of an infinite set of angular momentum states. The inversion theorem of an orthogonal series expansion tells us then that each angular momentum amplitude can be determined by itself, completely independently of the other amplitudes.

Now let us consider the realistic situation of a set of high energy scattering data at a sufficiently large, but discrete set of angles (at a fixed energy), with some experimental errors, and an analysis of these data in terms of a large but finite number of angular momentum states. In this case, although

we cannot count any longer on a simple determination of each amplitude by inversion, independently of the other amplitudes, we will approach that situation in the sense that we can expect to be able to determine each amplitude with the help of only very rough information about the other amplitudes. The practical procedure therefore consists of dividing up the total range of significant angular momenta into bands of partial waves. The analysis begins by determining the uppermost band of partial wave amplitudes in the usual way, but with the lower bands of partial waves represented only through a collective description in terms of a few parameters only. Once the uppermost band is thus determined, it can be fixed, and with its help the next lower band of partial wave parameters is determined, with the lower bands still only collectively represented. An iteration of the above two steps can assure that the top two bands are determined in a self-consistent fashion. We can then proceed to the next lower band, keeping the top two fixed and the even lower ones in their collective representations. This sequence can be continued until all angular momentum parameters are determined in a self-consistent fashion. The method in fact replaces the simultaneous determination of a very large number of parameters by a sequence of determinations of a small number of parameters. If one is patient enough and is willing to follow a long sequence, therefore, each step can be a small enough problem to be feasible even on the smallest computer.

The method is the better the more partial waves one deals with, since the more one approximates the idealized situation of simple orthogonal inversion that was discussed above.

In order to avoid an apparently common misunderstanding, we should emphasize that the possibility of determining each partial wave amplitude almost independently of each other does not mean that there is an absence of

correlations among the various partial wave amplitudes. The easiest way to see this is to recall that although the Fourier coefficients of a function can be determined one by one, independently of each other, there is of course a very strong correlation among the coefficients.

Phase band analysis has not been applied yet to N-N or K-N scattering data, only to the pion-nucleon data already mentioned above. It would be quite appropriate, for example, to try the phase band method on the 600-1,200 MeV nucleon-nucleon scattering data already in existence. It would appear from the success of the application to pion-nucleon scattering that as soon as one has significant contributions up to at least $\ell = 6$ or so, the phase band method is applicable.

There is a possibility that the optimalized expansion method and the phase band method can be combined into an even more powerful tool of phenomenological analysis. In other words, it is possible that an application of the phase band method to the parametrization in the conformally transformed space will also constitute a convergent and iterable procedure. Although a priori this is very likely to be true, it must be tried on actual data.

Now let me turn to the specific question of what type of experiments should be performed for partial wave analysis, taking into account the above outlined new developments.

Let us first note that the problem of determining the partial wave parameters contains two different components: The determination of the invariant amplitudes from the various polarization measurements, and the decomposition of these amplitudes into partial waves. At very low energies, when only very few partial waves are present and the scattering is purely elastic, both aspects are not necessarily present. We remember, for example, that in the early days of pion physics, the pion-nucleon phase shifts could be determined at very low energies almost unambiguously without any polarization experi-

ments, only from the differential cross section. At higher energies, however, both aspects are indispensable, and no amount of improvement on one can eliminate the necessity of the other.

The first conclusion is, therefore, that for partial wave decomposition, top priority must go to various types of polarization experiments. This is of course easier for the K-N interaction where there are only three independent polarization experiments, and where up till now we have managed to get by performing mostly two of them. In the N-N interaction, the situation is more difficult, and one must be prepared to be able to perform six or seven different types of experiments.

The second comment pertains to the angular range of the experiments. In recent years it has become common to measure particle reaction cross sections mainly in the very forward and very backward directions. There were two reasons for this. First, in many reactions there were peaks in these directions, sometimes several orders of magnitude larger than the average differential cross section, and hence experimentally the measurements in these directions were much easier. Second, the most fashionable model of recent years, the Regge pole scheme, has claimed applicability mainly in these directions. With the improved experimental techniques, however, as well as with the continuing decline of Reggeism, attention has been shifting to include the complete angular range. From the point of view of partial wave analysis, this trend is indispensable. In partial wave decompositions the diffraction peak, unless measured with extreme precision, is a highly uninteresting phenomenon, since in it all partial waves add constructively and hence the delicate interplay of the various partial wave amplitudes is washed out.

Thus, as a second conclusion, we must place high priority on cross section and polarization measurements in the complete angular range, and in

particular at the intermediate angles.

As a third conclusion, let me suggest, purely on empirical grounds, that probably the best mix of various experiments would be to have a rather complete angular coverage for the polarizationwise simpler experiments, and then measurements at a smaller number of angles, widely spaced, of some of the more involved polarization experiments.

In general, sets of experiments at given, fixed energies are easier to handle, since our understanding of the angular variation of reaction amplitudes at fixed energies is more advanced than our understanding of the energy variation of amplitudes at a given angle or the energy variation of partial wave amplitudes. There is, however, a variant of the Cutkosky-Deo-Ciulli work which might also be helpful in connecting partial wave amplitudes at neighboring energies.

Finally, let me say a few words about hunting for so-called exotic resonances. Actually, this subject is just a special case of the search for resonances in general. There are basically three ways to find traces of resonances in particle reactions: a) in terms of direct intermediate state resonances (Figure 1); b) in terms of a crossed channel intermediate state resonance (Figure 2); and c) in terms of a decaying resonance produced in the final state (Figure 3). Of these, only the first method is directly pertinent to a partial wave analysis, since in the second situation the resonance will contribute to all angular momentum states and hence will not be easily separable from the background. In the third situation the obvious method of detection determination of the quantum numbers of such a resonance a more detailed angular momentum analysis of the final state might be necessary. In any case, such a resonance might show up in the partial wave analysis of the elastic channel at best as a sudden dip in one or several of the inelasticity

parameters at a given energy, an indecisive indication indeed.

In the first situation, however, the existence of the resonance should in fact produce a loop in the Argand diagram, superimposed on some background of unknown magnitude. For the K-N reaction, such a resonance, if exotic, would have to have S = +1 (i.e., in K^* - N scattering), or be double charged (i.e., in K^* - p scattering). The search for such so-called Z^* resonances has been underway, and summaries of it are available.[3]

Although it does not pertain to partial waves, it might be mentioned that a resonance in the K^*p direct channel would of course be a cross channel resonance in the K^-p channel, and as such would give a backward peak in the latter reaction. To look for some backward peak in itself, however, would not be very convincing, because some enhancement in the backward direction might come about simply by the combination of ordinary direct channel resonances also. If, however, one could establish in some manner (for example, by the traditional extrapolation to the pole in the unphysical region) that the shape of the backward resonance is of the type which is characteristic of such a cross channel resonance (for example, the residue obtained from the extrapolation is energy independent) then one might acquire more definite evidence for the existence of an exotic resonance.

For the N-N reaction, on the other hand, such an exotic resonance would have a baryon number of two, but otherwise non-exotic quantum numbers, except possibly double charge (in the case of p-p scattering). This area has not been explored very much, because of the added complexity of the N-N system, and would be a good subject for exploration.

One should also remember that, at least according to some classifications,[3] resonances can also be called exotic if they have permissible quantum numbers but do not fit into known SU_3 multiplets or do not form new complete multiplets

(i. e., do not fit the quark dynamics scheme). These might occur in many reactions at the lower or intermediate energies.

In conclusion, there is much to be done in the intermediate energy range in terms of experiments helpful in partial wave analysis, and with the help of recent advancements in phenomenological methods such experiments should contribute substantially to our detailed knowledge of particle interactions at intermediate energies. In particular, they should give information on one of the central problems of particle physics, namely whether resonances continue indefinitely or not as we get to higher and higher energies.

References

1. The literature of the optimalized expansion and related studies include the following papers:
For the Pittsburgh group: Cutkosky and Deo, Phys. Rev. Letters 20, 1272 (1968); Phys. Rev. 174, 1859 (1968); Phys. Rev. D1, 2547 (1970); Cutkosky, Ann. Phys. (N. Y.) 54, 350 (1969); Yung-An Chao, Phys. Rev. Letters 25, 309 (1970). There are also two abstracts in the 1971 New York APS meeting bulletin.
For the Ciulli group, see Ciulli, Nuovo Cimento A61, 787 (1969) and A62, 301 (1969); Ciulli and Fischer, Nuclear Phys. 24, 465 (1961); Ciulli, Ciulli, and Fischer, Nuovo Cimento 23, 1129 (1962).
For related references, see also Pisut and Presnajder, Nucl Phys. B12, 110 (1969) and B12, 586 (1969), Presnajder and Pisut, Nucl. Phys. B14, 489 (1969) and B22, 365 (1970). Furthermore see Pfister, Nucl. Phys. B20, 320 (1970) and B22, 327 (1970); Viano, Nuovo Cimento A58, 628 (1969) and A63, 581 (1969); Bertero and Viano, Nuovo Cimento 38, 1915 (1965); Nielsen et al. Nucl. Phys. B32, 294 (1970).

2. M. J. Moravcsik, Phys. Rev. 177, 2587 (1969); Bridges, Moravcsik and Yokosawa, Phys. Rev. Letters 25, 770 (1970) and 26, 155 (1971).

3. See e. g. Gerson Goldhaber, UCRL-19832 (1970) for Z^*'s, and Jonathan Rosen, CALT-68-262 (1970) on exotic bosons. The latter discusses various "types" of exotics.

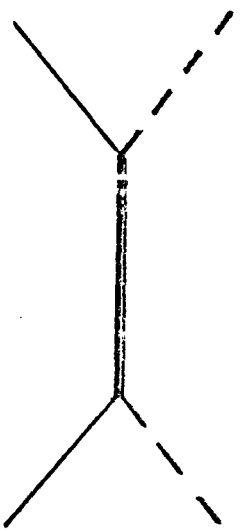

Fig. 1.

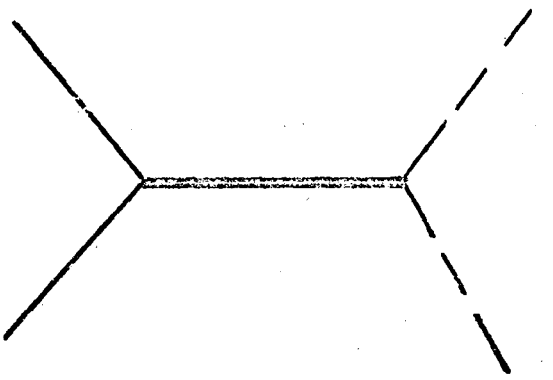

Fig. 2.

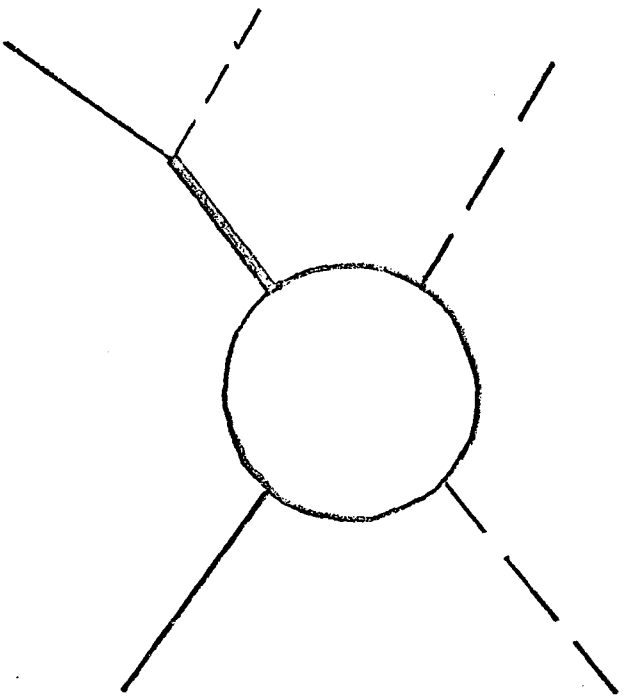

XBL 714-714

Fig. 3.

Discussion

Moravcsik (Oregon):

1. In connection with phase shift analysis: There are two important requirements for being able to be engaged in large scale computer type analysis: Generous access (financially and physically) to computer time, and the availability of auxiliary personnel to assist in computer operations and data handling. Both of these are better available at national laboratories than at universities, and hence such projects should be encouraged by the national laboratories as their special contribution to physics.
2. In connection with reported ambiguities in the partial wave analysis of three-body final state reactions: There is a theorem [see Phys. Rev. Letters 14, 861 and 1056 (1965)], according to which in a reaction involving more than four particles it is in general impossible to determine the intrinsic parity of one of the particles even if the intrinsic parities of all other particles is known, and even if all possible polarization experiments are allowed. This theorem might have some consequences in the partial wave analysis of three-particle final states.
3. In connection with high energy phenomenology in general: It is very essential to be able to measure the amplitudes of high energy reactions, and not only a few of the simplest experimental observables such as differential cross section and polarization. The recent history, for example, of the Regge schemes shows that new type of polarization quantities (charge-exchange polarization,

photoproduction with polarized photons, etc.) can be much more helpful to weed out bad theories than increased accuracy in already measured observables. Measuring amplitudes cannot help but being useful, no matter what the ultimate theory will turn out to be.

4. In connection with the future of intermediate energy machines: Intermediate energy machines, through careful experimentation and particularly through the use of polarization techniques, can supply more essential information on strong interactions than the information most likely to come out of superhigh energy machines. In this respect, the present machines in the 5-10 GeV range should be forerunners of meson factories (i.e., high current machines) in the same energy range, to be built a decade hence, which might in fact hold the key to our understanding of particle physics.

Yokosawa (Argonne): How can one determine the phase between resonant amplitudes and background amplitudes, and what does this phase mean?

Moorhouse (LRL): One normally assumes that the Pomeron (background) is purely imaginary at $t = 0$, but as you go away from the forward direction, the amount of the real part of the Pomeron will probably increase.

Schmid (CERN): I'd like to make a simple comment about the meaning of phases. Let me remind you that phases are very important in dispersion relations. If you know the imaginary part of the

amplitude, you can calculate the real part and hence determine the whole amplitude. The phases are well defined, the imaginary parts are more fundamental, they correspond to the spectral function. It is the imaginary part which must vanish for exotic, inelastic channels, (e.g., K^+n charge exchange), while the real part does not vanish.

LOW AND INTERMEDIATE ENERGY $\bar{K}N$ EXPERIMENTS

R. D. Tripp

Lawrence Radiation Laboratory
Berkeley, California 94720

LOW AND INTERMEDIATE ENERGY $\bar{K}N$ EXPERIMENTS

R. D. Tripp

Lawrence Radiation Laboratory
Berkeley, California 94720

I shall present an experimental view of K^- formation experiments at low and intermediate energies -- what has been done and what are some of the further needs in this field.

A. Bubble Chamber Experiments

Fig. 1 shows the path lengths for the seven major hydrogen bubble chamber experiments[1-6] below 500 MeV/c of the past decade. Notice that the vertical scale is logarithmic so that certain momentum regions are covered vastly better than others. This figure contains only those experiments which were analyzed for strong interactions. For momenta below 250 MeV/c there exists (in stopping K^- film used primarily for Σ leptonic decays an order of magnitude more path length than shown. The region from 250-350 MeV/c may need additional path length if experiments now in progress indicate any interesting structure. From 350 to 420 MeV/c, the domain of $\Lambda(1520)$, there is a great abundance of film, whereas beyond that lies a depression in the path length which extends up to 650 MeV/c. This can be seen in Fig. 2 which is an updated version of a figure constructed last year by Levi-Setti[7] for the Duke Conference on hyperon resonances. Here at higher energies, individual momentum settings are not subdivided into 10 MeV/c momentum intervals as in Fig. 1. That certain momentum regions have been neglected is immediately apparent. In addition to the 420 to 650 MeV/c interval one

sees from the figure that the region from 1.0 to 1.15 GeV/c has also been sparsely covered. Apart from these gaps which have occurred for various historical reasons of beam limitations, and scheduling pressures, and not for any lack of interest, K^- formation experiments up to 2 GeV/c in hydrogen bubble chambers have for the present probably been pushed to the limit of their usefulness in resonance physics.

A more promising approach for bubble chambers would be to put more effort into getting good K^0_L beams at these momenta. This would be extremely valuable for both the I = 1 $\bar{K}N$ system and the I = 0 KN system. The most important $K^0_L p$ bubble chamber exposures have been:

1)	LRL (1966)	100-500 MeV/c
2)	SLAC	1-10 GeV/c
3)	DESY	Intermediate momenta

These experiments are in beams with large momentum spreads, although the SLAC experiment has electronic time of flight information to determine the incident momentum. Electron machines seem to have the edge over proton machines with regard to a good K^0_L to neutron ratio, which is the major experimental obstacle with K^0_L beams.

B. Electronic Experiments

1. Kp polarization experiments

As a means of elucidating hyperon resonances, elastic polarization experiments have so far not been very fruitful. This is partially

due to the fact that they have only been done at higher energies where the resonance structure is quite complex. (The lowest momenta measured up to now have been 980 MeV/c for K^- and 870 MeV/c for K^+, both at CERN.) The problem is that for good polarization experiments one needs beam fluxes well in excess of 1000 K per pulse and this is difficult to achieve below 1 GeV/c. These experiments should be pursued more vigorously in the future in conjunction with other experiments. However I do not expect them to have the revolutionary impact on hyperon physics that the corresponding polarization experiments had on nucleon resonances. This is because most of the important structure has already been clarified by means of bubble chamber experiments using $\Lambda\pi$, $\Sigma\pi$, and $\Lambda(1520)\pi$ reaction channels where the hyperon decay analyzes the polarization in the final state.

2. $K^-p \rightarrow \bar{K}^0n$

A counter experiment (CERN - 1970) has been done on the total charge exchange cross section from 1 to 3 GeV/c. It would be more valuable to also have good differential cross sections for this reaction since bubble chamber experiments usually have fewer events here than in any other two body reaction. Resonances are invariably more prominent in this channel than in the elastic since it is given by the difference in the I = 0 and I = 1 amplitudes so that the absorptive background largely cancels.

3. Elastic differential cross sections

As a general rule, bubble chamber statistics are usually adequate for K^-p elastic scattering, amounting to several thousand events per momentum. However, for large angle scattering where the differential cross section is very small, good counter experiments would be of interest.

A CERN experiment is in preparation to study the K^-n differential cross section from 1 to 2 GeV/c using a deuterium target. This will isolate the I = 1 elastic amplitude.

Another region of elastic K^-p scattering inaccessible to bubble chambers but easily explored by electronic means, is the very forward direction -- the region of Coulomb-nuclear interference. This if of course of great interest for the dispersion relation evaluation of the $\bar{K}N\Lambda$ and $\bar{K}N\Sigma$ coupling constants which has had an unsettled history for over a decade. A particularly vivid example of the difficulty encountered in bubble chamber evaluations of ratio of the real to imaginary part of the forward scattering amplitude is seen in Fig. 3. In the region below 1 GeV/c even the same experiment evaluated by different procedures[8,9] gives very conflicting results.

C. Multichannel Analysis

Multichannel partial wave analyses have so far been unique to $\bar{K}N$ reactions. This type of analysis has been indispensable up to 500 MeV/c

in fixing the scattering lengths and effective range parameters. Here only the reactions $K^- p \rightarrow \bar{K}N$, $\Sigma\pi$, $\Lambda\pi$, $\Lambda\pi\pi$ are important. Above 500 MeV/c new channels such as $\bar{K}N\pi$, $\Sigma\pi\pi$, $\Lambda\pi\pi\pi$, $\Lambda\eta$, $\Sigma\eta$ become significant so that the constraint of unitarity becomes much less restrictive.

Multi-channel type analyses have been used:

1. Universally below 500 MeV/c.
2. By the CERN-Heidelberg-Saclay[10] collaboration in the region of 750 MeV/c for an analysis of the reaction $K^- p \rightarrow \Lambda(1670) \rightarrow \Lambda\eta$, $\bar{K}N$, $\Sigma\pi$. Here the advantage of a multichannel analysis is that it gives a simultaneous best fit value for the mass, width, and branching fractions for a resonance observed in several channels.
3. By Kim[11] for a study of the $\bar{K}N$, $\Sigma\pi$, and $\Lambda\pi$ amplitudes from 500 to 1200 MeV/c.

In resonance investigations, the unitarity constraint is less useful for a state with visible structure only in a reaction channel than for one showing structure in the elastic channel. The reason for this is as follows. The elastic and reaction amplitudes for a Breit-Wigner resonance are given by:

$$T_e = \frac{x_e}{\epsilon - i} \quad , \quad T_r = \frac{\sqrt{x_e x_r}}{\epsilon - i} \quad \text{where} \quad \epsilon = \frac{2}{\Gamma}\,(E - E_R)$$

$$x_e = \frac{\Gamma_e}{\Gamma} \quad , \quad x_r = \frac{\Gamma_r}{\Gamma} \quad , \quad \text{and} \quad \sum_i x_i = 1$$

Suppose small structure thought to be a resonance is found in the elastic channel (x_e small). Then in some reaction channel it must have a much larger effect since $T_r > T_e$ for x_e small. If this is not found, then one is led to suspect the resonance interpretation of the elastic structure which otherwise might have been acceptable interpreted as a resonance in a single channel analysis. The converse argument cannot be used to exclude a resonance interpretation for small structure in a reaction channel because in this case the smallness of the structure could be attributed to an extremely small elasticity x_e whose effect would be undetectable in the elastic channel.

An example of the latter situation can be seen in some preliminary and uncertain evidence for an I = 1 resonance we have observed in the $\Lambda\pi$ state at a K^- momentum of about 325 MeV/c. Fig. 4 shows the differential cross section for backward produced lambdas in the reaction $K^-p \rightarrow \Lambda\pi^0$ obtained from an extrapolation of the differential cross section measured over all angles. The figure also contains curves obtained from a multichannel fit to all the K^-p reactions in this region, fitting simultaneously the energy dependence of all the polynomial coefficients for the angular distributions and polarizations under different assumptions for the spin-parity of the presumed resonance. The best improvement is obtained with a D_{15} resonance as indicated in the figure. With no resonance the ratio of measured χ^2 to expected χ^2 is 2.3 for all $\Lambda\pi$ data from 300-350 MeV/c. Introduction of a D_{15} resonance

reduced this ratio to 1.0. Despite this dramatic improvement we are still suspicious that it may result from a subtle bias since these angular distribution data are the only substantial evidence for the resonance. The best fit required that the resonance decay 72% into $\Lambda\pi$, 28% into $\Sigma\pi$ and only 0.1% back into the $\bar{K}N$ channel. The smallness of the observed effect is a result of its very weak coupling to the incident channel and the constraint of unitarity is of little value.

REFERENCES

1. J. K. Kim, Phys. Rev. Letters 14, 29 (1965).

2. M. Sakitt et al., Phys. Rev. 139, B719 (1965).

3. J. Chan and J. Kadyk, private communication of an unpublished Berkeley experiment.

4. M. B. Watson, M. Ferro-Luzzi, and R. D. Tripp, Phys. Rev. 131, 2248 (1963).

5. D. Berley et al., Phys. Rev. (to be published).

6. Some of the $\Sigma^{\pm}$ data appears in R. Bangerter et al., Phys. Rev. Letters 17, 495 (1966) and R. Bangerter, Lawrence Radiation Laboratory Report UCRL-19244, July 1969.

7. R. Levi-Setti in Hyperon Resonances - 70; E. C. Fowler, et al., (Moore Publishing Co., Durham, N.C. 1970).

8. R. Armenteros et al., Nuclear Physics B21, 15 (1970).

9. B. Conforto et al., Nuclear Physics B (in press).

10. R. Levi-Setti, in Proceedings or the Lund International Conference on Elementary Particles, 1969 (Berlingska Boxboktryckeriet, Lund, Sweden, 1969).

11. J. Kim in Hyperon Resonances - 70; E. C. Fowler, et al., (Moore Publishing Co., Durham, N.C. 1970).

FIGURE CAPTIONS

Fig. 1: Path lengths for the seven major hydrogen bubble chamber experiments on K^-p interactions from 0 to 500 MeV/c. The abbreviations are as follows: K(Kim[1]), MB(Maryland-Berkeley[2]), CK(Chan and Kadyk[3]), WFT(Watson, Ferro-Luzzi, and Tripp[4]), BMY(Brookhaven, Massachusetts, and Yale[5]), K-65(unpublished Berkeley experiment[6]), and CHS(CERN, Heidelberg, and Saclay[7]). The BMY path length shown corresponds only to that part which has been analyzed for certain strong interactions; their total path length in the egion of $\Lambda(1520)$ is comparable with K-65.

Fig. 2: Path lengths for various K^-p bubble chamber experiments from 436-2000 MeV/c. "Old" refers to experiments whose data were published prior to 1971.

Fig. 3: Ratio of the real to the imaginary parts of the K^-p forward scattering amplitude. Only the magnitude of the ratio is determined by experiment. The sign is chosen to agree with partial wave analyses as indicated by the curves. Solid circles are from the CHS experiment as interpreted in reference 8 while solid squares are the same data as interpreted in reference 9. Open circles are preliminary data from the LRL experiment K-65.

Fig. 4: Preliminary differential cross sections for the reaction $K^-p \rightarrow \Lambda\pi^0$ at the lambda c.m. angle given by $\hat{K}\cdot\hat{\Lambda} = -1$ from the K-65 experiment.

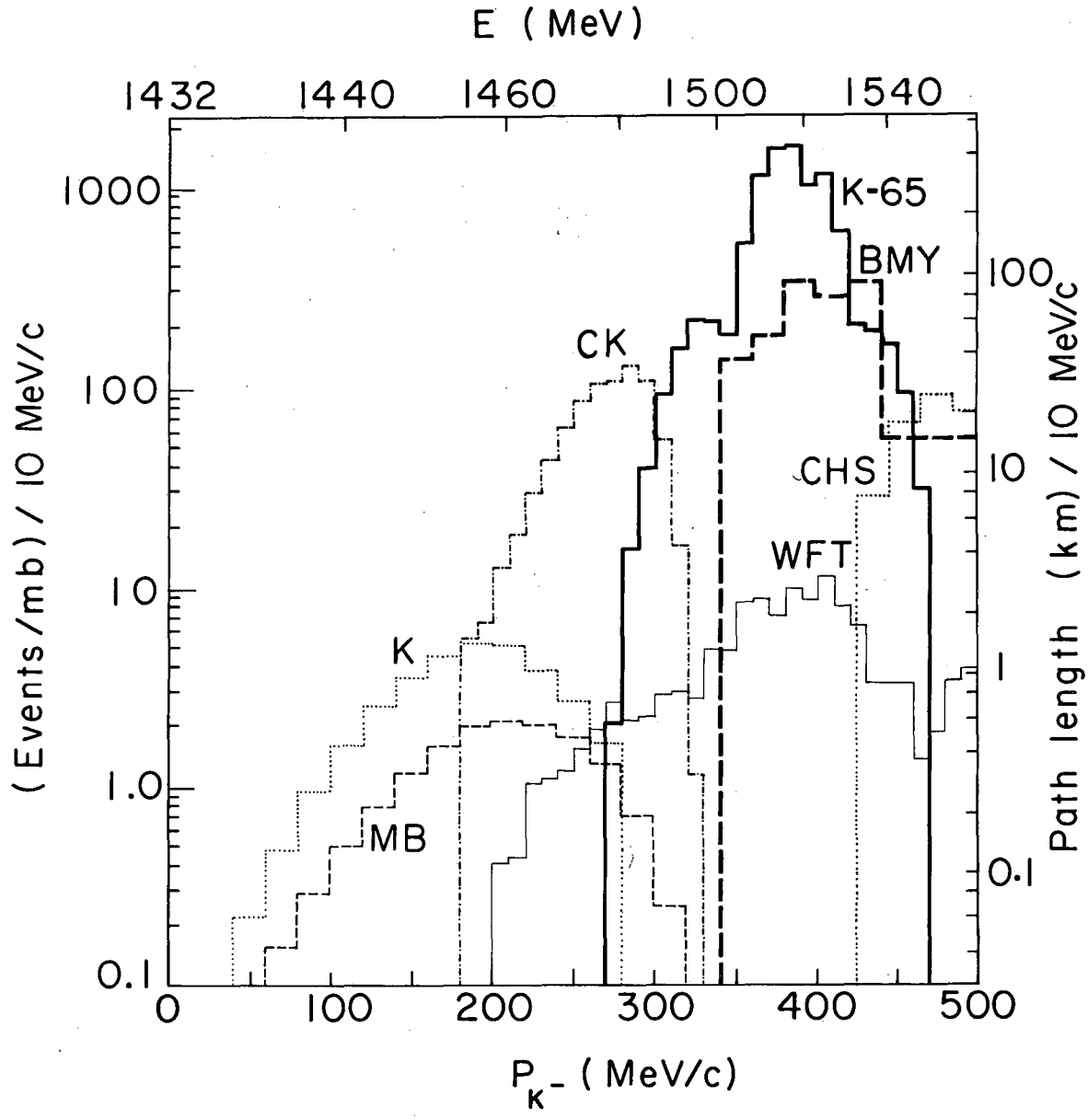
E (MeV)
1432
1440
1460
1500
1540
1000
100
10
1.0
0.1
(Events/mb) / 10 MeV/c
K-65
BMY
CK
CHS
WFT
K
MB
100
10
1
0.1
Path length (km) / 10 MeV/c
0
100
200
300
400
500
P_K- (MeV/c)
XBL704-2694

Fig. 1.

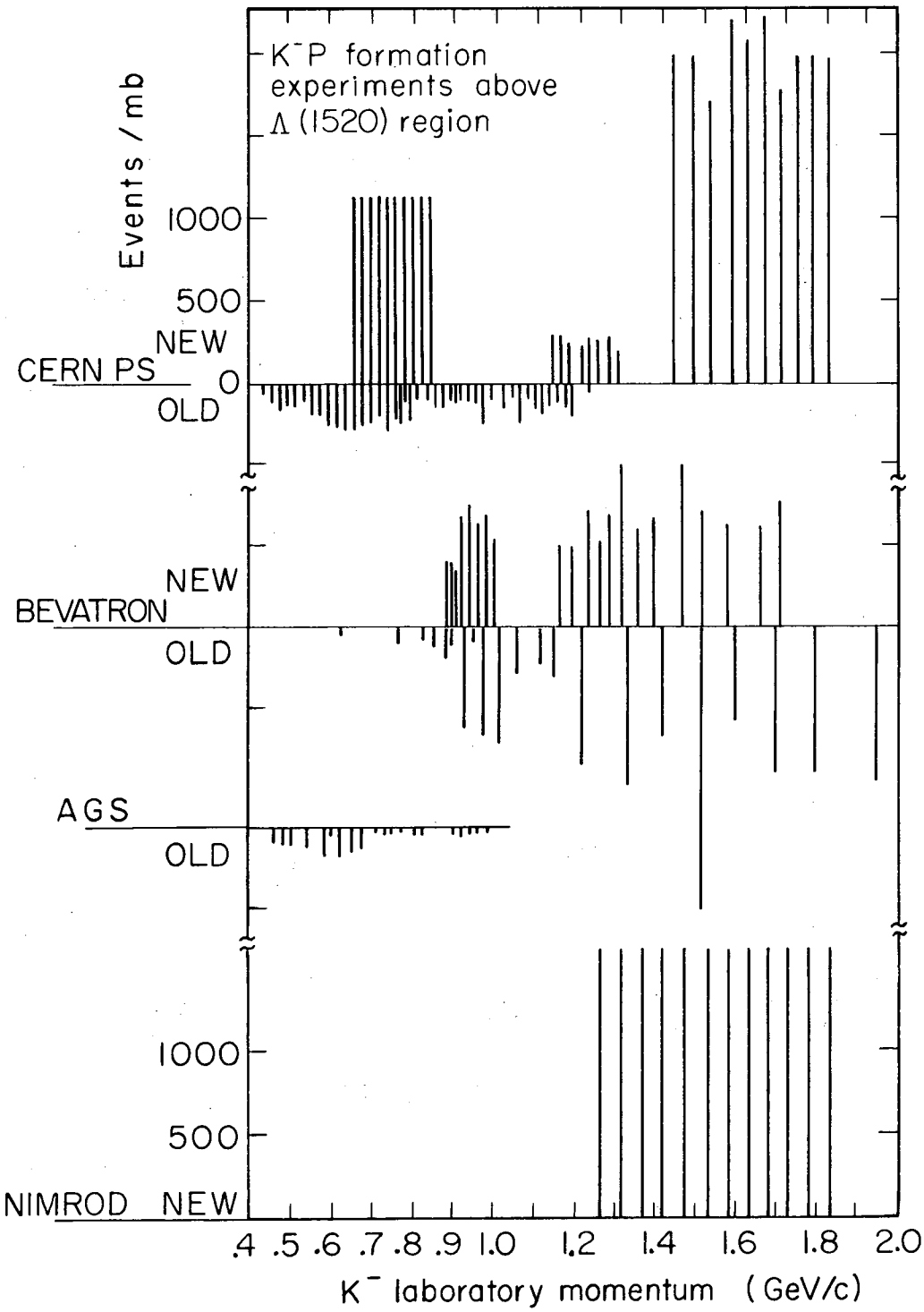

XBL713-3156

Fig. 2.

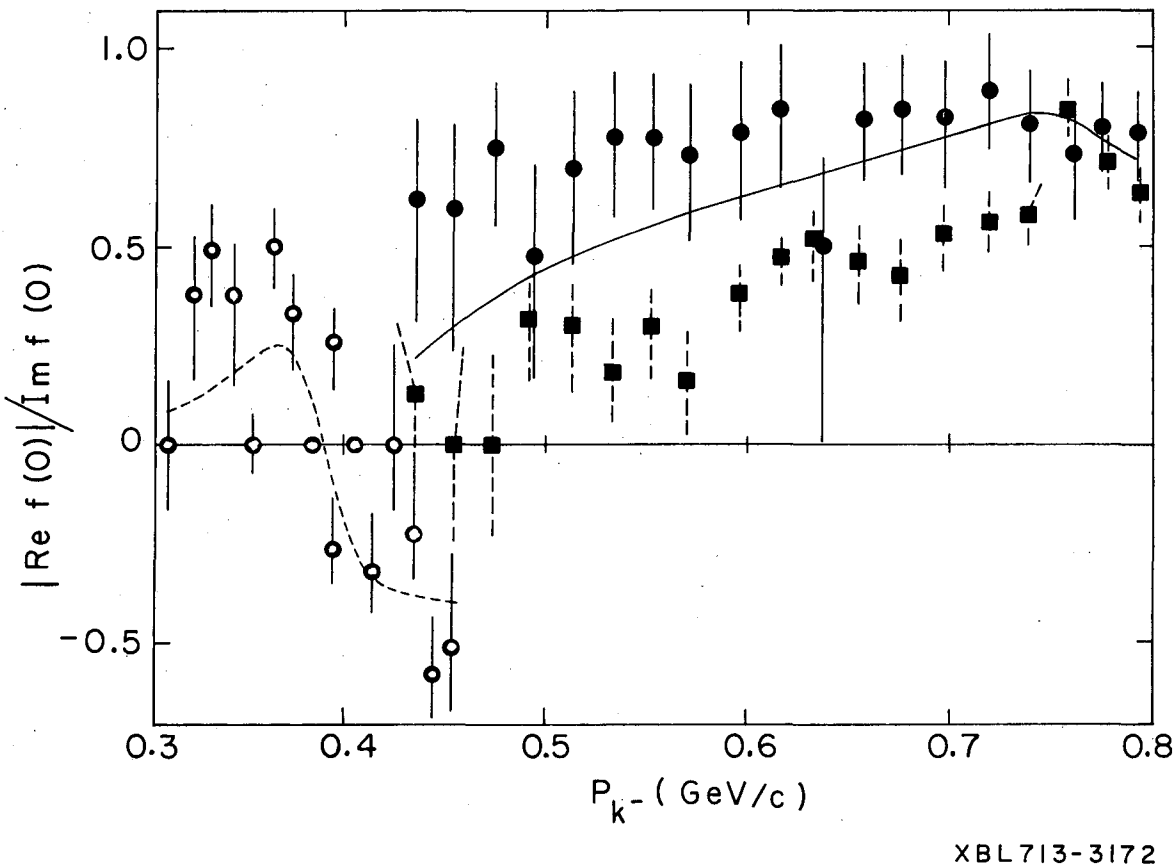

Fig. 3.

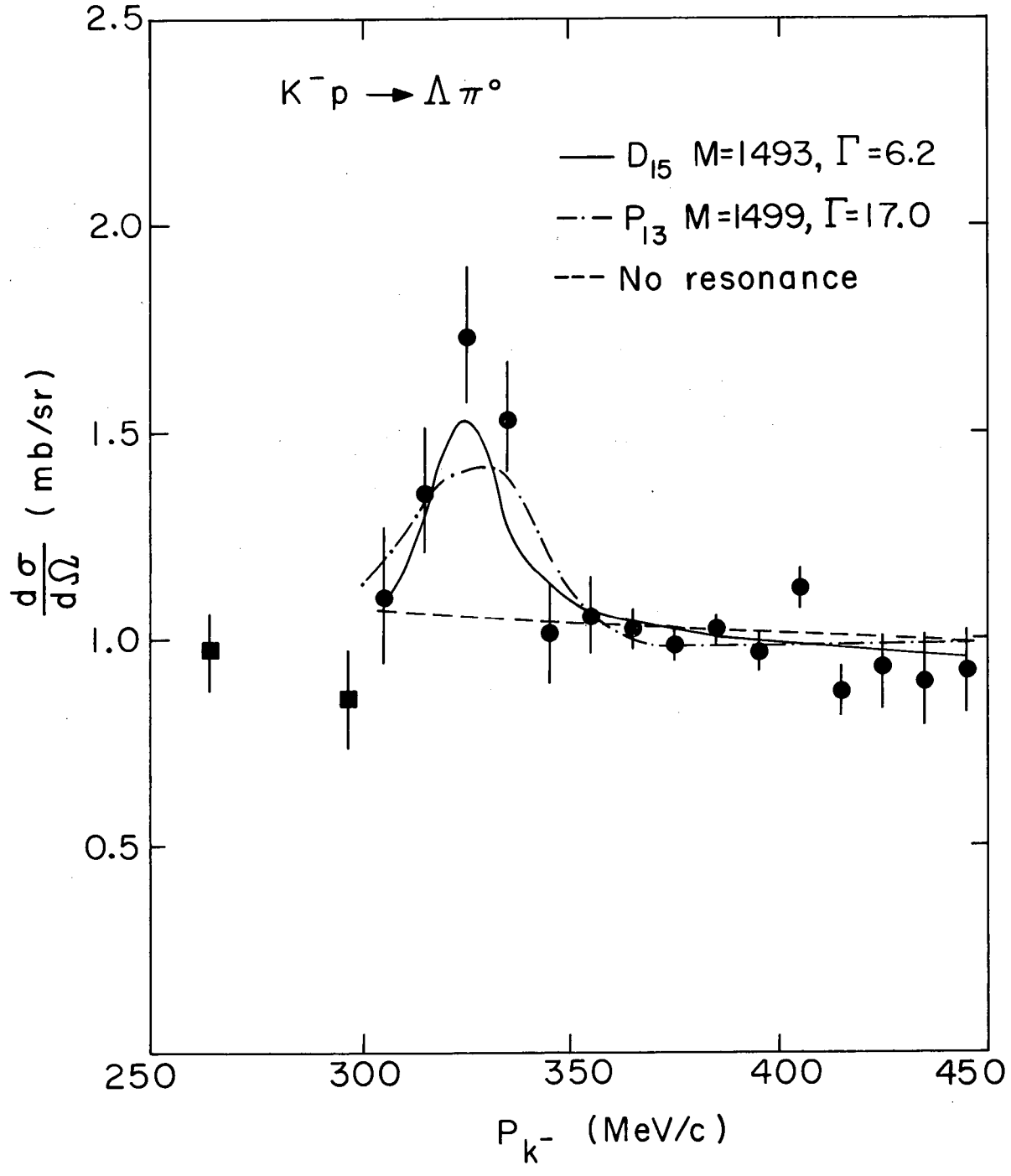

Fig. 4.

XBL713-3171

SESSION III

WORKSHOP TALK ON WEAK INTERACTIONS

L. Wolfenstein

WORKSHOP TALK ON WEAK INTERACTIONS

L. Wolfenstein

To obtain perspective I have listed in Table 1, thirty significant experimental results on weak interactions between 1957 and 1969. The list is somewhat arbitrary but serves to illustrate several points of interest: (1) even after high energy accelerators came into use, important results on weak interactions continued to come from low-energy and synchrocyclotron experiments; (2) with the exception of the neutrino experiment, the high-energy experiments involved kaons and hyperons at low energy and could be done in most cases at the PPA as well as Brookhaven; and (3) there is often a strong interrelationship between experiments at lower and higher energies--for example, the failure to find $\mu \rightarrow e + \gamma$ at synchrocyclotrons was the forerunner of the discovery of two neutrinos by the first BNL neutrino experiment. From both an intellectual and political point of view it is very healthy to have this kind of common interest between physicists in the different energy ranges.

A list of the important results likely to be found in the next twelve years is obviously even more arbitrary. I have tried to list some of these in Table 2. Some of those listed have already been carried out, but I list them for the future because the results at present are not sufficiently accurate or definitive to be entered in Table 1. I shall limit my discussion to the first four general items.

1. Tests of the Cabibbo Theory

When the Cabibbo theory of the $\Delta S = 1$ current was first published in 1963, the most striking feature to me was the prediction of the V/A ratios for the different hyperon decays. Until that time there was very little idea of what these should be except the feeling that probably all decays were V-A like the neutron. The Cabibbo theory on the other hand makes definite predictions given that $g_A/g_V = -1.23$ for the neutron and fitting the d/f ratio from experimental rates:[1]

$$\Lambda \rightarrow pe\,\nu \qquad g_A/g_V = -0.73$$

$$\Sigma \rightarrow ne\,\nu \qquad g_A/g_V = +0.26$$

$$\Xi \rightarrow \Lambda e\,\nu \qquad g_A/g_V = -0.24$$

Since Cabibbo's original paper the values of the decay rates have been determined to greater accuracy confirming Cabibbo's original analysis in terms of a single Cabibbo angle--indeed it works better than is theoretically to be expected. But there has been very little direct experimental confirmation of the g_A/g_V ratios. These require the decay of polarized hyperon with a study of the electron and neutrino asymmetries with respect to the hyperon spin, as well as the e-ν correlation. During the last year there have been two experiments on polarized Λ decay from CERN and Argonne and the measured asymmetries have not all agreed very well with the Cabibbo predictions but the accuracy is such that the disagreement is not really significant. More statistics are sorely needed. There is still less known about the Σ decay where there is the interesting prediction of the opposite sign for g_A/g_V. With more accurate experiments one might hope to check the Cabibbo predictions for the two less important forms factors:

(1) the weak magnetism predicted by the SU(3) generalization of CVC; and (2) the pseudotensor (the term of the form $g_T\ \sigma_{\mu\nu}\gamma_5 q_\nu$) predicted to vanish in the SU(3) limit if there are no second class currents.

2. Second-Class Currents

It is usually assumed that the hadronic $\Delta S = 0$ current has well-defined G transformation properties ($\approx$ means "transforms like")

$$V_\mu \approx \rho \qquad J^{PG} = 1^{-+}$$
$$A_\mu \approx A_1 \qquad J^{PG} = 1^{+-}$$

A second-class axial current would have

$$A_\mu^{II} \approx B \qquad J^{PG} = 1^{++}$$

The origin of this assumption came from the specific form for the current in terms of proton and neutron fields as in the Feynman-Gell-Mann paper:

$$J_\mu = \bar{P}\ \gamma_\mu(1 + \gamma_5)n$$

in which case there is no second-class current. This remains true in a later version in which p and n are quarks. It should be noted that the assumption is not only that the current can be written in terms of quarks but that there are no derivative couplings. Since the B meson can be made out of quarks so can the second-class axial current.

So the question is really experimental. Interest has recently been aroused in this question because of the advertising efforts of Wilkinson.[2] It has been known for almost a decade that there is a difference in the ft values of the mirror betta-decays:

$$B^{12} \rightarrow C^{12} + e^- + \bar{\nu}$$

$$N^{12} \rightarrow C^{12} + e^+ + \nu$$

The difference parameter

$$\delta = \frac{ft(e^+)}{ft(e^-)} - 1$$

is about 10%. Wilkinson has surveyed δ for a number of cases and finds they can all be fitted (although most of the data is rather poor) to a single straight line as a function of the energy release in agreement with some theoretical predictions. It is quite possible that this difference can be explained as being an electromagnetic effect, but if it is not then it is evidence for a second-class axial current.

There are three other places we can look for second-class currents. In muon capture $\mu^- + p \rightarrow n + \nu$ the induced-tensor coupling could make a significant contribution to the rate, although it is not distinguishable from a change in the value of the induced pseudoscalar coupling. The present rate for muon capture on hydrogen[3] agrees perfectly with theory assuming CVC, $g_p = 7g_A$, and no second-class current to the experimental accuracy of about 10%. The second-class current would make a large contribution to the elastic high-energy neutrino reaction $\nu_\mu + n \rightarrow \mu^- + p$ at large values of q^2, although it takes detailed experiments to isolate this factor in the presence of contributions from the unknown first-class axial form factor $g_A(q^2)$.

An important possibility mentioned in Weinberg's original paper[4] is to compare the rates for the mirror decays:

$$\Sigma^+ \rightarrow \Lambda\, e^+ \nu$$

$$\Sigma^- \rightarrow \Lambda\, e^- \nu$$

If there are no second-class currents these should have the same ft-values, which means the rate ratio is given by phase space. Here there is the advantage that there are no coulomb corrections, although I do not know whether the radiative corrections have been investigated. At present the rate ratio agrees with theory within an experimental error of about 25%. It is clearly very desirable to improve this. If there were second-class currents and these had octet transformation properties then in the SU(3) limit they would contribute only to the pseudotensor-type coupling. This presumably could be observed by a detailed study of the correlations and polarization-dependence of these decays.

3. CP and T Violation

At present the only evidence for CP or T violation comes from K^o decays. The limited information available, the phase and magnitude of η_{+-} and the charge asymmetry in the $K_{\ell 3}$ mode, agree with a simple one-parameter model in which all CP violation is confined to the dispersive part of the K^o mass matrix. Then the only CP violating effects are associated with the mixing of the wrong CP state in the K_L and K_S state vectors. The simplest realization of this model is the superweak-theory in which CP violation is associated with a very weak interaction which allows $\Delta S = 2$ transitions in lowest order. In this case CP violation outside the K^o system is too small to be observed in foreseeable experiments.

Since proposing the superweak theory I have spent a good deal of effort urging people not to accept it too readily. The point is that there are many other theories which give quite similar results but that are very different in their implications. To distinguish these it is necessary

either (1) to find small discrepancies in the values of Φ_{+-} or η_{oo} relative to the superweak predictions; or (2) to find CP violation in other processes. While it is very important to obtain precision values of the CP-violation parameters in K_L decay it seems unlikely that discrepancies of the order of 1^o in Φ_{+-} or 5% in η_{oo} will be believed in the near future even if some experimenters uncover them.

It therefore remains important to search for small amounts of CP or T violation in other processes. It is still true that no experiments searching for CP or T violation have obtained the accuracy of parts per thousand that characterizes the observed CP violation in K_L decay. It is natural to look in non-leptonic strange-particle decays, which is where CP violation was first found. At present the best test is in the slopes of the Dalitz plot of τ^+ and τ^- decays

$$\Delta = \frac{a(\tau^+) - a(\tau^-)}{a(\tau^+) + a(\tau^-)} = -.007 \pm .005$$

from a recent experiment of Piroué and others.[5] This is at the 1% level. In hyperon decay the best limit comes from the β_Λ parameter in $\Lambda \to p\pi^-$ which agrees with the prediction based on pion-nucleon phase shifts to accuracy of about 10%.[6] This could be improved to a great extent although improvements in knowledge of pion-nucleon scattering at 37 MeV pion energy would be needed. The CP-violating amplitude for $K_S \to 3\pi$ is still almost completely unknown; at best present experiments say that it is not greater than the CP-conserving amplitude $K_L \to 3\pi$.

For liptonic decays the best limits come from the relative phase of V and A in beta-decay and the transverse muon polarization in $K_{\mu 3}$. These are both around the 2% level. At an order-of-magnitude lower one should

see a definite non-zero transverse polarization in $K_L \to \pi\mu\nu$ due to the electromagnetic final-state interaction. This, however, is predictable and depends very little on the poorly-determined form factors of the decay.[7] Finally there is the possibility of electromagnetic CP violation which can be tested from the rates of $K^{\pm} \to \pi^{\pm}\pi^{o}\gamma$, the transverse polarization in $K \to \mu\nu\gamma$, or in η-meson decays.

4. "Forbidden" Decays

By this I mean decays that are not forbidden by absolute selection rules but are forbidden in lowest order by the usual weak interaction Hamiltonian. Examples are:

$\Delta S = 2$	$\Xi \to N\pi$
	$\Xi \to Ne\nu$
$\Delta Q = \Delta S$	$K^+ \to \pi^+\pi^+e^-\nu$
4 Leptons	$K^+ \to \mu^+ + 3\nu$
"Neutral Currents"	$K_L \to \mu^+\mu^-$
	$K \to \pi + e^+ + e^-$
	$K \to \pi + \nu + \bar{\nu}$

There are several reasons for interest in these. One is the possibility that there are small corrections to the usual weak interaction, sometimes called milliweak interactions, that violate these selection rules; perhaps they are of the same order as CP violation. A second possibility suggested by Pontecorvo and others is that these may be due to the weak interaction plus new unknown interactions.[8] An illustrative, though very unlikely, possibility is a four-neutrino reaction which would allow (A) $K \to \mu + \nu + \nu + \nu$ and also (B) $\nu_\mu + p \to \mu^+ + \nu_\mu + \nu_\mu + n$. An interesting comparison calculated by Pontecorvo et al. is that a measurement

of a branching ratio of 10^{-5} for (A) would be equal in sensitivity to a measurement of a cross-section for (B) of about 10^{-41} cm^2 at 10 GeV as far as detecting the $\nu\nu\nu\nu$ interaction is concerned.

To me by far the most important reason for studying "forbidden decays" comes from the desire to understand the expansion parameter for weak interactions. The lowest order for the usual Hamiltonian gives a matrix element

$$M^{(1)} \approx \frac{Gm_p^2}{4\pi} \approx 10^{-6}$$

The next term is

$$M^{(2)} \approx \frac{Gm_p^2}{4\pi} \lambda .$$

How large is λ ? If we use the $\Delta S = 2$ nonleptinic transition as determined from the mass difference $m(K_L) - m(K_S)$ as a measure we find $\lambda \approx 10^{-6}$. The recent limit on $K_L \rightarrow \mu^+\mu^-$ determined by the Berkeley group[9] sets λ as less than 10^{-4} to 10^{-5}. The significance of λ depends on theoretical models and in many models λ is expected to be quite different for different processes. If we think of the term $M^{(2)}$ as coming from the second-order of the usual weak interaction then

$$\lambda \approx \frac{G\Lambda^2}{4\pi}$$

where Λ is the needed cutoff. The mass difference gives a limit on Λ of ≈ 4 GeV, whereas the limit on $K_L \rightarrow \mu^+\mu^-$ gives a limit on Λ of about 20 GeV. There are other possible models for $M^{(2)}$. Thus in the model of Kummer and Segrè elaborated by Christ[10] the expansion parameter is $\frac{q^2}{M^2}$ where q^2 is defined in terms of the external momenta and M is the mass of the intermediate particles (two bosons and two fermions) that mediate the weak interaction. In the Okubo model of CP violation[11] $M^{(2)} \alpha g^3$ where g is the semiweak coupling so that:

$$\lambda \approx \sqrt{\frac{Gm_p^2}{4\pi}} = 10^{-3}.$$

This model predicts a rate[12] for $K_L \to \mu^+\mu^-$ of about 5×10^{-8} and so would seem to be ruled out by the recent data.

In models such as that of Christ decays like $K \to \pi e^+e^-$ and $K \to \pi\nu\bar{\nu}$ would be characterized by lepton nonlocality because the limit in which the usual interactions become local (intermediate masses $M \to \infty$) is just the limit in which these days are forbidden. The decay $K^+ \to \pi^+e^+e^-$ should be seen in the near future from the weak-electromagnetic one-photon exchange contribution alone. Once seen it would be important to look for an electron-positron asymmetry which would be a sign of an admixture of a nonlocal interaction.[13]

REFERENCES

1. F. Eisele, et al., Zeits f. Physik 225, 383 (1969).

2. D. H. Wilkinson, Phys. Letters 31B, 44-7 (1970).

3. A. Quarrenta, et al., Phys. Rev. 177, 2118 (1969).

4. S. Weinberg, Phys. Rev. 112, 1375 (1958). For a further discussion, see P. Hertal, Zeits f. Physik 202, 383 (1967).

5. W. T. Ford, et al., Phys. Rev. Letters 25, 1370 (1970).

6. Overseth and Roth, Phys. Rev. Letters 19, 391 (67).

7. Details are given in the thesis of J. Brodins, Carnegie-Mellon University (1971).

8. Okun, et al., Revue Romaine de Physiques, Tome 11, 819 (1966), Pontecorvo et al., Phys. Letters 32B, 121 (1970).

9. A. B. Clark, et al., submitted to Phys. Rev. Letters.

10. N. Christ, Phys. Rev. 176, 2086 (1968).

11. S. Okubo, Nuovo Cimento 54A, 491 (1968), Ann. of Phys. 49, 219 (1968).

12. R. E. Marshek, et al., submitted to Phys. Rev.

13. S. K. Singh and L. Wolfenstein, Nuc. Phys. B24, 77 (1970).

TABLE 1.

30 Major Experimental Results in Weak Interaction Physics from 1957 - 1969

Parity violation	
Beta - decay	L
π - μ - e decay	S
Non-leptonic hyperon decay	H
Nuclear γ-rays	L
CP violation	
η_{+-}	H
Φ_{+-}	H
Charge asymmetry in $K_{\ell 3}$	H
Limits on neutron E 1 moment	L
V-A Interaction	
e ν Correlation in β-decay	L
Helicity of β-decay ν	L
ρ parameter in mu decay	S
Spectrum of K_{e3} decay	H
Determination of coupling constants G_V, G_A, θ	
Neutron lifetime	L
Superallowed β transitions	L
Polarized neutron decay	L
Muon precision lifetime	S
Rates of hyperon leptonic decays	H
Rates of K^+ leptonic decays	H

Selection rules on lepton number	
Limits on $\mu \rightarrow e + \gamma$	S
Discovery of muon neutrino	H
Discovery of double beta-decay	L
Tests of conserved current theory	
Rate of $\pi^+ \rightarrow \pi^o$ e ν	S
B^{12}, N^{12} beta spectra	L
Tests of muon-electron universality	
Rate of $\pi \rightarrow$ e + ν	S
Rate of $\mu^- + p \rightarrow n + \nu$	S
Rate of $K \rightarrow e + \nu$	H
Isotopic spin selection rules	
K^o leptonic decay rates	H
Non-leptonic hyperon decay branching ratios and asymmetries	H
Rates and Dalitz plots for $K \rightarrow 3\pi$	H
Mass difference between K_L and K_S	H

10 are L = low energy (ratioactive sources, reactors)

7 are S = synchrocyclotron energies (1 BeV > E > 300 MeV)

13 are H = high energy (> 1 BeV)

TABLE 2.

Some Major Experiments in Weak Interaction Physics for the Next Decade

Tests of Cabibbo Theory of $\Delta S = 1$ currents	
Hyperon leptonic decay parameters	I
Ξ leptonic decays	H
Second class currents	
Tests in beta-decay	L
Muon capture	S
$\Sigma^{\pm} \rightarrow \Lambda\, e^{\pm}\, \nu$	I
Neutrino elastic reaction	H
CP and T violation	
Precision values for the K_L decay parameters	I
Lower limits on neutron dipole moment	L
Transverse polarization in $K_{\mu 3}$	I
Tests in hyperon leptonic and non-leptonic decays	I
Amplitude for $K_S \rightarrow 3\pi$	I
Neutrino experiments	H
Asymmetric in η and η' decays	I
$\pi \rightarrow e + \nu + \gamma$ and $\pi \rightarrow e^+ \nu e^+ e^-$	S
"Forbidden" processes	
Detection of neutral currents $K_L \rightarrow \mu^+ \mu^-$ $K \rightarrow \pi \bar{e} e$, $K \rightarrow \pi \nu \bar{\nu}$	I
Limits on $\nu + p \rightarrow \nu + p$	H
Search for $\Delta Q = -\Delta S$ and $\Delta S = 2$ in neutrino reactions	H
Limits on $\Delta Q = -\Delta S$ in kaon decays	I

Form factors	
Determination of $g_A(q^2)$ in elastic neutrino reactions	H
Induced pseudoscalar in muon capture and radiative muon capture	S
Form factors in $K_{\ell 3}$ decay	I
Lepton selection rules	
Observations of double beta-decay	L
Forbidden muon decays as $\mu \rightarrow e + \gamma$	S
Neutrino reactions	H
Observations of neutrinos from muon decay	S
Isotopic spin selection rules	
$\Delta I = 1$ rule in $\nu + N \rightarrow N^* + \mu$	H
Violations of $\Delta I = 1/2$ rule in non-leptonic K and hyperon decays	I
Tests of the self-current	
Parity violation in $n + p \rightarrow d + \gamma$	L
$\nu + e \rightarrow \nu + e$	L
Structure of the weak interaction	
Locality tests in neutrino reactions	H
Search for the IVB	H
Precision measurements of muon decay	S
Tests of CVC	
$g_v(q^2)$ and $g_\mu(q^2)$ in neutrino reactions	H
More precise value of $\pi^+ \rightarrow \pi^o e \nu$	S
Muon capture	S
Form factors in $\Sigma \rightarrow \Lambda e \nu$	I

The high energy is here broken up as

I : 1 to 12 BeV
H : > 12 BeV

Discussion

Jovanovic (Argonne): If the intermediate vector boson is discovered would its mass provide a cut-off for weak interaction theories.

Wolfenstein (Carnegie-Mellon): If the intermediate vector boson is discovered it will be a very important result. For some processes it might provide a cut-off. On the other hand, the intermediate vector boson theory itself is divergent so it is not clear how the W-boson mass can in general be identified with the necessary cut-off.

Quigg (Stony Brook): I would like to mention a couple of electromagnetic decays I think are interesting. As you know the $K_L^0 \to \mu^+\mu^-$ is smaller than one would expect. It is in fact smaller than one expects the electromagnetic background to be. It is interesting to study decays in the theoretically simpler case where there is no weak interaction to confuse the calculation, namely: $\eta \to \mu^+\mu^-$ and $\pi^0 \to e^+e^-$. In these two decays, only the $\gamma\gamma$ intermediate state is important, so the theoretical estimate of a lower bound on the rate is (almost) ironclad. [Such estimates are contained in a paper I wrote with Jackson, UCRL-18487 (1968).]

Gidal (LRL): There are several theories concerning the origin of the Cabibbo angle. Are there any experimental areas where one can test these theories?

Wolfenstein (CMU): I think the explanations of the origin of the Cabibbo angle raise more questions than they answer. Some of the theories raise the question of whether there exists a sizable

non-electromagnetic isospin violating interaction. This is not so easy to test experimentally because we do not know how to calculate the E + M part. Nevertheless, it increases the interest in looking for violations of isotopic spin.

It is interesting to study the $|\Delta I| = \frac{1}{2}$ rule. One would like to increase the accuracy of the experimental results on $\Lambda \to n\pi^0$ to the point where one sees the level at which the $|\Delta I| = \frac{1}{2}$ rule is violated. Also I feel the radiative decays such as $\Sigma^+ \to p\gamma$ will be of interest in the future.

Conforto (RHEL): I would like to make a comment in regard to the test of T-invariance in Λ-decay. The πN phase shifts at the decay energy (≈ 40 MeV) are not known very accurately. One would have to improve on the πN phase shifts at ≈ 40 MeV if one desires to make tests on $\Lambda \to n\pi^0$.

Wolfenstein (CMU): Oh Yes! I thought I said that in addition to increasing the accuracy of the decay $\Lambda \to n\pi^0$ one has to increase the accuracy of the πN phase shifts.

PARTIAL WAVE ANALYSES IN MULTIPARTICLE FINAL STATES

R. J. Cashmore

Partial Wave Analyses in Multiparticle Final States

R. J. Cashmore

Introduction

So far in this workshop we have heard little discussion of processes other than 2 body reactions, even though elastic phase shift analyses predict appreciable inelasticities at low energies. For example, phase shift analyses of πN elastic scattering data indicate that $\sim 50\%$ of the total cross-section in the resonance region is in inelastic channels and this inelasticity is far from accounted for by ΛK, ΣK, ηK. This lack of study of the inelastic channels also means that we have essentially no measurements of resonance branching ratios into $\pi\Delta$, $N\rho$, etc. Such numbers will be important for a greater understanding of resonance classification schemes.

Thus there are two major reasons for studying inelastic channels:

1. To identify resonances.
2. To measure branching ratios.

At this moment the only other inelastic channels receiving any systematic investigations are those containing a 3 body final state. There are two major sources of 3 body final states.

1. Production experiments
2. Formation experiments

In this talk formation experiments will be the major topic but the importance of production reactions needs some emphasis.

Production Experiments

In a production reaction the 3-body system is produced via some mechanism schematically indicated in Fig. 1. Such reactions are important for the following reasons.

(a) It is the only way to observe 3-body meson systems (except in $\bar{p}p$ and e^+e^- annihilation) and thus the only way to identify many meson resonances and hence measure their properties ie. spin-parity, isospin, branching ratios etc.

(b) Many of the recently proposed baryon isobars are predicted to have small couplings to the elastic channel. These types of experiment allow their production by other mechanisms than coupling to the elastic channel, and thus the possibility that they can be more clearly seen.

Of course an enormous amount of information on the methods of production of these resonances is obtained at the same time.

U. Kruse[1] has discussed the analyses of 3-meson systems at length and clearly partial wave analyses will be vital for the eventual decision between the resonance and kinematic interpretations of many enhancements presently observed.

Formation Experiments

A formation experiment is schematically represented by Fig. 2. Such reactions are of interest for the identification of N^*, Δ, Y_0^*, Y_1^* and possibly Z^* resonances.

Figs. 3 and 4 demonstrate many of the characteristic properties of 3 body final states. They are from the reactions[2]

$$\pi^- p \rightarrow \pi^- \pi^+ n$$

$$\pi^- p \rightarrow \pi^- \pi^o p$$

where copious resonance production can be seen in the Dalitz plots. The production angular distributions are characteristic of resonance production at lower energies, becoming far more peripheral at the higher energies.

The major problem confronting anyone with 3-body data is how to extract any physics information from it. There are essentially two procedures usually followed

(i) make cuts on the data to select a quasi two body reaction

(ii) attempt to use all of the data at once.

(i) Selections of 2 body reactions

From Fig. 3 it is clear that if one selects the $\pi^- n$ to be in a Δ^- an enriched sample of the reaction

$$\pi^- p \rightarrow \pi^+ \Delta^-$$

is obtained. A conventional partial wave analysis can then be made of the Δ production angular distributions[3] (and possibly its decay distribution).

However, there are two major limitations.

1. A large amount of background is included by the selection. This problem can be reduced somewhat by making subtractions from adjacent areas of the Dalitz plot but even this may be very unsatisfactory due to the possible (most likely) presence of interference between Δ and the background.

2. The decay distributions are more susceptible to interferences and hence not as reliable as one would like.

These limitations and the small quantity of data make it essentially impossible to do an energy independent partial wave analysis and thus energy dependent analyses are used to extract the major partial wave amplitudes.

Fig. 5 represents the results of such an analysis[3]. There are at least two solutions but in both cases the F_{15} (P5 wave) and D_{15} (D5 wave) are required in order to make a fit. These represent the first measurements of the decay of the F_{15} and D_{15} into an inelastic channel. However, if solution A is correct we still have no knowledge of decay channels other than $\pi\Delta$ for the F_{15}.

(ii) Analysis of the whole final state

In general, four variables are required to describe a 3 body final state at a given cms energy. These 4 variables are usually chosen to be

(a) Two angles Θ and Φ expressing the relative orientation of the incident beam and the normal to the plane of the three final state particles.

(b) Two invariant masses ω_1, ω_2 specifying the relative position of the particles within the plane.

Two methods are used to extract information from this information in four variables.

(1) Model Independent

The cross-section is written[4] as

$$\frac{d^4\sigma}{d\omega_1^2 d\omega_2^2 d\cos\Theta d\Phi} = \sum_{LM} W_L^M(\omega_1^2,\omega_2^2) Y_L^M(\Theta,\Phi)$$

where the W_L^M are products of partial wave amplitudes. Thus these W_L^M are analogous to the expansion coefficients A and B of elastic scattering differential cross-section and polarization distributions. They have many similar properties[4].

(a) interference of waves of the same parity lead to terms of even L

(b) interference of waves of opposite parity lead to terms of odd L

(c) if j_1 and j_2 are the maximum angular momenta present $L_{max} \leq j_1 + j_2$ (if $j_1 = j_2 = j_m$, which is a half integer, then (a) tells us that $L_{max} < 2j_m - 1$)

This approach has been applied by a number of groups but due to the lack of data the Dalitz plot has either not been subdivided at all or just divided into 2 or 3 sections. Clearly this will lose information. Figs. 6 and 7 demonstrate the results of such measurements in the reaction

$$\pi^- p \rightarrow \pi^+ \pi^- n \ .$$

The large non zero W_1^1 moments indicate the presence of waves of opposite parity while the non-zero W_4^0 around 1700 MeV is due to the presence of the D_{15} and F_{15} resonances. However, the W_5 moments which should represent interference between these two states are zero indicating the loss of information in integrating over the Dalitz plot.

We can make the following comments about this method:

(1) At present it can only serve as a guide.

(2) Measurements with polarized targets are necessary to give enough W_L^M to allow a determination of the partial waves.

(3) Without measurements of the final baryon spin, parity ambiguities still exist.

(4) The overall phase is undetermined.

(5) If certain partial wave amplitudes show resonant behavior a model of their variation over the Dalitz Plot is still needed to extract couplings to various decay channels.

(6) ~ 1000-2000 events/region are necessary to make reasonable measurements of the W_L^M.

However it does have the distinct advantages that:

(1) It is model independent.

(2) It represents a complete description of the data.

(3) The reactions $K^- p \to \Lambda\pi\pi$, $\Sigma\pi\pi$ using polarized targets allow measurements of the final baryon polarization and hence sufficient quantities to determine the partial wave amplitudes.

(2) Model Dependent

The model conventionally used is the isobar model which is schematically represented in Fig. 8. The main ingredients of such a model are

(a) Include a large no. of final state interactions, eg. Δ, ρ, σ,

$I = 2$ $\pi\pi$, N^*'s etc.

(b) Include a large number of partial waves for the production of each quasi two body system.

(c) Ensure Bose symmetry for the two pions.

(d) Add amplitudes coherently.

This prescription then gives the amplitude and hence the cross-section as a function of the 4 variables ω_1^2, ω_2^2, Θ and Φ.

The advantages of this procedure are:

(a) the calculations are comparitively easy

(b) different final states differ only by Clebsch Gordon coefficients and hence it is easy to fit them simultaneously

(c) the couplings to different channels are automatically obtained

(d) the problems of background are removed (only within the model's validity of course)

There are disadvantages too:

(a) it is model dependent

(b) in order to keep the calculations reasonably simple, different angular momentum bases are used

(c) the introduction of the final state interactions as

$$\frac{e^{i\delta}\sin\delta}{q^{L+1}} \quad \text{or} \quad \text{Breit-Wigner}$$

while probably reasonably correct near a resonance are more doubtful when far away from the central value or when the resonance is very broad eg. σ. (s-wave $\pi\pi$)

(d) even though the calculations are reasonably simple there is

still immense scope for error. At present we are now reasonably convinced that the major groups involved in such analyses do agree on their calculations.

Having made this model, it is necessary to decide how to fit the data and this has been approached in a different manner by the different groups.

(a) Saclay[5]: Fits are made to the W_L^M, described previously, as functions of $\pi\pi$ mass bands in the Dalitz Plot.

(b) Oxford[6],[7]: Fits are made to projections of the data. Figs. 9, 10 and 11 demonstrate the sort of results obtained in fits to the reactions

$$\left.\begin{array}{l} \pi^+ p \to \pi^+ p\pi^o \\ \pi^+\pi^+ n \end{array}\right\} \text{ at 800 MeV/c}$$

while Fig. 12 demonstrates the variation of different solutions as a function of energy. (These analyses are energy independent.) In general, it is found that the moduli of the partial wave amplitudes vary smoothly while the phases are far less well determined.

In Fig. 13 the values of $\sqrt{1 - \eta^2}$ determined by this method are compared with predictions of the CERN EXP phase shifts.

(c) LRL/SLAC: The most efficient use of the data in a 4-D space is made by using a maximum likelihood method of analysis. At LRL we are at present applying such techniques to analyse the reactions.

$$\pi^- p \to \pi^+\pi^- n$$
$$\pi^-\pi^o p$$
$$\pi^+ p \to \pi^+ p\pi^o$$

Table 1 shows very preliminary results of such an analysis in the CM energy region 1680-1700 MeV. (Deliberately chosen so that identification of the D_{15} and F_{15} resonances should be made. The inelastic partial wave cross-sections are compared with the predictions of an average of the elastic phase shift analyses (EPSA). Clearly the agreement is good. Table 1 also contains the D_{15} and F_{15} branching fractions obtained by the method.

Finally, measurement of the final baryon polarization has been demonstrated to be useful in analyses of the reaction[8]

$$K^- p \rightarrow \Lambda\pi\pi$$

in the region of the Y*(1520), where more continuous solutions as a function of CMS energy have resulted.

Thus I think we conclude that:

(1) It is possible to obtain reasonable solutions to the 3 body data within the isobar model.

(2) The method leads to measurements of branching ratios of resonant states.

(3) The method could be applied to analyze

$$K^+ p \rightarrow K\pi N$$

(4) Measurements of final nucleon polarization and scattering from polarized targets will improve the analyses.

General Conclusions

In general, a better understanding of the 3-body reactions is being steadily obtained. The improvement in polarized targets should

allow measurements that will enable a model independent calculation of the important partial waves as a function of Dalitz plot variables.

Finally, it would be naive to think that we will understand the strong interaction by looking at elastic scattering or two body reactions alone. However, 3-body final states are more difficult to analyze and thus I think it would be valuable for theoreticians to work a little harder (ie. leave simple 2-body reactions) in an attempt to fill this theoretical gap while the experimentalists fill the obvious data gaps.

References

1. U. Kruse, Proceedings of Conference on the Phenomenology of Particle Physics 1971.
2. A. D. Brody et al., SLAC PUB 861.
3. A. D. Brody et al., SLAC PUB 788 (to be published in Phys. Letters).
4. D. Branson, P. V. Landshoff and J. C. Taylor, P.R. 132, 902 (1963),
   D. Morgan, P.R. 166, 1731 (1968),
   R. J. Cashmore, D. Phil Thesis, Oxford (unpublished).
5. M. De Beer et al., Nuclear Physics B12, 599 (1969).
6. M. G. Bowler and R. J. Cashmore, Nuclear Physics B17 (1970).
7. W. Chinowsky et al. Phys. Rev. 2D, 1790 (1970).
8. T. Mast, Private Communication.

Table 1

A comparison of inelastic partial wave cross-sections with the predictions of elastic phase shift analyses and the D_{15} and F_{15} branching fractions.

	EPSA	$\pi\pi N$
D_{15}	6.92 ± 0.17	5.54 ± 0.80
F_{15}	6.75 ± 0.32	7.01 ± 0.75
P_{33}	4.40 ± 1.72	5.58 ± 0.70
S_{31}	3.50 ± 0.40	2.63 ± 0.60
D_{33}	3.40 ± 2.00	4.44 ± 0.90
F_{35}	2.56 ± 1.56	0.0
D_{13}	2.43 ± 0.20	2.01 ± 0.50
P_{11}	2.24 ± 0.20	1.45 ± 0.40
D_{35}	1.80 ± 1.40	1.05 ± 0.25
P_{31}	1.60 ± 1.00	1.16 ± 0.45
P_{13}	1.43 ± 0.26	0.55 ± 0.20
S_{11}	1.37 ± 0.40	2.35 ± 0.50
F_{37}	0.48 ± 0.84	0.40 ± 0.15
F_{17}	0.15 ± 0.24	0.06 ± 0.05

D_{15}: $\frac{\pi\Delta}{\pi\pi N} \sim 1$	F_{15}: $\frac{\pi\Delta}{\pi\pi N} \sim 0.5$ $\frac{N\rho}{\pi\pi N} \sim 0.25$ $\frac{N\sigma}{\pi\pi N} \sim 0.25$

Figure Captions

1. Production Experiments.

2. Formation Experiments.

3. Dalitz Plots for the reactions $\pi^- p \to \pi^+ \pi^- n$, $\pi^- p \to \pi^- \pi^o p$.

4. Production angular distributions of each particle in the reaction $\pi^- p \to \pi^+ \pi^- n$.

5. Variation of partial wave amplitudes in two solutions A and B obtained in an energy dependent partial wave analyses of the reaction

$$\pi^- p \to \pi^+ \Delta^-$$

in the C.M. energy region 1647 MeV - 1760 MeV.

6. The moments W_L^M as a function of energy in the final state $\pi^+ \pi^- n$ for $L \leq 4$.

7. The moments W_L^M as a function of energy in the final state $\pi^+ \pi^- n$ for $4 \leq L \leq 5$.

8. The Isobar Model.

9. The projections of the Dalitz plot for the final state $\pi^+ \pi^o p$ on the three mass squared axes. The points are the values obtained from our solution B (0.8 GeV/c data).

10. Three projections of the angular distribution of the incident proton in the $\pi^+ \pi^o p$ c.m. Here θ is the polar angle with respect to the normal to the decay plane, ϕ_1 is the azimuthal angle measured from opposite the π^o direction and ϕ_2 is the azimuthal angle measured from opposite the π^+ direction. The points are values obtained from our solution B (0.8 GeV/c data).

11. The distributions fitted in the final state $\pi^+ \pi^+ n$. The points are values obtained from our solution B (0.8 GeV/c data).

12. The amplitudes for DS3, DD3, SS1 and PP3 are plotted for each of our three solutions. The radii are $\sqrt{\sigma_{JL'L}}$ and the azimuthal angles

Figure Captions (Cont'd)

give the relative phases of the $V^{JL'L}$ to $V^{\frac{3}{2}\,0\,2}$ (DS3). Typical errors are shown for solution B.

13. A comparison of the values of $\sqrt{(1 - \eta^2)}$ obtained from our model and the values obtained from the CERN phase shift analysis. We show the values from our solution B: values from solutions A and C are consistent with these results.

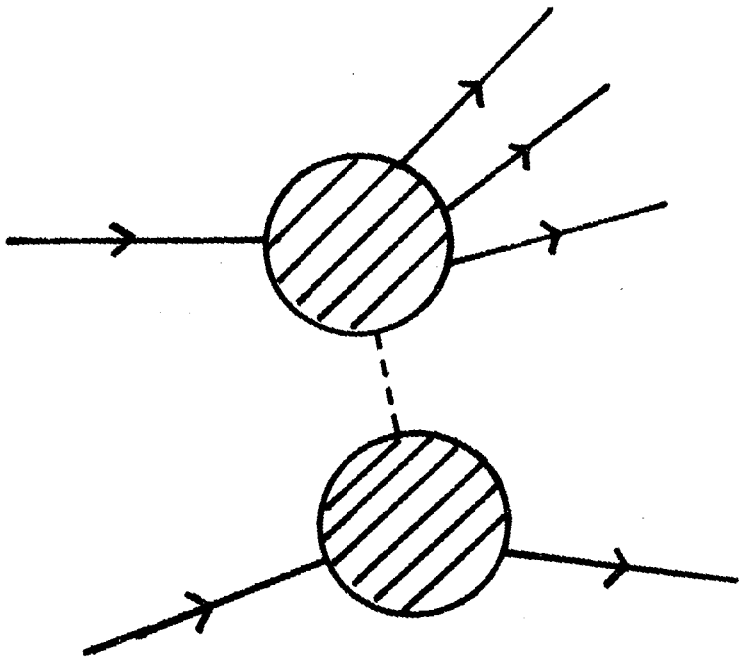

Eg. $\pi p \rightarrow p A_1$
$\rightarrow p A_2$
$\rightarrow p A_3$
$\pi p \rightarrow \pi N^*$

XBL 714-701

Fig. 1.

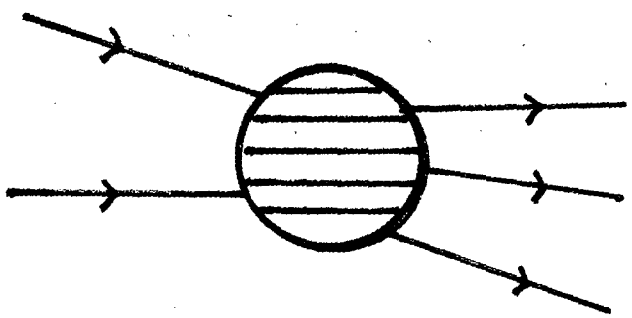

Eg. $\pi N \to \pi\pi N$
$\bar{K}N \to \bar{K}\pi N$
$\to \Lambda\pi\pi$
$\to \Sigma\pi\pi$
$KN - K\pi N$

XBL 714-702

Fig. 2.

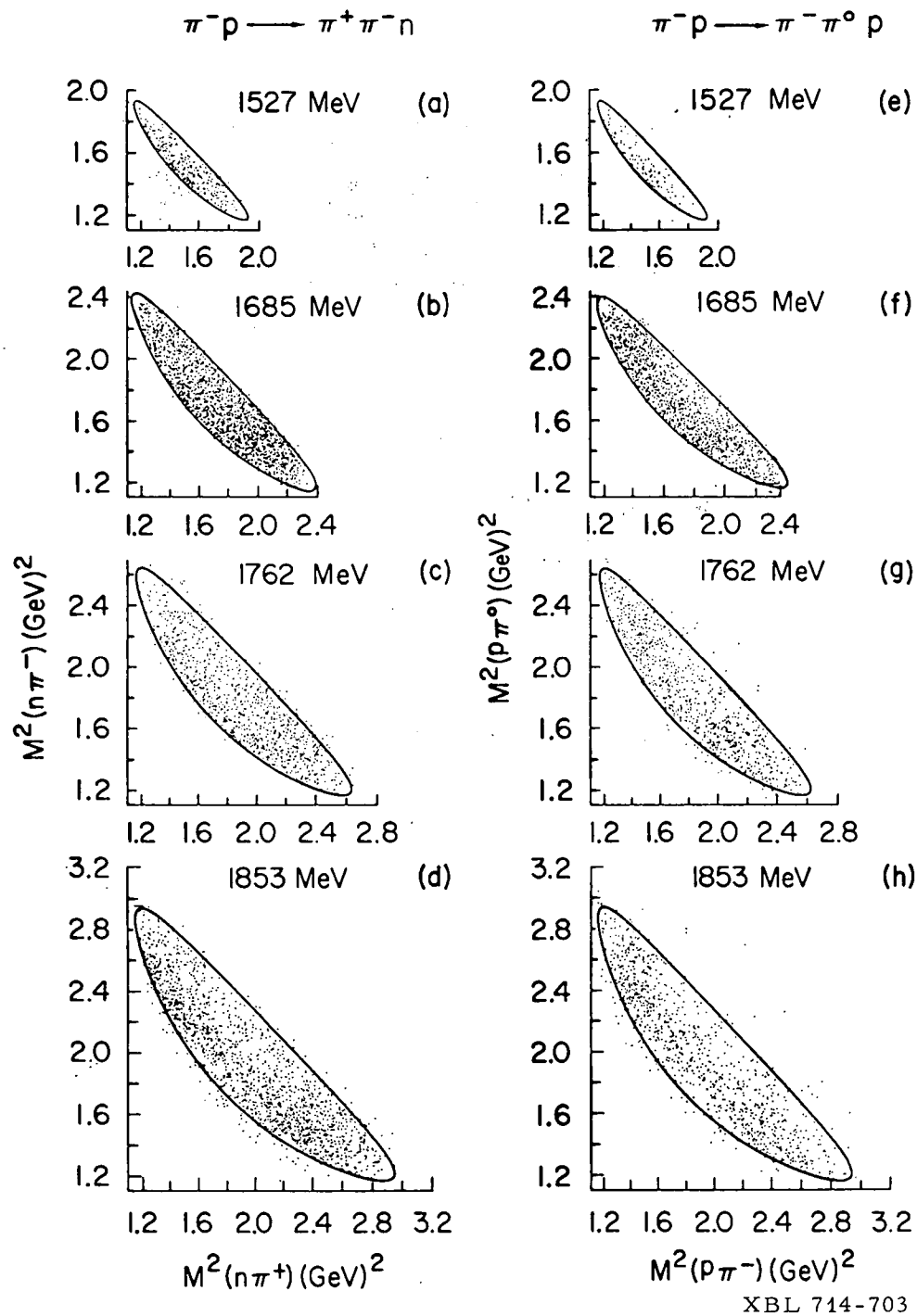
$\pi^- p \longrightarrow \pi^+ \pi^- n$
$\pi^- p \longrightarrow \pi^- \pi^\circ p$
1527 MeV (a)
1685 MeV (b)
1762 MeV (c)
1853 MeV (d)
1527 MeV (e)
1685 MeV (f)
1762 MeV (g)
1853 MeV (h)
$M^2(n\pi^-)$ (GeV)^2
$M^2(p\pi^\circ)$ (GeV)^2
$M^2(n\pi^+)$ (GeV)^2
$M^2(p\pi^-)$ (GeV)^2
XBL 714-703

Fig. 3.

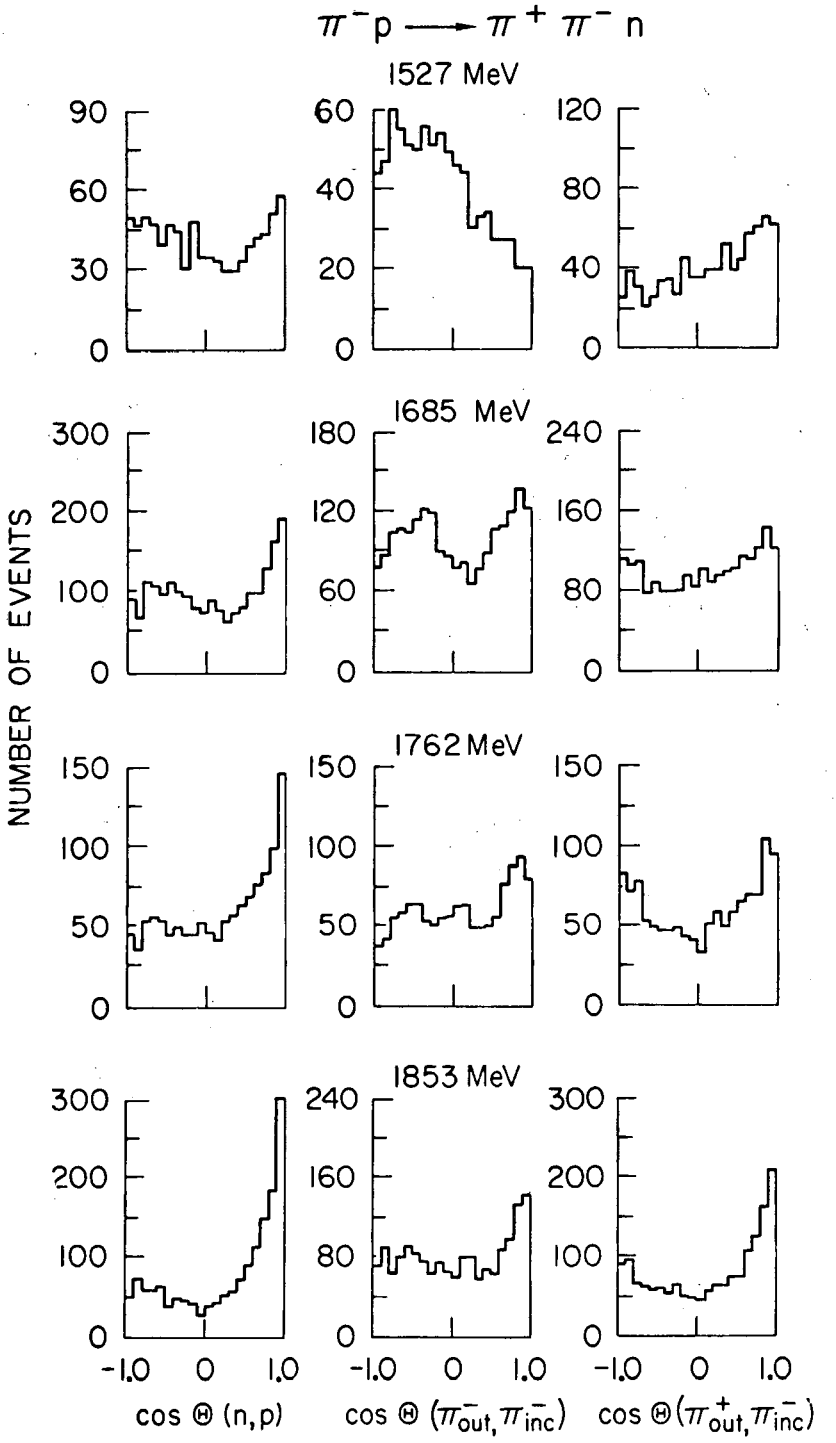
$\pi^- p \longrightarrow \pi^+ \pi^- n$
1527 MeV
1685 MeV
1762 MeV
1853 MeV
NUMBER OF EVENTS
cos Θ (n,p)
cos Θ (π^-_{out}, π^-_{inc})
cos Θ (π^+_{out}, π^-_{inc})
XBL 714-704

Fig. 4.

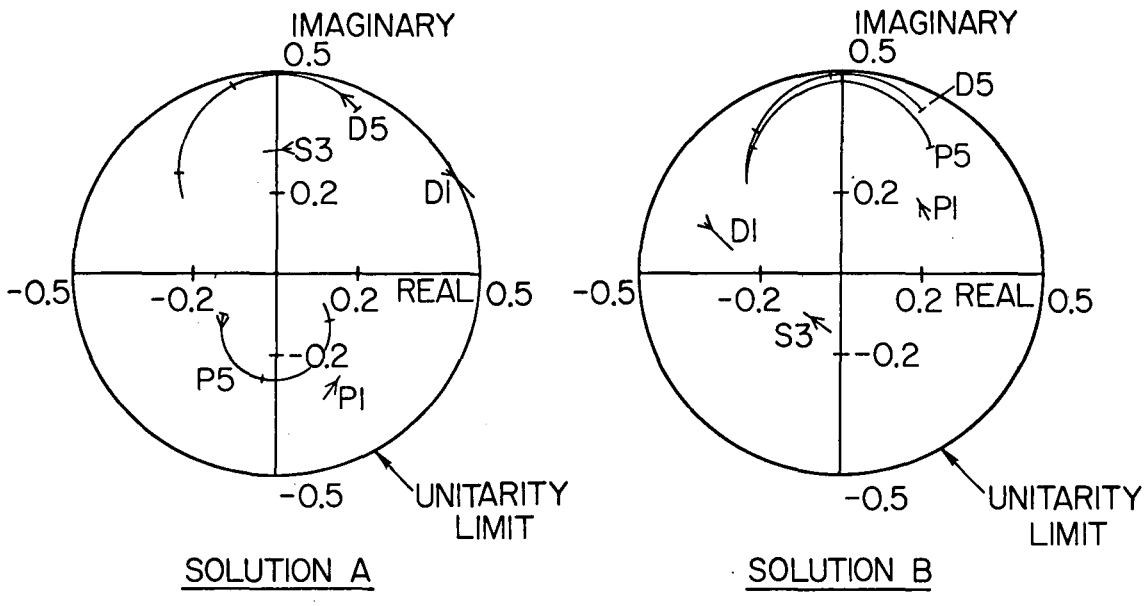

XBL 714-705

Fig. 5.

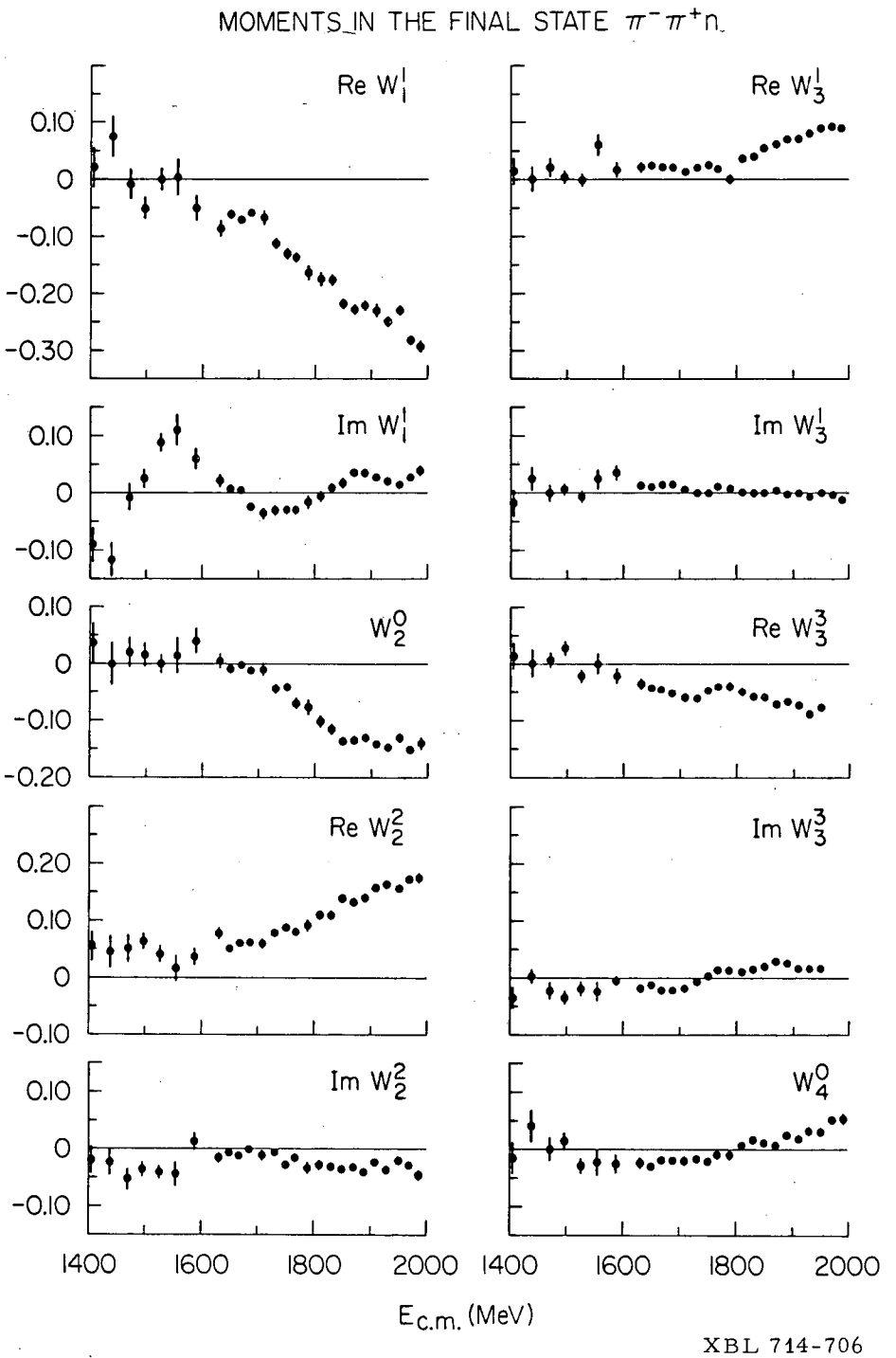
MOMENTS IN THE FINAL STATE $\pi^-\pi^+n$
Re W_1^1
Re W_3^1
Im W_1^1
Im W_3^1
W_2^0
Re W_3^3
Re W_2^2
Im W_3^3
Im W_2^2
W_4^0
0.10
0
-0.10
-0.20
-0.30
0.20
1400
1600
1800
2000
$E_{c.m.}$ (MeV)
XBL 714-706

Fig. 6.

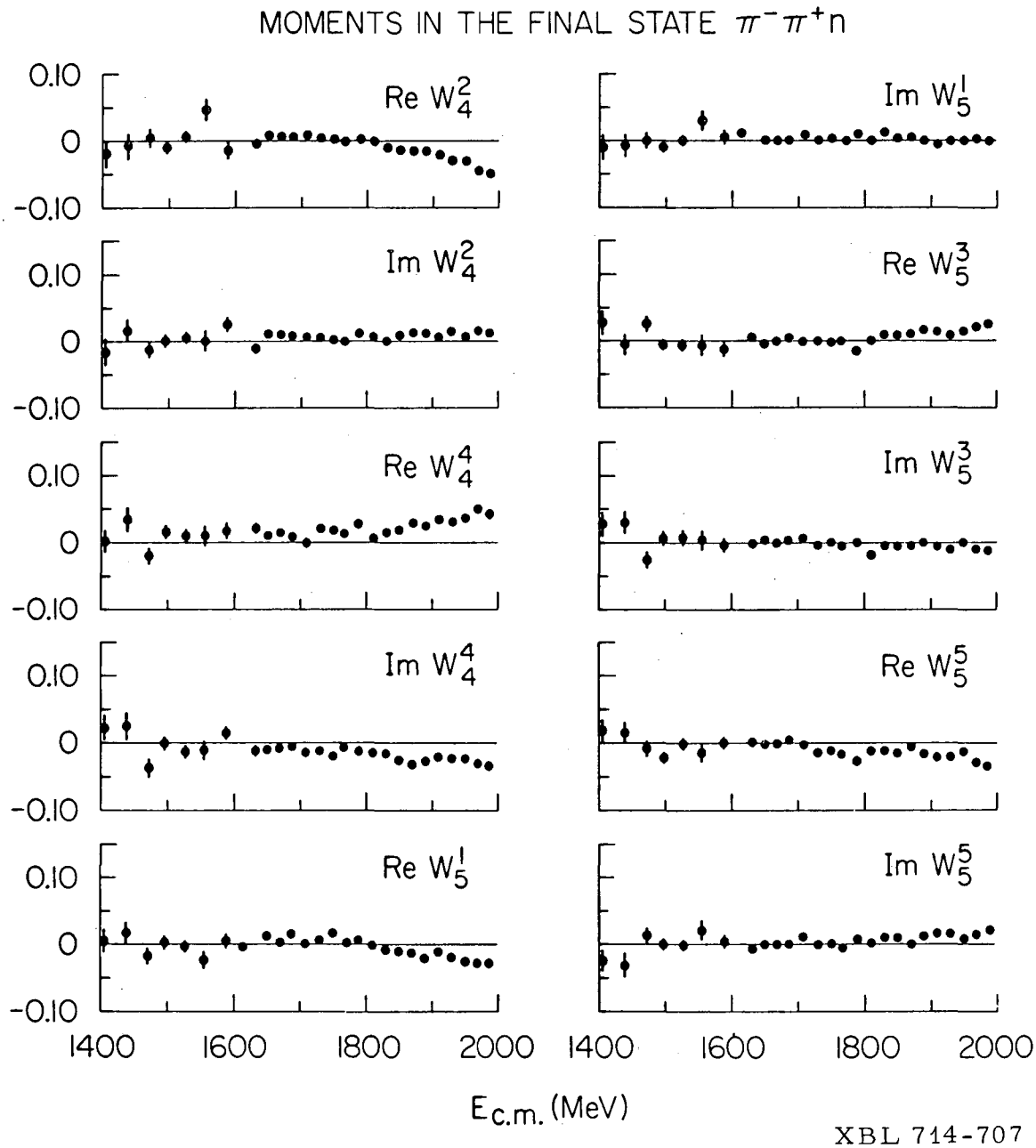
MOMENTS IN THE FINAL STATE $\pi^-\pi^+n$
Re W_4^2
Im W_5^1
Im W_4^2
Re W_5^3
Re W_4^4
Im W_5^3
Im W_4^4
Re W_5^5
Re W_5^1
Im W_5^5
0.10
0
-0.10
1400
1600
1800
2000
$E_{c.m.}$ (MeV)
XBL 714-707

Fig. 7.

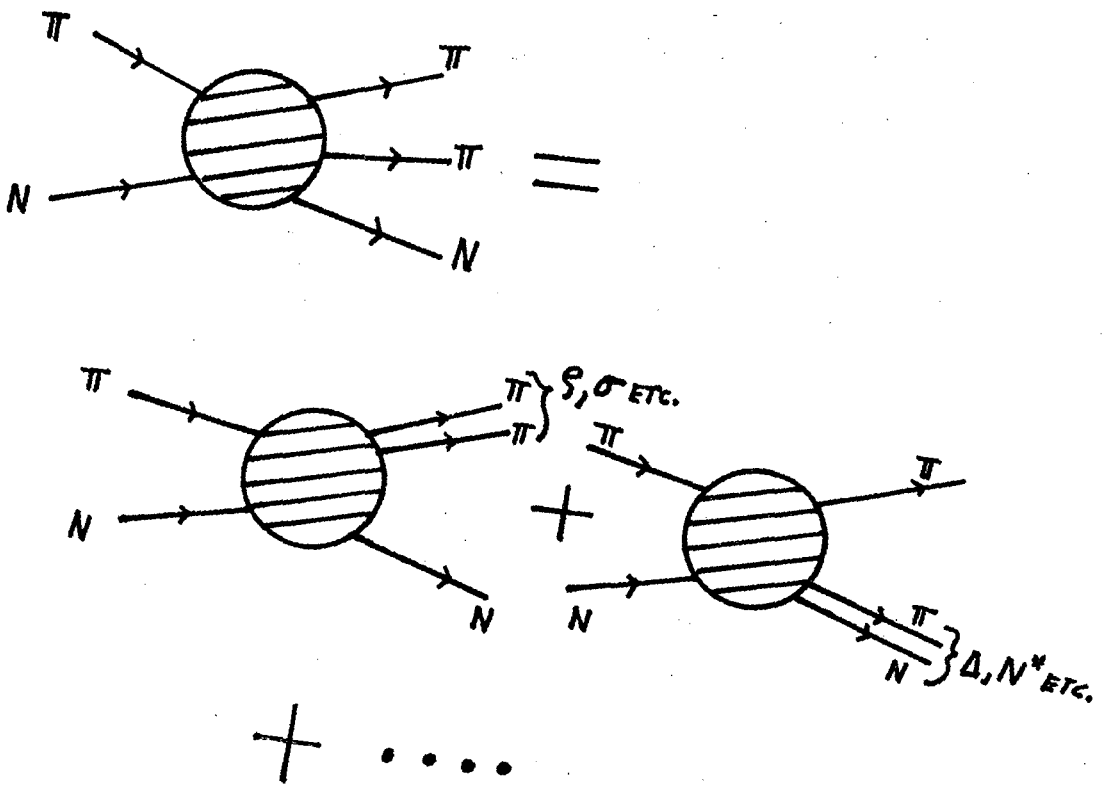

XBL 714-708

Fig. 8.

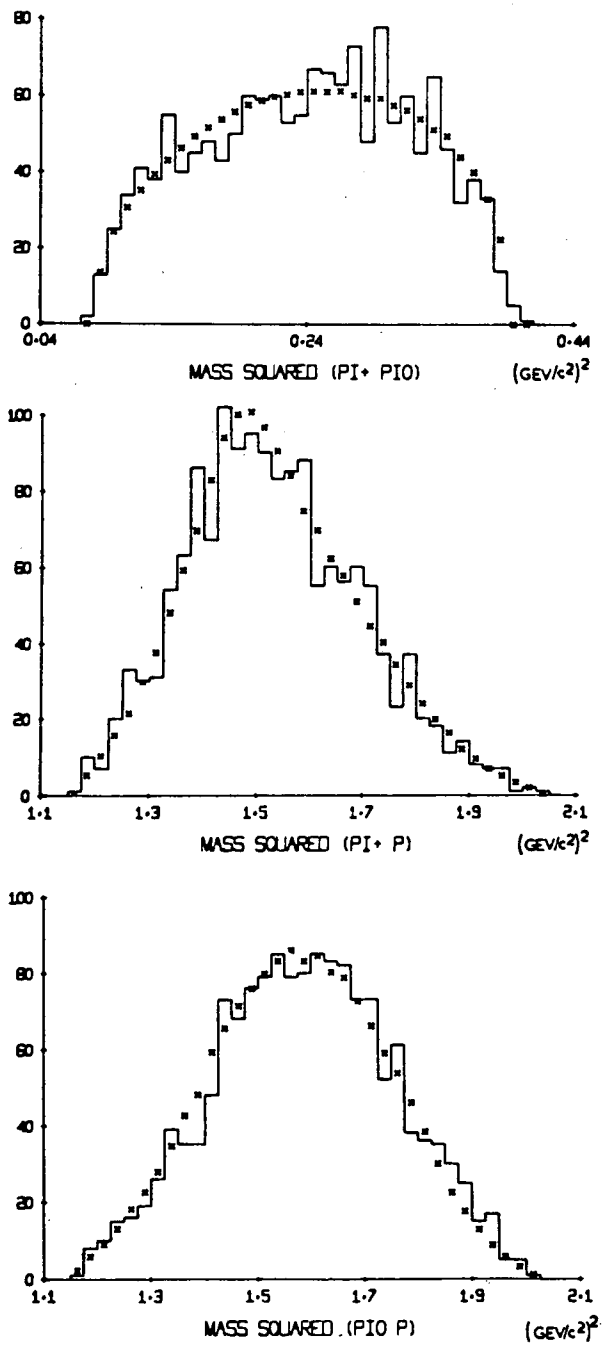

XBL 714-709

Fig. 9.

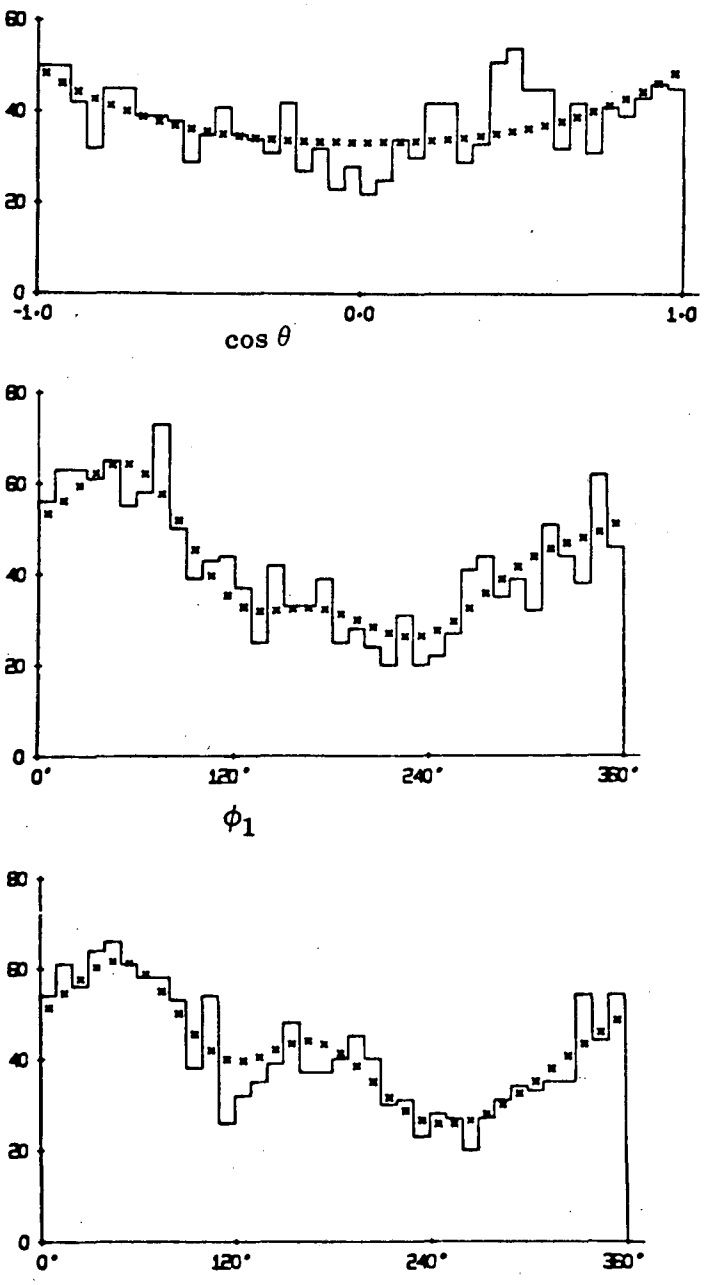

XBL 714-710

Fig. 10.

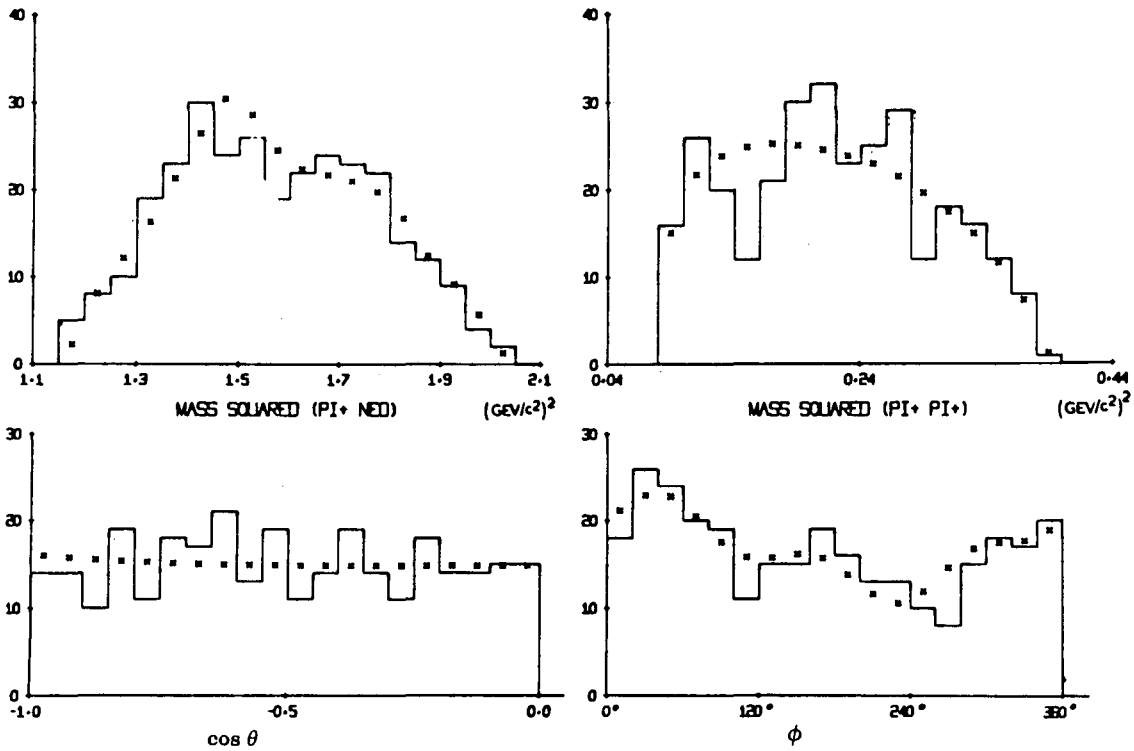

XBL 714-711

Fig. 11.

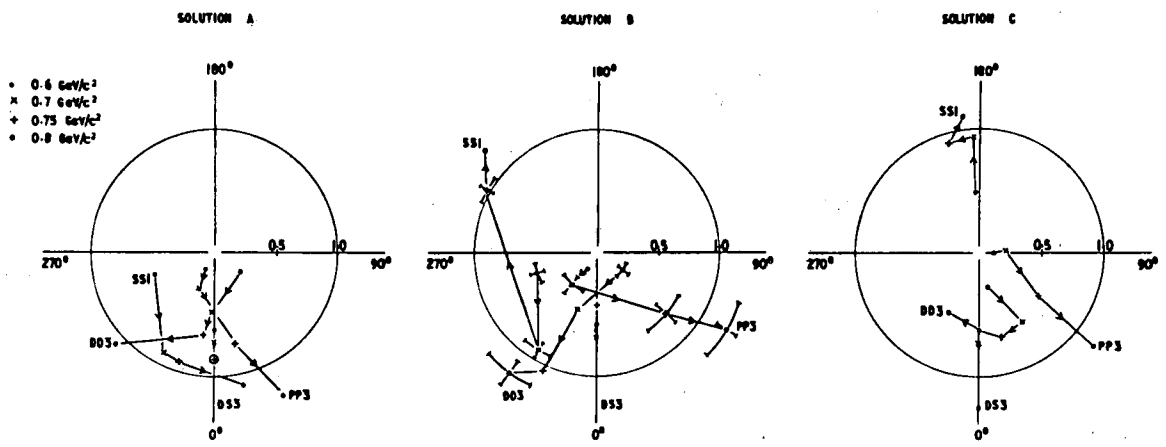

XBL 714-712

Fig. 12.

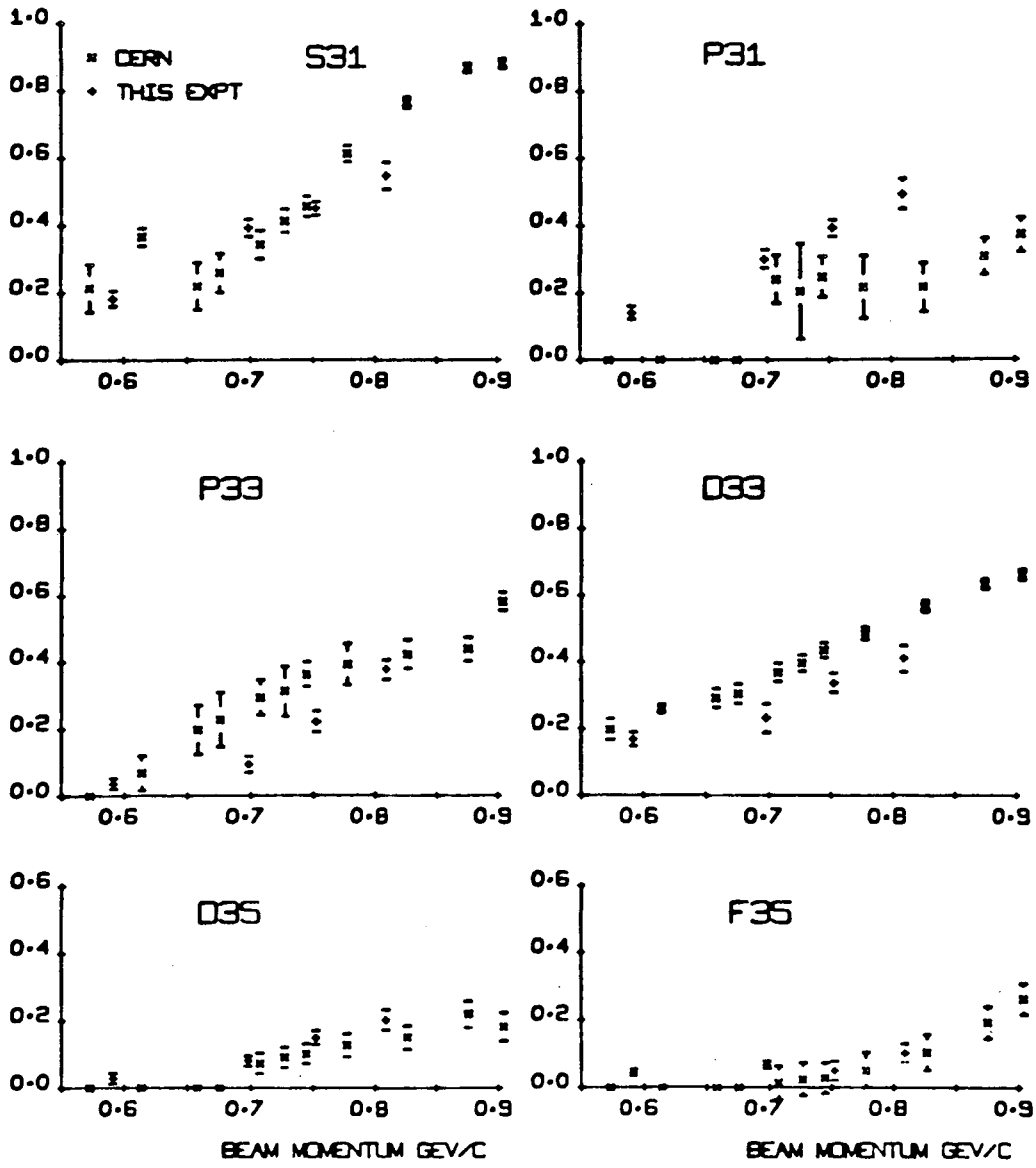

XBL 714-713

Fig. 13.

Discussion

LOVELACE: There is one three-particle process that is really understood, namely $n + d \rightarrow n + n + p$ at low energies. Here you have overlapping effects between various final channels, where two particles form a deuteron or singlet virtual bound state. The theory is nevertheless very successful. You can find out about it in recent conference reports on three-body nuclear physics [e.g., I. Duck, Advances in Nucl. Phys. Vol. I (1969)]. Any theorist who is planning to help Dr. Cashmare, should be sure he understands the above reaction first.

BERGER: I would like to make some theoretical remarks which I think are relevant to the isobar model. They involve how duality can be used to strengthen the analysis of two to three particle processes. At the present time, duality constraints are essentially ignored by experimenters in their analyses of $2 \rightarrow 3$ body data. A few years ago, in $2 \rightarrow 2$ scattering, the lesson was learned that it is illegitimate to express a scattering amplitude as a sum of resonance terms and Regge-pole exchange terms. To do so is to count the same effect twice ("doubling-counting"; Dolen, Horn, Schmid). Analogous statements apply for $2 \rightarrow 3$ body reactions. Terms which represent resonance (and background) contributions in different two-body channels of the $2 \rightarrow 3$ final state should not simply be added together to form an overall reaction amplitude. This popular type of analysis generally involves serious double counting.

Dual models do not now provide a complete quantitative alternative to present procedures, but they can at least serve as a qualitative guide. For example, they may be exploited for the restrictions they impose on scattering amplitudes in the vicinity of the intersection point of two prominent resonances on the plot. These restrictions will be qualitatively different in different reactions. Indeed, in $K^+p \to K^o\pi^+p$ (which has exotic quantum numbers in the initial state), terms corresponding to K^* and Δ resonances in the final state are additive in the overall production amplitude. Duality specifies the the relative phase of K^* and Δ poles. However, in $K^-p \to \bar{K}^o\pi^-p$, duality imposes a much stronger constraint; as discussed at greater length in my talk last week,* the $\bar{K}^*$ and N^* resonance poles occur in the same dual B_5 function.

In their examination of Dalitz plots, it would be valuable if experimenters would develop a systematic table of signs and magnitude of interference effects between resonances on the Dalitz plot. This information could be confronted fairly directly with predictions of dual models.

As a second example of the use of dual models, suppose we look briefly at A_1 decay. There is now experimental evidence that A_1 decays into both $\rho\pi$ and $\epsilon\pi$, where ϵ is the 0^+ daughter of the ρ. Dual models

---

* "Phenomenological Applications of Dual Models" (ANL/HEP 7110), to be published in Proceedings of the Caltech Conference on the Phenomenology of Particle Physics.

suggest that the relative phase of ϵ and ρ should be the same as it is in $\pi\pi$ (off-shell) elastic scattering, viz. +1. For $\pi^+\pi^-$ pairs which are decay products of A_1, this means that the angular distribution in the $\pi^+\pi^-$ rest frame should be peaked forward. On the other hand,

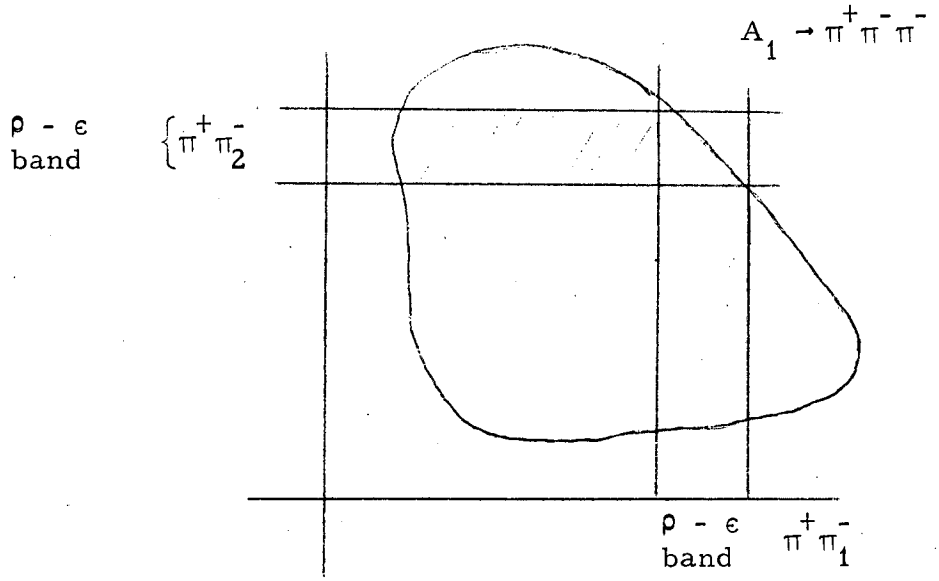

purely experimentally, the Dalitz plot sketched above shows that a forward peaked angular distribution may also be attributed to <u>destructive</u> interference between the two crossing ρ bands, with the crossing ϵ bands doing what they please, and the ρ/ϵ phase being, perhaps, 90°. I'm not sure there is an unambiguous purely empirical way to decide which answer is correct -- dual model constructive interference of ρ/ϵ or the empirical ρ/ρ destructive interference -- for explaining the observed $\pi^+\pi^-$ angular distribution. However, an unguided computer search can give both answers, maybe with equal χ^2. Perhaps experimenters should build in the dual model suggestion from the start, to reduce ambiguity.

INTERFERING BOSON RESONANCES AS A TOOL IN STRONG INTERACTIONS AND SEARCH FOR C VIOLATION IN THE ELECTROMAGNETIC OR SEMI-STRONG INTERACTIONS

Gerson Goldhaber

Department of Physics and Lawrence Radiation Laboratory
University of California, Berkeley, California 94720

INTERFERING BOSON RESONANCES AS A TOOL IN STRONG INTERACTIONS AND SEARCH FOR C VIOLATION IN THE ELECTROMAGNETIC OR SEMI-STRONG INTERACTIONS

Gerson Goldhaber

Department of Physics and Lawrence Radiation Laboratory
University of California, Berkeley, California 94720

In my talk I will concentrate on a few specific ideas for future experiments. The ideas are not complete as yet, in that they are not yet ready for the Bevatron Scheduling Committee. In part, some experiments await further technical developments; in part, some experiments are intricate and lengthy so that they involve a long-range program.

Much of the material in my talk has been developed in conjunction with various of my colleagues; in particular, Dr. Gerald Abrams.[1,2]

My discussion will center on two resonances, the ω and ρ^o, for which interference effects have been clearly established. However, there is no reason why similar effects should not occur between other overlapping resonances which bear a similar relation to each other such as the f^o and A_2^o. In this case interference in the respective $K\bar{K}$ modes may have been observed already, but EM or other type of mixing, yielding f^o interference in the $A_2^o \to \pi^{\pm}\rho^{\mp}$ decay or A_2^o interference in the $f^o \to \pi^+\pi^-$ decay, could also occur.

First let us look back at the question of ω-ρ interference. Basically when one studies the two companion reactions

$$\pi^+ n \to \rho^o p \qquad (1)$$

$$\pi^- p \to \rho^o n \qquad (2)$$

one sees a dip in the $\pi^+\pi^-$ mass spectrum at the ω mass in the π^+ reaction and a peak in the π^- reaction. Actually the dip was originally not observed in reaction (1) but rather in the similar reaction $\pi^+ p \to \rho^o \Delta^{++}$.

Let me now remind you of some of the experimental data. In Fig. 1 we show the $\pi^+\pi^-$ mass spectrum for the reaction $\pi^+ p \to \pi^+\pi^-\Delta^{++}$, at a beam momentum of 3.7 GeV/c. In addition to a Δ^{++} selection, only events with $t' < 0.14$ $(\text{GeV/c})^2$ are plotted ($t' = |t - t_{min}|$). A clear dip can be seen in the $\pi^+\pi^-$ mass spectrum at the ω mass. This dip is the result of a destructive interference effect and can be explained in terms of the relative production phase β between ω and ρ being 90° ($\beta \approx 90^\circ$).

When we obtained this data Alfred Goldhaber, Fox and Quigg[3] (GFQ) suggested an analysis using a simple first-order theory. Namely, the $\pi^+\pi^-$ mass spectrum in the ρ region is given by

$$\frac{dN}{dm} = |B_\rho(m)A_\rho|^2 F(m)$$

where

$$F(m) = \left|1 + \frac{A_\omega}{A_\rho}\frac{\delta}{m_\omega - m - i\Gamma_\omega/2}\right|^2 .$$

Here $F(m)$ is a modulating factor multiplying the Breit-Wigner distribution

$$B_\rho(m) = \frac{\sqrt{\Gamma_2/2\pi}}{m_\rho - m - i\Gamma_\rho/2}$$

which describes ρ production. A_ρ and A_ω are the amplitudes for ρ and ω production, δ is the ω-ρ mass mixing parameter, $\frac{1}{m_\omega - m - i\Gamma_\omega/2}$ is the propagator of the ω. The production amplitudes A_ρ, A_ω are related to N_ρ and N_ω, the experimental number of ρ,ω events observed in the t' interval studied, by the following expression:

$$(A_\omega/A_\rho) = \sqrt{N_\omega/N_\rho}\, e^{i\beta}$$

where β is the relative production phase.

GFQ also pointed out that if the experiment were repeated using a π^- beam, there would be a change in sign at the ρ vertex and hence a change in the value

of β from 90° to 270°, which would then correspond to a constructive interference effect.

At the time we carried out our experiment another experiment was performed independently at Berkeley by Rangaswamy, Wenzel et al. They looked at the reaction $\pi^- p \to \pi^+ \pi^- n$ in a diboson spectrometer, at a number of beam momenta between 3 to 5 GeV/c. In Fig. 2 their $\pi^+\pi^-$ mass spectrum for events with t between 0.2 to 0.4 $(\text{GeV/c})^2$ and $\cos \theta_{\pi\pi}$ between (-0.6) and (-0.3) is shown. A peak at the ω mass can be seen; if this is interpreted as ω-ρ interference it corresponds to a value of $\beta \cong 270^{\circ}$.

An experiment done later on by Hagopian et al. shows the same results more clearly. They study the reaction $\pi^- p \to \pi^+ \pi^- n$ at 2.3 GeV/c. In Fig. 3 we present their $\pi^+\pi^-$ mass spectrum for events in the t region $3\mu^2 \leq t \leq 12\mu^2$; a clear peak in the ω mass region is observed. (Here $\mu = m_{\pi}$.)

Another π^- experiment done at CERN by Abramovich et al. analyzed the reaction $\pi^- p \to \pi^+ \pi^- \pi^- p$ at 3.9 GeV/c. They noted (see Fig. 4a) that the interference effect which is seen in the $\pi^+\pi^-$ mass spectrum (2 combinations per event) is considerably enhanced if one restricts the $\pi^+\pi^-$ combination to one combination per event by selecting the ρ° to be more forward than the bachelor π^-. (See Fig. 4b.) The effect is further enhanced by restricting the sample to events with $t_{p\text{-}p} \leq 0.35$ $(\text{GeV/c})^2$ (see Fig. 4c). The ω-ρ interference observed here suggests $\beta \approx 180^{\circ}$.

Another experiment which has observed this interference effect is an experiment done at Daresbury by Biggs et al. The reaction studied was diffraction photoproduction of carbon:

$$\gamma C \to \pi^+ \pi^- C \quad \text{for} \quad \langle E_{\gamma} \rangle = 4.2 \text{ GeV} \ .$$

In Fig. 5 we show their result, which clearly deviates from a Breit-Wigner shape for the $\pi^+\pi^-$ mass spectrum. Their result is consistent with a relative

production phase $\beta \cong 0$. Very recently similar results have been observed in H, C and Pb by the DESY-MIT group. In this photoproduction case there are some problems in determining the value for β. In the analysis of the reaction $\gamma C \rightarrow e^+e^- C$ in a companion experiment a different value of β is obtained. I do not want to go into the details of this point here, however.[4]

My main point here is that by choosing different production mechanisms, you can obtain different values for β and observe different interference patterns. That much is well known; as for the future, I would like to suggest that a very accurate experiment could be done on the reactions

(a) $\pi^+ n \rightarrow \pi^+\pi^- p$

(b) $\pi^- p \rightarrow \pi^+\pi^- n$

to study the breakdown of charge symmetry induced by ω-ρ mass mixing. Furthermore, one should investigate ω production in the reaction

(c) $\pi^+ n \rightarrow \pi^+\pi^-\pi^o p$

(d) $\pi^- p \rightarrow \pi^+\pi^-\pi^o n$.

In reactions (c) and (d) one can examine the effect of $\rho \rightarrow 3\pi$ on ω production.

In the case of ω production, the modulating function which multiplies the ω Breit-Wigner distribution can be given as:

$$F(m)_{3\pi} = \left| 1 + \frac{A_\rho}{A_\omega} \frac{\delta}{m_\rho - m - i\Gamma_\rho/2} \right|^2 .$$

Here A_ω, A_ρ, δ are as defined previously, $\frac{1}{m_\rho - m - i\Gamma_\rho/2}$ is the ρ propagator. For our purposes the ω Breit-Wigner can be considered as a delta function and then $F(m_\omega) \cong$ constant.

The influence of the 3π decay of the ρ on the ω thus has the effect of changing the amplitude for ω production. In that case one expects a larger value for the ω production cross section in $\pi^+ n$ than in $\pi^- p$ reactions. In particular:

$$\rho_{oo}\left(\frac{d\sigma}{dt}\right)_{\pi^+ n \to \omega p} > \rho_{oo}\left(\frac{d\sigma}{dt}\right)_{\pi^- p \to \omega n} .$$

Thus one should do both the π^+ and the π^- experiments in order to measure this difference. This should show a clear case of the breakdown of charge symmetry; i.e., a very marked difference in cross section for ω production in $\pi^+ n$ and $\pi^- p$ reactions. This would also be the first complete test of the mass mixing theory which we now accept, to the best of my knowledge, without complete experimental verifications.

In order to eliminate experimental biases, the experiment has to be done on deuterium. Thus we have to detect the two reactions

$$\pi^+ d \to \omega pp$$

and

$$\pi^- d \to \omega nn .$$

There are experimental difficulties in detecting the two nucleons in the final state. One will probably have to do the experiment by detecting the three outgoing mesons; i.e., detecting the π^+ and π^- directly and the π^o via its 2γ decay mode.

In Fig. 6 we show the natural parity contribution to ω production in the reaction $\pi^+ p \to \omega^o \Delta^{++}$ at 3.7 GeV/c $\left(\rho_{oo}\left(\frac{d\sigma}{dt}\right)_{\pi^+ p \to \omega^o \Delta^{++}}\right)$. The distribution is flat in the forward direction. There is a dip at $t' \cong 0.14$ $(\text{GeV}/c)^2$. So far we have succeeded in establishing coherence between ρ and ω for $t' < 0.14$ $(\text{GeV}/c)^2$. There were not enough events to establish whether or not coherence is present beyond this point. The data in Fig. 6 show what the $\pi^+ p$ differential cross sections look like; we expect a lower cross section for the $\pi^- p$ case. The question is, increase or decrease relative to what? The curve in Fig. 6 represents an absolute prediction of a model proposed by G. Abrams and U. Maor,[5] which does not take into account ρ-ω interference. The model suggests that there are an excess of events in the forward direction,

but one has to measure the π^- reactions to see if this is indeed the case.

The dip at $t' \cong 0.14$ $(GeV/c)^2$ is not understood as yet. It might be related to ρ-ω interference, and this is another reason we want to see what the $\pi^- p$ reaction looks like. Will it show a peak or a dip at $t' \cong 0.14$ $(GeV/c)^2$? An answer to these questions demands a study of the two reactions I mentioned.

I would like to discuss another topic based upon the same general ideas; namely, a search for C violation in ρ decay using the ρ-ω interference effect. In looking for the effects of the $\rho \to 3\pi$ decay on ω decay we observe a charge asymmetry on the ω Dalitz plot. It occurred to us[1] that there is an opportunity here, in principle, to look for C violation in electromagnetic or sub-strong interactions.

The question is how does the ρ meson decay into 3π's? There are four possible ways.

(a) Electromagnetic decay with $\Delta I = 1$ to $I = 0$. Here the ρ turns into an ω via an electromagnetic interaction with $\Delta I = 1$. In this case the final state which decays into 3π's has the same quantum numbers as the ω: $I = 0$, $J^{PC} = 1^{--}$. Thus there is no interference which alters the shape of the matrix element on the Dalitz plot.

(b) C violating decay with $\Delta I = 0$ to $I = 1$. Here the ρ decays into 3π's with $\Delta I = 0$. From the relation $G = C(-1)^I$, since G changes from +1 to -1 and $\Delta I = 0$, C must change sign. The final state $I = 1$, $J^{PC} = 1^{-+}$ has a matrix element that vanishes along the y axis ($T_+ - T_- = 0$) of the Dalitz plot and hence will give rise to a left-right asymmetry on interference with the ω.

(c) Electromagnetic decay with $\Delta I = 1$ to $I = 2$. Here the final state after decay has $I = 2$, $J^{PC} = 1^{--}$. The matrix element for such a state vanishes

along the $x = 1/3$ line ($T_0/Q = 1/3$). This gives rise to an asymmetry along the y axis of the Dalitz plot on interference with the ω.

(d) C violating decay with $\Delta I = 2$ to $I = 3$. Here the final state is $I = 3$, $J^{PC} = 1^{-+}$. The matrix element for such a decay vanishes along the lines of sextant symmetry. This will give rise to an asymmetry between adjacent sextants. This is illustrated in Table I.

Let me concentrate on the search for a C violating effect with $\Delta I = 0$. First, why is it important to look for other C-violation effects besides η decay for which careful measurements are already being done? There is an important difference between the two cases. The interference between the (normal) $\Delta I = 1$ electromagnetic decay of the η and the conjectured $\Delta I = 0$ C-violating decay gives rise to a sextant asymmetry on the Dalitz plot. As T. D. Lee pointed out[6] there are strong angular momentum barriers suppressing the $I = 0$ final state in η decay. Thus what is being searched for in the current measurements is only the $\Delta I = 2$ C-violating effect. The best value for the asymmetry that Wonyong Lee et al.[7] has at present is $\alpha = 1.5 \pm 0.5\%$ corresponding to the $\Delta I = 2$ transition. Suppose C violation does occur for $\Delta I = 0$ rather than $\Delta I = 2$. In such a case the study of $\eta \to \pi^+\pi^-\pi^0$ decay might <u>not</u> lead to a definitive result, because of the angular momentum barriers. In fact, no evidence for a sextant asymmetry is seen here. As I have outlined in the ω-ρ interference case one can look for a possible $\Delta I = 0$ C-violating transition.

Now let me say a few words about what could be the significance of the asymmetry we observed. There are at least four mechanisms which can give rise to an asymmetry:

(1) C violation in ω decay. This will proceed via $\Delta I = 1$. There is good evidence against this hypothesis as I will show below.

(2) C violation in $\rho \to 3\pi$ via $\Delta I = 0$.

(3) Background amplitude with spin parity $J^{PC} = 1^{-+}$ which is coherent with the ω (Yuta-Okubo effect).[9]

(4) Existence of an exotic state $\tilde{\rho}$ near the ω mass with $J^{PC} = 1^{-+}$. The question is, can one distinguish among these four possibilities? We propose that in our experiment looking for C violation using the ρ-ω interference effect one must first measure the production phase β from ω-ρ interference in the $\pi^+\pi^-$ mass spectrum and determine the interval of coherence in t. After that a fit to the asymmetry on the ω decay Dalitz plot would measure β_1, the characteristic phase of C violation in the decay of the $\rho \to 3\pi$ with $\Delta I = 0$. The asymmetry is related to

$$\sim \mathrm{Re}\left\{\frac{\epsilon_\omega - i}{\epsilon_\omega^2 + 1} e^{i(\beta' - \beta + \beta_1)}\right\}$$

where:

β' ≡ phase angle of the ρ amplitude at the ω mass $\beta' \cong 106^\circ$;

β ≡ relative ω,ρ production angle;

β_1 ≡ characteristic C violation phase for $\Delta I = 0$ decay of $\rho \to 3\pi$; and

$\epsilon_\omega = (m_\omega - m)/(\Gamma_\omega/2)$.

Once β_1 has been measured in one reaction you can predict the expected asymmetry in other reactions. We thus expect different types of asymmetries on the ω decay Dalitz plot depending on the value of β_1.

Let me now show you some data from our $\pi^+ p$ experiment at 3.7 GeV/c. The reaction studied is

$$\pi^+ p \to \pi^+\pi^+\pi^-\pi^0 p \qquad 16{,}000 \text{ events} .$$

In Fig. 7a,b we show the $\pi^+\pi^-\pi^0$ mass spectrum in the interval near the η and ω masses. Figure 7a corresponds to the left side of the Dalitz plot ($x < 0$); Fig. 7b corresponds to the right side of the Dalitz plot ($x > 0$). If there

were any left-right asymmetry, you would expect a different number of ω events in the two plots. The background level is somewhat different, but there is no statistically significant difference in the ω signal above background. From this one concludes that there is no $\Delta I = 1$ C violation in the ω decay itself. Similar results were observed earlier by Flatté et al.

In Fig. 8a we show the ω Dalitz plot decay for about 4000 ω events. In Fig. 8b,c we show the projection on the x,y axis and note that there is no overall asymmetry. The curves represent the expected number of events assuming no asymmetry.

Next, we restrict ourselves to the reaction

$$\pi^+ p \rightarrow \pi^+ \pi^- \pi^o \Delta^{++} \quad ,$$

and study the question of asymmetry as a function of t'. In Fig. 9 we show $(\frac{d\sigma}{dt'})_{\pi^+ p \rightarrow \omega \Delta^{++}}$, where + (cross) corresponds to events with $x > 0$ and $\cdot$ (dot) corresponds to events with $x \leq 0$. Notice that in the very low t' region, $t' < 0.14$, where ρ-ω coherence has been established, we find only a very slight difference (if any) in the two differential cross sections. However, in the t' interval $0.08 \leq t' < 0.2$ $(\text{GeV}/c)^2$ for $\pi^+ p \rightarrow \pi^+ \pi^- \pi^o \Delta^{++}$ we have observed a difference. In Fig. 10a,b we show the three meson invariant mass for $x > 0$ and $x < 0$. Note that the background level is very low but nonzero, and that the difference in the number of events is not in the background but in the ω signal. The asymmetry is $\alpha = 0.18 \pm 0.05$ and its statistical significance is clear to everyone; it could conceivably be a statistical fluctuation, but that is very unlikely. In Fig. 11a we show the Dalitz plot distribution for these events. In Fig. 11b,c we show the x,y projection and note that there are more events with $x > 0$ than $x < 0$. The two curves on the x projection represent no asymmetry (dotted line) and a fit to an asymmetry of the form $\vec{q} = \vec{p}_{\pi^+} \times \vec{p}_{\pi^-}$ is the matrix element for ω decay and $b \equiv$ asymmetry

parameter. For no asymmetry $b = 0$. The result of the best fit are reproduced by the solid curve, and correspond to $b = 0.67 \pm 0.22$. Note that the fits are not influenced by the spike near $x = 0$ and that the effect is there even if this spike is removed. The chisquare for the two fits are (binning the data in 8 bins)

$$b = 0 \qquad \chi^2 = 18.7$$

$$b = 0.67 \pm 0.22 \qquad \chi^2 = 9.7 \ .$$

If the asymmetry should be due to the Yuta-Okubo effect, this implies, however, in view of the low background intensity, that about 50% of the background is entirely in one state, namely, $J^{PC} = 1^{-+}$. The other two more-far-reaching possibilities are the existence of an exotic particle $\tilde{\rho}$ with $J^{PC} = 1^{-+}$ and production cross section at about the 1% level compared to ω production, or C violation in $\rho \rightarrow 3\pi$ decay with $\Delta I = 0$. We certainly do not claim to have observed either of these two more exciting possibilities but we feel this is a very promising field for further investigation.

In conclusion, I have suggested a number of experiments today. Being an experimentalist you may ask why do I not just carry out these experiments myself? Well, what I proposed is really a series of experiments which have to be done. We are actually repeating our $\pi^+ p$ experiment to increase the statistics 10-fold, but at the same time to really identify the asymmetry the experiment needs to be done under several different conditions as I have outlined.

REFERENCES

1. G. S. Abrams, G. Goldhaber, and B. H. Hall, UCRL-20617, submitted to Phys. Rev.

2. G. S. Abrams, K. W. J. Barnham, W. R. Butler, D. G. Coyne, G. Goldhaber, B. H. Hall, and J. MacNaughton, UCRL-20618, submitted to Phys. Rev.

3. A. S. Goldhaber, G. C. Fox, and C. Quigg, Phys. Letters 30B, 249 (1969).

4. References to these papers as well as a more complete description can be found in G. Goldhaber, Experimental Results on the ω-ρ Interference Effect, in Experimental Meson Spectroscopy, edited by C. Baltay and A. H. Rosenfeld (Columbia University Press, New York, 1970), p. 59.

5. G. S. Abrams and U. Maor, Phys. Rev. Letters 25, 621 (1970).

6. T. D. Lee, Phys. Rev. 139, B1415 (1965).

7. M. Gormley, E. Hyman, W. Lee, T. Nash, J. Peoples, C. Schultz, and S. Stein, Phys. Rev. Letters 21, 402 (1968); see also Phys. Rev. Letters 22, 108 (1969).

8. S. M. Flatté, D. O. Huwe, J. J. Murray, J. Button-Shafer, F. T. Solmitz, M. L. Stevenson, and C. Wohl, Phys. Rev. 145, 1050 (1966).

9. H. Yuta and S. Okubo, Phys. Rev. Letters 21, 781 (1968).

Table I. Distribution of zeros for matrix elements corresponding to $\pi^+\pi^-\pi^o$ decay for $J^P = 1^-$ with I = 0 to 3.

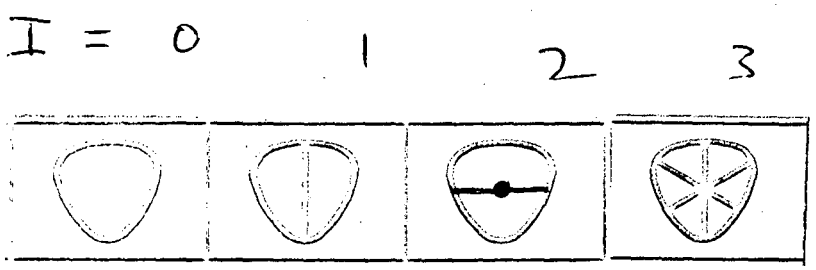

XBL 715-984

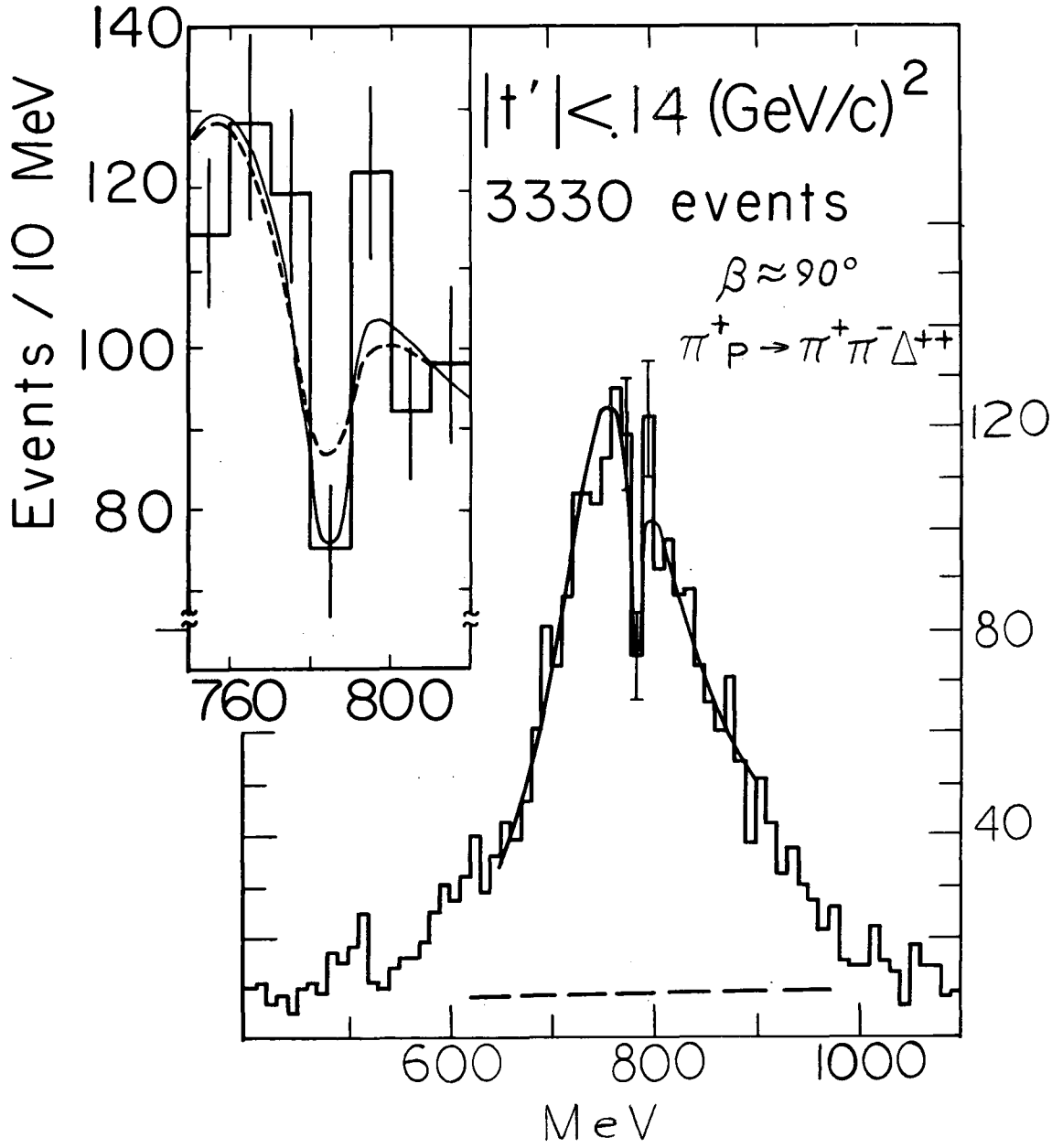
Events / 10 MeV
140
120
100
80
760
800
|t'|<.14 (GeV/c)²
3330 events
β≈90°
π⁺p→π⁺π⁻Δ⁺⁺
120
80
40
600
800
1000
MeV

Fig. 1.

DI BOSON SPECTROMETER

RANGASWAMY, WENZEL et al. LRL $\pi^- p \to n\, \pi^+ \pi^-$

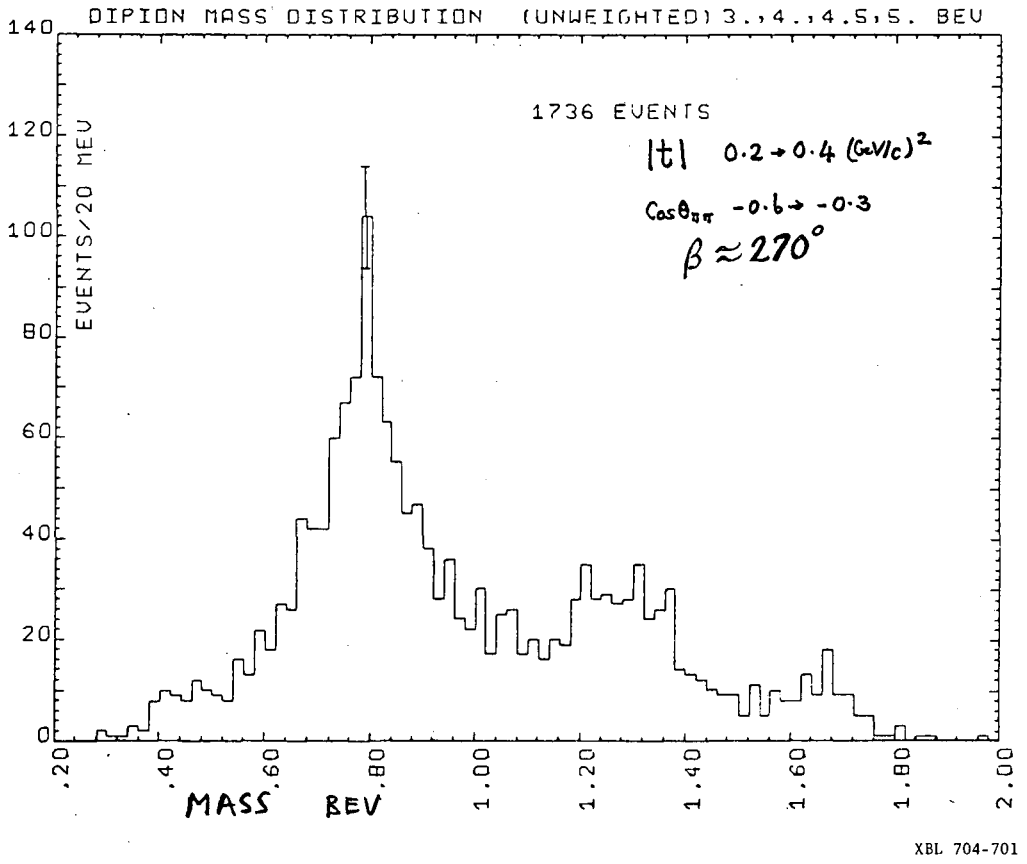

Fig. 2.

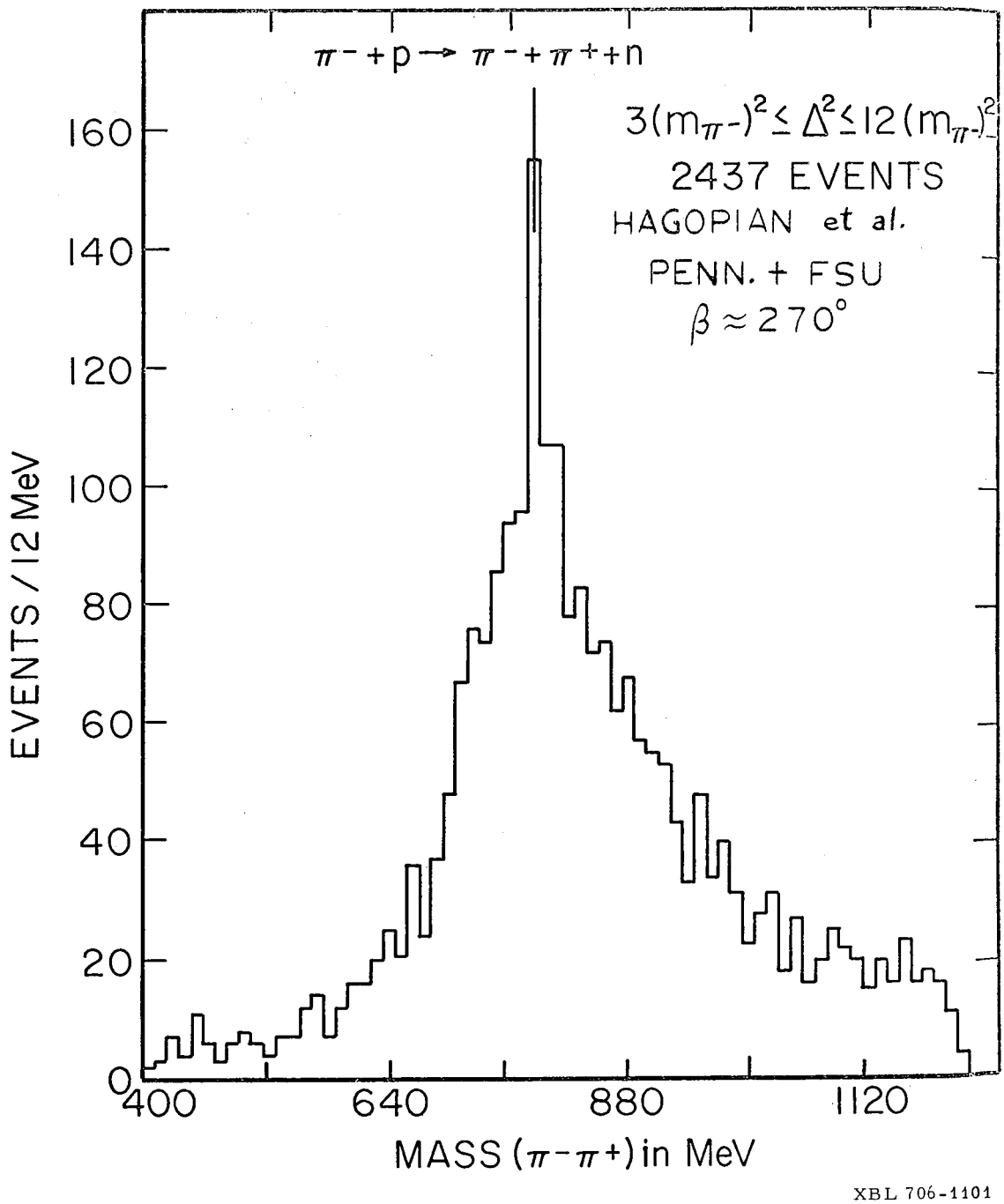
$\pi^- + p \rightarrow \pi^- + \pi^+ + n$
$3(m_{\pi^-})^2 \leq \Delta^2 \leq 12(m_{\pi^-})^2$
2437 EVENTS
HAGOPIAN et al.
PENN. + FSU
$\beta \approx 270°$
EVENTS / 12 MeV
0
20
40
60
80
100
120
140
160
400
640
880
1120
MASS ($\pi^-\pi^+$) in MeV
XBL 706-1101

Fig. 3.

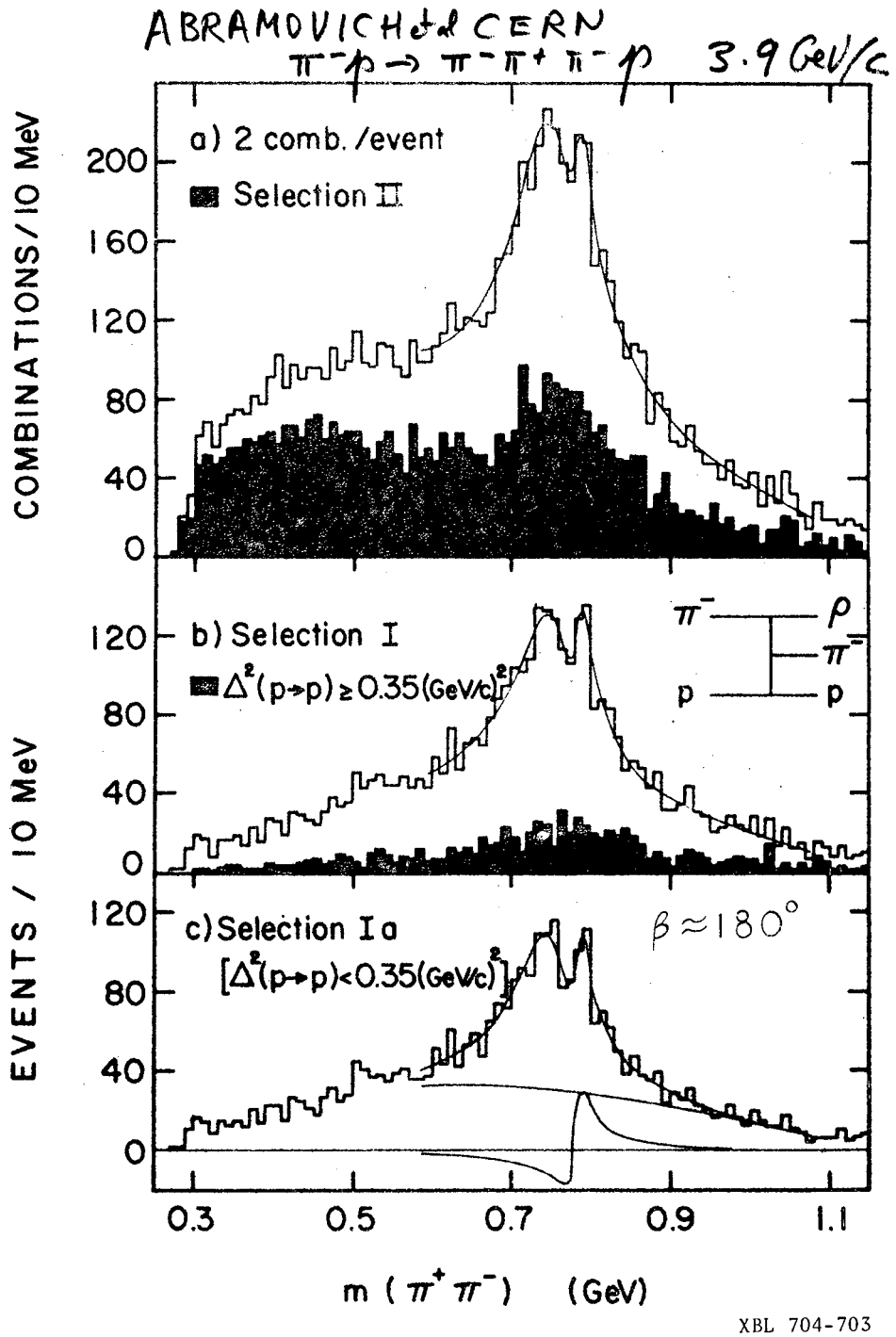
ABRAMOVICH et al CERN
π⁻p → π⁻π⁺π⁻p 3.9 GeV/c
a) 2 comb./event
Selection II
b) Selection I
Δ²(p→p) ≥ 0.35(GeV/c)²
c) Selection Ia
[Δ²(p→p) < 0.35(GeV/c)²]
β ≈ 180°
π⁻ ρ
π⁻
p p
COMBINATIONS/10 MeV
EVENTS / 10 MeV
0
40
80
120
160
200
0.3
0.5
0.7
0.9
1.1
m (π⁺π⁻) (GeV)
XBL 704-703

Fig. 4.

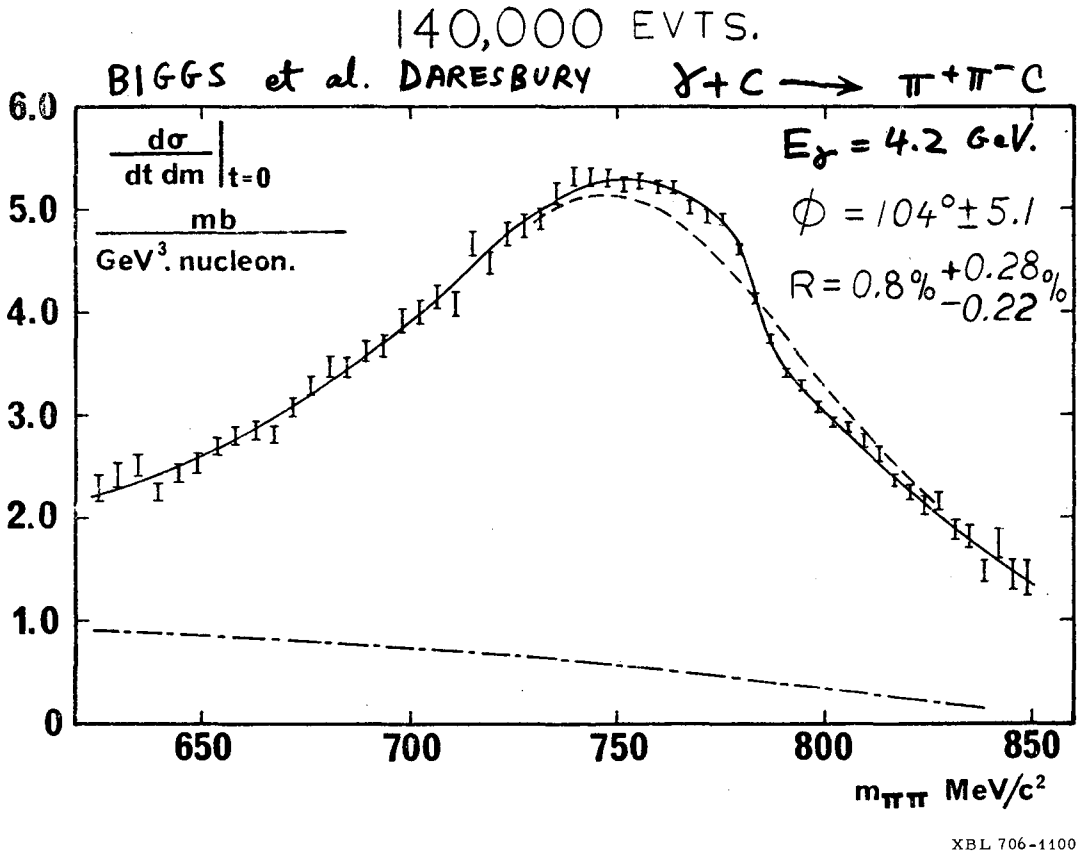
140,000 EVTS.
BIGGS et al. DARESBURY
γ + C → π⁺π⁻C
dσ/dt dm |t=0
mb
GeV³. nucleon.
Eγ = 4.2 GeV.
φ = 104° ± 5.1
R = 0.8% +0.28% −0.22%
6.0
5.0
4.0
3.0
2.0
1.0
0
650
700
750
800
850
mππ MeV/c²
XBL 706-1100

Fig. 5.

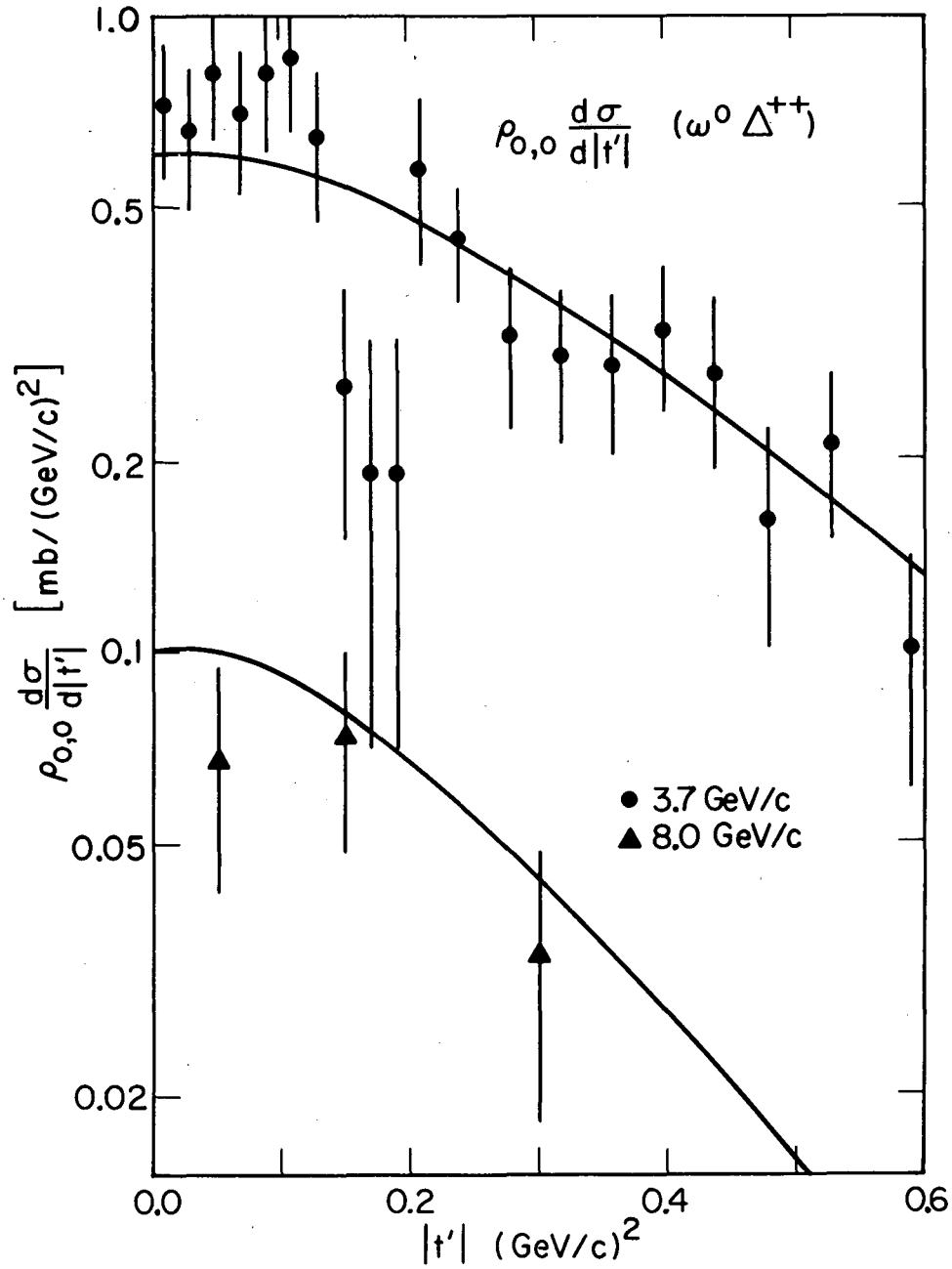

XBL 705-2889

Fig. 6.

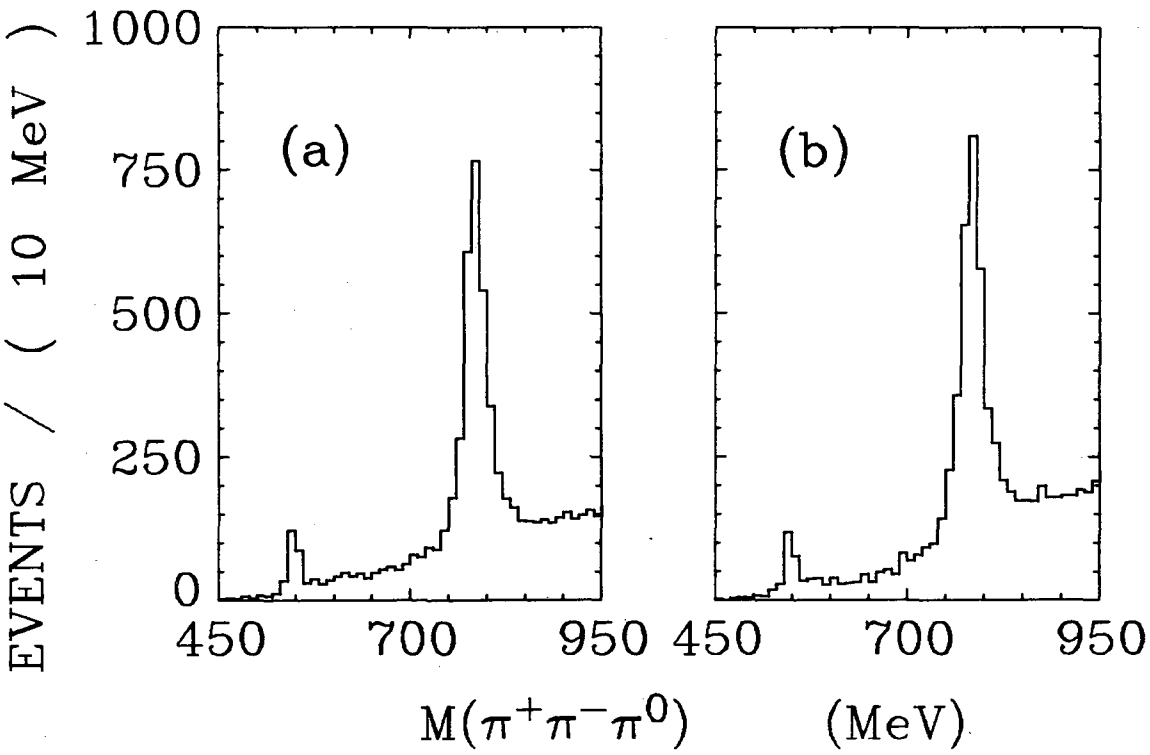

XBL 712-169

Fig. 7.

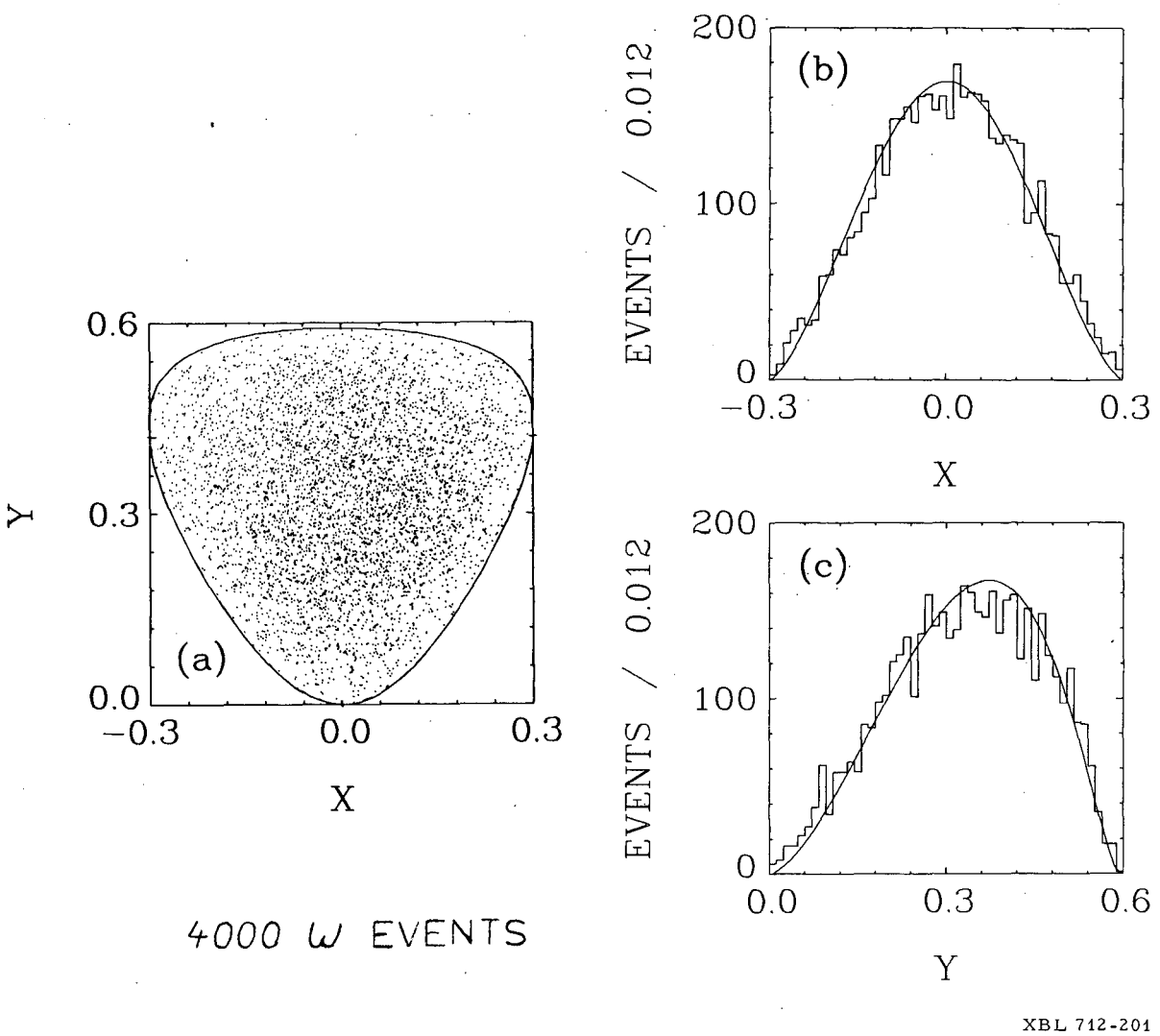
0.6
0.3
0.0
Y
(a)
−0.3
0.0
0.3
X
4000 W EVENTS
200
100
0
EVENTS / 0.012
(b)
−0.3
0.0
0.3
X
200
100
0
EVENTS / 0.012
(c)
0.0
0.3
0.6
Y
XBL 712-201

Fig. 8.

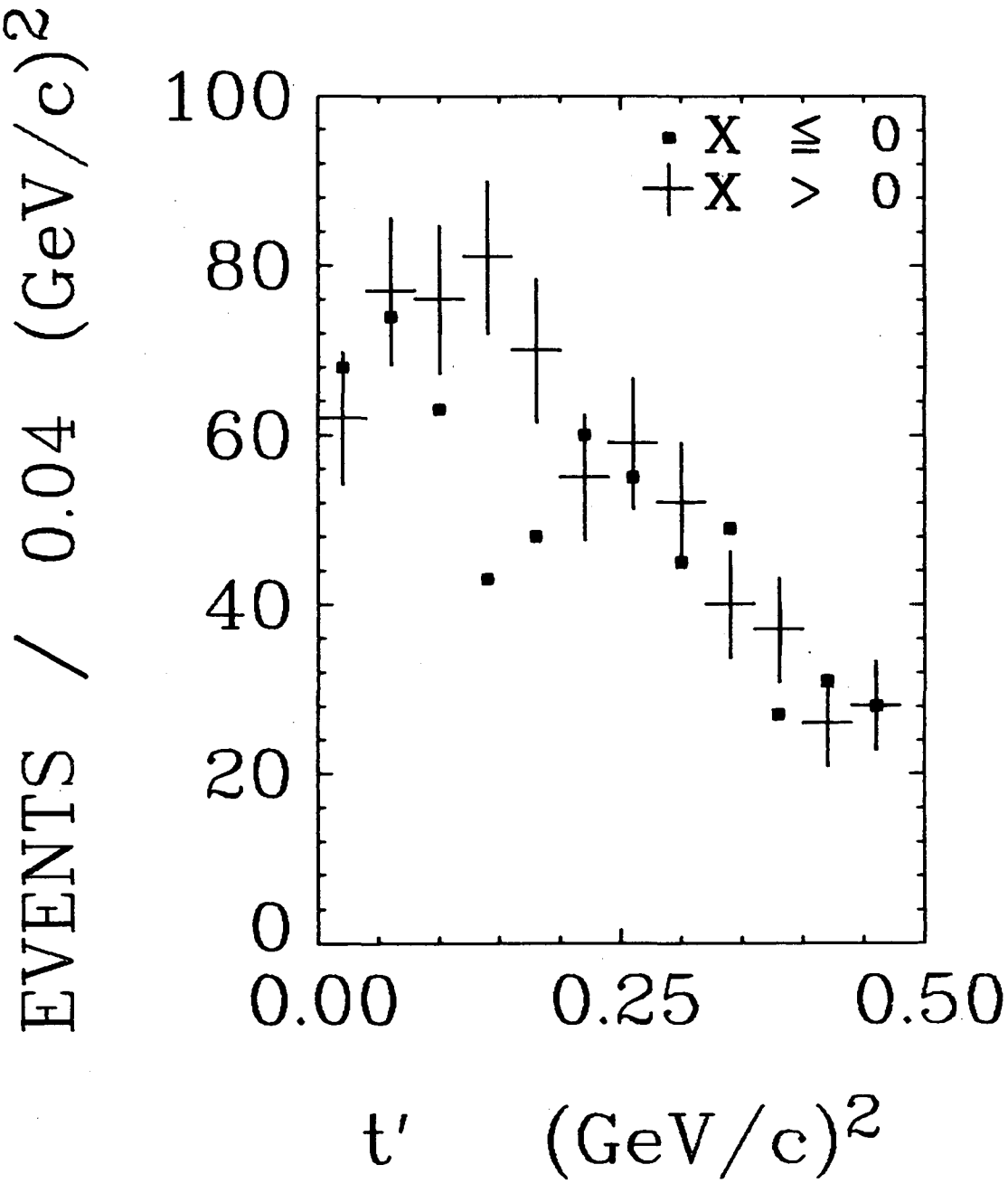

XBL 712-171

Fig. 9.

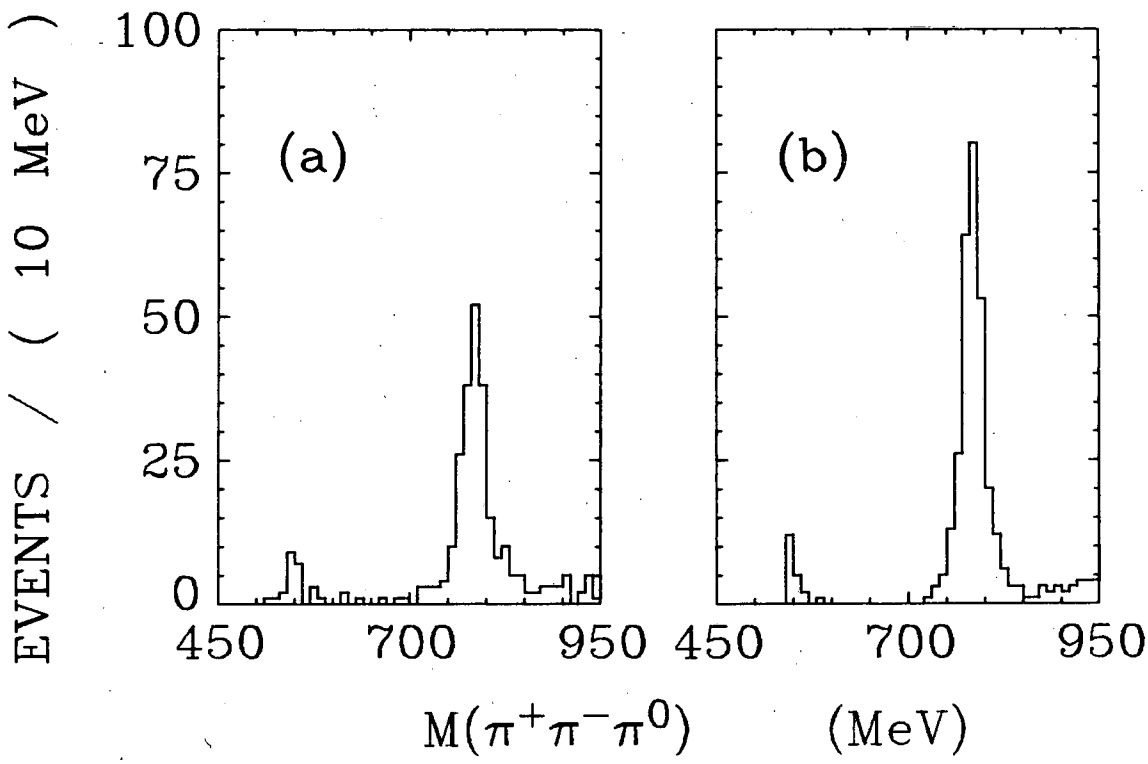

XBL 712-168

Fig. 10.

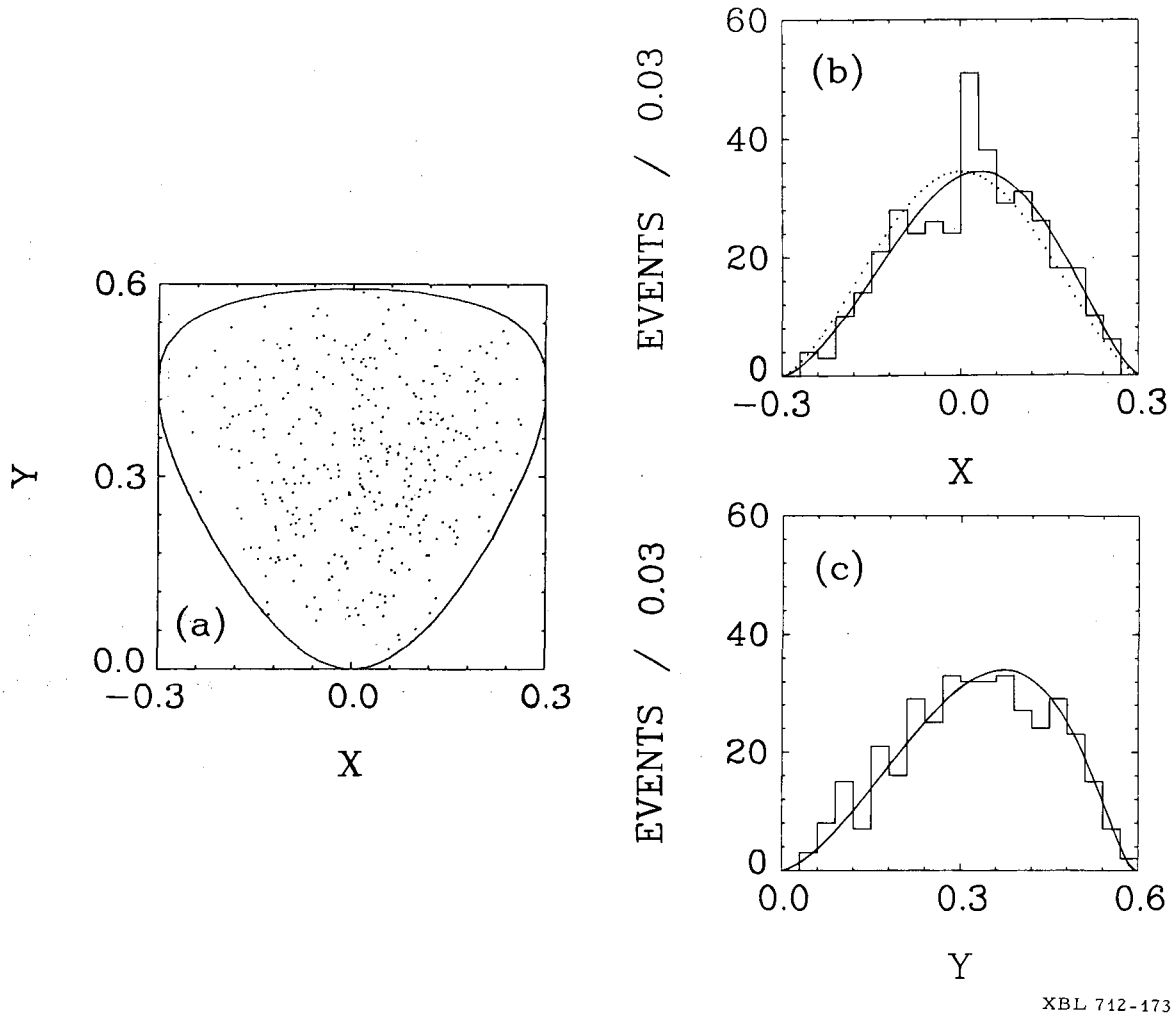
(a)
0.6
0.3
0.0
−0.3
0.0
0.3
X
Y
(b)
60
40
20
0
−0.3
0.0
0.3
X
EVENTS / 0.03
(c)
60
40
20
0
0.0
0.3
0.6
Y
EVENTS / 0.03
XBL 712-173

Fig. 11.

DISCUSSION FOLLOWING G. GOLDHABER'S TALK

Berger (Argonne): Observation of charge asymmetry in the ω Dalitz plot is very intriguing. Some theorists have been quick to invent esoteric explanations. However, I think a mundane background effect explains everything which Gerson just reported. I communicated this to him and to other people at Berkeley, so I'm surprised he doesn't mention the calculation.

First of all, let me draw a diagram which represents peripheral production of ω:

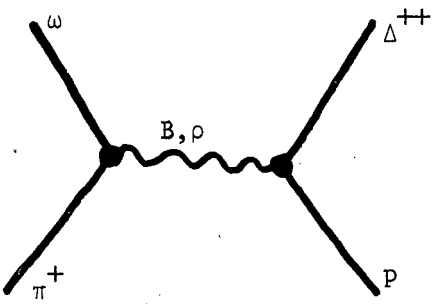

Fig. A

Exchange of B and ρ is indicated. There is good evidence from dσ/dt and density matrix elements that both of these exchanges are present.

Second, I'll draw a background graph (actually two graphs):

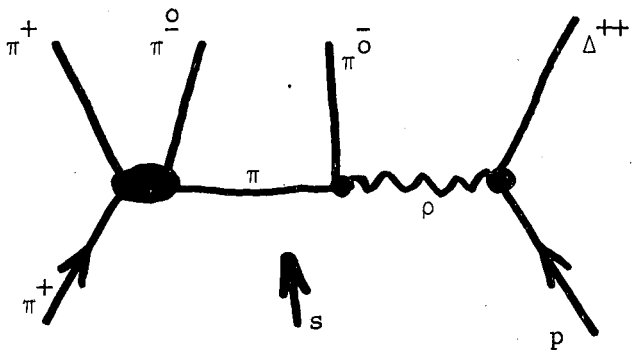

Fig. B

The shaded oval represents the full ππ scattering amplitude, which is known quite well at least up to the ρ position (I'll only be concerned with values of ππ mass up to $M_{\pi\pi} \simeq M_{\rho}$). The idea is that the (3π) system produced by Fig. B is coherent background under the ω signal produced by Fig. A. A virtue of Fig. B is that its absolute normal-

ization and phase relative to (the ρ exchange part of) Fig. A is known a priori. This statement is based on 5 facts:

1) the $\rho\bar{\Delta}p$ vertex is common in Figs. A and B;
2) the $\pi\pi\rho$ coupling constant at the central vertex in Fig. B is well known;
3) the pion exchange propagator in Fig. B is well known;
4) the magnitude and phase of the $\pi\pi$ (off-shell) scattering amplitude in Fig. B is well known; and
5) fits by Fox and others to $\pi p \to \omega N$ and $\pi p \to \omega\Delta$ data tell us the relative amounts of the cross sections for these processes which should be assigned to B and ρ exchange, respectively, in Fig. A.

The upshot of all this is that Fig. B gives a background distribution having the general shape sketched here:

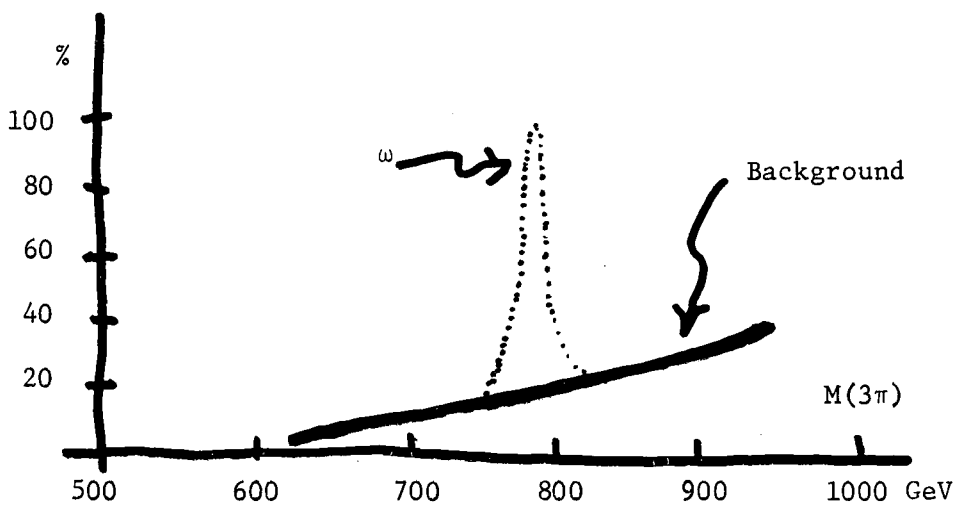

Fig. C

The background rises gradually with increasing (3π) mass. Its magnitude in the vicinity of ω is 15 to 20% of the ω cross section.

Of course, all of this background does not contribute to the Dalitz plot asymmetry; only the fraction with $J^{PC} = 1^{-+}$ is effective. Projecting out the various J^{PC} components of background is not easy; however, we can imitate Nature by letting the ω pick out the part of the background it wants to interfere with. To do this, I add the amplitudes corresponding to Figs. A and B, and then I compute experimental

observables. I obtain an asymmetry value

$$\alpha = 0.14 ,$$

after making the same selections made by Goldhaber and co-workers.

It is easy to see qualitatively why the background mechanism works. Because the incident beam is π^+, the angular distribution of the final $\pi^+\pi^-$ pair in Fig. B will tend to be peaked forward in the $(\pi\pi)$ rest frame. When a Lorentz transformation to the ω rest frame is performed, this angular effect is translated into a statement that $T_{\pi^+} > T_{\pi^-}$, as observed. Note that if the incident beam were π^- (in, say, $\pi^- n \to \omega\Delta^-$) I predict an asymmetry with opposite sign.

A second qualitative remark concerns the fact that the asymmetry vanishes at small t'. I expect this to be true because the ρ exchange amplitude vanishes at t=0. Only ω production by B exchange survives at small t. Because B exchange produces helicity 0 ω, and ρ exchange populates helicity 1 ω, the asymmetry effect ought to be large for helicity 1 ω, and essentially non-existent for helicity 0 ω. It would be useful to verify this experimentally.

Third, from the point of view of the background mechanism, it is reasonable that the asymmetry effect should arise primarily from interference with the imaginary part of the ω Breit-Wigner. A glance at Fig. B shows that the phase of the background is determined by the (known) phase of $\pi\pi$ scattering, for $\pi\pi$ mass values in the range 400-600 MeV. In this range, the $\pi\pi$ amplitude has a large imaginary part. In Goldhaber's notation, $\alpha \neq 0$ but $\alpha' \simeq 0$. This is true in my calculation also.

Goldhaber (LRL): I think that if Ed Berger is able to reproduce our results quantitatively this is very interesting and should be presented in detail. Before this I had only heard a handwaving argument from Ed via telephone. Furthermore if the model works quantitatively we can also ask what is the projection on the $I = 0$, $J^{PC} = 1^{--}$ state? This should interfere with the ω intensity and could in principle be measured as well. For instance the fact that the dip in $\rho_{oo} \frac{d\sigma}{dt}(\omega)$ occurs in the same t' region as the asymmetry we observe may be related. As we state in our paper[2] we have realized that the t' region in which we observe the asymmetry is very suggestive of ρ exchange. However a thorough study of the background outside the ω region does not give any indication of π^+ versus π^- asymmetry with the very meager statistics available to us in this region so far.

Finally, Ed has an opportunity to make additional quantitative predictions for the $\pi^+ p$ reaction at about 2.6 GeV/c where George Gidal of LRL Powell-Birge Group has extensive data as well as at 7 GeV/c where Stan Flatté and coworkers of LRL Group A have extensive data.

MULTIPARTICLE REACTIONS AT INTERMEDIATE ENERGIES*

C. Quigg

Institute for Theoretical Physics
State University of New York
Stony Brook, Long Island, New York 11790

(Invited paper for the Pasadena Meeting
on Hadron Physics at Intermediate Energies, 1971)

ABSTRACT

Recently developed concepts and model which can be used to study multiparticle production in hadron collisions are reviewed. The need to draw upon experience and intuition gained from quasi two-body collisions is emphasized, and some simple ways to make use of two-body data are suggested. A theoretical framework based upon an optical theorem analogue is described, which permits the application of the accumulated wisdom of two-body Regge phenomenology to the study of inclusive reactions. The new Regge phenomenology leads to many predictions which may be tested at energies below 20 GeV. Valuable studies which take advantage of existing data are outlined, together with some new experiments to illuminate the physics of production reactions. Brief summary remarks are made about the outlook for medium-energy studies of inclusive reactions in the immediate future.

* Work supported in part under Contract No. AT(30-1)-3668B of the United States Atomic Energy Commission.

I. INTRODUCTION

The enormous progress toward an understanding of two-body reactions which has occurred in the past decade has been made possible by sustained and intimate interaction between theory and experiment, between theorists and experimenters. Three types of theoretical contributions come easily to mind. There is first, the recognition of new ways to extract important information from the data. In this vein one thinks of the Treiman-Yang test[1] and the classic work of Gottfried and Jackson[2] on the connection between production mechanisms and decay angular distributions of resonances. A second contribution is the construction of a model or viewpoint which permits the correlation of a large number of experimental observations. Of many such useful schemes, Regge theory[3] is no doubt the best known, and most fruitful. Finally there is the phenomenon of confrontation, wherein a theory makes specific predictions which experiment can confirm or deny. The success or failure of model predictions is of secondary importance; posing interesting questions which stimulate valuable experiments is of primary significance.

Interaction between theory and experiment has been much less characteristic of the study of production $(2 \rightarrow n)$ reactions. Until quite recently the only theorists in the field were those visionaries who build untestable (but probably correct) theories. Likewise most theoretical students of production reactions have had little appreciation for the general features, the pleasing consistencies, and the tantalizing puzzles of two-body interactions. Happily, theorists and experimenters are beginning to talk about multiparticle reactions in specific terms.

I shall confine my attention in this paper to what happens at finite, intermediate energies and have nothing to say about high (NAL and ISR) energies.*

Putting to work some of our knowledge about 2-to-2 reactions is the first topic I shall discuss in detail, in Sec. II. In Sec. III, I formulate Mueller's picture of inclusive reactions[5] which enables us to use the tools of two-body Regge phenomenology to study production processes at medium energies. Using the Regge language I discuss in Sec. IV what kind of experimental information will be of value in developing a basic understanding of multiparticle collisions. The last section contains some brief speculations on what the near future will bring.

II. TWO-BODY ASPECTS OF MULTIPARTICLE REACTIONS

1. Transverse Momentum Distributions

I have already stated my belief that the fund of experience and intuition developed in the study of two-body reactions has to a large extent remained untapped by physicists studying production reactions. It is obvious that a knowledge of two-body physics should be useful (if only through unitarity) in understanding at least some features of 2-to-n scattering. A trivial example of a feature of multiparticle reactions which is foreshadowed in two-body scattering is the energy-independence of the mean transverse momentum of secondaries. The constancy of $\langle q_\perp \rangle$ is, as is well known, related to the multiperipheral idea.[6] That a peripheral two-body cross section implies a limiting behavior for $\langle q_\perp \rangle$ is clear, but the appropriate question is, how is the limit reached? According to folklore,[7] $\langle q_\perp \rangle \approx 0.35$ GeV/c independent of s and roughly independent of the entrance channel. The same feature is present in 2-to-2 reactions at quite low energy.

Consider a typical elastic scattering cross section of the form

$$d\sigma/dt = f(s)e^{at} \tag{1}$$

where $a \approx (6 - 8)(\text{GeV/c})^{-2}$. In terms of center of mass variables,

$$t = 2p^2(\cos\theta - 1), \tag{2}$$

$$q_\perp = p \sin\theta. \tag{3}$$

Therefore,

$$\langle q_\perp \rangle = \frac{p \int_0^\pi \sin^2\theta \, d\theta \, e^{2ap^2(\cos\theta - 1)} f(s)}{\int_0^\pi \sin\theta \, d\theta \, e^{2ap^2(\cos\theta - 1)} f(s)} \tag{4}$$

$$= \frac{\pi p}{2} I_1(2ap^2)/\sinh(2ap^2).$$

Now, using the asymptotic form of the Bessel function

$$\lim_{|z| \to \infty} I_1(z) \sim e^z (2\pi z)^{-\frac{1}{2}} (1 - 3/8z - \cdots), \tag{5}$$

we find

$$\langle q_\perp \rangle \to (\pi/4a)^{\frac{1}{2}} (1 - 3/16ap^2 - \cdots). \tag{6}$$

This function, which approaches its limit quite swiftly, is sketched in Fig. 1 for $a = 6$ $(\text{GeV/c})^{-2}$. The limit is attained for center of mass momentum $p^* = 1$ GeV/c which corresponds, for usual combinations of projectile and target to $p_{Lab} = 2.5 - 3$ GeV/c, a very low incident momentum. It is in addition quite amusing that the limiting value of $\langle q_\perp \rangle$ calculated in this manner is the same value found in multiparticle reactions:

a, $(\text{GeV/c})^{-2}$	$\langle q_\perp \rangle_\infty$, GeV/c
6	0.36
8	0.32 .

This coincidence is admittedly not (yet) a theory. What is of possible interest in this simple example is that a limiting behavior

seen in high-energy 2-to-n collisions is already seen in two-body reactions at very modest energies.

2. Longitudinal Momentum Distributions

There are likely to be other similarities between two-particle and n-particle final states. To look for analogies in the longitudinal momentum distributions, I propose the following exercise. Plot the invariant cross section $\omega d\sigma(p_{||})/dp_{||}$ for pions and protons in specific, quasi-two-body channels, e.g.,

$$\pi N \rightarrow \rho N$$
$$\rho N^*$$
$$\pi N^*$$
$$\omega N$$
$$\omega N^*$$

vs. $p_{||}^{Lab}$, $p_{||}^{Projectile}$, and $p_{||}^*$. I do not know what the results will be, or whether they will enable us to feel comfortable with gross features of multiparticle collisions. But it is easy enough to look at existing bubble chamber events this way, and we will learn nothing by not looking.

3. Other Two-body Features

Even if the compilation just suggested fails to give information which accounts for the bulk of the longitudinal momentum spectrum, it will certainly reveal something about what multiperipheralists call "end effects" or, in other language, about the characteristics of low multiplicity events. Recently, several groups[8] have noticed that the spectrum of secondary pions $d\sigma/dp_{||}^*$ is in a number of cases not

symmetrical about $p^*_{||} = 0$. Figure 2 shows the Rochester data on the π^- spectra in π^+p and K^+p collisions. [The asymmetry itself is no great surprise, since I know of no serious model which predicts a symmetric distribution. The physics, if any, lies in the observation that the distributions are symmetric in the "quark frame" in which all five quarks ($q\bar{q}$ from a meson projectile, qqq from a proton target) have the same momentum. This seems to be the case for $\pi^-p \to \pi^+$ + anything at 25 GeV/c, $\pi^+p \to \pi^-$ + anything at 7 GeV/c, and $K^+p \to \pi^-$ + anything at 11.8 and 12.7 GeV/c.] In all the cases studied, the observed secondaries are thought not to be "leading particles." However, resonance formation in low-multiplicity events can blur the distinction between leading and nonleading particles. For example, a fast ρ^0 formed in a π^+p collision can decay with π^- going forward to produce a "leading π^-" with momentum nearly equal to that of the beam π^+. In Fig. 3, which[9] shows the front-back asymmetry in π^+-π^- scattering as a function of $s^{\frac{1}{2}}$, I remind you that this sort of double charge exchange does occur in the resonance region with significant probability, although above $s = 4\ (\text{GeV/c})^2$ it is completely forbidden. The "forbidden" forward π^- peak in $d\sigma/dp^*_{||}$ for the reaction $\pi^+p \to \rho^0\Delta^{++}$ at 3.7 GeV/c is shown in Fig. 4. The number of "leading" π^- mesons is <u>not small</u>.[10] It is quite evident from this discussion that more good information on virtual meson-baryon or meson-meson scattering and on resonance production and decay is always welcome, even if one is mainly interested in understanding 2-to-n reactions.[11]

III. A PICTURE OF INCLUSIVE REACTIONS

1. Inclusive Reactions--Why?

Feynman[12] and Yang[13] have emphasized the importance of inclusive experiments in which, in a collision of particles a and b we look for particular particles with specific momenta in the final state but we allow anything else to be produced also. The simplest inclusive experiment is the measurement of the total cross section (σ_t)

$$a + b \rightarrow \text{anything} \tag{7}$$

in which we look for no special particles in the final state. The first nontrivial inclusive experiment is the measurement of the single-particle spectrum, i.e., of the invariant cross section

$$\omega \frac{d^3\sigma(\underset{\sim}{p}; s)}{d^3\underset{\sim}{p}} = f(\underset{\sim}{p}; s) \tag{8}$$

for production of particle c with momentum $\underset{\sim}{p}$ and energy ω in the reaction

$$a + b \rightarrow c + \text{anything}. \tag{9}$$

The inclusive reaction (9) is intuitively analogous to the total cross section measurement (7), and with the empirical knowledge that σ_t is a constant at high energies one is led to the hypothesis of limiting fragmentation:

$$\lim_{s\rightarrow\infty} \omega \frac{d^3\sigma(\underset{\sim}{p}; s)}{d^3\underset{\sim}{p}} = \rho_1(\underset{\sim}{p}) > 0. \tag{10}$$

Indeed, one may be tempted to extend the conjecture to more complicated inclusive reactions such as

$$a + b \rightarrow 1 + 2 + \cdots + n + \text{anything}, \tag{11}$$

for which the statement of limiting is

$$\lim_{s\to\infty} \frac{d^{3n}\sigma(\underset{\sim}{p}_1,\underset{\sim}{p}_2,\cdots,\underset{\sim}{p}_n;\ s)}{\sum_{i=1}^{n} (d^3\underset{\sim}{p}_i/\omega_i)} = \rho_n(\underset{\sim}{p}_1,\underset{\sim}{p}_2,\cdots,\underset{\sim}{p}_n) > 0. \tag{12}$$

The possibility of making these general hypotheses is one reason for discussing inclusive reactions; the ease of measuring inclusive cross sections is another. As we shall discuss shortly, one is also able to make quite detailed predictions for inclusive cross sections if he is willing to pay the price of making additional theoretical assumptions. Before taking up detailed predictions let us notice that, in principle, knowledge of all the functions ρ_n is equivalent to knowledge of all inclusive experiments. The distributions ρ_n have counterparts in many-body theory. For example $\rho_1(\underset{\sim}{p})$, which is proportional to the density of secondary particles in momentum space is analogous to the density of molecules in position space, in the theory of liquids. Similarly $\rho_2(\underset{\sim}{p}_1,\underset{\sim}{p}_2)$ which is proportional to the probability of finding one secondary with momentum $\underset{\sim}{p}_1$ and another with momentum $\underset{\sim}{p}_2$ has its analog in position space. The many-body-theory analogy has not yet been exploited to any great degree, but it may prove to be a promising line of inquiry.

2. Inclusive Reactions in S-Matrix Theory

In hadron physics it has been possible to give a theoretical description of the total cross section without understanding the individual channels represented collectively by "anything" in (7). This is so because, as indicated in Fig. 5 (a), unitarity relates the total cross section to the imaginary part of the forward elastic scattering amplitude by means of the familiar optical theorem. Mueller[5] recognized that in a similar way the "anything" in (9) allows one to use unitarity to relate the single-particle spectrum to the discontinuity in missing mass of an analytic continuation of the forward 3-to-3 elastic scattering amplitude for

$$a + b + \bar{c} \rightarrow a + b + \bar{c} \tag{13}$$

as depicted in Fig. 5 (b). Furthermore, one can generalize the argument in an obvious way to relate the n-particle spectrum (11) to the discontinuity in missing mass of an analytic continuation of the forward (n+2)-to-(n+2) elastic scattering amplitude for

$$a + b + \bar{1} + \bar{2} + \cdots + \bar{n} \rightarrow a + b + \bar{1} + \bar{2} + \cdots + n. \tag{14}$$

We shall be interested mainly in the single-particle spectrum. Unfortunately, unlike the optical theorem, Mueller's optical theorem analog relates not to the physical amplitude for the process (13) but only to an analytic continuation of it. Nonetheless if, as proposed by Mueller, one assumes that the continued amplitude is dominated by the same Regge singularities as the physical amplitude, one is led to extremeley interesting results. Our purpose in the next section will

be to investigate the phenomenological consequences of this hypothesis, and to clarify the experimental conditions under which they may be tested. Notice that a forward 3-to-3 amplitude depends on 3 independent variables* which we may choose to be

$$\left.\begin{aligned} s &= (a+b)^2, \\ \text{the missing mass squared } \mathcal{M}^2 &= (a+b-c)^2, \\ \text{and either } t_a &= (a-c)^2 \quad \text{or} \\ t_b &= (b-c)^2. \end{aligned}\right\} \tag{15}$$

Four interesting kinematical regions, corresponding to different Regge limits, have been identified:[14]

(i) Fragmentation region (single-Regge limit). This is illustrated in Fig. 6 (a) for the fragmentation of a. It is the limit

---

* Lorentz invariance says a 2n-point function at general angles depends on 6n - 6 parameters, after imposition of 2n mass shell constraints, 3 rotation constraints, and 3 boost constraints. The requirement of forward elastic scattering, $p_i(\text{in}) = p_i(\text{out})$, imposes 3n additional constraints which simultaneously ensure Poincaré invariance. Thus a forward n-to-n amplitude depends on 3n - 6 parameters. In particular, the forward 3-to-3 amplitude depends on 3 parameters.

$s \to \infty$, $t_b \to -\infty$, t_a fixed, s/m^2 fixed, which is equivalent to fixing $\underset{\sim}{p}^{(a)}$ (the momentum of c, measured in the rest frame of a) since

$$\begin{aligned} t_a &= m_a^2 + m_c^2 - 2m_a\omega_c^{(a)} \\ s/m^2 &= [1 - (\omega_c^{(a)} - p^{(a)})/m_a]^{-1} \end{aligned} \tag{16}$$

Note the presence of three independent variables, e.g., s, $p^{(a)}$, and $p_\perp$.

(ii) Central region (double-Regge limit). The central region is usually defined to be that range of $p_{||}^*$ (longitudinal momentum of c, measured in the center of mass) in which, for fixed values of $p_\perp$ and s, the invariant cross section is independent of $p_{||}^*$. The double-Regge diagram is indicated in Fig. 6 (b). The appropriate kinematical limit is $s \to \infty$, t_a and $t_b \to -\infty$, while $t_a t_b/s = p_\perp^2 + m_c^2$.

(iii) Phase space boundary of the fragmentation region. This special case of (i) occurs for $s/m^2 \to \infty$, and may be represented by the triple-Regge limit of Fig. 6 (c). In this case only two variables, for example s and $|\underset{\sim}{p}^{(a)}|$ remain.

(iv) Region of fixed missing mass. Represented by direct channel resonances in Fig. 6 (d), the region of fixed missing mass defines an elliptical ring in the phase space of $\underset{\sim}{p}$, which moves toward the phase space boundary as $s \to \infty$.

Of these four regions, we shall only be concerned with the single-Regge limit, which is easily accessible at medium energies, and about which two-body phenomenology has much to say.

3. A New Regge Phenomenology[15]

Despite its inherent weaknesses,[16] the Regge pole model has proved to be a most useful tool for a qualitative description of the energy dependence of total cross sections for energies up to 30 GeV. Figure 7 is representative of the many impressive fits which have been made to total cross section data with Regge poles.[17] The application of Regge theory to total cross sections is based on unitarity which relates to the imaginary part of the forward elastic amplitude. The Regge behavior of the elastic amplitude then implies the same for the total cross section.

Assume now that the 3-to-3 amplitude (13) related to the single-particle spectrum of reaction (9) is dominated by the usual Regge singularities

(i) the Pomeranchuk trajectory with $\alpha_P(0) = 1$;

(ii) the approximately exchange degenerate meson trajectories $(\rho, P' = f, \omega, A_2)$ with $\alpha_M(0) \approx 0.5$.

The preceding observations then imply that the invariant cross section (8) corresponding to single particle spectra should have the Regge behavior

$$f(p_{||}^{(a)}, p_{\perp}^{2}; s) = A(p_{||}^{(a)}, p_{\perp}^{2}) + B(p_{||}^{(a)}, p_{\perp}^{2}) s^{-\frac{1}{2}} . \qquad (17)$$

In (17), $p_{||}^{(a)}$ is the longitudinal momentum of particle c measured in the rest frame of a, corresponding to a fixed value of the invariant mass t_a of the system $(a\bar{c})$ as specified above. The function f may thus conveniently be interpreted as the distribution of particles c

due to the fragmentation of the projectile a. Obviously, the same statement can be made about the fragmentation products of the target b.

In spite of its simple appearance, Eq. (17) is an extremely powerful statement. It yields not only the limiting fragmentation hypothesis,[12,13] but also a definite prediction for the manner in which this limit is approached. Moreover, by relating single-particle spectra to Regge-behaved amplitudes, it allows the full armory of Regge phenomenology to be applied here also. There being a full distribution to study, instead of only one point at each energy, it can mean a whole new branch of Regge phenomenology at least as rich as two-body collisions.

To illustrate this point we cite as examples the following predictions derived from:

(a) Charge Conjugation. Consider the reactions

$$\pi^+ p \to c + \text{anything} \tag{18}$$

$$\pi^- p \to c + \text{anything}, \tag{19}$$

where c may be π, K, N, or $\bar{N}$. The distribution of c from the fragmentation of the target proton has the form (17) with

$$B = B_{P'} + B_\rho \tag{20}$$

corresponding respectively to P' and ρ exchange. The coupling functions A and B for reactions (18) and (19) are related to one another by charge conjugation at the pion vertex, so that

$$A^+ = A^-, \qquad B_{P'}{}^+ = B_{P'}{}^-, \qquad B_\rho{}^+ = -B_\rho{}^-. \tag{21}$$

As a result, for the distributions f^+ and f^- corresponding respectively to (18) and (19), we have

$$f^+(s; p_{||}^{lab}, p_\perp^2) - f^-(s; p_{||}^{lab}, p_\perp^2) = 2B_\rho^+(p_{||}^{lab}, p_\perp^2)s^{-\frac{1}{2}}. \quad (22)$$

In other words, one expects the distributions from reactions (18) and (19) to approach each other as $s^{-\frac{1}{2}}$. Similar conclusions can be drawn for the pairs of reactions initiated by (i) K^+ and K^-, or (ii) p and $\bar{p}$ as projectiles.

(b) Duality. For reactions in which the direct channel has exotic quantum numbers, duality implies, through exchange degeneracy, that the imaginary parts of meson exchanges $(\rho, P' = f, \omega, A_2)$ should cancel in the crossed channel. The imaginary part of the forward amplitude is then due entirely to Pomeranchuk exchange, which would in turn imply that cross sections for such processes are virtually independent of energy. A familiar example of this effect is the total cross section for K^+p scattering which is practically constant above 1.5 GeV/c. Apply now the same arguments to the reaction

$$K^+p \to \pi^\pm + \text{anything}. \quad (23)$$

This is related by means of Fig. 5 (b) to the three-body reactions

$$K^+p\pi^\mp \to K^+p\pi^\mp \quad (24)$$

which is exotic in the direct channel. The preceding observations then suggest that the invariant distributions f of pions from both projectile and target in (23) are practically constant as functions of incoming energy. In contrast, the distributions of pions from the reaction

$$K^- p \rightarrow \pi^{\pm} + \text{anything} \qquad (25)$$

are expected to be quite strongly energy dependent. For reference, I have listed 84 such predictions in Table I. (Our criterion that the missing mass have exotic quantum numbers is a sufficient but not necessary requirement for the absence of meson contributions.) The reader may easily supply the corresponding predictions for the double-Regge limit by drawing six-point duality diagrams.[18]

(c) Factorization. If the Pomeranchuk singularity is a simple pole, factorization of its residues implies that the limiting distributions of the fragmentation products of the target should be independent of the projectile, apart from the normalization. To test this experimentally, one needs in general high incoming energies (say > 30 GeV) to guarantee that the limit has indeed been reached. However, according to the duality arguments given in (b), such high energies are unnecessary for those reactions with exotic direct channels. If the $K^+ p$ total cross section can be accepted as a reliable guide, Pomeranchuk exchange should already dominate at beam momenta as low as 1.5 GeV/c. Thus, for example, for the reactions

$$K^+ p \rightarrow \pi^- + \text{anything}, \qquad (26)$$

$$\pi^+ p \rightarrow \pi^- + \text{anything}, \qquad (27)$$

both of which are exotic in the direct channel, we expect that pion fragments from the target proton should have similar distributions already at moderate energies, for which data are immediately available.

To the extent that limiting behavior is reached, it is unnecessary that reactions (26) and (27) be compared at the same energy s.

The idea that the Pomeranchuk singularity is factorizable is qualitatively supported by two-body data on elastic scattering and diffractive excitation of N^* resonances in πN and NN collisions,[19] but the tests are not at all definitive. The predictions we are about to consider for single-particle spectra depend only on the assumption that the Pomeranchuk factorizes at $t = 0$, where the evidence in favor of factorization is strongest in the two-body case. It is appropriate to point out that a study of the reactions $K^+p \to K^+N^{*+}$ at intermediate energies would provide conclusive new information on the nature of the Pomeranchuk singularity in two-body collisions.

Stone, et al.[20] of the University of Rochester have bubble chamber data on the reactions $K^+p \to \pi^-$ + anything at 12.7 GeV/c and $\pi^+p \to \pi^-$ + anything at 7 GeV/c with which they have tested the factorization predictions. Let us adopt the notation $a \xrightarrow{b} c$ to mean the fragmentation of particle a into particle c (and anything else) under impact of particle b.[21] Denote by f_x the invariant cross section for $p \xrightarrow{x} \pi^-$. Then, applying Pomeranchuk factorization to (17), we have

$$\left.\begin{aligned} f_K &= g_{K\bar{K}P}(t=0)\tilde{A}(p_{\parallel}^{Lab}, p_{\perp}^2), \\ f_\pi &= g_{\pi\pi P}(t=0)\tilde{A}(p_{\parallel}^{Lab}, p_{\perp}^2), \end{aligned}\right\} \qquad (28)$$

where the constants g are the Pomeranchuk residues, evaluated at $t = 0$. These may be obtained from the total cross sections at infinite energy, for

$$\left.\begin{aligned} \sigma_{t,\infty}(K^+p) &= g_{K\bar{K}P}(0)g_{ppP}(0) \approx 17.4 \text{ mb.} \\ \sigma_{t,\infty}(\pi^+p) &= g_{\pi\pi P}(0)g_{ppP}(0) \approx 23.0 \text{ mb.} \end{aligned}\right\} \tag{29}$$

Thus we predict

$$f_\pi(p_{||}^{Lab}, p_\perp^2) = \frac{\sigma_{t,\infty}(\pi^+p)}{\sigma_{t,\infty}(K^+p)} f_K(p_{||}^{Lab}, p_\perp^2). \tag{30}$$

This relation remains valid when integrated over any region of phase space within the fragmentation region.

In Fig. 8 we show the prediction for $\omega d\sigma/dp_{||}$ based on the $p \xrightarrow{K^+} \pi^-$ data, together with the $p \xrightarrow{\pi^+} \pi^-$ data points, as functions of $p_{||}^{Lab}$. The agreement is spectacular throughout the fragmentation region, which is confined to $p_{||}^{Lab} \lesssim 1$ GeV/c. Let me emphasize that, given the $p \xrightarrow{K^+} \pi^-$ data at 12.7 GeV/c, we are making an <u>absolute</u> prediction of $p \xrightarrow{\pi^+} \pi^-$ at 7 GeV/c. The agreement obtained supports both the assumption of factorization and the duality argument that both channels are Pomeranchuk-dominated. Another representation of the same information is given in Fig. 9, where we plot the ratio

$$\omega \frac{d\sigma}{dp_{||}}(p \xrightarrow{\pi^+} \pi^-)/\omega \frac{d\sigma}{dp_{||}}(p \xrightarrow{K^+} \pi^-)$$

which should be equal to the ratio $\sigma_{t,\infty}(\pi^+p)/\sigma_{t,\infty}(K^+p) = 1.32$. The points in the fragmentation region indeed cluster about this value. Figure 10 is similar to Fig. 8, except that a cut has been made on the

transverse momentum, $p_\perp^2 < 0.1$ (GeV/c)^2. The agreement is again impressive. In Fig. 11 we compare $\omega d\sigma/dp_\perp^2$ for $p \xrightarrow{\pi^+} \pi^-$ with the prediction based upon $p \xrightarrow{K^+} \pi^-$ as before. We restrict ourselves to the fragmentation region $p_{||}^{Lab} < 1$ GeV/c, and plot as a function of $p_\perp^2$. The two sets of points are nearly indistinguishable. Figure 12 is the same as Fig. 11, except that we now include events up to $p_{||}^{Lab} < 1.5$ GeV/c. The distribution is slightly flatter than in the previous figure, but the success of the prediction is unchanged.

If the evidence complied here is a fair test, Pomeranchuk factorization seems to be a very useful concept indeed. (The evidence cited here is much stronger than that which has been compiled in two-body scattering.) I will show later that not all fragmentation distributions are the same, which demonstrates that the agreement found here is not utterly trivial. There is also some indication that factorization fails in nonexotic cases.[22] Consider the preliminary data of the Stony Brook Track Chamber Group on the reaction $K^-p \to \pi^-$ + anything at 9 GeV/c.[23] This channel is nonexotic and therefore we expect $f(p \xrightarrow{K^-} \pi^-)$ to have marked energy dependence and to approach $f(p \xrightarrow{K^+} \pi^-)$ from above at very high energies. Moreover, no factorization argument predicts that the shapes of $f(p \xrightarrow{K^\pm} \pi^-)$ should be identical. Because of the difficulty in separating pions from kaons, the shape of the K^--initiated spectrum is only tentative. This shape, shown in Fig. 13, is qualitatively similar to that for the exotic channel, but the normalization is clearly different. The nonexotic cross section lies a factor of ~ 1.6 above the exotic cross section, in support of the

exotic v. nonexotic distinction. The shape of the transverse momentum distributions, $\omega d\sigma/dp_\perp^2$, plotted in Fig. 14, bears a qualitative resemblance to that for $K^+p \to \pi^-$ + anything.

To test the factorization of residues for secondary trajectories such as ρ, one may either make an overall fit as Barger and Phillips did for total cross sections or attempt to isolate the contribution of a single trajectory by forming judicious combinations of distributions from several reactions. For example, the ρ-exchange contribution to reactions (18) and (19) can be isolated as in (22). Similarly, from Kp and $\bar{K}p$ collisions, one can isolate the ρ-exchange contribution by forming the linear combination

$$\{f(K^+p) - f(K^-p)\} + \{f(K^0p) - f(\bar{K}^0p)\} \tag{31}$$

where in deriving (31) one has used charge conjugation and isospin. Further, one may replace the last two distributions in (31) by their charge-symmetric partners which are more accessible experimentally. One then has the relation

$$\{f(\pi^+p \to c + \text{anything}) - f(\pi^-p \to c + \text{anything})\} =$$

$$= Z\{[f(K^+p \to c + \text{anything}) - f(K^-p \to c + \text{anything})]$$

$$+ [f(K^+n \to \tilde{c} + \text{anything}) - f(K^-n \to \tilde{c} + \text{anything})]\} \tag{32}$$

between the distributions of the target fragments. The constant of proportionality Z is predicted to be unity by $SU(3)$, and $\tilde{c}$ is the charge-symmetric partner of c. The total cross section analog of the

SU(3) sum rule (32) for ρ-exchange has already been verified by Barger[17] within rather large errors which reflect the smallness of the ρ contribution. This is shown in Fig. 15. The $\omega N\bar{N}$ helicity nonflip coupling is quite large, so a more stringent test is possible for ω factorization in two-body reactions. Such a test[17] is shown in Fig. 16; the agreement is satisfying.

4. Photon Fragmentation

In two-body phenomenology it has proved fruitful to regard photoproduction reactions as hadronic processes by means of vector meson dominance, and it is natural to extend this philosophy to inclusive reactions. I have already assumed this to be meaningful in constructing the last line of Table I which contains the predictions of duality for photoinduced reactions. Duality has been applied as if the photon were a real ρ^0. Since the photon is massless, we cannot look at its fragments in its rest frame as we did for massive projectiles. However, by fixing the scaled center of mass variable

$$x = p_{||}{}^*/p_a{}^* \tag{33}$$

(the asterisk denotes center of mass quantities), one closely approximates the kinematical conditions for the fragmentation region which were listed in Sec. III-2. Specifically, for x fixed near 1 and s large, both

$$s/\mathcal{M}^2 = \left[(1 - x) + \frac{m_c{}^2 - xm_b{}^2}{s} + \frac{2(p_\perp{}^2 + m_c{}^2)}{x^2(s - m_b{}^2)^2}\right]^{-1} \tag{34}$$

and

$$t_a = m_c^2 - \frac{(p_\perp^2 + m_c^2)}{x^2} + \frac{(p_\perp^2 + m_c^2)^2 s}{x^4 (s - m_b^2)^2} \qquad (35)$$

are fixed, up to terms of order $(1/s)$. This suggests that we can study photon fragments within the Regge pole scheme, by examining the invariant cross section for fixed values of $(x, p_\perp^2)$.

What will photon fragments look like? By vector dominance, we expect photon fragments to resemble ρ^0 and ω^0 fragments. But, lacking experience with vector meson projectiles, we must make further assumptions to say anything specific. Some time ago Satz[24] combined vector dominance with the quark model to predict multipion photoproduction cross sections from the corresponding pion-nucleon scattering data. From the usual vector meson dominance decomposition of the elctromagnetic current, and ignoring interference effects, we may write

$$\sigma(\gamma p \to X) = \sum_V \frac{\alpha_\pi}{\gamma_V^2} \sigma(V_p \to X) \qquad (36)$$

where the sum runs over the vector mesons, γ_V is the vector meson-photon coupling constant, and $\sigma(V_p \to X)$ is the cross section for transversely-polarized vector mesons. The ϕ contribution is negligible compared to those of ρ^0 and ω. From the simple quark model,

$$\sigma_t(\rho^0 p) = \sigma_t(\omega p) = \frac{1}{2}\left(\sigma_t(\pi^+ p) + \sigma_t(\pi^- p)\right) = \sigma_t(\pi^0 p). \qquad (37)$$

Satz assumed that this identity holds term by term for the integrated partial cross sections that make up the total cross section:

$$\sigma(\rho^0 p \to X) = \sigma(\omega p \to X) = \sigma(\pi^0 p \to X). \qquad (38)$$

Using $\gamma_\rho^2/4\pi = \frac{1}{2}$ and $\gamma_\omega^2/\gamma_\rho^2 = 9$, we obtain from (37)

$$\sigma(\gamma p \to X) = 4.1 \times 10^{-3}\, \sigma(\pi^0 p \to X). \qquad (39)$$

Figure 17 displays the excellent agreement between Satz's predictions and experiment for the five-prong cross section $\gamma p \to 2\pi^+ 2\pi^- p$. Although it is based on extreme assumptions, the work of Satz lends qualitative support to the guess that photon fragments should resemble ρ^0 fragments, which should be useful in assessing whether the results of photoproduction experiments are "surprising" or "expected."

IV. SPECIFIC EXPERIMENTAL SUGGESTIONS

1. Beam Survey Experiments

While I was a student in Berkeley, I became so adept at pestering experimenters with questions about what kinds of experiments they could do, that in self-defense they presented me with a "Bevatron Experimenter's Handbook" and instructed me to read it carefully. In fact I did read it, and in preparing this review I looked through the section on secondary beam characteristics to see whether any information on multiparticle final states was hidden there. To my great glee, I found Fig. 18 which shows the relative production of π^+ and π^- in 7 GeV/c pp collisions as a function of p_{Lab} and θ_{Lab}. This comes very close to being a portion of a single-particle spectrum as it stands and I imagine somewhat optimistically that it could be converted into a map of ρ_1 without undue effort. It is frequently wondered whether old beam surveys might contain interesting inclusive experiments, and this figure encourages me to believe that the answer is yes. Members of the audience who have built beams are encouraged to reclaim theiry survey data for modern uses.

2. Old Bubble Chamber Experiments

The great advantage of the bubble chamber for inclusive experiments is its ability to map the whole of a single-particle spectrum. Even with marginal statistics, the shapes of fragmentation distributions are of enormous interest. I recommend that inclusive cross sections be made out of old, medium-energy exposures in order to investigate the dependence of the shape of $\rho_1(a \xrightarrow{b} c)$ on the particles involved in the

fragmentation. It is of obvious importance for fabricating a theory to know the qualitative rules that govern single-particle spectrum shapes.

That some intuition will be gained by regarding quasi-two-body data as fragmentation distributions has already been suggested in Sec. II. I simply remark here that it should take about one week for a bright graduate student to satisfy his (and my) curiosity by doing the exercise.

3. Old Counter Experiments

Unless geometrical biases are particularly weird, missing mass counter data can usefully be converted into single-particle spectra. Spectra thus obtained may be of great interest because they are likely to involve beam-target combinations for which inclusive experiments have not yet been performed.

4. New Bubble Chamber Experiments

Much fascinating information about multiparticle reactions is coming out of bubble chamber experiments at the present time. I am aware of high-statistics inclusive experiments in the π^+p, π^-p, K^+p, K^-p, and pp channels which are beginning to pour out results. Only the $\bar{p}p$ channel (among those accessible in a Hydrogen chamber) seems neglected. Probably some groups hoarding large exposures have not yet started to study many-body final states; I hope to tempt them into beginning analysis. Again I will show examples from the 7 GeV/c π^+p and 12.7 GeV/c K^+p exposures of Stone, et al.[20] at the University of Rochester. As a check of factorization, I showed a comparison of $p \xrightarrow{\pi^+} \pi^-$ with $p \xrightarrow{K^+} \pi^-$ in Figs. 8-12. By observing slow particles in the rest frame of the beam (projectile frame) one can also study

$\pi^+ \underset{\Rightarrow}{p} \pi^-$ and $K^+ \underset{\Rightarrow}{p} \pi^-$. This enables us to compare the fragmentation distributions of protons, positive kaons, and positive pions into negative pions. [Assuming Pomeranchuk dominance in these exotic reactions, plus Pomeranchuk factorization, I can regard the fragmentation as independent of the other initial state particle.] The longitudinal momentum distributions $\frac{\omega d\sigma}{dp_{||}}(p_{||}^{\text{Projectile}}, p_\perp^2)$ for $K^+ \underset{\Rightarrow}{p} \pi^-$ is shown in Fig. 19. It is similar to the $p \to \pi^-$ spectrum of Fig. 8. In contrast, the same distribution for $\pi^+ \underset{\Rightarrow}{p} \pi^-$, plotted in Fig. 20, seems to be qualitatively <u>different</u> from both the proton and the kaon fragmentations. Similarly, the distribution $\frac{\omega d\sigma}{dp_\perp^2}(p_{||}^{\text{Proj}}, p_\perp^2)$ for the kaon fragmentation (Fig. 21) closely resembles that for the proton fragmentation, but is drastically different from that for the pion fragmentation (Fig. 22). I find these data very exciting, and appetizing food for theoretical thought. In Fig. 23 I have estimated (quite roughly) the cross section $\omega d\sigma/dp_{||}^{\text{Proj}}$ for π^- mesons in $\pi^+ p \to (\rho^0, \omega)\Delta^{++}$ at 3.7 GeV/c.[10] The shape of the distribution is quite similar to the shape shown for the pion fragmentation in Fig. 22. The possibility that resonances characterize the shapes of fragmentation distributions should be studied more carefully in bubble chamber experiments, both in this case and in the others we have seen. Indeed, many other distributions are measurable, and <u>all</u> combinations of $a \underset{\Rightarrow}{b} c$ should be studied. We have seen so few of these pictures until now, that each new one represents a large fractional increase in our knowledge.

5. New Counter Experiments

Those dubious about the invocation of Regge poles are probably wondering by now why I didn't examine the energy dependence of ρ_1 before indulging in a subtlety like factorization. Of course I did check the energy dependence, but I found that existing experiments are insufficiently accurate to measure it. Three data points taken at different energies are needed for each point $(p_{\parallel}^{Proj}, p_{\perp}^2)$ at which one wants to study the energy dependence. All[25] the elegant counter experiments on the inclusive reaction $pp \to p$ + anything overlap at only 11 points, many of which lie outside a strict definition of the fragmentation region in which the single-Regge limit is thought to apply. For the points of overlap, the data are plotted in Fig. 24. Relative normalization uncertainties are much too large to allow one to draw any quantitative conclusions. The measurements by Anthony, et al.[26] of $\pi^- p \to \pi^+$ + anything from 2 to 6 GeV/c, shown in Fig. 25, are likewise consistent with the predicted energy dependence but too coarse to test it severely. Consequently I suggest a series of measurements of single-particle spectra from 2 to 20 GeV/c with 2% relative normalization uncertainty, for any beam and any secondary. For developing an understanding of multiparticle production, this set of experiments is equally as important as measurements of total cross sections.

Double-arm spectrometers are ideally suited for measurements of the two-particle correlation function

$$\rho_2 = \omega_1 \omega_2 \frac{d^6\sigma(p_{1\parallel}, p_{1\perp}^2 : p_{2\parallel}, p_{2\perp}^2; s)}{d^3p_1 \, d^3p_2}$$

in the reaction $a + b \rightarrow c + d +$ anything. Such measurements should certainly be made, but I am embarrassed to report that there are no very strong theoretical expectations to guide experiment design.

6. Cross Sections at 90°

I cannot resist mentioning a group of experiments which lack a direct connection with multiparticle reactions but which will be useful in determining hadron structure, knowledge of which will in turn guide our thinking about inclusive reactions. Measurements of differential cross sections at 90° in the center of mass must necessarily be carried out at intermediate energies because, as the pp elastic cross section plotted in Fig. 26 shows, the differential cross section drops very rapidly with increasing energy. Existing data on elastic and inelastic two-body channels are so scanty as to be consistent with the hypothesis that, for fixed energy, all 90° cross sections are approximately equal. This idea is extremely significant if true, but independently of any theory, the experimental situation deserves to be clarified.

V. OUTLOOK

To conclude, I want to hazard a few guesses about where we are in the study of multiparticle reactions at intermediate energies, and what directions we will be taking in the near future. It seems clear that the major thrust of effort will be the study of inclusive reactions. Among the good reasons for the primacy of inclusive experiments are these facts:

1. At very high energies (those available at NAL or ISR) it will be difficult to study individual multiparticle channels. To match the intermediate energy program with the very high energy possibilities requires the study of inclusive reactions.

2. Inclusive experiments are theoretically tractable and interesting. Important qualitative statements, such as the hypothesis of limiting fragmentation, can be made.

3. The potential utility of a Regge phenomenology of inclusive reactions makes possible quantitative comparisons among different inclusive experiments. Duality arguments suggest that the asymptotic ideas of limiting fragmentation may already apply in some channels at intermediate energies.

Despite the well-deserved popularity of inclusive experiments, it is evident that at medium energies one can do more to study how fragmentation distributions are built up of particular exclusive channels. This enterprise is likely to be frustrating for the experimenter, who will find little guidance from heavily advertised theoretical models, and whose results may be greeted at first by theoretical yawns. I am sorry that this is the case, for I feel it reflects misjudgement, and sorrier

still that I have no predictions of my own to offer. I can only urge experimenters to persevere in the face of indifference and if necessary to make their own models for guidance.

If the Regge pole framework described in Sec. III lives up to its promise, then the energy dependence of the single-particle spectrum can be understood, and the factorization of Pomeranchuk residues will enable us to relate fragmentation distributions in different inclusive reactions. Assuming this to be so, the next theoretical step is to try to explain the shapes of fragmentation distributions. Experimental input is desperately needed here. For example, a catalog of the shapes of $a \xrightarrow{b} c$ for all particles a, b, c is desirable. To the extent that Pomeranchuk factorization is useful, we can speak of $a \to c$, without reference to the exciting particle b. There is a general theoretical expectation, enunciated by Chou and Yang,[21] that two qualitatively different kinds of fragmentation distributions should exist, namely "favored" and disfavored" distributions. A favored fragment is one that has the same quantum numbers (other than spin) as the initial state particle of which it is an artifact, i.e., one which can be produced by diffractive excitation of the incident particle. Other fragments are disfavored. A disfavored distribution is expected to vanish on its kinematical boundary, whereas a favored distribution should not vanish on its boundary. All the distributions I have shown in this paper are "disfavored." Experimenters should look carefully for exceptions to these rules, and should try to discover whether several types of disfavored distributions might exist. Perhaps there are "forbidden" fragmentations!

A final area I wish to single out for study is the measurement of more complicated inclusive distributions such as the two-particle correlation function ρ_2. This is another instance in which we have only vague theoretical expectations, which I will not discuss. I do expect theoretical ideas to progress to an experimentally useful stage within the next year. All sorts of crude but instructive model calculations are possible, and many of my colleagues are screwing up their courage to carry the computations out.

I hope first that I have convinced you that the study of multiparticle reactions at intermediate energies is a young and rapidly-changing subject from which we can learn exciting and unexpected new physics, and second that many experimenters will join the game. The more, the merrier!

ACKNOWLEDGMENTS

Many of the ideas contained in this paper were evolved in conversations with Professor Chan Hong-Mo, whom I am pleased to thank for a most pleasant and stimulating collaboration, still in progress. I am grateful to Professor C. N. Yang for a number of instructive discussions, and to many of my colleagues at Stony Brook for helpful comments. I am particularly happy to acknowledge the enormous contribution of Professor Tom Ferbel and Mr. Sheldon Stone who, by their generosity with new and as yet unpublished data, have made it possible for us daily to test and refine our developing ideas. Similarly, I thank Dr. G. S. Abrams for producing a number of plots from the LRL (Trilling-Goldhaber Group) 3.7 GeV/c $\pi^+ p \to V^0 \Delta^{++}$ experiment. Finally, I thank Dr. Geoffrey Fox for inviting me to prepare this review.

REFERENCES

1. S. B. Treiman and C. N. Yang, Phys. Rev. Letters 8, 140 (1962).

2. K. Gottfried and J. D. Jackson, Nuovo Cimento 33, 309 (1964).

3. See, for example, V. Barger and D. B. Cline, Phenomenological Theories of High Energy Scattering (W. A. Benjamin, Inc., New York, 1969), or P. D. B. Collins and E. J. Squires, Regge Poles in Particle Physics, Springer Tracts in Modern Physics No. 45 (Springer-Verlag, Berlin, 1968).

4. K. G. Wilson, Some Experiments on Multiple Production, Cornell Preprint CLNS-131, Nov., 1970.

5. A. H. Mueller, Phys. Rev. D2, 2963 (1970).

6. D. Amati, A. Stanghellini, and S. Fubini, Nuovo Cimento 26, 896 (1962).

7. F. Turkot, CERN 68-7.

8. J. W. Elbert, A. R. Erwin, and W. D. Walker, Evidence for the Internal Structure of Hadrons..., Wisconsin Preprint, 1970; S. Stone et al., Ref. 14; W. Ko and R. Lander, Symmetric π^- Production from $K^+p \to \pi^-$ + anything at 12 GeV/c, University of California, Davis Preprint, 1971.

9. This compilation by J. Veillet is quoted by G. Goldhaber in Proceedings XIII International Conference on High Energy Physics, Berkeley, 1966, ed. by M. Alston-Garnjost (University of California Press), p. 130.

10. G. S. Abrams, et al., Phys. Rev. Letters 25, 617 (1970); G. S. Abrams (Lawrence Radiation Laboratory, Berkeley), private communication.

11. In a similar vein, see E. Yen and E. L. Berger, Phys. Rev. Letters 24, 695 (1970).

12. R. P. Feynman, Phys. Rev. Letters 23, 1415 (1969); High Energy Collisions, ed. by C. N. Yang, et al (Gordon and Breach, Science Publishers, New York, 1970).

13. J. Benecke, T. T. Chou, C. N. Yang, and E. Yen, Phys. Rev. 188, 2159 (1969); C. N. Yang, High Energy Collisions, ed. by C. N. Yang et al. (Gordon and Breach, Science Publishers, New York, 1970).

14. C. E. DeTar, K. Kang, C.-I Tan, and J. H. Weis, MIT Preprint CTP-180 (1971).

15. Chan Hong-Mo, C. S. Hsue, C. Quigg, and J. M. Wang, Phys. Rev. Letters 26, 672 (1971).

16. G. C. Fox, High Energy Collisions, ed. by C. N. Yang et al. (Gordon and Breach, Science Publishers, New York, 1970).

17. V. Barger and R. J. N. Phillips, Phys. Rev. 187, 2210 (1969); V. Barger CERN Report 68-7.

18. H. Harari, Phys. Rev. Letters 22, 562 (1969); J. L. Rosner, ibid. 22, 689 (1969).

19. For example, E. W. Anderson et al., Phys. Rev. Letters 16, 855 (1966); 24, 683 (1970); 25, 699 (1970); P. G. O. Freund, Phys. Rev. Letters 21, 1375 (1968).

20. S. Stone, et al., Bull. Am. Phys. Soc. 16, 136 (1971); Longitudinal Momentum Distributions of π^- Mesons produced in 12.7 GeV/c K^+p and 7 GeV/c π^+p Interactions, Rochester Preprint UR-875-335 (1971), submitted to Nucl. Phys. B. S. Stone (University of Rochester), private communication.

21. T. T. Chou and C. N. Yang, Phys. Rev. Letters 25, 1072 (1970).

22. Factorization is being studied in $p \xrightarrow{p} \pi^-$ (exotic) at 28.5 GeV/c and in $p \xrightarrow{\pi^-} \pi^-$ (nonexotic) at 25 GeV/c, as well as in the cases reported here, by a Brookhaven-Rochester-Wisconsin consortium. [R. Panvini and L. L. Wang (Brookhaven National Laboratory), private communication.

23. M. Foster (Stony Brook Track Chamber Group), private communication.

24. H. Satz, Phys. Letters 25B, 27 (1967).

25. At. 12.4 GeV/c: J. L. Day et al., Phys. Rev. Letters 23, 1055 (1969); at 18.8 GeV/c: D. Dekkers et al., Phys. Rev. 137, B962 (1965); at 19.2 GeV/c: J. Allaby et al., CERN 70-12 (1970); at 30 GeV/c: E. W. Anderson et al., Phys. Rev. Letters 19, 198 (1967).

26. R. W. Anthony et al., Phys. Rev. Letters 26, 38 (1971).

Table I. Reactions (of the type projectile + target $\rightarrow$ secondary + anything) to which the meson trajectories contribute in the single-Regge limit are denoted by the entries p or n, for proton or neutron target. Absence of an entry indicates an exotic channel, for which the cross section is expected to be energy-independent.

Projectile	Secondary					
	π^+	π^-	K^+	K^-	p	$\bar{p}$
π^+	p,n	n	p,n		p,n	
π^-	p	p,n	p		p	
K^+			p,n		p,n	
K^-	p	p,n	p	p,n	p	
p					p,n	
$\bar{p}$	p	p,n	p	p,n	p,n	p,n
γ	p,n	p,n	p,n		p,n	

FIGURE CAPTIONS

Fig. 1. Average transverse momentum $\langle q_\perp \rangle$ as a function of CM incident momentum for a two-body elastic cross section of the form $d\sigma/dt \propto e^{at}$.

Fig. 2. Longitudinal momentum distributions of π^- mesons in the K^+p and π^+p centers of mass, respectively (from Ref. 20).

Fig. 3. A compilation by Veillet on the $(F - B)/(F + B)$ ratio as a function of $\pi^+\pi^-$ mass (from Ref. 9).

Fig. 4. Center of mass longitudinal momentum distribution of π^- mesons from $\pi^+p \to \rho^0\Delta^{++}$ at 3.7 GeV/c. Note the forbidden forward peak. (From Ref. 10.)

Fig. 5. (a) The usual optical theorem connection for total cross sections.

(b) Mueller's optical theorem analog for single-particle spectra.

Fig. 6. Four kinematic limits of the Mueller diagram. (a) Single-Regge limit; (b) Double-Regge limit; (c) Triple-Regge limit; (d) Regime of fixed missing mass.

Fig. 7. Representative Regge pole fits to total cross sections below 30 GeV/c (from Ref. 17).

Fig. 8. Comparison of $f(p \xrightarrow{\pi^+} \pi^-)$ with $f(p \xrightarrow{K^+} \pi^-)\sigma_{t\infty}(\pi^+p)/\sigma_{t\infty}(K^+p)$ integrated over $p_\perp^2$ (from Ref. 20).

Fig. 9. The ratio $\frac{\omega d\sigma}{dp_{||}}(p \xrightarrow{\pi^+} \pi^-)/\frac{\omega d\sigma}{dp_{||}}(p \xrightarrow{K^+} \pi^-)$, from Ref. 20.

Fig. 10. Same comparison as in Fig. 8, for $p_\perp^2 < 0.1$ (GeV/c)^2, from Ref. 20.

Fig. 11. Comparison of the cross sections in Fig. 8 as functions of $p_\perp^2$, integrated over $p_{||}^{Lab} < 1.0$ GeV/c, from Ref. 20.

Fig. 12. Same as Fig. 11, for $p_{||}^{Lab} < 1.5$ GeV/c, from Ref. 20.

Fig. 13. Invariant cross section for $p \xrightarrow{K^-} \pi^-$ at 9 GeV/c, as a function of $p_{||}^{Lab}$ (from Ref. 23).

Fig. 14. The data of Fig. 13, as a function of $p_\perp^2$, integrated over $p_{||}^{Lab} < 1$ GeV/c.

Fig. 15. Test of ρ^0 factorization in total cross sections (from Ref. 17).

Fig. 16. Test of ω^0 factorization in total cross sections (from Ref. 17).

Fig. 17. Quark-vector dominance model predictions for five-prong cross sections (from Ref. 24).

Fig. 18. Beam survey invormation from the Bevatron Experimenter's Handbook which can be converted into single-particle spectra.

Fig. 19. Fragmentation distribution $\omega d\sigma/dp_{||}^{Proj}$ of $(K^+ \xrightarrow{p} \pi^-)$ at 12.7 GeV/c (from Ref. 20).

Fig. 20. Same for $(\pi^+ \xrightarrow{p} \pi^-)$ at 7 GeV/c (from Ref. 20).

Fig. 21. Fragmentation distribution $\omega d\sigma/dp_\perp^2$ of $(K^+ \xrightarrow{p} \pi^-)$ at 12.7 GeV/c, integrated over $-p_{||}^{Proj} < 1.0$ GeV/c (from Ref. 20).

Fig. 22. Same for $(\pi^+ \xrightarrow{p} \pi^-)$ at 7 GeV/c (from Ref. 20).

Fig. 23. A crude estimate of the invariant cross section $\omega d\sigma/dp_{||}^{Lab}$ for π^- from $\pi^+ p \to (\rho^0, \omega)\Delta^{++}$ at 3.7 GeV/c, based on the data of Ref. 10.

Fig. 24. Energy dependence of the invariant cross section in $pp \to p$ + anything. The data are from Ref. 25.

Fig. 25. Energy dependence of $d^2\sigma/dp_{||}^{Proj}\, dp_{\perp}^2$ in $\pi^- p \to \pi^-$ + anything (from Ref. 26).

Fig. 26. Energy dependence of $d\sigma/dt$ at 90° in the center of mass for pp elastic scattering.

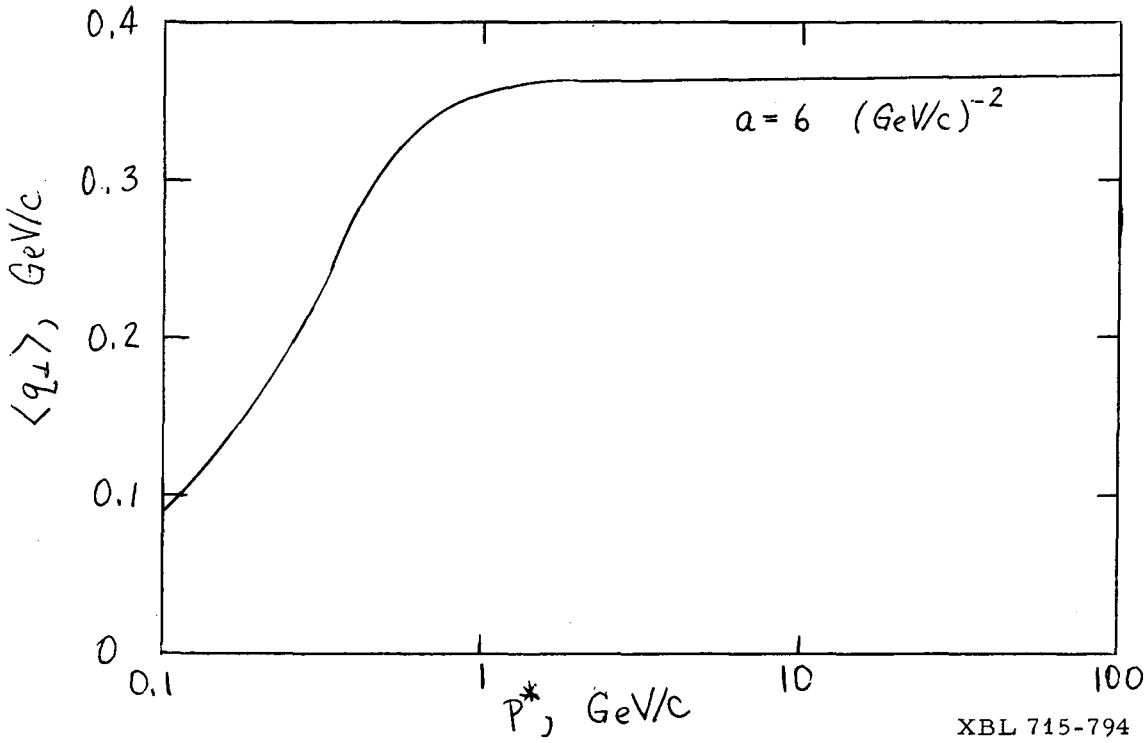
0.4
0.3
0.2
0.1
0
$\langle q_\perp \rangle$, GeV/c
$a = 6 \quad (GeV/c)^{-2}$
0.1
1
10
100
P^*, GeV/c
XBL 715-794

Fig. 1.

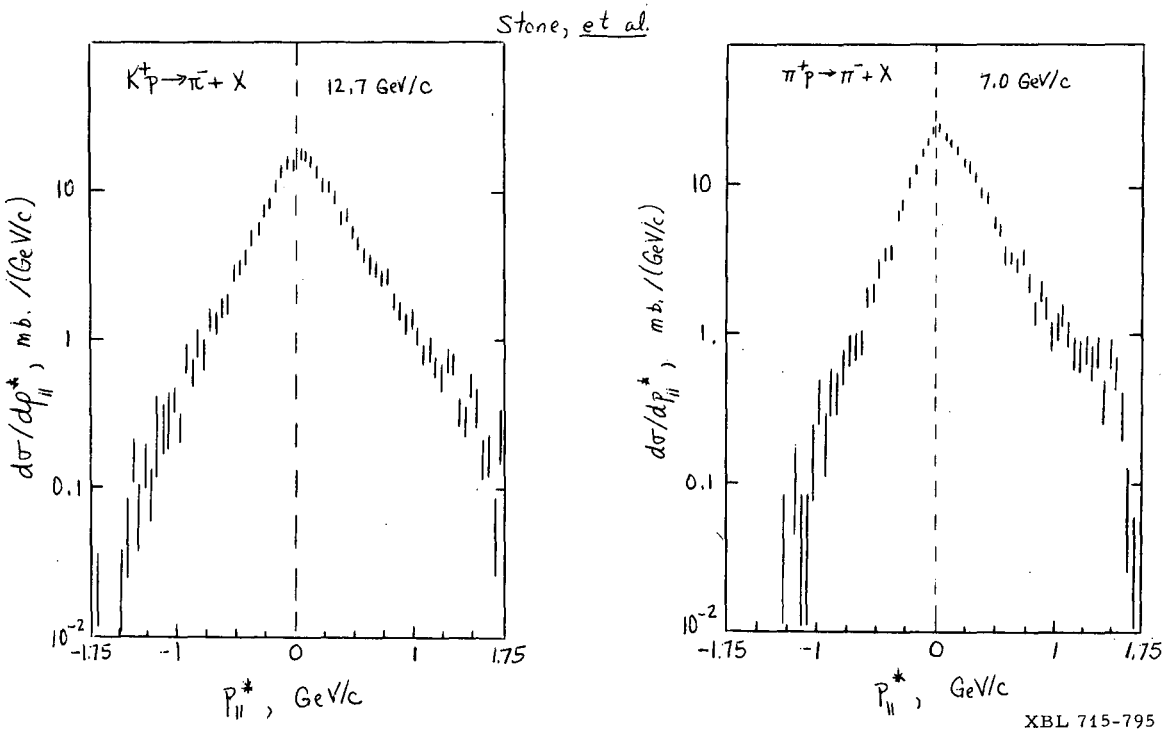
Stone, et al.
$K^+p \to \pi^- + X$
12.7 GeV/c
$\pi^+p \to \pi^- + X$
7.0 GeV/c
$d\sigma/dp_{\parallel}^*$, mb./(GeV/c)
$p_{\parallel}^*$, GeV/c
10
1
0.1
10^{-2}
-1.75
-1
0
1
1.75
XBL 715-795

Fig. 2.

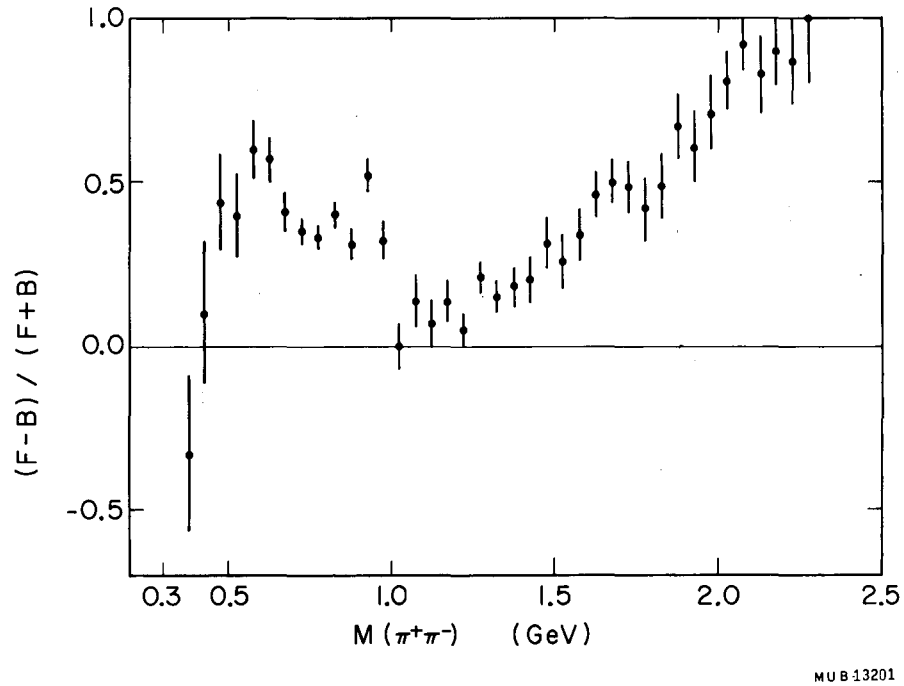

Fig. 3.

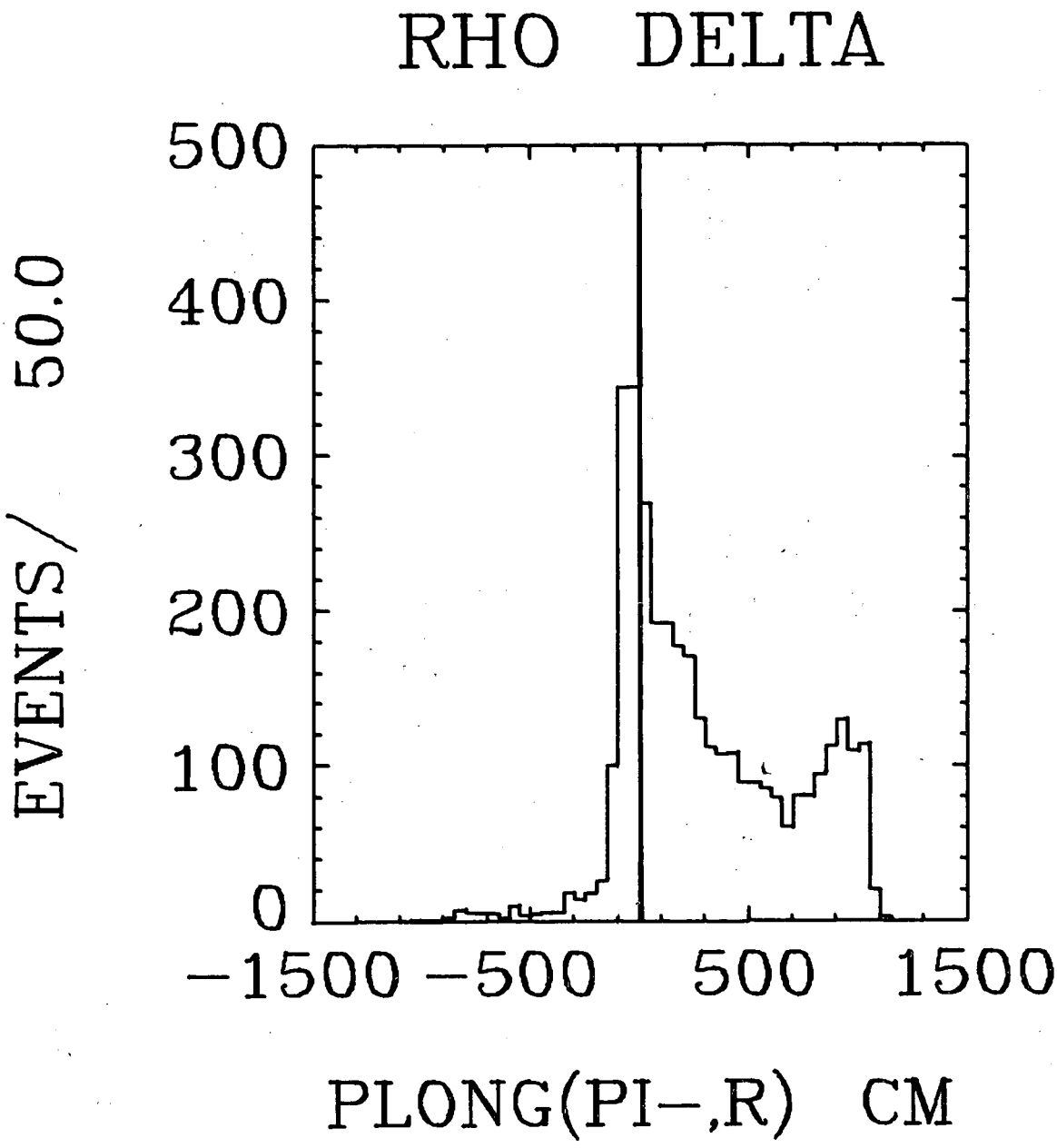
RHO DELTA
EVENTS/ 50.0
500
400
300
200
100
0
-1500
-500
500
1500
PLONG(PI-,R) CM
XBL 715-796

Fig. 4.

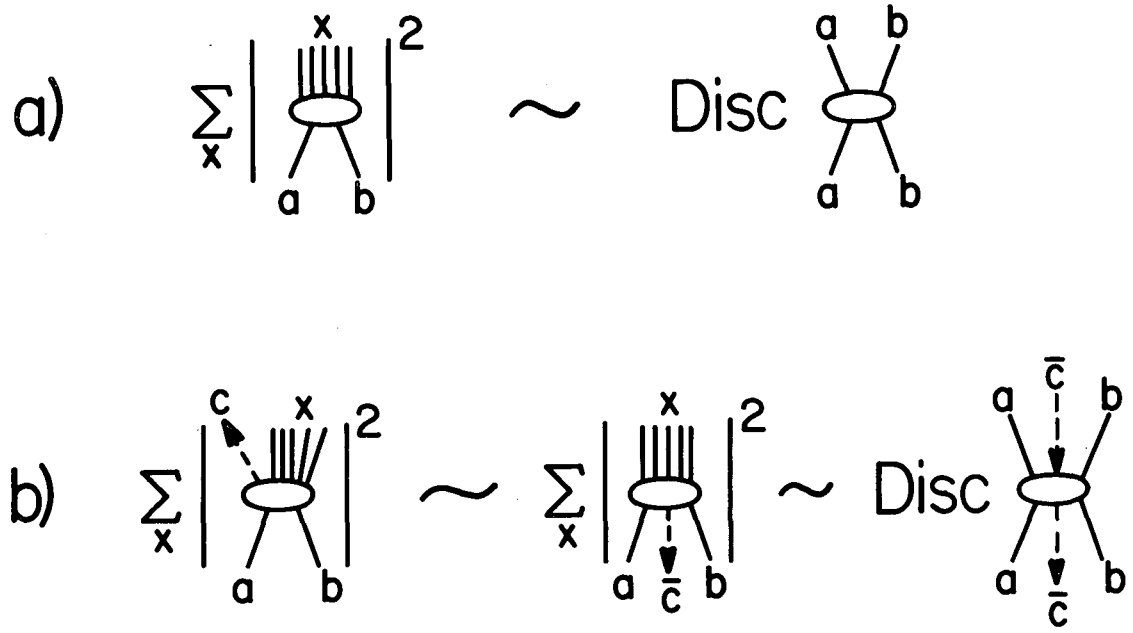

XBL 715-797

Fig. 5.

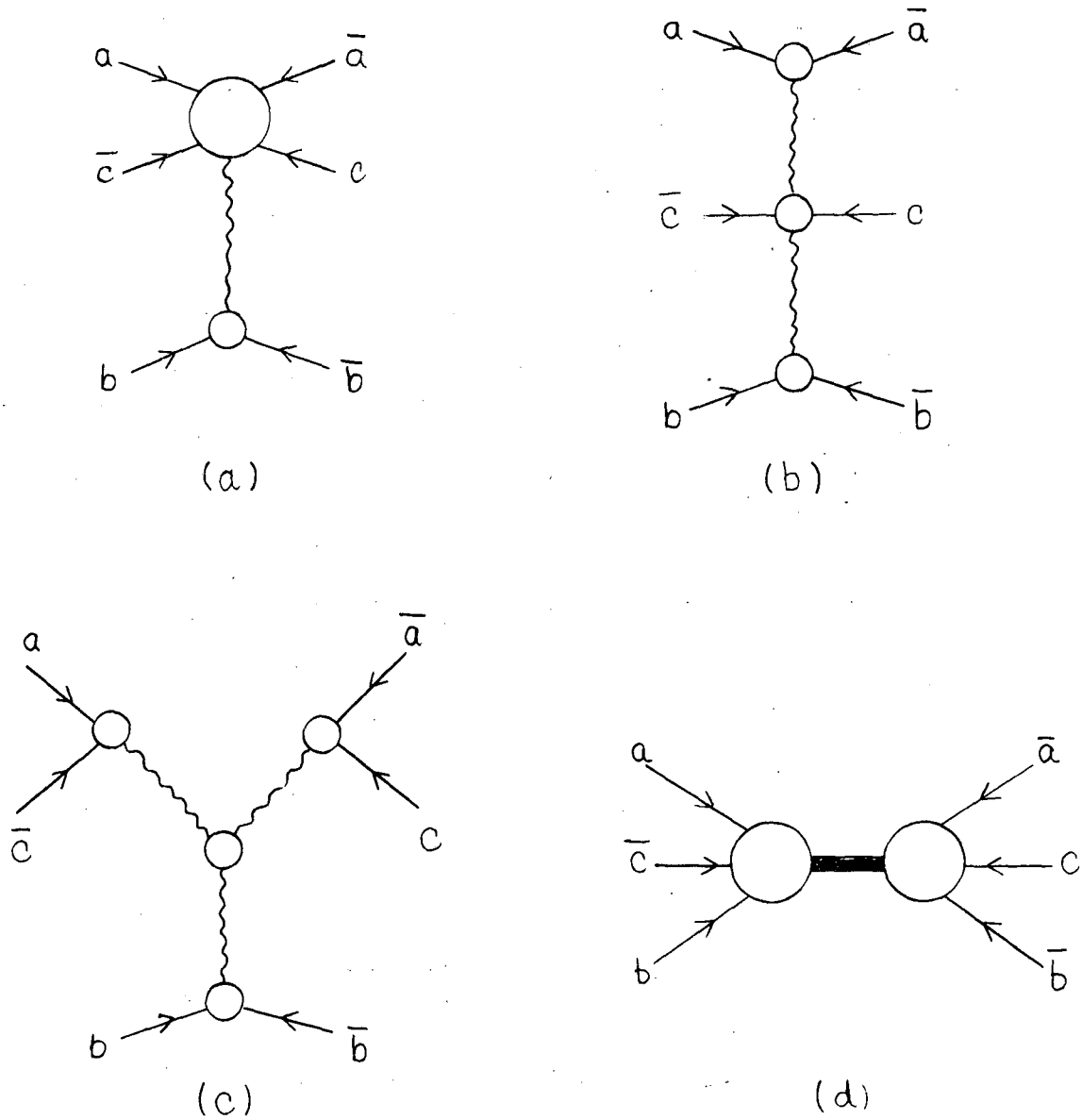

XBL 715-798

Fig. 6.

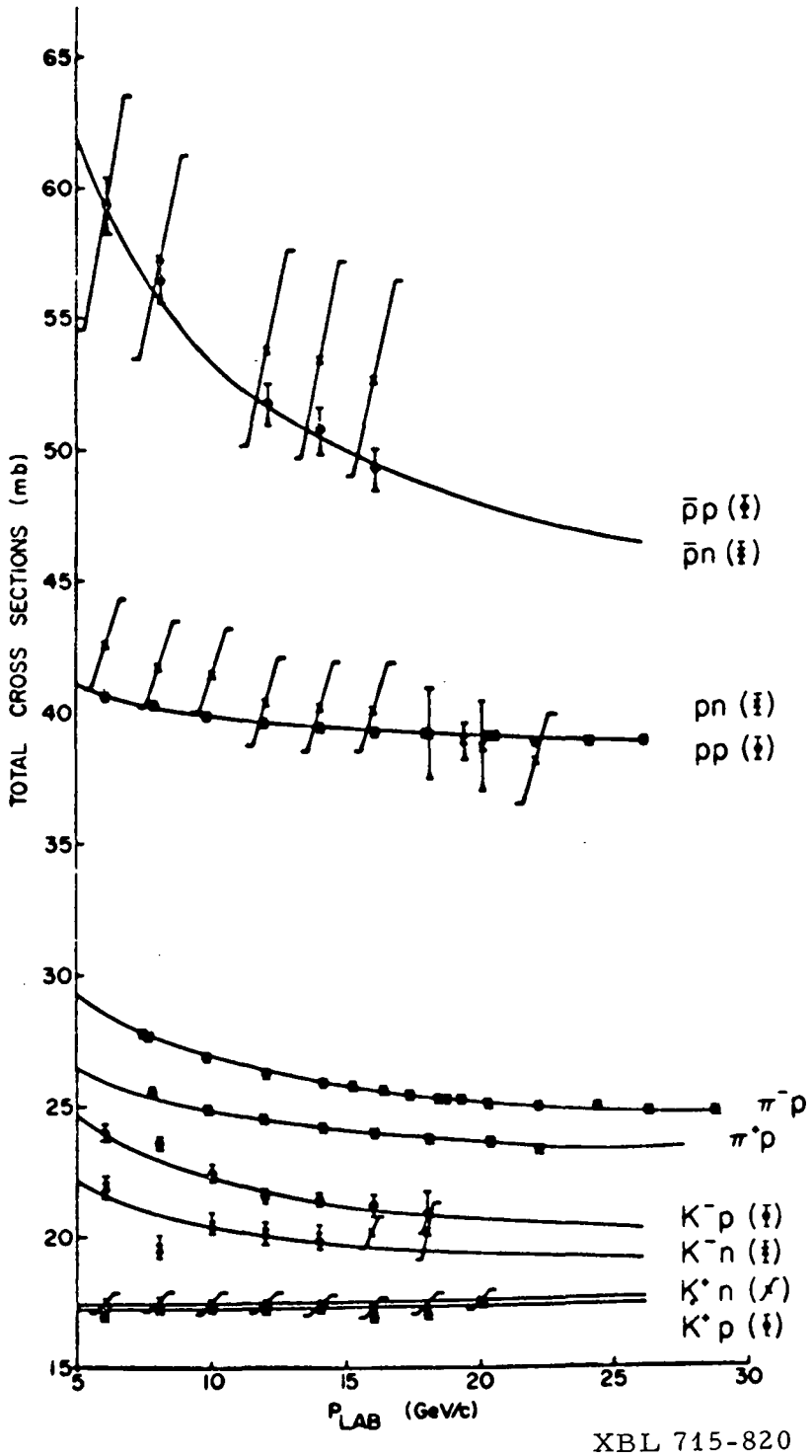
TOTAL CROSS SECTIONS (mb)
65
60
55
50
45
40
35
30
25
20
15
5
10
15
20
25
30
P_LAB (GeV/c)
p̄p (I)
p̄n (I)
pn (I)
pp (I)
π⁻p
π⁺p
K⁻p (I)
K⁻n (I)
K⁺n (I)
K⁺p (I)
XBL 715-820

Fig. 7.

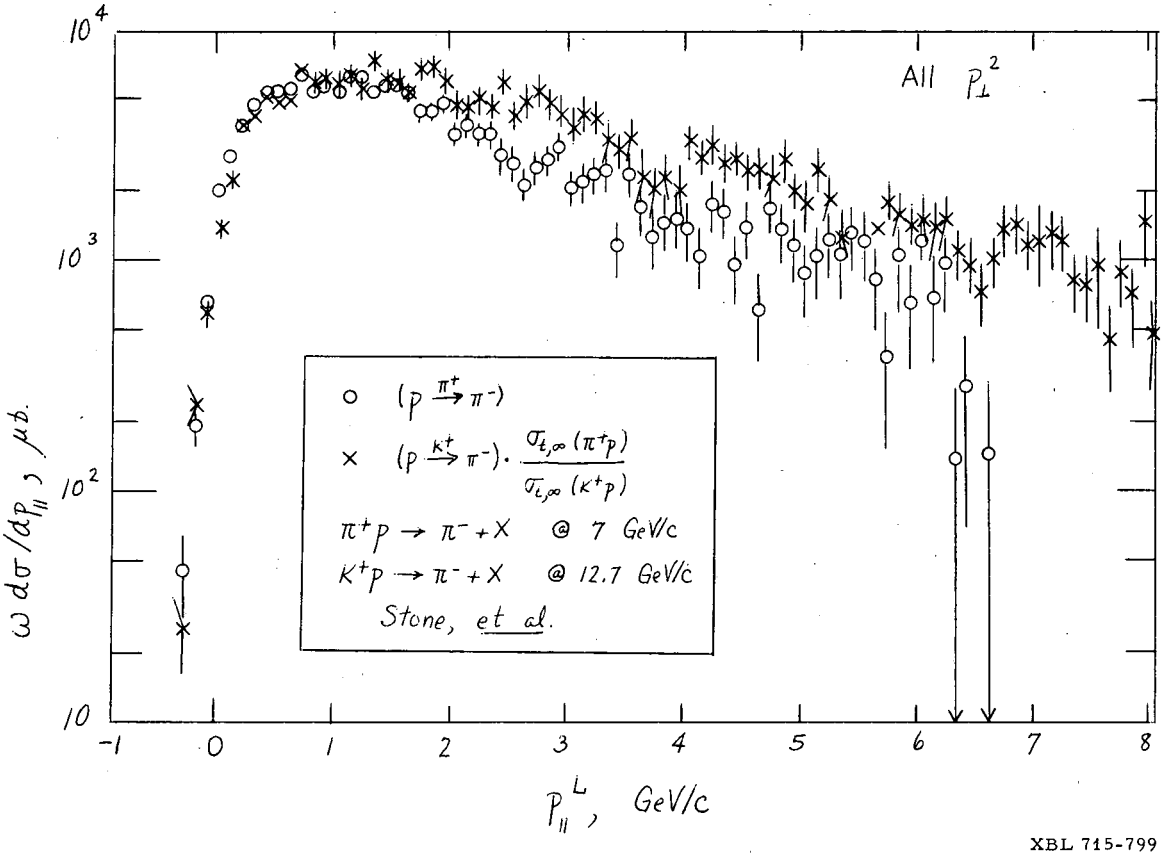
All $P_\perp^2$
$(p \xrightarrow{\pi^+} \pi^-)$
$(p \xrightarrow{K^+} \pi^-) \cdot \frac{\sigma_{t,\infty}(\pi^+ p)}{\sigma_{t,\infty}(K^+ p)}$
$\pi^+ p \to \pi^- + X$ @ 7 GeV/c
$K^+ p \to \pi^- + X$ @ 12.7 GeV/c
Stone, et al.
$\omega\, d\sigma/dp_{\parallel}$, μb.
$P_{\parallel}^L$, GeV/c
10^4
10^3
10^2
10
-1
0
1
2
3
4
5
6
7
8
XBL 715-799

Fig. 8.

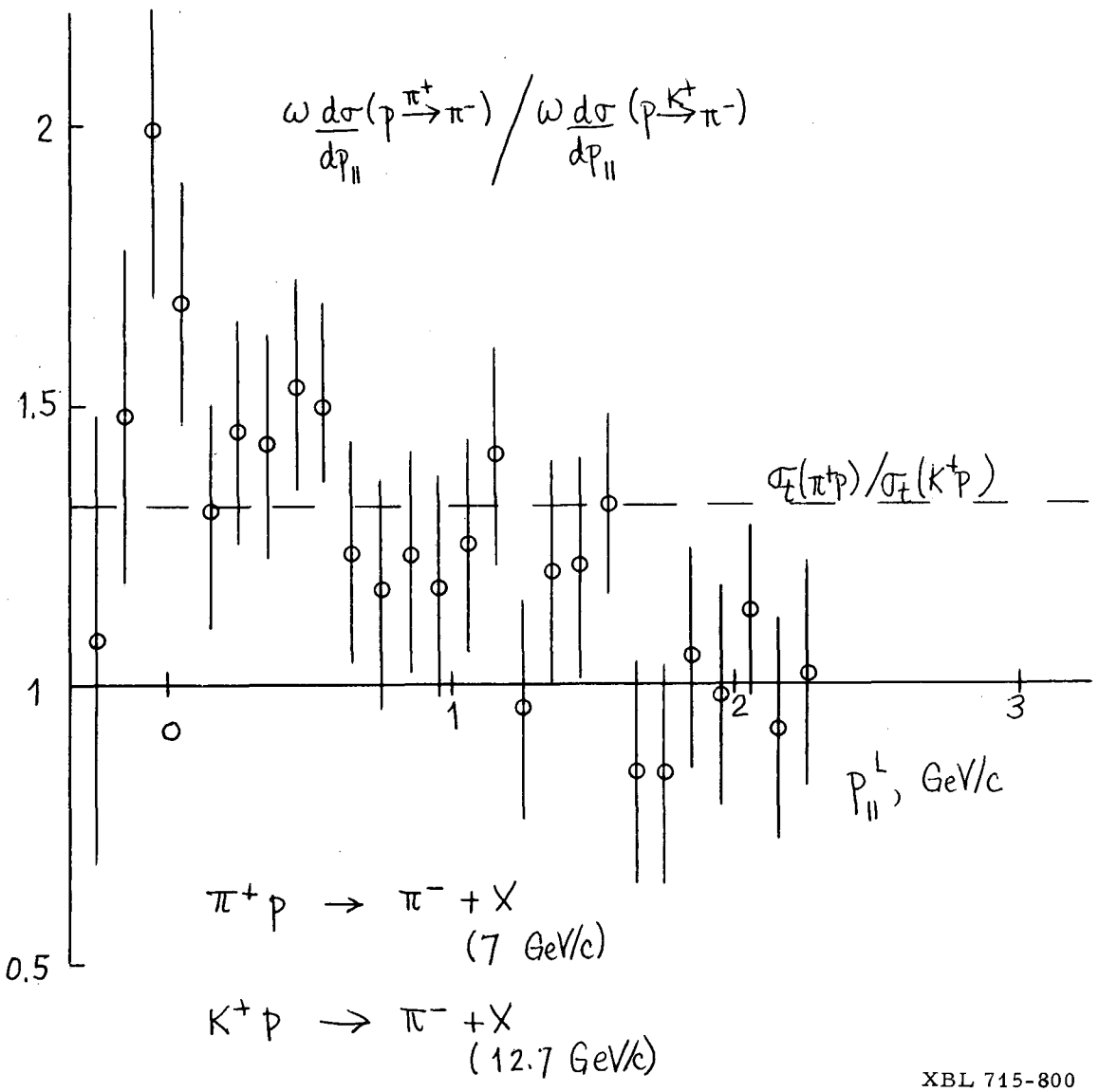
$\omega \frac{d\sigma}{dp_{\parallel}}(p \xrightarrow{\pi^+} \pi^-) \Big/ \omega \frac{d\sigma}{dp_{\parallel}}(p \xrightarrow{K^+} \pi^-)$
$\sigma_t(\pi^+p)/\sigma_t(K^+p)$
2
1.5
1
0.5
0
1
2
3
$p_{\parallel}^L$, GeV/c
$\pi^+ p \rightarrow \pi^- + X$
(7 GeV/c)
$K^+ p \rightarrow \pi^- + X$
(12.7 GeV/c)
XBL 715-800

Fig. 9.

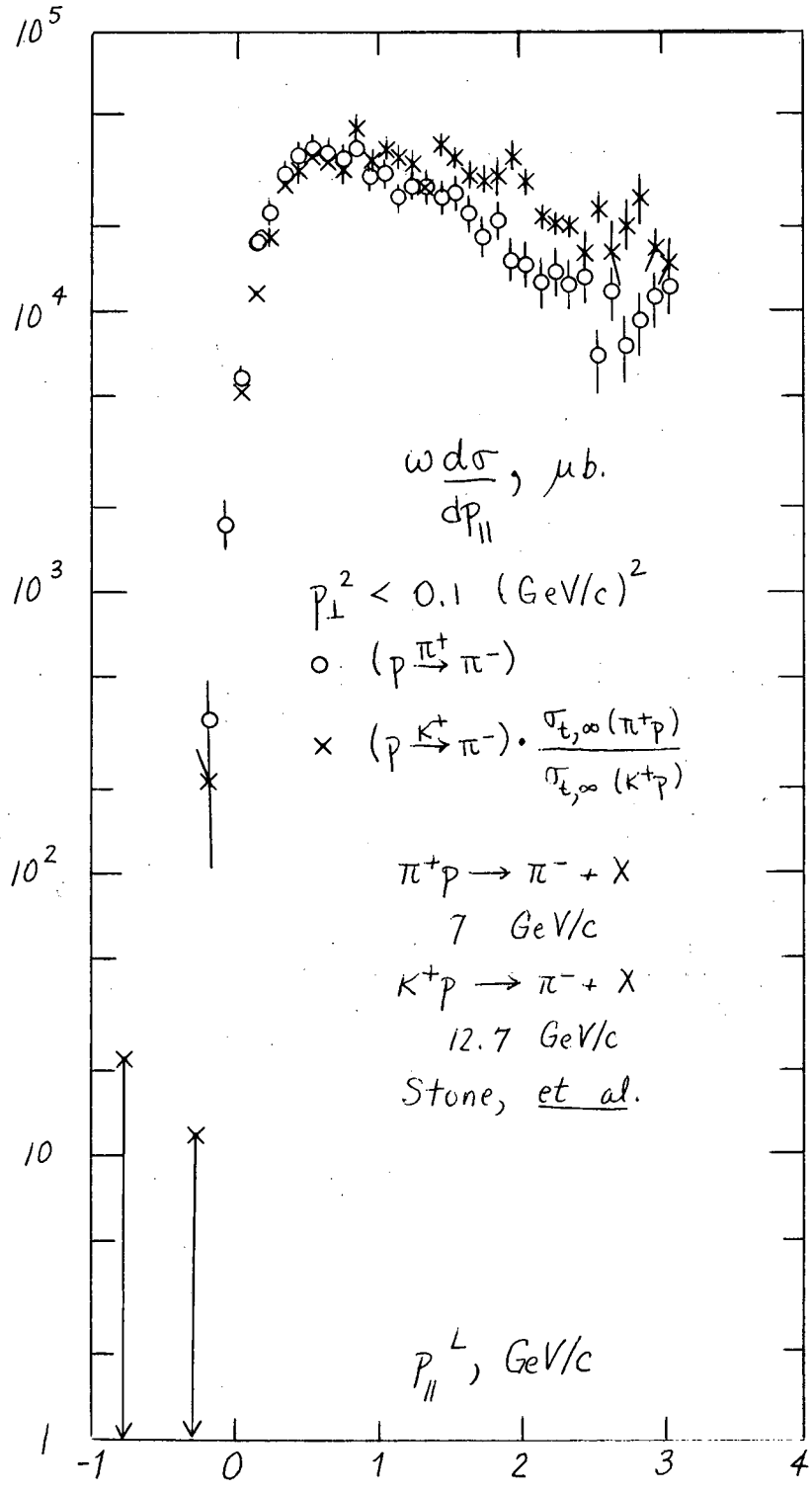
10^5
10^4
10^3
10^2
10
1
-1
0
1
2
3
4
$\omega \frac{d\sigma}{dp_{\parallel}}$, $\mu b.$
$p_\perp^2 < 0.1$ (GeV/c)^2
o $(p \xrightarrow{\pi^+} \pi^-)$
× $(p \xrightarrow{K^+} \pi^-) \cdot \frac{\sigma_{t,\infty}(\pi^+ p)}{\sigma_{t,\infty}(K^+ p)}$
$\pi^+ p \rightarrow \pi^- + X$
7 GeV/c
$K^+ p \rightarrow \pi^- + X$
12.7 GeV/c
Stone, et al.
$p_\parallel^L$, GeV/c
XBL 715-801

Fig. 10.

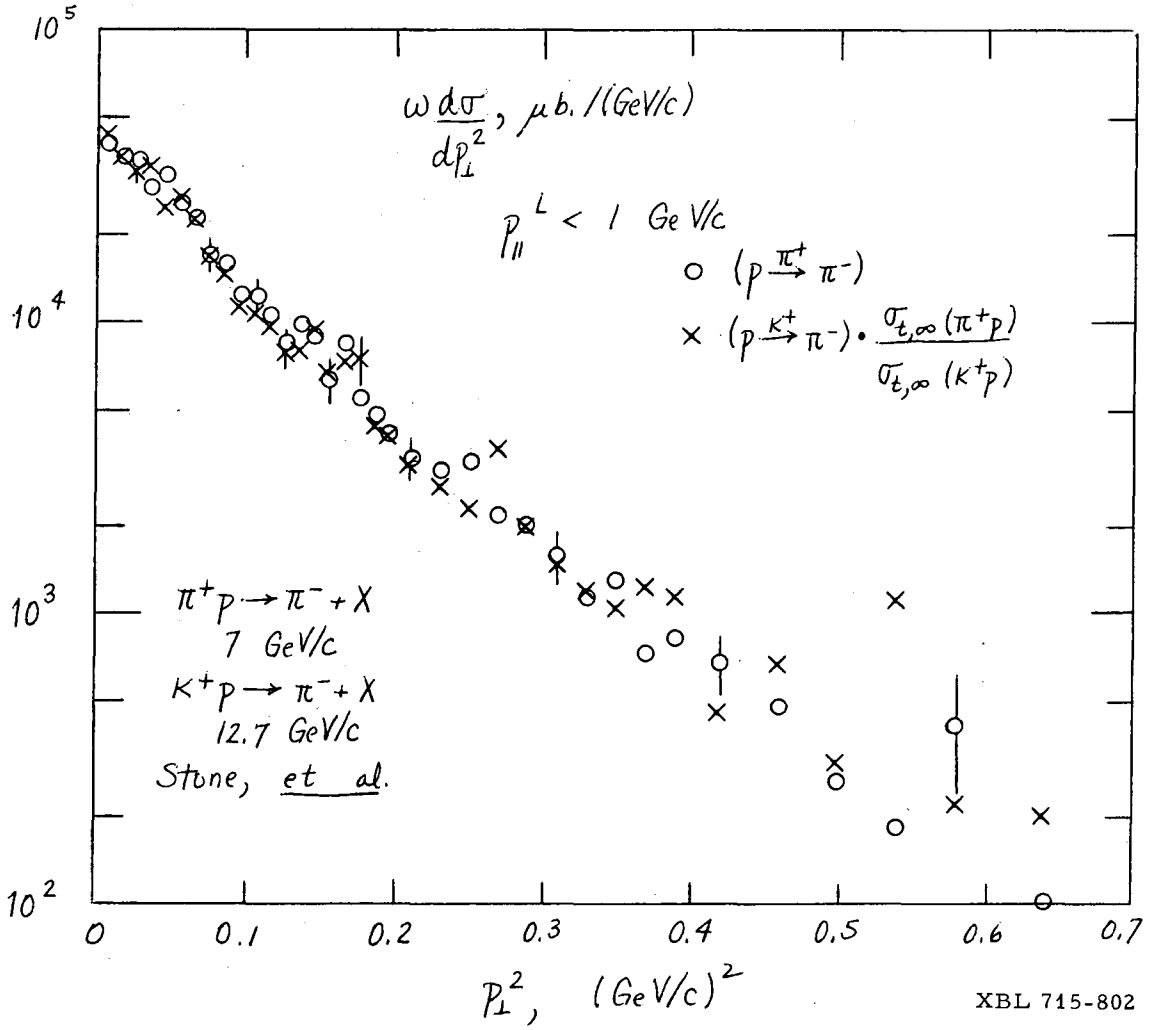
10^5
10^4
10^3
10^2
$\omega \frac{d\sigma}{dp_\perp^2}$, μb./(GeV/c)
$p_\parallel^L < 1$ GeV/c
$(p \xrightarrow{\pi^+} \pi^-)$
$(p \xrightarrow{K^+} \pi^-) \cdot \frac{\sigma_{t,\infty}(\pi^+ p)}{\sigma_{t,\infty}(K^+ p)}$
$\pi^+ p \to \pi^- + X$
7 GeV/c
$K^+ p \to \pi^- + X$
12.7 GeV/c
Stone, et al.
0
0.1
0.2
0.3
0.4
0.5
0.6
0.7
$p_\perp^2$, $(GeV/c)^2$
XBL 715-802

Fig. 11.

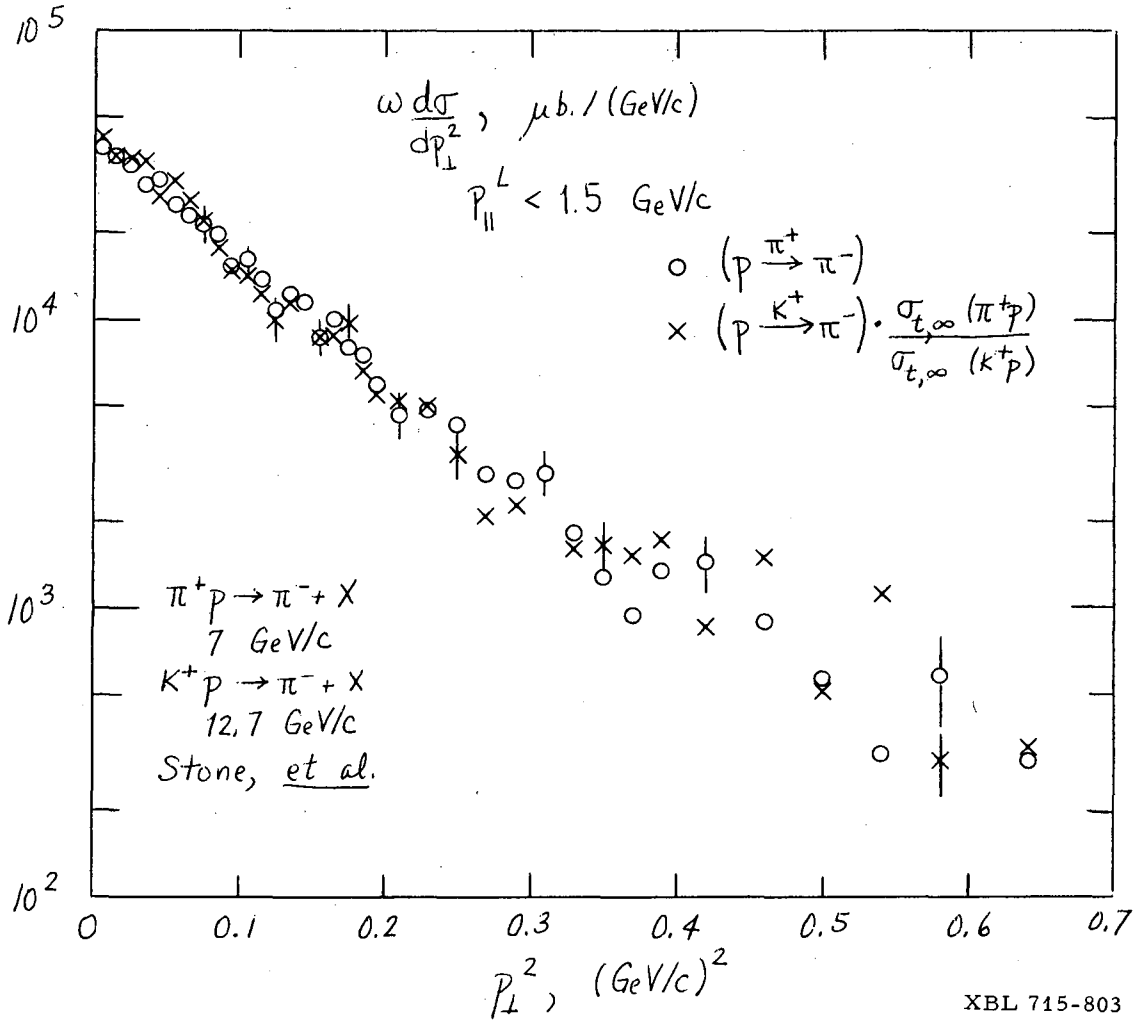
10^5
10^4
10^3
10^2
$\omega \frac{d\sigma}{dp_\perp^2}$, $\mu b./(GeV/c)$
$p_{||}^L < 1.5$ GeV/c
$(p \xrightarrow{\pi^+} \pi^-)$
$(p \xrightarrow{K^+} \pi^-) \cdot \frac{\sigma_{t,\infty}(\pi^+ p)}{\sigma_{t,\infty}(K^+ p)}$
$\pi^+ p \to \pi^- + X$
7 GeV/c
$K^+ p \to \pi^- + X$
12.7 GeV/c
Stone, et al.
0
0.1
0.2
0.3
0.4
0.5
0.6
0.7
$p_\perp^2$, $(GeV/c)^2$
XBL 715-803

Fig. 12.

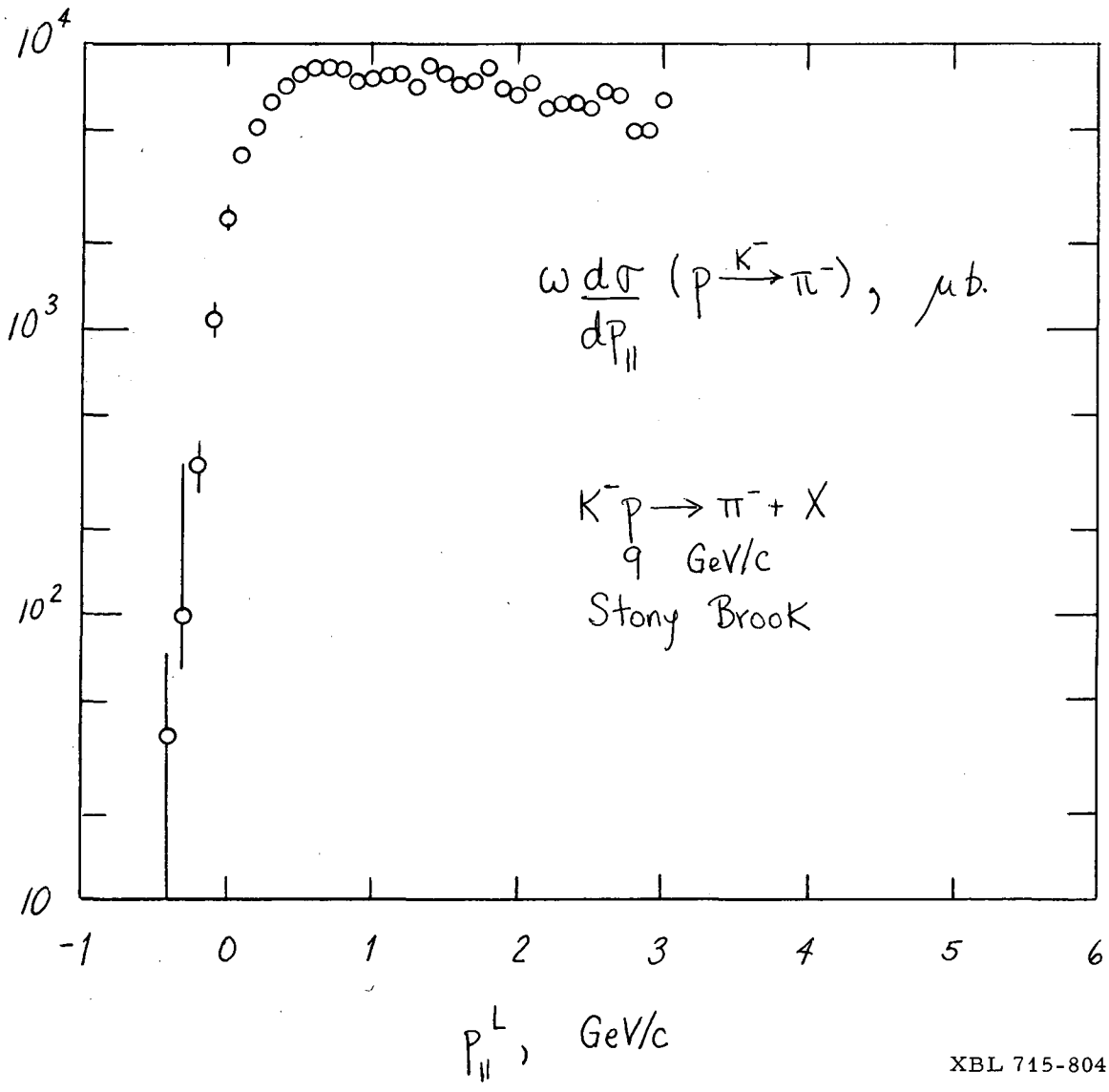
10^4
10^3
10^2
10
$\omega \frac{d\sigma}{dp_{\parallel}} (p \xrightarrow{K^-} \pi^-)$, $\mu b.$
$K^- p \rightarrow \pi^- + X$
9 GeV/c
Stony Brook
-1
0
1
2
3
4
5
6
$p_{\parallel}^L$, GeV/c
XBL 715-804

Fig. 13.

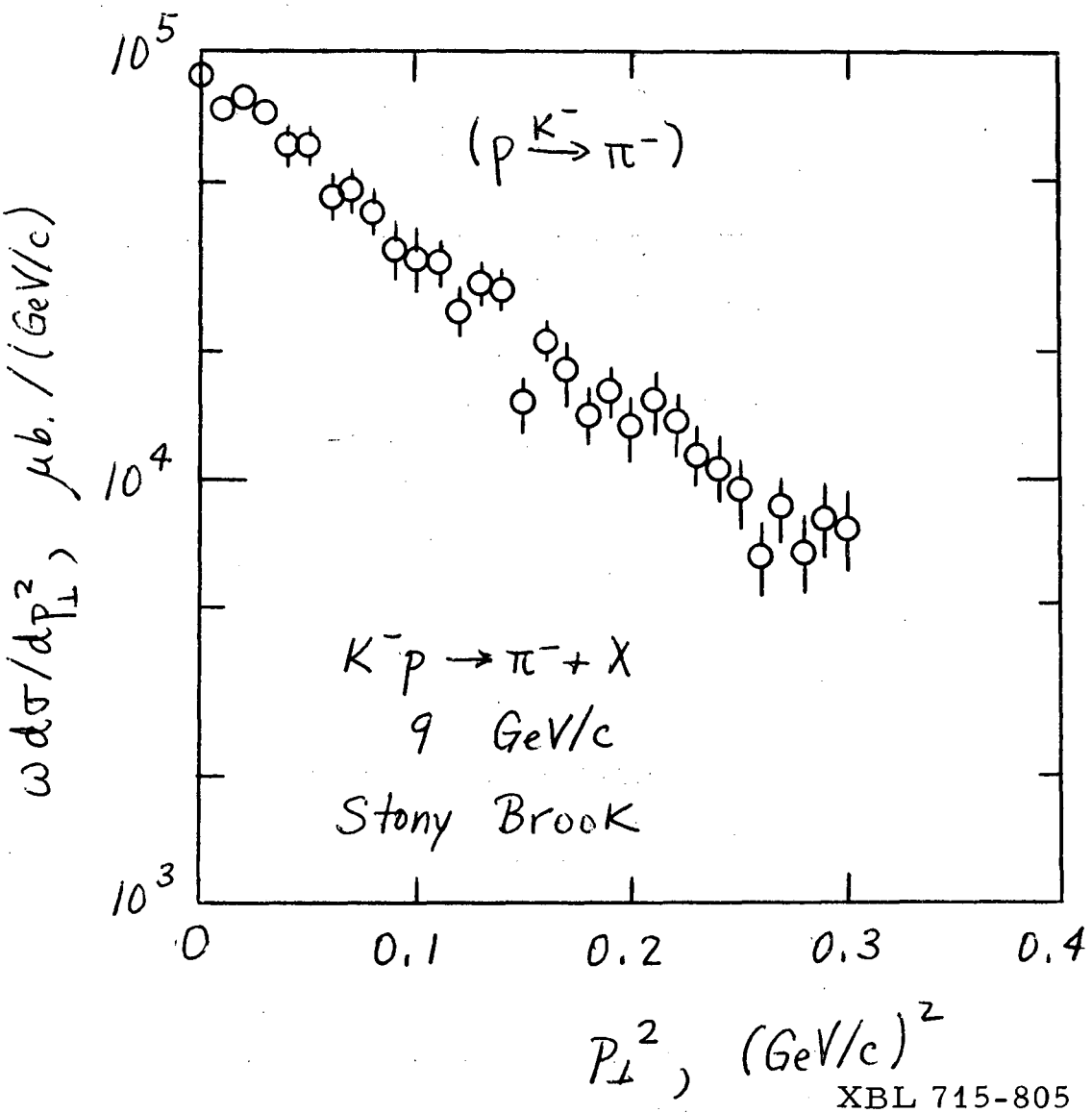
10^5
10^4
10^3
$(p \xrightarrow{K^-} \pi^-)$
$K^- p \to \pi^- + X$
9 GeV/c
Stony Brook
$\omega d\sigma/dp_\perp^2$, μb./(GeV/c)
0
0.1
0.2
0.3
0.4
$p_\perp^2$, $(GeV/c)^2$
XBL 715-805

Fig. 14.

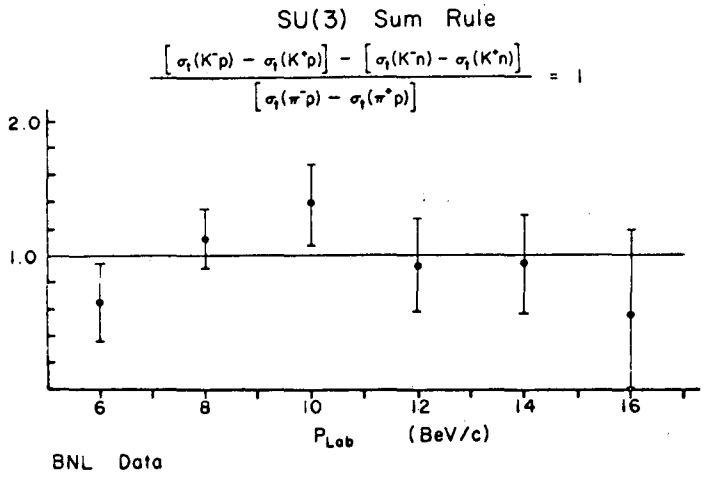

Fig. 15.

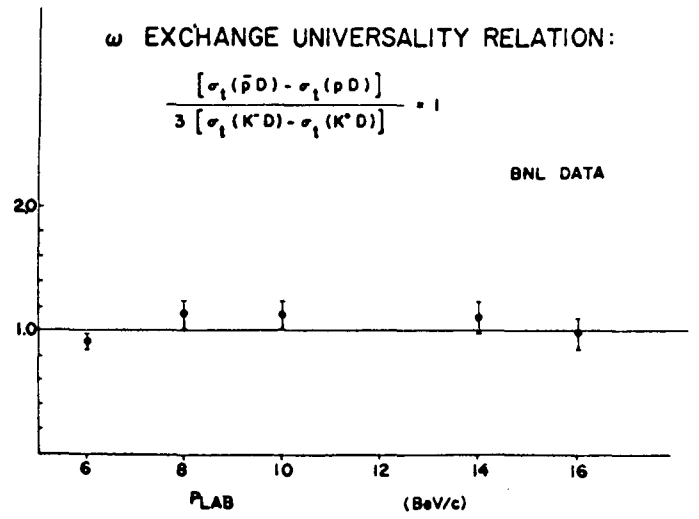

XBL 715-806

Fig. 16.

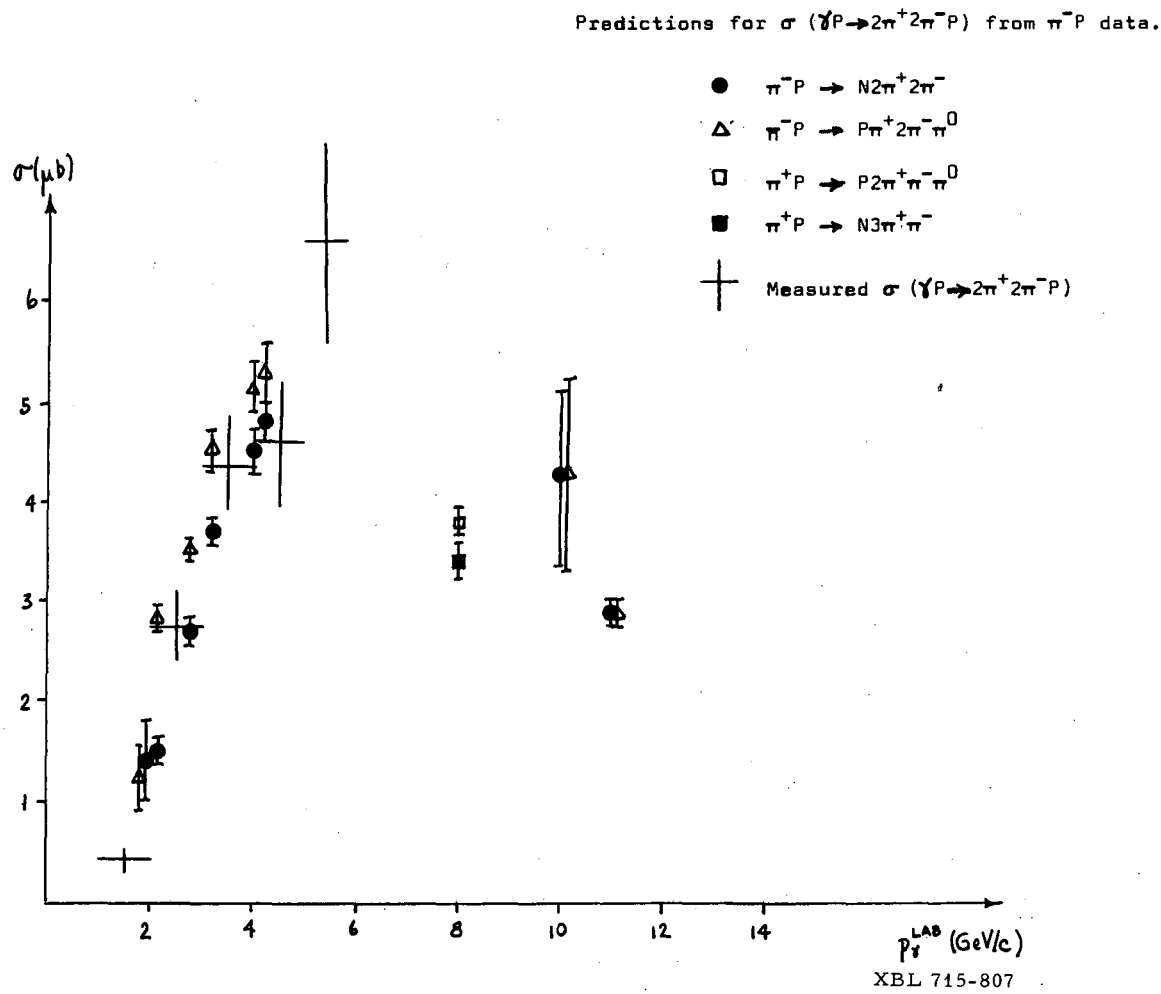
Predictions for σ (γP→2π⁺2π⁻P) from π⁻P data.
π⁻P → N2π⁺2π⁻
π⁻P → Pπ⁺2π⁻π⁰
π⁺P → P2π⁺π⁻π⁰
π⁺P → N3π⁺π⁻
Measured σ (γP→2π⁺2π⁻P)
σ(μb)
1
2
3
4
5
6
2
4
6
8
10
12
14
p_γ^{LAB} (GeV/c)
XBL 715-807

Fig. 17.

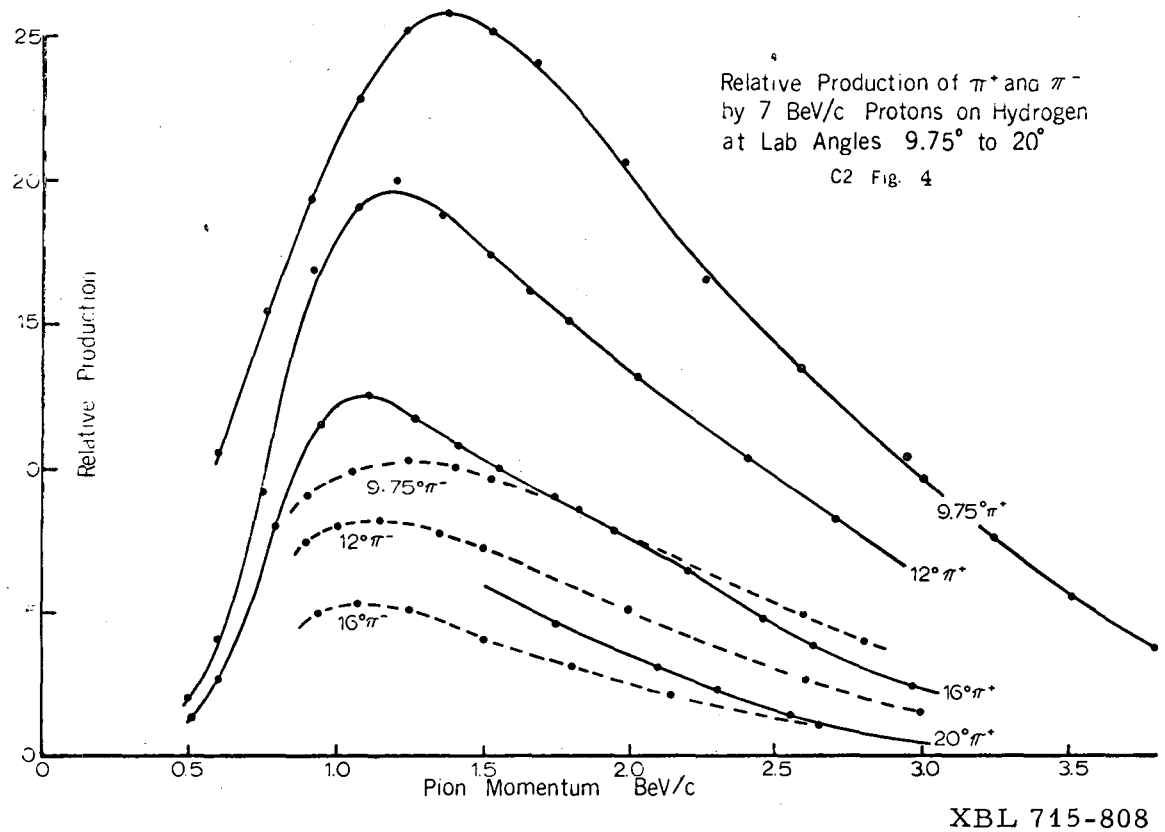
Relative Production of π⁺ and π⁻
by 7 BeV/c Protons on Hydrogen
at Lab Angles 9.75° to 20°
C2 Fig. 4
Relative Production
Pion Momentum BeV/c
9.75°π⁻
12°π⁻
16°π⁻
9.75°π⁺
12°π⁺
16°π⁺
20°π⁺
XBL 715-808

Fig. 18.

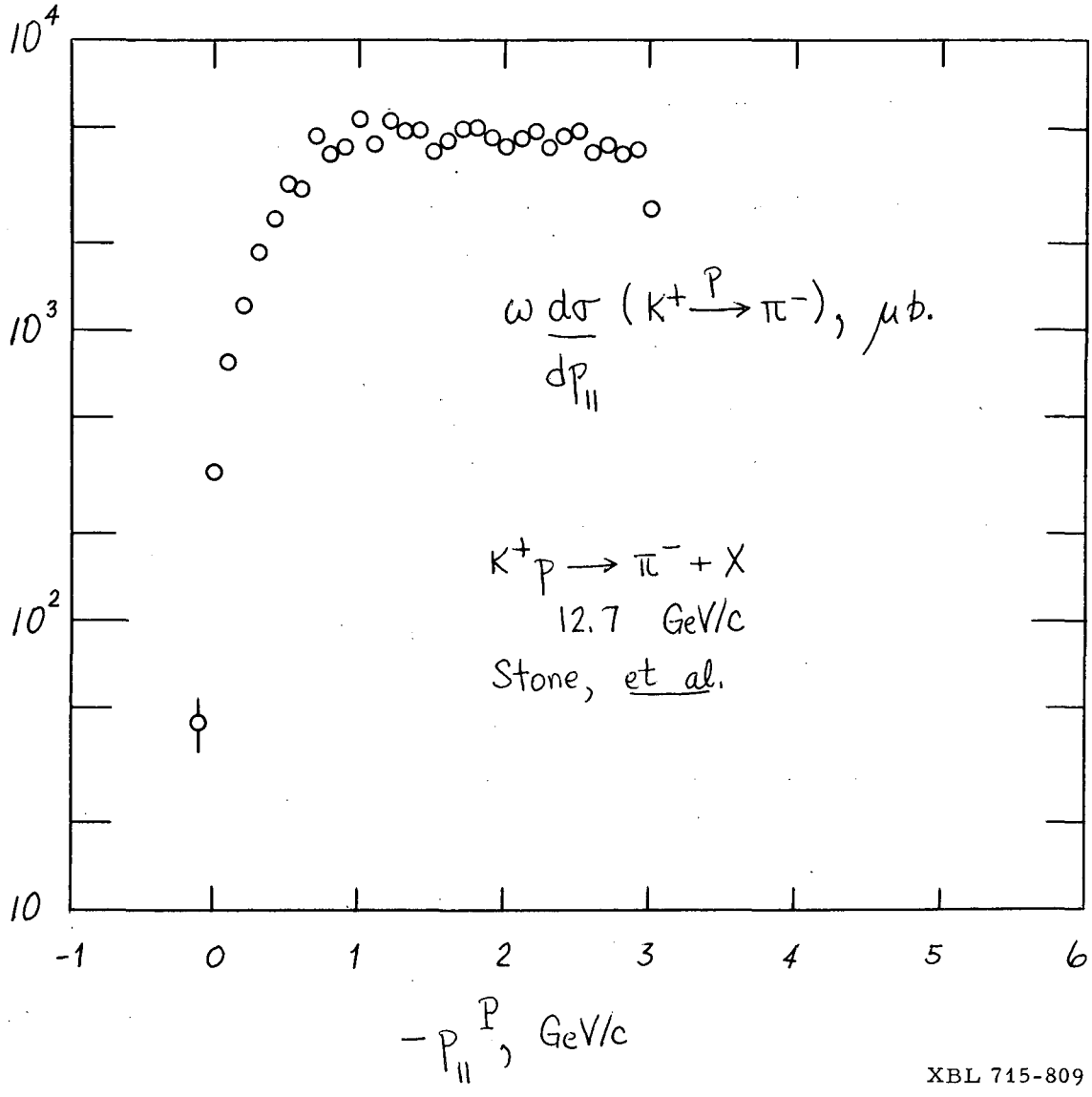
10^4
10^3
10^2
10
$\omega \frac{d\sigma}{dp_{\parallel}} (K^+ \xrightarrow{p} \pi^-)$, μb.
$K^+ p \rightarrow \pi^- + X$
12.7 GeV/c
Stone, et al.
-1
0
1
2
3
4
5
6
$-p_{\parallel}^{p}$, GeV/c
XBL 715-809

Fig. 19.

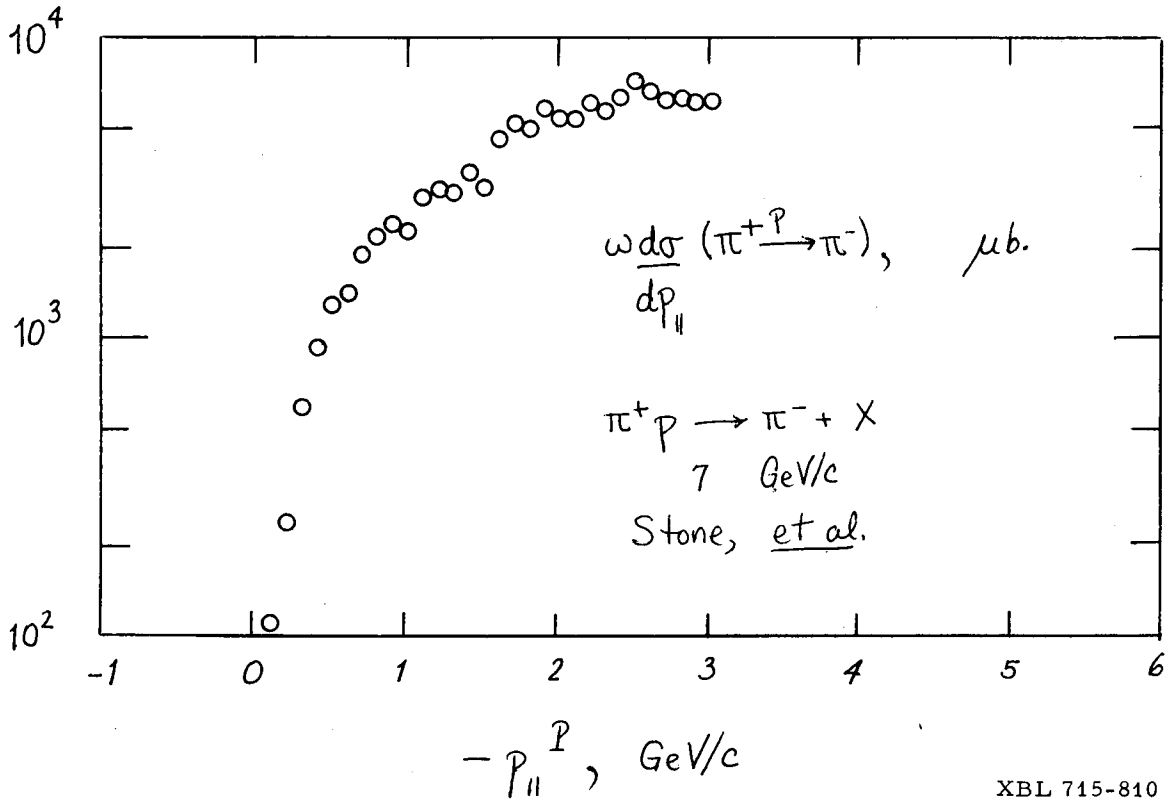
10^4
10^3
10^2
$\omega \frac{d\sigma}{dp_{\parallel}} (\pi^+ p \to \pi^-)$, $\mu b.$
$\pi^+ p \to \pi^- + X$
7 GeV/c
Stone, et al.
-1
0
1
2
3
4
5
6
$-p_{\parallel}^{p}$, GeV/c
XBL 715-810

Fig. 20.

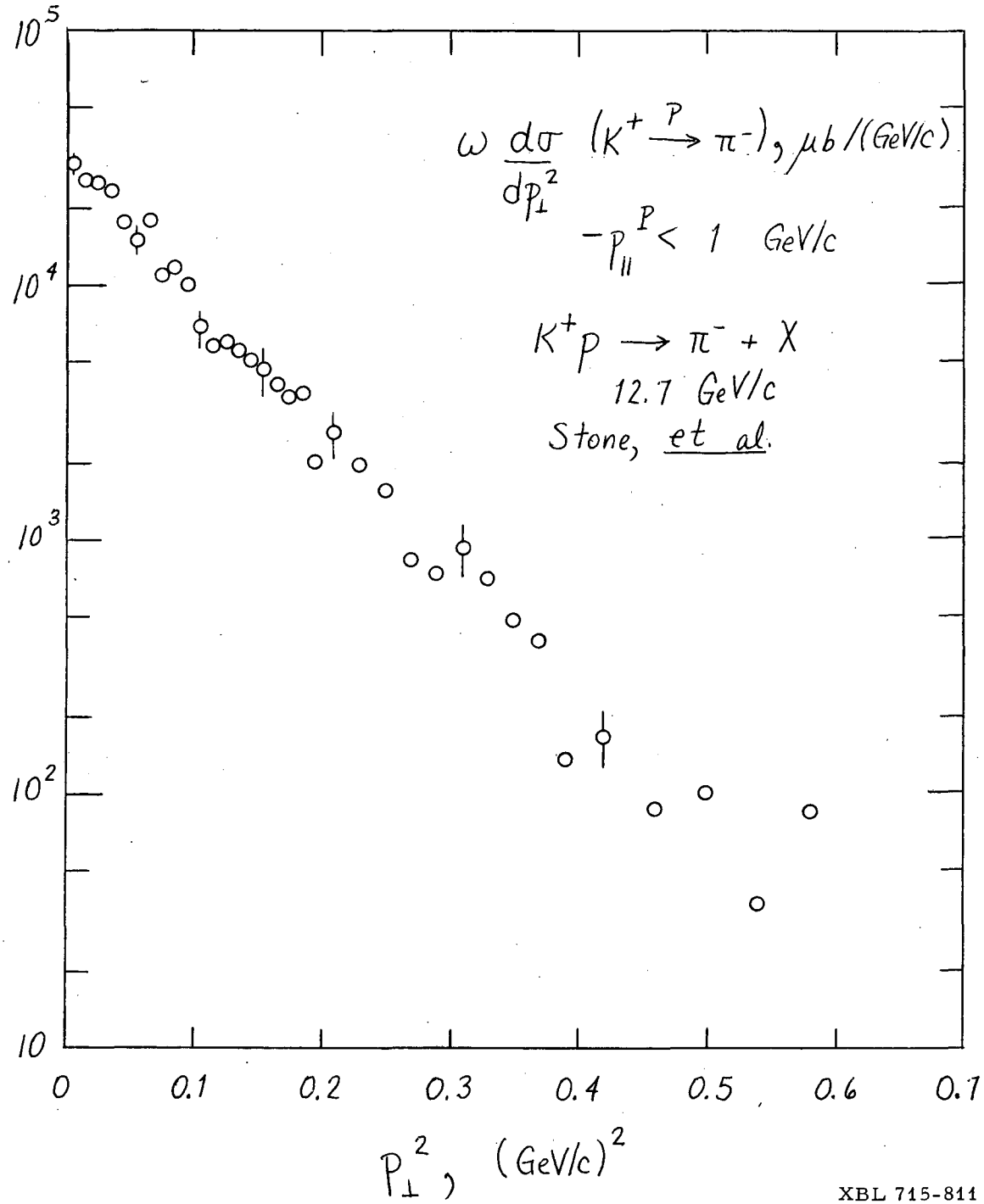
10^5
10^4
10^3
10^2
10
0
0.1
0.2
0.3
0.4
0.5
0.6
0.7
$\omega \frac{d\sigma}{dp_\perp^2}(K^+ \xrightarrow{P} \pi^-)$, $\mu b/(GeV/c)$
$-p_\parallel^P < 1$ GeV/c
$K^+ p \longrightarrow \pi^- + X$
12.7 GeV/c
Stone, et al.
$p_\perp^2$, $(GeV/c)^2$
XBL 715-811

Fig. 21.

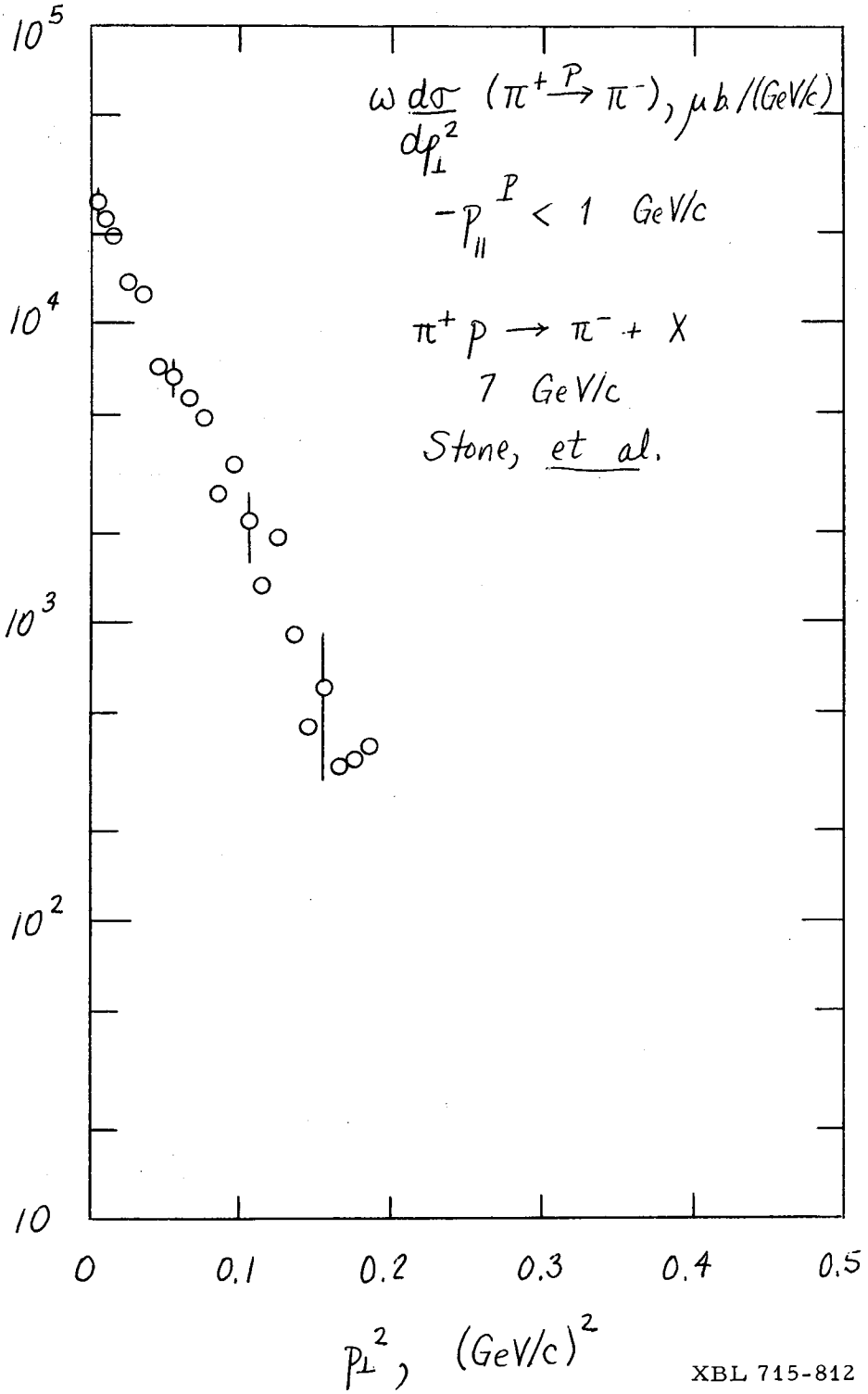
10^5
10^4
10^3
10^2
10
$\omega \frac{d\sigma}{dp_\perp^2}$ $(\pi^+ \xrightarrow{p} \pi^-)$, $\mu b/(GeV/c)$
$-p_\parallel^{\,p} < 1$ GeV/c
$\pi^+ p \rightarrow \pi^- + X$
7 GeV/c
Stone, et al.
0
0.1
0.2
0.3
0.4
0.5
$p_\perp^2$, $(GeV/c)^2$
XBL 715-812

Fig. 22.

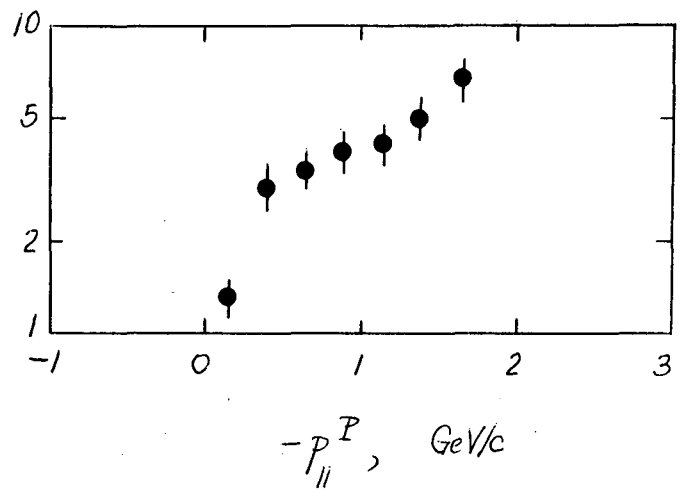
10
5
2
1
-1
0
1
2
3
$-p_{\parallel}^{P}$, GeV/c
$\omega \frac{d\sigma}{dp_{\parallel}} (\pi^+ p \to \pi^-)$ ESTIMATED
$\pi^+ p \to (\rho^0, \omega) \Delta^{++}$
3.7 GeV/c
Abrams, et al.
XBL 715-813

Fig. 23.

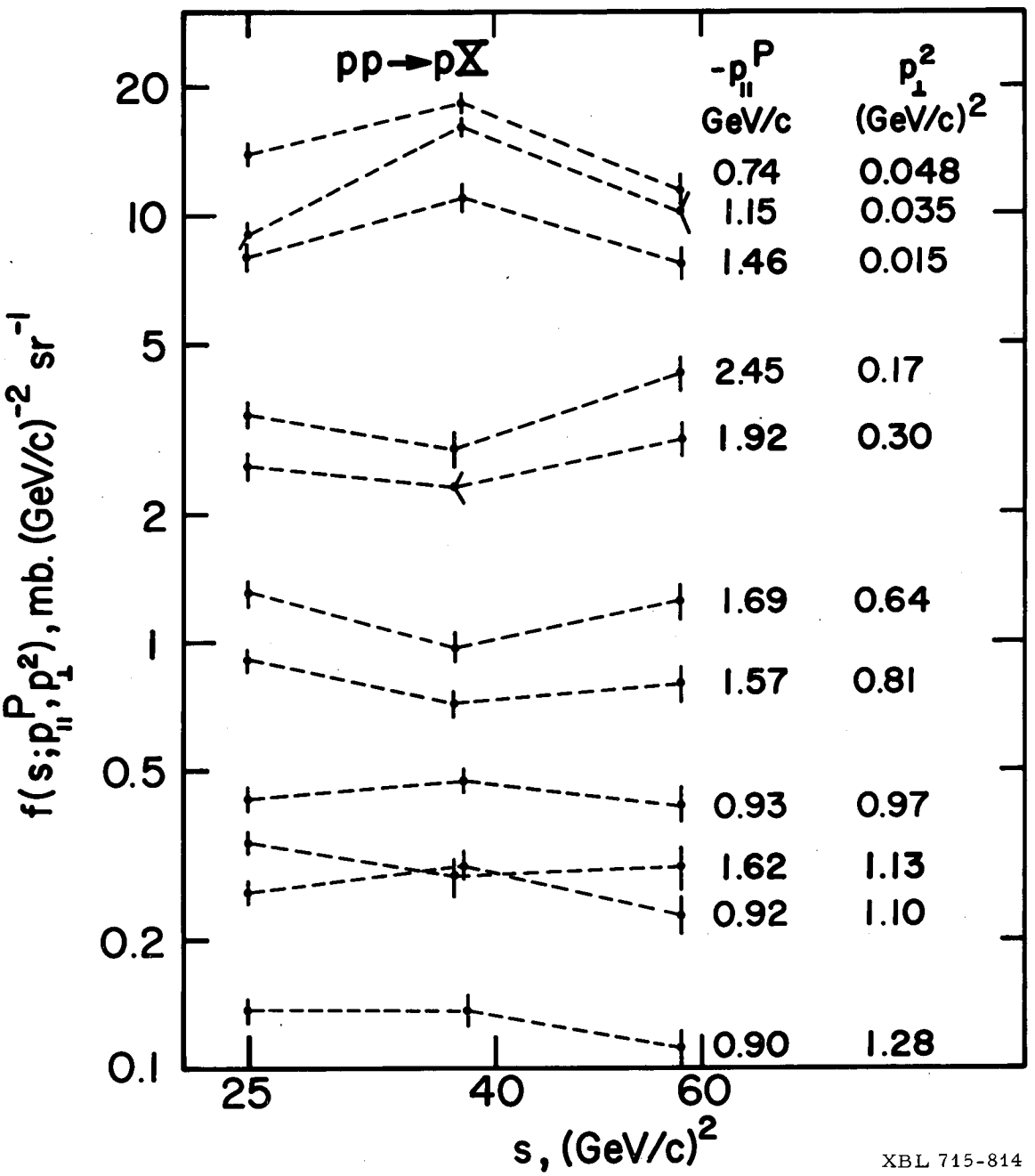
pp→pX
$-p_{\parallel}^{P}$ GeV/c
$p_{\perp}^{2}$ (GeV/c)^2
0.74 0.048
1.15 0.035
1.46 0.015
2.45 0.17
1.92 0.30
1.69 0.64
1.57 0.81
0.93 0.97
1.62 1.13
0.92 1.10
0.90 1.28
$f(s;p_{\parallel}^{P},p_{\perp}^{2})$, mb. (GeV/c)$^{-2}$ sr^{-1}
20
10
5
2
1
0.5
0.2
0.1
25
40
60
s, (GeV/c)^2
XBL 715-814

Fig. 24.

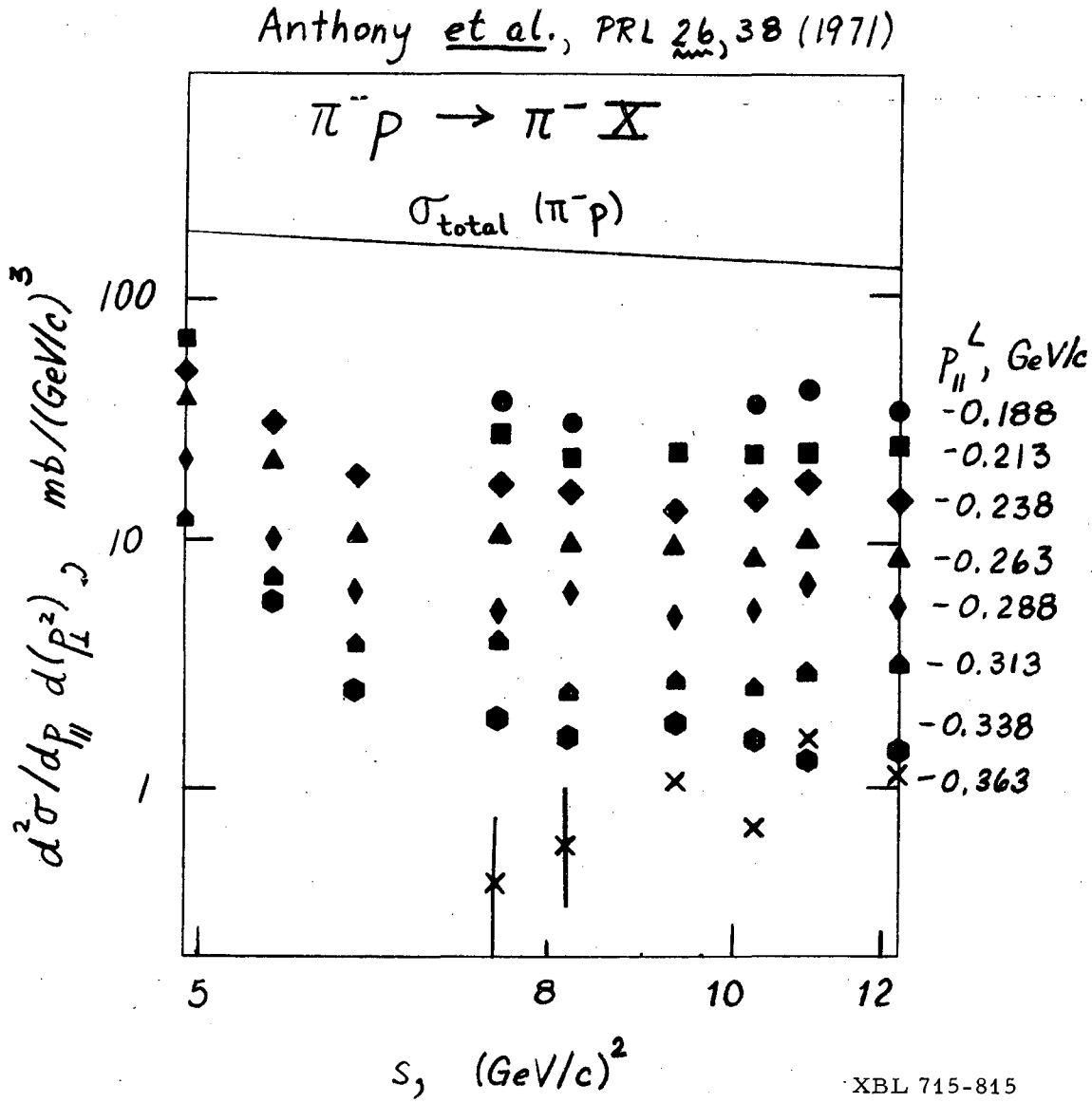
Anthony et al., PRL 26, 38 (1971)
$\pi^- p \to \pi^- X$
$\sigma_{total}(\pi^- p)$
$d^2\sigma/dp_{\parallel} d(p_\perp^2)$, mb/(GeV/c)^3
100
10
1
5
8
10
12
s, (GeV/c)^2
$p_\parallel^L$, GeV/c
-0.188
-0.213
-0.238
-0.263
-0.288
-0.313
-0.338
-0.363
XBL 715-815

Fig. 25.

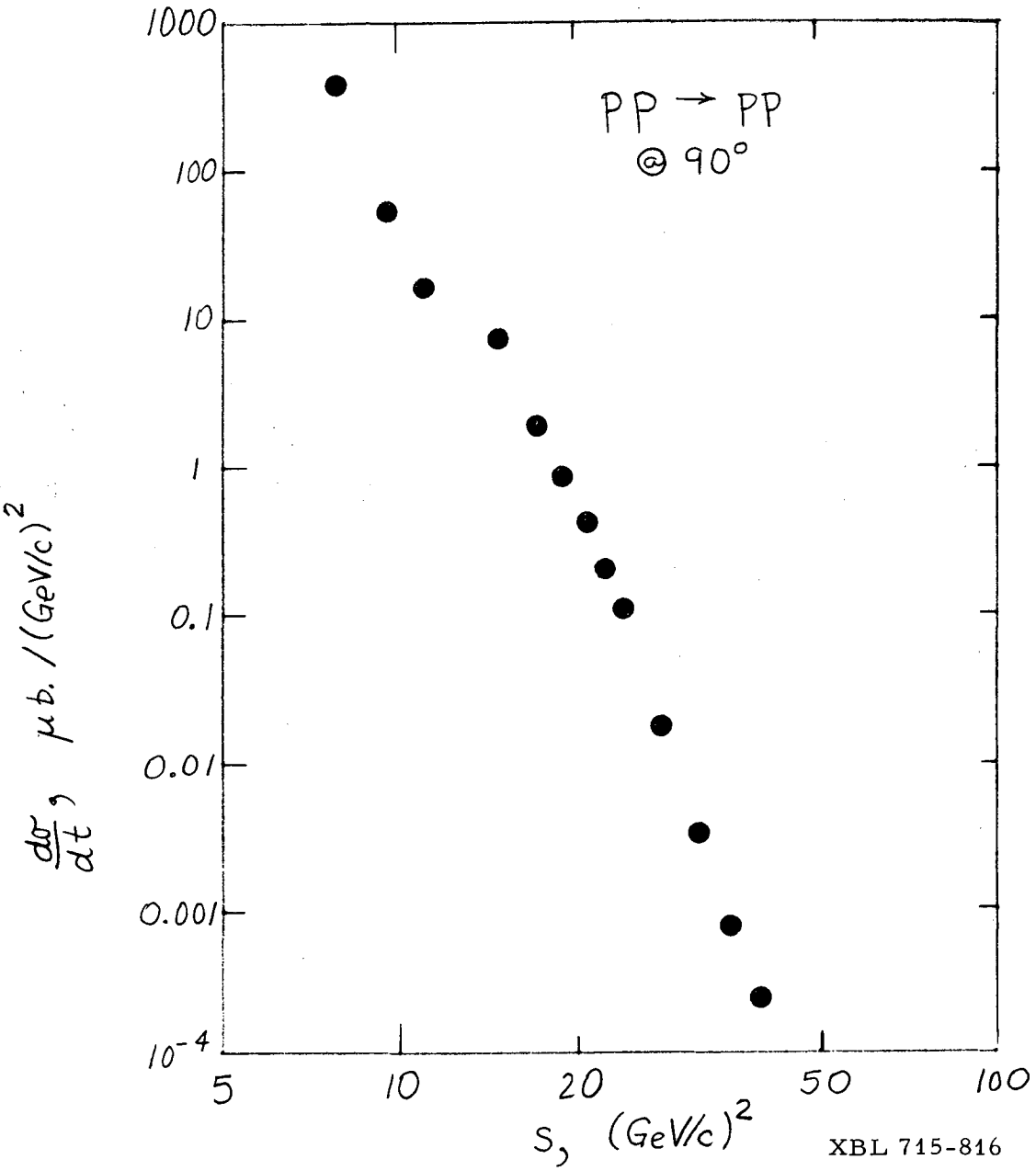
1000
100
10
1
0.1
0.01
0.001
10^{-4}
5
10
20
50
100
PP → PP
@ 90°
$\frac{d\sigma}{dt}$, μb. /(GeV/c)^2
s, (GeV/c)^2
XBL 715-816

Fig. 26.

SESSION IV

INTERMEDIATE ENERGY EXPERIMENTS ON QUASI-TWO-BODY PRODUCTION

R. Diebold

High Energy Physics Division
Argonne National Laboratory

Intermediate Energy Experiments on Quasi-Two-Body Production*

R. Diebold

High Energy Physics Division

Argonne National Laboratory

Several types of experiments giving useful information on production mechanisms at intermediate energies are discussed in this note. Such experiments in the range 3 to 12 GeV/c incident momentum have generally been interpreted in terms of t-channel exchange, although the region at the low end of this range may be enriched (or complicated) by s-channel effects.

Since this energy region has been accessible for many years, most of the easy experiments have been done and future experiments will in general require considerable effort. This tends to favor large general purpose setups and long-range programs over experiments designed to study one small specific piece of physics. There are exceptions, of course, based on cleverness or new advances in technology.

The various experiments have been grouped according to experimental method in the following sections. The list is far from complete, and should be taken as a sampling of the many things yet to be done.

---

*Work supported by the U. S. Atomic Energy Commission.

MISSING-MASS AND TWO-ARM SPECTROMETERS

There are basically two types of missing-mass spectrometers. The first looks at a slowly recoiling particle and allows the calculation of the missing mass of forward produced particles. Such a spectrometer has been used at CERN to study Boson spectroscopy.[1] The 1.6-GeV/c spectrometer at SLAC has been used by the Ritson Group to study production mechanisms for photoproduction.[2] Perhaps the time is ripe for a carefully constructed experiment of this type which would study both spectroscopy and production mechanisms. For example, at the recent Phenomenology Conference Fox discussed the importance of cross sections at large t; a missing-mass spectrometer set in a high intensity beam could give such information on

$$\pi^- p \to \rho^- p$$

$$\to A_2^- p, \text{ etc.}$$

In his talk at this conference, Manning mentioned that a missing mass experiment is underway at the Rutherford Laboratory.

The second type of missing-mass spectrometer looks at a fast forward-going particle from which one can calculate the missing mass of the recoiling system. Such spectrometers have been used at

several laboratories to study N^* production by protons rather thoroughly.[3] Similar experiments using other beams and deuterium as well as hydrogen targets might be appropriate. A BNL (Collins)-Carnegie Mellon collaboration also used a forward spectrometer to obtain results on a large number of processes including various backward scattering reactions.[4]

Both types of missing mass spectrometers can be embellished with the addition of equipment detecting other particles. A whole range of sophistication is possible: one can simply measure the number of particles; or their angles; or both angles and momenta. In the latter case, one would then have a two-arm spectrometer giving four constraints for two-body final states, or a double missing mass spectrometer for events of the type

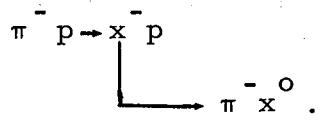

An example of the latter type of spectrometer is presently being constructed on the floor of the ZGS by an Indiana Group.[5]

Another spectrometer which should still do considerable useful work at medium energies is the 3-C spectrometer with which one measures the production angles of both particles from two-body final states as well as the momentum of one of those particles. Such a spectrometer was built by an Argonne-Michigan collaboration around one of the three Argonne SCM-105 magnets. These magnets

have an aperture 84 inches wide, up to 30 inches high, and an effective length of about 40 inches. While the primary interest of the collaboration was the reaction $\pi^+ p \to K^+ \Sigma^+$, they simultaneously obtained results on other reactions such as $\pi^+ p$ elastic scattering,[6] as shown in Fig. 1. The Lundby Group at CERN had a recent run at 5 GeV/c with a 3-C spectrometer looking at a large number of reactions. Among other things they were able to see the first-forbidden backward peaks

$$K^- p \to p K^-$$
$$\bar{p}p \to K^+ K^-$$
$$\bar{p}p \to p\bar{p} .$$

Such reactions are of course very interesting from the point of view of duality, Regge-cut models, etc. As shown in Fig. 2, taken from the compilation by Akerlof,[7] these cross sections fall off very rapidly with energy and little data is available above 3 GeV/c. The Lundby results are somewhat higher than the lines shown, and it would be interesting to study both the magnitudes and slopes of these backward peaks in this energy region.

While the rates for any one reaction in the large t or backward region tend to be a dismally low, such experiments are made worthwhile by the fact that one can study many reactions simultaneously. As an example of rates, consider an unseparated beam having a ratio of $\pi^-/K^-/\bar{p} = 100/1.3/.15$ (as expected at

4 GeV/c for Argonne Beam 21). For 3×10^8 beam particles per hour incident on a 20-inch liquid hydrogen target, one expects 600/8/1 events/hour/effective μb for reactions initiated by π, K, and $\bar{p}$, respectively. Typical cross sections at 5 GeV/c for the first-forbidden backward reactions are 0.1 μb, and the big t cross section for $\pi^{\pm}$ elastic scattering is about 0.1 μb/GeV^2. For a spectrometer azimuthal acceptance of 5% and a run of about 200 hours, the number of events for a given backward peak or for a 1-GeV^2 t bin would thus be 600, 8, 1 for π^-, K^-, $\bar{p}$ initiated reactions, respectively.

To pick up the K^- and $\bar{p}$ reactions will clearly take considerable patience as well as a good Cerenkov counter system so that the many reactions can be simultaneously studied. Eventually, one might even use a polarized target with such a 3-C spectrometer. With higher energy as well as the higher intensities expected to result from the AGS improvement program, the medium energy machines may not be competitive for K^- and $\bar{p}$ reactions. For example, a collaboration between Carnegie-Mellon University, University of Pittsburgh, and University of Michigan has proposed a missing mass spectrometer at Brookhaven which would study many of these reactions. They hope to use an enriched beam of 10^6 per burst, with π/K or $\pi/\bar{p}$ ratios of ≤ 10. This would seem to be at least 10 times the available flux at Argonne at present and one would want to consider ways for obtaining a high-intensity beam, enriched if

possible, before embarking upon the experiments described in this section.

EFFECTIVE MASS SPECTROMETERS

Many high energy reactions result in the forward production of two charged particles. Figure 3 shows a system with spark chambers on both sides of a large aperture magnet to measure the angles and momenta of the two particles; from this information the two-particle effective mass can be calculated with good precision. If filmless readout of the spark chambers is used, the data can go directly onto magnetic tape, ready for processing without scanning and measuring. Large statistics experiments are thus possible with computer programs typically processing from 1 to 30 events per second from raw data through physics histograms. This can be compared with the automatic measuring of bubble chamber events at 100 per hour, two orders of magnitude slower, after which the events must still be analyzed on a computer. The disadvantage of such a spectrometer is of course its less-than-4π solid angle.

Recent Experiments and Comparison of Intermediate and High Energies

The concept of such a spectrometer is old, but recently there has been increasing interest in the technique. At the moment, there are well instrumented setups at both Brookhaven (Lindenbaum) and CERN (Hyams). At SLAC (Leith) such a spectrometer has been used

to study photoproduction processes and more recently pion-induced reactions; they are now moving to an rf-separated K beam. At Argonne Poirier et al. recently did several experiments with such a spectrometer, and my group, together with that of Jovanovic, are assembling the spectrometer sketched in Fig. 3. There are at least two other approved Argonne experiments which will use similar spectrometers to study specific interactions. All of these spectrometers use magnetostrictive wire spark chambers and the high-energy experiments have (or are getting) threshold Cerenkov counters after the magnet to aid in identifying the reaction.

Are medium energy effective-mass spectrometers competitive with those at higher energies? The answer is yes, but a better word might be complementary. First of all, one would like production cross sections as a function of energy and the BNL, SLAC, and CERN spectrometers are running in the range 8 to 20 GeV/c, outside of our range of 3 to 6 GeV/c. The high-energy spectrometers have better acceptance, especially at the higher effective masses, but somewhat worse resolution. When designing these systems there is always some tradeoff available between resolution and acceptance; but once the geometry is fixed, there is an optimum momentum at which to run, lower momenta having increasingly worse acceptance and higher momenta having bad momentum resolution with the separation between various reaction hypotheses becoming blurred.

The useful range of incident momentum is roughly a factor of two. Thus, the existing experiments at the high-energy laboratories cannot directly compete at our energies without extensive modifications.

There are other complementary aspects: while the high-energy experiments can study high mass resonances, the cross sections for many reactions, such as ρ^o, f, K^*_{890} production, are maximum in the medium energy range 3 to 6 GeV/c and we can more easily accumulate large numbers of these events. With better resolution and higher cross sections, we can provide better searches for anomalies in the $\pi\pi$ and $K\pi$ mass spectra, while the better acceptance at high energies may provide more reliable decay angular distributions. Since we span the region between resonance dominance and t-channel dominance, our energy dependence is potentially rich and with sufficient data may eventially yield considerable insight into both phenomena and their relation to one another.

Neutral Trigger

There are basically two types of triggers. The first requires a forward neutral particle which then decays, giving two particles detected by a hodoscope behind the magnet. This trigger is relatively easy in that there is a clear and definite signature, not easily imitated by various backgrounds. The reactions which

immediately spring to mind are

$$\pi^- p \rightarrow K^o(\Lambda, \Sigma^o \ldots) .$$

These are the first reactions to have been reported (Kiev Conf.) from the Brookhaven spectrometer and will be the first reactions studied by the Jovanovic group at Argonne.[8] In addition to understanding the production amplitude for these particular processes, one can try to relate them to other hypercharge exchange reactions.

The Jovanovic group will replace the target veto counters shown in Fig. 3 with spark chambers to observe the decay proton from $\Lambda \rightarrow p\pi^-$, thus measuring the Λ polarization. About 6000 $K\Lambda$ events with decay protons are expected from a 40 shift run at 5 GeV/c; data from the other reactions will be recorded simultaneously. Some forward going Λ's from baryon exchange $\pi^- p \rightarrow \Lambda K^o$ will also be recorded. Another experiment planned for Argonne will be optimized for this backward reaction.[9]

Reactions such as

$$K^- p \rightarrow K^o n$$
$$\rightarrow \Lambda \pi^o, \rho^o, \text{ etc.}$$
$$\bar{p}p \rightarrow \bar{\Lambda}\Lambda, \text{ etc.}$$

can also be studied with a neutral trigger. At 4 GeV/c a short unseparated beam typically has 1% K^- and .2% $\bar{p}$, so the rate for these processes will be low. However, they come for free along

with the pion reactions if one has sufficient Cerenkov-tagging power in the beam; a production run of 100 shifts should yield several hundred $\bar{\Lambda}\Lambda$ events plus a few thousand of the K reactions.

A variation of the neutral trigger is to use a $\frac{dE}{dx}$ counter to require only one forward-going charged particle just after the target together with three charged particles in a later hodoscope. Using such a trigger the CERN[10] and Brookhaven[11] groups studied

$$\pi^- p \rightarrow A_2^- p$$
$$\hookrightarrow K^- K^o$$
$$\hookrightarrow \pi^+ \pi^-$$

at 17 and 20 GeV/c, respectively. Their results do not show structure in the A_2 as seen in the earlier data at 7 GeV/c on the same reaction and decay mode by the CERN Boson Spectrometer Group.[1] Figure 4 compares the two sets of CERN data. The effective-mass data is superior both in statistics and in resolution on the A_2 mass, ±6 MeV instead of ±10 MeV.

Charged Trigger

The second type of trigger for effective mass spectrometers simply requires an interaction giving two charged particles through the spectrometer. In addition to the neutral reactions discussed above, such a trigger will pick up the many reactions giving final states such as

$$\pi^- p \rightarrow \pi^- \pi^+ n,$$

$$K^- p \rightarrow K^- \pi^+ n.$$

For these particular reactions, one can improve the trigger rate with arrays of veto counters around the target to suppress events in which additional pions are produced. In our experiment,[12] we will have three layers of scintillator interspersed with two layers of lead around the target plus single-layered counters lining the magnet aperture. Such vetoes must be used judiciously to avoid biases from vetoing the slow recoil neutrons from events of interest. The SLAC group used such counter information only in the software and not in hardware veto; they found that ~30% of the good $\pi^+ \pi^- n$ events had a count from the neutron at small t. Delta rays produced in the target may also be a problem.

The charged trigger is easily faked by delta rays or reactions produced in the spectrometer or by randoms in the trigger hodoscope. Some of these problems can be solved with a hole counter or $\frac{dE}{dx}$ counter immediately following the target and/or a counter to veto noninteracting beam particles. With a very tight veto system, the CERN group was able to get one $\pi^- \pi^+ n$ event every four triggers.

The combination of high statistics and good resolution which we expect in our experiment is ideal for detailed studies of the $\pi\pi$ and $K\pi$ mass spectra. For example, one can study $\rho\omega$ interference

with the $\pi^+\pi^-$ mass distribution. We expect an effective-mass resolution of typically ± 3 MeV at the ρ, about half the natural width of the ω. At 4GeV/c, we expect an error on the missing neutron mass of ± 30 MeV/c which should give a clean separation from events with additional pions. At 6 GeV/c, this becomes ±60 MeV/c and should still be more than adequate. Events will be accepted over a wide range of decay angles, the average acceptance at 4 GeV/c is about 30% with decays near 90° being somewhat favored.

Assuming that the trigger rate holds no surprises, we hope to be able to collect one half million events in the ρ region in 40 shifts of production running. For comparison, the Goldhaber Group had 7000 $\pi^+ p \to \rho^0 \Delta^{++}$ events at 3.7 GeV/c. As shown in Fig. 5 they split their data into two t intervals, one having no significant effect and the other with a 3.5 standard deviation dip at the ω mass.[13] With our large statistics, we should be able to study the interference in detail as a function of t. If we take the $\omega \to \pi^+\pi^-$ decay amplitude as known from other experiments, the interference effects should help considerably in our understanding of the ρ and ω production amplitudes. The problem is somewhat complicated (or rich) since there are six helicity amplitudes contributing to vector meson production:

$$\frac{d\sigma}{dt} = \sum_{\lambda=1}^{6} |F_\lambda|^2.$$

A separation into three pairs of amplitudes can be accomplished by considering the three products $\rho_{oo} \frac{d\sigma}{dt}$, $(\rho_{11}-\rho_{1-1}) \frac{d\sigma}{dt}$ and $(\rho_{11}+\rho_{1-1}) \frac{d\sigma}{dt}$ where ρ_{ij} is the vector meson density matrix element. In a simple Regge pole picture the leading terms in the amplitudes for the first two products come from unnatural parity exchange, $P = -(-1)^J$ such as π, B and A_1, while the last product corresponds to natural parity exchanges such as ρ and A_2.

Another subject having to do with anomalies in mass spectra is the question of structure in the 2^+ nonet. The $f(1250) \rightarrow \pi^+\pi^-$ and $K^{*o}(1420) \rightarrow K^-\pi^+$ decays can be studied with the spectrometer; the acceptance at these masses is less than for the ρ^o, about 14% at 6 GeV/c after taking into account the unfavorable decay angular distribution. Since the f and K^*_{1420} cross sections and acceptance are comparable, one would ordinarily collect about 1% as many K^*'s as f's, reflecting the beam K^-/π^- ratio of 1%. This situation can be improved by increasing the beam rate, ignoring some of the pion triggers but taking all the K triggers. A comparison of the effective mass spectrometer technique with bubble chamber results is made in the Table.

Table. Comparison of Berkeley (Group A) bubble chamber (Ref. 14) with projected results from effective mass spectrometer (40 shifts)

	Resolution	f Events	$K^*(1420)$ Events
HBC	± 7 MeV	5000	2000
EMS	± 4 MeV	60000	6000

High statistics together with good resolution can also be used to look for new narrow resonances. It is not hard to find several 3 to 5 standard deviation effects in the literature, both for $\pi\pi$ and $K\pi$. Such resonances would upset various symmetry apple carts and it would be very exciting to firmly establish such beasts. The $K\pi$ spectrum between the 890 and 1420 is an especially popular region. The Goldhaber Group,[15] for example, recently reported the 5 standard deviation effect at $M_{K\pi} = 1250$ with width $\Gamma = 20 \begin{smallmatrix}+9\\-6\end{smallmatrix}$ MeV shown in Fig. 6. A 10 shift run at 6 GeV/c should give us 20 times the number of events.

High statistics should also allow better studies of $\pi\pi$ and $K\pi$ scattering. As shown by the recent ρ^o results[16] from SLAC a believable extrapolation to the pion pole requires several t bins inside of m_π^2, but in the past statistics have not allowed such fine binning. Small t bins with good statistics are also needed to check the vector dominance prediction of a sharp forward peak in

$\rho_{11}\frac{d\sigma}{dt}$ for ρ^o production. Theoretical controversy exists over the effects of frame used to evaluate ρ_{11}; Harari, et al.[17] have claimed that a sharp forward peak will not show up in the Jackson frame.

K^- charge exchange is interesting both theoretically and experimentally and we expect to collect a few hundred events per shift. As usual, one can apply his favorite brand of Regge theory to the process; in this case, however, fits to K^-p and K^-n elastic scattering should be directly applicable to the charge exchange data and all three reactions should be fit at once, hopefully giving a much tighter constraint to the models than possible with the reactions separately considered.

Experimentally K^o's can be used for delightful checks of the experimental system, both hardware and software: a) the K^o peak position may indicate systematic troubles; b) the K^o peak width directly measures the effective mass resolution; and c) the decay distribution (after corrections for geometric efficiency) should be isotropic.

MANY - PARTICLE EXPERIMENTS

Streamer Chambers

Large streamer chambers have been used successfully at DESY and SLAC for several years. Similar setups are now under construction at the Bevatron by a UCLA group and at Argonne by a

group from the University of Illinois. The Argonne chamber will be 1.5 x 1.0 x 0.6 m^3 and will likely be located in the old 500-liter bubble chamber magnet.

The principle advantage of streamer chambers over bubble chambers is triggerability. A good trigger is the heart of a successful streamer chamber experiment and this technique works best for reactions with distinctive signatures. The University of Illinois plans to look at various backward scattering processes by triggering on the fast forward-going proton from $\pi^- p \to p x^-$ at 5 and 8 GeV/c.[18] They will detect the x^- decay products in the streamer chamber, the decay correlations being useful for identifying resonances and their quantum numbers as well as for understanding the production amplitudes. They will be sensitive to boson masses up to about 2400 MeV. Another type of process which could be studied with such a device is $\pi^- p \to \pi^- N^*$. By momentum analyzing the fast outgoing pion, one could choose a particular N^* mass region and again study the decay correlations with the streamer chamber. For example, one could look to see if diffractively produced N^*'s conserve s-channel helicity. Another type of trigger would be to look for reactions with K^- in and K^+ out; such a trigger would allow a study of Ξ^*'s and Ω's. Rare decay modes of mesons or baryons involving γ-rays, leptons, etc., can be identified with trigger counters and the decays studied in detail

with a streamer chamber.

Bubble Chambers

Up to now most studies of many-particle reactions have been done with bubble chambers. After the 30-inch bubble chamber moves from Argonne to NAL, the Argonne 12-foot chamber and the British 1.5-m chamber will be left as the only operating bubble chambers at the medium-energy laboratories. In his talk at this Conference, Manning mentioned that the emphasis on the 1.5-meter chamber will be a track-sensitive hydrogen target in a neon-hydrogen mixture, appropriate for reactions giving γ rays.

The long path length in the 12-foot bubble chamber will give many interactions; the precision for physics quantities is comparable to that obtained with other bubble chambers. As an example of this use for the 12-foot chamber, we consider an approved experiment[19] for 1,000,000 pictures of 6.5 GeV/c K^- in an rf separated beam. Such an exposure will give 100 events/μb, more than all of the K^- exposures previously taken above 5 GeV/c. In addition to studying resonance properties, one can use this exposure to look at production mechanisms; in particular, density matrixes, hyperon polarizations, etc., will be available. A few hundred events for backward peaks such as $K^-p \to \Lambda\rho$ are expected. There should be about 3000 examples of $K^-p \to \bar{K}^0 n$; the polarization of the recoil

neutron can be measured to 10% by observing np scatters in the chamber.

SLAC is now advertising[20] a 15-inch diameter bubble chamber which will cycle at 60 times per second. The machine cycle at SLAC will allow continuous useful running instead of being limited by a flat-top spill. One may still, however, have a better duty cycle for the counters and spark chambers surrounding the target at proton machines. Would such a device be useful at a medium energy proton machine?

EXPERIMENTS IN EXTERNAL PROTON BEAMS

Considerable work has been done both on elastic and inelastic pp reactions in external proton beams. This work could well be extended with a polarized target (discussed in another section). Further, a deuterium target could be used to study reactions off neutrons, elastic scattering from the deuteron as a whole, and double scattering reactions.

Further work on reactions such as

$$pp \rightarrow d\pi^+$$
$$\rightarrow d\rho^+, \text{ etc.},$$

might also be contemplated. Such reactions are, of course, interesting as a means for studying baryon exchange.

Polarized Proton Beam

It appears likely that polarized protons can be accelerated in a weak-focusing machine such as the ZGS but not in the strong-focusing machines such as those at Brookhaven and CERN. Even in the ZGS this is not trivial and one will probably have to jump the machine tune several times during acceleration to avoid depolarization conditions. A polarized proton source with guaranteed 75% polarization can be purchased for $225,000. Less than 10% depolarization is expected during acceleration and an extracted beam of 10^9 per pulse should be possible. One would use a second pre-accelerator (750 KeV) to allow fast changeover of sources; the pieces for this second pre-accelerator already exist.[21]

One would presumably run several experiments simultaneously with polarized targets to look at the spin dependence of total pp cross sections, elastic scattering, and so on, and a bubble chamber to study the spin dependence of more complicated processes.

Λ-Beams

Akerlof et al. (University of Michigan) have proposed[22] to use an external proton beam of 10^8 per pulse to produce a 10 GeV/c Λ-beam. Such a beam would be used to study elastic scattering and total Λ-proton cross sections. These cross sections are clearly fundamental but the experiments are rather hard; backgrounds will have to be brought under control, but are expected to be manageable.

POLARIZED TARGETS

An enormous amount of work remains yet to be done at medium energies with polarized targets. Thus far, these targets have been used primarily to measure the polarization parameter P for elastic scattering. Recent advances in polarized target technology should allow these measurements not only to be extended to other reactions but also to the parameters R and A. The advances of particular interest are the following: a) the use of hydro-carbon targets with a factor of four fewer bound protons per polarizable hydrogen atom (recent results with ammonia indicate that an additional factor of 3/2 is now available); b) the large polarizations of 60 to 70% obtainable from hydro-carbon targets with the use of He^3 refrigerators; c) the polarization of deuterons in a butanol target to 22% (Ref. 23); and d) the frozen-spin targets now under development which can be used in low-quality magnetic fields allowing greater access (especially important for the R and A measurements). Progress in detectors such as proportional wire chambers should also allow considerable improvement over previous experiments.

One of the most productive and efficient ways for exploiting polarized targets is collaborations between a polarized target group and other groups with particular experiments and techniques which have been thoroughly understood with less exotic targets. Such

collaborations between the Chamberlain group and the in-house SLAC groups were highly successful for both electron scattering[24] and photoproduction[25] experiments.

Elastic Scattering

The medium-energy polarization data for elastic scattering could probably stand the general improvement now possible with the better techniques discussed above. In particular backward πp scattering information scarcely exists above the resonance region. The polarized target group at Argonne is planning to study $\pi^- p$ backward scattering within the next year or so; this reaction is the most readily interpretable since it involves pure $I = 3/2$ amplitudes in the t channel. As pointed out by Berger and Fox,[26] the currently popular models give rather different predictions for this quantity.

A study of polarization effects in pp elastic scattering with a high intensity extracted beam appears most attractive at the present time. Such studies were not feasible with the old LMN targets which were easily radiation damaged. The new hydrocarbon targets are much more resistant; Borghini et al.[27] report a $1/e$ loss of polarization for 4×10^{14} electrons/cm^2. It was found that the polarization could be largely recovered by annealing the target for a few minutes at 140°K. Neal et al. (Indiana University) have an approved Argonne experiment[28] which will use 5×10^{10} protons per

pulse to cover momentum transfers up to 10 GeV^2 at four energies from 3 to 12.5 GeV/c. The differential cross section in this region shows various changes of slope which may be reflected in the polarization. They will use two magnetic spectrometers with proportional wire chambers to identify the elastic events. The depolarization parameter will be studied at a few points using a carbon scatterer in one of the spectrometers to measure the polarization of one of the recoil protons. This setup may also be used later for other experiments in the external proton beam.

Inelastic Reactions

Pion charge exchange $\pi^- p \rightarrow \pi^o n$ has been previously studied[29] out to momentum transfers of about -.4 GeV^2. The polarized target group at Argonne plans to extend these measurements out to 1.2 GeV^2 with a large array of lead-glass counters to detect the two γ rays.[30] They hope to avoid having to use neutron counters because of the factor-of-5 loss in counting rate due to neutron counter efficiency. Without the angular constraints from the neutron, they will be unable to distinguish between events from free protons and those from complex nuclei. This is unpleasant, of course, but not as bad as one might have first thought for several reasons: (a) The Fermi motion in the nucleus will result in some kinematic smearing which may allow one to throw away a portion of the unwanted events. (b) The protons in a carbon nucleus are not as efficient as free protons since

they are partially shadowed by the other nucleons (for example, the effective number of protons in carbon for π^+ photoproduction was found to be four). (c) At small momentum transfers (less than 0.1 GeV^2), the events from complex nuclei are suppressed by the Paul-exclusion principle. (d) Veto counters around the target may be able to partially suppress the events from complex nuclei by detecting nuclear debris.

For π^+ photoproduction (also a charge-exchange reaction), it was found that with no veto counters near the target and detecting only the π^+ the total number of events in the appropriate kinematic region was four times that from the free protons.[25] This means that if one has a target with nominal polarization of 60%, the effective polarization for such experiments is 15%, comparible with target polarizations of a few years ago. This situation might be further improved up to a factor of 1.5 with an ammonia target. An alternate method would be to use a polarized deuteron target to study $\pi^+ n \rightarrow \pi^o p$, detecting both the γ rays and the recoil proton.

With minor modifications, the Argonne charge-exchange experiment will be able to study the reaction $\pi^- p \rightarrow \eta n$. This reaction is of great interest since only the A_2 can be exchanged in the t channel and the interpretation is relatively direct.

Polarization Studies with an Effective Mass Spectrometer

Assuming that our effective mass spectrometer lives up to expectations, it should be straight forward to simply replace the liquid hydrogen target with a polarized target. The geometry does not easily allow for neutron counters and we will simply have to accept the lower effective polarization of about 15%. Since absolute normalizations are not a worry in this case, we would probably use a very tight set of veto counters around the target and this may give some improvement on the effective polarization. If we want to measure the polarization parameter to ± 10%, we need a statistical precision of ± 1.5% or $1/0.015^2 \approx 5000$ events/bin.

In 60 shifts of production running, one should obtain about three million triggers of which 25,000 would be K charge exchange; thus the data could be split into five momentum transfer bins, each with the desired 10% statistical error. At the same time, one would get three times as many K^*_{890}'s and 20 times as many ρ^o's. With this many ρ^o's the polarization effects on the various amplitudes could be studied using the ρ^o density matrixes. The general theory was worked out long ago by Byers and Yang;[31] Jackson also discusses such things with a somewhat different treatment.[32] In addition to simply trying to understand production amplitudes, one can make a vector dominance comparison with the already existing polarization data for π^+ photoproduction[25] (this reaction showed large

polarization effects at both 5 and 16 GeV).

A and R Measurements

For reactions such as

$$\pi^+ p \rightarrow K^+ \Sigma^+,$$

three quantities can be determined as a function of s and t: the magnitudes of the flip and nonflip amplitudes and their relative phase. In terms of helicity amplitudes[33]

$$\frac{d\sigma}{dt} = |F_{++}|^2 + |F_{+-}|^2,$$

$$P \frac{d\sigma}{dt} = 2\,\mathrm{Im}(F_{++}F_{+-}^*).$$

Two other quantities can be obtained by measuring components of polarization in the scattering plane for both incident and final baryons:

$$A \frac{d\sigma}{dt} = 2\,\mathrm{Re}(F_{++}F_{+-}^*),$$

$$R \frac{d\sigma}{dt} = |F_{++}|^2 - |F_{+-}|^2.$$

This gives us four equations for the three unknowns; the relation between the parameters can be expressed as the constraint

$$P^2 + A^2 + R^2 = 1.$$

As pointed out by Berger and Fox,[34] there is great interest in determining A and R. The various models currently in vogue have very different amplitude structure, and the different models predict quite different structure for A and R. This is illustrated in

Fig. 7 for the reaction

$$\overline{K}N \rightarrow \pi \Sigma$$

where 4-GeV/c predictions are shown for both the strong-cut Regge-absorption model and exchange degenerate Regge-pole model. Even a relatively low-precision experiment should be able to distinguish between the models.

The usual polarization parameter P is not as useful as A and R since it is mainly sensitive to small terms which are difficult to calculate reliably.

If we define our coordinate system in the standard way,

$$\hat{x} = \hat{y} \times \hat{z},$$

$$\hat{y} = \text{production normal (in x out)},$$

$$\hat{z} = \text{baryon direction},$$

then the quantities A and R relate the initial and final polarization components as[33]

$$P^f_{x'} = AP^i_z + RP^i_x$$

$$P^f_{z'} = RP^i_z - AP^i_x$$

where the primes refer to the outgoing baryon coordinate system (see Fig. 8). The directions are usually defined by theorists in the center of mass system, while experimentalists sometimes quote results in the laboratory frame. This involves a rotation of $(\theta_{cm} - \theta_{lab})_{baryon}$; this angle is large at small t.

Experimentally, the polarized target is oriented to give an initial component of polarization along x or z. The Σ^+ decay with decay asymmetry $\alpha = -1$ is then used to measure the components of P^f. In the laboratory frame, measurements of $P^f_{x'}$ are generally more reliable than those of $P^f_{z'}$, and if only one target orientation is to be used, detailed studies should be made to determine which orientation will yield the most useful data. A more elegant method would be to use orientations of the target along both x and z, in each case getting measurements of both A and R. This would allow checks of systematic errors, and together with the constraint equation, would allow an overall reduction in both systematic and statistical errors.

The geometry of existing targets make it very hard to measure A and R. With a frozen spin target one should be able to operate in a low-quality field with considerable free space through which the particles can pass to the detectors. One would "cook" the target in a standard high-quality field and then cool the target down to say, $0.24^{\circ}K$, where the relaxation time for butanol is two days.[35] The target would then be transferred to the low-quality field. Such targets are being developed at both Rutherford and CERN.

Since the Σ^+ decays too fast (L_{mean} = 2 cm/GeV/c) to measure its direction, it will not be possible to distinguish between events from free-protons and those from complex nuclei; the effective

polarization again is expected to be about 15%. In a previous experiment at Argonne, Pruss et al,[36] took 40,000 events with a 12-inch hydrogen target during a relatively short run; the results are shown in Fig. 9. It should not be difficult to get three times this number of events. The statistical error in left-right decay asymetry will give

$$\sigma_{A,R} = \frac{2}{P^{i}_{eff}\sqrt{N_{events}}}$$

A ± 15% error, would thus require about 8,000 events; and one would expect to be able to get at least half a dozen measurements as a function of t for each of the two target orientations (along x and z).

PHYSICS FROM DEUTERIUM TARGETS

By studying reactions from both protons and neutrons, considerably more information can generally be obtained than if only one reaction is studied. Much tighter constraints on theoretical models can often be obtained when information is available from several related reactions. Depending on the experimental setup, running with deuterium often involves no modification of the experiment, only a change of liquids in the target. Given the amount of time, effort, and money which normally goes into a high energy experiment, it is unfortunate that people have not always fully exploited the potentialities of their equipment by running with deuterium.

Deuteron Complications

The kinematic smearing from Fermi motion in the deuteron often frightens people. This smearing is not troublesome, however, for experiments which measure forward-going particles from peripheral reactions.[37] The momentum transfer t in such reactions is not smeared at all since one directly measures the quantities which define t. The effective center of mass energy s is smeared by the Fermi momenta, an average value for deuterium being about ± 4%; at high energies, this should have very little effect on the data. The worst effect of smearing comes when one tries to calculate the missing mass of the recoiling nucleon to ensure that additional pions have not been produced. For deuterium, this smearing is given approximately by

$$\sigma_{M_n^2} = \pm 0.08 \ |\Delta\vec{p}| \ \mathrm{GeV}^2,$$

where $\Delta\vec{p}$ is the difference between the three momenta of the beam and the forward going particles; for small t, $|\Delta\vec{p}| \approx \sqrt{-t}$. Thus, at small t, one should not have troubles distinguishing between reactions with and without additional pion production: at large t, say 1 GeV^2 and greater, there will be ambiguities.

At small t the recoil nucleon can't always find a home and the reaction is suppressed by the Pauli-exclusion principle. The amount of suppression depends upon the relative amounts of spin-flip and spin-non-flip. For charge-exchange reactions, the cross section on

deuterium is related to that on free nucleons by[38]

$$\left(\frac{d\sigma}{dt}\right)_D = \left[1-F(q^2)\right]\left(\frac{d\sigma}{dt}\right)_{nf} + \left[1-\frac{1}{3}F(q^2)\right]\left(\frac{d\sigma}{dt}\right)_f .$$

$F(q^2)$ is the deuterium form factor which starts from unity at $q^2 = 0$ and falls to about 0.45 at $q^2 = m_\pi^2$. Comparing charge-exchange reactions off protons in hydrogen and deuterium thus allows a determination of the relative amounts of flip and nonflip amplitudes near the forward direction.

A third type of complication comes from the Glauber-shadow correction terms and final state interactions involving the "spectator" nucleon. These corrections are typically 10% and to a very good approximation should be the same for π^+ and π^- reactions. For $K^\pm$ the corrections may differ slightly, but are calculable and should largely cancel when taking ratios.

When comparing reactions from protons and neutrons, it is clearly best to do both reactions off deuterium so that the various effects will cancel when taking ratios. This has tended not to be the case for bubble-chamber studies where a hydrogen reaction may be studied by one group and then compared with the deuterium reaction studied by a different group with different criteria, different bubble chambers and different analysis programs.

Physics

Measurements of $\rho\omega$ interference can be made with an

effective mass spectrometer to look at the reactions

$$\pi^- d \rightarrow \pi^- \pi^+ n(n_s),$$

$$\pi^+ d \rightarrow \pi^+ \pi^- p(p_s).$$

These reactions are charge symmetric ($I_z \rightarrow -I_z$) and their comparison ordinarily would be rather dull since one would expect the cross sections to be equal. However, the decay $\omega \rightarrow \pi^+ \pi^-$ violates isotopic spin and we have the general result

$$\frac{d\sigma^{\pm}}{dt} = \sum_{\lambda=1}^{6} \left| a e^{i\phi} F_\lambda^\omega \pm F_\lambda^\rho \right|^2$$

where the F_λ's are the six helicity amplitudes and include the appropriate Breit-Wigner amplitudes; the $\pm$ refers to the sign of the incident pion. The $\omega \rightarrow \pi^+ \pi^-$ decay is described by a and ϕ. Taking the sum of the two cross sections will cause the interference terms to cancel, leaving two pure Breit-Wigner peaks from which the $\omega \rightarrow \pi^+ \pi^-$ branching ratio can be deduced. The difference between the two cross sections should be 0 except near the ω mass where the interference terms are present. Again one can try to isolate the interference effects by looking at quantities such as

$$\left(\rho_{oo} \frac{d\sigma}{dt}\right)_+ - \left(\rho_{oo} \frac{d\sigma}{dt}\right)_- = \sum_{\lambda=1}^{2} 4 \mathrm{Re}\left(a e^{i\phi} F_\lambda^\omega F_\lambda^{\rho *}\right).$$

Reactions such as

$$K^- p \rightarrow K^o n$$

$$K^+ n \rightarrow K^o p$$

are not charge symmetric and having information from both reactions can put severe constraints on the theoretical models. Differences between these two cross sections are again due to interference terms, in this case between amplitudes corresponding to t channel exchange of opposite signature, for example, $\mathrm{Re} F_\rho F^*_{A_2}$. Exchange degeneracy predicts the ρ-exchange amplitude F_ρ to be 90^o out of phase with the A_2 exchange amplitude; thus the two cross sections are predicted to be equal. The present experimental results have large uncertainties, but as shown in Fig. 10 (ref. 39) the cross sections approach one another at 5.5 GeV/c. Similar arguments apply for $K^\pm \rightarrow K^*$. As in the case of ρ production, one can try to isolate the helicity amplitudes with density matrix elements.

HEAVY TARGETS

The use of targets of complex nuclei for high-energy beams can give information on both nuclear physics and on the properties of elementary particles. For example, a recent high statistics experiment[40] on ρ^o photoproduction at DESY gave quite precise results on both nuclear radii (see Fig. 11) and on the total cross section for ρ^o-nucleon interactions (27 ± 2 mb).

Elastic scattering of protons on complex nuclei was studied several years ago at CERN by the Cocconi Group at 10 GeV.[41] Their results were discussed in many subsequent theoretical papers.[42] Such an experiment would be relatively easy to repeat at medium energies with proportional wire chambers;[43] it would be interesting to try to observe differences between π, K, and proton elastic scattering from complex nuclei.

If an effective mass spectrometer were placed in a neutral beam, one could study diffraction dissociation for the reaction

$$nA \rightarrow N^{*o} A$$
$$\qquad\quad \lfloor \rightarrow p\pi^- .$$

Since the incident neutron energy cannot be readily determined, nor the recoil easily observed, such an experiment cannot directly distinguish the above process from those in which additional pions are produced. In the diffraction dissociation model certain of the N^* resonances are expected to be produced coherently from the entire nucleus, and this will result in a very sharp peak at small momentum transfers sitting on a slowly varying background coming from other types of reactions including those in which additional pions are produced. Taking only events with high apparent energy, should help to reduce this background, but in any case the sharp forward peak should be easy to distinguish.

Incoherent reactions can also give useful information. At Berkeley the Santa Barbara Group recently ran an experiment to look at the processes

$$\pi^- A \rightarrow \pi^o A^*$$

$$\rightarrow \eta A^*.$$

They took data from 2 to 4 GeV/c on various elements from hydrogen through copper. Since one knows the π^o-nuclear amplitudes, one can use the first reaction to understand the nuclear physics. After this has been done, information on the η-nucleon cross section can be extracted. Similarly, an effective mass spectrometer could be used to measure the reaction

$$K^{\pm} A \rightarrow K^o A^*.$$

By using both K^+ and K^-, one may obtain information on the relative distributions of neutrons and protons in the various nuclei. Once the K^o data has been understood, one can then look at other reactions to get the total cross sections on nucleons for K^*_{890}, K^*_{1420}, ρ, f, etc.

REFERENCES

1) Baud et al., Experimental Meson Spectroscopy (Philadelphia 1970), pages 311, 437, and 557.

2) For example, R. L. Anderson et al., Phys. Rev. Letters 23, 721 (1969).

3) For example, Ankenbrandt et al., Phys. Rev. 170, 1223 (1968); Blair et al., Phys. Rev. Letters 17, 789 (1966).

4) E. W. Anderson et al., Phys. Rev. Letters 20, 1529 (1968); 22, 102 (1969); 22, 1390 (1969); 25, 1748 (1970).

5) Heinz et al., Spin and Parity of the A_2 Meson, ZGS Experiment 266.

6) Rust et al., Phys. Rev. Letters 24, 1361 (1970).

7) Akerlof, Double Charge Exchange Reactions, invited paper presented at the APS-DPF Meeting, Austin (Nov. 1970).

8) Ward et al., Study of the Reactions $\pi^- p \rightarrow K^o \Lambda^o$ and $\pi^- p \rightarrow K^o \Sigma^o$ in the Range 3 to 6 GeV/c, ZGS Experiment 271.

9) Jenkins et al., Study of the Backward Peak of the Reaction $\pi^- p \rightarrow \Lambda^o K^o$, ZGS Experiment 282.

10) Grayer et al., Phys. Letters 34B, 333 (1971).

11) Foley et al., Phys. Rev. Letters 26, 413 (1971).

12) Diebold et al., Study of Meson Production with a Wire-Spark-Chamber Spectrometer, ZGS Experiment 268.

13) Goldhaber et al., Phys. Rev. Letters 23, 1351 (1969).

14) Davis et al., Phys. Rev. Letters 23, 1071 (1969); Flatté et al., UCRL-20273 (Jan. 1971).

15) Firestone et al., UCRL-20091 (Aug. 1970).

16) F. Bulos et al., SLAC-PUB-884 and 885; also presented by Leith at the Phenomenology Conference.

17) Harari et al., Phys. Letters 29B, 314 (1969); Phys. Rev. Letters 23, 262 (1969).

18) O'Halloran et al., Proposal to Study Backward Meson Production in $\pi^- p$ Interactions between 5 and 8 GeV/c, ZGS Proposal 297.

19) Derrick, Smith, et al., Study of Ξ States and $K^- p$ Interactions in the 12-Foot Chamber, ZGS Experiments 289 and 292.

20) Ballam and Blumberg, SLAC Users Bulletin No. 21 (Dec. 1970).

21) I would like to thank R. Moffett for polarized beam information; in his talk to this Conference Cork also discussed the possibilities of a polarized beam.

22) Akerlof et al., Two Proposals to Study Λp Interactions, ZGS Proposals 301 and 302.

23) Borghini and Scheffler, CERN Preprint (Jan. 1971).

24) Rock et al., Phys. Rev. Letters 24, 748 (1970); Powell et al., Phys. Rev. Letters 24, 753 (1970).

25) Morehouse et al., Phys. Rev. Letters 25, 835 (1970).

26) Berger and Fox, Nuc. Phys. B26, 1 (1971).

27) Borghini et al., Nucl. Instrum. Methods 84, 168 (1970).

28) Neal et al., Polarization in Large Angle p-p Elastic Scattering from 3 to 12.5 GeV/c, ZGS Experiment 280.

29) Drobnis et al., Phys. Rev. Letters 20, 274 (1968).

30) Koehler et al., Measurement of the Polarization Parameter in πp Charge-Exchange Scattering at 4.5, 3.7, and 3.2 GeV/c, ZGS Experiment 306.

31) Byers and Yang, Phys. Rev. 135, B796 (1964).

32) Jackson, Proc. of Int. Conf. on Polarized Targets and Ion Sources, Saclay (1966), p. 3.

33) Jacob, Proc. of Int. Conf. on Polarized Targets and Ion Sources, Saclay (1966), p. 235.

34) Berger and Fox, Phys. Rev. Letters 25, 1783 (1970).

35) See the talks given by Borghini and by Thresher at a meeting at Cosener's House on Physics with the Omega Spectrometer (June 1970).

36) Pruss et al., Phys. Rev. Letters 23, 189 (1969).

37) Diebold, Smearing of Kinematic Parameters by Deuterium Fermi Motion, Report RD-16 (1968), unpublished.

38) Butterworth et al., Phys. Rev. Letters 15, 734 (1965).

39) Cline et al., Phys. Rev. Letters 23, 1318 (1969).

40) Alvensleben et al., Phys. Rev. Letters 24, 792 (1970).

41) Bellettini et al., Nuc. Phys. 79, 609 (1966).

42) See for example Matthiae, Nuc. Phys. 87, 809 (1967); Frahn and Wiechers, Ann. of Physics 41, 442 (1967); Dar and Varma, Phys. Rev. Letters 16, 1003 (1966).

43) Koester et al., $K^{\pm}$, $\pi^{\pm}$ Cross Sections on Complex Nuclei, ZGS Proposal 190 (plus addendum).

FIGURE CAPTIONS

1. Elastic scattering data for $\pi^+ p$ at 5 GeV/c from Rust et al., (ref. 6).
2. Energy dependence of first-forbidden peaks compiled by Akerlof (ref. 7).
3. Sketch of effective mass spectrometer under construction at Argonne (refs. 8 and 12).
4. Comparison of data obtained by missing-mass (ref. 1) and effective mass (ref. 10) techniques.
5. Data on $\rho\omega$ interference (ref. 13).
6. $K^+ \pi^-$ enhancement at 1250 MeV (ref. 15).
7. Predictions for A and R in the process $\bar{K} N \rightarrow \pi \Sigma$ at 4 GeV/c (ref. 34).
8. Components of polarization giving A and R.
9. Data obtained from a short run looking at $\pi^+ p \rightarrow K^+ \Sigma^+$ (ref. 36).
10. Comparison of $K^\pm$ charge exchange (ref. 39).
11. Nuclear radii obtained from ρ photoproduction (ref. 40).

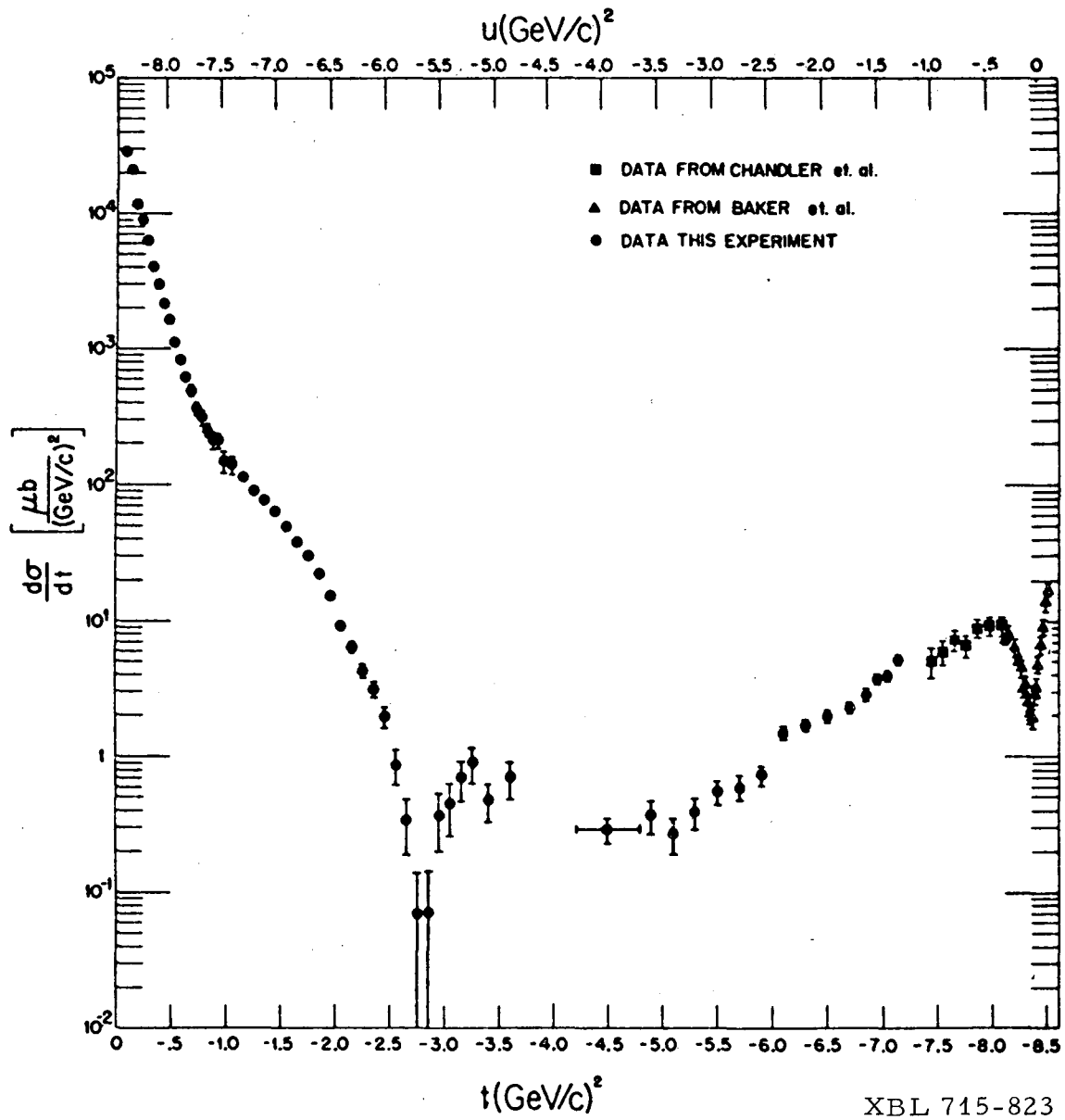
u(GeV/c)²
-8.0 -7.5 -7.0 -6.5 -6.0 -5.5 -5.0 -4.5 -4.0 -3.5 -3.0 -2.5 -2.0 -1.5 -1.0 -.5 0
DATA FROM CHANDLER et. al.
DATA FROM BAKER et. al.
DATA THIS EXPERIMENT
dσ/dt [μb/(GeV/c)²]
10⁵
10⁴
10³
10²
10¹
1
10⁻¹
10⁻²
0 -.5 -1.0 -1.5 -2.0 -2.5 -3.0 -3.5 -4.0 -4.5 -5.0 -5.5 -6.0 -6.5 -7.0 -7.5 -8.0 -8.5
t(GeV/c)²
XBL 715-823

Fig. 1.

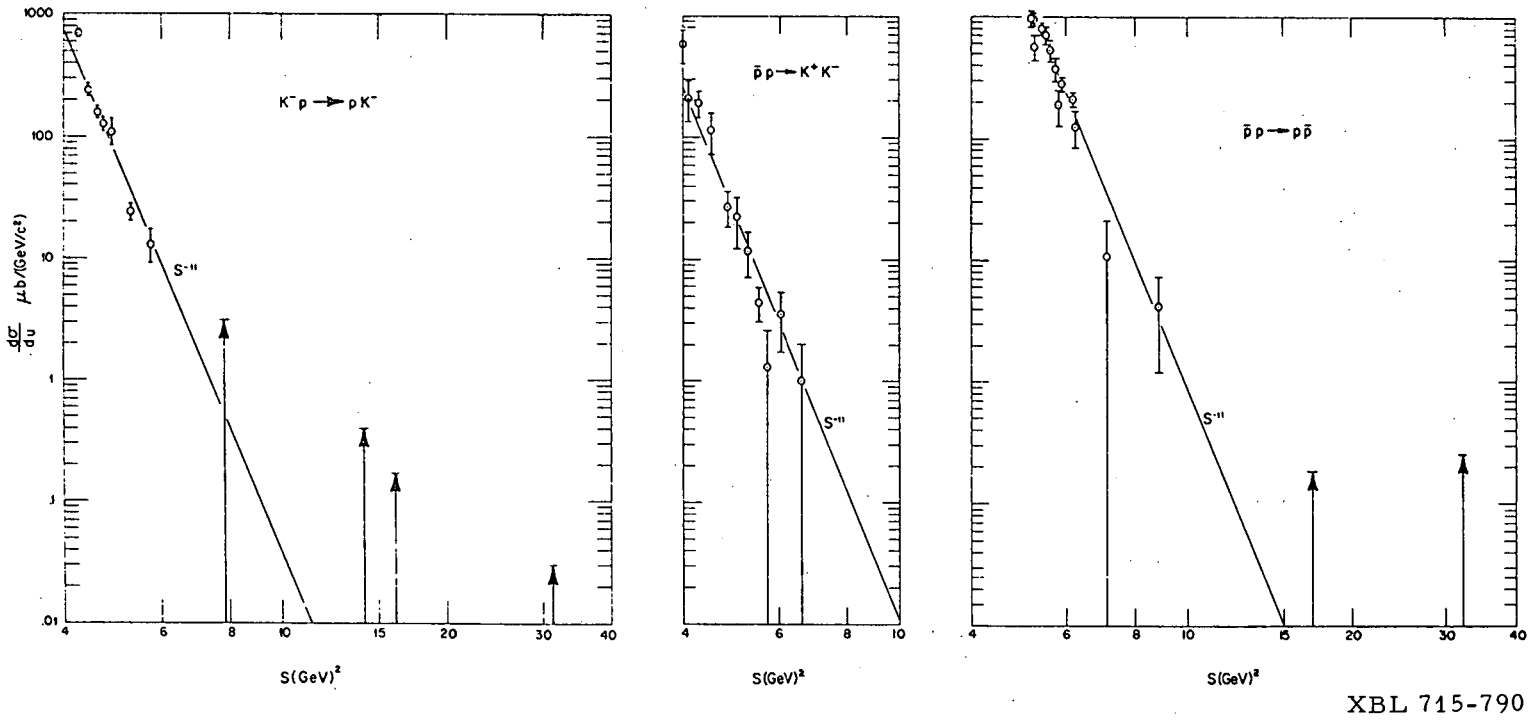
$K^-p \rightarrow pK^-$
S^{-11}
$\frac{d\sigma}{du}$ μb/(GeV/c)²
S(GeV)²
$\bar{p}p \rightarrow K^+K^-$
S^{-11}
S(GeV)²
$\bar{p}p \rightarrow p\bar{p}$
S^{-11}
S(GeV)²
XBL 715-790

Fig. 2.

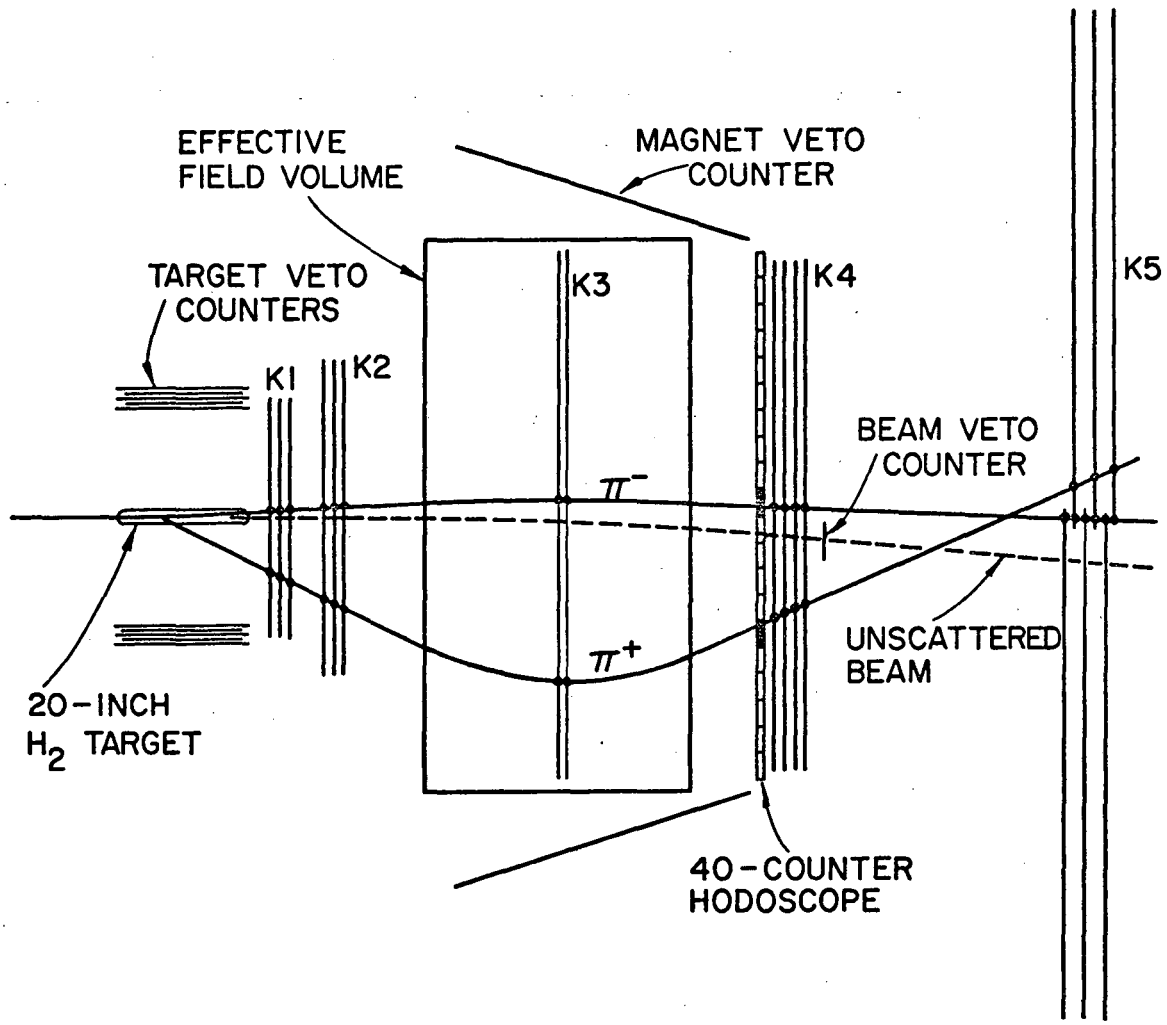

Fig. 3.

XBL 715-791

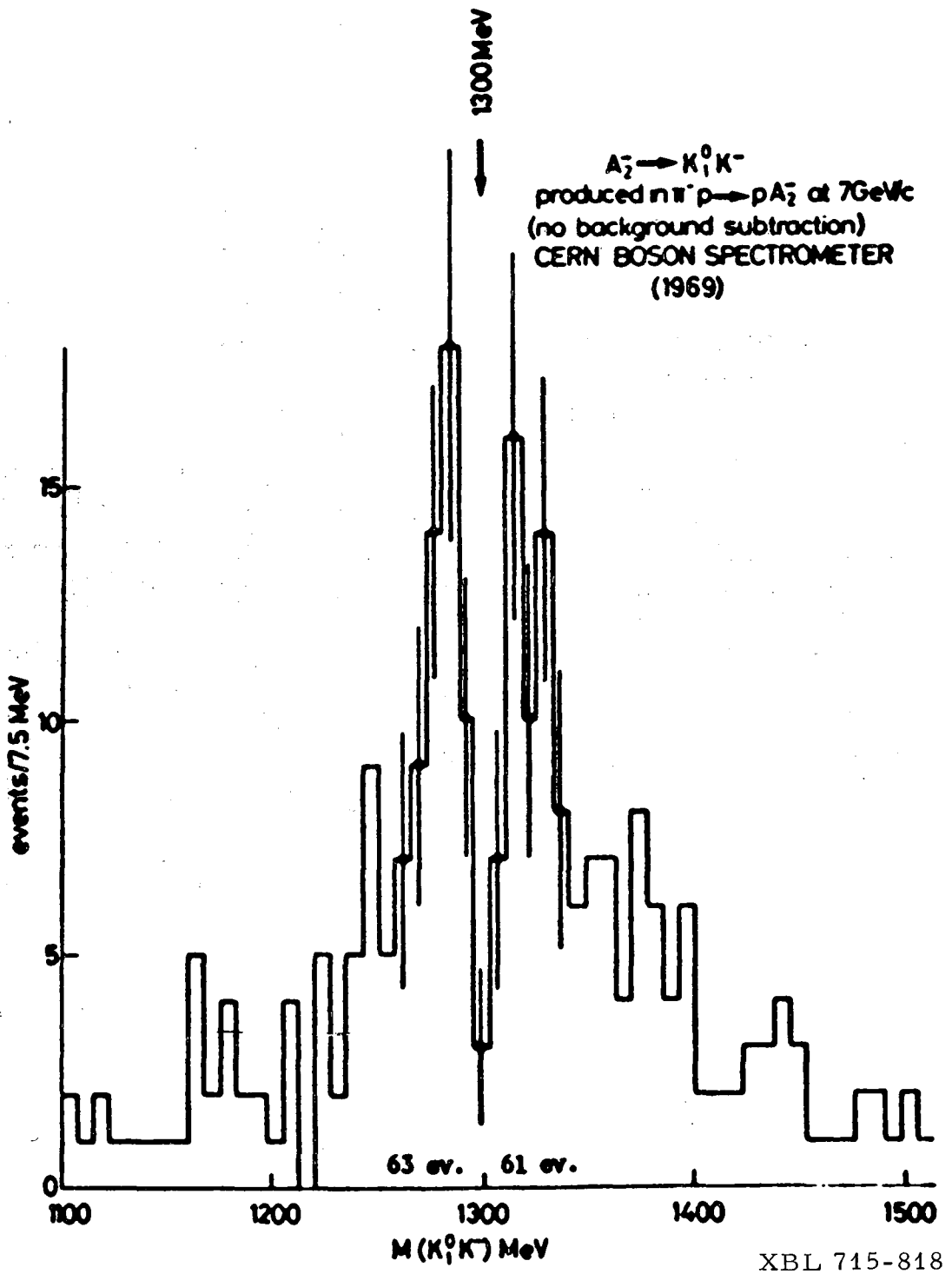
1300 MeV
$A_2^- \rightarrow K_1^0 K^-$
produced in $\pi^- p \rightarrow p A_2^-$ at 7GeV/c
(no background subtraction)
CERN BOSON SPECTROMETER
(1969)
events/7.5 MeV
15
10
5
0
63 ev.
61 ev.
1100
1200
1300
1400
1500
M ($K_1^0 K^-$) MeV
XBL 715-818

Fig. 4a.

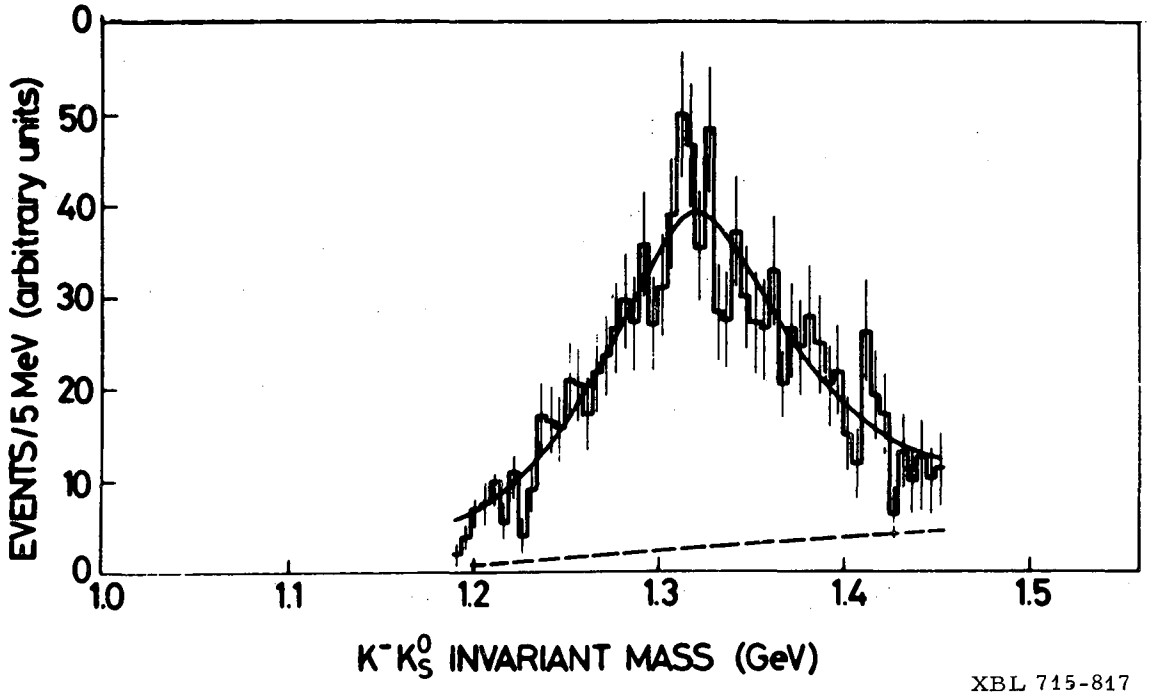
EVENTS/5 MeV (arbitrary units)
0
50
40
30
20
10
0
1.0
1.1
1.2
1.3
1.4
1.5
K⁻K⁰S INVARIANT MASS (GeV)
XBL 715-817

Fig. 4b.

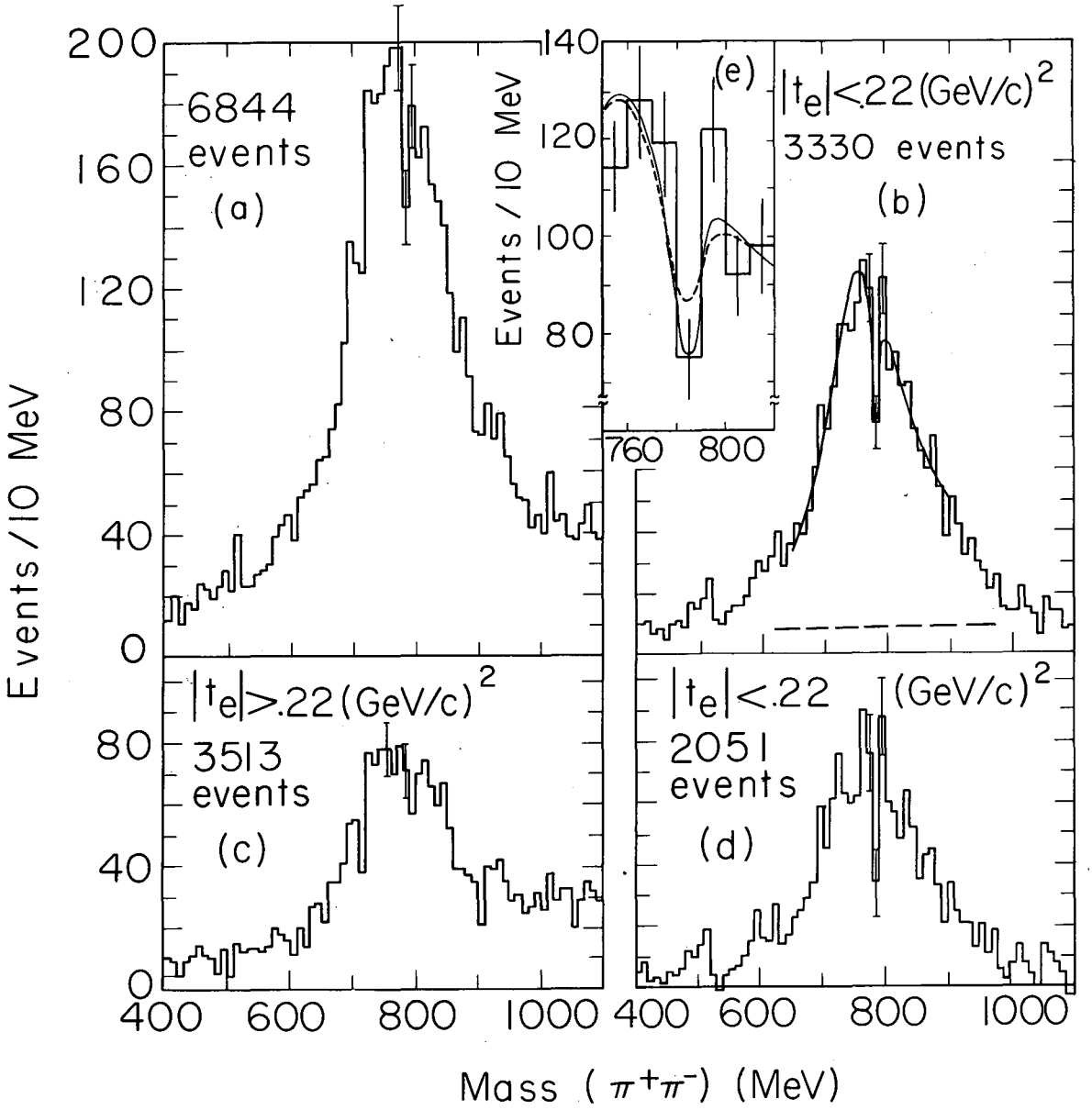

XBL699-3797

Fig. 5.

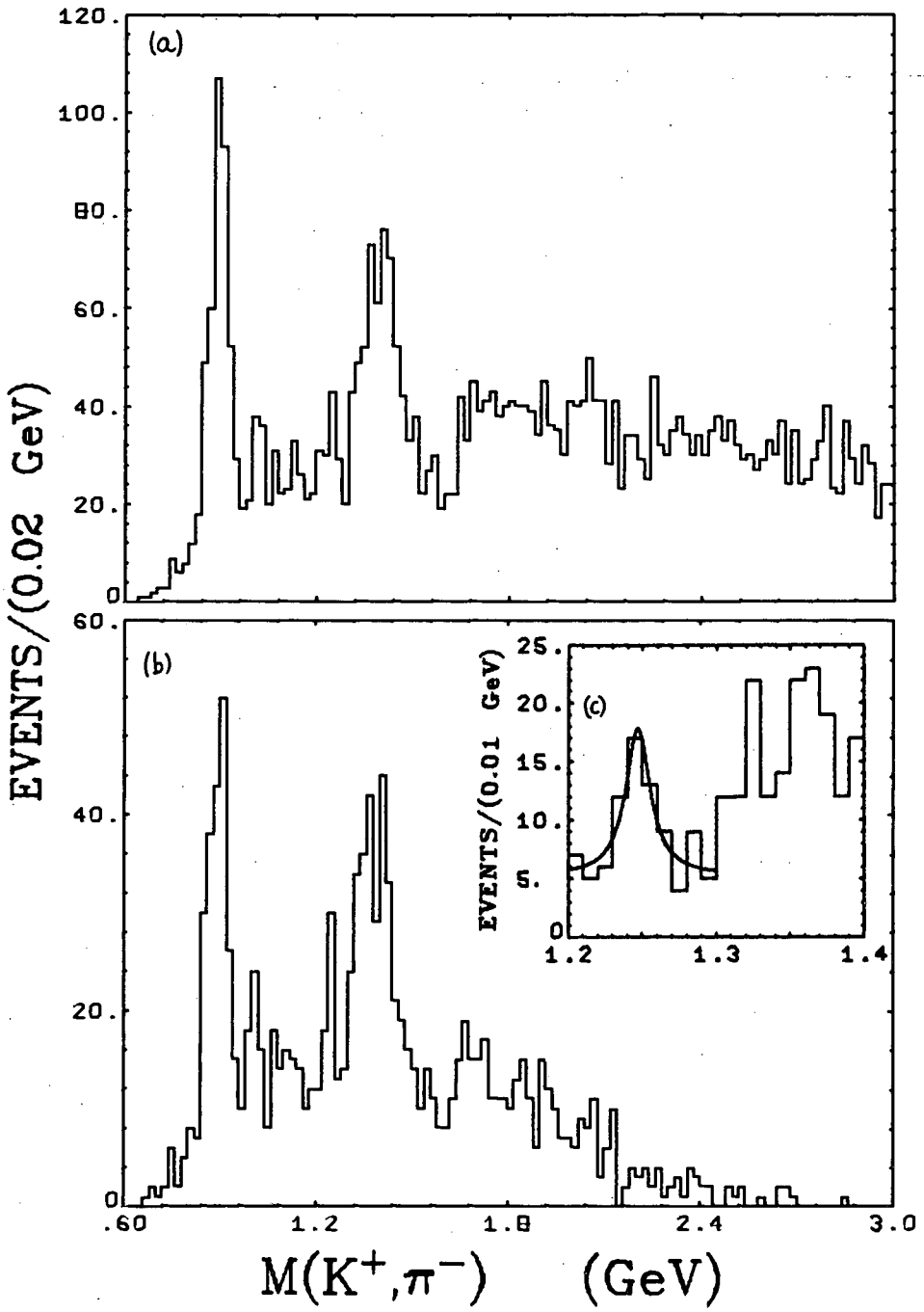

XBL 708-1782

Fig. 6.

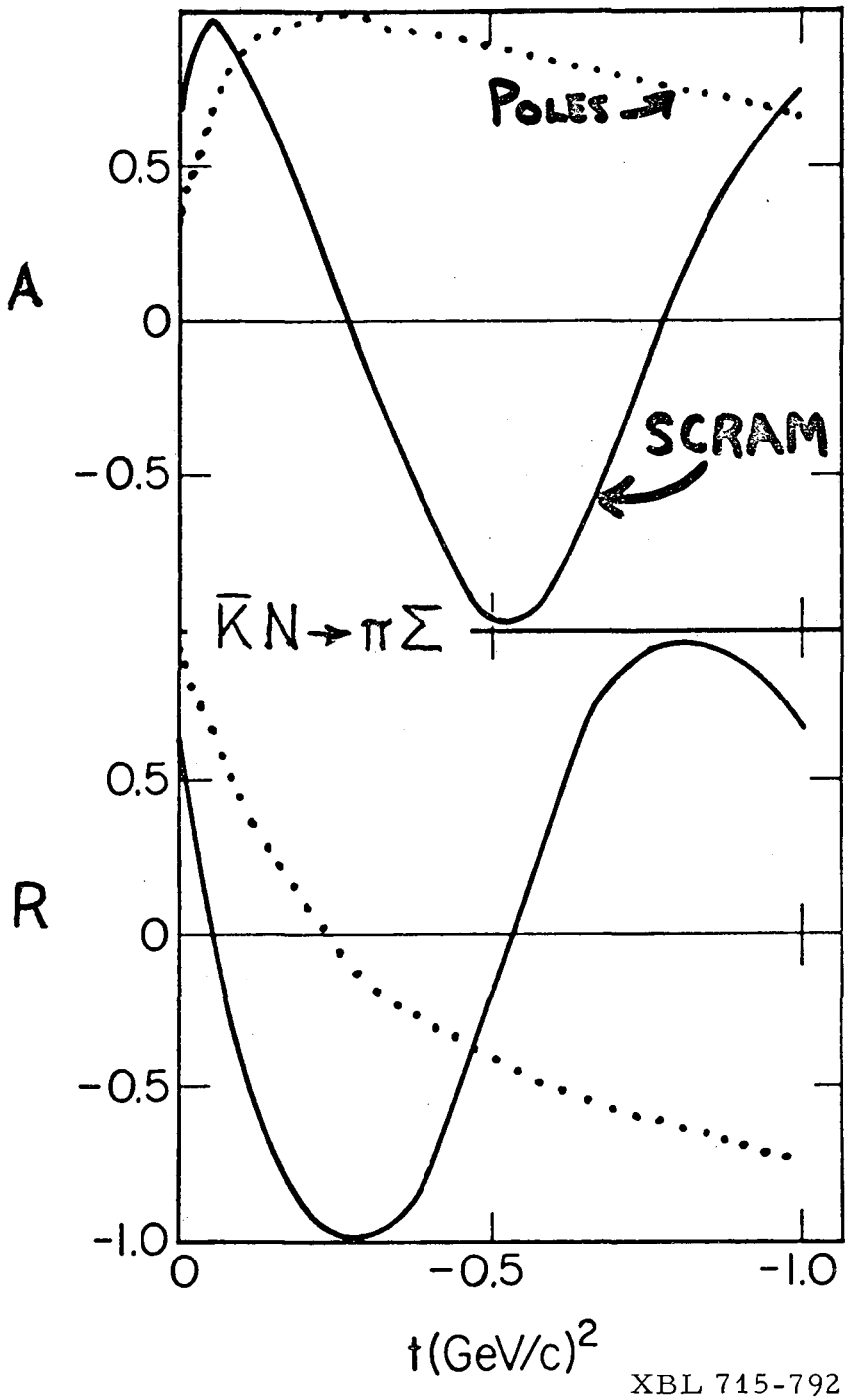
POLES
SCRAM
$\bar{K}N \to \pi\Sigma$
A
R
0.5
0
-0.5
-1.0
0
-0.5
-1.0
t(GeV/c)^2
XBL 715-792

Fig. 7.

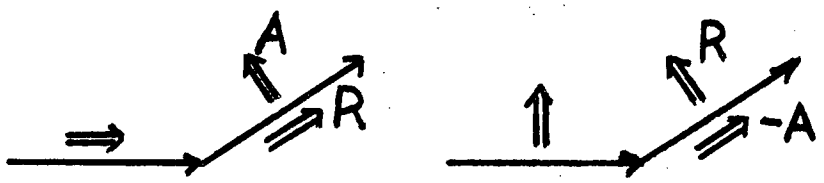

XBL 715-793

Fig. 8.

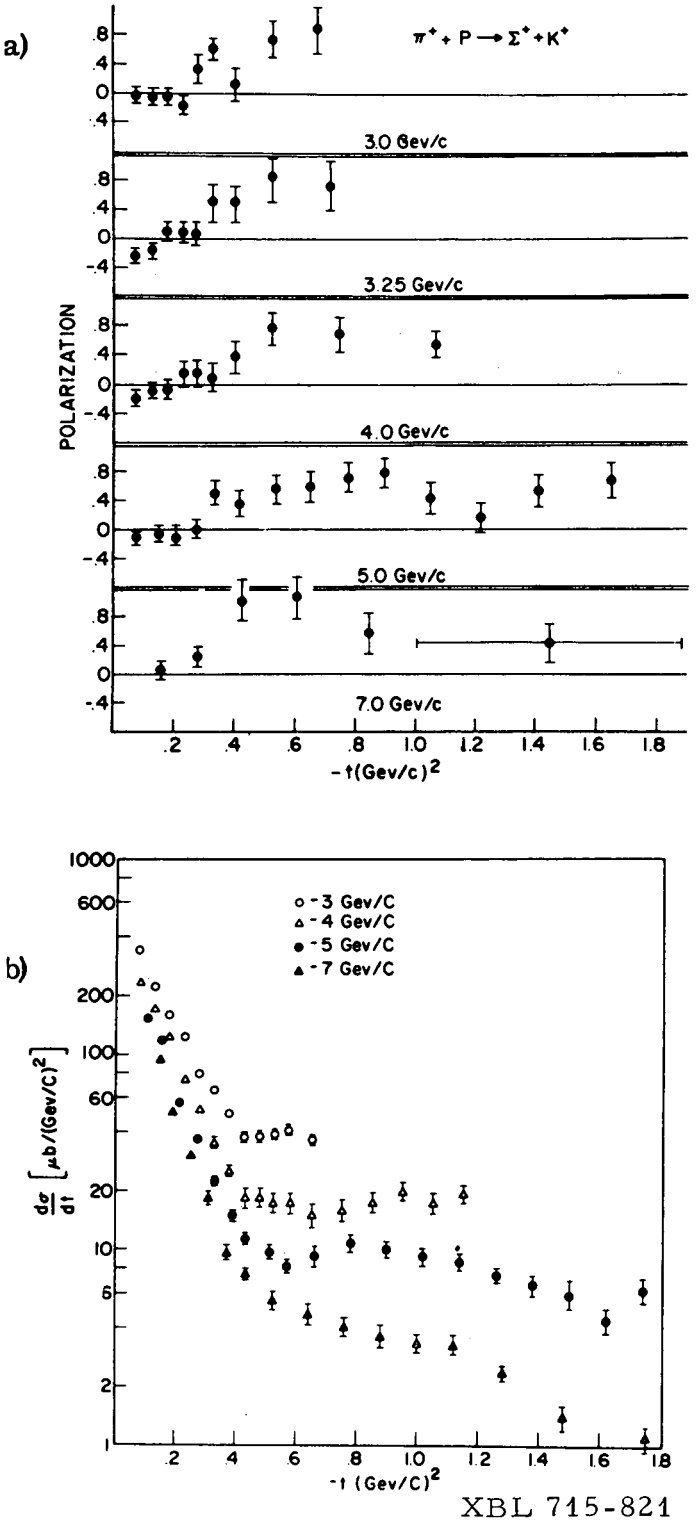
a)
$\pi^+ + P \rightarrow \Sigma^+ + K^+$
3.0 Gev/c
3.25 Gev/c
4.0 Gev/c
5.0 Gev/c
7.0 Gev/c
POLARIZATION
$-t(Gev/c)^2$
b)
o - 3 Gev/C
Δ - 4 Gev/C
● - 5 Gev/C
▲ - 7 Gev/C
$\frac{d\sigma}{dt}$ [μb/(Gev/c)²]
$-t\ (Gev/C)^2$
XBL 715-821

Fig. 9.

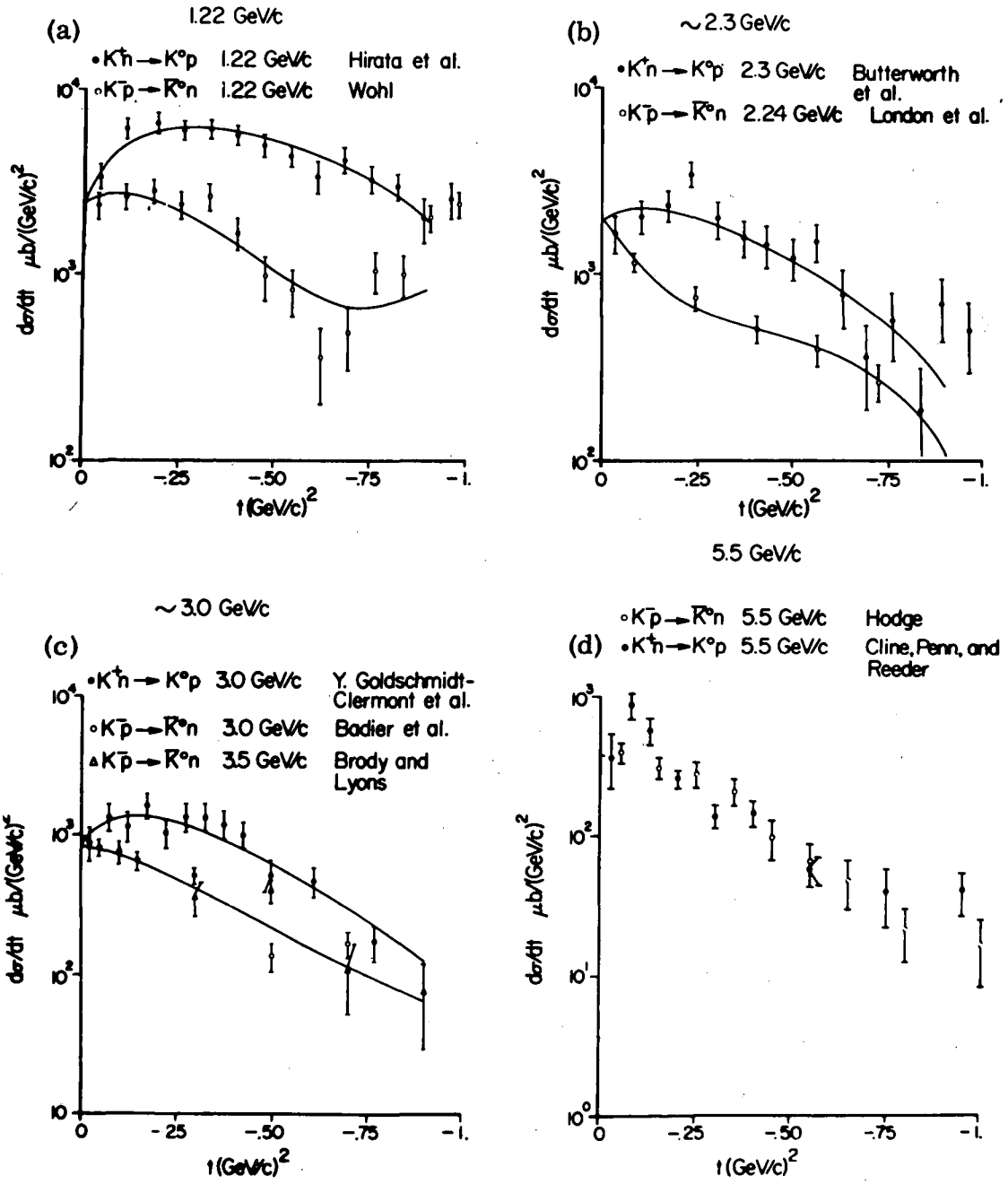
(a)
1.22 GeV/c
•K⁺n → K°p 1.22 GeV/c Hirata et al.
◦K⁻p → K̄°n 1.22 GeV/c Wohl
(b)
~2.3 GeV/c
•K⁺n → K°p 2.3 GeV/c Butterworth et al.
◦K⁻p → K̄°n 2.24 GeV/c London et al.
5.5 GeV/c
◦K⁻p → K̄°n 5.5 GeV/c Hodge
•K⁺n → K°p 5.5 GeV/c Cline, Penn, and Reeder
(c)
~3.0 GeV/c
•K⁺n → K°p 3.0 GeV/c Y. Goldschmidt-Clermont et al.
◦K⁻p → K̄°n 3.0 GeV/c Badier et al.
▲K⁻p → K̄°n 3.5 GeV/c Brody and Lyons
dσ/dt μb/(GeV/c)²
t(GeV/c)²
XBL 715-819

Fig. 10.

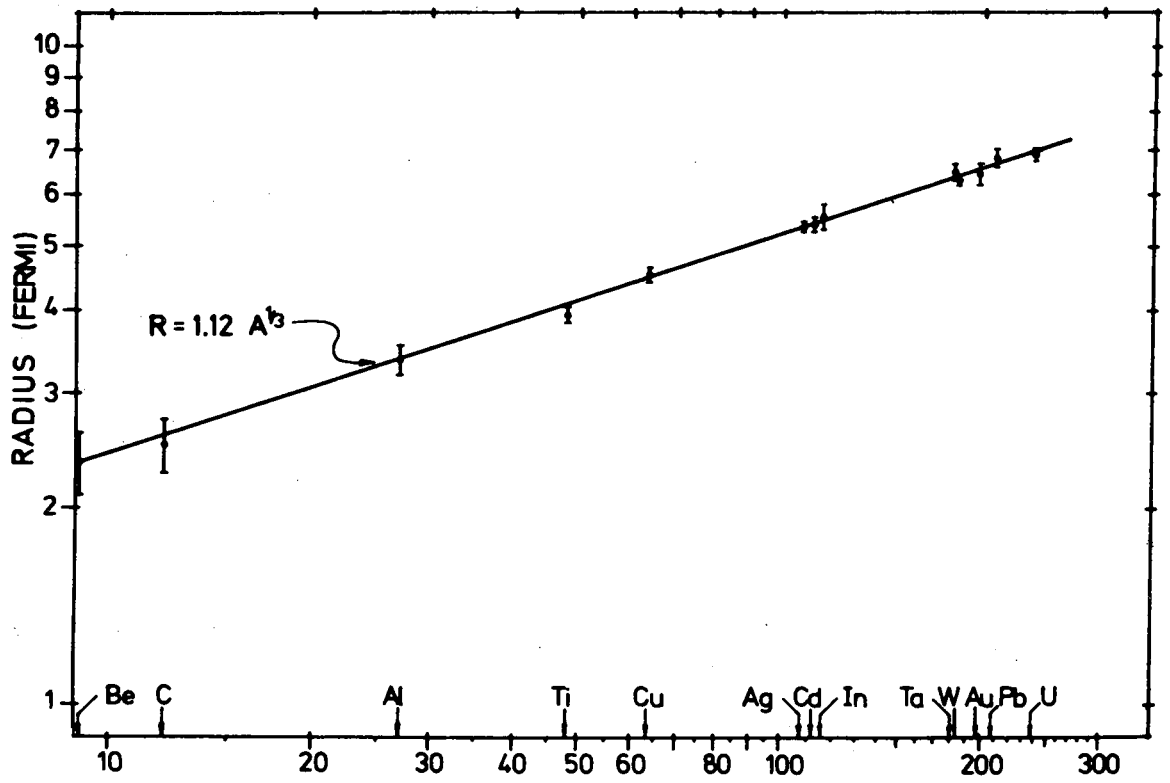

XBL 715-822

Fig. 11.

Discussion

Lovelace (Rutgers): It is very interesting to do phase shift analysis on $\pi\pi$, $K\pi$, $K\bar{K}$, $\pi\eta$, etc. and to get the density matrix elements for ρ and f production. I would also like to point out that if $K^-p \to K^+\Xi^-$ could be measured with good statistics around 6 GeV/c, it would be extremely useful in studying Regge-Regge cuts.

Galtieri (LRL): At 6 GeV/c the cross section for $K^-p \to K^+\Xi^-$ is very small.

Lovelace (Rutgers): Perhaps the streamer chamber people can do it.

Jovanovic (Argonne): Suppose you knew all the amplitudes for a given reaction up to 3 GeV what would you do then?

Lovelace (Rutgers): I would use finite-energy sum rules to find out about the high-energy amplitudes. One learns about the Regge amplitudes from the Low Energy amplitudes through the use of FESR.

Rosner (Minnesota): It may be that when you are working with hyperon beams (e.g., Λ,Σ) the uncertainties in our knowledge of the absorption in nuclei are less of a problem than the actual experimental uncertainties. If you use carbon or aluminum targets you might learn something about the total cross section of hyperon on nucleons. This would be easier than using a 6-foot hydrogen target.

Lovelace (Rutgers): Are Λp cross sections really worthwhile? It took thirty years to unravel pp.

Rosner (Minnesota): If you found a highly energy dependent Λp cross section it would be very surprising. If you could measure $\sigma_T(\Lambda p)$ to better than 10% you would have an independent check of SU(3) breaking of the pomeron, which is something that we have a handle on only from πp and Kp cross sections.

Fox (CIT): There are some striking polarization experiments in resonance production experiments.

(i) $\rho_{00}\, d\sigma/dt$ in $\pi N(\uparrow) \to \rho N$. Any polarization observed in this reaction would at once indicate that both π and A_1 exchange were present. This is by far the cleanest test of A_1 exchange--there is much dispute over its resonance interpretation; the discovery of the A_1 trajectory would settle the argument. Note a Slope 1 trajectory through the A_1 gives similar energy dependence to π exchange. It would lead--after absorption corrections--to energy independent polarizations.

(ii) The measurement of R and A (final Λ polarizations) for $\pi N(\uparrow) \to KY^*\ (\to \pi\Lambda)$ and $\bar{K}N(\uparrow) \to \pi Y^*\ (\to \pi\Lambda)$ is of great interest. It tests (a) t-dependence of double flip amplitudes--these cannot be seen, of course, in simple (!?) $\pi N \to K\Sigma$ measurements, (b) quark model additivity frame [cf. Bialas and Zalewski, Nucl. Phys. B6, 449 (1968) and G. C. Fox in "Phenomenology in Particle Physics 1971" (Caltech, 1971)]. Thus usual Stodolsky-Sakurai distribution $\rho_{33} = 3/8$, $\rho_{3-1} = \sqrt{3/8}$, $\rho_{31} = 0$ is rotation invariant. It could correspond to simple (M1) amplitude structure in any frame.

Usually one thinks of the t-channel--however, current absorption pictures have emphasized importance of s-channel. Experimentally one can best tell by these R and A measurements which are no longer rotation invariant and so are sensitive to the particular frame.

CALT-68-300
AEC RESEARCH AND
DEVELOPMENT REPORT

Tests of an Empirical Rule for Cuts and Discussion of Line Reversal Relations*

CHARLES B. CHIU

California Institute of Technology, Pasadena, California 91109

Paper presented at the
Workshop on Particle Physics at Intermediate Energies
California Institute of Technology
March 29-30, 1971

*Work supported in part by the U. S. Atomic Energy Commission. Prepared under Contract AT(11-1)-68 for the San Francisco Operations Office, U. S. Atomic Energy Commission.

ABSTRACT

The empirical rule, that cuts are important in the s-channel nonflip amplitude and relatively unimportant in the flip amplitude, consistently distinguishes the success and the failure of the Regge pole model for natural parity meson exchanges. Measurements on the density matrix elements of the ω in the reaction $\pi^+p \to \omega\Delta^{++}$ will be helpful in understanding the underlying reason for such systematics. A discussion on the line reversal relation is also presented. A prediction of the absorption model on the Λ and the Σ polarizations in $\pi^+p \to K^+\Sigma^+$ and $\pi^-p \to K^0\Lambda$ and the line reversed reactions is discussed. Measurement of polarizations at high energies will provide us with a direct test on the present absorption picture.

1. INTRODUCTION

It is by now a well-known fact that the leading Regge pole contribution alone is inadequate in explaining hadron scattering data. However, the qualitative feature of the data can be understood in terms of poles plus cuts. In spite of the fact that a priori we know very little theoretically about the properties of cuts, an empirical rule on the cut contribution for natural parity meson exchanges has emerged from models as well as phenomenological analyses of the data.[1] To state this rule, let us consider the s-channel scattering $1+2 \to 3+4$. As usual, we define the quantity $n = |(\lambda_1-\lambda_3) - (\lambda_2-\lambda_4)|$, where λ_i are the helicities of the external particles defined in the s-channel c.m. system. We restrict ourselves to those cases where $|\lambda_1-\lambda_3| = 0$ or 1 and $|\lambda_2-\lambda_4| = 0$ or 1. Then $n = 0$, 1, and 2 corresponds to respectively

the nonflip-, flip-, and double flip-helicity amplitudes. This rule says that away from $t = 0$, for $t > -1$ GeV^2 and $P_L \gtrsim 5$ GeV/c:

> cuts dominate the $n = 0$ amplitude and they are relatively unimportant in the $n = 1$ amplitude (1)

The qualitative features of the rule are contained in the weak and the strong absorption model,[2] the dual absorptive model,[3] and also the Carlitz and Kislinger model.[4]

Experimental evidence which suggests such a rule was reviewed in some detail in Ref. 1. There the relative importance of the cut contribution was phrased in terms of the t-channel helicity amplitudes. Presently we find that it appears to be more natural to state the situation in terms of the s-channel helicity amplitudes. We have only stated our conclusion for $n = 0$ and 1. We will comment on the $n = 2$ amplitude later on. In Section 2 we shall repeat some of the relatively well-known arguments for and against the Regge pole model to demonstrate experimental evidence for this empirical rule and we shall stress experiments which can further test this rule and make it more quantitative.

In Section 3 we discuss the line reversal relations. These relations are well-known. They follow directly from the assumption of the Regge pole dominance together with the exchange degeneracy for the Regge pole parameters. They are

$$\frac{d\sigma}{dt}(R) = \frac{d\sigma}{dt}(M) \quad \text{and} \quad P(R) = P(M) = 0 \quad , \qquad (2)$$

where R designates the fact that the relevant direct channel is exotic with the exchanged Regge pole amplitude being purely real, and M the

line-reversed reaction with the Regge pole amplitude having a moving phase $-\exp(-i\pi\alpha)$. If one assumes SU(3) for the vertex function, the "R" channels are extended to include all the channels specified by those duality diagrams with crossed quark lines. The "M" channels correspond to those with planar duality diagrams.[5] Large polarization is observed in $\pi^+p \to K^+\Sigma^+$ (an M channel) up to 14 GeV/c.[6] This clearly indicates the breaking of the line reversal relation. However, the large polarization can be naturally accounted for by rule (1) as due to the interference effect between the expected large cut contribution in the nonflip amplitude and the flip Regge pole amplitude. The breaking of the line reversal relation (BLRR) in the differential cross section involves a comparison between the cross sections for the pair of channels. For most cases, experimental tests are only available at low energies. Typically, say at 5 GeV/c, one finds that for the integrated cross section,[7]

$$\sigma_M/\sigma_R \sim 0.45 \text{ to } 0.7$$

It was stressed by Michael some time ago[8] that the BLRR in the differential cross section observed cannot be accounted for by the breaking of the exchange degeneracy for the leading Regge poles, nor by Pomeron-Reggeon cuts. This breaking must be attributed as due to the lower lying J-plane singularities, such as the Reggeon-Reggeon cut which is, near the forward direction, at least half a unit below the Regge pole. At this stage, we do not have a detailed enough theory on Reggeon-Reggeon cuts to explain the observed breaking. However, we do expect that, as energy increases, the Reggeon-Reggeon cut contribution should fall off considerably faster than the Pomeron-Reggeon cut contribution. Based on the general properties of the Pomeron-Reggeon cut, we review the qualitative prediction on the t-dependence of the polarization for the

hypercharge exchange reactions and the general expectation of the BLRR in the differential cross section. Future experiments on $\pi^+p \to K^+\Sigma^+$, $K^-p \to \pi^-\Sigma^+$, $\pi^-p \to K^0\Lambda$, and $K^-n \to \pi^-\Lambda$ measuring the differential cross sections and polarizations at the intermediate and high energies are useful in checking these detailed predictions.

2. EVIDENCE FOR THE EMPIRICAL RULE FOR CUTS AND FURTHER EXPERIMENTAL TESTS

In this section we shall repeat some of the arguments given in Ref. 1 and add some more arguments to demonstrate the empirical rule and at the same time to stress further experimental checks.

2.1. Successes of the Regge Pole Model. We note at the very beginning here that these are cases where the Regge pole property in the flip amplitude is tested; in turn, these are evidences for supporting the rule.

2.1.1. The eight reactions.[1] They are:

$$\begin{array}{llll} \pi^-p \to \pi^0n & , \quad \pi^+p \to \pi^0\Delta^{++} & , \quad \rho & , \\ \pi^-p \to \eta^0n & , \quad \pi^+p \to \eta^0\Delta^{++} & , \quad A_2 & , \\ K^-p \to \bar{K}^0n & , \quad K^-n \to \bar{K}^0\Delta^- & , \quad A_2 + \rho & , \\ K^+n \to K^0p & , \quad K^+p \to K^0\Delta^{++} & , \quad A_2 - \rho & . \end{array} \tag{3}$$

With the simplifying assumption such as SU(3), exchange degeneracy, the dominance of the flip couplings, and the $SU(6)_W$ symmetry for the vertex functions, all the eight differential cross sections are correlated by one t-dependent function in the following manner:

$$\frac{d\sigma}{dt}(\pi^o n) = C_1 \frac{d\sigma}{dt}(\pi^o \Delta^{++}) = C_2 \sin^2 \frac{\pi\alpha}{2} F(t)\, s^{2\alpha-2} \quad ,$$

$$\frac{d\sigma}{dt}(\eta^o n) = C_1 \frac{d\sigma}{dt}(\eta^o \Delta^{++}) = C_3 \cos^2 \frac{\pi\alpha}{2} F(t)\, s^{2\alpha-2} \quad , \qquad (4)$$

$$\frac{d\sigma}{dt}(\bar{K}^o n) = \frac{d\sigma}{dt}(K^o p) = C_1 \frac{d\sigma}{dt}(\bar{K}^o \Delta^-) = C_1 \frac{d\sigma}{dt}(K^o \Delta^{++}) = F(t)\, s^{2\alpha-2} \quad ,$$

where $\alpha = 0.5 + 0.9\ t$, a nominal trajectory function and C_i's are known constants. For completeness, we illustrate the comparison between the t-dependence of the predicted differential cross section and the data in Figs. 1, 2, and 3. The relative normalization for the different reactions are in agreement with the theory in the symmetry limit to better than a factor of 2. From the comparisons, one sees that the correlation of the different t-dependence is indeed relatively successful.

We would like to make a few comments here.

(i) The line reversal equality for $K\Delta$ production and KN charge exchange is satisfied to 60-70% at 5 GeV/c.[9] So there is perhaps a 10-15% background contribution in the flip amplitude. In the KN charge exchange case, the line reversal equality is quickly restored as the energy increases. We shall look at the situation more closely in Section 3.

(ii) The $K^o\Delta^{++}$ data points in Fig. 2 near $t = -1$ deviate significantly from the prediction. The same deviation does not occur in the other three reactions. Further measurement will certainly be helpful in clarifying the situation here.

(iii) The $\eta^o n$ data do not shrink as much as that predicted by the nominal Regge trajectory function used. The data plotted has $\alpha_{eff} = 0.34 + 0.35\ t$.[10] Recent data give $\alpha_{eff} = 0.43 + 0.64\ t$.[11] Further measurement on this reaction, especially in the large $|t|$ region, will be useful in giving a quantitative estimate on the breaking of the Regge pole dominance picture.

(iv) The $\eta^0\Delta^{++}$ data from 2.3 - 8 GeV/c have been reported as giving an enormously steep trajectory function.[12] We observe that data points above 3 GeV/c (which is presumably still too low in energy) are compatible with the nominal trajectory function. In Fig. 4 we illustrate the quantity $\frac{d\sigma}{dt}/(P_L/5)^{2\alpha-2}$. We see within the experimental error, points at three energies certainly are consistent with being equal.

(v) The fact that in these reactions the $n = 1$ amplitude dominates is extracted out mainly from the turnover of the differential cross section near the forward direction, the Δ decay density matrix elements, the $\pi^{\pm}p$ polarization data, and the SU(3) couplings. There is strong evidence for the dominance of the $n = 1$ amplitude up to $t = -0.6$ GeV^2 or so.[1] Future data on the Δ matrix elements extended to larger momentum transfer, allowing analysis of the spin structure for the ρ and A_2 couplings in the same region, will certainly be useful in checking the spin flip dominance assumption used above.

2.1.2. The elastic polarizations. These are again the well-known examples for the success of Regge theory. We illustrate the $\pi^{\pm}p$ polarization data in Fig. 5.[13] The nearly mirror symmetric $\pi^{\pm}p$ polarizations are well-known to be associated with the interference effect between the predominantly imaginary nonflip contribution and the flip amplitude of the ρ. The double zero in the polarization is caused by the corresponding double zero in the real part of the Regge pole amplitude (i.e., $\mathrm{Re}\, A_F^{\rho} \propto \sin^2 \frac{\pi\alpha}{2}$).[14] Again we stress here that one is testing basically the Regge phase of the ρ in the flip amplitude. In Fig. 6 we illustrate the $K^{\pm}p$ polarization.[15] Here both polarizations correspond to what one expects from the interference between again the predominantly imaginary nonflip amplitude and the exchange degenerate ρ and A_2 contribution in the

flip amplitude.[16] For the K^+p case, the flip amplitude is purely real, giving rise to a relatively smooth and structureless polarization. For the K^-p case, the $\exp(-i\pi\alpha)$ factor gives the characteristic t-dependence indicated by the data. The sign change near $t = -1\ GeV^2$ has been argued to be correlated with the point $\alpha = -1/2$. If this is so, the flip amplitude would have approximately the exchange degenerate Regge pole phase, even at $t = -1\ GeV^2$. However, future confirmation on the phase of the nonflip amplitude is necessary in order to make it conclusive.

Thus far we have confined our discussion to the ρ and A_2 exchange. The analysis can be conveniently extended to reactions such as

$$\pi^+p \to K^+Y^{*+} \quad , \quad K^-p \to \pi^-Y^{*+} \quad ,$$

studying, e.g., α_{eff}, the density matrix elements, and line reversal tests. According to SU(3), the $n = 1$ amplitude should again dominate here. Finally, the Regge pole model is expected to work well, e.g., for the quantity

$$(\rho_{11} + \rho_{1-1}) \ \frac{d\sigma}{dt} \ (\pi N \to \rho N,\ I_t = 0)$$

Detailed measurement on this quantity can again provide a quantitative test for the rule.

2.2. The Success of the Strong Absorption Model. Now we proceed to look at the $n = 0$ amplitude, where the Regge pole model has repeatedly failed and where the strong absorption model has claimed its success; this in turn implies again the success of the empirical rule.

2.2.1. The crossover zero. This is one of the well-known difficulties in the Regge pole model which occurs in the nonflip amplitude where the cut contribution dominates. We illustrate the plot by Davier

and Harari here.[17] They considered the quantity

$$y = \left[\frac{d\sigma}{dt}(K^- p) - \frac{d\sigma}{dt}(K^+ p)\right] \Big/ \left[\frac{d\sigma}{dt}(K^+ p)\right]^{1/2} \quad . \tag{5}$$

Assuming that the Pomeron is predominantly imaginary and is contributing to the helicity nonflip amplitude, one arrives at

$$y \propto \mathrm{Im}\, A_{NF}^{(-)} \quad , \tag{6}$$

where $A_{NF}^{(-)}$ in the Regge pole model is dominated by the ω. This quantity for KN and NN is illustrated in Fig. 7.[18] Notice that the zero of the y occurs near $t = -0.2$ GeV^2. This differs considerably from the position predicted by the Regge pole model which should be around $t = -0.5$ GeV^2. So the cut contribution near $t = -0.2$ GeV^2 must have a comparable size as that of the pole to give rise to this zero. We expect the cut to dominate in the larger $|t|$ region.

It is interesting to look at the recent SLAC data on $K_L^0 p \to K_S^0 p$.[19] This is illustrated in Fig. 8. Both the ρ and the ω contribute here, with the ρ contributing mainly to the $n = 1$ amplitude while the ω contributes to the $n = 0$ amplitude. The dip structure near $t = -0.2$ GeV^2 in the 2 - 4 GeV/c region is presumably associated with the pole plus cut contribution in the nonflip amplitude, since from Fig. 7 we have already learned that there is a zero in the imaginary part of this amplitude. In the pure pole model, the dip should be at $t \sim -0.5$ GeV^2.

2.2.2. The πN charge exchange polarization. In the pure pole model, this polarization is zero. The observed non-vanishing polarization in the small $|t|$ region can plausibly be attributed to the interference effect between the cut in the nonflip amplitude and the ρ in the flip amplitude.[20]

2.2.3. The f^o trajectory. Although the Regge pole appears to work reasonably well at $t = 0$ in the $n = 0$ amplitude, it is quite curious, so far as we are aware, associated with meson exchange, there has never been any clean evidence suggesting the success of Regge pole model in the nonflip amplitude. To fit the πN elastic data, within the framework of the Regge pole model, for the f^o contribution to the $n = 0$ amplitude one needs to invoke the no-compensation mechanism, or the cyclic residue function.[21] If we assume that all trajectories choose the universal nonsense choosing mechanism, this can be considered as additional evidence against the f^o dominance assumption in the nonflip amplitude.

2.2.4. Polarization in $\pi^+p \to K^+\Sigma^+$. As mentioned in Section 1, a large polarization is observed in $\pi^+p \to K^+\Sigma^+$ at 14 GeV/c. This is naturally explained as due to the interference between the absorbed nonflip contribution and the flip Regge pole contribution. We will discuss this in more detail in Section 3.

2.2.5. The one-pion-exchange quartet. The structure in these differential cross sections near the forward direction has been explained successfully by the absorption model.[22] The comparison between an evasive pion pole prediction, the absorption model prediction, and the data is as follows:

	Data	"Evasive" Pion	Absorption Model
$\pi^-p \to \rho^o n$	dip	dip	dip
$\gamma p \to \pi^+ n$	peak	dip	peak
$pn \to np$	peak	dip	peak
$\pi^+p \to \rho^o\Delta^{++}$	peak	peak	peak

The crucial point here is that in the second and the third cases, it is precisely the cut contribution in the $n = 0$ amplitude which alters the pole prediction and successfully explains the data. Associated with the unnatural parity exchange, we have seen that there is evidence that cuts are important in the $n = 0$ amplitude. At this stage, we do not have a qualitative estimate of its importance in the $n = 1$ amplitude. So the corresponding rule for the unnatural parity exchange is unclear at the moment. We refer the reader to a recent review of Fox[23] for further discussion along this line.

2.3. The Double-Flip Amplitude. What is the empirical rule for the relative importance of cuts in this amplitude? Probably cuts are weak here. The data are inconclusive on this point. Motivated by the absorption model, one would expect that the $n = 2$ amplitude should have a cut contribution even weaker than that in the $n = 1$ amplitude. On the other hand, the dual absorptive model suggests a strong cut contribution here at least associated with, for example, the ρ exchange. The reason is as follows. In this model, one assumes that the imaginary part of the direct channel partial wave amplitude has a peripheral profile peaking around 1 Fermi. This in turn implies that

$$\text{Im } A_{n=2} \sim J_2(R\sqrt{-t}) = 0 \qquad \text{at} \quad t \approx -1 \text{ GeV}^2 \tag{7}$$

Since the ρ Regge pole term has a nonsense-wrong-signature zero at $t \sim -0.5$, a strong cut contribution here is required to shift the zero from -0.5 to -1 GeV^2. We mention that a strong cut is also predicted in the Carlitz-Kislinger model here.

Consider the reaction $\pi^+ p \to \omega^0 \Delta^{++}$. The density matrix element

$$\rho_+ = \rho_{11} + \rho_{1-1} \tag{8}$$

projects out the natural parity contribution in the exchange channel which is contributed by the $n = 0$ and $n = 2$ amplitudes. The ρ Regge pole is the relevant contributor here. It vanishes at $t = -0.5$ GeV^2. If the ρ dominates, there should again be a dip at this t value. The data are illustrated in Fig. 9. There seems to be some indication for a suppression especially in Fig. 9b near $t = -0.6$. Such a suppression, if indeed present, would imply the existence of a nonsense-wrong signature zero in the $n = 2$ amplitude, which in turn suggests that the cut in $n = 2$ amplitude is relatively weak. The differential cross section $(\rho_{11} + \rho_{1-1}) \frac{d\sigma}{dt}$ for $p_L = 3 - 4$ GeV/c is illustrated in Fig. 10.[24] For comparison, in the same figure we also illustrate a typical Regge pole fit to the data. Notice that the significant deviation between the Regge prediction and the data beyond $t = -0.3$ GeV^2 indicates the presence of a large background. The data are consistent with a slight suppression in the dip region. However, more accurate data are needed in order to make a definitive statement. An alternative way to see whether cuts are important in the $n = 2$ amplitude is to look at the density matrix element ρ_{1-1}.

From parity argument, it can be shown that at the point where the $n = 2$ amplitude vanishes, the contribution of the natural parity exchange and that of the unnatural parity exchange have to be equal, i.e.

$$\rho_+ = \rho_{11} + \rho_{1-1} = \rho_- = \rho_{11} - \rho_{1-1} \quad \text{or} \quad \rho_{1-1} = 0 \ . \tag{9}$$

Thus if the $n = 2$ amplitude is dominated by the ω exchange contribution at its nonsense-wrong-signature point, $\rho_{1-1} \approx 0$. Present data available are insufficiently accurate to extract this information. So the

determination of the t-dependence of the elements ρ_+ and ρ_{1-1} will be useful in clarifying the systematics here. From the pion photoproduction data, we expect that the contribution of the B should be relatively small in the $n = 2$ amplitude. However, to avoid the ambiguity of the B contamination, it is best to determine the quantity ρ_{1-1} at several energies.

2.4. Phenomenological Amplitudes. Let us reiterate our conclusion here. Apart from the BLRR in the differential cross section, which (as mentioned in the Introduction) we do not understand at the moment and will be discussed in some detail in the following section, qualitative features of the high energy data, say for P_L above 5 GeV/c, can be understood in terms of the following pole-cut structure:

$$\begin{aligned} &\text{EXD Regge pole + strong cuts in the } n=0 \text{ amplitude} &&, \\ &\text{EXD Regge poles in the } n=1 \text{ amplitude} &&, \qquad (10) \\ &\text{EXD Regge poles + (?) in the } n=2 \text{ amplitude} &&. \end{aligned}$$

Again, here we only consider the simple cases: $|\lambda_1-\lambda_3| = 0, 1$ and $|\lambda_2-\lambda_4| = 0, 1$. Notice that this prescription is similar to that of the Michigan model in the $n = 0$ amplitude although not in the $n = 1$ amplitude. On the other hand, it is similar to the Argonne model and the Regge pole model in the $n = 1$ amplitude but not in the $n = 0$ amplitude. So far as the detailed parameterization for the strong cut in the $n = 0$ amplitude is concerned, the possibilities are still left open so long as the cut is strong, and its energy dependence, and perhaps also its phase near $t = 0$, although not necessarily the t-dependence, are similar to those of the strong absorption model. Usually in the strong absorption

model, say the Michigan model, the central partial waves are over-absorbed. Perhaps it is desirable to avoid this by increasing the absorption radius. Anyway, quantitative analysis of the data is necessary before we can completely specify this cut parameterization.

Now we come to some possible differences between the rule stated in (1) and the dual absorptive model. In the dual absorptive model, the strength of the cut term required is determined by whether the pole term itself is already peripheral or not. If it is, then the cut is weak. If it is not, then the cut is strong. This in turn implies that the strength of the cut is sensitive to the zero intercept of the exchanged trajectory. For example, within this framework, one expects the cut strength, say in the $n = 1$ amplitude, to vary between the ρ, the K^*, and the ϕ exchange. The most convincing examples which we have considered are associated with the ρ, A_2, and ω^0 exchanges. So these examples also support the dual absorptive model. Future detailed study on the properties of cuts associated with the K^*, K^{**} exchange and also the ϕ, f' exchange are needed before we can resolve the ambiguities here.

The cut strength in the Carlitz-Kislinger model also has the same pattern as that given by Eq. (8) for $n = 0$ and 1, and it is strong for $n = 2$.[1,4] There are two comments here: (1) When the cut is strong, the CK model also predicts an asymptotic behavior $s^{\alpha(0)}$ for the amplitude. There is no experimental evidence for such a behavior. (2) Recently, Ellis showed that in his dualized version of the CK model, similar pole cut systematics also appear, although the underlying reason for such systematics is different.[25] There is an unfortunate feature in Ellis' version. It gives a wrong sign for the pion-nucleon charge exchange polarization. It remains to be seen whether both the CK model and Ellis model can be modified to agree with the data.

3. LINE REVERSAL RELATIONS

3.1. Experimental Survey. The experimental situation for the line reversal relations on the differential cross sections for the natural parity meson exchange reactions are summarized in Table 1. A review on the situation was given earlier by Lai and Louie.[26] We refer the reader to this paper for a complementary discussion. The substantial data points which are not contained in their review are:[27] the K^+n charge exchange data at 3.8 and 12 GeV/c, the K^-p charge exchange data at 3.95 GeV/c, the new SLAC $\bar{K}^0p \to K^-\Delta^{++}$ data, and some new information on the Stony Brook-Wisconsin $\pi^+p \to K^+\Sigma^+$ data. We mainly concentrate on two quantities: the ratio of the integrated cross sections and the ratio of the exponential slopes in the differential cross section. For convenience, we shall refer to the differential cross sections in the R and M channels as $|R|^2$ and $|M|^2$ respectively (remember R and M were defined in the Introduction).

Let us go through Table 1 briefly. First, the KN charge exchange data.[27] The cross sections σ_M and σ_R converge on each other rapidly, as the energy increases from 4 to 12 GeV/c, while the corresponding slopes for these reactions at each energy are about the same within the accuracy of the data. For the $K\Delta$ and $\bar{K}\Delta$ productions,[27] the ratio does not vary much with energy for data points, say, between 3 - 6 GeV/c (see Fig. 11). The ratio b_M/b_R is about the same. We mention here that in the B_5 model there are cases where unstable final state particles are treated on a different footing as compared to the stable final particles. Berger and Fox found that[28] using this model for $K\Delta$ and $\bar{K}\Delta$ productions, the difference $|R|^2 - |M|^2$ is proportional to the width of the Δ, and this difference

falls off with the usual Regge pole power law. Unfortunately, they observed that their formalism violates the unitarity relation. So the quantitative prediction of the B_5 model should not be trusted. Nevertheless, one should keep in mind that, in principle, dealing with BLRR there could be a difference between the stable particle case and the unstable particle case.

For the KY^* production,[27] the situation is illustrated in Fig. 12. Note that the error bars are quite large. Taking the trend of the data, there is apparently a factor of two difference. For the Σ production, data points only up to 7 GeV/c were considered.[27] The higher energy points included in Lai and Louie's review were preliminary results from the Stony Brook-Wisconsin group. There are large uncertainties. Presently there are indications that the cross sections, say above 10 GeV/c, could be consistent with no BLRR.[29] Unfortunately the final results are not available at this stage.

The polarization data for the Λ and the Σ productions are illustrated in Fig. 13.[30] Large polarizations are observed in all these reactions at around 3 - 4 GeV/c. The Σ polarization in $\pi^+p \to K^+\Sigma^+$ has been measured up to 14 GeV/c. There the polarization is again large. We will come back to the curves later on.

Next, the Λ production differential cross section data. The situation at 4 GeV/c is illustrated in Fig. 14.[27] Here the slope for the M reaction is substantially larger than that for the R reaction. In the energy region between 3 - 6 GeV/c, the σ_M is again smaller than σ_R.

For these reactions, the trend for the BLRR can be summarized as follows:

(1) The ratio $\sigma_M/\sigma_R < 1$ and $b_M/b_R \gtrsim 1$. Notice that there are different ways to give rise to $\sigma_M/\sigma_R < 1$. For most reactions the breaking is strong in normalization and is relatively weak in the exponent, while for the Λ production case, the breaking is strong in the slopes, while relatively weak in the absolute values of the differential cross section near $t = 0$. It is useful to confirm these systematics and find out if this trend persists at higher energies. We mention here that for all these cases considered, the differential cross sections do not exhibit a simple crossover phenomenon between $|R|^2$ and $|M|^2$ in the $|t|$ interval, say between 0.2 to 0.6 GeV^2. This turns out to be crucial in eliminating the possibility of explaining the observed BLRR in terms of the breaking of the exchange degeneracy in the pole parameters.

(2) The energy dependence. For some reactions, there is the trend for the convergence of $|R|^2$ and $|M|^2$. This is definitely observed for the KN charge exchange and there is some indication of convergence to equality in the Σ data.[30]

(3) Large polarizations are observed in the Λ and Σ productions.

To contrast with these pure natural parity exchange data, in the last row we indicate the situation for np and $\bar{p}p$ charge exchange reactions, where both natural and unnatural parity can be exchanged. The apparent "BLRR pattern" is reversed. Here $\sigma_M/\sigma_R > 1$ and $b_M/b_R < 1$. This is illustrated in Fig. 15.[31] This last pair of reactions turned out to be relatively well understood in terms of the interference effect between the ρ and A_2 contributions and the pion cut contribution in the $n = 0$ amplitude. The behavior of the np charge exchange reaction near $t = 0$ has already been quoted as an example for the success of the strong absorption model.

3.2. Regge Cuts. In the last section we have seen that the ratio σ_M/σ_R at 5 GeV/c is 0.45 to 0.7. If the Regge poles were strictly exchange degenerate, this ratio typically will require, say, about 10 - 15% background contribution having constructive and destructive interference with the pole contribution. In spite of the fact that the background required is not terribly big, at this stage we do not have a convincing model to account for the observed effect. In this subsection we will indicate the problems involved and in the following subsection we will discuss the experiments which can be helpful in checking our understandings.

3.2.1. Regge pole model. Within the pole dominance picture, the breaking means

$$\beta_+ \neq \beta_- \qquad \text{and} \qquad \alpha_+ \neq \alpha_- \tag{11}$$

where $A_\pm \sim -\beta_\pm (e^{-i\pi\alpha} \pm 1)\ s^{\alpha_\pm}$.

Then

$$|R|^2 - |M|^2 \sim -16\,\beta_+\beta_-\cos\frac{\pi\alpha_+}{2}\sin\frac{\pi\alpha_-}{2}\sin\frac{\pi}{2}(\alpha_+ - \alpha_-)\,s^{\alpha_+ + \alpha_- - 2} \tag{12}$$

and

$$P_M = -P_R \propto -8[\beta_+^{n=0}\beta_-^{n=1} - \beta_+^{n=1}\beta_-^{n=0}]\cos\frac{\pi\alpha_+}{2}\sin\frac{\pi\alpha_-}{2}\cos\frac{\pi}{2}(\alpha_+ - \alpha_-). \tag{13}$$

Within the pole dominance picture, $|R|^2 - |M|^2$, the difference of the differential cross sections must vanish at the point where $\alpha_- = 0$, since the odd signature pole amplitude vanishes here. But we have pointed out earlier that this does not occur in the data. So the observed BLRR cannot be explained within pole dominance framework. Also, according to Eq. (12), the difference on the left-hand side should have a comparable energy dependence as that for the ρ. This apparently is not the case for KN charge

exchange where the difference approaches zero rapidly. Of course, more accurate data are needed before one can make a more quantitative statement on the specific rate of approach. The Regge pole model also predicts $P(M) = - P(R)$. This prediction is not favored by the data, especially for $|t| \lesssim 0.2$ GeV^2 (see Fig. 13). Again the observed BLRR cannot be explained within the pole dominance framework. We need the interference between backgrounds and poles to achieve the observed BLRR. Once we have given up the explanation of the observed BLRR in terms of poles, there is no reason for us to believe that the pole parameters have to necessarily break the exchange degeneracy. For simplicity we shall continue to assume the exchange degeneracy for the pole parameters.

3.2.2. The Pomeron-Reggeon cut vs. the Reggeon-Reggeon cuts. It was pointed out by Michael[8] that the Pomeron-Reggeon (PR) cut calculated using the absorption model prescription gives a correction which is in the opposite direction from the observed BLRR effect. The argument is, in essence, as follows. The PR cut for the R channel is stronger than that for the M channel, since the latter has oscillations in t while the former does not. Also we recall that the PR cut interferes destructively with the pole term. So the cut gives more correction in the R channel than in the M channel. Therefore,

$$\sigma_M(R+PR) > \sigma_R(R+PR) \quad . \tag{14}$$

On the other hand, Michael observed that the Reggeon-Reggeon (RR) cut, using the same prescription (later on this will also be referred to as the box diagram prescription) gives corrections in the right direction for, e.g., the KN charge exchange case. In the original work of Michael, there is some ambiguity in specifying the intermediate states. This

becomes more obvious if we look at the $\pi^+p \to K^+Y^{*+}$ scattering. In particular, for the RR cut contribution, there is no reason to include only those box diagrams having one of the two amplitudes being an elastic amplitude. Presumably one should at least include all the possible members of the meson octet and the baryon octet and the decouplet in the intermediate states. Perhaps it is also tempting to include the vector meson nonets. This complication does not affect Michael's argument so long as the R channel is exotic. However, for those cases where the R channel is not exotic, one has to look at the various contributions explicitly. No results of this sort have been reported so far. We do not know within this framework whether or not one can account for those BLRR in, for example, the hypercharge exchange reactions. Recently, Finkelstein[32] has cast some doubts on using the box diagram prescription to estimate the normalization for the RR cut. We turn to his work next.

3.2.3. The dual-third double spectral function selection rules. By combining the expectation that diagrams which generate Regge cuts must contain third double spectral functions with the requirement of exchange degeneracy, Finkelstein derived the following selection rule for the cut. Consider the cut in the amplitude $a+b \to c+d$ due to the exchange of the two trajectories R_1 and R_2 (see Fig. 16). Let r_1 and r_2 be any particle lying on the R_1 and R_2 trajectories. The R_1R_2 cut is absent from the amplitude unless there exists a planar duality diagram connecting the process $a+r_1 \to c+r_2$ with the process $\bar{c}+r_1 \to \bar{a}+r_2$. The cuts that have been found in the non-planar dual loops of Kikkawa[33] also obey this rule. Finkelstein further argued that this rule implies, for example, that the RR cut should not contribute to the Kp elastic scattering which might be

correlated with the remarkably flat Kp cross section. The same selection rule also implies that the RR cut is absent in KN charge exchange but not in $\pi^+p \to K^+\Sigma^+$, for example. Since the box diagram prescription does not contain this selection rule, one would certainly feel somewhat uncomfortable, at this stage, to blindly estimate the strength of the RR cut using the box diagram. Apparently we have now lost Michael's argument. It remains a challenge to account for the observed BLRR, especially in the low energy regions. This is also the reason why we have to ignore the BLRR in the differential cross section in stating our prescription in Section 2.4.

Despite the uncertainties in the details of the RR and the higher order cut corrections, if it is high enough in energy, we expect that the PR cut should dominate over the other cut contributions. There it is ideal to look at the interference effect between the PR cut in the nonflip amplitude, with its phase dictated by the absorption model prescription (incidentally, there is no selection rule against a PR cut), and the Regge pole in the flip amplitude. In the following subsection we will look at the detailed prediction on the polarization for hypercharge exchange reactions from this interference effect.

3.3. The Hypercharge Exchange Reactions and the Line Reversal Tests.

3.3.1. Predictions on the polarization and the differential cross section at high energies. First we consider the spin structure in the $K^*N\bar{\Lambda}$, $K^{**}N\bar{\Lambda}$, $K^*N\bar{\Sigma}$, and $K^{**}N\bar{\Sigma}$ couplings. The situation for the quark model and for the assumptions that the $\omega N\bar{N}$ coupling is pure nonflip + SU(3) and exchange degeneracy is given as follows:

$$\text{t-channel: quark model } \left.\frac{F}{D}\right|_{++} = \infty \ , \quad \left.\frac{F}{D}\right|_{+-} = \frac{2}{3} \ ,$$

$$(\gamma_\Lambda^{++}/\gamma_\Sigma^{++})/(\gamma_\Lambda^{+-}/\gamma_\Sigma^{+-}) = -3 \ , \tag{15}$$

$$\text{s-channel: } \alpha\bar{N}N \text{ pure NF, etc., } \left.\frac{F}{D}\right|_{++} = \infty \ , \quad \left.\frac{F}{D}\right|_{+-} = \frac{1}{3} \ ,$$

$$(\gamma_\Lambda^{++}/\gamma_\Sigma^{++})/(\gamma_\Lambda^{+-}/\gamma_\Sigma^{+-}) = -1/3 \ .$$

The upshot is that if we normalize the nonflip couplings of Σ and Λ to be the same, then the sign of the flip amplitude for Λ is opposite to that for Σ. If the t-dependence of the nonflip amplitudes for these two cases is comparable, we expect the Λ polarization should have the sign opposite to that for the Σ.[30]

The theoretical prediction on the t-dependence of the polarization for the small momentum transfer region, say $|t| \lesssim 0.4$ GeV^2, is quite clean. Let us go into the argument in some detail here.[34] First for the M channel, for example $\pi^+p \to K^+\Sigma^+$, the Regge pole has the moving phase $-e^{-i\pi\alpha}$. At $t = 0$, it is in the second quadrant in the Argand plot for the amplitude (see Fig. 17a). According to the usual absorption prescription, the PR cut contribution has a phase slightly more than 180° ahead of that of the pole. To start with, the polarization is negative. As $|t|$ increases, both the pole and the cut vectors rotate in a counterclockwise manner. The pole rotates with a faster rate. When the pole is 180° out of phase with respect to the cut, the polarization vanishes. This should occur typically around $t = -0.2$ to -0.3 or so. (As energy increases, this zero should slowly move inward toward $t = 0$.) From then on, the angle subtended between the two vectors gradually decreases and the polarization becomes large and positive. For the line reversed reaction, e.g., $K^-p \to \pi^-\Sigma^+$, the Regge

pole contribution is purely real and it has the phase angle π (see Fig. 17b). For the PR cut, we first look at the case where the Pomeron is a moving pole.[35] At $t = 0$ the PR cut is again slightly more than 180° ahead of the pole. So it is above the real axis in the first quadrant, as illustrated in Fig. 17b. Near $t = 0$, the polarization is negative. As $|t|$ increases, the pole phase stays fixed while the cut phase will rotate in again a counterclockwise manner and the polarization gradually becomes large in magnitude. There is no sign change here. The solid curves in Fig. 13 are the results of Irving et al.,[30] using $\alpha_p' = 0.5$. The significance of the agreement between their prediction and the low energy data is unclear, since these predictions are expected to be valid where all the lower lying singularities are not important, while the BLRR in the differential cross section observed at these energies indicated otherwise. Nevertheless, these curves illustrate what we could anticipate at high energies. On the other hand, if $\alpha_p' = 0$, the polarization arises only through the interference effect between the pole term and the RR cut term. Thus for a flat Pomeron, at high energies, small polarization is expected in $K^- p \to \pi^- \Sigma^+$ and also in $\bar{K}N \to \pi\Lambda$. This should be the case throughout the $|t|$ region considered.

It is interesting to do accurate polarization measurements for these real reactions at high energies to distinguish between these two possibilities and also to check the detailed predictions from the PR and R interference effect. For example, a large polarization near $t = -0.2$ GeV^2 in either the R or the M channels will be incompatible with either one of the two models. The fact that the high energy polarization for the real reactions can shed some light on the slope of the Pomeron also means that

we can learn something about the phase of the diffraction amplitude from these polarization measurements.

How should the line reversal relation in the differential cross section work when the PR cut dominates? We reiterate here that we expect

$$\sigma_M^{NF} \gtrsim \sigma_R^{NF} \tag{14}$$

In the flip amplitude, since the Regge pole is assumed to dominate, we expect either the equality $|M|_F^2 = |R|_F^2$ or the crossover between $|M|_F^2$ and $|R|_F^2$ if they turned out to be not equal. It will be interesting to check these predictions.

3.3.2. Measurements on the breaking of the line reversal relations as a function of energy. We conclude our discussion on BLRR with Table 2. This table contains some of these reactions at which we have already looked. These reactions are given in column 1. In columns 2 and 3 we indicate respectively the relevant Regge trajectories exchanged and the dominant helicity amplitudes. In column 4, we indicate the experimental value of σ_M/σ_R at 5 GeV/c; again they range from 0.45 to 0.7. We want to stress that although the numbers are within a factor of 2, the similarity of these numbers is quite fortuitous. In fact, in the following discussion, we show that they are to be associated with different energy dependence. This point has been stressed recently by Finkelstein[32] and also by Irving et al.[30] So it is useful to measure the BLRR as a function of energy to confirm or deny this.

For the purpose of our discussion, it is convenient to divide the poles and cuts into two categories: those having the J-plane singularities near α at $t = 0$ (leading singularities) and those which are at least 1/2 unit below the leading ones (non-leading singularities).

The leading singularities: (a) Poles. In the limit of exchange degeneracy, poles give $\sigma_M/\sigma_R = 1$. Presently we do not know the amount of this breaking. The difference in the breaking, say, between ρA_2 and $K^* K^{**}$, will reflect itself in the difference between the BLRR for the first two and the last two reactions of Table 2. Next, the B_5 model distinguishes the ΔY^* productions from the other two reactions.
(b) Pomeron-Reggeon cuts. The PR cut dominates the nonflip amplitude, thus giving a relatively large cut correction to the ratio σ_M/σ_R making it bigger. In the table, we indicate this by two arrows pointing upward. The PR cut contribution to the flip amplitude is relatively weak, so the flip amplitudes receive only one arrow, again pointing upward.

The non-leading singularities: They contain higher order cuts in R, daughter trajectories, and other lower lying trajectories. These contributions are presumably the ones which are responsible for the observed pattern in the BLRR in the differential cross sections around 5 GeV/c. In the first two reactions of Table 2, the RR cuts are absent, while they are present in the last two reactions. The lower lying trajectories can also further confuse the issue here.

A glance at Table 2 reveals that hidden beneath the simple observed ratio "0.45 to 0.7" there appear to be many different mechanisms operating. Despite the fact that BLRR systematics appear to be simple -- i.e., a strong "absorption" in the M channel and a relatively weak "absorption" in the R channel; or alternatively a strong "absorption" in the imaginary part of the amplitude and a relatively weak "absorption" in the real part of the amplitude -- our present knowledge on poles and cuts indicates that the energy dependence of σ_M/σ_R for the different reactions is expected to

be different. If the pole-cut picture is relevant here, future accurate measurements on the energy dependence of the difference $|M|^2 - |R|^2$ should reveal this complexity. These measurements will also be useful in determining at what stage the leading singularities should begin to dominate. This will also facilitate the interpretation of the polarization measurements suggested in the previous subsection.

4. SUMMARY

In the first part of this paper, we are interested in the empirical systematics in the hadron scattering data. We have reviewed the experimental situation and have seen that there is a relatively simple empirical pattern, which correctly describes the success and the failure of the Regge pole model in the $n = 0$ and 1 amplitudes. This pattern has been most extensively demonstrated for the natural parity meson exchange. As mentioned in the Introduction, the qualitative feature of this pattern can be understood in terms of various absorption models and also the Carlitz-Kislinger model. However, if we want to be more quantitative, the dual absorptive model is, by far, most successful in "explaining" these empirical systematics. At this stage, the empirical pattern for the $n = 2$ amplitude is unclear. This can be established through the study of the ω density matrix elements in the reaction $\pi^+ p \to \omega^o \Delta^{++}$. The importance of this particular measurement can hardly be overemphasized. It can help us to uncover the underlying reason for the systematics, in particular, whether the importance of cuts is simply related to the number n: i.e., it is important in $n = 0$, less important in $n = 1$, and least important in $n = 2$; or whether it is connected with the dual optical picture; or with something else.

We have also discussed the breaking of the line reversal relations and looked at our present theoretical understanding, or rather the lack of understanding, for the systematics of the breaking in the differential cross section. Future experiments studying the energy variation of this breaking can help us to verify or deny our present theoretical viewpoint. Confirmation on the different systematics for the Λ and Σ differential cross sections will also be desirable. At high energies, there are relatively simple predictions on the Λ and Σ polarizations based on the absorption model. Measurements on these polarizations can test directly the presently popular absorption picture.

5. ACKNOWLEDGEMENTS

I would like to thank Geoffrey Fox for his encouragement of the present work, enlightening discussions, and the critical reading of the manuscript. Thanks also to George Gidal, Robert Worden, and Yair Zarmi for useful conversations.

TABLE 1. Experimental Data

M	R	Trajectories	P_L	σ_M/σ_R	b_M/b_R	Figures	Ref.
$K^-p \to \bar{K}^o n$	$K^+n \to K^o p$	$\rho\ A_2$	3.95, 3.8	0.55 ± 0.1*			a,b
			5, 5.5	0.7 ± 0.15	~ 1		c,d
			12.3, 12	1 ± 0.15			c,e
$K^-n \to \bar{K}^o\Delta^-$ $\bar{K}^o p \to K^-\Delta^{++}$	$K^+p \to K^o\Delta^{++}$	$\rho\ A_2$	3 - 6†	~ 0.65	~ 1	11	f
$\pi^+p \to K^+Y^{*+}$	$K^-p \to \pi^-Y^{*+}$	$K^*\ K^{**}$	4 - 6†	~ 0.5 (?)	$\gtrsim 1$	12	g
$\pi^+p \to K^+\Sigma^+$	$K^-p \to \pi^-\Sigma^+$ $K^-n \to \pi^-\Lambda$	$K^*\ K^{**}$	4 - 7†	0.45	$\gtrsim 1$		h
$\pi^-p \to K^o\Lambda$	$K^-p \to \pi^o\Lambda \times 2$ $\bar{K}^o p \to \pi^+\Lambda$	$K^*\ K^{**}$	3 - 6†	~ 0.3 to 0.5	~ 2	14	g
$\bar{p}p \to \bar{n}n$	$pn \to np$	$\pi\ \rho\ A_2$	8	> 1	< 1	15	i

REFERENCES FOR TABLE 1

* The integrated cross sections are:

K^+n		K^-p	
3.8 GeV/c	475 ± 90 μb**	3.95 GeV/c	258 ± 15 μb
5.5	193 ± 30 μb	5	151 ± 18 μb
12	44.5 ± 5.1 μb	12.3	45 ± 5 μb

**We have assumed 8% deuterium correction for the K^+n data.

† Experimental situation at higher energies is not clear at this stage.

a. L. Moscoso et al., Physics Letters 32B, 513 (1970).

b. B. Eisenstein et al., University of Illinois preprint, paper submitted to Kiev Conference (1970).

c. P. Astbury et al., Physics Letters 23, 396 (1966).

d. D. Cline et al., Nucl. Phys. B22, 247 (1970).

e. A. Firestone et al., Phys. Rev. Letters 25, 958 (1970).

f. A. D. Brody et al., SLAC-PUB-823 (1971), Fig. 22.

g. K. W.Lai and J. Louie, Nucl. Phys. B19, 205 (1970).

h. J. Kirz, Proceedings of Third International Conference on High Energy Collisions (Gordon and Breach Publishers, 1969), p. 59.

i. W. Beusch et al., CERN-Imperial College collaboration, paper submitted to Kiev Conference (1970).

TABLE 2. J-Plane Complications

	α	H-amps.	σ_M/σ_R	EXD R	B_5	RP	Sel. Rule	L.L. traj. daughters
$K^-p \to \bar{K}^o n$ $K^+n \to K^o p$	$\rho\ A_2$	$n = 1$	~ 0.7	1	1	$\uparrow$	RRR	
$K^-n \to \bar{K}^o \Delta^-$ $K^+p \to K^o \Delta^{++}$	$\rho\ A_2$	$n = 1$	~ 0.65	1	$\neq 1$	$\uparrow$	RRR	
$\pi^+p \to K^+\Sigma^+$ $K^-p \to \pi^-\Sigma^+$	$K^*\ K^{**}$	$n = 0$ $n = 1$	~ 0.45	1	1	$\uparrow\uparrow$ $\uparrow$	RR	no predictions
$\pi^+p \to K^+Y^{*+}$ $K^-p \to \pi^-Y^{*+}$	$K^*\ K^{**}$	$n = 1$	~ 0.5	1	$\neq 1$	$\uparrow$	RR	

REFERENCES

1. C. B. Chiu, "The Role of Regge Poles and Cuts in High Energy Phenomenology", Caltech preprint CALT-68-281 (1970), Nucl. Phys. (to be published).
2. For a review on the absorption models, see, for example, J. D. Jackson, Rev. Mod. Phys. 42, 12 (1970).
3. H. Harari, Proceedings of the Daresbury Conference (Liverpool, 1969), p. 107; "A Dual Absorptive Model for Dips in Inelastic Hadron Processes", SLAC preprint (1971); see also Ref. 17.
4. R. Carlitz and M. Kislinger, Phys. Rev. D2, 336 (1970).
5. H. Harari, Phys. Rev. Letters 22, 562 (1969); J. Rosner, Phys. Rev. Letters 22, 689 (1969).
6. See Fig. 13 for the polarization data.
7. See Table 1 for further details.
8. C. Michael, Nucl. Phys. B13, 644 (1969).
9. See Table 1.
10. R.J.N. Phillips and W. Rarita, Physics Letters 19, 598 (1965).
11. M. Spiro and A. Derem, Nuovo Cimento Letters 1, 81 (1971).
12. D. F. Grether and G. Gidal, Phys. Rev. Letters 26, 792 (1971).
13. R. J. Esterling et al., Phys. Rev. Letters 21, 1410 (1968).
14. C. B. Chiu, R.J.N. Phillips, and W. Rarita, Phys. Rev. 153, 1485 (1967).
15. The 6 GeV/c K^+p data: M. Borghini et al., Physics Letters 31B, 405 (1970). The 10 GeV/c K^-p data: L. Dick, "Some New Experimental Results with Polarized Targets", to be published in Phenomenology in Particle Physics (1971).

16. See, for example, R. C. Arnold and R. K. Logan, Phys. Rev. 177, 2318 (1969).

17. M. Davier and H. Harari, "Elastic $K^{\pm}p$ Scattering and a Dual Absorptive Model", SLAC-PUB-893 (197).

18. For the pp and $\bar{p}p$ plot, we have used the 5 GeV/c pp data in the Ph.D. thesis of A. R. Clyde, University of California at Berkeley (unpublished); the $\bar{p}p$ data is from CERN-Orsay-Paris-Stockholm collaboration (1971).

19. A. D. Brody et al., SLAC-PUB-888 (1971).

20. There is no quantitative fit to the πN charge exchange data in terms of the strong absorption model. This presumably should be attributed to the unrealistic strong cut in the $n = 1$ amplitude.

21. C. B. Chiu, S. Y. Chu, and L. L. Wang, Phys. Rev. 161, 1563 (1967); V. Barger and R.J.N. Phillips, Phys. Rev. Letters 20, 564 (1968).

22. See, for example, P. R. Stevens, Phys. Rev. D1, 2523 (1970).

23. G. C. Fox, "The Importance of Being an Amplitude", to be published in Phenomenology in Particle Physics (1971).

24. The $\pi^+p \to \omega^0\Delta^{++}$ data:

    (a) 2.67 GeV/c: W. Ko et al., UCRL-19779, paper submitted to the Kiev Conference (1970);

    (b) 2.95 - 4.08 GeV/c: D. Brown et al., Phys. Rev. D1, 3053 (1970);

    (c) 3.7 GeV/c: G. S. Abrams et al., Phys. Rev. Letters 25, 617 (1970);

    (d) 5 GeV/c: C. L. Pols et al., Nucl. Phys. B25, 109 (1970);

    (e) ABC Collaboration, Nucl. Phys. B8, 45 (1968).

25. S. Ellis, private communication (1971).

26. See Ref. g of Table 1.

27. For all data quoted here, see the references in Table 1.

28. E. L. Berger and G. C. Fox, "Broken Exchange Degeneracy and Interference Effects Between Resonances on a Dalitz Plot", Caltech preprint (1971).

29. A. Bashian et al., Stony Brook-Wisconsin preprint, paper submitted to the Kiev Conference (1970).

30. A. C. Irving, A. D. Martin, and C. Michael, CERN preprint TH-1304 (1971). For the polarization data points illustrated, we refer the reader to Ref. 3 of this paper.

31. W. Beusch et al., CERN-Zurich-Imperial College collaboration, paper submitted to the Kiev Conference (1970).

32. J. Finkelstein, CERN preprint TH-1306 (1971).

33. K. Kikkawa, Phys. Rev. 187, 2249 (1969).

34. See, for example, A. Krzywicki and J. Tran Thanh Van, Physics Letters 30B, 185 (1969); also Arnold et al. in Ref. 16 and Irving et al. in Ref. 30.

35. This case was considered, for example, by Krzywicki et al. of Ref. 34 and by Irving et al. of Ref. 30.

FIGURE CAPTIONS

Fig. 1: (a) A comparison between the predicted curves and the data at 5.9 and 18.2 GeV/c, from Ref. 1.

(b) A comparison between the $\pi^+ p \to \pi^0 \Delta^{++}$ data points and the $\pi^- p \to \pi^0 n$ experimental cross section indicated by the solid curves, from Ref. 1.

Fig. 2: A comparison between the predicted curves and the data, from Ref. 1.

Fig. 3: A comparison between the predicted curves and the data, from Ref. 1. The dashed line in (a) corresponds to what one obtains when there is no shrinkage, and that in (b) corresponds to a pure flip contribution near $t = 0$, from Ref. 1.

Fig. 4: The differential cross sections for $\pi^+ p \to \eta^0 \Delta^{++}$. The ordinate corresponds to the quantity $(\frac{d\sigma}{dt})/(\frac{P_L}{5})^{2\alpha-2}$ with $\alpha = 0.5 + 0.9\ t$. Data points: O 3.64 GeV/c, Δ 5 GeV/c, and $\square$ 8 GeV/c. See Ref. 12 for further information on the data.

Fig. 5: The proton polarization in $\pi^{\pm} p$ elastic scattering. See Ref. 13 for the data.

Fig. 6: The $K^{\pm} p$ polarization vs. t. See Ref. 15 for the data.

Fig. 7: The differences of $K^- p$ and $K^+ p$ and of $\bar{p}p$ and pp differential cross sections vs. t. The solid line corresponds to

$$y = \left[\frac{d\sigma}{dt}(K^- p) - \frac{d\sigma}{dt}(K^+ p)\right] \Big/ \left[\frac{d\sigma}{dt}(K^+ p)\right]^{1/2} ,$$

and the solid points correspond to

$$y = \left[\frac{d\sigma}{dt}(\bar{p}p) - \frac{d\sigma}{dt}(pp)\right] \Big/ \left[\frac{d\sigma}{dt}(\bar{p}p) + \frac{d\sigma}{dt}(pp)\right]^{1/2} ,$$

with both curves normalized to 1 at $t = 0$. The dashed line illustrates the Regge pole contribution to the same quantity.

Fig. 8: The differential cross section for $K_L^o p \to K_S^o p$, from Ref. 19.

Fig. 9: The density matrix element $\rho_+ = \rho_{11} + \rho_{1-1}$ from the reaction $\pi^+ p \to \omega^o \Delta^{++}$: (a) 2.7 GeV/c, Ref. 24a; (b) $\square$, 3.7 GeV/c, Ref. 24c, $\triangle$, 3 - 4 GeV/c, Ref. 24b; (c) 5 GeV/c, Ref. 24d; and (d) 8 GeV/c, Ref. 24e.

Fig. 10: The quantity $\rho_+ \frac{d\sigma}{dt}$ at $P_L = 3 - 4$ GeV/c plotted vs. t. The dashed curve is drawn to guide the eye. The solid curve is a typical Regge pole prediction, where $|A| = \alpha\, t\, C\, e^{at}$ with $a = 4$, $c = 16$, and $\alpha = 0.5 + 0.9\, t$. Circles are data points multiplied by ρ_+ of the solid curve in Fig. 9b. The crosses indicate the corresponding quantities when multiplied by ρ_+ of the dashed curve in the same figure.

Fig. 11: Cross sections for $K\Delta$ production vs. P_L, from Brody et al. of Ref. f in Table 1.

Fig. 12: Comparison between the reactions $\pi^+ p \to K^+ Y^{*+}(1385)$ and $K^- p \to \pi^- Y^{*+}(1385)$: (a) b vs. P_L or s; (b) σ vs. P_L, from Lai and Louie of Ref. g in Table 1.

Fig. 13: Polarization for Λ and Σ productions. Curves are results from the pole plus Pomeron-Reggeon cut model at $s = 11$ GeV^2, from Irving et al. of Ref. 30.

Fig. 14: (a) Comparison between the differential cross section of $K^- n \to \Lambda\pi^-$ at 3.9 GeV/c (data points) and that of $\pi^- p \to \Lambda K^o$ at 4 GeV/c (shaded area).

(b) The polarization of Λ for the reaction $K^- n \to \Lambda\pi^-$ at 3.9 GeV/c, from Lai and Louie of Ref. g in Table 1.

Fig. 15: Differential cross section of $\bar{p}p \to \bar{n}n$ (solid points) and $np \to pn$ (open points) at 8 GeV/c, from Beusch et al. of Ref. 31.

Fig. 16: (a) The R_1R_2 cut diagram.

(b) The particle-Reggeon amplitude drawn in two equivalent ways.

Fig. 17: Argand diagrams illustrating the phase of the exchange degenerate Regge pole R and the Pomeron-Reggeon cut:

(a) in the M-channel,

(b) in the R-channel.

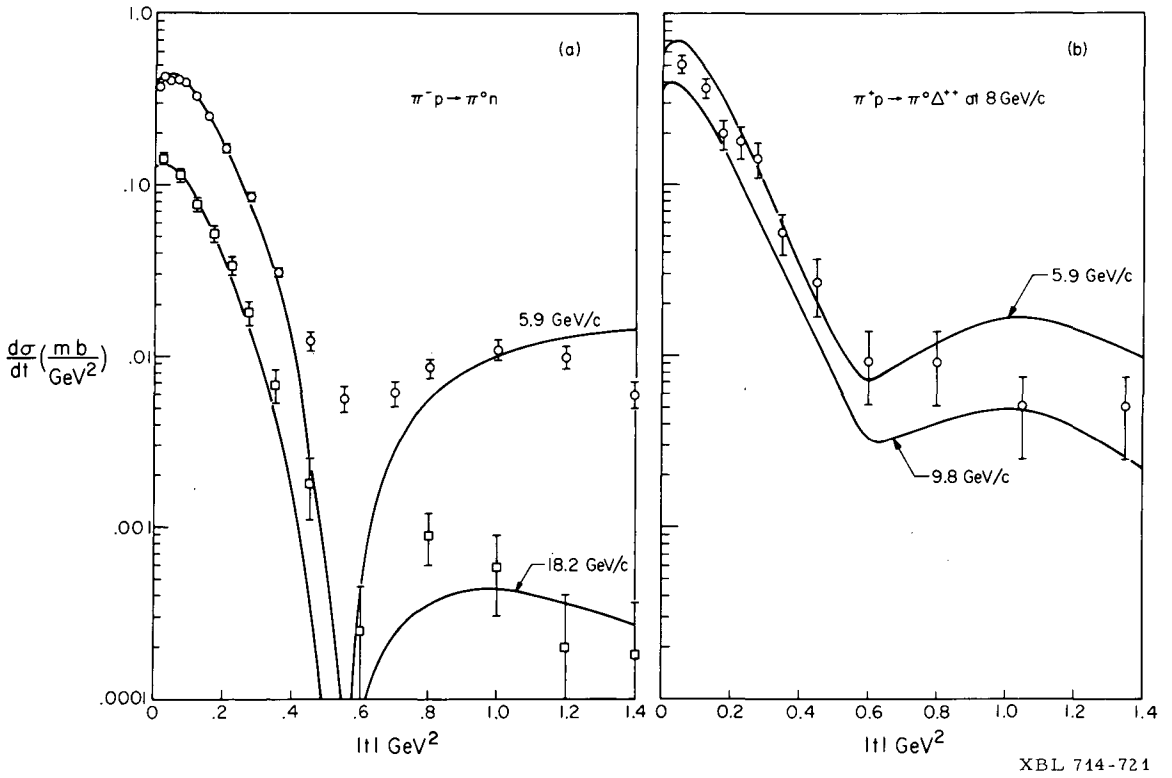
(a)
$\pi^- p \to \pi^0 n$
5.9 GeV/c
18.2 GeV/c
$\frac{d\sigma}{dt}\left(\frac{mb}{GeV^2}\right)$
1.0
.10
.01
.001
.0001
0
.2
.4
.6
.8
1.0
1.2
1.4
$|t|$ GeV^2
(b)
$\pi^+ p \to \pi^0 \Delta^{++}$ at 8 GeV/c
5.9 GeV/c
9.8 GeV/c
0
0.2
0.4
0.6
0.8
1.0
1.2
1.4
$|t|$ GeV^2
XBL 714-721

Fig. 1.

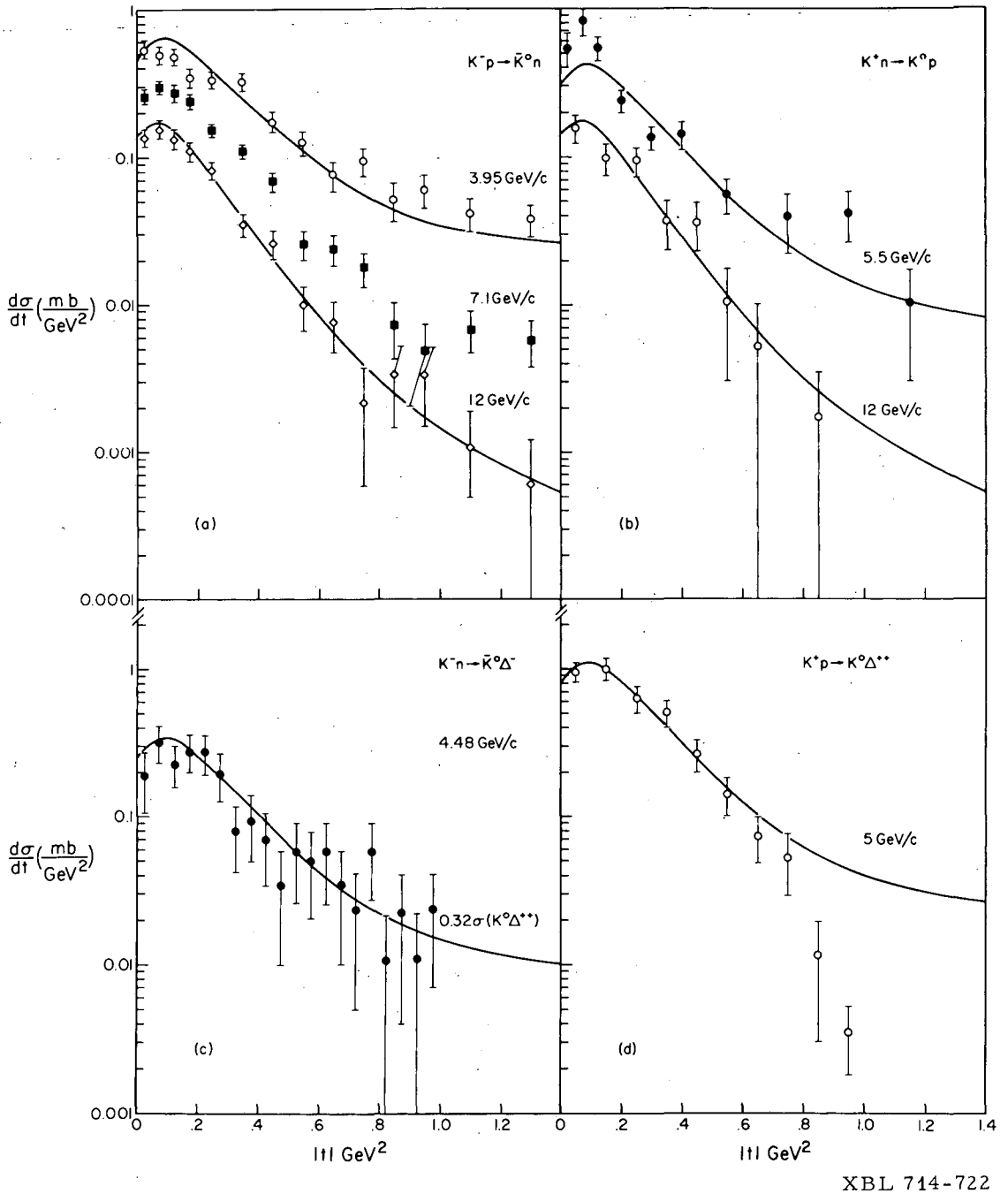
K⁻p→K̄°n
3.95 GeV/c
7.1 GeV/c
12 GeV/c
(a)
K⁺n→K°p
5.5 GeV/c
12 GeV/c
(b)
K⁻n→K̄°Δ⁻
4.48 GeV/c
0.32σ(K°Δ⁺⁺)
(c)
K⁺p→K°Δ⁺⁺
5 GeV/c
(d)
dσ/dt (mb/GeV²)
|t| GeV²
XBL 714-722

Fig. 2.

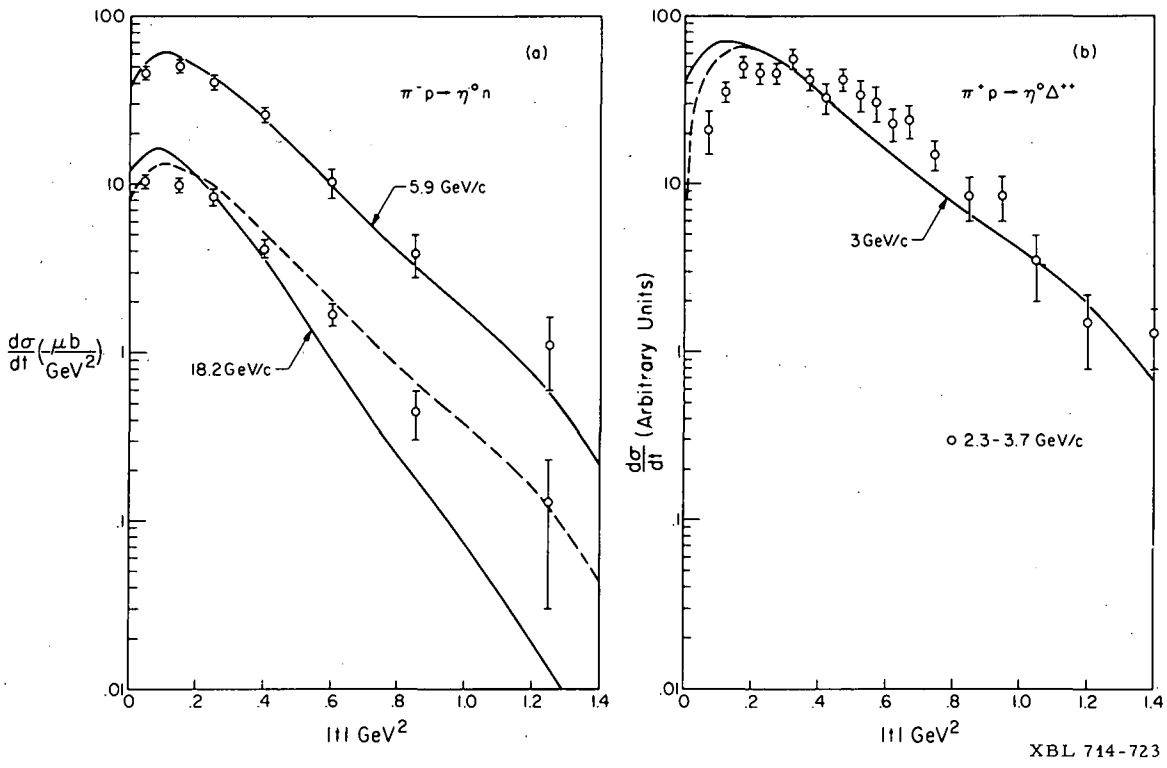
(a)
$\pi^- p \to \eta^0 n$
5.9 GeV/c
18.2 GeV/c
$\frac{d\sigma}{dt}\left(\frac{\mu b}{GeV^2}\right)$
$|t|$ GeV^2
(b)
$\pi^+ p \to \eta^0 \Delta^{++}$
3 GeV/c
o 2.3-3.7 GeV/c
$\frac{d\sigma}{dt}$ (Arbitrary Units)
$|t|$ GeV^2
XBL 714-723

Fig. 3.

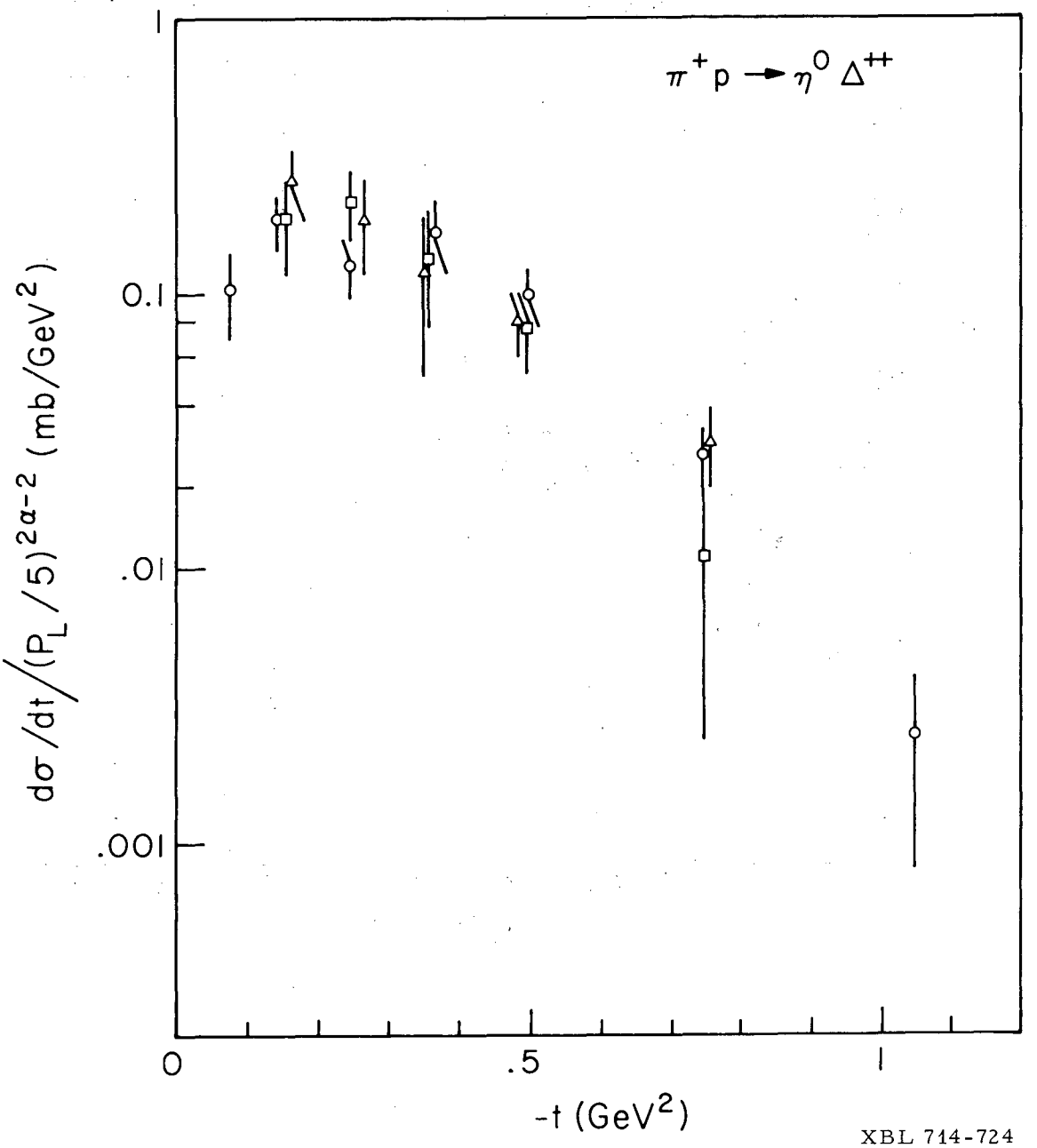
$\pi^+ p \rightarrow \eta^0 \Delta^{++}$
1
0.1
.01
.001
$d\sigma/dt/(P_L/5)^{2\alpha-2}$ (mb/GeV^2)
0
.5
1
-t (GeV^2)
XBL 714-724

Fig. 4.

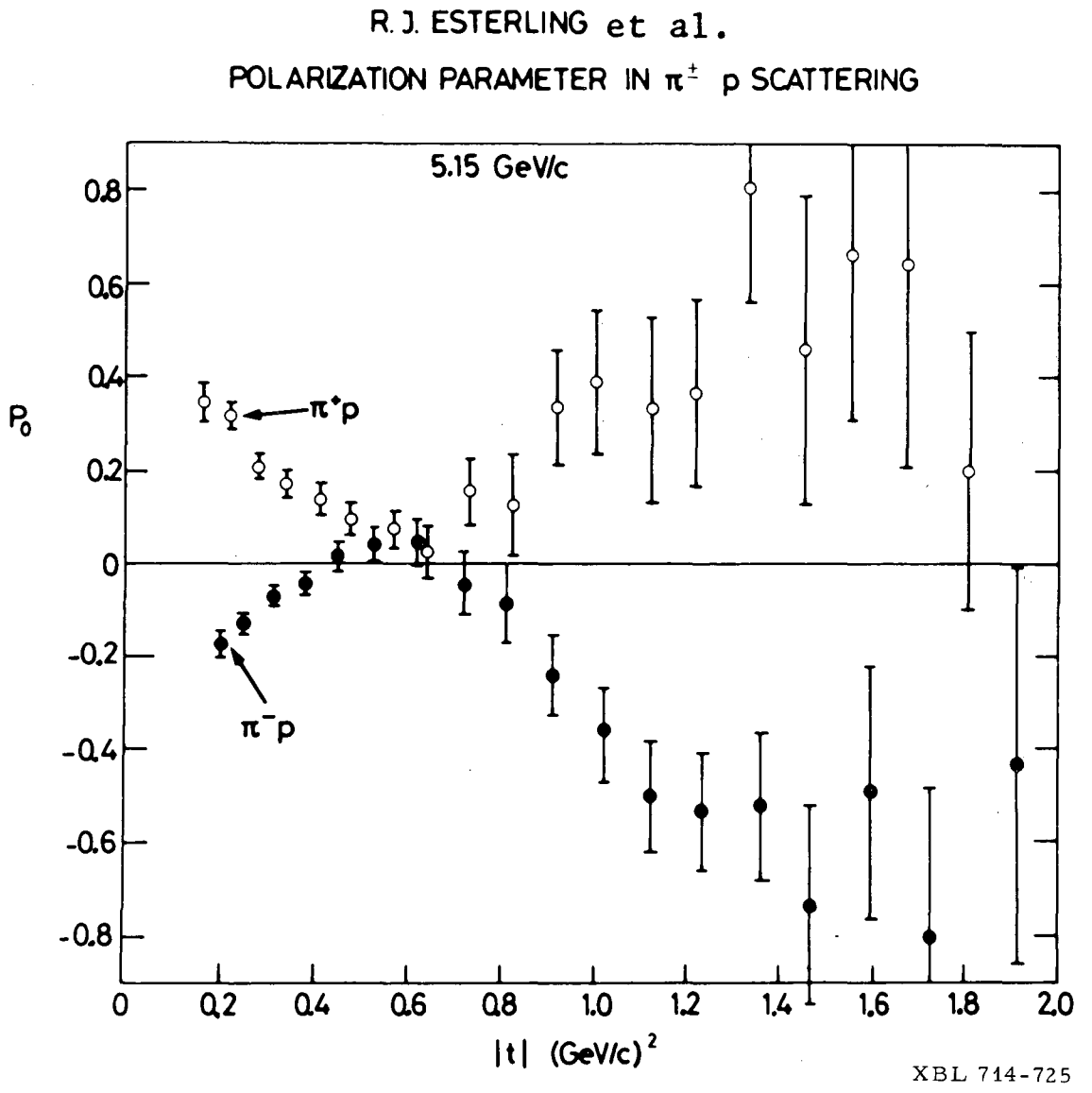
R. J. ESTERLING et al.
POLARIZATION PARAMETER IN π± p SCATTERING
5.15 GeV/c
π⁺p
π⁻p
P0
0.8
0.6
0.4
0.2
0
-0.2
-0.4
-0.6
-0.8
0
0.2
0.4
0.6
0.8
1.0
1.2
1.4
1.6
1.8
2.0
|t| (GeV/c)²
XBL 714-725

Fig. 5.

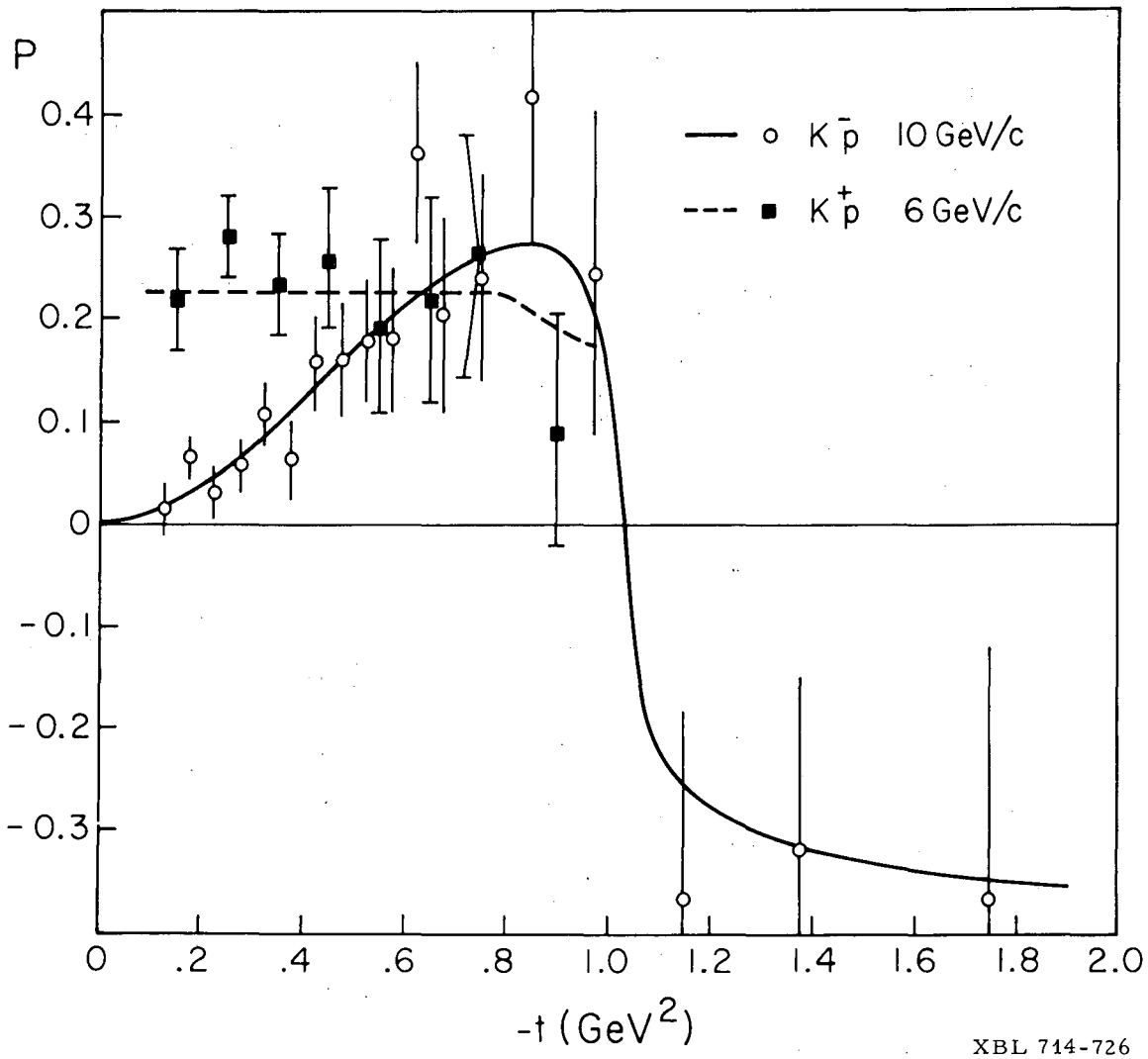
P
0.4
0.3
0.2
0.1
0
-0.1
-0.2
-0.3
0
.2
.4
.6
.8
1.0
1.2
1.4
1.6
1.8
2.0
-t (GeV²)
K⁻p 10 GeV/c
K⁺p 6 GeV/c
XBL 714-726

Fig. 6.

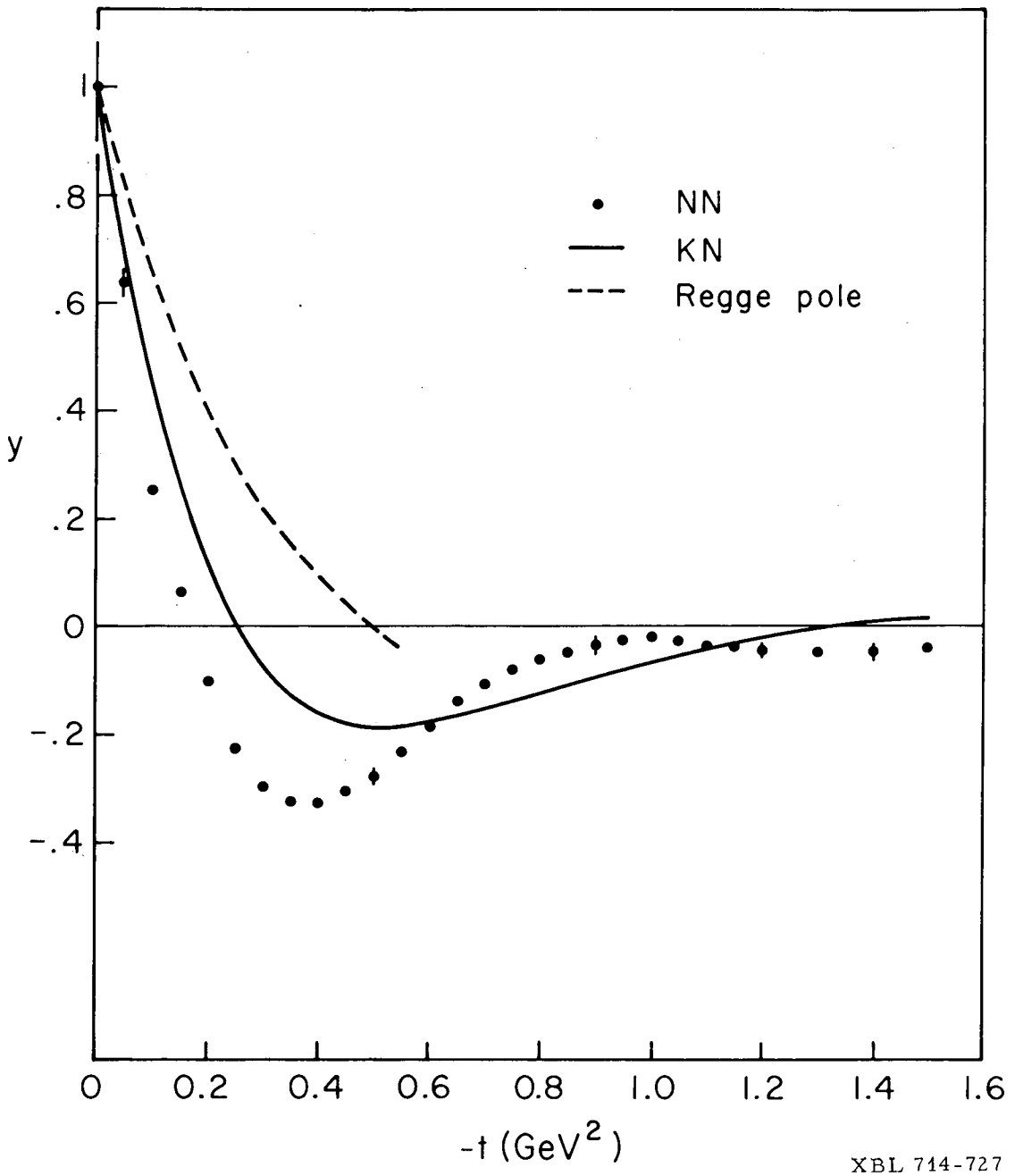
NN
KN
Regge pole
y
1
.8
.6
.4
.2
0
-.2
-.4
0
0.2
0.4
0.6
0.8
1.0
1.2
1.4
1.6
-t (GeV^2)
XBL 714-727

Fig. 7.

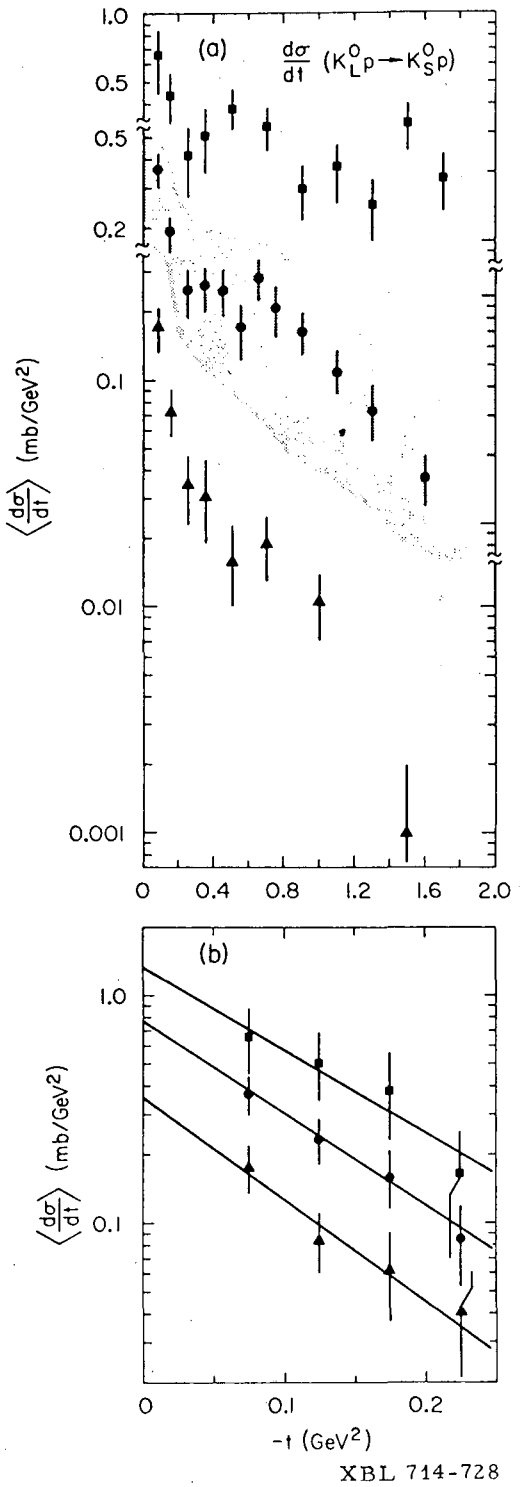
(a)
$\frac{d\sigma}{dt}$ ($K_L^0 p \to K_S^0 p$)
$\left\langle \frac{d\sigma}{dt} \right\rangle$ (mb/GeV^2)
1.0
0.5
0.5
0.2
0.1
0.01
0.001
0
0.4
0.8
1.2
1.6
2.0
(b)
$\left\langle \frac{d\sigma}{dt} \right\rangle$ (mb/GeV^2)
1.0
0.1
0
0.1
0.2
-t (GeV^2)
XBL 714-728

Fig. 8.

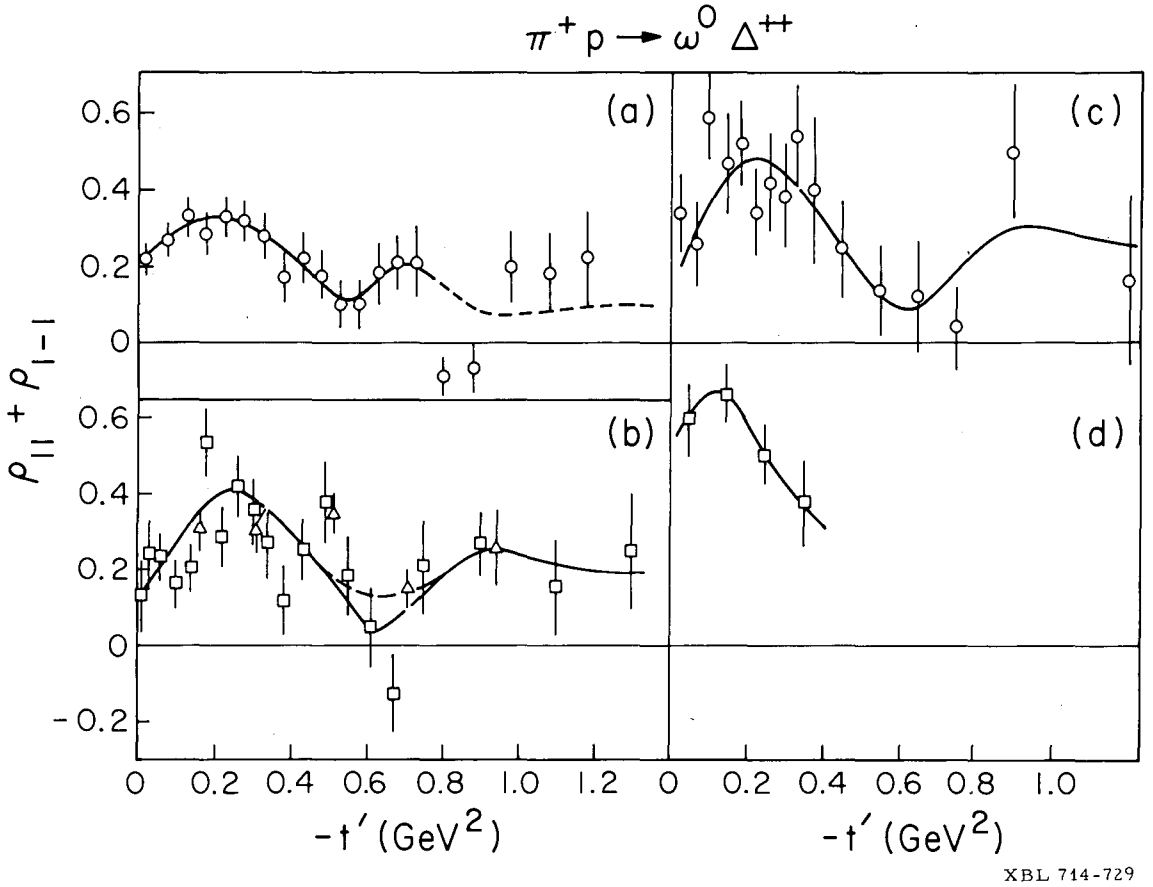
$\pi^+ p \rightarrow \omega^0 \Delta^{++}$
(a)
(b)
(c)
(d)
$\rho_{11} + \rho_{1-1}$
0.6
0.4
0.2
0
-0.2
0 0.2 0.4 0.6 0.8 1.0 1.2
$-t'(GeV^2)$
XBL 714-729

Fig. 9.

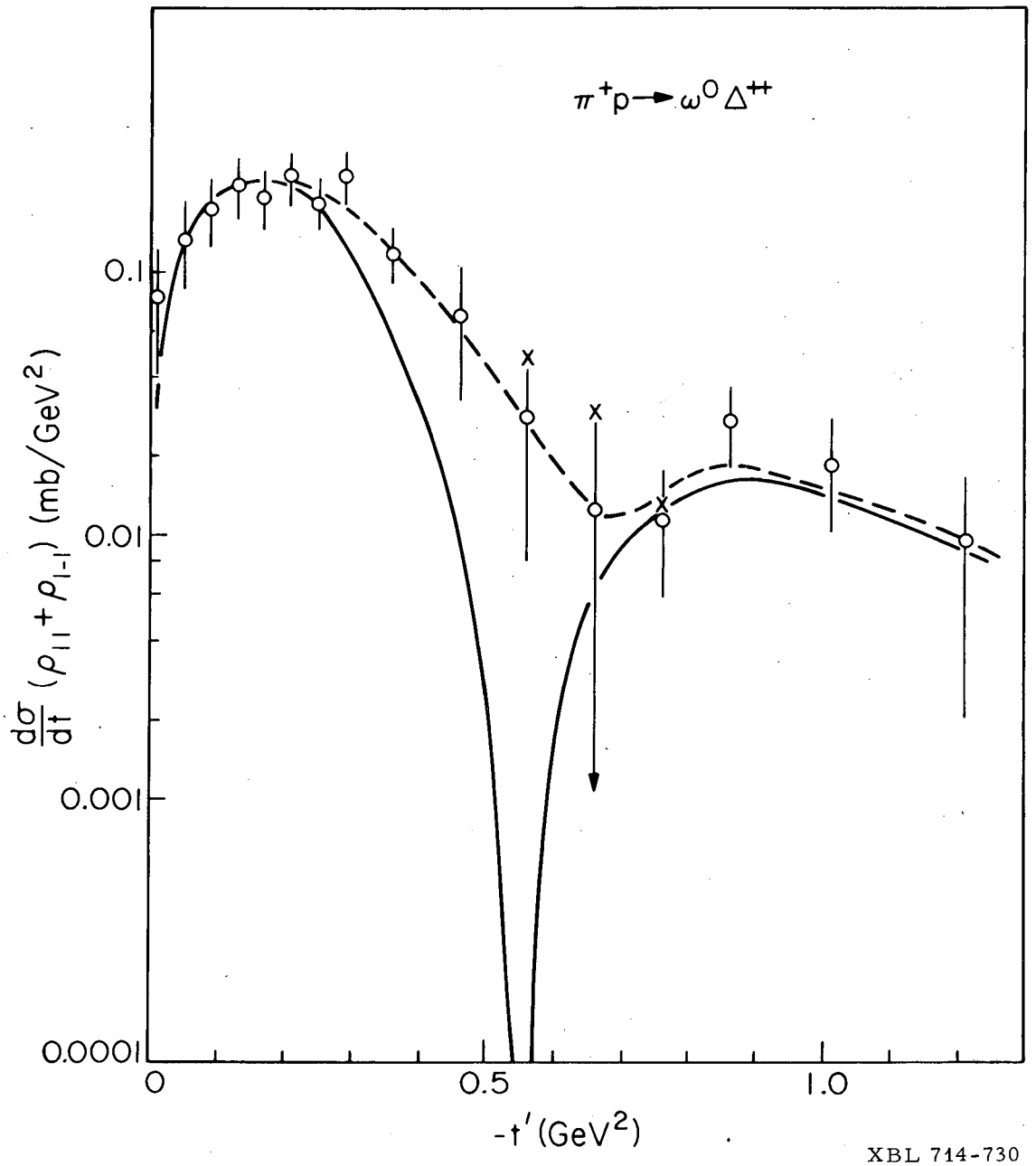
$\pi^+ p \rightarrow \omega^0 \Delta^{++}$
$\frac{d\sigma}{dt}(\rho_{11}+\rho_{1-1})$ (mb/GeV^2)
0.1
0.01
0.001
0.0001
0
0.5
1.0
$-t'$(GeV^2)
XBL 714-730

Fig. 10.

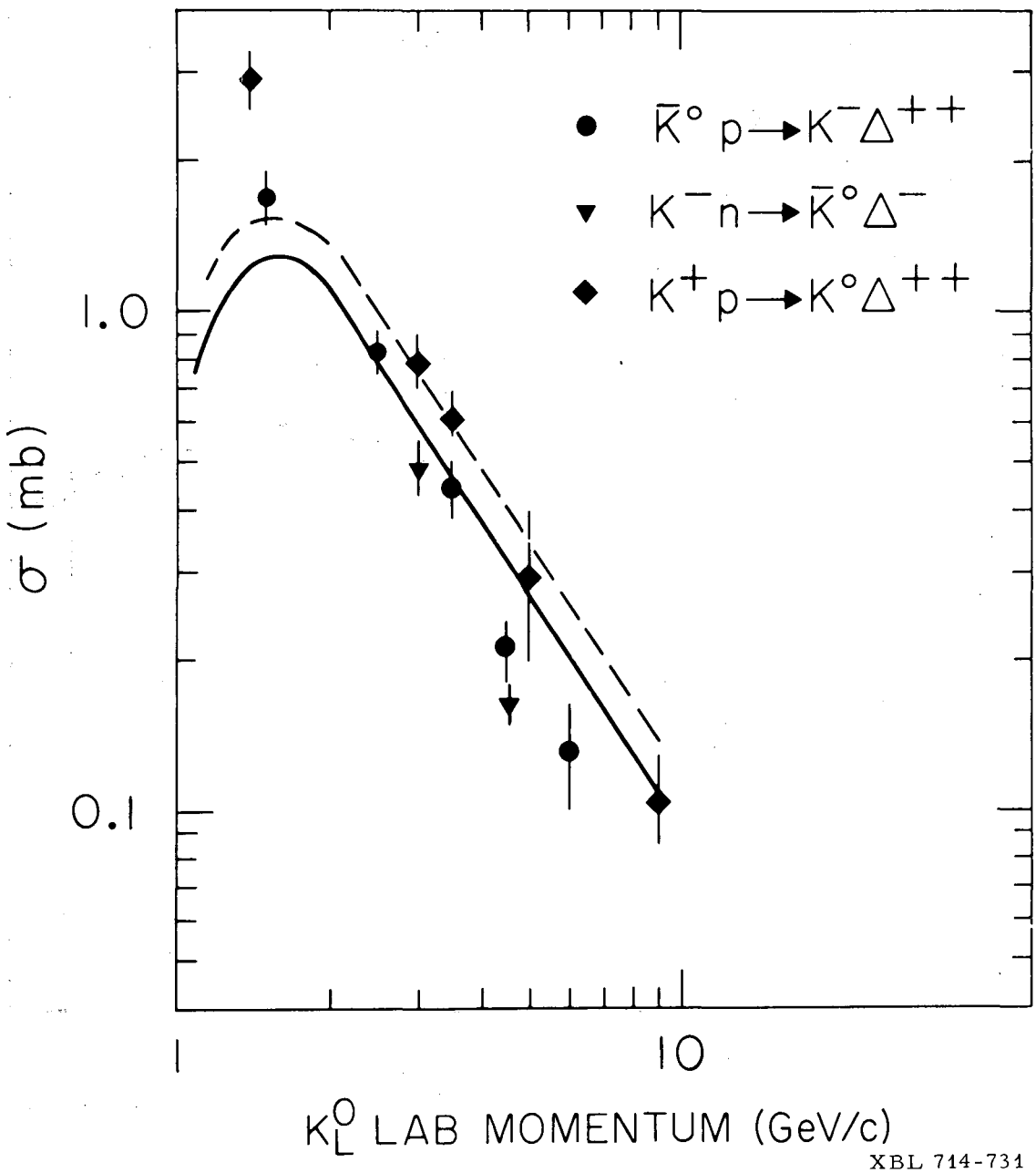
$\bar{K}^0 p \rightarrow K^- \Delta^{++}$
$K^- n \rightarrow \bar{K}^0 \Delta^-$
$K^+ p \rightarrow K^0 \Delta^{++}$
1.0
0.1
σ (mb)
1
10
K_L^0 LAB MOMENTUM (GeV/c)
XBL 714-731

Fig. 11.

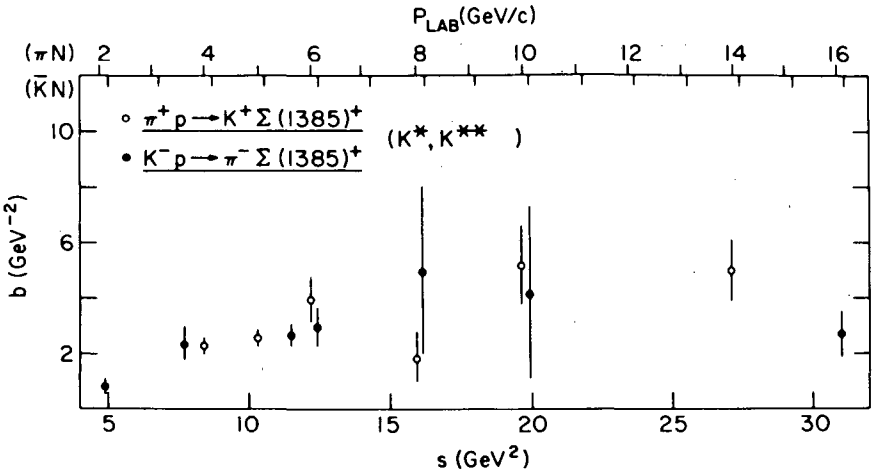
P_LAB(GeV/c)
(πN) 2 4 6 8 10 12 14 16
(K̄N)
10
6
2
b (GeV⁻²)
π⁺p → K⁺Σ(1385)⁺
K⁻p → π⁻Σ(1385)⁺
(K*, K**)
5 10 15 20 25 30
s (GeV²)

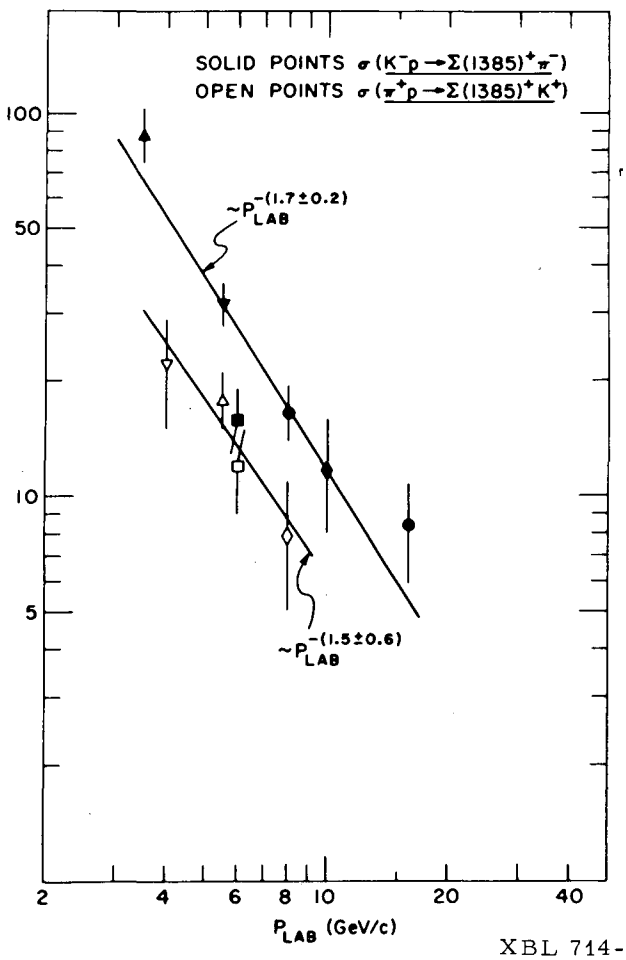
SOLID POINTS σ(K⁻p → Σ(1385)⁺π⁻)
OPEN POINTS σ(π⁺p → Σ(1385)⁺K⁺)
100
50
10
5
~P_LAB^-(1.7±0.2)
~P_LAB^-(1.5±0.6)
2 4 6 8 10 20 40
P_LAB (GeV/c)
XBL 714-732

Fig. 12.

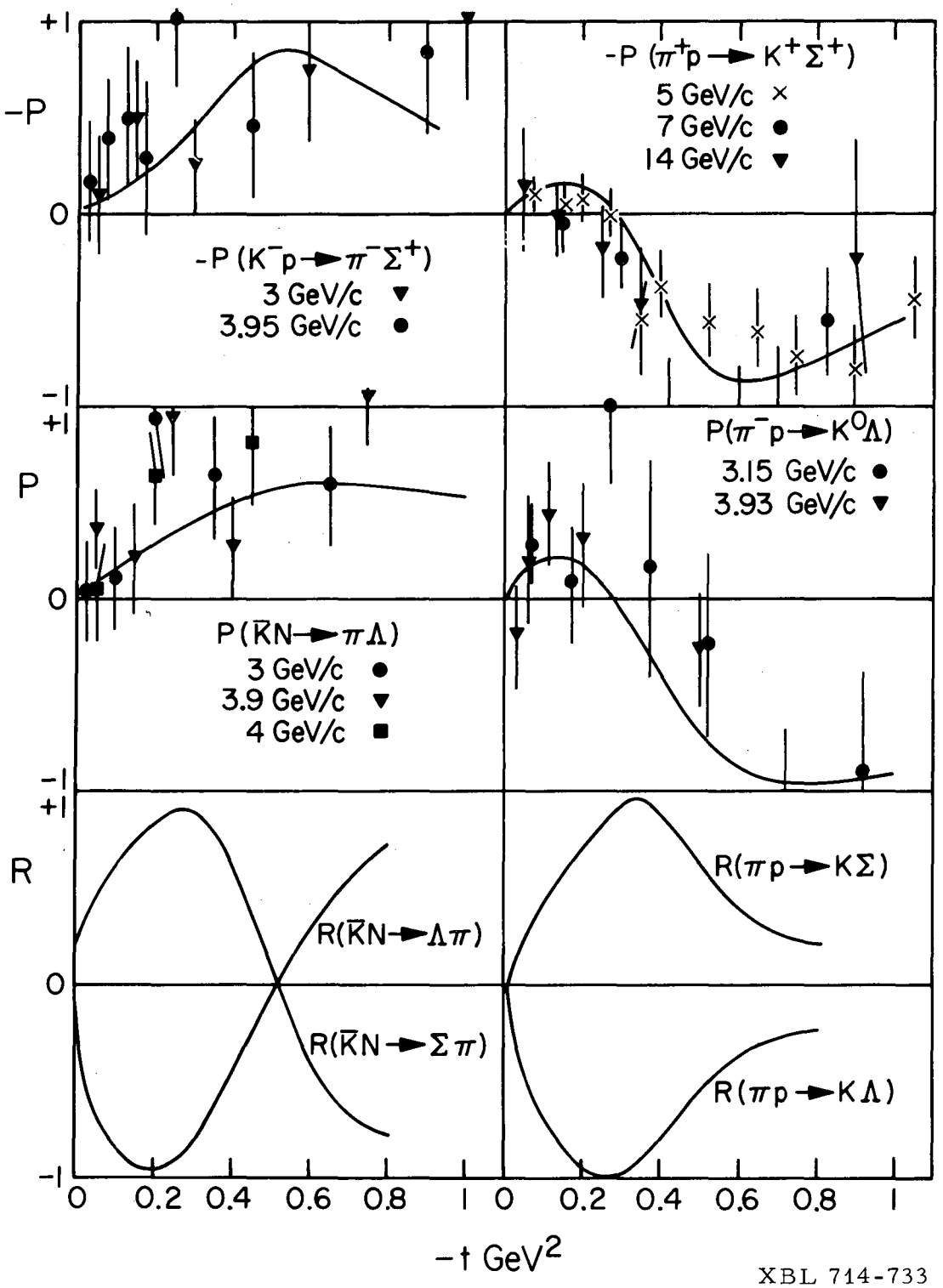

XBL 714-733

Fig. 13.

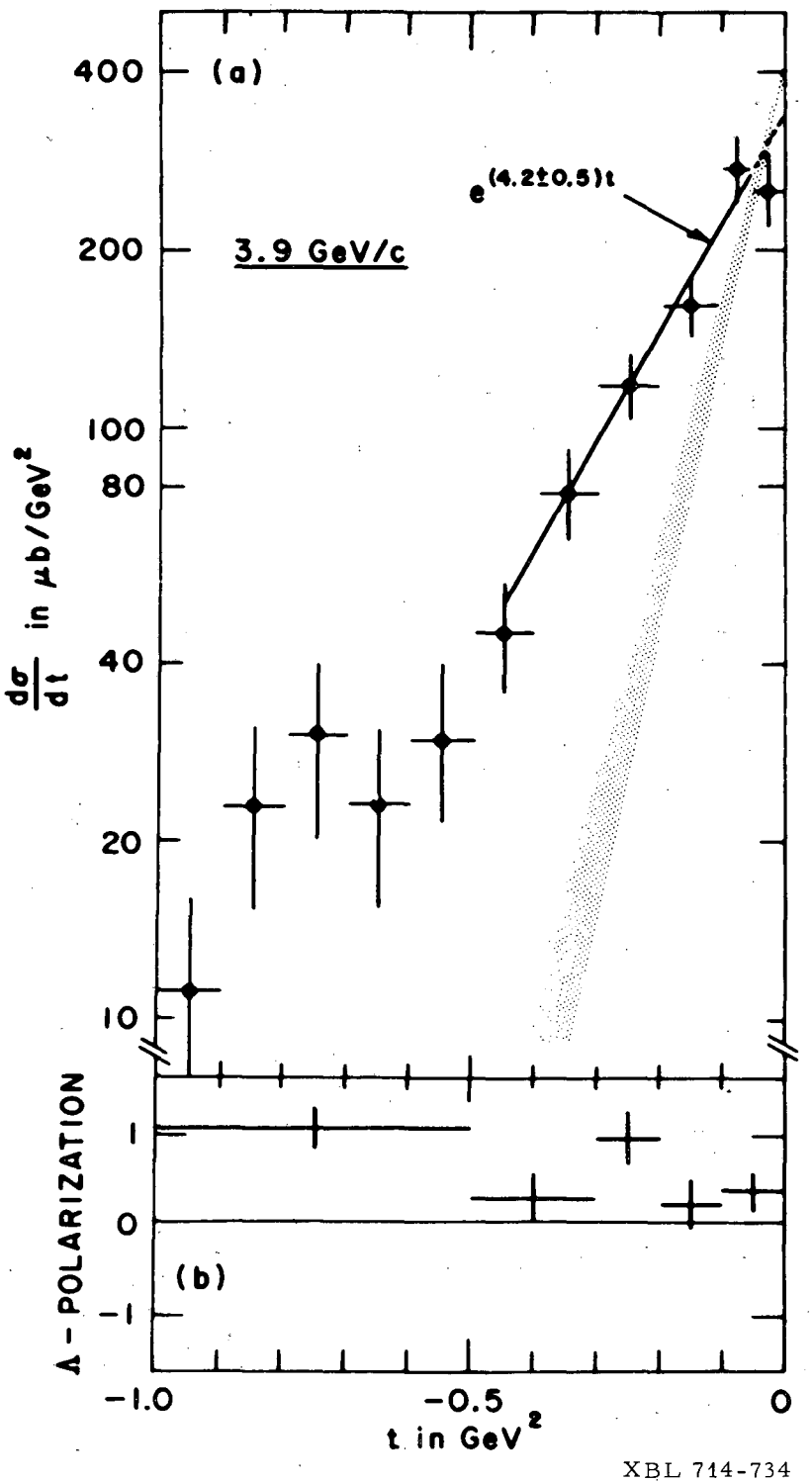
400
(a)
$e^{(4.2\pm0.5)t}$
200
3.9 GeV/c
100
80
$\frac{d\sigma}{dt}$ in μb/GeV²
40
20
10
A - POLARIZATION
1
0
(b)
-1
-1.0
-0.5
0
t in GeV²
XBL 714-734

Fig. 14.

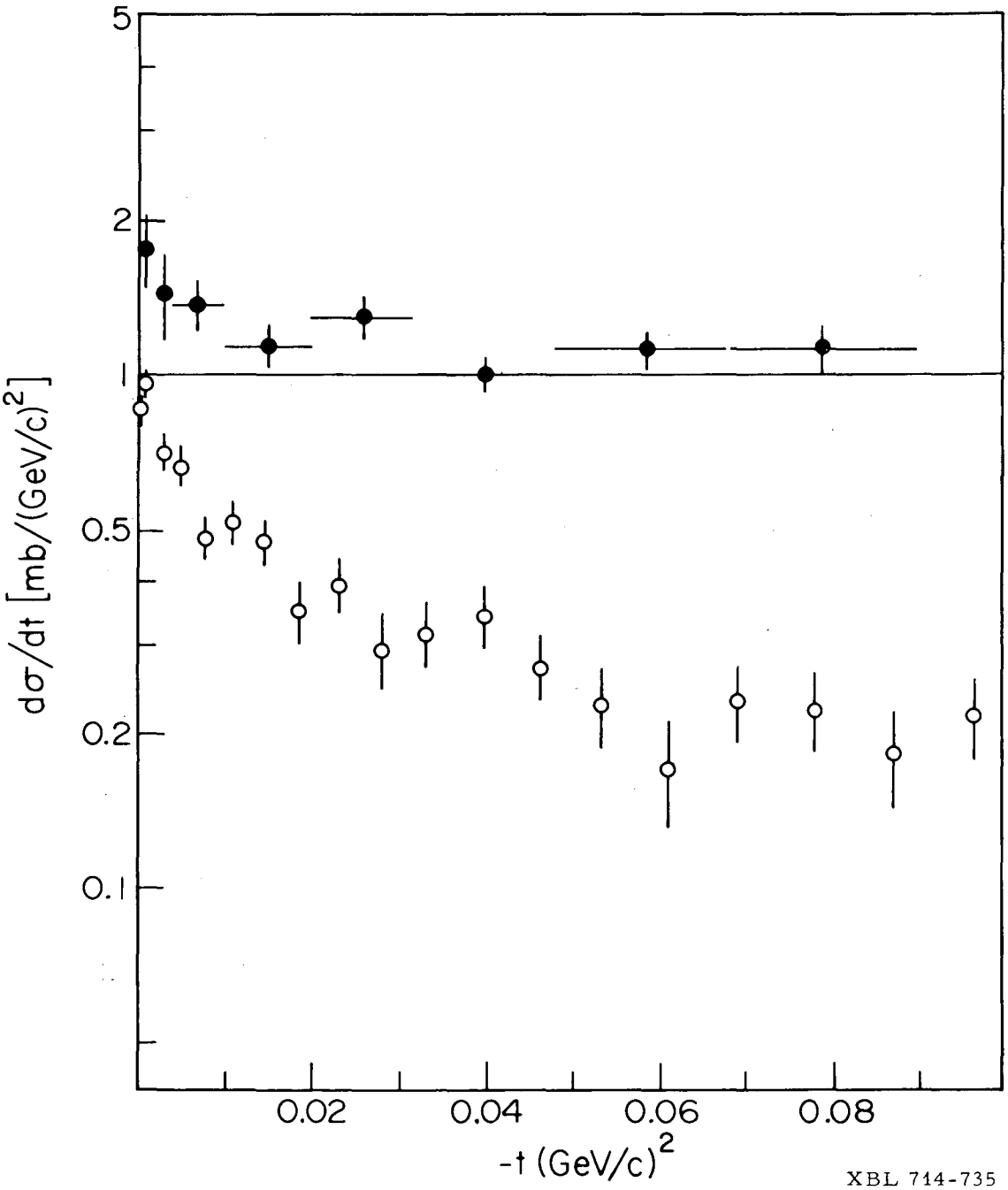

Fig. 15.

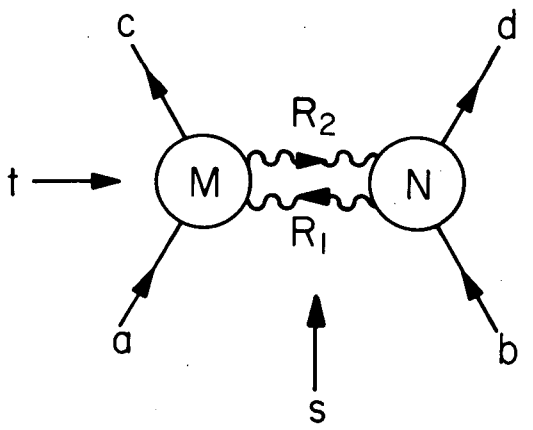

(a)

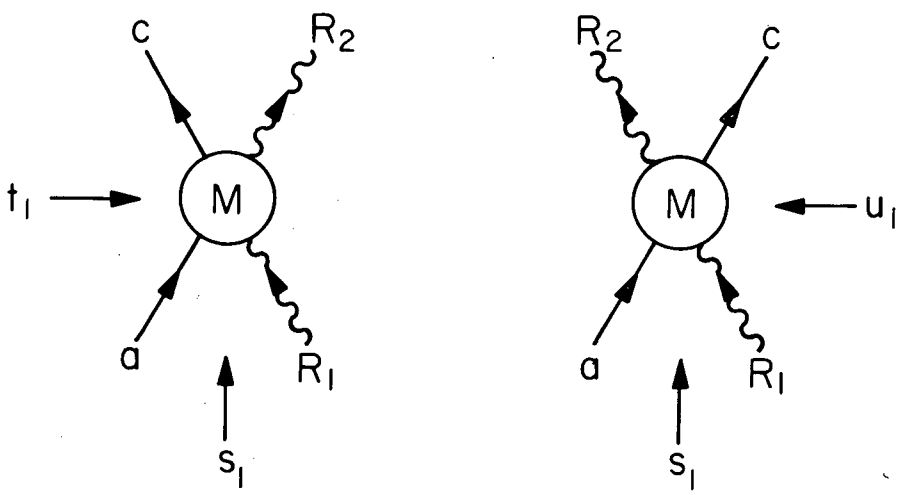

(b)

XBL 714-736

Fig. 16.

M – channel

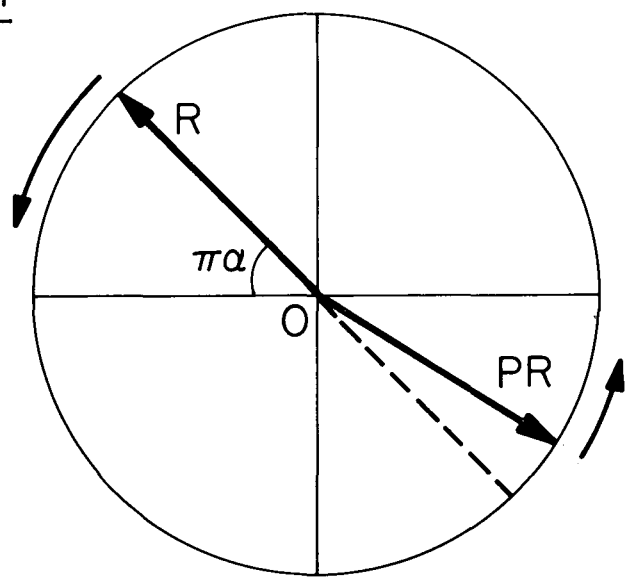

(a)

R – channel

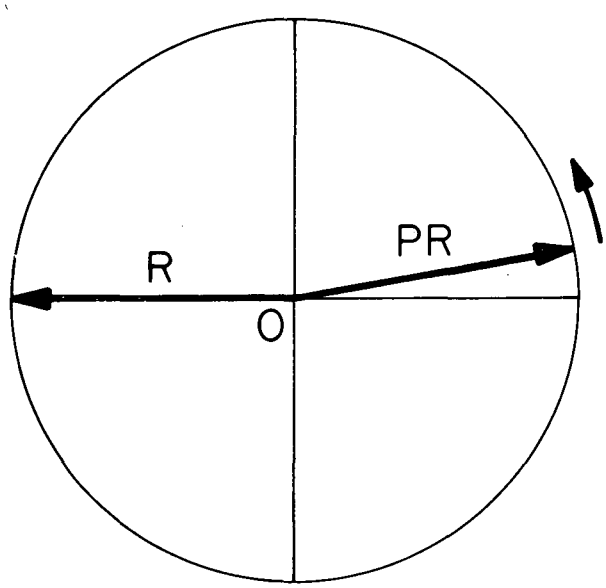

(b)

XBL 714-737

Fig. 17.

Discussion

Schmid (CERN): One interesting thing in strong interactions is clearly the connection between low energy and high energy through duality. The surprising fact has been that the high energy features are observed experimentally, depending on the channels, down to 1.5 - 3.0 GeV in the lab system. Therefore experiments at comparatively low energy are important for Reggeology. The second experimental point about why it is interesting to do high energy experiments at low energies is that we are also interested in the behaviour of processes at large t values, that is for $1 \leq |t| \leq 3$ $(\mathrm{GeV/c})^2$, and if you want to get an acceptable rate, particularly for measuring polarizations, you will have to go to rather low lab energies. It is also interesting theoretically to do experiments at relatively low energies, because, at low and intermediate energies, crossing is a very effective concept while it is not very useful at high energies because the crossed channel is very far away. For example, there are letters of intent for the Ω project at CERN to measure the differential cross-section, R, A, and P for the reactions $\pi^+ p \to K^+ \Sigma^+$ and $K^- p \to \pi^- \Sigma^+$ in the resonance and Regge regions in both channels. Because of the crossing relations between these two channels such experiments should give far more information than the study of four unrelated experiments.

Ringland (RHEL):

1. An important question is how high in Plab can the techniques of phase shift analysis (PSA) be applied, and what experiments (e.g., A and R, P) are required. It would be good if phenomenologists give some kind of well based answer--it would be a tragedy if experiments gave out at too low a Plab. Computer experiments on data "faked" from some of the more realistic models may well be the best way of answering these questions. Herb Steiner has already started this by faking A and R data from different πN phase shifts, to decide how relevant these measurements would be. It is certainly ridiculously conservative to believe PSA should stop at 2.0 GeV/c.

2. We should stress that PSA is relevant to things other than just the enumerating of resonances. Obvious points we want to find from PSA, particularly outside the very low energy region are:

   a. How do resonances and/or background add to build amplitudes smooth in s?

   b. How do resonances build structure in t for some channels, and not for others.

   c. The nature of the background--how true is the Harari-Freund hypothesis?

   d. Perhaps most important of all, PSA (particularly if pursued to high Plab) helps via FESR to understand high energy data. So in this way the medium energy domain is completely

complementary to the high energy domain. But we must stress that both s and u channels are required, e.g., good $\pi N \to K\Lambda$ data cries out for good $\bar{K}N \to \pi\Lambda$ data. All this implies that in picking channels to study one should not just consider the resonance properties in isolation.

3. Though PSA may be forced up to say 3.5 GeV/c or higher it is possible even probable--that there will exist a region between the phase shift region and the high energy region--the intermediate region. What should one do here?

Experiments with good statistics are surely of interest--but one expects that the small intervals in Plab required for PSA will not be required.

Presumably A and R measurements will be particularly important--focusing attention on reactions with a Λ or Σ^+ in the final state.

Lovelace (Rutgers): One can push phase shift analysis to higher energies by including some theoretical information, and the higher you wish to go, the more theoretical input you will need. People who rely on a wrong theory, will find it hard to get a consistent fit. Phenomenology is very much survival of the fittest.

R. L. Kelly (Carnegie-Mellon University): As Ringland mentioned, it is important to know which A and R measurements would be most useful in distinguishing various phase shift solutions. It is also important to realize that there may be energy regions where all phase shift solutions for a particular reaction agree

in spite of the fact that the parameters are poorly determined by the existing cross-section and polarization measurements in that region. In such an energy region it would not be particularly surprising to measure the spin-rotation parameters and find disagreement with all existing phase shift solutions.

I can mention a specific example of this that has turned up in the CMU-Argonne-Northwestern phase-shift analysis of K^+p scattering. Nearly all analyses of this reaction find the $P_{3/2}$ amplitude to be fairly inelastic and moving in a counter-clockwise loop in the fourth quadrant of the unitarity circle for momenta between about 1100 and 1300 MeV/c. We have found that the elasticity in this region is not at all well determined, and that there exist very elastic solutions in which the loop is squashed down close to the edge of the unitarity circle. The other partial waves are not changed much. The A and R parameters in the forward hemisphere are quite sensitive to the $P_{3/2}$ elasticity in this energy region, and their measurement would help to decide about the existence of a Z^*.

Concerning the actual measurement of A and R, there seems to be a fear among some experimentalists, particularly with regard to intermediate and high energies, that they may try to measure A or R or some linear combination of A and R, and get a null result, therefore getting no information out of their experiment. In this connection I want to repeat a remark of Cutkosky's. Once the polarization is measured one

can regard the spin-rotation parameters as a vector (A,R) of known length, $\sqrt{1 - P^2}$, but unknown orientation in the "AR-plane." It's easy to see that the orientation of a vector of known length is better determined by the measurement of a small component of the vector than by a comparably accurate measurement of a large component. So the measurement of a linear combination of A and R which turns out to be small is actually more informative than the measurement of a large linear combination.

SOME USEFUL HADRONIC EXPERIMENTS AT INTERMEDIATE ENERGIES

E. L. Berger, G. C. Fox, C. Quigg, and G. A. Ringlund

SOME USEFUL HADRONIC EXPERIMENTS AT INTERMEDIATE ENERGIES

Introduction. Here we list some experiments of obvious importance. The list is of course not complete, nor will everyone agree that all the entries are equally valuable, but we hope our outline will catalyze the discussion. We have itemized broad classes of experiments as well as specific reactions. Additional ideas will surely emerge from the workshop. Essentially all exploratory experiments have been done at intermediate energies. (In fact, this is true up to 30 GeV/c.) Hence the proposed experiments will require high statistics and significant logistical effort. The most useful incident momenta, ranges of momentum transfer, and required statistical precision must be determined through critical appraisal of the already completed survey experiments, together with the physics objectives. The values suggested here are only rough estimates.

A. Stable Particle Channels: Phase Shift Region. This region encompasses threshold up to ?? GeV/c; the value ?? must be defined. Differential cross section measurements on the order of 10-50 Kevents/momentum, and polarization data of comparable quality to the best existing pion-nucleon polarization data (±0.05 for 30 angular bins) will be required. The significance of A and R measurements in discriminating solutions must be studied, and where the measurements prove crucial they should be done. The associated production reactions listed below are particularly accessible to A and R measurements as the weak hyperon decay analyzes its polarization. Typical reactions:

(i) πN elastic and CEX for $p_{lab} > 2 \to 3$ GeV/c.

(ii) $\bar{K}N$ elastic and CEX: there are glaring gaps in the low energy polarization measurements, particularly below $p_{lab} = 900$ MeV/c.

(iii) $\pi N \to KY$, $\bar{K}N \to (\gamma,\eta)Y$: $d\sigma/dt$, P, R, A

(iv) $K^- p \to K^+ \Xi^-$

B. Multiparticla channels in the phase shift region. Lack of polarization data has hampered phase shift analyses of multiparticle final states. Experiments on polarized targets (with what techniques?) are (a) $KN \to K\pi N$; (b) $\bar{K}N \to \Lambda\omega$; (c) $\pi N \to \pi\pi N$; (d) polarized proton beam on p,d $\to NN\pi$ is sensitive to dibaryon exotics, as (a) is to Z*'s. These measurements should be backed up by very high statistics unpolarized measurements.

C. Bubble Chamber Program. 1. Intensive analysis at 5 GeV/c. A coordinated series of very high statistics (100 events/μb) bubble chamber experiments at ∿5 GeV/c will clarify many issues raised by existing exposures. Detailed examination should be made of all observable quantities in all processes initiated by K, $\bar{K}$, $\pi^{\pm}$, and protons on both hydrogen and deuterium. The payoff from such experiments is reasonably clear, as 5 GeV/c is essentially the beginning

of the energy range in which quasi-two-body processes have attained smooth, asymptotic behavior. 2. Complementarity. (Counter and Bubble Chamber Techniques). Bubble chamber results from experiments discussed above may be used in conjunction with high statistics counter experiments. For instance, complementary studies can improve understanding of universal features of inclusive processes (e.g. $d\sigma/dp_\perp^2 \propto \exp(-3p_\perp^2)$). 3. Low energy. (a) Stable-particle final states phase shift analysis, see A; (b) Multiparticle final states phase shift analysis, see B(a). 4. Polarized Proton Beams. (a) Low energy ($\sim 1 \rightarrow 2$ GeV/c) polarized p on p, $d \rightarrow NN\pi$ as in B(d). (b) ~ 5 GeV/c polarized p on p, d will supplement C1 with a new class of measurements. For instance, one can study the variation of the polarization asymmetry with the final state. 5. Deuterium. Bias or other effects associated with the "spectator" nucleon should be examined carefully. Validity of neutron data obtained from deuteron exposures may be tested precisely by comparison of neutron spectator events with direct proton data for a variety of processes.

D. "High Energy" Counter Physics. All possible two-body and quasi-two-body cross sections should be measured from 5 to 15 GeV/c. As in A, these should be done with polarized and unpolarized beams and targets.

E. It is likely that there will exist a region too high in energy for phase shift analysis, but below the high energy region. This region will almost certainly be above 3.0 GeV/c. Here high statistics experiments should be done, but not at the close spacings in energy required for phase shift analysis. Channels where A and R are comparatively easy to measure are particularly interesting, but all channels will be of significance.

E. L. Berger
G. C. Fox
C. Quigg
G. A. Ringland

CALT-68-305

AEC RESEARCH AND
DEVELOPMENT REPORT

Quantum Numbers of Cross-Channel Exchanges

J. MANDULA,* J. WEYERS,*† and G. ZWEIG*‡

California Institute of Technology, Pasadena, California 91109

and

F. HALZEN

CERN, Geneva, Switzerland

Paper presented at the

Workshop on Particle Physics at Intermediate Energies

California Institute of Technology
March 29-30, 1971

* Work supported in part by the U. S. Atomic Energy Commission. Prepared under Contract AT(11-1)-68 for the San Francisco Operations Office, U. S. Atomic Energy Commission.

† On leave of absence from CERN, Geneva, Switzerland and the University of Louvain, Louvain, Belgium.

‡ Alfred P. Sloan Foundation Fellow.

Most phenomenological analyses of high energy scattering describe reactions in terms of their crossed channel exchanges. It is therefore desirable to organize scattering data so that the contributions of each set of crossed channel quantum numbers are isolated. We know from examination of reactions where only exotic quantum numbers are exchanged that exchanges with these quantum numbers are strongly suppressed. Their size is not known quantitatively, however. A sensitive way to measure these exotic exchanges is to interfere them with the dominant non-exotic exchanges. We catalogue here all relations following from the absence of exotic exchanges which have the property that their violation is proportional to the interference between an exotic and a non-exotic exchange, rather than to the square of an exotic exchange.

Many of these relations have been described previously and are included here only for completeness.[1] The compendium, which is in Table I, contains two classes of relations. Class I relations depend only on the absence of exotic exchange while Class II relations depend in addition on exact SU_3 symmetry. We have omitted relations between reactions with different crossed channel isotopic spins, since they, of course, are expected to have different energy dependences.

An instructive way to present the data correlated by these relations would be to calculate their percentage of violation as a function of energy and angle for each reaction. A "contour map", with percentage violation plotted as height on the s-t plane, would clearly show the limits of the purely non-exotic exchange approximation, and might give clues about what are the important dynamical effects in various parts of the physical region.

We would like to make several remarks about possible uses of these relations and about expectations based on currently popular models.

(a) It would be especially interesting to compare reactions that involve currents (photoproduction, Compton scattering, and inelastic electron and neutrino scattering at various fixed q^2) to purely hadronic reactions. If the "contours of constant percentage violation" have the same shape in both kinds of reactions, one would be fairly confident that the same dynamical approximations could be applied to both. But if the contour maps were qualitatively different, then different dynamical descriptions of each type of reaction would have to be sought.

(b) If the Class I relations are very accurately satisfied in some region of energy and angle, then one could assume that in that part of the physical region the approximation of no exotic exchange is very accurate. In the same part of the physical region the violation of Class II relations will then constitute a measurement of the violation of SU_3 symmetry. Examination of reactions involving currents may allow one in addition to examine SU_3 symmetry breaking as a function of the mass of the current.

(c) At low energies where there are prominent resonances with definite direct channel quantum numbers, these relations must be strongly violated. It is possible that the relations correlating baryon number two reactions are more accurate at low energies since there are no strong resonances in this channel.[2)]

The remaining remarks are made within the Regge phenomenological framework:

(d) Regge poles and their associated diffractive cuts have the same internal quantum numbers and so these cuts do not lead to any violation of the "no-exotics" relations.

(e) Regge asymptotic behavior asserts that lines of fixed t on the s-t plane will cross contours of constant percentage violation. For fixed t, the relations will become exact as s goes to infinity. If the potential theoretic intuition that the magnitude of the crossed cosine determines the accuracy of the Regge asymptotic formula is correct, then the contours of constant violation will asymptote to rays of fixed t/s, at least for small t/s.

One of the authors (J.W.) would like to thank Professor Murray Gell-Mann for his hospitality at the California Institute of Technology.

TABLE I

The relations given are between the cross sections of the indicated processes. Class I reactions depend only on the absences of crossed channel exotic contributions, while Class II reactions depend on exact SU_3 symmetry as well. Except for the two relations involving four cross sections, they are all the squares of relations between amplitudes and so the polarizations of the particles in related reactions should be equal. The particle names denote only the internal quantum numbers of the indicated particles so that π^+, for example, may stand for $\pi^+(140)$, $\rho^+(765)$, $A_1^+(1070)$, $A_2^+(1305)$ . . . . An octet of mesons is denoted by M, an octet of baryons by B, and a decuplet of baryons by Δ. Σ^* and Ξ^* denote members of a decuplet. The relations enclosed in $\{\ \}$ are the squares of relations which could be obtained by isotopic rotations from other amplitude relations whose squares appear in the table. However, because the relative phases of the isospin eigenamplitudes are unknown, these cross section relations are in fact independent. The Cabibbo angle is denoted by θ.

Reaction	Class
$\underline{MB \to M'B'}$	
$\pi^+p \to K^+\Sigma^+ = 2(\pi^-p \to K^0\Sigma^0)$	
$K^-p \to \pi^-\Sigma^+ = 2(K^-n \to \pi^-\Sigma^0)$	I
$\{K^-p \to \pi^-\Sigma^+ = 4(K^-p \to \pi^0\Sigma^0)\}$	
$(K^-p \to \bar{K}^0n) + (K^+n \to K^0p) = (\pi^-p \to \pi^0n) + 3(\pi^-p \to \eta n)$	II
$\underline{MB \to B'M'}$	
$\pi^-p \to p\pi^- = K^-p \to \Sigma^+\pi^-$	II

TABLE I (cont.)

Reaction	Class
$MB \to M'\Delta$	
$\pi^+p \to \pi^+\Delta^+ = \pi^-p \to \pi^-\Delta^+$	
$\{\pi^+p \to \pi^+\Delta^+ = 2(\pi^-p \to \pi^o\Delta^o)\}$	
$\pi^+p \to K^+\Sigma^{*+} = 2(\pi^-p \to K^o\Sigma^{*o})$	I
$K^-p \to \pi^-\Sigma^{*+} = 2(K^-n \to \pi^-\Sigma^{*o})$	
$\{K^-p \to \pi^-\Sigma^{*+} = 4(K^-p \to \pi^o\Sigma^{*o})\}$	
$(K^+p \to K^+\Delta^+) + (K^-p \to K^-\Delta^+) = \frac{1}{2}(\pi^+p \to \pi^+\Delta^+) + (\pi^+p \to \eta\Delta^{++})$	II
$MB \to \Delta M'$	
$\pi^-p \to \Delta^+\pi^- = K^-p \to \Sigma^{*+}\pi^-$	
$\pi^-p \to \Delta^o\pi^o = 2(K^-p \to \Sigma^{*o}\pi^o)$	
$\pi^-p \to \Delta^-\pi^+ = 3(K^-p \to \Sigma^{*-}\pi^+)$	
$\{\pi^+p \to \Delta^+\pi^+ = 2(K^-n \to \Sigma^{*-}\pi^o)\}$	II
$\pi^+p \to \Delta^{++}\eta = 6(K^-p \to \Sigma^{*o}\eta)$	
$\pi^-p \to \Sigma^{*-}K^+ = K^-p \to \Xi^{*-}K^+$	
$\pi^-p \to \Sigma^{*o}K^o = \frac{1}{2}(K^-p \to \Xi^{*o}K^o)$	
$\pi^+p \to \Sigma^{*+}K^+ = K^-n \to \Xi^{*-}K^o$	
$BB \to B'B''$	
$\Sigma^+p \to p\Sigma^+ = 2(\Sigma^-p \to n\Sigma^o)$	I

TABLE I (cont.)

Reaction	Class
$BB \rightarrow B'\Delta$ and $BB \rightarrow \Delta B'$	
$\Sigma^+p \rightarrow \Sigma^+\Delta^+ = \Sigma^-p \rightarrow \Sigma^-\Delta^+$	
$\{\Sigma^+p \rightarrow \Sigma^+\Delta^+ = 2(\Sigma^-p \rightarrow \Sigma^o\Delta^o)\}$	
$\Sigma^+p \rightarrow p\Sigma^{*+} = 2(\Sigma^-p \rightarrow n\Sigma^{*o})$	I
$\Sigma^+p \rightarrow \Delta^+\Sigma^+ = \frac{1}{3}(\Sigma^-p \rightarrow \Delta^-\Sigma^+)$	
$\{\Sigma^+p \rightarrow \Delta^+\Sigma^+ = 2(\Sigma^-p \rightarrow \Delta^o\Sigma^o)\}$	
$pp \rightarrow p\Delta^+ = \frac{4}{3}(\Lambda p \rightarrow \Sigma^{*o}p)$	
$pp \rightarrow p\Delta^+ = 2(\Sigma^-p \rightarrow \Sigma^{*o}n)$	II
$\Sigma^+p \rightarrow p\Sigma^{*+} = \Sigma^+p \rightarrow \Delta^+\Sigma^+$	
$BB \rightarrow \Delta\Delta'$	
$pn \rightarrow \Delta^{++}\Delta^- = 3(pp \rightarrow \Delta^{++}\Delta^o)$	
$\{pn \rightarrow \Delta^{++}\Delta^- = \frac{9}{4}(pn \rightarrow \Delta^+\Delta^o)\}$	
$\Sigma^+p \rightarrow \Sigma^o\Delta^{++} = 3(\Sigma^-p \rightarrow \Sigma^{*o}\Delta^o)$	
$\{\Sigma^+p \rightarrow \Sigma^o\Delta^{++} = \frac{3}{2}(\Sigma^-p \rightarrow \Sigma^{*-}\Delta^+)\}$	I
$\Sigma^+p \rightarrow \Delta^{++}\Sigma^o = \frac{1}{2}(\Sigma^+n \rightarrow \Delta^{++}\Sigma^{*-})$	
$\{\Sigma^+p \rightarrow \Delta^{++}\Sigma^o = 3(\Sigma^-p \rightarrow \Delta^o\Sigma^{*o})\}$	
$pn \rightarrow \Delta^{++}\Delta^- = 3(\Lambda p \rightarrow \Sigma^{*o}\Delta^+)$	II
$pn \rightarrow \Delta^{++}\Delta^- = 6(\Sigma^+p \rightarrow \Sigma^{*o}\Delta^{++})$	
$\bar{B}\bar{B} \rightarrow \bar{B}'\bar{B}''$	
$\bar{p}p \rightarrow \bar{\Sigma}^+\Sigma^+ = 4(\bar{p}p \rightarrow \bar{\Sigma}^o\Sigma^o)$	I
$\{\bar{p}p \rightarrow \bar{\Sigma}^+\Sigma^+ = 2(\bar{p}n \rightarrow \bar{\Sigma}^+\Sigma^o)\}$	

TABLE I (cont.)

Reaction	Class
$\bar{B}B \to \bar{B}'\Delta$	
$\bar{p}p \to \bar{\Sigma}^{+}\Sigma^{+} = 4(\bar{p}p \to \bar{\Sigma}^{o}\Sigma^{*o})$	I
$\{\bar{p}p \to \bar{\Sigma}^{+}\Sigma^{+} = 2(\bar{p}n \to \bar{\Sigma}^{+}\Sigma^{*o})\}$	
$\bar{B}B \to \bar{\Delta}\Delta'$	
$\bar{p}p \to \bar{\Delta}^{++}\Delta^{++} = 9(\bar{p}p \to \bar{\Delta}^{o}\Delta^{o})$	I
$\{\bar{p}p \to \bar{\Delta}^{++}\Delta^{++} = 3(\bar{p}n \to \bar{\Delta}^{++}\Delta^{+})\}$	
$\bar{p}p \to \bar{\Sigma}^{+}\Sigma^{+} = 4(\bar{p}p \to \bar{\Sigma}^{*o}\Sigma^{*o})$	
$\{\bar{p}p \to \bar{\Sigma}^{+}\Sigma^{+} = 2(\bar{p}n \to \bar{\Sigma}^{*+}\Sigma^{*o})\}$	
$\gamma B \to MB'$	
$\gamma p \to K^{o}\Sigma^{+} = 2(\gamma n \to K^{o}\Sigma^{o})$	I
$\gamma p \to K^{+}\Sigma^{o} = \frac{1}{2}(\gamma n \to K^{+}\Sigma^{-})$	
$\gamma B \to B'M$	
no relation	
$\gamma B \to M\Delta$	
$\gamma p \to \pi^{-}\Delta^{++} = 3(\gamma n \to \pi^{-}\Delta^{+})$	
$\gamma p \to \pi^{+}\Delta^{o} = \frac{1}{3}(\gamma n \to \pi^{+}\Delta^{-})$	
$\{\gamma p \to \pi^{o}\Delta^{+} = \gamma n \to \pi^{o}\Delta^{o}\}$	I
$\gamma p \to K^{o}\Sigma^{+} = 2(\gamma n \to K^{o}\Sigma^{*o})$	
$\gamma p \to K^{+}\Sigma^{o} = \frac{1}{2}(\gamma n \to K^{+}\Sigma^{*-})$	
$\gamma p \to \pi^{o}\Delta^{+} = \frac{1}{3}(\gamma p \to \eta\Delta^{+})$	II

TABLE I (cont.)

Reaction	Class
$\gamma B \to \Delta M$	
$\gamma p \to \Delta^{0}\pi^{+} = 2(\gamma n \to \Delta^{0}\pi^{0})$ $\gamma p \to \Delta^{++}\pi^{-} = 4(\gamma n \to \Delta^{-}\pi^{+})$	II
$\nu(\bar{\nu})B \to \mu M B'$	
$\nu p \to \mu^{-}K^{+}\Sigma^{+} = 2(\bar{\nu}p \to \mu^{+}K^{0}\Sigma^{0})$ $\bar{\nu}p \to \mu^{+}\pi^{-}\Sigma^{+} = 2(\bar{\nu}n \to \mu^{+}\pi^{-}\Sigma^{0})$ $\{\bar{\nu}p \to \mu^{+}\pi^{-}\Sigma^{+} = 4(\bar{\nu}p \to \mu^{+}\pi^{0}\Sigma^{0})\}$	I
$(\bar{\nu}p \to \mu^{+}\bar{K}^{0}n) + (\nu n \to \mu^{-}K^{0}p) = \tan^{2}\theta\left[(\bar{\nu}p \to \mu^{+}\pi^{0}n) + 3(\bar{\nu}p \to \mu^{+}\eta n)\right]$	II
$\nu(\bar{\nu})B \to \mu B'M'$	
$\bar{\nu}p \to \mu^{+}\Sigma^{+}\pi^{-} = \tan^{2}\theta\ (\bar{\nu}p \to \mu^{+}p\pi^{-})$	II
$\nu(\bar{\nu})B \to \mu M'\Delta$	
$\nu p \to \mu^{-}\pi^{+}\Delta^{+} = \bar{\nu}p \to \mu^{+}\pi^{-}\Delta^{+}$ $\{\nu p \to \mu^{-}\pi^{+}\Delta^{+} = 2(\bar{\nu}p \to \mu^{+}\pi^{0}\Delta^{0})\}$	
$\nu p \to \mu^{-}K^{+}\Sigma^{*+} = 2(\bar{\nu}p \to \mu^{+}K^{0}\Sigma^{*0})$ $\bar{\nu}p \to \mu^{+}\pi^{-}\Sigma^{*+} = 2(\bar{\nu}n \to \mu^{+}\pi^{-}\Sigma^{*0})$ $\{\bar{\nu}p \to \mu^{+}\pi^{-}\Sigma^{*+} = 4(\bar{\nu}p \to \mu^{+}\pi^{0}\Sigma^{*0})\}$	I
$(\nu p \to \mu^{-}K^{+}\Delta^{+}) + (\bar{\nu}p \to \mu^{+}K^{-}\Delta^{+}) = \tan^{2}\theta\left[\frac{1}{2}(\nu p \to \mu^{-}\pi^{+}\Delta^{+}) + (\nu p \to \eta\Delta^{++})\right]$	II

TABLE I (cont.)

Reaction		Class
	$\underline{\nu(\bar{\nu})B \rightarrow \mu\Delta M'}$	
$\bar{\nu}p \rightarrow \mu^+\Sigma^{*+}\pi^-$	$= \tan^2\theta \ (\bar{\nu}p \rightarrow \mu^+\Delta^+\pi^-)$	
$\bar{\nu}p \rightarrow \mu^+\Sigma^{*o}\pi^o$	$= \frac{1}{2}\tan^2\theta \ (\bar{\nu}p \rightarrow \mu^+\Delta^o\pi^o)$	
$\bar{\nu}p \rightarrow \mu^+\Sigma^{*-}\pi^+$	$= \frac{1}{3}\tan^2\theta \ (\bar{\nu}p \rightarrow \mu^+\Delta^-\pi^+)$	
$\{\bar{\nu}n \rightarrow \mu^+\Sigma^{*-}\pi^o$	$= \frac{1}{2}\tan^2\theta \ (\nu p \rightarrow \mu^-\Delta^+\pi^+)\}$	
$\bar{\nu}p \rightarrow \mu^+\Sigma^{*o}\eta$	$= \frac{1}{6}\tan^2\theta \ (\nu p \rightarrow \mu^-\Delta^{++}\eta)$	II
$\bar{\nu}p \rightarrow \mu^+\Xi^{*-}K^+$	$= \tan^2\theta \ (\bar{\nu}p \rightarrow \mu^+\Sigma^{*-}K^+)$	
$\bar{\nu}p \rightarrow \mu^+\Xi^{*o}K^o$	$= 2\tan^2\theta \ (\bar{\nu}p \rightarrow \mu^+\Sigma^{*o}K^o)$	
$\bar{\nu}n \rightarrow \mu^+\Xi^{*-}K^o$	$= \tan^2\theta \ (\nu p \rightarrow \mu^-\Sigma^{*+}K^+)$	

REFERENCES

1. V. Barger and D. Cline, Phys. Rev. 156, 1522 (1967); A. M. Boyarski, R. Diebold, S. D. Ecklund, G. E. Fisher, Y. Murata, B. Richter, and M. Sands, Phys. Rev. Letters 25, 695 (1970); M. Abramovich, H. Blumenfeld, V. Chaloupka, S. U. Chung, J. Diaz, L. Montanet, J. Pernegr, S. Rencroft, J. Rubio, and B. Sadoulet, CERN preprint PHYS 70-61, to be published in Nucl. Phys. B.

2. If non-diffractive baryon number two amplitudes are real, then

$$\sqrt{pn \to np} = \left| \sqrt{\tfrac{1}{2}(\Sigma^- p \to \Sigma^0 n)} \pm \sqrt{\tfrac{3}{2}(\Sigma^- p \to \Lambda n)} \right|$$

$$\sqrt{pp \to p\Delta^+} = \left| \sqrt{\Sigma^+ p \to \Sigma^{*+} p} \pm \sqrt{\Sigma^- p \to \Sigma^{*-} p} \right|$$

$$= \left| \sqrt{\tfrac{1}{4}(\Sigma^+ p \to \Sigma^+ \Delta^+)} \pm \sqrt{\tfrac{1}{2}(\Lambda p \to \Sigma^- \Delta^{++})} \right|$$

The ambiguity in sign is, of course, related to the ambiguity in the sign of the amplitude.